

Investigating the role of the centromeric histone variant CENP-A in cancer

Charlène Renaud

▶ **To cite this version:**

Charlène Renaud. Investigating the role of the centromeric histone variant CENP-A in cancer. Cellular Biology. Sorbonne Université, 2024. English. ⟨NNT : 2024SORUS349⟩. ⟨tel-05013526⟩

HAL Id: tel-05013526

https://theses.hal.science/tel-05013526v1

Submitted on 31 Mar 2025

HAL is a multi-disciplinary open access archive for the deposit and dissemination of scientific research documents, whether they are published or not. The documents may come from teaching and research institutions in France or abroad, or from public or private research centers.

L'archive ouverte pluridisciplinaire **HAL**, est destinée au dépôt et à la diffusion de documents scientifiques de niveau recherche, publiés ou non, émanant des établissements d'enseignement et de recherche français ou étrangers, des laboratoires publics ou privés.



HAL Authorization

Sorbonne Université

École doctorale Complexité du Vivant (ED n° 515)

Laboratoire Dynamique de la chromatine
Dynamique du noyau (UMR 3664)
Institut Curie, CNRS

Investigating the role of the centromeric histone variant CENP-A in cancer

Étude du rôle du variant d'histone centromérique CENP-A dans le cancer

Par Charlène RENAUD-PAGEOT

Thèse de doctorat de Biologie moléculaire et cellulaire

Co-dirigée par Geneviève ALMOUZNI et Jean-Pierre QUIVY

Présentée et soutenue publiquement le 27 septembre 2024
Devant un jury composé de :

Renata BASTO Directrice de Recherche, Institut Curie, Paris	Présidente du jury
Florian STEINER Directeur de Recherche, Université de Genève	Rapporteur
Reini FERNANDEZ DE LUCO Directrice de Recherche, Institut Curie, Orsay	Rapportrice
Benoît MIOTTO Directeur de Recherche, Institut Cochin, Paris	Examinateur

To my sister,
A ma sœur.

"Alone we can do so little
together we can do so much."
Helen Keller

"Every individual matters.
Every individual has a role to play.
Every individual makes a difference."
Jane Goodall

"Je suis de ceux qui pensent que la science est d'une grande beauté [...]
Si je vois quelque chose de vital autour de moi,
c'est précisément cet esprit d'aventure,
qui me paraît indéracinable et
s'apparente à la curiosité."
Marie Skłodowska-Curie

ACKNOWLEDGEMENTS

REMERCIEMENTS

Et voilà. Here I am, at the conclusion of this beautiful journey. I recall my first experience in a lab during my bachelor's (licence) internships in Nantes – what a challenge, and what a joy it was! Early on, I knew that pursuing a PhD in cellular biology was my objective. Before diving in, I prepared myself for the journey ahead: the inevitable ups and downs, moments of doubt, and the stress and anxiety that are part of the process (Friedrich et al. 2023). However, I was confident that I would love working on my PhD project. From the moment I began as an M2 intern, I was captivated by the subject. As expected, the PhD experience has been a challenging endeavor, yet incredibly rewarding. If given the chance, I would do it all over again, without hesitation or regret. Along the way, I've had the privilege of meeting extraordinary people! Shared many moments of joy, pride and laughter with them! Felt the thrill of discovering something for the first time! And the satisfaction that comes with learning – and understanding – new concepts! I've also witnessed my own growth as a scientist. I had the chance and privilege to conduct research in a great environment. I could participate in stimulating courses, teach, communicate science and engage in many events as a member (then President) of the Training Advisory Board (TAB) of the Labex DEEP. For all these reasons, I've enjoyed every step of the journey and my PhD experience will forever hold a special place in my heart, filled with cherished memories. I am happy to have reached this milestone, an accomplishment that would not have been possible without the support of the incredible people I've been fortunate to meet. To all of you, I want to express my deepest gratitude.

First, I thank Reini De Luco and Florian Steiner for accepting to review this manuscript, along with Renata Basto and Benoît Miotto for kindly agreeing to take part in the jury for my PhD defense. Finding experts in our field who are both available and willing to dedicate their time to reviewing a thesis is no small feat, and I am truly grateful for your generosity. Thanks for your interest and positive feedback when I first introduced my project, and thanks for the time and expertise you have generously shared throughout this process. I would like to extend my sincere gratitude to the members of my thesis committee: Frédéric Devaux, Daniele Fachinetti and Pascal Pineau. You have provided me with great advice and feedback during our meetings, while being attentive and positive… You have done a great, great job!

I also want to express my gratitude to the Ecole Doctorale Complexité du Vivant and Sorbonne Université for providing the training and financial support that made it possible for me to pursue my PhD. I am also thankful to the Fondation pour la Recherche Médicale (FRM) for their generous funding, which supported me during the fourth year of my doctoral studies. Thanks also to the Intercept-MDS network and Marcus Buschbeck for inviting and warmly welcoming me into your community. The excellent courses on leukemia, epigenetics, single-cell genomics and bioinformatics have allowed me

to get invaluable knowledge and meet wonderful friends! Finally, I thank the Institut Curie for welcoming me and providing me with excellent courses and conferences throughout my PhD studies.

I also want to thank my collaborators on the project: Laura Cantini and Daniele Capocefalo at Institut Pasteur. Your motivation, your insightful feedback and, of course, your great "multiomic" contribution have made this collaboration both fruitful and rewarding! Exchanging ideas with you has always been a fun and inspiring experience. I would also like to thank Krastan Blagoev for consistently sharing new exciting ideas. Your enthusiasm and energy toward the project have also been truly inspiring!

Je souhaite également remercier ma directrice de thèse, Geneviève, ainsi que mon co-directeur de thèse, Jean-Pierre. Geneviève, merci de m'avoir accueillie dans ton équipe. Merci également de m'avoir offert de nombreuses opportunités à tous les niveaux. Enfin, un grand merci pour la confiance que tu m'as accordée ; j'espère ne pas t'avoir déçue. Jean-Pierre et Geneviève, merci à tous les deux de m'avoir formée, conseillée et corrigée. Merci aussi d'avoir été patients avec moi au cours du processus ! Merci pour avoir partagé vos connaissances, mais aussi pour votre esprit critique, votre rigueur et votre exigence ; J'ai énormément appris à vos côtés (sans exagérer), et j'en suis profondément reconnaissante. En bref: **mille mercis**.

A special thank you to Daniel, my mentor in the lab from the very beginning. You have truly been the best mentor a student could ask for, really. Thanks for being who you are: smart, kind, patient and invested in my training without ever placing undue pressure on me. I am grateful for the opportunity to work with you and for all that you taught me: not only science, but also all the valuable aspects in a lab: the communication, the organization, and more. As David wrote, you are "the most Canadian" person we could have met, and I couldn't agree more (that's a compliment)! In short, **thanks for being a great teacher**. I've learned so much from you, and I hope to become a great teacher like you, one day.

Many thanks to all my (past and present) colleagues from the UMR 3664 for these wonderful ~4 years and a half together! I will always be thankful to you for your kindness, warmth, and support! Without a doubt, I can say that the atmosphere in our unit is among the best one could ever hope to experience in any work environment. It has been one of the main reasons I've come to the lab each day with a smile on my face. In particular, I want to thank Marie, Caroline, and Marion for your invaluable help with administrative matters and your constant kindness, patience, and support. Vous êtes géniales. Special thanks to Isabelle for becoming a great friend, for always looking out for us, and for being such a kind soul. Thanks, Héloïse, for your kindness, fun discussions (often really needed!) and your positive energy. I am really happy that I could get to know you more! Thanks also to Inês for your energy, advice and kindness towards us – TAB members – when organizing events. It was great working with you and preparing the Art & Science exhibition together! Thank you to all team leaders in the unit: Antoine for always being here to help students, Ines for your smile, kindness and for having taken some of your time to teach me about Lepidoptera! Thanks, Angela, for being such a great support to the students,

including during our efforts to get and secure university and visa fee reimbursements! Thanks, Nathalie, for your invaluable help with administrative matters related to the Ecole Doctorale and the University, for ensuring students' voting rights, and for being a reassuring and cheerful presence during UMR meeting presentations! And thank you, Léonid, for your positivity and for sharing exciting hypotheses with me after watching my UMR meeting presentation – it was really motivating!

I want to extend my heartfelt thanks to everyone in the Chromatin Dynamics team: you are all amazing and an endless source of knowledge. First, a huge thank you to Alodie for your tremendous help with administration and so much more! Your good advice and unwavering kindness and positivity have made a significant impact. Thanks to Sébastien and Weitao for your passion and energy, and for always being ready to share some exciting scientific news. Thanks, Dominique, for your advice; I appreciate your willingness to provide feedback after my presentations and for your steadfast support! Many thanks to Delphine and Christele for the fun discussions and for your support! David, merci pour ton humour, ta joie de vivre et pour tes encouragements depuis ton retour dans l'équipe. Thérèse, thanks for your interest and questions during lab meetings. Thanks also for checking on me when I started writing my thesis, I really appreciated that you made sure I stay hydrated and fed (hahaha)! Thank you, Audrey, for becoming my new neighbor in the lab, for being helpful and full of ideas, thanks also for your contributions on the project. It has been great working with you and learning from you! Iva, a special thank you for regularly sharing pictures of your cat Mirko (very important, 10/10 for the support!), for motivating me to attend stretching sessions with you, for reminding me about lunch, and for becoming a good friend. Your fun and positive spirit, along with your insightful feedback after my presentations, have meant a lot to me. In addition, I want to thank you for giving me the opportunity to teach during my PhD: it has been a great experience! Many thanks to you Nicole for your infinite kindness, for your support and your patience… You are a wonderful friend, and I wish you all the best. I also want to thank some special alumni: Kamila and Marina, it was great meeting you in the lab. Thanks a lot for your support, advice and jokes.

Additional special thanks are absolutely required for the students of the team/unit. I will definitely miss you all. You have been a great support and a source of joy and laughs! In particular, Tina, thank you so much for your kindness, your advice, and for being so patient. I admire your intelligence and rigor; you are a great scientist, and I am convinced you will do great! Thank you for being such a good friend; it is always a joy being around you! Stefano, my former neighbor in the lab, thanks for being so nice and patient with my (and Florian's) Italian food jokes! It has been great having you in the lab, you really were a source of joy and knowledge about birds and Italian food… To the new "babies" of the lab: thank you first Shubhamay (Shub) for your joy, your jokes and your positivity in the lab. I am extremely happy I could get to know you! You'll be a great scientist! Thank you Asya, it is a joy having your positivity and enthusiasm in the team. You're smart and I have no doubt your PhD will be successful!

Manuela, merci pour ta bienveillance constante, ton soutien, ton amitié. Tu as été une super représentante pour les étudiants ! Tu es une amie formidable, prends soin de toi. Colin, merci pour ta gentillesse et tes efforts pour améliorer les choses autour de toi. Gonçalo, I truly appreciated your unwavering support and valuable advice during challenging times. Gertjan, thank you for your kindness, engaging debates, and mutual encouragement while writing our theses; it was a pleasure getting to know you! Yang, thanks for your enthusiasm, positivity, and kindness! Thanks also for the delicious sweets! Samuele, a big thank you for being a little sun in the lab, with your positivity and your jokes! Take care. Abhro, thanks also for always bringing so much humor and joy into every conversation… Keep this optimism! Martin, I just wanted to say thank you for your positive energy (truly one of a kind!) which reminded me to focus on the good things in life - I'm glad we had you around when writing the thesis! All the best for your next adventures. Special thanks to Lucas and Ana: thanks for the party and the discovery of Brazilian food. It was great meeting you both, and I hope we can stay good friends in the future! I wish you both great success in the next steps of your careers! Erica, I am so happy to have had the chance to meet you. It was a real pleasure to go through all the stages of writing a thesis with you, Gertjan and Lucas. I wish you all the best. Special thanks go to Fadma; you are an amazing friend. I can't wait to see you again in the lab and have our little fun lunches and discussions together. Merci pour tes avis honnêtes et tranchés, pour les débats sans fin, pour les bons restaurants et les fous rires… Thank you to the students and postdocs of Labex DEEP. I am deeply grateful for the opportunity to serve as your TAB president for the past 2 years (time has flown)! I hope I did not disappoint you, and that you appreciated being part of the TAB! I also want to extend my thanks to the students I met during ITN-MDS trainings. Ollie, merci pour ton amitié, ton soutien et ta bienveillance. C'était top de rencontrer un autre fan d'histones dans le groupe. J'ai hâte de venir te rendre visite à Barcelone ! Je te souhaite le meilleur. De manière générale, à vous tous, chers collègues et amis, je vous souhaite tout le bonheur du monde.

Je souhaite continuer en français pour remercier des personnes qui ont joué un rôle-clé dans mon parcours : Merci à mes anciens maîtres de stages. J'ai commencé à me former avec vous, j'ai beaucoup appris de vous et mon passage chez vous a fortement influencé la scientifique que je suis devenue. Vous avez contribué à alimenter la passion scientifique qui m'alimente (et ne cesse de grandir) encore aujourd'hui. Pour cela, merci à Vehary Sakanyan pour m'avoir offert mon premier stage, j'ai découvert l'univers de la recherche à vos côtés. Merci à Paul Déléris pour avoir été un professeur et un maître de stage aussi motivant ; c'est en stage avec toi que j'ai réalisé « Ouah, c'est vraiment ça que je veux faire. » Finalement, je ne suis pas tombée si loin de tes traces, j'ai quand même bien fini par faire de la signalisation cellulaire (au moins en partie)… Elle est partout ! Enfin, merci à Evelyne Lauret pour m'avoir permis de fortifier mes compétences en clonage (par la force des choses !), et pour m'avoir encouragée dans mon choix de carrière. Mes plus sincères remerciements, à vous, et à tous les professeurs merveilleux rencontrés depuis le début de ma scolarité.

Mélo, un grand merci pour ta gentillesse et ta patience, même quand je suis tellement focalisée sur mon boulot que je ne donne pas signe de vie. Tu es la meilleure des amies, prends toujours soin de toi. Béatrice, merci de m'avoir accueillie lorsque les circonstances étaient dramatiques. Tu m'as offert une porte de sortie, un toit sur la tête et de quoi me nourrir, sans contrepartie. Grâce à toi, je ne me suis jamais sentie seule. Grâce à toi, j'ai terminé le lycée presque normalement. J'ai compris qu'on a toujours plus d'une option, et qu'une main tendue peut tout changer. Je te souhaite de rester en bonne santé, que le crabe ne réapparaisse jamais. Quant à moi, je continuerai de rester forte et de rendre la pareille. Un très grand merci également à Stéphane et Christelle ! Merci de m'avoir accueillie dans votre famille. Je vous serai toujours reconnaissante pour votre gentillesse et votre soutien. Merci d'avoir été bons avec moi et de m'avoir encouragée et aidée à aller à Paris pour mes études alors même que vous me connaissiez à peine.

Merci à ma sœur, Nelly, ainsi qu'à Kévin. Avec Mathys et Thiago, vous êtes ma famille. Nelly, merci d'avoir été une grande sœur qui faisait de son mieux malgré les circonstances. Merci pour ton soutien lorsque j'ai commencé à faire des études supérieures, merci d'avoir fait l'effort de me retrouver, de venir vers moi. Tu t'es assurée que j'ai de quoi manger et que je puisse continuer mes études. Merci d'avoir cru en moi, et de continuer m'encourager. Merci d'être patiente lorsque je donne trop peu de nouvelles car je suis obnubilée par le travail. Merci. Merci de me connaître si bien. **Merci d'être toi.** Je t'aime fort. Je remercie également nos grands-parents. Vous nous avez quitté lorsque je commençais à peine ma thèse, par un triste concours de circonstances. Alors que ma thèse se termine, mes pensées ne peuvent s'empêcher de se tourner vers vous. Mamie, merci d'avoir été la bonté incarnée. Merci de m'avoir encouragée. Tes appels quotidiens me manquent. Je vous aime fort.

Enfin, Florian, mon amour, la douceur incarnée derrière une façade d'enfant farouche… Merci d'avoir bousculé tes habitudes et d'avoir quitté Nantes pour me rejoindre. Merci pour ta patience quand j'avais du mal à prendre une décision et à planifier des congés, où que je finissais par retourner au labo pour une expérience. Merci de croire en moi et de m'encourager tout en me rappelant qu'il y a aussi une vie en dehors du labo ! Plus généralement, merci d'être si gentil et généreux avec moi… Et de faire de ton mieux pour être un soutien au quotidien. Tu as su me rassurer dans les moments difficiles et partager ma joie dans les moments de bonheur – et je suis heureuse d'avoir pu les partager avec toi. J'ai hâte de découvrir ce que l'avenir nous réserve. Merci de prendre soin de nous. **Je t'aime.**

~

Je souhaite conclure avec une photo du Jardin Marie Curie, à l'Institut Curie (Paris). On peut voir la façade du bâtiment Pasteur, cadre de mon parcours de doctorat, ainsi que les statues de Marie Skłodowska-Curie et Pierre Curie. Ce fut une joie et un privilège de passer chaque jour de mes études doctorales dans cet endroit historique… et inspirant.



"Nothing in life is to be feared, it is only to be understood."
"Rien dans la vie n'est à craindre, tout doit être compris."

Marie Skłodowska-Curie.

ABBREVIATIONS

ASF1	Anti silencing factor 1 protein
ATRX	α-thalassemia/mental retardation syndrome X-linked protein
ATAC	Assay for transposase-accessible chromatin
bHLH	Basic helix-loop-helix
Bp	Base pair
CABIN1	Calcineurin-binding protein cabin 1
CAF	Cancer-associated fibroblast
CAF-1	Chromatin assembly factor-1 complex
CAL1	Chromosomal alignment defect 1 protein
CAP	Chromatin architectural protein
CATD	CENP-A targeting domain
CCAN	Constitutive centromere-associated network
CDE	Cell cycle-dependent element
CDK	Cyclin dependent kinase
CenH3	Centromeric histone H3 variant
CENP-A	Centromeric protein A
ChIP	Chromatin immunoprecipitation
CHR	Cell cycle genes homology region
CID	Centromere identifier
CIN	Chromosomal instability
CpG	5'-cytosine-guanine-3' dinucleotide
CREST	Calcinosis, Reynaud's syndrome, esophageal dysmotility, sclerodactyly, telangiectasia syndrome
CRISPR	Clustered regularly interspaced short palindromic repeats
DAXX	Death domain-associated protein
DDR	DNA damage response
DMSO	Dimethyl sulfoxide

DN	Dominant Negative
DNA	Deoxyribonucleic acid
DNAme	DNA methylation
DNAse	Deoxyribonuclease
DNMT	DNA methyltransferase
DREAM	Dimerization partner, Rb-like, E2F, And MuvB
DSB	Double-strand break
DSC	DNA synthesis-coupled histone incorporation
DSI	DNA synthesis-independent histone incorporation
EdU	5-ethynyl-2'-deoxyuridine
EMT	Epithelial-mesenchymal transition
ERK	Extracellular signal-regulated kinases
ESC	Embryonic stem cell
EZH2	Enhancer of Zeste 2 protein
FACT	Facilitates chromatin transcription complex
FGF	Fibroblast growth factor
FISH	Fluorescent in situ hybridization
GAPDH	Glyceraldehyde phosphate dehydrogenase
GFP	Green fluorescent protein
GIC	Glioblastoma initiating cell
HAC	Human artificial chromosome
HAT	Histone/lysine acetyltransferase
HDAC	Histone/lysine deacetylase
HFD	Histone fold domain
HGF	Hepatocyte growth factor
Hi-C	High-throughput chromosome conformation capture
HIF	Hypoxia-inducible factor
HIRA	Histone regulator A protein/complex

HJURP	Holliday junction recognition protein
HLB	Histone locus body
HMT	Histone methyltransferase
HOR	Higher-order repeat
HP1	Heterochromatin protein 1
HRP	Horseradish peroxidase
IF	Immunofluorescence
IHC	Immunohistochemistry
IL	Interleukin (e.g., IL-6 for Interleukin 6)
Kb	Kilobase
KD	Knockdown
KO	Knockout
MAPK	Mitogen-activated protein kinases (= MEK)
Mb	Megabase
MEF	Mouse embryonic fibroblast
MET	Mesenchymal-epithelial transition
miRNA	microRNA
MNase	Micrococcal nuclease
NAP1	Nucleosome assembly protein 1
NASP	Nuclear autoantigenic sperm protein
NCP	Nucleosome core particle
ncRNA	non-coding RNA
NPM1	Nucleophosmin 1 protein
PCNA	Proliferating cell nuclear antigen
PHC	Pericentric heterochromatin
PLK1	Polo-like kinase 1
POLE	DNA polymerase epsilon catalytic subunit
PRC	Polycomb Repressive Complex

PTM	Post-translational modification
rDNA	Ribosomal DNA
RNA Pol II	RNA polymerase II
RSF	Remodeling and spacing factor protein
RT-qPCR	Reverse transcription quantitative polymerase chain reaction
SAC	Spindle assembly checkpoint
SIM	Structured illumination light sheet microscopy
siRNA	small interfering RNA
SLBP	stem-loop binding protein
snRNA	small nuclear RNA
SRCAP	Snf2-related CREBBP activator protein
STORM	Stochastic optical reconstruction microscopy
TAD	Topologically associated domain
TCGA	The Cancer Genome Atlas
TEMTIA	The Epithelial-Mesenchymal Transition international association
TF	Transcription factor
TGF	Transforming growth factor
TNF-α	Tumor necrosis factor α
TP53	Tumor protein 53
TSS	Transcription start site
UBN1	Ubinuclein 1 protein
UTR	Untranslated Transcribed Region
WB	Western blotting
WT	Wild type
ZEB	Zinc finger E-box-binding homeobox

LIST OF PUBLICATIONS

Research article: Jeffery D, Gatto A, Podsypanina K, Renaud-Pageot C, Ponce Landete R, Bonneville L, Dumont M, Fachinetti D, Almouzni G. CENP-A overexpression promotes distinct fates in human cells, depending on p53 status. Commun Biol. 2021 Mar 26;4(1):417. doi: 10.1038/s42003-021-01941-5. PMID: 33772115; PMCID: PMC7997993.

Review: Renaud-Pageot C, Quivy JP, Lochhead M, Almouzni G. CENP-A Regulation and Cancer. Front Cell Dev Biol. 2022 Jun 2;10:907120. doi: 10.3389/fcell.2022.907120. PMID: 35721491; PMCID: PMC9201071.

News & Views: Renaud-Pageot C, Almouzni G. Tipping the balance in histone supply puts genome stability at stake. EMBO J. 2024 Jun;43(11):2091-2093. doi: 10.1038/s44318-024-00112-6. Epub 2024 May 2. PMID: 38698217; PMCID: PMC11148134.

Research article (in preparation): C. Renaud-Pageot, D. Capocefalo*, S. Lemaire*, A. Forest, J.-P. Quivy, L. Cantini & G. Almouzni. CENP-A overexpression is an epigenetic regulator of cell plasticity and heterogeneity during epithelial-mesenchymal transition in human cells.

TABLE OF CONTENTS

PREAMBLE

A pinch of history: Science tales 19

INTRODUCTION

Chromatin, dynamic support of genetic and epigenetic information 24

1. Chromatin organization: a multi-scale nuclear complex 24

1.1. From DNA to chromatin 24

1.2. Modulation of the nucleosome composition 29

1.3. Higher-order chromatin organization 38

2. Chromatin replication: maintaining or remodeling the epigenetic landscape 42

2.1. Replication initiation and pattern of origin firing 42

2.2. Chromatin dynamics during replication fork progression 46

CENP-A chromatin in normal and diseased states 53

1. Centromere architecture and function: A region like no other 53

1.1. Centromere function and organization 53

1.2. Role and structure of CENP-A chromatin 58

2. CENP-A regulation and cancer 64

2.1. Introduction 65

2.2. Regulation of CENP-A 66

2.3. CENP-A levels increase in cancer 69

2.4. CENP-A overexpression leads to mislocalization and heterotypic nucleosomes 70

2.5. Impact of CENP-A overexpression on kinetochore and chromosome segregation 72

2.6. CENP-A overexpression and cell fate reprogramming 73

2.7. CENP-A nuclear distribution in health and cancer 76

2.8. Clinical interest for CENP-A in cancer treatment 78

2.9. Concluding remarks 80

The epithelial-mesenchymal transition and its plasticity 81

1. Epithelial-mesenchymal transition states 81

1.1. Defining the EMT: epithelial and mesenchymal markers 81

1.2. Discovery of the EMT 83

1.3. Involvement of intermediate states 84

2. Different EMT types 85
2.1. Type 1 EMT: Development 85
2.2. "Type 2" EMT: Wound healing and fibrosis 89
2.3. "Type 3" EMT: Cancer 90
3. Regulating the epithelial-mesenchymal plasticity: key programs 97
3.1. EMT transcription programs 97
3.2. Epigenetic mechanisms 108

QUESTION 115

RESULTS

General approaches and methodology 118

PART 1. CENP-A overexpression promotes distinct fates in human cells, depending on p53 status 121

1. Rationale and contribution 121
2. Results 122
3. Discussion 144
4. Material and Methods 147

PART 2. CENP-A overexpression is an epigenetic regulator of cell plasticity and heterogeneity during epithelial-mesenchymal transition in human cells 157

1. Rationale and contribution 157
2. Abstract 158
3. Introduction 159
4. Results 161
5. Discussion 181
6. Supplementary figures 184
7. Materials and Methods 194

Additional results (preliminary data) 199

DISCUSSION 201

CONCLUSION.....217

REFERENCES.....219

SUMMARY.....321

APPENDIX.....327

PREAMBLE

A PINCH OF HISTORY: SCIENCE TALES

Cell Theory

Historically, microscopy was the primary method for studying nuclear organization. The first recorded observation of a cell dates back to 1665 when Robert Hooke, who improved the design of the existing compound microscope, examined cork tissue and observed tiny pores (Hooke 1665). Hooke coined the term “cells” as the boxlike structures he saw reminded him of the cells of a monastery. Hooke subsequently identified similar structures in wood and other plants. Later, Antonie van Leeuwenhoek used a single-lens microscope he built himself to observe microscopic organisms such as bacteria and protozoa, which he termed “animalcules”. He went on to be the first to observe and describe spermatozoa, along with nuclei in 1682 while observing blood cells of cod and salmon. In his letter to the Royal Society of London he reported seeing some cells containing “a little round body or globule” (Cole and J 1949). In the nineteenth century, biologists began taking a closer look at both animal and plant tissues, perfecting cell theory. Theodore Schwann and Mattias Schleiden studied cells of animals and plants; they identified key differences between the two cell types and put forth the idea that cells were the fundamental units of both plants and animals (Nyhart 1995).

The term nucleus and its more detailed description arose from the observations of the botanist Robert Brown (Brown 1833). Nuclei were subsequently observed in both plant and animal cells, but for a long time they were thought to have no functional significance and were considered dispensable to the cell. Although Dumortier first observed plant cell divisions in 1832 (Dumortier 1832), it was Robert Remak who recognized the importance of his own observations of cell division in animal tissues in 1852 (reviewed in (Bolduc et al 2021)). His work established a crucial link between cell theory and the processes of reproduction and development. By the time of Remak’s work, significant progress had already been made in the field. For instance, Jean-Louis Prévost and Jean-Baptiste Dumas documented the fertilization and segmentation of the frog egg, while Karl Ernst von Baer described similar processes in mammalian eggs (reviewed in (Müller-Wille 2010)). Remak himself demonstrated that the frog egg was initially a single cell and showed that its segmentation involved successive divisions from one cell to two, then to four, and so on. Altogether, these observations culminated in the understanding that embryonic development proceeds through a series of cell divisions. Rudolf Virchow expanded upon Remak’s findings, asserting that all living cells arise from pre-existing cells: *omnis cellula e cellula* (Virchow 1858). Finally, in 1859, Louis Pasteur conducted a series of experiment which disproved Aristotle's theory of spontaneous generation of life (reviewed in (Farley et Geison 1974)), further solidifying the foundations of modern biology.

Inside the nucleus

The genome of eukaryotic cells was visible over a century before it was sequenced and several decades before chromosomes and chromatin were understood to be the physical carrier of genetic information.

Walther Flemming studied the process of cell division, focusing on the distribution of chromosomes to daughter nuclei – a process he named “mitosis”, derived from the Greek word for “thread” (Flemming 1882). Flemming also introduced the term “chromatin” to describe the substance within the nucleus that absorbs dyes when treated with nuclear stains (Figure 2A). Additionally, he coined the term “centromere” to define the primary constriction on chromosomes, where spindle fibers connect during cell division. Flemming proposed that chromatin could correspond to the “nuclein” previously isolated by Friedrich Miescher from lymphocyte nuclei – the first purified form of deoxyribonucleic acid (DNA). Beyond nuclein, Miescher had also isolated positively charged proteins from salmon sperm, which he named “protamines” (reviewed in (Lamm, Harman, and Veigl 2020)), and Albrecht Kossel biochemically purified histones from goose erythrocytes in 1884, further defining chromatin as a complex of nucleic acids and proteins (Kossel 1884). These discoveries led to the hypothesis that chromatin was the hereditary material of the cell. This theory gained validation in the early 1900s with the rediscovery of Mendelian genetics (Mendel 1866), the identification of chromosomes as the carriers of hereditary information (De Vries 1900; Sutton 1900), along with the concept of genes as units of heredity (Johannsen 1909; Morgan 1910) and the discovery of the transforming principle (Griffith 1928). In 1927 Nikolai Koltsov proposed that each chromosome consists of two chromatids, each composed of a double-stranded giant hereditary molecule containing genes. He suggested that these two complementary strands could replicate in a semi-conservative manner, using each other as templates, ensuring the inheritance of traits during cell division (Soyfer 2001). Koltsov’s pioneering ideas were later confirmed. In 1944, DNA was definitively identified as the carrier of genetic information (Avery, Macleod, and McCarty 1944). Subsequent discoveries, including the elucidation of DNA's structure (Franklin and Gosling 1953; Watson and Crick 1953; Wilkins, Stokes, and Wilson 1953), further reinforced the central role of DNA in heredity.

Meanwhile, chromatin research converged with the broader field of epigenetics. The embryologist Conrad Waddington first coined the term "epigenetics" (1942) as a fusion of the words “Epigenesis” and “Genetics” to refer to the complex interaction between the genome and the environment. Indeed, the earlier concept of “epigenesis” (Aristotle, 343 BC; William Harvey, 1651) posits that complexity emerges progressively during the development of an organism from a naïve entity – the egg – in opposition to the theory of preformation. Waddington investigated the inheritance of characteristics acquired by a population in response to environmental stimuli. He described this developmental process as a series of “decisions” which he visualized as “valleys” and “forks” within a conceptual developmental landscape (Figure 1). He suggested that during development, cells follow specific paths down this “epigenetic landscape” (Figure 1) that is influenced by the actions of particular genes (Waddington 1952, 1957). This way, Waddington proposed that epigenetics links the “genotype” to the “phenotype”, requiring the integration of inherited genetic information with environmental signals. Since then, the definition of epigenetics has evolved and is now defined as the study of mitotically

and/or meiotically heritable changes in gene function that are not attributable to changes in the DNA sequence (Russo, Martienssen, and Riggs 1996).

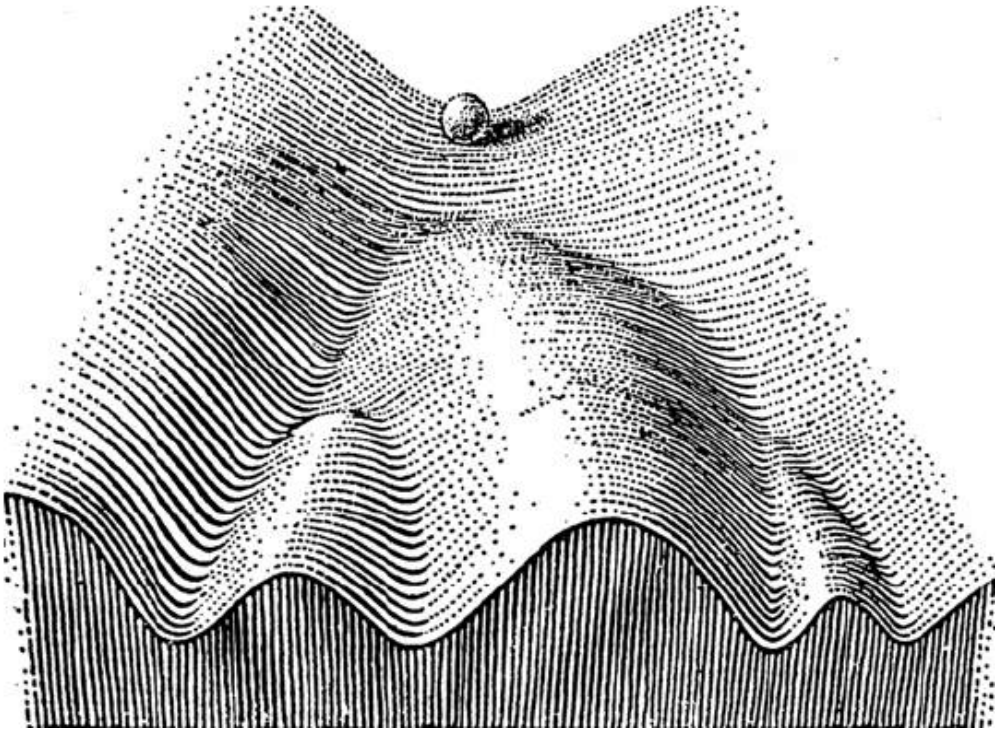


Figure 1. Part of an epigenetic landscape.
The epigenetic landscape was a visual metaphor introduced by Conrad Waddington to illustrate the natural restriction of cell differentiation potential during embryonic development.
The path followed by the marble (a stem cell) when it rolls down corresponds to the developmental history of the egg across successive cell divisions. Final points represent the eventual cell fates, that is, tissue types. Below, a complex system of interactions underly the epigenetic landscape to illustrate how gene regulation modulates development (not shown). (Waddington 1957).

In contemporary usage, and in relation to my project, the term "epigenetics" generally refers to modifications in chromatin that regulate gene expression programs in a reversible manner, without changing the underlying DNA sequence. For instance, the regulation of physical access to DNA, a highly dynamic property of chromatin, plays an essential role in establishing and maintaining cellular states that can be reversed or inherited through multiple cell divisions. The field of chromatin biology, closely tied to the concept of cell fate, has made significant strides, driven in part by the advent of single-cell analysis techniques. In this context, my thesis investigates the role of CENP-A, an important protein component of chromatin, in regulating cell fate decisions in cancer.

INTRODUCTION

PART 1.

CHROMATIN, DYNAMIC SUPPORT OF GENETIC AND EPIGENETIC INFORMATION

The genome of eukaryotic cells is organized within the nucleus into chromatin, a complex structure composed of DNA, RNA, and associated proteins. Chromatin is organized hierarchically, from its fundamental repeated unit, the nucleosome, to higher-order structures. These structures play a crucial role in regulating cell fate decisions and cell identity. This first part provides an overview of the key aspects of chromatin architecture and dynamics.

1. CHROMATIN ORGANIZATION: A MULTI-SCALE NUCLEAR COMPLEX

1.1. From DNA to chromatin

1.1.1. DNA structure and modifications

Deoxyribonucleic acid (DNA) is a long biopolymer encoding the hereditary genetic information in living organisms. Nucleobases (or nitrogenous bases) – adenine (A), thymine (T), cytosine (C) and guanine (G) – form nucleosides which, in turn, compose the nucleotides of DNA (Chargaff 1950). Their ability to form complementary base pairs (A and T or G and C, held together by two or three hydrogen bonds, respectively) and to stack upon each other leads to a double helix structure, with two antiparallel polynucleotides filaments and a sugar-phosphate backbone (R. E. Franklin and Gosling 1953; J. D. Watson and Crick 1953; Wilkins et al. 1953). In eukaryotic cells, nuclear DNA is transcribed in RNA in the nucleus, RNA molecules are then transported into the cytoplasm where they are translated into proteins.

Modifications of DNA bases in eukaryotes have been first documented in 1948 (Hotchkiss 1948). Many types of DNA modifications have been discovered. The most studied modification, DNA methylation (DNAme), defined by the addition of a methyl (-CH3) group by dedicated enzymes called methyltransferases (DNMT), is a universal mechanism of epigenetic regulation existing in all kingdoms of life (Seong, Han, and Sul 2021). In mammalian cells, this modification occurs mostly at cytosines preceding a guanine (the pair being called CpG dinucleotides) on both strands of DNA (A. P. Bird 1986). The most common base modification detected in mammalian genomes, the 5-methylcytosine (5mC), corresponds to the methylation of the fifth carbon of a cytosine (Razin and Cedar 1977) and is concentrated in CpG islands (A. Bird et al. 1985).

CpG islands are enriched at the transcriptional start sites of genes and their hypermethylation is associated with gene silencing, by recruiting repressing factors with a methyl-binding domain (Boyes and Bird 1991, 1992) or impeding the binding of transcription factors (Watt and Molloy 1988). A well-

known example illustrates the impact of DNAme on gene expression: pregnant mice exposed to bisphenol A led to an increased number of obese yellow individuals among the offspring (Waterland and Jirtle 2003), due to disrupted DNAme patterns (Dolinoy, Huang, and Jirtle 2007). DNAme is essential to preserve genome stability by controlling both gene expression and chromatin structure; DNAme is thus enriched at most DNA repeated sequences to maintain a repressed state (Lehnertz et al. 2003; Pappalardo and Barra 2021), it contributes to X-chromosome inactivation during female mammalian development (Mohandas, Sparkes, and Shapiro 1981) and it is crucial for genomic imprinting during mammalian development (Monk 1987), a process whereby only one gene copy is expressed in a parent-of-origin-specific manner. Finally, while it generally correlates with repression of gene expression, DNAme is also found at actively transcribed gene bodies where it contributes to gene expression regulation, although its precise function remains elusive (reviewed in (Greenberg and Bourc'his 2019)).

DNAme is a stable mark that can be transmitted through cell division or lost, either actively or passively: Active demethylation in mammals involves TET methylcytosine dioxygenases catalyzing several consecutive oxidations of 5mC until its conversion to 5caC, which is recognized by thymine DNA glycosylases and exchanged with an unmodified base by base excision repair (Lio et al. 2020). Passive DNA methylation occurs by dilution through cell divisions if methylation patterns are not maintained by the methylation machinery (Greenberg 2020). Such a process occurs for example during early mammalian development: fertilization is followed by the progressive and passive erasure of parental DNA methylation patterns during cleavage division (Monk, Boubelik, and Lehnert 1987; Sanford et al. 1987), before the establishment of the embryonic methylation pattern (Okano et al. 1999).

Perturbation of DNAme can associate with diseased states: Hypomethylation of DNA repeats is associated with many neurodevelopmental and neurodegenerative diseases, while mutations in DNMT and TET genes (affecting methylation patterns of the genome) can lead to genetic diseases such as the immunodeficiency, centromeric instability and facial anomalies (ICF) syndrome (G. L. Xu et al. 1999; Greenberg and Bourc'his 2019). Finally, the genome of cancer cells is commonly extensively hypomethylated relative to cells from healthy tissues (Feinberg and Vogelstein 1983). Thus, DNAme pattern in the genome changes as a result of dynamic processes involved during development or diseased states. Importantly, in addition to its modifications, DNA is organized into a highly ordered structure involved in the modulation of the genome: chromatin.

1.1.2. Chromatin organization

a) Chromatin components

Chromatin, first identified as "threadlike structures" in the cell nucleus by Walter Flemming (Figure 2A), is a nucleoprotein complex of DNA, RNA and associated proteins. They contribute together to

generate distinct properties, termed epigenetic modifications, to regulate gene expression (Adrian Bird 2007). Epigenetic regulation involves various factors, including proteins and non-coding RNAs, that influence how genes are expressed without altering the underlying DNA sequence. The epigenome (or "chromatin landscape") refers to the complete set of chemical modifications and proteins interacting with the genome to regulate gene expression in a cell. Most of chromatin-associated proteins are directly implicated in DNA packaging, thus providing the most fundamental level of chromatin organization. All living organisms use scaffolding proteins to protect, compact and organize their DNA. Prokaryotes store their DNA as a single circular molecule in a region of their cytoplasm called the nucleoid. Bacteria rely on nucleoid associated proteins (NAPs) (Dillon and Dorman 2010) and Archaea use NAPs and/or archaeal histones, depending on the species (Laursen, Bowerman, and Luger 2021). In contrast, in the nuclei of eukaryotic cells, DNA is organized into linear molecules termed chromosomes, which are themselves composed of DNA tightly wound around histone proteins (Yadav, Quivy, and Almouzni 2018). This packaging into a more compact structure allows DNA to fit in the nucleus. As an illustration, somatic cells of the human body normally contain 23 chromosomes, which are present in two copies, making the genome diploid with 23 pairs of chromosomes (Tjio and Levan 1956). This makes a total of 6 billion base pairs (bp) of nucleotides. Because each bp is around 0.34 nanometers (nm) long, in total almost 2 meters (m) in length of DNA is contained in the microscopic space of each nucleus. The packaging of DNA into chromatin leads to a shorten (about sevenfold) length for the "beads-on-a-string" 10 nm chromatin fiber (Olins and Olins 1974) (Figure 2B). In addition, chromatin is further coiled into a shorter and thicker fiber, the 30 nm chromatin fiber, when assembled on purified DNA *in vitro* (Finch and Klug 1976; Rattner and Hamkalo 1979).

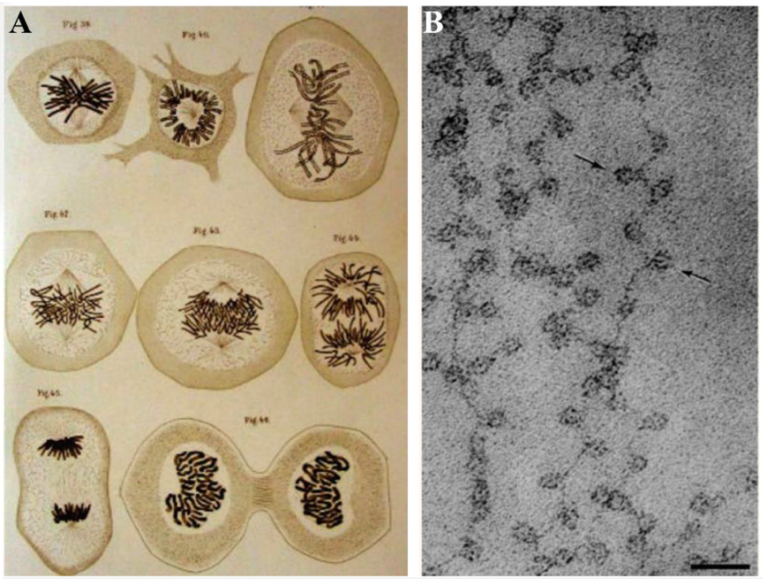


Figure 2. Early visualizations of chromatin.
(A) Drawings of mitotic chromosomes (chromatin) by Walter Flemming, 1882.
(B) Electron micrographs of ν bodies (nucleosomes), pointed by arrows, arranged as "beads on a string" from chromatin spreads at low ionic strength. Scale bar = 30nm. (Adapted from Olins and Olins, 2003).

The fundamental unit for this extreme level of compaction is the nucleosome. The composition of the nucleosome was determined with biochemical and X-ray diffraction experiments (Kornberg 1974; Luger et al. 1997): Each nucleosome is comprised of a core particle, linker DNA and a linker histone (Figure 3). The nucleosome core particle (NCP) contains approximately 147 bp of DNA wrapped 1.65 times around an octamer of histones. The histone octamer contains two copies of each histone H2A, H2B, H3 and H4 assembled into a core tetramer $(H3\text{-}H4)_2$ flanked by two H2A-H2B dimers. Between two core particles, the linker histone H1 binds the linker DNA, whose length varies between 10 and 90 bp depending on the organism or the cell type. Thus, the NCP typically repeats every 160-240 bp over the genome (McGhee and Felsenfeld 1980); the nucleosome is the basic, repeated unit of chromatin. In its simplest form, the repeating nucleosomal units of chromatin adopt the decondensed "beads-on-a-string" configuration of individual chromatin fibers observed by electron microscopy (Olins and Olins 1974) (Figure 2B).

Histones, the "building blocks" of chromatin, are small basic proteins of about 20 kilodaltons (kDa) in size which represent the major protein component of chromatin (reviewed in (Sitbon et al. 2017)). Core histones (H2A, H2B, H3 and H4) are highly evolutionary conserved across all eukaryotes. They contain a characteristic histone fold domain (HFD) of 80-90 amino acids which is implicated in histone dimerization (Figure 3). The HFD comprises 3 α-helices connected by flexible loops, and is flanked by a C-terminal core domain and an extensive, less-structured and flexible N-terminus tail of about 10-40 amino acids (Arents and Moudrianakis 1995) that extends at the surface of the nucleosome (Luger et al. 1997). The histone H2A is the only core histone that contains an additional unstructured and flexible C-terminal extension consisting of 15 amino acids beyond the globular domain, leaving the nucleosome at the entry/exit site of the nucleosomal DNA (Luger et al. 1997). The histone H1 is quite distinct, and the least conserved of the histones. In Metazoans, it exhibits a globular domain with a winged-helix fold, in addition to its short N-terminal tail and long C-terminal tail (Allan et al. 1980; Chapman, Hartman, and Bradbury 1976; Graziano et al. 1990). H1 completes the nucleosome by binding on the surface of the NCP to the entry/exit site of DNA (An et al. 1998; An, van Holde, and Zlatanova 1998; Noll and Kornberg 1977), contributing to reducing nucleosome mobility and promoting compaction of chromatin (C. Pan and Fan 2016; Prendergast and Reinberg 2021).

The HFD of each core histone mediates histone-histone interactions and their interactions with DNA. Thus, H2A-H2B and H3-H4 dimers form through the "handshake" interaction of their HFDs in an anti-parallel orientation (Arents et al. 1991; Richmond, Searles, and Simpson 1988). Then, the H3-H4 tetramer is formed *via* a bundle of α2 and α3 helices of H3, and a similar interaction occurs between H4 and H2B. This results in a histone core with a pseudo-dyad symmetry (Luger et al. 1997). Due to their abundant lysine and arginine residues, about two-thirds of which are concentrated in their tails, histones are highly basic. Their positive charges are neutralized by the negatively charged phosphate backbone of the DNA. However, since a major part of the histone positive charges reside in their tails outside of

the NCP, charge-charge interactions contribute little to the stability of the NCP itself (Lorch, Kornberg, and Maier-Davis 2023). Instead, hydrogen bonding between histones' amino acids and DNA phosphates, and nonpolar contacts of their side amino acid chains with deoxyribose, contribute to form stable NCPs (Davey et al. 2002; Luger et al. 1997).

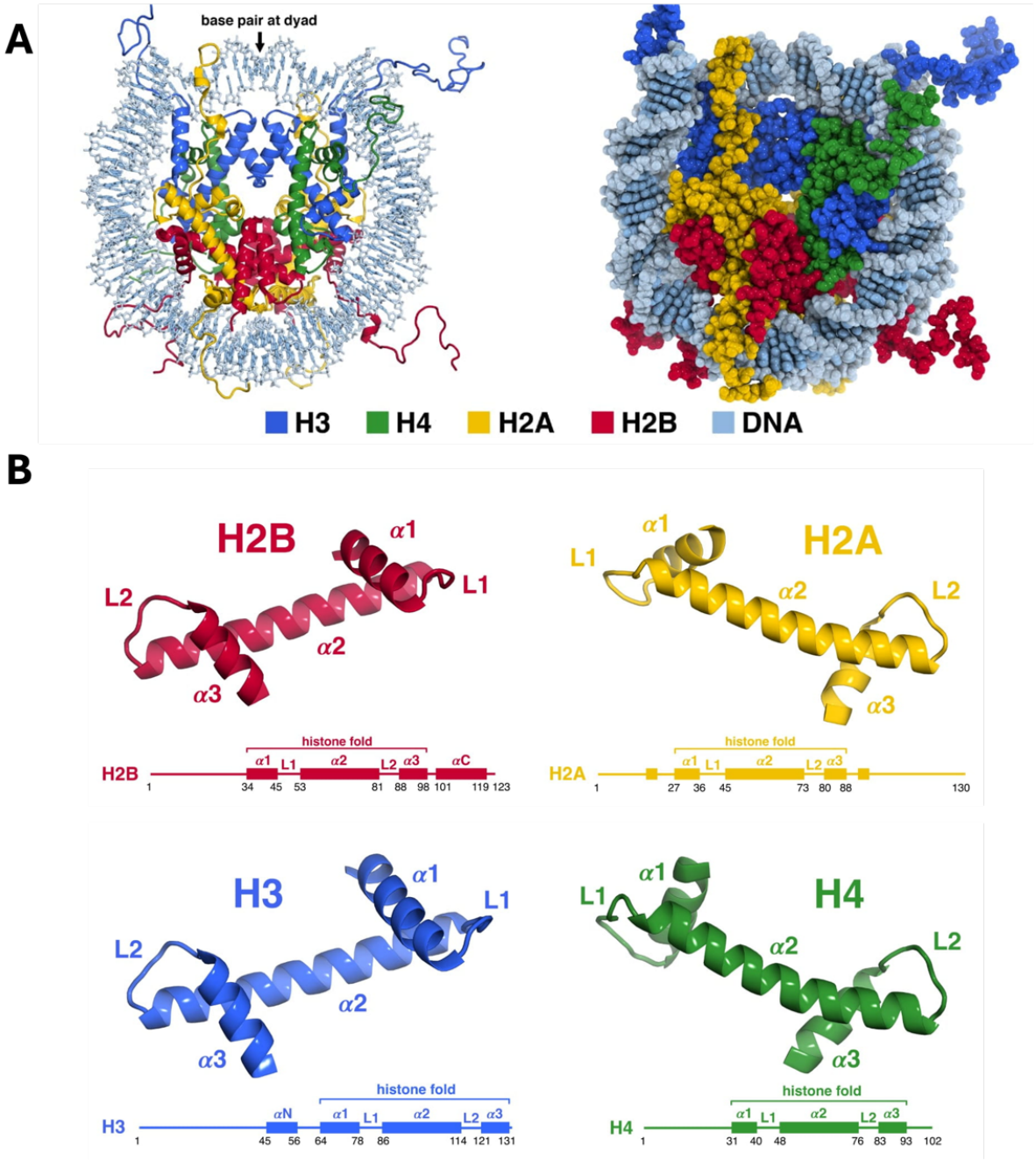


Figure 3. Nucleosome structure.
(A) Crystal structure of the nucleosome core particle, viewed from the top, at 2.8Å resolution (adapted from Luger et al., 1997).
(B) Histone fold as dimerization motif. The histone fold is comprised of a short helix (α1), followed by a loop (L1), a longer helix (α2), a second loop (L2) and another short helix (α3).
(Adapted from Tan Lab at Penn State website (https://sites.psu.edu/tanlab/)).

c) Forming the nucleosome

Before their incorporation into chromatin, free histones could, due to their charge, engage into promiscuous interactions with any acidic partner and even could form aggregates in the cell. This is prevented by dedicated proteins called histone chaperones, which escort non-nucleosomal (free) histones in the cell throughout all their cellular life and ensure their deposition into chromatin (reviewed in (Sitbon et al. 2017)). The first protein to be characterized as a "histone chaperone" was the Nucleoplasmin, a prominent protein in the *X. laevis* oocyte that promotes chromatin assembly (Laskey, Mills, and Morris 1977). Histone chaperones are now considered to be proteins that associate with histones and are involved in their transfer, without being necessarily part of the final product (De Koning et al. 2007).

Nucleosome deposition can be modulated by DNA methylation patterns which affect chromatin structure and flexibility (S. Li, Peng, and Panchenko 2022). Indeed, DNA methylation leads to stiff DNA segments that are refractory to nucleosome binding (Pérez et al. 2012; Zaichuk and Marko 2021). In addition, high levels of DNA methylation generally induce a narrowing of the "nucleosome-free" regions (linker DNA between core nucleosome units), as well as an increased chromatin condensation and a decrease in nucleosome dynamics (Buitrago et al. 2021). This represents a typical mark of gene inactivation due to altered DNA accessibility. In addition, histone N-terminal tails, which extend outside the NCP, modulate nucleosome structure and function (Davey et al. 2002; Davey and Richmond 2002; Luger et al. 1997); Their positive charges may contribute to chromatin condensation (D. J. Clark and Kimura 1990; Dorigo et al. 2003), and neutralizing these charges promotes a more open chromatin structure (Dueva et al. 2019). Thus, nucleosomes have been implicated in regulating both *access to* and *interpretation of* their associated DNA, by shaping chromatin local organization but also by providing a scaffold for the binding of several proteins, including TFs (Ballaré et al. 2013; Bartke et al. 2010; Zhu et al. 2018) and pioneer factors (Soufi et al. 2015).

1.2. Modulation of the nucleosome composition

1.2.1. Histone post-translational modifications

Beyond their role in DNA packaging, histone proteins carry epigenetic information. Histones are modified both at their protruding N-terminal tails (Arents et al. 1991; Arents and Moudrianakis 1995; Davey and Richmond 2002; Luger et al. 1997) and within their HFD (Cosgrove, Boeke, and Wolberger 2004; Mersfelder and Parthun 2006), thus providing an additional layer of epigenetic control. These diverse post-translational modifications (PTMs) are proposed to constitute a "histone code" that regulatory proteins can read and interpret, and which influences the local chromatin environment (Jenuwein and Allis 2001). Most PTMs are addition of relatively small, yet structurally distinct, chemical groups. They can be dynamically added or removed by enzymes throughout the histone's

lifespan, from its production to its degradation (Loyola et al. 2006). These modifications have the potential to modify interactions between histones and DNA, histones themselves, and histones and other proteins (H. Huang et al. 2015). Consequently, PTMs can transiently modify the nucleosome conformation, but also impact chaperone binding, histone deposition, and/or the final chromatin state (Cosgrove, Boeke, and Wolberger 2004). Thus, PTMs can exert direct effects on chromatin, by changing the physical properties of nucleosomes, which in turn affects chromatin structure. Additionally, they can also direct changes indirectly, by influencing the binding of alternative protein partners that impact chromatin states. Histones are subject to over a dozen distinct types of PTMs that can alter more than 60 amino acid residues (Tan et al. 2011). Despite the large number of potential modification sites, only a subset of these residues – such as lysine (K), serine (S), arginine (R), threonine (T), tyrosine (Y), histidine (H), and glutamic acid (E) – are known to be covalently modified (reviewed in (Taverna et al. 2007)). The N-terminal tails of histones, in particular, are subject to extensive PTMs which can modulate transcriptional activity through both positive and negative regulatory mechanisms (Lorch, Kornberg, and Maier-Davis 2023) (Figure 4). Among the most studied histone PTMs are acetylation, methylation, phosphorylation, ubiquitylation, and ribosylation.

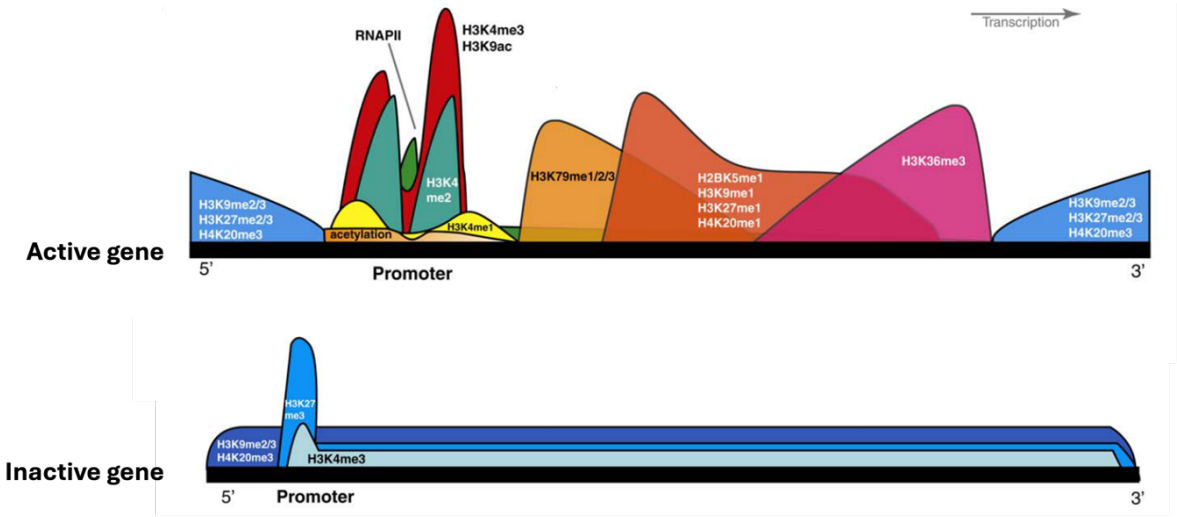


Figure 4. Histone PTM distribution at active and inactive gene.
Profiles of histone PTM enrichment at "active" (top) and "inactive" (bottom) genes. (Adapted from Barth and Imhof, 2010).

Specific enzymes, often referred to as "writers", "erasers" and "readers", have been identified to add, remove, or interpret these modifications, respectively. The connection between histone modifications and transcription was first suggested by the discovery that hyperacetylated histones correlate with gene expression (Allfrey, Faulkner, and Mirsky 1964). Lysine acetylation of histones (e.g., H3K56, H3K64, H3K122) neutralizes their positive charge, reducing their affinity for the negatively charged DNA. The loosened interaction with DNA leads to reduced nucleosome stability and/or increased spontaneous DNA unwrapping (nucleosome "breathing"), making the DNA locally more accessible to transcription

factors (Shahbazian and Grunstein 2007; Bowman and Poirier 2015). In addition to this process, bromodomain-containing proteins, which recognize acetylated lysine residues on histone tails, are associated with ATP-dependent chromatin remodeling enzymes that can reposition or evict nucleosomes from promoters, facilitating access for the RNA polymerase II transcription machinery (reviewed in (B. Li, Carey, and Workman 2007)). This example highlights the pivotal role of histone PTMs in mediating interactions between transcription-associated factors and DNA.

Furthermore, the distribution and function of histone PTMs are complex and cannot be simply categorized as either activating or repressive. H3K4me3 is commonly found at active promoters in mammals (Bernstein et al. 2005) and yeast (Pokholok et al. 2005), while H3K36me3 is enriched in gene bodies (Barski et al. 2007), and H3K27ac and H3K4me1 are associated with active enhancers (Creyghton et al. 2010; Heintzman et al. 2009; Rada-Iglesias et al. 2011) (Figure 4). Conversely, certain PTMs, such as H3K27me3 and H3K9me3, are associated with the repression of gene expression, although they display distinct genomic distributions (A. H. F. M. Peters et al. 2003). For example, H3K9me3 is enriched in constitutive heterochromatin, including repetitive DNA sequences like pericentromeres, telomeres, and retroviral elements (Mikkelsen et al. 2007; Nicetto and Zaret 2019; A. H. Peters et al. 2001), while H3K27me3 marks facultative heterochromatin, such as the inactive X chromosome in female mammals (reviewed in (Aranda, Mas, and Di Croce 2015)). The role of a histone PTM should not be considered in isolation but within the context of its surrounding chromatin landscape. Many PTMs can indeed coexist, resulting in a variety of combinations. For example, bivalent domains around poised promoters can combine both activating and repressive histone marks, such as the co-enrichment of H3K27me3 and H3K4me3. Genes for which transcription factors are expressed at low levels frequently have bivalent domains (Bernstein et al. 2006). These domains are essential for modulating developmental gene programs during development. Additionally, histone PTMs can interact with other epigenetic regulatory mechanisms. For instance, broad genome-wide enrichment in H3K4me3 prevents *de novo* DNA methylation in human and mouse early embryos, thereby preventing inappropriate DNAme (Ooi et al. 2007; B. Zhang et al. 2016). Conversely, DNAme prevents the deposition of H3K4me3 in oocytes (Hanna et al. 2018). This exemplifies how a PTM may not always recruit readers to actively stimulate processes like transcription but may instead prevent the binding of inhibitory factors (Millán-Zambrano et al. 2022).

In summary, chromatin is organized into arrays of nucleosomes whose building blocks, histones, are subject to various PTMs (Figures 2-5). These modifications influence chromatin structure and function. The combinatorial diversity of histone modifications plays a critical role for transcriptional regulation.

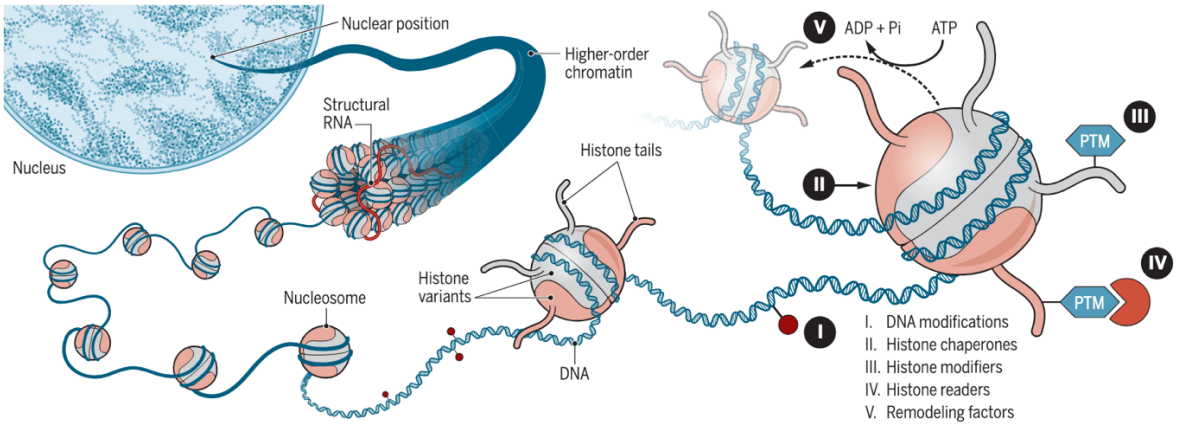


Figure 5. Chromatin plasticity.
The hierarchy of chromatin organization in an interphase nucleus is shown along with factors acting at each level. Arrays of nucleosomes fold into higher-order chromatin structures, and noncoding RNA participates in local organization. On the right, the basic repeated unit of chromatin, the nucleosome, is detailed. The nucleosome core particle comprises double-stranded DNA wrapped around an octamer consisting of a (H3-H4)2 tetramer flanked by two H2A-H2B dimers. Variations of this basic module by dynamic combinations include the choice of histone variants, modifications of DNA bases, and reversible posttranslational modifications of histone tails, enabling chromatin plasticity. (Adapted from Yadav et al. 2018).

1.2.2. Histone variants

a) Classification of histone variants in mammals

In addition to PTMs, nucleosome composition is diversified by the incorporation of distinct histone variants, defined based on differences in their amino acid sequence, expression patterns during the cell cycle, and selective loading by dedicated histone chaperones (reviewed in (Sitbon et al. 2017)) (Figure 5). All histones from the NCP (S. G. Franklin and Zweidler 1977) and the linker histone H1 (Kinkade and Cole 1966) exist as several non-allelic variants. The incorporation of specific histone variants into chromatin plays a key role in establishing distinct epigenetic states, contributing to the control of transcriptional activity and cell identity (reviewed in (Yadav, Quivy, and Almouzni 2018)) (Figure. 5). Histone variants can be classified into two main groups: replicative and non-replicative, based on their expression patterns during the cell cycle and their mode of incorporation into chromatin. Replicative variants (also referred to as “canonical” histone variants) have a peak of expression during the S-phase of the cell cycle and their deposition is DNA synthesis-coupled (DSC). This coupling ensures the immediate assembly of newly replicated DNA into chromatin (reviewed in (Corpet and Almouzni 2009)), thereby protecting it from damage (Xiaofen Ye et al. 2003). In mammals, replicative histone genes exhibit several distinctive features: they have short Untranslated Transcribed Regions (3’-UTRs), lack introns, and possess a conserved stem-loop structure at their 3' end instead of a poly-A tail (reviewed in (Marzluff 2005)). Thus, their transcripts exhibit a peculiar architecture, as their maturation, stability, and translation are regulated by a 3′ stem-loop rather than by polyadenylation (poly-A) signals. Replicative histone mRNAs are processed by specific factors such as the stem-loop binding protein

(SLBP), which is required for the cleavage of their 3' stem-loop (Sànchez and Marzluff 2002). Importantly, since most transcriptomic analyses to date have used poly-A detection, changes in replicative histone transcripts could have been missed. Furthermore, these histone genes are organized into clusters: in humans, HIST1 on chromosome 6 (6p21-p22) contains 55 histone genes, HIST2 on chromosome 1 (1q21) contains 6 genes, and HIST3 on chromosome 1 (1q42) contains 3 histone genes. These histone clusters are spatially compartmentalized within the nucleus in structures known as histone locus bodies (HLBs). HLBs persist throughout the S phase and are enriched with factors required for the transcription and processing of replicative histone genes (reviewed in (Mendiratta, Gatto, and Almouzni 2019)). The tight coupling between cell cycle progression and the expression of replicative histones is partly due to this unique gene organization.

In contrast, the expression of non-replicative histone variants does not peak during the S phase, and their deposition onto chromatin is DNA synthesis-independent (DSI). This process is crucial for maintaining chromatin integrity, as nucleosomes can be displaced during DNA-templated processes outside S-phase, such as transcription or DNA repair, and must be reassembled (Ray-Gallet et al. 2011). The incorporation of non-replicative variants also plays a key role in establishing specific chromatin landmarks. For instance, the centromeric H3 variant CENP-A (CenH3) defines the position of the centromere in most eukaryotes (Fachinetti et al. 2013).

Mammalian histone families show a great diversity of variants (Table 1). In addition to the core histone variants described in Table 1, linker histone H1 has five replicative histones (H1.1-H1.5) and many variants. There is considerable sequence variability between its replicative variants, which is conserved among species, suggesting they carry out different functions (Prendergast and Reinberg 2021). H1 has long been associated with gene repression and chromatin compaction. Generally, replicative H1 variants are enriched in heterochromatin, while its two somatic replacement variants, H1.0 and H1x, tend to be enriched in more open chromatin regions (Millán-Ariño, Izquierdo-Bouldstridge, and Jordan 2016). H1 has three testis-specific variants (H1t, H1T2, HILS1) and an oocyte-specific (H1oo) variant (Pérez-Montero, Carbonell, and Azorín 2016).

a) Notion of oncohistones

Intriguingly, the expression of histone variants and histone chaperones is deregulated in various cancers, highlighting the critical link between chromatin and genome integrity (reviewed in (Filipescu, Müller, and Almouzni 2014; Buschbeck and Hake 2017)).

Histone	Chaperones, chromatin remodelers (role)	General function (genome distribution)
H2A (replicative)	NAP1 (import & deposition) FACT, Nucleolin (deposition & exchange) POLA1 (recycling at replication fork)	Chromatin integrity (genome-wide)
H2A.X	FACT (deposition & exchange)	DNA damage response & chromatin remodeling (genome-wide)
H2A.Z.1	p400/SRCAP (deposition) ANP32E/INO80 (eviction) POLA1 (recycling at replication fork)	Binding of regulatory complexes (regulatory regions: promoters & enhancers, heterochromatin)
H2A.Z.2.1	p400/SRCAP (deposition) ANP32E (eviction) POLA1 (recycling at replication fork)	
H2A.Z.2.2		
macroH2A1.1	ATRX (antagonizes deposition) FACT (eviction)	Gene silencing & higher-order compaction (heterochromatin)
macroH2A1.2		
macroH2A2		
H2A.B (H2A.Bbd)	NAP1 (deposition and removal)	Nucleosome destabilization for transcription & splicing (euchromatin), testis and brain only
H2A.L	NAP2L4 (H2A.L2 splice form)	Histone-to-protamine transition, in various mammals, not in humans, testis only
H2B (replicative)	Co-chaperoned with H2A as a dimer	Chromatin integrity (genome-wide)
H2B.W (H2BFWT)	SWI-SNF (remodeling)	Testis only
H2B.1 (TH2B)	ND	Histone-to-protamine transition, testis only
H3.1, H3.2 (replicative)	NAP1 (import), NASP1 (protection from degradation) ASF1 (transfer to CAF-1) CAF-1 (de novo deposition at DNA synthesis sites) Spt2 (deposition) FACT (exchange) MCM2/POLE3-4/POLA (replication fork recycling)	Chromatin integrity (genome-wide)
H3.3	NAP1 (import) NASP1 (protection from degradation) ASF1 (transfer to HIRA) HIRA-UBN-CABIN1 (de novo deposition & recycling at active sites) DAXX-ATRX (deposition at heterochromatin) DEK (supply to DAXX-ATRX at PML bodies) Spt2 (deposition) FACT (exchange) MCM2/POLE3-4/POLA (replication fork recycling)	Transcriptional activation (active genes and regulatory regions), heterochromatin formation & telomere stabilization (repetitive elements)
CENP-A	HJURP (deposition) MCM2 (recycling at replication fork)	Centromere identity & function (centromeres)
H3.Y (H3.Y.1)	HIRA-UBN-CABIN1 (deposition)	Regulation of cell cycle genes (euchromatin), primate-specific, testis and brain only
H3.X (H3.Y.2)		Primate-specific, testis and brain only
H3.4 (H3T, H3.1t)	NAP2 (deposition at euchromatin)	Histone-to-protamine transition, testis-specific
H3.5	ND	
H4 (replicative)	Co-chaperoned with H3 as a dimer	Chromatin integrity (genome-wide)
H4G	Nucleophosmin/NPM1	Upregulation of rDNA transcription

Table 1. Core histone variants and their chaperones in mammals. Histone variants from the NCP in mammals, classified depending on their family (H2A, H2B, H3, H4). The role of the chaperones or chromatin remodelers is specified in brackets in column 2, the genome distribution is given in brackets in column 3. Tissue-specific expression and species specificity are indicated in italics in column 3.
ATRX, α-thalassaemia mental retardation syndrome X-linked; CABIN1, calcineurin-binding protein cabin 1; CENP-A, centromeric protein A; DAXX, death domain-associated protein; FACT, facilitates chromatin transcription; HIRA, histone regulator A; HJURP, Holliday junction recognition protein; NAP, nucleosome assembly protein; ND, not determined; POLE, DNA polymerase epsilon subunit; rDNA, ribosomal DNA; SRCAP, Snf2-related CREBBP activator protein; UBN, ubinuclein.
(Modified from (Martire and Banaszynski 2020)).

The discovery of H3 mutations in pediatric glioblastomas has brought significant attention on the role of histone variants in cancer development (Khuong-Quang et al. 2012; Schwartzentruber et al. 2012; G. Wu et al. 2012). Mutations of histone (H3K27M and G34V/R) have been termed “oncohistones”, a term specifically referring to histone alterations implicated in cancer development, and emerged as major drivers of glioblastoma, the most common and aggressive malignant brain tumor (Fontebasso et al. 2014; Nikbakht et al. 2016; Harutyunyan et al. 2019). Since then, a greater number of histone mutations have been identified in human tumors (Nacev et al. 2019). The amino acid substitutions often occur in the conserved N-terminus of the H3 tail (K27, K36, and G34). The loss of H3K27me3 in K27M mutants, for example, is associated with inhibition of Polycomb repressor complex 2 (PRC2) activity, which in turn leads to upregulation of genes involved in neurodevelopmental progression (Bender et al. 2013; Lewis et al. 2013; Mohammad et al. 2017). H3G34R gives rise to recurrent hemispheric-specific brain tumors through inhibition of the KDM4 demethylase and upregulation of the MYCN oncogene (Behjati et al. 2013; Bjerke et al. 2013). Interestingly, the chromatin landscapes differ from each other depending on whether the mutation affects H3.1 or H3.3; H3.1K27M is distributed genome wide, while H3.3K27M is mainly found at sites of active histone turnover (Sarthy et al. 2020). Such specificity towards particular tissues might be explained by the different gene expression dynamics of H3 variants depending on the cell type.

Thus, mutations occurring on replicative variants, rather than non-replicative, affect predominantly chromatin landscapes of proliferating cells such as stem cells, in contrast with mutations of non-replicative variants (Jessa et al. 2022; Mackay et al. 2017). Since the discovery of H3 mutations in cancer, increased interest has thus arisen in investigating the histone variants of the H3 family.

b) Organization of the histone H3 family

In mammals, the histone H3 family comprises two replicative variants and various non-replicative H3 variants. Its replicate variants, H3.1 and H3.2, differ from each other at a single amino acid at position 96 in the α2 helix of their HFD. The presence of a Cysteine (C) in H3.1 instead of the Serine (S) found in H3.2 has been suggested to enable the formation of disulfide bridges in H3.1-containing nucleosomes (Hake and Allis 2006). In human cells, methylation on K9 and K27 has also been detected between in these two variants using mass spectrometry (Hake et al., 2006). Like other replicative variants, their

transcripts both display a stem-loop structure at their 3' end (Figure 6). However, under stressful conditions, such as exposure to carcinogens, the H3.1 mRNA can be polyadenylated (D. Chen et al. 2020). This has been proposed to cause the transformation of human cells *in vitro*. The first reports of mutations in their genes linked them to the pediatric cancers glioblastoma (GBM) and diffuse intrinsic pontine glioma (DIPG). They both exhibit a heterozygous mutation in a single allele – 1 of all 15 genes producing H3 histones – which implies that H3 oncohistones operate in a dominant-negative manner (Schwartzentruber et al. 2012; G. Wu et al. 2012).

In addition, H3 exists as at least 6 non-replicative variants: H3.3 and CENP-A, which are expressed across tissues and the most well-studied (Table 1), H3.4 and H3.5, which are testis-specific, and H3.X and H3.Y, which are present only in primates (Figure 6). Histone H3.3 is the predominant non-replicative H3 variant in non-dividing cells, including post-mitotic or quiescent (Piña and Suau 1987; R. S. Wu, Tsai, and Bonner 1982). It is also required in the fertilized zygote to replace the paternal protamines before the first round of replication during embryo development (van der Heijden et al. 2005; Loppin et al. 2005; Torres-Padilla et al. 2006). In mammals, two genes (*H3F3A* and *H3F3B*) encode the exact same H3.3 protein (Figure 6). Double knockout (KO) of these genes results in embryonic lethality in mice (Jang et al. 2015), and sterility with reduced viability in flies (Hödl and Basler 2009; Sakai et al. 2009). In *Xenopus* (*Xenopus Laevis*), H3.3 depletion leads to gastrulation defects (Sitbon et al. 2020; Szenker, Lacoste, and Almouzni 2012), while mutation of the five H3.3 homologs present in *C. elegans* (*Caenorhabditis elegans*) is not lethal but alters its ability to modulate heat stress response in both soma and germ lines (Delaney et al. 2018). Finally, in *Arabidopsis* (*Arabidopsis thaliana*), H3.3 knockdown through the removal of three H3.3 genes (*HTR4*, *HTR5*, and *HTR8*) leads to defects in male gametogenesis and embryonic lethality (Wollmann et al. 2017). H3.3 has been implicated in a variety of biological processes such as embryonic stem cell differentiation (Banaszynski et al. 2013) and DNA damage response (Adam, Polo, and Almouzni 2013). Regarding its incorporation into chromatin, in mammalian cycling cells, the histone chaperone HIRA recognizes the H3.3 HFD containing AIG at residues 87-90 and promotes H3.3 deposition (reviewed in (Ricketts and Marmorstein 2017)) in actively transcribed regions, mainly at promoters and gene bodies (Goldberg et al. 2010). By contrast, the DAXX/ATRX chaperone complex promotes H3.3 enrichment at telomeric and pericentric heterochromatin (Drané et al. 2010; Goldberg et al. 2010; Lewis et al. 2010). Finally, at regions lacking H3.1, an alternative HIRA-dependent H3.3 deposition has been proposed as a gap-filling mechanism to prevent nucleosome-free DNA accumulation and to preserve chromatin stability (Ray-Gallet et al. 2011). Outside H3.3 HFD, on its N-terminal tail, S31 is the only amino acid residue that differs from the replicative variants (S31 instead of A31), in addition to the S96 residue that differs from the C96 on H3.1. This S31 residue is phosphorylated during mitosis (Hake et al. 2006; Wong et al. 2009), and at gastrulation (Sitbon et al. 2020). In addition, it is also phosphorylated at transcribed genes in mouse (Armache et al. 2020). Intriguingly, H3.3 phosphorylation at S31 then promotes the

acetylation of nearby residues, thus contributing to enhancer function; H3.3 depletion indeed reduces H3K27Ac at enhancers (Martire et al. 2019).

The centromeric variant of histone H3, CenH3, also called Cse4 (in budding yeast), CENH3 (in plants) or CENP-A (in mammals), epigenetically defines the centromere position and is critical for centromere function. CENP-A encodes a 140-amino-acid protein which shares less than 50% identity with the three other H3 variants; it is the most divergent variant from the H3 family (reviewed in (Müller and Almouzni 2017)). CENP-A is incorporated at centromeres in late M and early G1-phase by its dedicated chaperone, Holliday junction recognition protein (HJURP) (Dunleavy et al. 2009; Foltz et al. 2009). This histone variant is further detailed in **Part 2. CENP-A chromatin in normal and diseased states**.

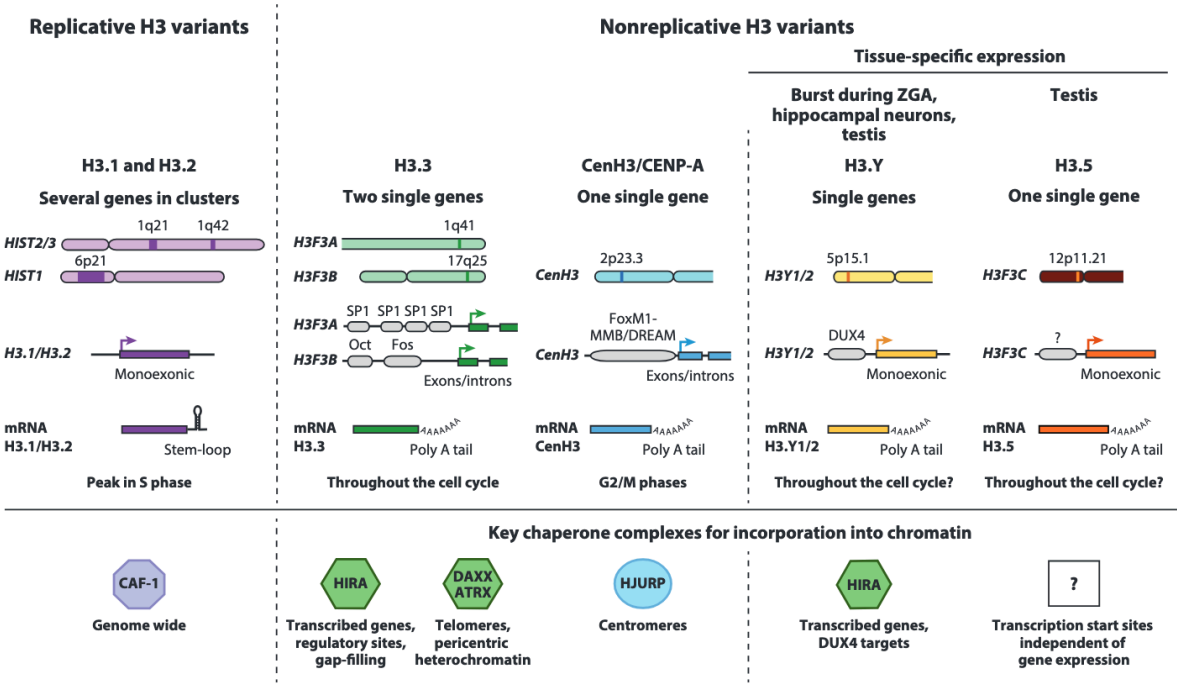


Figure 6. Histone H3 variants deregulated in cancers: genomic organization, mRNA structure, temporal expression in normal situations, and key chaperone complexes for incorporation into chromatin.
Replicative histones H3.1 and H3.2 are expressed from 15 intron-less genes organized into three clusters. Their expression peaks in S phase and their transcripts are regulated by a 3′ stem-loop.
Two single genes containing introns encode H3.3 proteins with identical amino acid composition, expressed throughout the cell cycle. Differences in the transcription factor binding sites account for specific regulation of H3.3 gene products.
A single gene encodes CENPA, which is expressed in G2/M phases. The shared FoxM1–MuvB/DREAM complex-binding motif ensures either CENPA transactivation or transcriptional repression.
The tissue-specific variants H3.Y1, H3.Y2, and H3.5 are encoded by single H3.3 pseudogene-derived intron-less genes. In normal tissues, H3.Y1 and H3.Y2 transcription is regulated by the zygotic homeobox transcription factor DUX4 in a short developmental window. (From Simeonova and Almouzni 2024).

1.3. Higher-order chromatin organization

1.3.1. Visualizing chromatin landmarks

The chromatin is highly dynamic, constantly altering its condensation state for gene regulation or chromosome segregation. The nucleosomal structure represents the first step in a series of higher-order chromatin structures. Electron microscopy enabled the discovery of the packing of DNA into nucleosomes as "beads-on-a-string" on chromatin fibers (Olins and Olins 1974), which organizes into a higher-order structure, further coiling of the flexible chains of nucleosomes: the 30 nm chromatin fiber, observed only when reconstituted *in vitro* from nuclear extracts (Dorigo et al. 2003, 2004; Finch and Klug 1976; Rattner and Hamkalo 1979; Robinson and Rhodes 2006; Song et al. 2014). The 30 nm fiber can form loops averaging 300 nm in length. When further folded and compressed, it produces a 250 nm-wide fiber, tightly coiled into the chromatid of a chromosome (Rattner and Hamkalo 1978). At the nucleus level, mitotic chromosomes (in which the DNA is compacted more than 10000-fold) represent the most obvious chromatin higher-order structure (Flemming 1882; Heitz 1928); they have characteristic localizations in the nucleus, locations of specific genes and banding patterns detected with dyes – such as quinacrine mustard or Giemsa – staining preferentially AT-rich areas (Ferreira et al. 1997; Carvalho et al. 2001). The analysis of the interphase nucleus reveals that genome organization is also highly structured, with specific chromatin landmarks that are distinguishable by imagery.

In the interphase nucleus, two condensation states co-exist: the eurochromatin and the heterochromatin (Lachner and Jenuwein 2002). The heterochromatin state is characterized by a tightly packed chromatin with no detectable gene expression. By contrast, the eurochromatin is marked by active gene expression (reviewed in (Felsenfeld and Groudine 2003; Messner and Hottiger 2011)). Over a hundred years ago, in addition to mitotic chromosomes, euchromatin and heterochromatin in interphase nuclei were also already observed. First, Emil Heitz (1928) observed heterochromatin as densely stained regions forming after mitotic exit in moss cells (Heitz 1928). Second, the use of light microscopy and chromatin dyes enabled to show that, in interphase, chromosomes occupy distinct territories in the nucleus (Boveri 1902). The maintenance of chromosome positioning is actually formed through the interaction between chromosomal DNA and the nuclear envelope, mediated by intermediate filament proteins called lamins and nuclear transmembrane proteins (Mekhail and Moazed 2010). Later, electron microscopy in rat liver cell slices enabled to further characterize the fine organization of the nucleus (Monneron and Bernhard 1969), demonstrating the enrichment of heterochromatin at the nuclear periphery and around the nucleolus previously observed in neurons (Cajal 1903). The development of a novel imaging technique named fluorescence in-situ hybridization (FISH) confirmed the connection between sequence identity and chromosomal arrangement (Bauman et al. 1980; Langer, Waldrop, and Ward 1981). This method enabled to visualize entire chromosomes (Bolzer et al. 2005; Lichter et al. 1988) and individual genes (Lawrence et al. 1988; Lawrence, Singer, and Marselle 1989). These analyses confirmed that,

following mitosis, mammalian chromosomes still occupy distinct territories in the cell nucleus (Bolzer et al. 2005) with significant levels of chromosome intermingling at territory edges (Branco and Pombo 2006). In human cell nuclei, inactive genes and gene-poor regions are predominantly located at the nuclear periphery, near the lamina, whereas active genes typically reside in the nuclear interior (Boyle et al. 2001; Croft et al. 1999) and preferentially at the periphery of chromosome territories (C. S. Osborne et al. 2004; Schoenfelder et al. 2010). In addition, activation or repression of single genes somewhat correlates with their location (T. Takizawa et al. 2008), providing direct evidence for function-related differential positioning of individual gene within the interphase nucleus. Finally, the use of antibodies to target specific proteins and PTMs (Köhler and Milstein 1975) enabled to map their distribution in the nucleus. For example, many nuclear entities, which were previously observed, could be formally characterized (reviewed in (Pueschel, Coraggio, and Meister 2016)). However, limitations remained to access genome organization at small loci, such as the spectral overlap of fluorophores, causing inability to distinguish many different regions simultaneously in the same cell, and the diffraction limit of light resulting in maximal optical resolution ~200-300nm. Over the past decade, significant progress has been made in addressing these challenges thanks to the development of advanced techniques such as super-resolution microscopy, which can distinguish individual objects separated by less than 200 nm (reviewed in (Boettiger and Murphy 2020)). Among these methods, the stochastic optical reconstruction microscopy (STORM) (Rust, Bates, and Zhuang 2006) and the structured illumination microscopy (SIM) (Schermelleh et al. 2008) techniques rely on the excitation of a type of fluorophore in the sample, once at a time, recording the distinct emissions over time to reconstruct a single image later, thus avoiding the problem of spatially dense labelling (reviewed in (Boettiger and Murphy 2020)). The application of STORM coupled to the labelling of histone variants and PTMs evidenced the heterogeneous organization of nucleosomes in the nucleus, which form “clutches” (Ricci et al. 2015) of varying compaction, density and/or volume throughout the cell cycle (Clément et al. 2018) and depending on their nuclear position (Jianquan Xu et al. 2018).

1.3.2. Sequencing-based study of chromatin 3D architecture

In parallel with imaging techniques, significant progress has been made in methods for characterizing chromatin structure, DNA-DNA interactions, and mapping chromatin-associated proteins. Early on, digestion experiments using restriction enzymes, endonucleases (like DNase I), and micrococcal nuclease (MNase) revealed the existence of “open” (nucleosome-free) hypersensitive sites at the 5' end of genes, typically corresponding to promoter regions (C. Wu 1980) and origins of replication (Varshavsky, Sundin, and Bohn 1978). These open chromatin regions are cell-type specific and can undergo changes in response to stress, emphasizing the relationship between gene expression and local chromatin organization (C. Wu 1984). Subsequent technological advances enabled the identification of “open” and “closed” chromatin regions with greater precision. DNase-sequencing analysis and, more

recently, assay for transposase-accessible chromatin (ATAC)-sequencing, have been developed. ATAC-sequencing utilizes a Tn5 transposase that inserts sequencing adaptors directly into accessible chromatin, allowing for efficient "tagmentation" and identification of open regions. These methods are frequently combined with protein mapping techniques, including those targeting histone variants, PTMs, and other chromatin-associated proteins. For example, the development of chromatin immunoprecipitation (ChIP)-sequencing, which allows the targeting of proteins and histone modifications, demonstrated the presence of histone H4 across genes even during transcription (Solomon, Larsen, and Varshavsky 1988). At another level, this approach also revealed that heterochromatin is typically marked by histone methylation signals, such as H3K9me2/3 and H3K27me3, and is bound by Heterochromatin protein 1 (HP1) (reviewed in (Allshire and Madhani 2018)). These findings have highlighted the intricate crosstalk between different layers of chromatin organization. Indeed, DNA methylation promotes chromatin condensation, decreases overall DNA flexibility, and favors the heterochromatin state (Buitrago et al. 2021). Thus, while "open" chromatin correlates with gene activity, "closed" chromatin generally associates with gene repression. More specifically, accessible chromatin tends to be enriched in H3.3 and H2A.Z variants, have high histone turnover and often corresponds to active promoters (marked by H4K4me3), enhancers (marked by H3K4me1 and H3K27ac) and early DNA replication origins. In contrast, inactive chromatin is typically organized in larger domains associated with the nuclear lamina and/or the nucleolus. Heterochromatin regions can be classified as either (1) facultative heterochromatin, marked by H3K27me3, bound by Polycomb repressive complex 1 (PRC1) and/or PRC2 and covering developmental genes, or (2) constitutive heterochromatin, enriched in DNAme and H3K9me3, bound by Heterochromatin protein 1 (HP1), spread over telomeres, centromeres and repetitive elements (reviewed in (Millán-Zambrano et al. 2022; Richards and Elgin 2002)).

Finally, a wide variety of tools has been developed to measure DNA-DNA interaction frequencies within three dimensions (3D) genomic configurations. High-throughput chromatin conformation capture (Hi-C) and its derivatives have become pivotal in studying genome organization, enabling insights at scales ranging from entire chromosomes to specific enhancer-promoter interactions. These methods have provided key confirmations: (1) the presence of chromosome territories which were observed decades ago (Lieberman-Aiden et al. 2009), (2) increased *in trans* contacts between small gene-rich chromosome clusters in the nuclear interior (Lieberman-Aiden et al. 2009), (3) distinct trans-interaction patterns in species with prominent centromere or telomere clustering, such as *Drosophila melanogaster* (*D. melanogaster*) (Sexton et al. 2012) and *Saccharomyces cerevisiae* (*S. cerevisiae*) (Duan et al. 2010), and (4) chromosome alignment along a centromere-to-telomere axis (Hoencamp et al. 2021). Furthermore, at the megabase (Mb) scale, mammalian Hi-C data reveals two distinct groups of large genomic segments that interact more frequently *within* their own set than *between* sets (Lieberman-Aiden et al. 2009). These compartments, known as A compartment (active, accessible,

early-replicating) and B compartment (repressed, closed, late-replicating) (Lieberman-Aiden et al. 2009) evolve with transcription programs. For instance, during the differentiation of human embryonic stem cells (hESCs), approximately 36% of the A and B compartments in the genome undergo switching (Dixon et al. 2015). A and B compartments roughly correspond to euchromatin and heterochromatin regions, respectively (Dixon et al. 2015; Lieberman-Aiden et al. 2009; Monneron and Bernhard 1969). However, this association has not been formally assessed and is not necessarily absolute. For instance, compartment B can contain active genes, while not all genes in compartment A are transcribed (Kempfer and Pombo 2020; Rowley and Corces 2018). Interestingly, various experimental (Arnould et al. 2023; Bantignies et al. 2011; Ogiyama et al. 2018; Schoenfelder et al. 2015) and modelling (Di Pierro et al. 2017) analyses suggest that a mechanism of phase separation likely contributes to this compartmentalization. In this model, chromatin compartments segregate based on their distinct physical properties, due to different composition/enrichment in chromatin-bound proteins, including histone variants and PTMs (Erdel and Rippe 2018; Gibson et al. 2019; McSwiggen et al. 2019). For example, developmental genes in facultative heterochromatin can be organized in foci termed Polycomb bodies in *Drosophila* and mammalian cells, *via* the establishment of long-range contacts when bound by the PRC1 complex (Bantignies et al. 2011; Ogiyama et al. 2018; Schoenfelder et al. 2015). Another recent example, following DNA double-stranded breaks (DSBs) in human cells in culture, ATM drives the formation of a new chromatin compartment (termed "D compartment") through the clustering of damaged topologically associating domains, along with γ-H2AX and 53BP1 (Arnould et al. 2023).

1.3.3. Topologically associated domains (TADs) and chromatin loops

At the scale of tens to hundreds of kilobases, chromatin is organized into topologically associating domains (TADs) to facilitate distal genomic interactions (Nora et al. 2012). A TAD is a self-interacting genomic region that often contains one or more genes, and where DNA elements interact more frequently with each other than with elements outside the TAD. Within TADs, chromatin forms DNA loops that are anchored by structural proteins, the CCCTC-binding factor (CTCF) homodimer and the cohesin complex, essential to maintain the looping. These CTCF-mediated loops constrain enhancer-promoter interactions, thereby contributing to regulating gene expression (Hnisz, Day, and Young 2016). CTCF, along with cohesin, facilitates loop extrusion (Saldaña-Meyer et al. 2014). In addition, CTCF can also regulate chromatin loop formation in cooperation with RNAs (Hansen et al. 2019; Saldaña-Meyer et al. 2019). Acting as an insulator at TAD boundaries, CTCF prevents unwanted interactions between regulatory elements on either side of the boundary.

In summary, the nuclear genome represents the most functional component of the cell. It is organized into chromatin, whose organization ranges from its basic unit, the nucleosome, to higher-level structures. Modulation at each level enables chromatin-based information to vary and represents a key regulator of gene expression in various biological processes, such as cell differentiation.

2. CHROMATIN REPLICATION: MAINTAINING OR REMODELING THE EPIGENETIC LANDSCAPE

2.1. Replication initiation and pattern of origin firing

2.1.1. Initiation control

At every cell cycle, the genome has to be fully and accurately duplicated in S-phase to ensure that the two daughter cells inherit equivalent genetic information. The replication machinery ensures to copy the genomic sequence. To achieve this, a number of factors collaborate to open the DNA and to "read" it. In parallel, tight cell cycle control exerted over this process ensures that all DNA is replicated completely and exactly once (reviewed in (Fragkos et al. 2015)). DNA replication proceeds in distinct enzymatically catalyzed and coordinated steps: initiation, elongation, and termination. Deregulation of DNA replication, including uncontrolled initiation and fork collapse or stalling, can promote DNA damage and genome instability (reviewed in (Branzei and Foiani 2010)). Replication stress, often triggered by oncogene activation, likely plays a key role in this process (reviewed in (Halazonetis, Gorgoulis, and Bartek 2008)). In particular, the timing of initiation and termination is key for preventing abnormal inheritance of genomic pool to daughter cells (reviewed in (L. Wu, Liu, and Kong 2014; Fragkos et al. 2015)). The steps of replication initiation are described below.

(1) Licensing (assembly of the pre-RC): As cells exit mitosis, the origin recognition complex (ORC), which consists of six subunits (ORC1-6), marks all the potential origins of replication (Kara et al. 2015). During G1, other factors bind the associated complex: cell division cycle 6 (CDC6) and CDC10-dependent transcript 1 (CDT1) (Miyazawa-Onami, Araki, and Tanaka 2017). They recruit the minichromosome maintenance (MCM) helicase, which is in complex with Cdt1 (Evrin et al. 2009). This is followed by a series of ATP hydrolysis reactions and conformational changes which lead to the ejection of CDC6 and CDT1, while ORC remains bound. A second complex is recruited to form a double MCM2-7 hexamer. Both complexes surround the dsDNA to form the pre-replication complex (pre-RC).

(2) Pre-initiation: After the G1-S transition, protein kinases coordinate the loading of complementary factors, the heterotetrametric ring-like complex GINS, CDC45, and the DNA polymerase ε (Pol ε), also known as leading strand polymerase (Yeeles et al. 2015). This results in the separation of the MCM2-7 double hexamer into two individual hexamers, each participating in the formation of an S-phase helicase CDC45-MCM2-7-GINS (CMG) complex. The two CMG helicases unwind 6-7 bp DNA concomitantly with their formation. The final step of the origin firing requires the binding of MCM10 and ATP hydrolysis to complete CMG activation. This results in the displacement of the lagging strand of DNA from the helicase channel (reviewed in (Costa and Diffley 2022)). Several additional factors are also recruited, such as the heterotrimeric complex replication A (RPA), which coats the lagging

single stranded DNA (ssDNA) for stabilization, and members of the replisome, a complex that ensures tethering and processing of the leading and lagging strand polymerases on the DNA template while orchestrating the activity of Pol ε (reviewed in (Attali, Botchan, and Berger 2021)).

(3) Replication initiation: In S-phase, Cdc45 and GINS activate the replicative helicases, which bind the ssDNA of the leading strands, thus creating a pair of bi-directional replication forks. At each fork, replication on both strands is initiated by the generation of a short RNA primer by Pol α and proceeds in 5'-3' direction.

(4) This results in the elongation: the processive *de novo* DNA synthesis on the leading strand by Pol ε, and the discontinuous synthesis of Okazaki fragments on the lagging strand by Pol δ. The CMG helicase travels along the template of the leading strand, unwinding the parental dsDNA and producing the ssDNA (Burgers and Kunkel 2017). The overall rate of DNA synthesis is controlled by the rate at which individual replication forks synthesize DNA and by changing the number of active forks in the S-phase. Importantly, Cdc45 is present in limiting amounts and recycled to a different origin after replication termination, which can contribute to the spatiotemporal control of origin firing (Tanaka and Araki 2013).

2.1.2. Definition of origins of replication

The average DNA replication fork speed is 2 to 3 kb/min (Conti et al. 2007), meaning it would take approximately three years to replicate the entire haploid human genome (~3100 Mb) if only a single origin of replication was used. The typical S-phase lasts only about 6-8 hours in human cells (G. M. Cooper 2000). To achieve this, DNA replication initiates from numerous replication origins during S-phase in a spatiotemporal sequence known as the replication timing (RT) program (Cairns 1966; Huberman and Riggs 1968).

Bacterial and archaeal genomes, usually consisting of a small circular chromosome, have generally a single replication origin (Barry and Bell 2006; F. Gao and Zhang 2007) while, by contrast, eukaryotic genomes contain significantly more replication origins, ranging from 400 in yeast to 30000-50000 in mammals (reviewed in (Cvetic and Walter 2005; Hu and Stillman 2023; Méchali 2010)). Although multiple replication initiation sites can be used, only a subset is activated during each S-phase. Origins of replication fire in a temporally defined order, giving rise to replication patterns characteristic of the cell type (reviewed in (Fragkos et al. 2015; Hiratani et al. 2008)).

In budding yeast, origins of replication are defined mainly based on the DNA sequence. Replication initiation starts at the autonomous-replicating sequence (ARS), which is recognized by ORC. Budding yeast origins have also a characteristic nucleosome organization comprising a nucleosome-depleted region (NDR) over the ARS, flanked by nucleosomal arrays, important for ORC1 binding and origin firing. By contrast, in metazoans, replication origins are not sequence-defined but instead rely on both

DNA- and chromatin-based information (reviewed in (Ganier et al. 2019)). Indeed, ORC1 does not exhibit sequence-specific binding but can recognize the H4K20me2 mark, deposited by the Suv420h1 enzyme, and has also been reported to associate with H3K9me3-, H3K27me3- and H4K20me3-marks (Costa and Diffley 2022; Vermeulen et al. 2010). In addition, origins of replication are enriched in G-rich elements such as G4 motifs, which may preclude nucleosome formation and promote chromatin accessibility at replication origins. Indeed, firing efficiency correlates with transcription and open chromatin regions (reviewed in (Hu and Stillman 2023)). It has been challenging to obtain a consensus mapping of replication firing origins at high resolution in mammalian cells, due to the fact they are likely used stochastically within initiation zones of approximately 20 up to 150 kb in length (Tian et al. 2023; W. Wang et al. 2021). Models of stochastic RT posit that the only difference between early- and late-firing origins is their relative probability of firing. More-efficient origins are more likely to fire first and thus on average, have earlier firing times (Rhind, Yang, and Bechhoefer 2010). Interestingly, measuring the relative probability of initiation in early-S phase was sufficient to accurately recapitulate genome-wide RT profiles obtained by optical replication mapping (ORM) (W. Wang et al. 2021). These findings support the model of a difference between early- and late-replicating initiation zones based on their relative initiation probability, likely influenced by chromatin structure. Early- and late-replication domains correlate with euchromatin and heterochromatin, respectively (Farkash-Amar et al. 2008). Furthermore, the conflict between transcription and pre-RC assembly (M. M. Martin et al. 2011; Nieduszynski, Blow, and Donaldson 2005) may explain why highly efficient origins are found at transcription start sites (TSSs), whereas origins at the end of transcriptional units are less efficient (Donato, Chung, and Tye 2006). The analysis of single-cell Repli-sequencing data, measuring the stochastic variation in genome-wide RT, revealed the emergence of the RT program during mouse (Nakatani et al. 2024; Halliwell et al. 2024) and bovine (S. Xu et al. 2024) early development. The RT is variable from zygote to 2-cell stage embryo; it then progressively acquires a well-defined partitioning (with early and late replication origins progressively more defined). Starting from the 2-cell stage, changes in RT correlate with chromatin accessibility but can occur independently of active transcription (RT patterns are established prior to embryonic genome activation), although it may contribute to the fine-tuning of initiation and termination sites.

Furthermore, recent work (Gatto et al. 2022) demonstrated that the dual deposition mode of H3.1 and H3.3 histone variants leads to the formation of boundaries defined by H3.3-enriched sites flanked by H3.1 genome-wide; these boundaries mark early replication initiation zones (Figure 7A). Knockout of the H3.3 chaperone HIRA led to two classes of effects on early-replicating sites. First, at boundaries associated with transcription, the patterns of both H3.3 and nascent DNA synthesis became less well-defined, therefore early initiation was termed blurred. Second, at H3.3/H3.1 boundaries with low or no transcriptional activity, a complete loss of both H3.3 enrichment and nascent DNA synthesis occurred; hence these early initiation zones became buried. Thus, HIRA proved critical for a chromatin-based

definition of early initiation zones to ensure precision in initiation in transcribed regions and allow initiation in non-transcribed regions (Figure 7B). These findings could indicate a potential role of H3.3/H3.1 boundaries in regulating early replication in mammals. In addition, during the induction of 2-cell-like cells from cultivated mouse ESCs, H3.3 enrichment increases alongside the earlier RT of the repetitive element MERVL (Nakatani et al. 2022). Also, during the transition from naïve to primed mouse ESCs, H3.3 enrichment changes represent the most accurate predictor of RT shifts (Gökbuget et al. 2023; Halliwell et al. 2024). These findings suggest a potential link between the incorporation of the H3.3 variant and early replication events during developmental transitions.

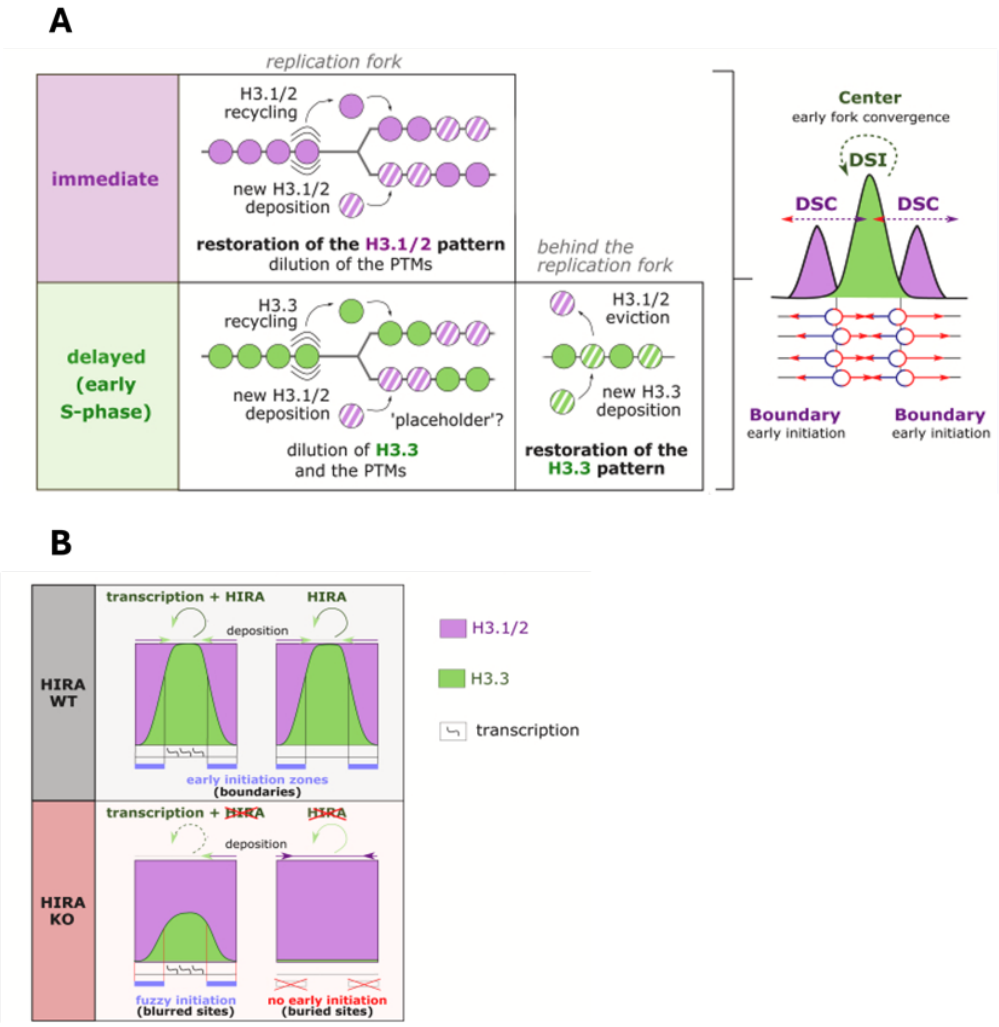


Figure 7. Deposition time and mode for variant landscape recovery.
(A) Scenario summary of dilution and recovery dynamics for H3.1/2 (top) and H3.3 (bottom). Right: scheme illustrating how the two distinct pathways, DSI deposition for H3.3 systematically at the same place combined with DSC deposition of H3.1, following the replication fork, create boundaries at early initiation zones of replication.
(B) Scheme depicting how HIRA removal, and by extension removal of HIRA-dependent H3.3 deposition, affects not only deposition but also early replication zones. Two types of effects occur, and they distinguish two types of regions: blurred sites show blurred incorporation and blurred initiation zones at regions with active transcription, and buried sites correspond to regions without significant transcription where incorporation of H3.3 is abrogated, and the initiation zone disappears. (Adapted from Delaney et al. 2023).

2.2. Chromatin dynamics during replication fork progression

2.2.1. Chromatin disruption

In S-phase, chromatin undergoes disruption at a rate of around 10 to 15 nucleosomes every minute ahead of a replication fork (reviewed in (Méchali 2010)). Indeed, when the replisome proceeds along DNA, it encounters nucleosomes, which are disassembled for the DNA replication machinery to travel, and subsequently reassembled in the daughter strands (McKnight and Miller 1977; A. T. Annunziato et al. 1981; Lucchini and Sogo 1995; Sogo et al. 1986). The mechanism underlying nucleosome disruption is not well understood. One possibility is that the collision with replicative helicases evict the nucleosome (reviewed in (Groth 2009)), but this is likely not sufficient for their complete eviction (A. T. Annunziato et al. 1981; Lucchini and Sogo 1995; Sogo et al. 1986). Chromatin remodelers and chaperones could be involved in this process. For example, the histone chaperone ASF1 has already been described to disrupt nucleosomes (English et al. 2006). In addition, artificial tethering of CDC45 to a chromosomal site can promote large-scale decondensation independently of DNA synthesis, suggesting a role for CDC45 in chromatin reorganization/decondensation for the progression of the replication fork (Alexandrow and Hamlin 2005). Another mechanism which could be involved, phosphorylation of linker histone H1 by the S-phase kinase cyclin A-CDK2 (Thomson, Gillespie, and Blow 2010), promotes H1 mobility and chromatin decompaction (Contreras et al. 2003). Consistently, in human cells, cyclin A-CDK2 is recruited to replication sites and interacts directly with both Proliferating cell nuclear antigen (PCNA) and MCM7 (Cardoso, Leonhardt, and Nadal-Ginard 1993; Chibazakura et al. 2011; Koundrioukoff et al. 2000). Moreover, the G2/M phase kinase cyclin A-CDK1, which also phosphorylates H1, can activate late firing origins if it is overexpressed in early S-phase (Katsuno et al. 2009). Finally, positive supercoiling ahead of the fork (Branzei and Foiani 2010) could potentially contribute to the disruption, as DNA superhelicity is important for nucleosome stability (Imre et al. 2017).

Parental nucleosomes, with their specific histone variants and PTMs, undergo a two-fold dilution with the replication fork passage (Alabert et al. 2015), posing a challenge for the maintenance of chromatin. Thus, in addition to DNA replication, cells must duplicate their chromatin to restore the epigenetic information and preserve cell identity and functions. This is accomplished by the concerted recycling of parental histones along with the deposition of newly synthesized histones, whose expression peak in S-phase (reviewed in (Ray-Gallet and Almouzni 2021)). Intriguingly, a recent study identified a defect of the 3' end processing of replicative histone pre-mRNAs in ASF1-depleted cells (Mendiratta et al. 2024). This result suggests a role for ASF1 in regulating the replicative histone transcript levels to ensure proper histone dosage and avoid imbalance in histone provision. The provision in replicative histones H3.1/2 in S-phase enables to restore full nucleosome occupancy but does not resolve the two-fold dilution of the parental variants and PTMs. Therefore, the time of replication provides a window

of opportunity for cellular reprogramming and has to meet the dual challenge of maintaining the epigenomic state and orchestrating changes in chromatin composition during cell differentiation and development (reviewed in (Stewart-Morgan, Petryk, and Groth 2020)). Three main categories of factors are involved during the duplication of chromatin: (1) chromatin remodelers, defined as large complexes using ATP hydrolysis to slide nucleosomes or remove histones from DNA (reviewed in (Becker and Workman 2013)); (2) histone chaperones, which associate with histones and promote their transfer to the replicated DNA (reviewed in (De Koning et al. 2007; Gurard-Levin, Quivy, and Almouzni 2014)); and (3) chromatin modifiers, which are involved in the establishment or removal of PTM marks on histones or DNA methylation (Van Rechem et al. 2021). Once established, PTMs can be maintained or spread by coupling of their read/write mechanisms with chromatin modifiers. For instance, this process has been well-characterized for the full restoration of heterochromatin marks, H3K9me3 and H3K27me3, upon chromatin replication. This is of major importance for genome stability, since defects in heterochromatin maintenance after replication can lead to chromosome instability (Taddei et al. 2001). In S-phase, K9me3 is "read" by HP1a, which recruits its writers SetDB1 and Suv39h1/2 (reviewed in (Allshire and Madhani 2018)). K27me3 is recognized by the PRC1 complex, which then deposits another mark, H2AK119ub, that is in turn recognized by the K27me3 writer complex PRC2, thus contributing to de novo deposition of K27me3 (reviewed (Schuettengruber et al. 2017)). In addition, H3 marks K9me3 and K27me3 allosterically stimulate the activity of their writers, thereby promoting their maintenance even in the absence of the original trigger (Escobar et al. 2022). This positive, feed-forward mechanism allows the formation of repressive facultative heterochromatin domains bearing H3K9me3 or H3K27me3 and is thought to contribute to their function in stable repression throughout the cell cycle. Importantly, the H3-H4 chaperone NPM1 is an integral component of this process, recycling parental nucleosomes (marked with H3K27me3) on the same chromatin domains during DNA replication to allow the allosteric activity. This exemplifies the importance, in addition to chromatin modifiers, to ensure histone (and other chromatin-bound factors) recycling from the parental strand to the daughter strands in order to reproduce a similar chromatin environment on new DNA. Read-write mechanisms indeed require the coordinated recycling of parental histones in S-phase.

2.2.2. Histone variants deposition during and after S-phase

a) Coordinated histone recycling at the replication fork

The current view involves the tight coordination of parental histone recycling and *de novo* histone deposition, along with reader-writer complexes re-establishing pre-existing marks (reviewed in (Delaney, Weiss, and Almouzni 2023)).

During the nucleosome core assembly at DNA replication forks, each histone is sequentially deposited into chromatin. H3 and H4 are deposited in a first time (Worcel, Han, and Wong 1978; Almouzni et al.

1990; S. Smith and Stillman 1991). Parental histone recycling on the leading and lagging strands involves distinct sets of chaperones, most of them being replisome components. On the leading strand, two Pol ε subunits (POLE3-4) handle H3-H4 tetramers (Bellelli et al. 2018; C. Yu et al. 2018). On the lagging strand, the replicative helicase subunit MCM2 (H. Huang et al. 2015; Petryk et al. 2018) cooperates with ASF1 (Groth et al. 2007), Pol α (Gan et al. 2018; Z. Li et al. 2020) and chromosome transmission fidelity 4 (Ctf4) (Gan et al. 2018) to recycle parental H3-H4 in a tetrameric or in a heterodimeric form (Groth et al. 2007). This is followed by the addition of two H2A-H2B dimers, transferred on the lagging strand by Pol α while its recycling mechanism on the leading strand remains unclear (Flury et al. 2023). Therefore, during nucleosome assembly, H3-H4 tetramers contain either two new or two recycled dimers but they can "mix" with either old or newly synthesized H2A-H2B (Jackson 1988; Yamasu and Senshu 1990). Subsequent work confirmed this for H3.1-H4 tetramers precisely, but revealed that a small fraction (~10%) of H3.3-H4 split in a manner associated with replication (M. Xu et al. 2010), supporting the hypothesis that a fraction of H3.3-H4 may be handled as dimers instead of tetramers, as mentioned above.

ASF1, the first histone recycling factor identified, can form a bridge with the MCM2 subunit of the replicative helicase from both nuclear and cytosolic extracts (Groth et al. 2007) (Figure 8A). Thus, disrupting the balance between histone supply and ASF1 levels (either by ASF1 knockdown or overexpression of H3.1 and H4) impaired DNA unwinding. In agreement with these findings, ASF1 depletion led to a reduced retention of parental histones at sites of DNA synthesis (Clément et al. 2018). In addition to the MCM2-H3-H4-ASF1 complex, MCM2 may transfer histones onto DNA directly without requiring an interaction with ASF1. In this case, MCM2 can bind all H3 variants (H. Huang et al. 2015), including H3.1/2, H3.3 (corroborated by (X. Xu et al. 2022)) and CENP-A together with its chaperone HJURP (corroborated by (Zasadzińska et al. 2018)). Thus, MCM2 provides a mechanism to couple histone recycling to replication progression genome wide.

After eviction from chromatin, histones retain their PTMs, preserving a memory of the local epigenetic state and providing an opportunity to maintain it. Their PTMs can then be used as a seed for read-write mechanisms, to be propagated on nearby *de novo* assembled nucleosomes (Escobar et al. 2022; Stewart-Morgan, Petryk, and Groth 2020). This requires the symmetric recycling of old histones in order to maintain the epigenetic landscape without affecting overall nucleosome occupancy (reviewed in (Stewart-Morgan, Petryk, and Groth 2020)). Early *in vitro* experiments indicated that during replication, chromatin-bound histones are indeed randomly recycled to the two daughter strands (Jackson and Chalkley 1985; Russev and Hancock 1982). More recent studies confirmed that genome-wide, new and old histones are largely randomly and symmetrically deposited on the leading and lagging strand at the replication fork (Gan et al. 2018; Petryk et al. 2018; C. Yu et al. 2018).

Several studies have investigated the influence of the parental nucleosome assembly pathway on cellular differentiation and development. Interestingly, both MCM2 and POLE3 deletion in mouse ES cells have shown to reduce their ability to differentiate, without affecting cell growth (Wen et al. 2023; Wenger et al. 2023; X. Xu et al. 2022). Similarly, mutations at the histone binding motif of MCM2 leads to defects in the silencing of pluripotent genes and in the induction of lineage-specific genes. Given these observations, along with the distinct RT in early embryogenesis contrasting with the RT in cell differentiation, with major replication changes correlating with H3.3 redistribution, H3.3 contributes to reshaping replication and cellular plasticity.

b) *De novo* histone deposition

In addition, new histones are incorporated to maintain nucleosome density (Figure 8). Newly synthesized histones, prior to their incorporation, show distinct PTMs compared to their incorporated forms. These PTMs are generally involved in their processing, nuclear import and differential recognition by histone chaperones directing their assembly pathway on chromatin (Anthony T. Annunziato 2015; Burgess and Zhang 2013). Thus, PTM signature of new histones is changed and become assimilated to the nearby "chromatin landscape", i.e., old histone marks in the local chromatin environment. As an example, HAT1-mediated acetylation of both new H3 (K9, K18) and H4 is required for DSC incorporation and genome stability in mouse embryonic fibroblasts (Nagarajan et al. 2013). Following deposition on chromatin, H4 is deacetylated within 20-30min (Cousens and Alberts 1982; Jackson et al. 1976; Ruiz-Carrillo, Wangh, and Allfrey 1975).

Coordination of parental histone recycling and deposition of newly synthesized histones at the fork requires a proper control of the supply of both new and parental histones. This involves the chaperone ASF1, implied in histone recycling and *de novo* deposition (reviewed in (Ray-Gallet and Almouzni 2021)). The DSC assembly is mediated by Chromatin assembly factor 1 (CAF-1) (S. Smith and Stillman 1989), which deposits new H3.1/2-H4 dimers into nascent DNA (Tagami et al. 2004). This coordination involves a direct interaction between the CAF-1 subunit p150 and PCNA (Moggs et al. 2000; Shibahara and Stillman 1999). In addition to the DSC, the DSI assembly of newly synthesized H3.3-H4 is mediated by HIRA and also takes place in S-phase. In normal conditions, HIRA continuously targets H3.3 to its pre-existing sites of enrichment (Gatto et al. 2022). Additionally, HIRA may perform a "gap-filling" function (Figure 8), depositing new H3.3 to maintain nucleosome density (Ray-Gallet et al. 2011).

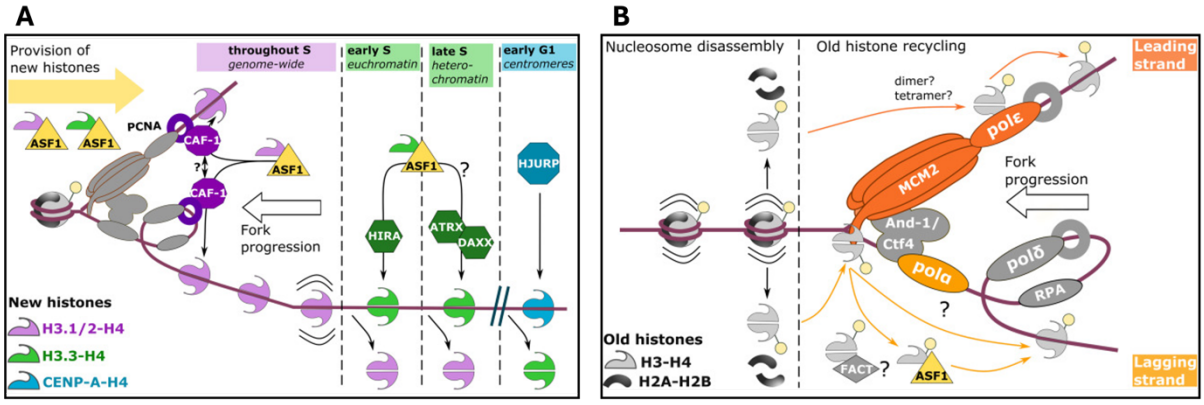


Figure 8. Histone dynamics during replication.
(A) *De novo* deposition of histones, mostly in S phase, involves dedicated histone chaperones at distinct locations and time.
(B) Recycling old histones: replisome is a "chaperone hub" at the replication fork. Ahead of the replication fork, nucleosomes are disassembled into an H3–H4 tetramer and two H2A-H2B dimers. Their recycling onto newly synthesized DNA is largely mediated by replisome components, which do not discriminate between the H3 variants. (Adapted from Karagyozova et al. 2024).

c) Centromere-specific aspects

CENP-A, the centromere-specific H3 variant, is stably inherited across multiple generations; this indicates that CENP-A nucleosomes are faithfully retained through DNA replication (Bodor et al. 2013). This stable CENP-A retention at centromeres involves CENP-A association with certain proteins from the constitutive centromere associated network (CCAN), notably CENP-C (Falk et al. 2015; Guo et al. 2017), as described below.

During centromeric DNA replication in mid/late S-phase (Zasadzińska et al. 2018), CENP-A is redistributed to each "daughter centromere" (Bodor et al. 2014; Jansen et al. 2007). CENP-A-H4 recycling on both strands involves the chaperone HJURP and its interaction with MCM2 (H. Huang et al. 2015; Zasadzińska et al. 2018). Intriguingly, removal of CENP-C during S-phase leads to massive loss of CENP-A by G2 at the centromere, suggesting that CENP-C could directly participate in CENP-A maintenance (Nechemia-Arbely et al. 2019). In addition, CAF-1 has been copurified with CENP-A in late-S-phase-derived chromatin (Nechemia-Arbely et al. 2019). Taken together, these results suggest a model wherein the local CENP-C/CCAN promotes CENP-A retention to the replication fork, thereby stabilizing CENP-A binding to HJURP, MCM2 and potentially CAF-1, for precise CENP-A reassembly within each "daughter centromere", ensuring the maintenance of centromere identity (see **Part 2. CENP-A chromatin in normal and diseased states**). In parallel, the provision in replicative histones H3.1/2 in S-phase partially restores nucleosome occupancy. However, the deposition of new CENP-A does not occur until late mitosis/early G1-phase in human cells (Jansen et al. 2007). CENP-A dilution at centromeres thus results in "CENP-A gaps" that are occupied by H3.3, deposited in S-phase as a placeholder for newly assembled CENP-A in late mitosis/early G1-phase (Dunleavy, Almouzni, and Karpen 2011). The histone chaperone(s) or exchange factor(s) involved in this process however remain

uncharacterized. A similar placeholder model has been shown in fission yeast, involving H3 deposition in S-phase at centromeres and subsequent removal in G2, when new CENP-A^{Cnp1} is deposited (Shukla et al. 2018).

In human cells, following the peak of CENP-A expression in G2/M phase (R. D. Shelby, Vafa, and Sullivan 1997), new CENP-A incorporation starts during late mitosis (telophase)/early G1 phase (Jansen et al. 2007). This timing differs across species and between somatic and germline cells. For instance, its new loading occurs in G2 in fission yeast, as described above (Lando et al. 2012; Shukla et al. 2018), and in *Arabidopsis* (Lermontova et al. 2006), while it takes place from metaphase to G1 in *Drosophila* cell cultures (Mellone et al. 2011; Schuh, Lehner, and Heidmann 2007) and late telophase-G1 in *Drosophila* somatic tissues (Dunleavy et al. 2012). Interestingly, CENP-A loading has been shown to occur at two distinct cell cycle phases in *Drosophila* meiosis for both male (prophase I and after exit from meiosis II) and female (prophase I) gametes (Dunleavy et al. 2012). Specific CENP-A deposition (and recycling) at centromeres relies on the CENP-A-targeting domain (CATD), which enables recognition of CENP-A by HJURP. HJURP mediates the deposition of CENP-A-H4 (Dunleavy et al. 2009; Foltz et al. 2009), which will replace placeholders H3.3-H4 at centromeres (Dunleavy, Almouzni, and Karpen 2011).

Finally, it is worth mentioning two points relative to centromeres:

First, due to their highly repetitive structure, human centromeres are difficult-to-replicate regions and hotspots for rupture and whole-arm chromosome translocation under replication stress. Thus, centromeres harbor specialized replication dynamics characterized by the presence of repair factors such as TOP2A and SMC5/6, that are required for faithful centromere duplication (Scelfo et al. 2024). In addition, CENP-A nucleosomes are essential to prevent the formation of R-loop – which can interfere with the replication fork – and subsequent replication stress (Giunta et al. 2021).

Second, DNA replication also functions to correct errors in CENP-A deposition by removing ectopic CENP-A from non-centromeric sites in human cells (Nechemia-Arbely et al. 2019). Most ectopic sites of CENP-A deposition in human cells are found in early and mid-replicating regions. As the replication fork progresses, ectopic CENP-A is removed from the replicating chromatin. While several E3 ligases promote the degradation of CENP-A^{Cse4} in budding yeast (Au et al. 2020; Cheng, Bao, and Rao 2016; G. Hewawasam et al. 2010; G. S. Hewawasam et al. 2014; Ohkuni et al. 2016; Ranjitkar et al. 2010), CENP-A^{Cnp1} in fission yeast (Kitagawa et al. 2014) and CENP-A^{CID} in flies (Moreno-Moreno et al. 2011; Moreno-Moreno, Torras-Llort, and Azorín 2006), such mechanism has not been identified in human cells. Therefore, in human cells, concomitant removal of CENP-A from non-centromeric sites, along with retention of CENP-A at centromeric sites, both achieved during DNA replication, function to restrict CENP-A localization to centromeres.

In summary, during chromatin replication, nucleosomes are disassembled ahead of the replication fork and reassembled, together with newly synthesized histones, on the daughter DNA strands. Chromatin modifications are copied from the parental chromatin onto the daughter chromatin strands. However, at the same time, replication provides an opportunity for chromatin modifications to be altered as cells change their differentiation state.

PART 2.

CENP-A CHROMATIN IN NORMAL AND DISEASED STATES

Centromeres are key structural components of eukaryotic chromosomes, playing a critical role in ensuring accurate chromosome segregation during cell division. The histone H3 variant CENP-A (CenH3) is the epigenetic mark that defines centromeres in most eukaryotes and is essential for their proper function. This section focuses on the role and regulation of CENP-A-containing chromatin, examining its dynamics in normal and pathological contexts.

1. CENTROMERE ARCHITECTURE AND FUNCTION: A REGION LIKE NO OTHER

1.1. Centromere function and organization

1.1.1. Studying centromere function

Following replication, proper chromosome segregation is essential for the equal distribution of replicated DNA to the daughter cells during cell division to ensure faithful genome inheritance. In eukaryotic cells, this task is executed by the kinetochore, a multiprotein complex which assembles at a single, specific site on each sister chromatid to orient and regulate contacts between chromosome and spindle apparatus. Once all chromosomes achieve amphitelic attachment – each sister chromatid oriented towards a different spindle pole – components of the spindle assembly checkpoint (SAC) signal the onset of anaphase. During anaphase, spindle microtubules contract, separating sister chromatids toward opposite poles to form the two future daughter nuclei (reviewed in (McKinley and Cheeseman 2016)). The centromere, distinguished as the primary constriction between sister chromatids of the condensed chromosome in most eukaryotes (Flemming 1882), is the chromosomal region where the kinetochore assembles during mitosis or meiosis (Darlington 1936).

In 1985, using autoantibodies targeting human centromeres (Moroi et al. 1980) from the serum of patients with systemic sclerosis (scleroderma), a rare auto-immune disease involving the fibrosis (hardening and tightening) of the skin, along with problems in the blood vessels, internal organs and digestive tract, William Earnshaw and Naomi Rothfield identified the first centromere proteins: CENP-A, -B, and -C (Earnshaw and Rothfield 1985). Among these centromeric proteins, CENP-A proved to be a variant of histone H3 (Palmer et al. 1987, 1991; K. F. Sullivan, Hechenberger, and Masri 1994). To date, CENP-A is considered the epigenetic mark of most centromeres. The study of CENP-A/centromere chromatin holds both fundamental and applied significance. On the one hand, it offers a framework for understanding how a chromatin component, a variant of histone H3, can interact at different levels to form a functional domain with distinct dynamics throughout the cell cycle. On the other hand, centromere dysfunction is linked to chromosomal instability, a hallmark of cancer (reviewed in (Barra and Fachinetti 2018; Nassar, Thompson, and Fouquerel 2023)), and centromere proteins

emerged as prognostic markers and potential therapeutic targets (reviewed in (Aldwaik et al. 2023; Shi et al. 2023; W. Zhang et al. 2016)). CENP-A itself, the H3 variant marking centromeres in most eukaryotes, is an epigenetic mark that can directly perturb both genetic stability and chromatin (epigenetic) information when overexpressed, both being hallmarks of cancer (Hanahan 2022).

1.1.2. An introduction to centromere diversity: Different types of centromeres

The concept of possessing a single regional centromere per chromosome is not universal in eukaryotic organisms. Despite their essential function in mediating chromosome segregation, centromere architectures and sequences are highly diverse among different organisms, with a length ranging from 120 bp to up to several Mb (reviewed in (Steiner and Henikoff 2015)). In most eukaryotes, cenH3 (termed CENP-A in mammals) is an essential centromere component. The distinct types of centromeres can be categorized as follows: Monocentromeres (point and regional centromeres), meta-polycentromeres and holocentromeres (Figure 9).

(i) Point centromeres were the first type of centromere to be isolated, ~44 years ago, by Louise Clarke and John Carbon (Clarke and Carbon 1980, 1985). They represent the "simplest type" of centromere and are found in budding yeast (Furuyama and Biggins 2007; Pluta et al. 1995). Point centromeres consist of a single cenH3 (Cse4) nucleosome binding a particular DNA sequence of ~120 bp length and connecting a single microtubule in mitosis. Their centromeric DNA is organized into 3 domains termed centromere DNA elements I-II-III (CDE I-II-III). CDE II is AT-rich and contains the Cse4 nucleosome, while CDE I-III are binding sites for protein complexes that bend DNA and constrain the Cse4 nucleosome.

(ii) Regional centromeres are found in most other organisms including humans; they consist of several cenH3 nucleosomes localized in a specific region of the chromosome encompassing several kb to Mb of DNA (Karpen and Allshire 1997; Logsdon et al. 2023; Pluta et al. 1995). Arrays of CenH3 nucleosomes are interspersed with blocks of H3 nucleosomes (Blower, Sullivan, and Karpen 2002). Depending on the relative centromere position, chromosomes are categorized into three types: Metacentric or submetacentric when the centromere is found roughly in a central position, acrocentric when the centromere is very close to the tip of a chromosome (telomere), and telocentric when the centromere is found at the terminal end of the chromosome. Human cells do not possess telocentric chromosome, in contrast with mouse cells where, interestingly, pericentric domains of several chromosomes unite and form structures termed chromocenters while centric domains remain individualized at their periphery (Guenatri et al. 2004).

(a) Certain regional centromeres form on one (or low copy) sequence(s) flanked by heterochromatin domains (Plohl, Meštrović, and Mravinac 2014). This type of centromere can be found, for example, in fission yeast (Polizzi and Clarke 1991), equines (Piras et al. 2010) and chicken (Shang et al. 2010).

(b) Satellite centromeres are larger, composed of particular families of tandemly repetitive satellite DNA and are often strongly enriched for transposons (reviewed in (P. B. Talbert and Henikoff 2022)). Their pericentric heterochromatin (PHC) is highly repetitive and has been shown to act as a regional boundary (Lam et al. 2006). The repetitive centromere sequences vary in size and sequence between species, and between chromosomes within a species. Repeat-length often lies between 100 and 200 bp, which corresponds to the approximate length of nucleosomal DNA (Melters et al. 2013).

(iii) Meta-polycentromeres (Macas et al. 2023) share a similar structure with satellite centromere but are organized as 3-5 distinct close centromeric domains which may function as one single domain. They are observed in peas, for example.

(iv) Holocentromeres cover the entire length of the chromosome. In most lineages, including that of *C. elegans*, cenH3 is present and preferentially incorporates at specific sites corresponding to accessible chromatin, coinciding with transcription factor hotspots (reviewed in (Steiner and Henikoff 2014)). In other lineages, such as in Lepidoptera, holocentromeres are cenH3-depleted and repressive chromatin states are sufficient for *de novo* centromere formation (Senaratne et al. 2021).

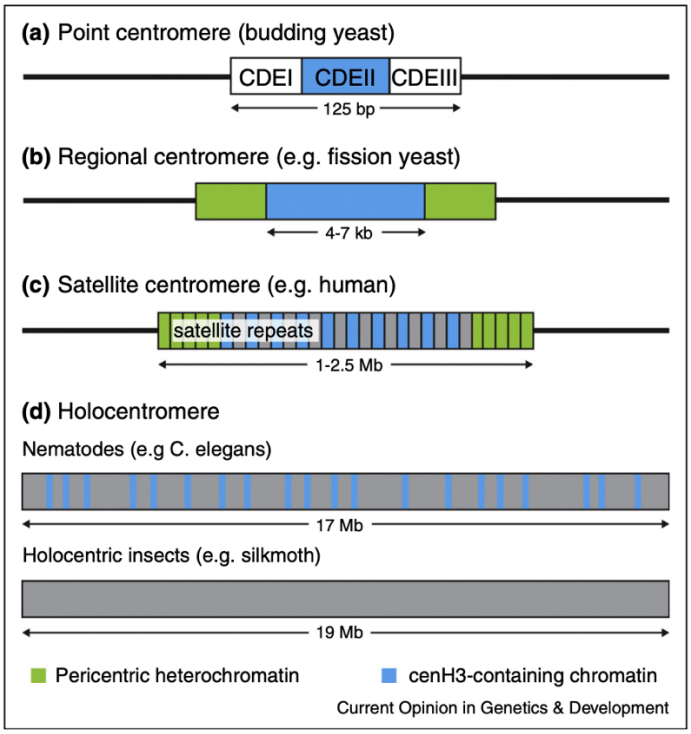


Figure 9. Diversity in centromere organization.
Diverse types of centromeres are found in different organisms. (a) The point centromere, found in budding yeast, consists of three DNA elements, CDE I–II–III. A single cenH3 nucleosome assembles on CDE II. (b) Regional centromeres, found for example in fission yeast, consist of a centromeric region that is usually flanked by pericentric heterochromatin. (c) Satellite centromeres, for example found in humans, are similar to regional centromeres in that they occupy contiguous regions of chromosomes flanked by pericentric heterochromatin, but they are composed of particular families of tandem repeats, occupied by alternating arrays of cenH3 and H3- containing nucleosomes. (d) Holocentromeres cover the entire length of the chromosomes. In most lineages, including that of nematodes, cenH3 preferentially incorporates at specific sites, whereas in holocentric insects, cenH3 has been lost. (From Steiner & Henikoff 2015).

1.1.3. Heterogeneity of the human centromere structure

a) Variable genetic features

In human centromeres, repeat arrays consist of primate-specific DNA units called alpha-satellite DNA (α-Sat), an AT-rich repeat family composed of ~171-bp monomers (reviewed in (Willard 1989)) which are highly divergent (Alkan et al. 2011). Accumulative sequences of α-Sat DNA monomers (2-16 monomers) form higher-order repeats (HORs) of 1 up to 3 kb length. Different monomer subtypes belong to HORs; for example, monomer subtypes "a", "b", and "c" repeating as "abc-abc-abc" could form a HOR (Waye et al. 1987). In turn, HORs are repeated multiple times, producing HOR arrays of ~200 kb to up to 5000 kb. These HOR arrays tend to homogeneous, often containing thousands of nearly identical units (reviewed in (Aldrup-Macdonald and Sullivan 2014)) (Figure 10).

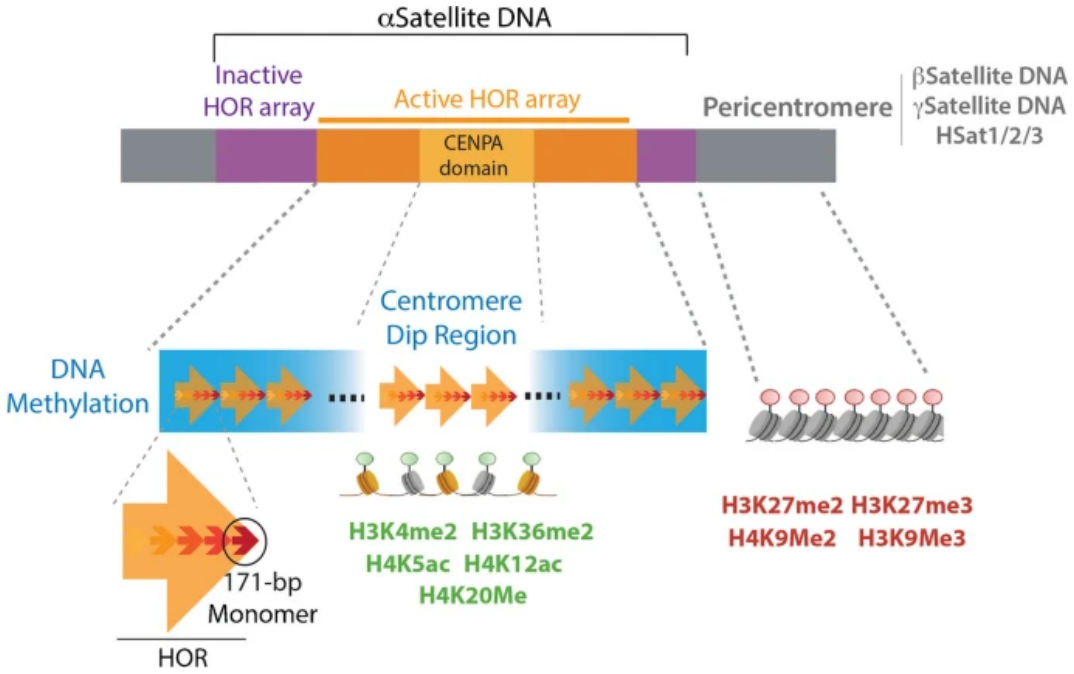


Figure 10. Genetic and epigenetic features of the centromere. Schematic of the genetic and epigenetic elements that compose the core centromere and pericentromere, indicating the inactive and active HOR arrays, and the CENP-A-binding domain. αSat monomers are portrayed as smaller arrows within the HORs. The DNA methylation pattern of the active array is shown in blue, and the centromere dip region (CDR) is indicated. Euchromatic (green) and heterochromatic (red) epigenetic marks present at the core centromere and pericentromere are depicted as circles located on top of the CENP-A (yellow) and H3 (gray) nucleosomes. (From Ruiz et al. 2024).

The highly repetitive DNA content of centromeres has posed a significant challenge for completing genomic maps. Indeed, mapping short reads in non-unique elements (Figure 10) gave rise to enormous ambiguity when assigning their positions along a chromosome. Therefore, centromeres have been referred to as the "dark matter" of the genome (Karpen and Allshire 1997). Recently, long-read sequencing and assembly methods enabled to produce the first complete assemblies of an entire human genome including the centromeres (Altemose 2022; Gershman et al. 2022; Hoyt et al. 2022; Logsdon et al. 2024; Nurk et al. 2022). In this context, recent analyses of human centromere sequences showed

evidence that they evolve through “layered expansions” involving repetitive variants that arise within each centromere and expand through mechanisms resembling successive tandem duplications. The most recently expanded repeats within each array are more likely to interact with CENP-A, whereas older flanking sequences shrink and diverge over time (Altemose 2022; Logsdon et al. 2023). CENP-A nucleosomes wrap discrete segments of centromeric DNA within a single HOR array and, while centromeres are hypermethylated, CENP-A enrichment corresponds to domains of reduced CpG methylation termed centromere dip regions (CDRs) (Logsdon et al. 2021; Miga et al. 2020).

b) Promoting CENP-A maintenance

In addition to centromere genetic features and structures, cenH3/CENP-A itself displays highly dynamic features including great diversity in length and sequence (J. L. Cooper and Henikoff 2004; Kursel et al. 2021; Malik and Henikoff 2001; Schueler et al. 2010) and tolerance to changes in position, as in the case of neocentromeres. However, its function is highly preserved across species. CenH3/CENP-A changes across evolution occur in parallel to its chaperone (HJURP in mammals), which is, thus, also highly divergent across species (Phansalkar, Lapierre, and Mellone 2012; Sanchez-Pulido et al. 2009). It is hypothesized that this rapid centromere evolution, both at the genetic and protein levels, represents an evolutionary “arms race” between selfish elements and mechanisms that suppress fitness costs (reviewed in (S. Henikoff, Ahmad, and Malik 2001; P. Talbert and Henikoff 2022)). In other words, according to the centromere drive model, centromere variants can compete in asymmetric female meiosis for inclusion in the egg rather than the polar body. If a satellite expansion results in the recruitment of more cenH3/CENP-A and other kinetochore proteins, that can preferentially orient towards the egg. This “stronger” centromere would then be favored for transmission to the next generation. Then, changes in cenH3/CENP-A can alter the binding to satellites in order to equalize centromere strength (and suppress the deleterious effects of centromere drive). This model has been reinforced by consistent studies in *Drosophila* (Dattoli et al. 2020; Ranjan, Snedeker, and Chen 2019) which highlight the importance of CENP-A for centromere function and strength. Thus, centromeric DNA co-evolve with cenH3/CENP-A and its chaperone.

α-Sat DNA contains a 17-bp sequence motif called CENP-B boxes. So far, the CENP-B protein is the only centromeric protein known with a sequence-specific DNA binding activity at centromeres, its N-terminal domain recognizing CENP-B boxes. CENP-B contributes to position and stabilize centromere nucleosomes, in particular CENP-A nucleosomes (reviewed in (Gamba and Fachinetti 2020)). They also regulate centromere topology, promoting the formation of DNA loops between repeats to favor centromere clustering in the nucleus and proper centromere positioning in mitosis (Chardon et al. 2022). CENP-B is considered as a kinetochore stabilizer through its interaction with CENP-A and CENP-C (Fachinetti et al. 2013, 2015; Fujita et al. 2007; Suzuki et al. 2004). Thus, CENP-B functions contribute

to ensure centromere fidelity, particularly upon CENP-A perturbation (Fachinetti et al. 2015; Hoffmann et al. 2020).

Furthermore, HOR arrays transcription by the RNA polymerase II produces low levels of non-coding RNAs (ncRNAs) (F. L. Chan et al. 2012) which promote CENP-A recruitment *in cis* (McNulty, Sullivan, and Sullivan 2017). Indeed, the specific depletion of ncRNAs transcribed from a CENP-A-bound HOR array, in turn, alters CENP-A localization at the centromere without affecting others. Because ncRNAs do not remain at centromere following transcription, it is likely that this *in cis* function relies on nascent RNA transcription (Bury et al. 2020). As a consequence, the centromere "epigenetic landscape" (epigenetic modifications) is essential to ensure proper transcription levels for proper CENP-A recruitment and maintenance (Bergmann et al. 2011; Bobkov, Gilbert, and Heun 2018; Molina et al. 2016; Nakano et al. 2008). On the one hand, H3K4me2 may promote centromere transcription and prevent the spread of H3K9me3 from PHC, which can block CENP-A assembly (Molina et al. 2016). On the other hand, high transcription levels displaces pre-established CENP-A and interferes with CENP-A loading by HJURP (Bergmann et al. 2011).

Despite the underlying DNA content is particularly variable among species and humans, owing to the action of unequal crossing over and amplification, a consensus for the centromere can be reached at two levels: the importance of CENP-A deposition and maintenance, which is maintained throughout evolution, and the conserved and essential function of centromeres, which are necessary for the correct inheritance of genetic material by enabling chromosome attachment to the spindle microtubules during each round of cell division (reviewed in (McKinley and Cheeseman 2016)).

1.2. Role and structure of CENP-A chromatin

1.2.1. CENP-A, the epigenetic mark of most centromeres

In contrast with centromeres that are genetically determined, such as point centromeres (Clarke and Carbon 1980, 1985), and potentially certain regional centromeres such as in the primitive red alga *C. merolae* (Maruyama et al. 2007) and in diatoms (Diner et al. 2017), for most centromeres (including humans), the underlying DNA sequence is neither sufficient nor necessary for centromere determination and function; this has long been indicating an epigenetic mechanism (reviewed in (Cleveland, Mao, and Sullivan 2003; Das et al. 2017)). However, in most eukaryotes studied to date, CENP-A and its orthologs are essential architectural components for chromosome segregation. CENP-A knockout is embryonic lethal (Howman et al. 2000) and depletion or conditional CENP-A knockout negatively impacts mitotic spindle pole integrity (Gemble et al. 2019), resulting in increased rates of chromosome segregation errors (Régnier et al. 2005). Thus, the presence of cenH3/CENP-A has been considered as the key epigenetic mark defining centromere sites (reviewed in (Balzano and Giunta 2020; Das et al. 2017)).

This idea has been reinforced by several observations. First, CENP-A binding is not-sequence-specific, CENP-A localization is not limited to a particular sequence motif (Aldrup-MacDonald et al. 2016; Hayden et al. 2013; Ross, Woodlief, and Sullivan 2016) and can even slide within an about 500 kb region in the same species, giving rise to "positional alleles" (Cappelletti et al. 2023). In human and *Drosophila* cells, targeting the chaperone of CENP-A/CID (HJURP/CAL1) to an ectopic location is sufficient for their stable assembly at the targeted locus in ~60 to 90% of the cases (Barnhart et al. 2011; Bassett et al. 2012a; Mendiburo et al. 2011). Robust CENP-A assembly and maintenance is further mediated by certain CCAN components, namely CENP-C and CENP-I (Shono et al. 2015). Second, neocentromeres – defined by the acquisition of a new centromere at a new location, and coupled with the inactivation of the original centromere in humans (reviewed in (O. J. Marshall et al. 2008)) – can support stable, fully functional centromeres in the presence of CENP-A, without requiring HOR arrays or pericentromeric repeats (reviewed in (Stimpson and Sullivan 2010)). Neocentromeres can be artificially generated in *Drosophila* by targeting CENP-A^{CAL1}in both actively transcribed chromatin and heterochromatin; this promotes the inactivation of the original centromere (Palladino et al. 2020). Generally, neocentromeres can arise naturally (Amor et al. 2004; Amor and Choo 2002; Tyler-Smith et al. 1999) or be artificially induced through the deletion of the endogenous centromere (Murillo-Pineda et al. 2021). Even in the absence of any detectable alpha satellite DNA, the establishment of stable human artificial chromosomes (HACs) with a functional centromere can be achieved, by targeting CENP-A or its chaperone HJURP, or even spontaneously (Logsdon et al. 2019). Thus, the centromere is a prime example of an epigenetically determined chromosomal domain.

The use of gene replacement in both human cells and fission yeast has enabled to confirm the mark to be CENP-A (Fachinetti et al. 2013), which maintains and propagates centromere function across cell divisions by recruiting CENP-C and other members of the constitutive centromere associated network (CCAN) (Foltz et al. 2006; Okada et al. 2006).

1.2.2. From the CENP-A nucleosome to the CCAN

Like other histones, CENP-A has a conserved HFD with three α-helices connected by two short loops. In normal conditions, CENP-A nucleosomes are octamers (Camahort et al. 2009; Hasson et al. 2013), most of them containing two molecules of CENP-A (homotypic nucleosomes) and less than 2% of them containing a CENP-A and a H3 histone (heterotypic nucleosomes) (Nechemia-Arbely et al. 2017; Padeganeh et al. 2013). Centromeric chromatin is comprised of both CENP-A- and H3-containing nucleosomes (Figure 12) (Blower, Sullivan, and Karpen 2002; B. A. Sullivan and Karpen 2004); CENP-A represents only ~0.1% of the total H3 variants in the human genome, with only 400 CENP-A nucleosomes per centromere on average by comparison with the ten thousands of α-Sat DNA copies (Bodor et al. 2014). In addition, following DNA replication, overall CENP-A amounts are reduced by half for each centromere, which means that human cells undergo mitosis with only half the maximal

CENP-A content at centromeres (reviewed in (Nechemia-Arbely, Fachinetti, and Cleveland 2012)). Furthermore, two CENP-A populations may co-exist in human cells, as two types of CENP-A nucleosomal complexes are detected by ChIP (J. G. Henikoff et al. 2015) and APEX-chromatin fibers mapping (Kyriacou and Heun 2018), one fraction being bound by CENP-C (and associated with other kinetochore proteins), the other being unbound. Whether these two CENP-A pools play a distinct role or not remains an open question. The proper balance between these populations might be important for centromere function, potentially enabling both centromeric transcription and new CENP-A deposition, and efficient/faithful chromosome segregation.

CENP-A stands out as the most divergent member of the histone H3 family (Figure 11) (Ali-Ahmad and Sekulić 2020; K. F. Sullivan, Hechenberger, and Masri 1994; Tachiwana, Kagawa, and Kurumizaka 2012). Thus, CENP-A and other H3 nucleosomes contain important differences.

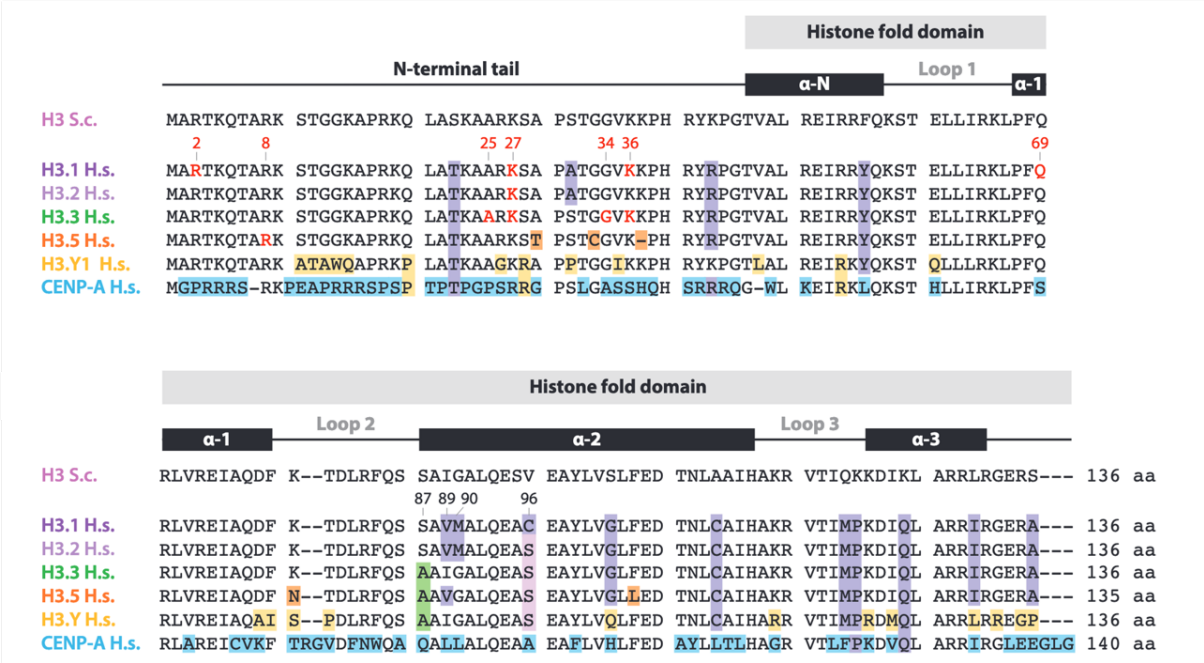


Figure 11. Multiple sequence alignment of H3 variants. Sequences of human H3 variants are compared to yeast H3 histones, showing a strong evolutionary conservation except for CENP-A. Differences are highlighted. (Adapted from (Simeonova & Almouzni 2024)).

In CENP-A nucleosomes, the L1 loop, positively charged, is more exposed, which facilitates interactions with other centromere factors (Ali-Ahmad and Sekulić 2020; Tachiwana et al. 2011). Furthermore, as a consequence of a sorter αN helix in CENP-A, which thus stabilizes less DNA at the entry/exit sites, CENP-A nucleosomes bind less DNA than H3 nucleosomes (Tachiwana et al. 2011), resulting in weaker binding by H1 and open and highly flexible DNA ends (Boopathi et al. 2020; Panchenko et al. 2011; Roulland et al. 2016; Sekulic et al. 2010; Zhou et al. 2019). This configuration leads to a less twisted conformation in tri-nucleosomes with two H3 nucleosomes bound to a central CENP-A nucleosome than in H3 tri-nucleosomes, promoting the exposition of the CENP-A

nucleosome, to be more accessible for kinetochore components (Y. Takizawa et al. 2020). This is consistent with studies showing transient DNA unwrapping at CENP-A chromatin (Conde e Silva et al. 2007; Hasson et al. 2013). In addition, CENP-B binding further opens the chromatin fiber structure and induces nucleosomal DNA unwrapping (Nagpal et al. 2023). How this local flexibility and CENP-A interactors together impact the higher-order structure of centromeric chromatin remains unclear. Overall, these specific features may lead to a dynamics structure, involving a global condensed chromatin state at centromeres with compact structures (Melters et al. 2019, 2023; Panchenko et al. 2011) while also loosening CENP-A nucleosomal DNA ends to increase the accessibility for CCAN binding. To date, the centromere community agrees with a model where the higher order structure of centromeres positions CENP-A towards the outer chromosome surface where they are maximally accessible for CCAN binding.

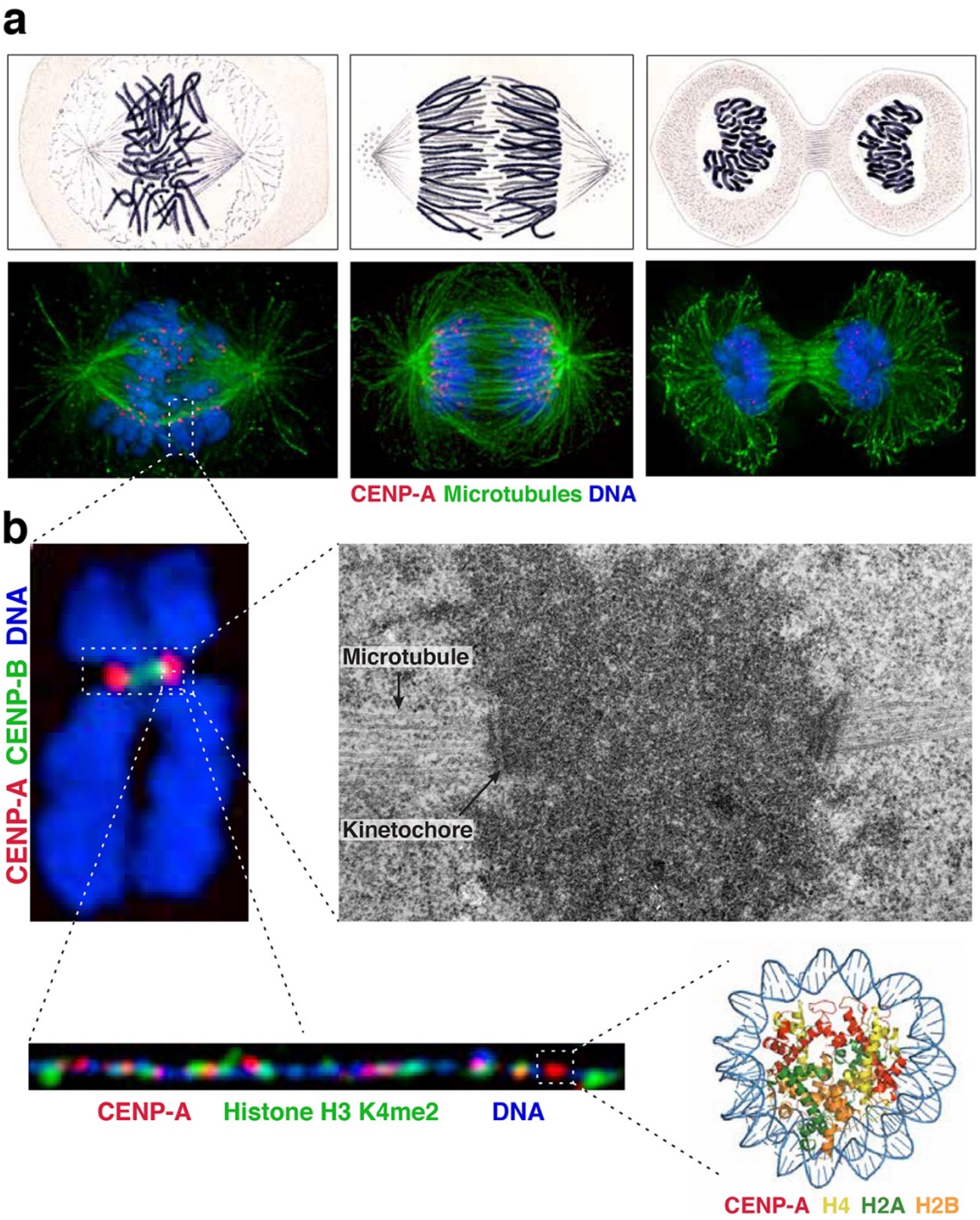


Figure 12. Visualization of the centromere. (A) Comparison of images of mitotic Salamander cells hand-drawn by Walther Flemming in 18822 (top) with immunofluorescence images of human cells (bottom) stained for microtubules (green), CENP-A (red) and DNA (blue). The images show cells at different phases of a mitotic cell cycle: late prometaphase-metaphase (left), anaphase (middle) and telophase (right). (B) Images of the centromere at increasing resolution. Top left: immunofluorescence image of a mitotic chromosome stained for DNA (blue), CENP-A (red) and CENP-B (a marker for the alpha-satellite DNA repeats present at most human centromeres, green). Top right: electron micrograph of centromeric region of a mitotic chromosome showing centromeric chromatin (dark cloud), kinetochore, and microtubules (indicated by arrows). Image courtesy of Conly Rieder. Bottom left: Immunofluorescence image of stretched centromeric chromatin fibers showing patches of CENP-A (red) interspersed with H3, in this case specifically H3 dimethylated on lysine 4 (H3K4me2, green). Image courtesy of Elaine Dunleavy. Bottom right: Crystal structure of the CENP-A nucleosome.
From (McKinley & Cheeseman 2015).

The CCAN consists of 16 proteins. Before mitotic entry, it links the centromere and spindle microtubules (Figure 12B) by nucleating kinetochore assembly (Figure 13). CCAN proteins can be grouped into five different sub-complexes: the CENP-H/I/K/M, the CENP-L/N, CENP-O/P/Q/U/R, CENP-T/W/S/X complexes, and CENP-C (reviewed in (Musacchio and Desai 2017)), which plays a central role since it can directly bind both CENP-A C-terminal tail and members of the outer kinetochore complex (Figure 13) (Ali-Ahmad et al. 2019; Falk et al. 2015, 2016; Guse et al. 2011; Kato et al. 2013; Klare et al. 2015; Milks, Moree, and Straight 2009; Screpanti, De Antoni, et al. 2011). CENP-C phosphorylation by Cyclin-dependent kinase 1 (CDK1) facilitates its interaction with CENP-A (R. Watanabe et al. 2019). Finally, CENP-C binding to CENP-A stabilizes centromeric chromatin, reshapes the octameric histone core of CENP-A nucleosomes, rigidifies both surface and internal nucleosome structure, and unwraps CENP-A DNA ends (Falk et al. 2015), thus facilitating interactions with the CCAN (Ali-Ahmad et al. 2019). CENP-C thus serves as an anchor that subsequently recruits other members of the CCAN at centromeres (Carroll, Milks, and Straight 2010; Klare et al. 2015; Tachiwana et al. 2015; Weir et al. 2016). Finally, during cell division, the recruitment of outer kinetochore proteins to the inner kinetochore CCAN complex ensures proper chromosome segregation (Q. Dong and Li 2022).

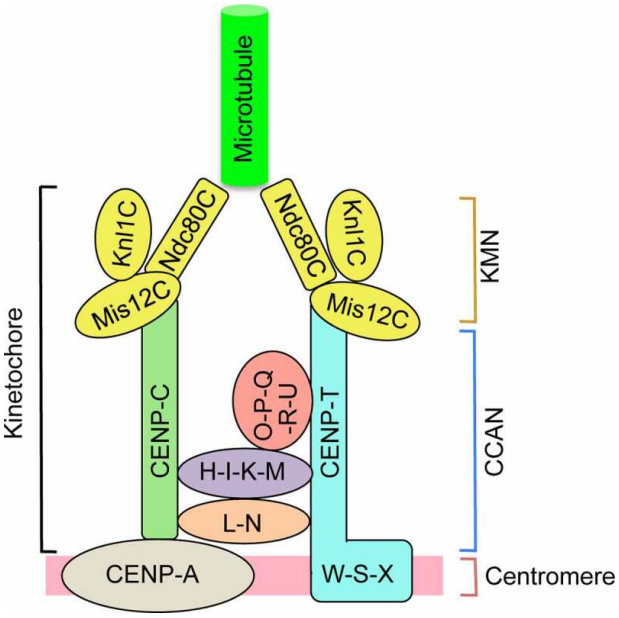


Figure 13. Schematic of a canonical kinetochore. The main structure of the kinetochore consists of constitutive centromere-associated network (CCAN), which includes five subgroups (CENP-L-N, CENP-H-I-K-M, CENP-O-P-Q-R-U, CENP-T-W-S-X and CENP-C), and the KMN (Knl1, Mis12, and Ndc80 complexes) network. Kinetochore position is specified by CENP-A-containing nucleosomes, upon which CCAN assembles. CCAN recruits KMN, which directly binds microtubules, during mitosis. Two independent pathways, CENP-C and CENP-T, link KMN to CCAN. (From Dong and Li 2022).

This is accompanied by chromosome condensation driven by condensing complexes (reviewed in (Antonin and Neumann 2016)), in particular at centromeres (Walther et al. 2018) to ensure centromere integrity. At this stage, the higher-level structure of the centromere comprises two main subdomains (bipartite centromere), each subdomain tightly associated with its neighboring pericentromeric region (Sacristan et al. 2024).

2. CENP-A REGULATION AND CANCER

Published in Front. Cell Dev. Biol. (2022)

Charlène Renaud-Pageot [1], Jean-Pierre Quivy [1], Marina Lochhead [1], and Geneviève Almouzni [1*]

[1]Institut Curie, PSL Research University, CNRS, Sorbonne Université, Nuclear Dynamics Unit, Équipe Labellisée Ligue contre le Cancer, 26 Rue d'Ulm, 75005 Paris, France

Keywords:

CENP-A histone variant, centromere, cancer, chromosome instability, chromatin organization

Abstract

In mammals, CENP-A, a histone H3 variant found in the centromeric chromatin, is critical for faithful chromosome segregation and genome integrity maintenance through cell divisions. Specifically, it has dual functions, enabling to define epigenetically the centromere position and providing the foundation for building up the kinetochore. Regulation of its dynamics of synthesis and deposition ensures to propagate proper centromeres on each chromosome across mitosis and meiosis. However, CENP-A overexpression is a feature identified in many cancers. Importantly, high levels of CENP-A lead to its mislocalization outside the centromere. Recent studies in mammals have begun to uncover how CENP-A overexpression can affect genome integrity, reprogram cell fate and impact 3D nuclear organization in cancer. Here, we summarize the mechanisms that orchestrate CENP-A regulation. Then we review how, beyond its centromeric function, CENP-A overexpression is linked to cancer state in mammalian cells, with a focus on the perturbations that ensue at the level of chromatin organization. Finally, we review the clinical interest for CENP-A in cancer treatment.

Main Text

2.1. Introduction

The first kinetochore proteins were described in 1985 using the sera of patients with an autoimmune disease called scleroderma (Moroi et al. 1980b). William Earnshaw and Naomi Rothfield purified the autoantibodies targeting the centromeres of the patients and identified three proteins, including the **Cen**tromere **P**rotein **A**: CENP-A (Earnshaw and Rothfield 1985). Since then, biochemical approaches demonstrated that CENP-A is a variant of histone H3 (Palmer et al. 1987, 1991; K. F. Sullivan, Hechenberger, and Masri 1994), which is one of the four major classes of histones (H2A, H2B, H3, H4) contributing to the basic unit of chromatin, the nucleosome. It is the only histone variant that is centromere-specific, its presence characterizing centromeric chromatin in most eukaryotes (Tromer et al. 2019). Within nucleosomes, CENP-A displays distinct features contributing to looser DNA binding and increased dynamics of the DNA ends in the nucleosome core particle (Ali-Ahmad et al. 2019; Arimura et al. 2019; Panchenko et al. 2011; Sekulic et al. 2010; Tachiwana et al. 2011). In addition, CENP-A-containing nucleosomes wrap only 121 bp of DNA, compared to the 147 bp in nucleosomes containing other H3 variants (Hasson et al. 2013; Lacoste et al. 2014; Tachiwana, Kagawa, and Kurumizaka 2012). These characteristics enable CENP-A to contribute to both the identity and function of centromeres. Centromeres are the loci where kinetochores assemble and dock to direct chromosome segregation during mitosis. Beyond this function during cell division, centromeres contribute to genome architecture as robust nuclear domains in interphase nuclei of mammalian cells (Dunleavy et al. 2009; Lacoste et al. 2014). Importantly, CENP-A has been involved as a key epigenetic determinant in defining the position of the centromere (Barnhart et al. 2011; Fachinetti et al. 2013). Furthermore, CENP-A is stably inherited across cell divisions, thereby helping to maintain centromere identity during cell proliferation (Jansen et al. 2007). Its inheritance through meiosis ensures a maintenance over organismal generations in mammals (Amor et al. 2004; Smoak et al. 2016; Tyler-Smith et al. 1999). CENP-A is also key for centromere function, establishing the interface necessary for the binding of components of the CCAN (constitutive centromere associated network) complex, such as CENP-C and CENP-N (Ali-Ahmad et al. 2019; Allu et al. 2019). At a chromatin level, CENP-A nucleosomes are interspersed with H3 nucleosomes along the arrays of repetitive DNA of the centromere (Dunleavy, Almouzni, and Karpen 2011). Additional kinetochore components, CENP-T and CENP-W, associate with H3 nucleosomes (Hori et al. 2008). Both CENP-C and CENP-T interact with Mis12 and the Ndc80 complex, which are components of the KMN network linking the kinetochore to microtubules (Malvezzi et al. 2013; Przewloka et al. 2011; Screpanti, Antoni, et al. 2011). The level of CENP-A is thus key to maintain genome integrity, as shown by experimental alterations in CENP-A levels where both depletion (K. Maehara, Takahashi, and Saitoh 2010) and overexpression (Shrestha et al. 2017) promote mitotic defects and chromosomal instability (CIN) in

human cells. Since alteration in CENP-A availability can alter both the formation of CENP-A-containing nucleosomes and centromere function, a link with cancer states is expected. Therefore, the control of CENP-A transcription, its turn-over/stability and its deposition into chromatin is central to ensure genome stability.

2.2. Regulation of CENP-A

Histone chaperones escort non-nucleosomal (free) histones and ensure their deposition into chromatin (reviewed in (Ray-Gallet and Almouzni 2021)). The timing of CENP-A deposition varies in different species. In mammals, the Holliday Junction Recognition Protein (HJURP) has been identified as the dedicated histone chaperone promoting CENP-A specific incorporation into centromeric chromatin, which in human occurs in late mitosis (outside S phase), to compensate for the replication-coupled dilution of CENP-A (Dunleavy et al. 2009; Foltz et al. 2009). Interestingly, in human cells, replication has been proposed as an error correction mechanism ensuring that CENP-A nucleosomes are retained at the centromere (Nechemia-Arbely et al. 2019). In addition, HJURP is involved in dealing with parental CENP-A displaced by the replication fork to ensure its recycling (Zasadzińska et al. 2018). This exclusive partnership is driven by the CENP-A targeting domain (CATD) in HJURP (Bassett et al. 2012; Shuaib et al. 2010). Furthermore, the presence of two C-terminal domains (HCTD1 and HCTD2) in HJURP is required for CENP-A deposition (D. Pan et al. 2019; Zasadzińska et al. 2013; H. Zhao et al. 2016).

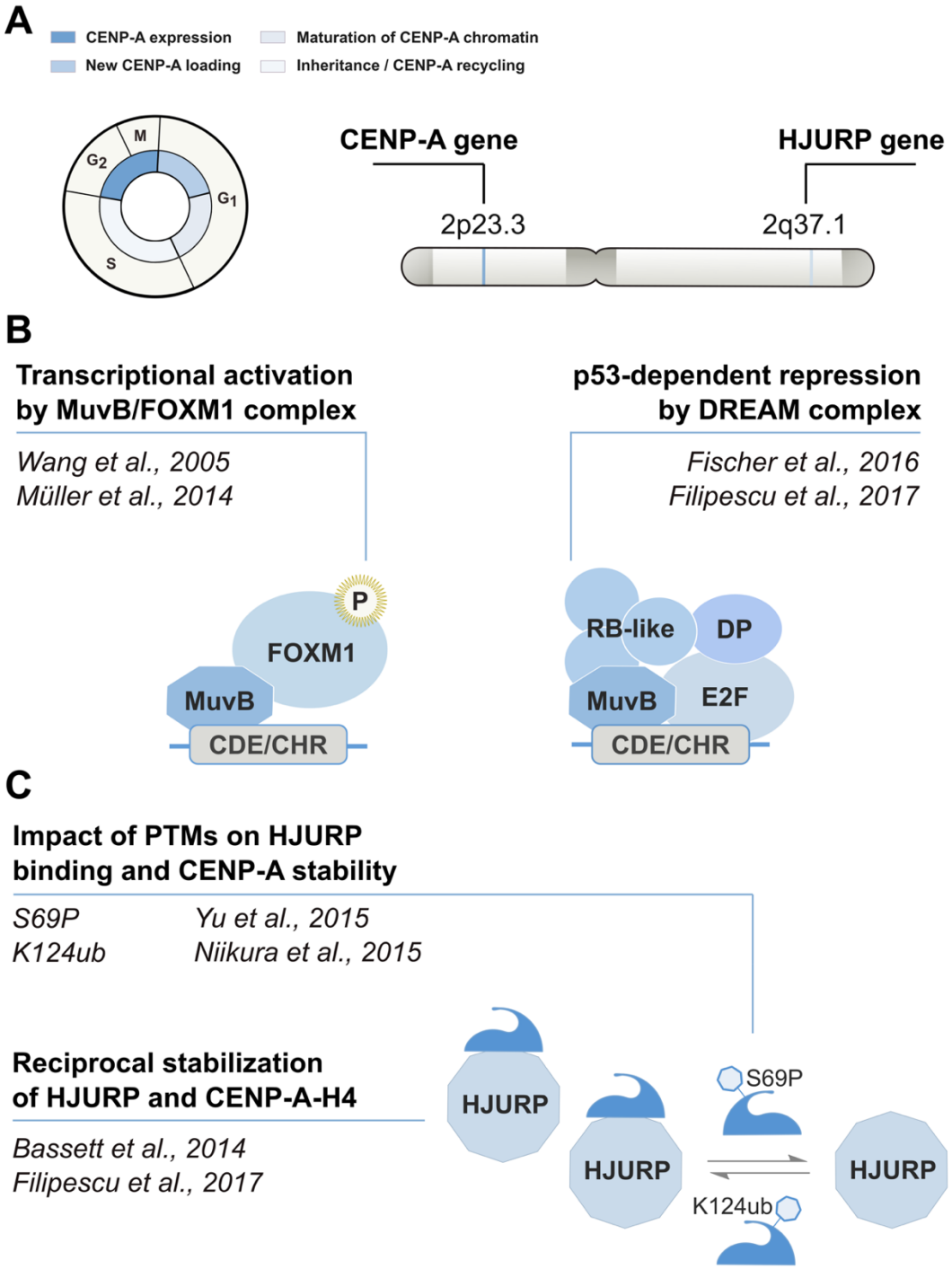


Figure 14. Cell cycle timing and regulation of CENP-A.
(A) CENP-A and its chaperone HJURP are regulated in a cell cycle–dependent manner. (B) Transcription is regulated in cis by the CHR/CDE motif in their promoter region. The recruitment of the DREAM complex at the CHR is thought to promote transcriptional repression during G1. At the beginning of S phase, the MuvB core of the DREAM complex remains bound to the CHR/CDE while other components dissociate and are replaced by B-MYB. The B-MYB-MuvB (MMB) complex recruits FOXM1 in late S phase. B-MYB is degraded upon phosphorylation, whereas the progressive phosphorylation of FOXM1 leads to its activation in G2/M. (C) CENP-A and HJURP mutually stabilize each other at the protein level. The reciprocal stabilization is affected by posttranslational modifications of CENP-A.

CENP-A is encoded by a single multi-exon gene located outside of the histone gene clusters (Figure 14). The CENP-A gene (*CENPA*) undergoes conventional pre-mRNA processing via splicing and polyadenylation. Expression levels of CENP-A and its chaperone HJURP are cell cycle regulated, with a peak of expression in G2/M (Richard D. Shelby, Vafa, and Sullivan 1997) (Figure 14A). *CENPA* and *HJURP* transcription involves a CDE/CHR motif in their promoters recognized by the transcriptional regulator FOXM1 (X. Chen et al. 2013; I.-C. Wang et al. 2005) and by the DREAM complex (M. Fischer et al. 2016). The DREAM complex is a transcriptional regulator binding to CDE/CHR sites to mediate indirect p53-p21-dependent repression, which can switch to an activator notably by recruitment of FOXM1 (reviewed in (Engeland 2018)). These regulatory mechanisms provide means to keep these genes under a p53-dependent transcriptional repression (Filipescu et al. 2017) (Figure 14B). CENP-A expression levels vary depending on the tissue, in a range up to 50-fold changes, with the highest CENP-A expression scores found in lymphoid, skin and gastrointestinal tissues according to the Human Protein Atlas (Uhlén et al. 2015). In addition to transcriptional regulation, CENP-A amounts are also controlled at the protein level and CENP-A and its chaperone HJURP mutually stabilize each other (Bassett et al. 2012; Filipescu et al. 2017). Their reciprocal stabilization is affected by posttranslational modifications on the N-terminal tail of CENP-A, which can further regulate the timing of deposition. CENP-A S69 phosphorylation prevents interaction with HJURP and premature loading, while K124 ubiquitylation favors HJURP binding and contributes to their stabilization (Figure 14C). Thus, the overexpression of either CENP-A or HJURP leads to an increase in the levels of their binding partner (Filipescu et al. 2017). Conversely, HJURP loss results in CENP-A depletion, and CENP-A knockdown leads to the proteasome-mediated degradation of HJURP. Specific enrichment of CENP-A at the centromere is achieved in telophase/early G1 by HJURP (Dunleavy et al. 2009; Foltz et al. 2009), which is recruited at the centromere during this critical time window by the Mis18 complex (composed of two subunits, Mis18α and Mis18β, and the Mis18-binding protein 1 (Mis18BP1)) (Dunleavy et al. 2009; Foltz et al. 2009; Jansen et al. 2007; Nardi et al. 2016; Zasadzińska et al. 2013). Specifically, during M phase, CDK1 phosphorylates CENP-C, which stabilizes its interaction with CENP-A nucleosomes (Ariyoshi et al. 2021; Watanabe et al. 2019). CENP-A-bound CENP-C can recruit Mis18 to centromeres (Dambacher et al. 2012; McKinley and Cheeseman 2014; Moree et al. 2011). Following this step, during anaphase, reduced CDK1/2 activity results in the dephosphorylation of HJURP, which in turn promotes its binding to Mis18 (Stankovic et al. 2017; Jianyu Wang et al. 2014). Finally, in the second part of the G1 phase, the RSF (remodeling and spacing factor) complex (Perpelescu et al. 2009) and MgcRacGap (a Rho family GTPase activating protein) (Lagana et al. 2010) interact transiently with centromeres via HsKNL2, a G1-specific CENP-A licensing factor, to stabilize newly deposited CENP-A nucleosomes and generate mature centromeric chromatin. When the cell transitions to S-phase, CDK1/2 activity levels increase, Mis18BP1 is phosphorylated, released from centromeric chromatin, and CENP-A deposition is inhibited (McKinley and Cheeseman 2014; D. Pan et al. 2017; Silva et al. 2012; Spiller et

al. 2017). Thus, under normal conditions, a combination of mechanisms, some of which exploit the partnership between CENP-A and its dedicated chaperone HJURP, ensure that CENP-A levels and deposition are restricted to the centromere to promote faithful chromosome segregation.

2.3. CENP-A levels increase in cancer

Interestingly, by comparison with healthy tissues, elevated CENP-A expression levels are documented in many cancer types in humans, including breast (X.-J. Ma et al. 2003; McGovern et al. 2012), colon (Tomonaga et al. 2003), liver (Y. Li et al. 2011), lung (Q. Wu et al. 2012), ovarian (Qiu et al. 2013), bone (X.-M. Gu et al. 2014), gastric (Yuan Xu et al. 2020), and prostate (Saha et al. 2020). Indeed, the analysis of matched normal-tumor transcriptomes from 101 datasets demonstrated that the overexpression of CENP-A is a common feature of more than 44% of human cancers (Lacoste et al. 2014). Additionally, Oncomine analysis of 51 studies showed that CENP-A expression is significantly upregulated in 20 types of solid tumors compared with healthy tissues (X. Sun et al. 2016). Among these studies, the most common cancer types showing CENP-A overexpression were breast, central nervous system, ovary, and lung cancers. By contrast, down-regulation of CENP-A expression has never been observed in cancer tissues. More recently, analysis using TCGA PanCancer Atlas confirmed the global increase in CENP-A levels in patient tumors relative to healthy tissues, which reaches over 1000-fold in the case of cholangiocarcinoma (Jeffery et al. 2021) (Figure 15). In line with their co-regulation (see above), the unusual level of CENP-A often occurs in parallel with upregulation of its chaperone HJURP (Dunleavy et al., 2009; Jeffery et al., 2021). Thus, on average CENP-A mRNA levels are significantly and positively correlated with those of HJURP in several cancer types as assessed based on gene expression profiling interactive analysis (W. Zhang et al. 2016). The negative regulation of *CENPA* and *HJURP* transcription under a p53 control (M. Fischer et al. 2016) is aligned with observations in mouse tumor cell line models where *TP53* loss-of-function mutations lead to high CENP-A and HJURP levels (Filipescu et al. 2017). However, according to TCGA PanCancer Atlas studies visualized on CBioPortal, CENP-A overexpression can be observed in many tumors displaying *TP53* loss of function mutation or wild-type (WT) *TP53* (Cerami et al., 2012). Notably, early studies did not consider the p53 status of the tumors when assessing CENP-A levels. As a result, two distinct situations (p53-WT or p53-defective) were combined in the data concerning CENP-A levels and its link with cancer, thereby masking potentially important distinctions. Thus, beside the direct loss of p53 function, other mechanisms underly aberrant expression levels of CENP-A in cancer. Genetic analysis indicated that the elevated CENP-A expression was not due to alterations in the sequence or an increased copy number of the *CENPA* gene (X. Sun et al. 2016) and other factors, apart from a direct impairment in p53, deserve to be explored to explain CENP-A overexpression in human cancers. Several hypotheses can be considered. First, the tumor suppressor protein pRb (retinoblastoma protein), whose inactivation leads to CENP-A upregulation (Amato et al. 2009), is frequently mutated or disabled

in cancer (reviewed in (Hickman, Moroni, and Helin 2002). Secondly, CENP-A and HJURP overexpression could be the result of a deregulation of FOXM1, a known oncogenic transcription factor and activator of *CENPA* and *HJURP* transcription (Thiru et al. 2014; Wang et al., 2005). Indeed, the upregulation of CENP-A strongly correlates with the expression of FOXM1 across many cancers and FoxM1 displays at least 100-fold relative enrichment at the *CENPA* promoter in cancer tissues compared with normal tissues (Thiru et al. 2014). Finally, *E2F8* and *E2F2* are also potential transcriptional regulators of *CENPA* with critical roles in tumorigenesis (X. Sun et al. 2016). Importantly, whichever underlying mechanism leads to CENP-A upregulation, an excess of this particular histone H3 variant leads to an unbalanced situation in histones with effects onto chromatin organization as we will now discuss.

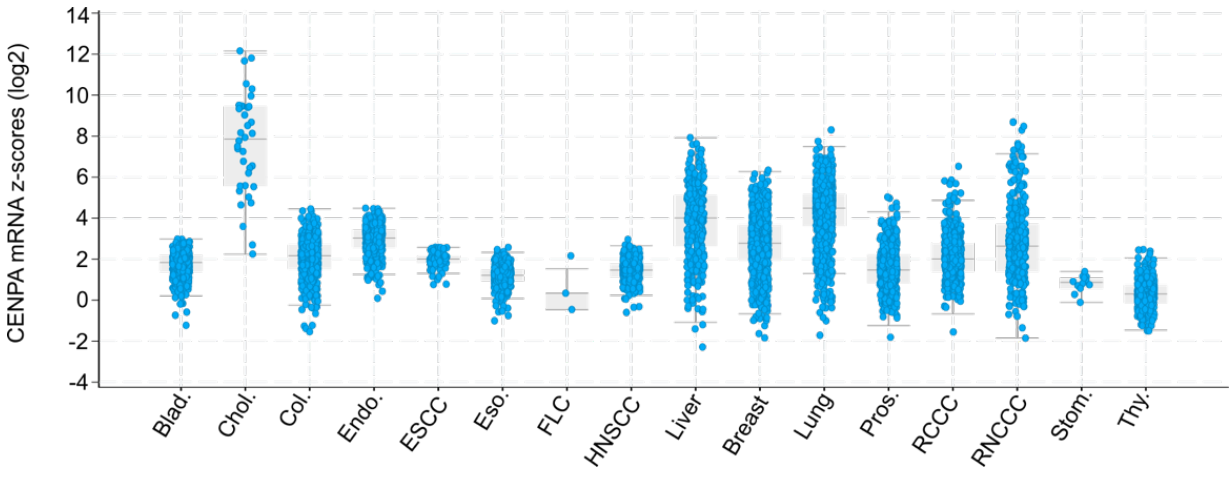


Figure 15. Box and dot plots indicating *CENPA* expression in patient tumors relative to normal samples (z-score, log2 RNA SeqV2 RSEM). (Modified from Jeffery et al., 2021).
Box and dot plots indicating CENPA mRNA expression levels in patient tumors relative to normal samples (z-score, log2 RNA SeqV2 RSEM) from cBioPortal (TCGA PanCancer Atlas studies) (Cerami et al., 2012; Gao et al., 2013). The plot was generated using the cBioPortal web interface. X-axis indicates Cancer Type: Bladder Urothelial Carcinoma (Blad.), Cholangiocarcinoma (Chol.), Colorectal Adenocarcinoma (Col.), Endometrial Carcinoma (Endo.), Esophageal Squamous Cell Carcinoma (ESCC), Esophagogastric Adenocarcinoma (Eso.), Fibrolamellar Carcinoma (FLC), Head and Neck Squamous Cell Carcinoma (HNSCC), Hepatocellular Carcinoma (Liver), Invasive Breast Carcinoma (Breast), Non-Small Cell Lung Cancer (Lung), Prostate Adenocarcinoma (Pros.), Renal Clear Cell Carcinoma (RCCC), Renal Non-Clear Cell Carcinoma (RNCCC), Undifferentiated Stomach Adenocarcinoma (Stom.), Well-Differentiated Thyroid Carcinoma (Thy.). TCGA: The Cancer Genome Atlas.

2.4. CENP-A overexpression leads to mislocalization and heterotypic nucleosomes

The localization of CENP-A at the centromere is normally controlled by HJURP. Thus, consistently, when HJURP is overexpressed, the increased levels of CENP-A that ensue result in an exclusive accumulation at the centromere, without ectopic localization (Filipescu et al. 2017). Strikingly though, exogenous overexpression or abnormal upregulation of endogenous CENP-A leads to its

mislocalization at non-centromeric regions (Athwal et al. 2015; Gascoigne et al. 2011; Lacoste et al. 2014; Van Hooser et al. 2001) (Figure 16). This is observed for overexpression of CENP-A either constitutive (Athwal et al. 2015; Lacoste et al. 2014; Shrestha et al. 2017, 2021) or inducible (Van Hooser et al., 2001; Gascoigne et al., 2011; Shrestha et al., 2017, 2021; Jeffery et al., 2021). Interestingly, the ectopic incorporation of CENP-A is abrogated when both CENP-A and HJURP are overexpressed in a coordinated fashion, as found following p53 inactivation by the oncogene E1A (adenovirus oncoprotein) and/or HRas-V12 (Ras oncogenic mutant). In this case, while CENP-A levels increase, its localization remains exclusive to the centromere (Filipescu et al. 2017).

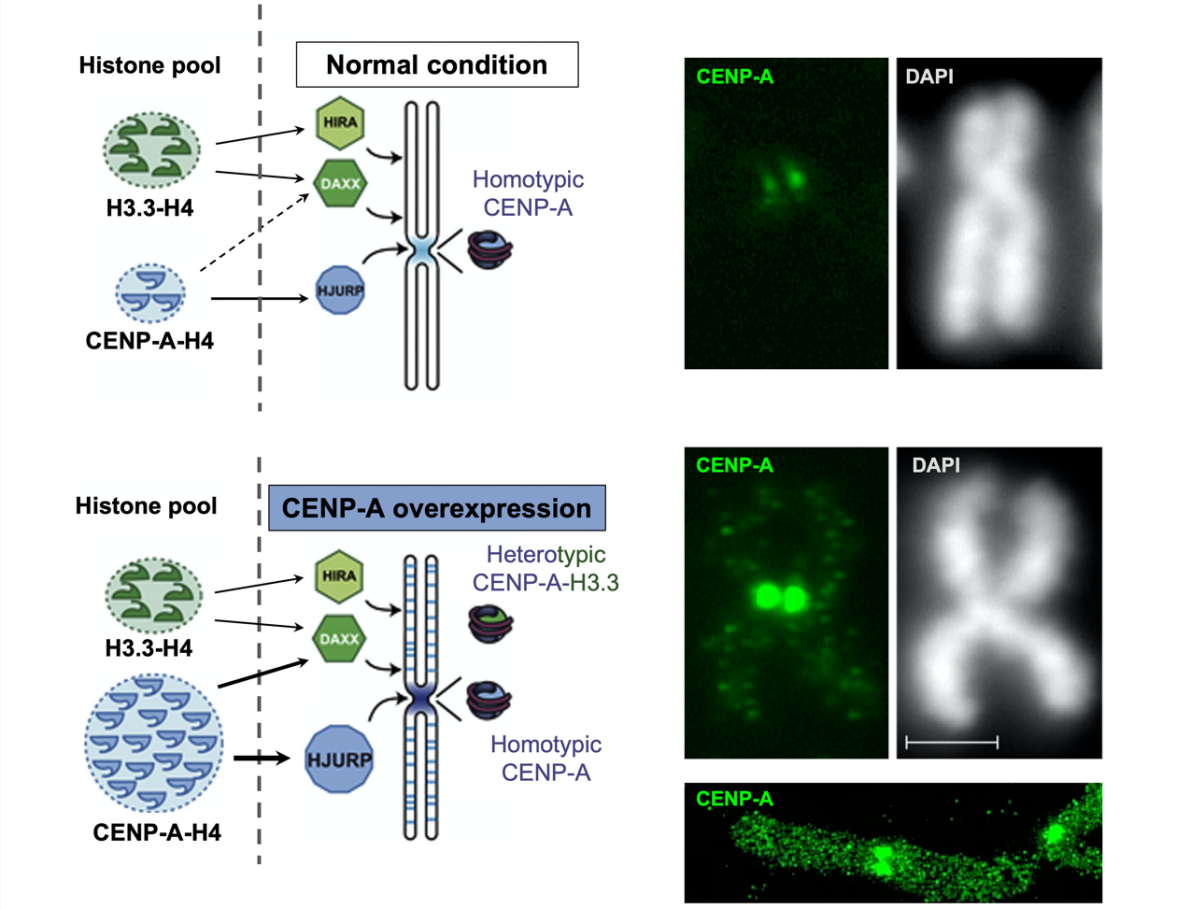


Figure 16. CENP-A overexpression leads to a mislocalization to chromosome arms with formation of heterotypic nucleosomes. (Modified from Lacoste et al., 2014).
Left, scheme: in the normal situation (top), CENP-A is deposited specifically at the centromere by its dedicated chaperone HJURP and forms homotypic particles. Upon overexpression (bottom), CENP-A get mislocalized in the chromosome arms in a manner that depends on a H3.3 chaperone, DAXX. In these loci, the CENP-A particle is heterotypic. Right, immunofluorescence images for CENP-A detection on a mitotic chromosome compare normal (top) and CENP-A overexpressing (bottom) HeLa cells along with a DAPI staining. Scale bar = 2 µm. Below, a super-resolution image (courtesy of Tristan Piolot and Nicolas Lacoste) further illustrates the mislocalized CENP-A in chromosome arms.

It is tempting, based on these findings, to propose that it could be when CENP-A overexpression exceeds the one of HJURP, that its mislocalization occurs (Athwal et al. 2015; Jeffery et al. 2021; Lacoste et al. 2014). This interdependence thus illustrates the functional importance of CENP-A and

HJURP partnership to restrict CENP-A localization at the centromere. In CENP-A overexpressing cells, when HJURP capacity to chaperone CENP-A gets saturated, the excess of CENP-A tends to associate with other histone H3 chaperones. Under these conditions, while HJURP still ensures a deposition of CENP-A at the centromere, the excess pool of CENP-A gets ectopically deposited within chromosome arms through a DAXX-dependent histone deposition pathway (Lacoste et al. 2014). Thus, in this case the DAXX-ATRX complex, normally responsible for depositing H3.3 at other chromatin sites (reviewed in (Ray-Gallet and Almouzni 2021)), is diverted to compensate for a saturation of HJURP. Other H3 chaperones like the HIRA complex have also been proposed to act as a means to compensate for CENP-A overexpression (Nye et al. 2018). The strict selectivity of histone-chaperone partners is thus weakened with unbalanced levels of CENP-A. Thus, reestablishing a correct balance between levels of HJURP and CENP-A can preclude ectopic assembly of CENP-A by H3.3 chaperones (Nye et al. 2018).

In addition to mislocalization, the excess of CENP-A which is ectopically incorporated show distinct properties in the corresponding nucleosomal core particles. Whereas at centromeric loci, homotypic particles with two CENP-A-H4 dimers form as $(CENP\text{-}A\text{-}H4)_2$ tetramers, at ectopic loci, heterotypic nucleosomes combining both CENP-A and H3 variant are observed (CENP-A-H4,H3.3-H4) (Lacoste et al. 2014). Accumulation of ectopic CENP-A particles is mainly observed at sites of high histone turnover (Lacoste et al. 2014; Mahlke and Nechemia-Arbely 2020) such as active promoters and enhancers (Lacoste et al. 2014), as well as subtelomeric and pericentromeric regions (Athwal et al. 2015; Nye et al. 2018). Moreover, ectopic CENP-A has also be found over CTCF binding sites, precluding proper CTCF localization at these sites (Lacoste et al. 2014). Given the importance of CTCF in 3D genome organization, how these CTCF displacements may impact chromatin architecture in the nucleus should be explored.

2.5. Impact of CENP-A overexpression on kinetochore and chromosome segregation

Assembling all components of the kinetochore is an important property of CENP-A to ensure a proper centromere function (Fachinetti et al. 2013; Liu et al. 2006). A major issue is thus to determine what happens at sites where CENP-A is mislocalized when overexpressed, since, in theory, this could potentially lead to the formation of neocentromeres competing with the original centromere. In fact, in human cells, ectopic CENP-A recruits only a subset of kinetochore proteins, namely CENP-C, CENP-N and the Mis18 complex (Gascoigne et al. 2011; Lacoste et al. 2014; Van Hooser et al. 2001), whereas the NDC80 complex has not been found. Therefore, overexpressing CENP-A is not sufficient to form stable neocentromeres in human cells. Since active neocentromere formation only occurs following inactivation of an endogenous centromere (O. J. Marshall et al. 2008), as long as the endogenous centromere is functional it may prevent the possibility for neocentromere to form. Indeed, following inactivation of endogenous centromere, ectopic CENP-A is capable of seeding stable neocentromere

formation (Shang et al. 2013). Recently, Murillo-Pineda et al., using a CRISPR-Cas9 approach to remove the initial centromeric region from a copy of chromosome 4 in human retinal pigment epithelium cells, observed the spontaneous formation of a neocentromere correlating with CENP-A seeding and eviction of H3K9me3 (Carty and Dunleavy 2021; Murillo-Pineda et al. 2021). These data support an important role of non-centromeric CENP-A deposition in neocentromere formation. However, conversely, the ectopic CENP-A traps a series of kinetochore components such as CENP-C, CENP-T and Nuf2 (a member of the Ndc80 complex) away from native centromeres, resulting in their weakening (Shrestha et al. 2017, 2021). Thus, these human cells exhibit mitotic defects such as lagging chromosomes, micronuclei formation, abnormal mitotic exit, and overall aneuploidy with karyotypic heterogeneity (Amato et al. 2009; Athwal et al. 2015; Shrestha et al. 2017, 2021). Of note, many of these chromosome segregation defects are suppressed when DAXX is depleted from CENP-A overexpressing cells (Shrestha et al. 2017, 2021). Altogether, these data indicate that ectopic incorporation of CENP-A into chromosome arms due to CENP-A overexpression represents a major source of mitotic stress that results in chromosomal instability (CIN) and aneuploidy. This in turn can lead to a large heterogeneity in the derived cell populations.

2.6. CENP-A overexpression and cell fate reprogramming

Since chromatin states have been associated with transcription regulation and cell fate, it is important to understand how CENP-A overexpression and its impact on chromatin could impact transcription and cell fate. Cancer cells generally activate transcriptional programs that ensure an upregulation of both core kinetochore components and genes required for cell cycle progression and DNA replication (Thiru et al. 2014). Analysis of gene expression dynamics associated with CENP-A overexpression showed major changes in most genes involved in cell-cycle progression, apoptosis, DNA repair and RNA metabolism (Jeffery et al. 2021; Y. Li et al. 2011; X. Sun et al. 2016). Interestingly, hotspots of ectopic CENP-A genomic localization had documented transcriptional start sites of genes, like *CDC25C* (Saha et al. 2020) and the oncogene *MYC* (Athwal et al. 2015). Furthermore, CENP-A mislocalization to the *MYCN* locus showed strong correlation with the amplification and overexpression of *MYC* (Nye et al. 2018). In addition, as mentioned above, aberrant CENP-A nucleosomes can occlude CTCF binding sites (Lacoste et al. 2014). This is particularly relevant when considering that the binding of CTCF is frequently altered in cancer and associated with tumorigenicity (Aitken et al. 2018; Katainen et al. 2015; Kemp et al. 2014; A. D. Marshall et al. 2017). However, while CENP-A overexpression could push/ facilitate a transition for cells to progress towards cancer, alone, its overexpression does not affect proliferation rate and is not sufficient for tumorigenic transformation, even with a loss of p53 function (Filipescu et al. 2017). Thus, the impact of CENP-A overexpression is likely to operate in combination with other events occurring during oncogenesis and be dependent on the cellular context. A first context to consider is the difference in p53 status, and recent work examining various cellular contexts

underlined the importance of the p53 status in the transcriptional reprogramming induced by CENP-A. This was achieved by comparing side by side, p53-WT cells and a counterpart where p53 status is altered with a dominant negative p53 (p53-DN). In the p53-WT cells, CENP-A upregulation could promote cell cycle exit and senescence whereas, in p53-defective cells, the shift from cycling to non-cycling cells was reduced and CENP-A overexpression lead to the emergence of a subpopulation of cells with downregulated epithelial genes but upregulated mesenchymal genes (Jeffery et al. 2021) (Figure 17). Thus, CENP-A, in a p53 dependent manner, can impact cell fate in two major ways: first with respect to cell cycle by evading from a senescence program, and second by promoting a cellular reprogramming favoring a change of cell identity, namely the epithelial-mesenchymal transition (EMT). EMT is an essential process during mammalian embryonic development and in wound healing (reviewed in (J. Yang, Antin, Berx, Blanpain, Brabletz, Bronner, Campbell, Cano, Casanova, Christofori, Dedhar, Derynck, Ford, Fuxe, García de Herreros, et al. 2020)). However, tumor cells hijack this process to migrate more efficiently and invade the underlying mesenchyme (J. Yang, Antin, Berx, Blanpain, Brabletz, Bronner, Campbell, Cano, Casanova, Christofori, Dedhar, Derynck, Ford, Fuxe, García de Herreros, et al. 2020; Xin Ye et al. 2017). Thus, in cancer, EMT has been associated with invasion, metastasis, and resistance to therapy (reviewed in (J. Yang, Antin, Berx, Blanpain, Brabletz, Bronner, Campbell, Cano, Casanova, Christofori, Dedhar, Derynck, Ford, Fuxe, García de Herreros, et al. 2020)). Similarly, high CENP-A levels correlate strongly with tumor aggressiveness, increased invasiveness and metastasis in cancer patient data (X.-M. Gu et al. 2014; X.-J. Ma et al. 2003; McGovern et al. 2012; Saha et al. 2020; X. Sun et al. 2016; W. Zhang et al. 2016). Of note, a recent study also linked CENP-A overexpression to invasion and metastasis via activation of the β-catenin pathway in clear cell renal cell carcinoma (Q. Wang et al. 2021). In cell culture, CENP-A overexpression has been associated with reduced expression of cell adhesion genes and higher cell invasion (Shrestha et al. 2021). Thus, the induction of EMT could explain the invasiveness and metastasis capacity of particular tumors overexpressing CENP-A. It will be important in the future to elucidate the exact mechanisms and pathways underlying EMT activation promoted by CENP-A. Indeed, CENP-A overexpression alone is not sufficient to induce EMT in any p53-defective cell line (Jeffery et al. 2021), only certain cells can undergo these transitions. Whether the effect on gene expression requires a certain threshold of CENP-A overexpression or is cell-type specific remains to be established. An attractive hypothesis to test is that CENP-A overexpression would function in the context of cells already in transition (e.g., cells in tumorigenic progression). Indeed, its targeting in active regions could particularly alter gene expression where both CTCF and the presence or absence of specific histone variants play a critical role (Goldberg et al. 2010; Szenker, Lacoste, and Almouzni 2012). The current emerging view is that CENP-A would help to maintain/stabilize the population of cells transitioning. How this is actually operating mechanistically remains to be determined. It is tempting to consider as well how CENP-A changes could impact the organization of the genome within

the nucleus to possibly contribute to changes in gene expression and function, thus affecting cell fate (Bonev and Cavalli 2016; Fritz et al. 2019; Krijger and de Laat 2013). However, this latter aspect has not yet been examined.

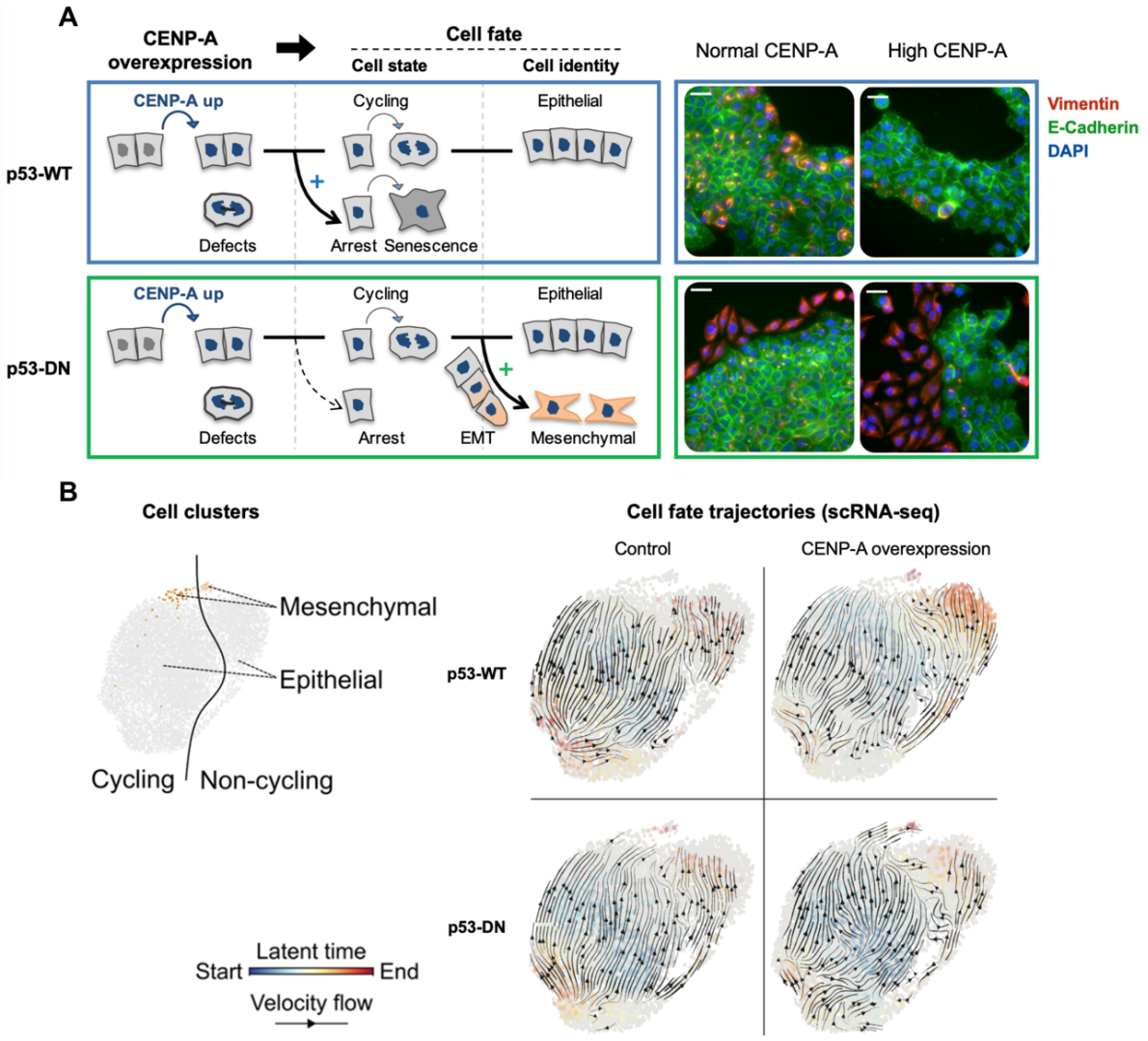


Figure 17. CENP-A overexpression promotes distinct cell fates depending on p53 status. Modified from (Jeffery et al., 2021).
(A) Scheme summarizing the consequences of CENP-A overexpression (in blue) on cell state and identity, in wild-type p53 (p53-WT, top panel blue) and p53-defective cells (p53-DN, dominant negative, bottom panel green). IF images show representative max intensity projections after 34 days with or without continuous CENP-A overexpression. DAPI (blue), E-cadherin (green, epithelial marker), and vimentin (red, mesenchymal marker). Scale bars = 40 µm. (B) Cell fate trajectories inferred by RNA velocity analysis of scRNA-seq samples. RNA velocities (black arrows) were calculated for each condition by stochastic modeling in individual samples. Each cell is colored by the estimated latent time from initial (blue, start) to terminal states (red, end).

2.7. CENP-A nuclear distribution in health and cancer

In the interphase nucleus, chromosomes are non-randomly arranged within the nuclear space. They are structurally and functionally organized into territories, and this nuclear organization is generally altered in cancer (Lever and Sheer 2010; Mai 2019; Zaidi et al. 2018). Notably, centromeres occupy particular subnuclear domains in interphase nuclei (review in (Muller, Gil, and Drinnenberg 2019)). Within this organization, the DNA-binding protein CENP-B favors loops between DNA repeats (Chardon et al. 2022). These subnuclear localization of centromeres provide information that can be followed according to the cell fate and differentiation (Feodorova et al. 2020; Jansz and Torres-Padilla 2019; Schlesinger and Meshorer 2019). To date, however, much of our knowledge comes from data collected in mammalian cultured cells. In these proliferating cells, CENP-A marks the centromere of the mitotic chromosomes and, during interphase, these marks are detected as numerous foci dispersed throughout the nucleus (Dunleavy et al. 2009; Lacoste et al. 2014; Verrelle et al. 2021). Importantly, these cultured cells derived from tumors provide a CENP-A localization in interphase that cannot necessarily reflect the situation in normal cells. Indeed, in normal human primary lymphocytes, the visualization of centromeres both by FISH (Skalníková et al. 2000; Weierich et al. 2003) and CENP-A staining (I. Alcobia, Dilão, and Parreira 2000; Weimer et al. 1992) provided very defined nuclear patterns quite distinct from the tumoral cells. Furthermore, in the cell nuclei of human normal solid tissues, CENP-A is detected in 9 to 18 foci corresponding to the clustering of the centromeres from 2 to 5 distinct chromosomes. These foci, homogenous in size and shape, localize equidistantly at the nuclear periphery and, in fewer cases, at the periphery of the nucleolus (Figure 18) (Verrelle et al. 2021). This very distinct organization represents a general feature shared by distinct cell types originating from various progenitors and along various different differentiation pathways irrespective of the fact that cells could be circulating or in tissues. Thus, in line with the hypothesis that centromeric regions are robust and stable chromosomal loci (Krijger and de Laat 2013), CENP-A labelling as foci at the nuclear periphery reflects a fundamental feature of centromeres organization and distribution in healthy cells. By contrast, in human tumor tissues, this discrete CENP-A subnuclear localization is drastically altered and, for invasive neoplastic lesions, similar to that detected in the cultured cell lines of tumoral origin (Verrelle et al. 2021). Interestingly, CENP-A subnuclear localization in breast lesions reveals distinct information. In healthy tissues, the normal reference pattern compares to benign lesions (Verrelle et al. 2021). By contrast, in neoplastic lesions, CENP-A foci localization in a regular distribution at the nuclear periphery is disrupted and clustering is altered or lost (smaller and many more foci) (Figure 18). Furthermore, the loss of CENP-A foci localization at the nuclear periphery with a high heterogeneity in terms of number, size, and shape within the nuclear volume can readily discriminate invasive from non-invasive neoplastic lesions. These major global change of centromere and nuclear organization in cancer reported recently (Verrelle et al. 2021) have not yet been related to ectopic localization of CENP-A in cancer (Lacoste et al. 2014). How these changes during oncogenic transformation and progression could

possibly relate thus remains to be assessed. Notably, tumor grade is reported to combine major perturbations that can lead to genome chaos (G. Liu et al. 2014). This destabilizing context might reach a threshold above which normal centromeric loci and CENP-A nuclear organization cannot be maintained. Whether the change of CENP-A subnuclear localization in tumor cells/tissues is a cause or a consequence of oncogenesis remains an open question (Finn and Misteli 2019; Maison et al. 2010; Muller, Gil, and Drinnenberg 2019). Given that the mechanisms involved in the clustering of centromeres and their link with the control of nuclear organization are yet to be discovered, the mechanisms contributing to the maintenance/loss of CENP-A nuclear organization during tumorigenesis represent an exciting avenue to explore.

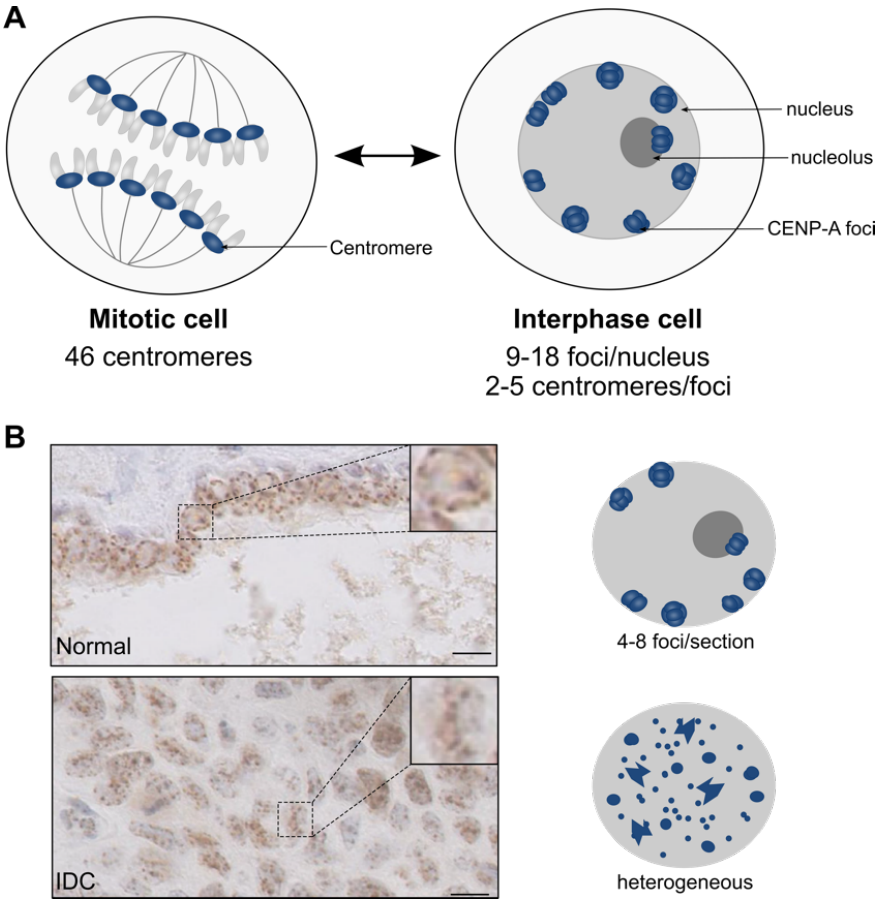


Figure 18. CENP-A localization patterns in normal tissues and neoplastic lesions. *Modified from Verrelle et al., 2021.*
(A) Schematic representation of nuclei from mitosis (left) and interphase (right) cells. In interphase cells, the clustering of centromeric CENP-A-enriched regions (blue) gives rise to CENP-A foci at the periphery of the nucleus and, in fewer cases, of the nucleolus. (B) CENP-A localization patterns visualized by IHC in breast tissues. Top: Normal duct; Bottom: Invasive Ductal Carcinoma (IDC). The boxed area shows the magnification of a representative nucleus. Scale bar = 10 µm. On the right is shown a schematic representation of the CENP-A localization pattern, with CENP-A foci (blue) within the nucleus (grey).

2.8. Clinical interest for CENP-A in cancer treatment

Elevated CENP-A levels correlate with cancer progression (Y. Li et al. 2011; X.-J. Ma et al. 2003; Qiu et al. 2013; X. Sun et al. 2016) and poor patient outcome (Gu et al. 2014; Li et al. 2011; Ma et al. 2003; McGovern et al. 2012; Qiu et al. 2013; Saha et al. 2020; Sun et al. 2016; Wu et al. 2012; Zhang et al. 2016). This correlation could reflect the CENP-A-induced CIN that leads to an increase in chromosomal rearrangements and mutagenesis rate, which both increase the heterogeneity of the cell population, thereby promoting the selection of advantageous clones. An alternative explanation could relate to the essential role of CENP-A in mitotic progression (Dunleavy et al. 2009; Fachinetti et al. 2013; Filipescu et al. 2017; Foltz et al. 2009). Following malignant transformation, hyperproliferative cells require sufficient expression of CENP-A along with its chaperone HJURP to ensure a proper CENP-A deposition enabling accurate chromosome segregation (Filipescu et al. 2017). This has led to the hypothesis according which such cells become "addicted" to CENP-A (Filipescu et al. 2017). In line with this hypothesis, in cancer cells overexpressing CENP-A, its depletion suppresses cell growth both *in vitro* and *in vivo*, blocks cell-cycle progression, and promotes apoptosis (Y. Li et al. 2011). Similarly, CENP-A partial depletion (Y. Li et al. 2011; Qing Wu et al. 2014) reduces proliferation, growth, migration, and invasiveness of cancer cells. Thus, CENP-A is required for tumor progression and its depletion may have anticancer effects which are likely mediated by genes involved in cell cycle control and apoptosis (Y. Li et al. 2011; Qing Wu et al. 2014). These two reports using cancer cell models show promising potential for targeting CENP-A as a cancer therapeutic, as an Achille's heel in addicted cells.

While CENP-A is generally associated with tumor aggressiveness, the correlation of high CENP-A levels with clear therapeutic response is not simple. Indeed, while a reduced therapeutic response is reported when CENP-A is overexpressed in osteosarcoma (X.-M. Gu et al. 2014), some reports in breast (McGovern et al. 2012; X. Sun et al. 2016; W. Zhang et al. 2016) and lung (W. Zhang et al. 2016b) cancers indicate a better clinical outcome. These discrepancies might reflect different cancer types / sub-types, various population of cells, possible heterogeneity in the samples and the methods of analyzing the therapeutic response. Considering the importance of the cellular context upon CENP-A overexpression, the p53 status clearly represented an important parameter to consider specifically (see discussion above). Indeed, CENP-A overexpression impacts cellular response to genotoxic stress, increasing the survival of p53-defective cells in the presence of DNA damage induced by a topoisomerase inhibitor (Lacoste et al. 2014). In addition, CENP-A overexpression strongly increases sensitivity to X-ray irradiation of several p53-WT cell lines but not of p53-defective cell lines (Jeffery et al. 2021). Importantly, the inactivation of p53 is sufficient to counteract the CENP-A induced radio-sensitivity phenotype (Jeffery et al. 2021). Thus, CENP-A acts as a double-edged sword: its overexpression enhances radio-sensitivity in cells with wild type p53, however, p53-defective cells show a more tolerant state to X-ray irradiation. This exemplifies how CENP-A overexpression could lead to either sensitivity or resistance to treatment depending on the p53 status. These findings highlight

the importance of integrating the p53 status when considering CENP-A for cancer treatment. Indeed, while tumors displaying high CENP-A levels in a wild-type p53 context would respond to radiotherapy, to treat tumors with defective p53 alternative options should be considered. These could include drugs that can recover an active p53 in combination with radiotherapy, and/or other DNA damaging agents. Importantly, a number of p53-targeted drugs are now being tested in clinical trials (Blandino and Di Agostino 2018; Bykov et al. 2018), including direct reactivators of mutant p53 (e.g. PRIMA-1MET/APR-246) and drugs designed to return functionality to wild-type p53 by inhibiting its upstream regulators (e.g. MDM2/X inhibitors) (Sanz et al. 2019). Interestingly, despite the impact on transcription of genes associated with DNA repair, CENP-A overexpression did not affect the rate of DNA repair (Jeffery et al. 2021), suggesting that sensitization or resistance observed is not related to repair efficiency.

Whether CENP-A can serve as a biomarker to improve stratification of cancer patients is also a crucial question. CENP-A overexpression has already been used as a general biomarker of poor patient prognosis and as a predictive biomarker for chemotherapy (X.-J. Ma et al. 2003; X. Sun et al. 2016; W. Zhang et al. 2016). It has been proposed as a biomarker for tumor aggressiveness in ovarian (Qiu et al. 2013), osteosarcoma (X.-M. Gu et al. 2014), lung (W.-T. Liu et al. 2018; Q. Wu et al. 2012), and breast estrogen receptor positive (McGovern et al. 2012; Montes de Oca et al. 2015) cancers. Interestingly, in breast cancer, identifying high levels of the CENP-A chaperone, HJURP, has been proposed as a prognostic marker of poor patient outcome, distinguishing aggressive tumors within the luminal A subtype (Montes de Oca et al. 2015). In addition to the use of CENP-A level, measured as a total amount in a bulk population to serve as a biomarker, given the discrete pattern observed, its nuclear distribution should also be considered. Indeed, CENP-A nuclear localization pattern in patient samples allows to directly interrogate the chromatin architecture in the nucleus by following centromeres and in breast could reveal changes between healthy, non-neoplastic and neoplastic lesions (Verrelle et al. 2021). CENP-A subnuclear pattern could also reveal clear alterations in chromatin architecture in the nucleus associated with resistance to treatments. The application of this strategy in head and neck squamous cell carcinoma (HNSCC) enabled to reveal a nuclear CENP-A localization pattern assessed by immunohistochemistry, as a predictive marker of local disease control at 2 years by concurrent chemoradiation therapy (CCRT) with 96% accuracy (Verrelle et al. 2021). This distinct CENP-A pattern, termed “Pattern-C” provided a strong prognostic marker of overall survival advantage, outperforming all other tumor characteristics usually examined including proliferation, HPV status and tumor stage. Given the general nature of CENP-A subnuclear patterns across tissues, extending the use of this simple staining method to predict sensitivity to concurrent chemoradiation may prove of interest for other cancers treated with genotoxic agents.

2.9. Concluding remarks

CENP-A is key for centromere function, a chromosome region with a fundamental role in cell division. However, recent work has demonstrated that beyond its centromeric role in mitosis, CENP-A may be related to tumor status through an impact on chromatin organization in interphase. We have presented recent studies concerning the regulation of CENP-A, and how aberrant expression affects mammalian cells in the context of cancer. The role of CENP-A in cancer progression is multifaceted, affecting both genome integrity and transcriptional reprogramming. These changes facilitate cancer progression and the acquisition of properties promoting metastasis. Furthermore, CENP-A levels could contribute to guiding therapy choice, notably when taking p53 status into account. Interestingly, in addition, CENP-A subnuclear pattern visualized on tissue sections represents a biomarker of potential prognostic value. Future work with new technological advances enabling to follow at a single cell level an integrated analysis of proteins, transcripts and spatial distribution in a tissue should help to further characterize the molecular mechanisms underlying the connections between CENP-A and cancer.

PART 3.

THE EPITHELIAL-MESENCHYMAL TRANSITION AND ITS PLASTICITY

1. EPITHELIAL-MESENCHYMAL TRANSITION STATES

1.1. Defining the EMT: epithelial and mesenchymal markers

The epithelial-mesenchymal transition (EMT) corresponds to the reprogramming of an epithelial cell into a mesenchymal cell (Figure 19). Epithelial cells are characterized by their close interactions with neighboring cells, which are maintained through protein structures like adherens junctions, tight junctions, gap junctions and desmosomes. They form the epithelial tissue by attaching to a basement membrane (basal lamina) – a specialized layer of extracellular matrix (ECM) proteins, mostly laminin and collagen type IV – through hemidesmosomes; hemidesmosomes contain integrins that bind to the basement membrane and connect to cytokeratins within epithelial cells. This structure supports the apical-basolateral (apicobasal) polarity of epithelial cells. However, epithelial cells can exhibit some degree of morphological variability and do not always possess fully formed cell-cell junctions. By contrast, mesenchymal cells are more isolated, lacking the basal lamina that separates them from adjacent tissues, and they do not maintain apicobasal polarity. Mesenchymal cells typically adopt a fibroblast-like morphology (Figure 19) and exhibit enhanced migratory capabilities (reviewed in (J. Yang, Antin, Berx, Blanpain, Brabletz, Bronner, Campbell, Cano, Casanova, Christofori, Dedhar, Derynck, Ford, Fuxe, García de Herreros, et al. 2020)).

During EMT, epithelial markers are downregulated while mesenchymal markers are upregulated (Figure 19). These changes encompass alterations in cell adhesion, cytoskeleton, transcription programs, and ECM components. Key epithelial markers are involved in maintaining cell-cell adhesion and communication by forming adherens junctions (reviewed in (Jean Paul Thiery et al. 2009)). E-cadherin, in complex with membrane-bound β-catenin, participate in the formation of these junctions, thereby ensuring the structural integrity of epithelial tissues (Gumbiner 2005). While the characteristics of fully epithelial cells are relatively well defined, defining the mesenchymal state remains challenging. There is currently no universal molecular marker that consistently characterize every mesenchymal cell resulting from an EMT program. To date, the most commonly used mesenchymal marker is vimentin, an important intermediate filament providing structural and functional support to the mesenchymal cell. More precisely, vimentin regulates cell migration by interacting with actin filaments to restrict actin flow and align traction stress (Jiu et al. 2015; Lanier, Kim, and Cooper 2015). It is also reported that vimentin expression is key to preserve mesenchymal cells from mechanical stresses during migration or squeezing through narrow spaces by providing a protective viscoelastic framework and by supporting the positioning and integrity of organelles, especially the nucleus (Patteson et al. 2019). In addition, vimentin could contribute to protecting cells from the stress induced by misfolded proteins, potentially

by directly binding to stress granules and aggregations of misfolded proteins to promote their destruction (Pattabiraman et al. 2020). Additional markers can include transcription factors involved in the EMT, which are context-dependent (**Part 3. Section 3.1.1. EMT transcription factors**). Finally, mesenchymal cells secrete specific extracellular proteases called matrix metalloproteinases (MMPs) that are involved in the proteolysis of basement membrane components, thereby facilitating migration and invasion (reviewed in (Lamouille, Xu, and Derynck 2014; Horejs 2016)).

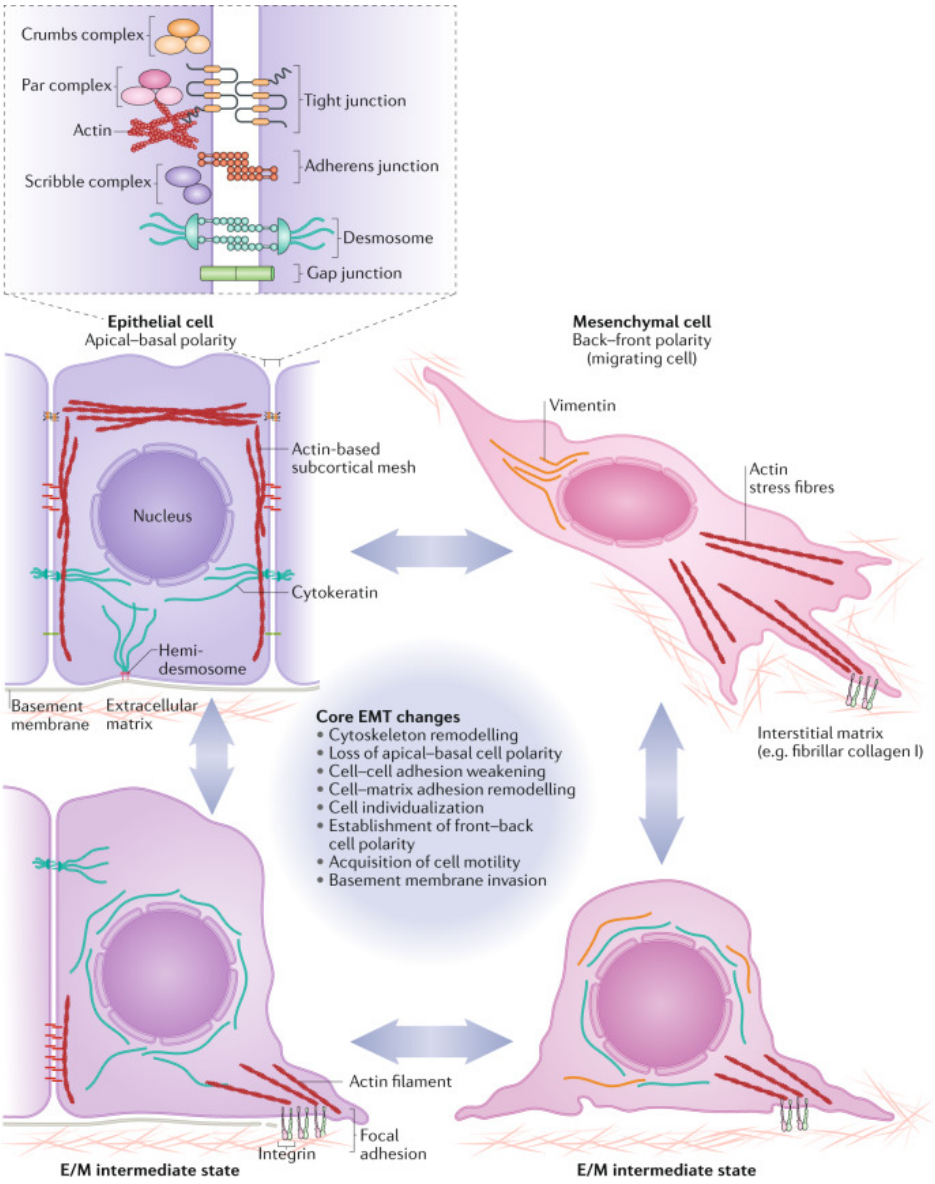


Figure 19. EMT diversity represented by an epithelial–mesenchymal plasticity model. Various cellular features associated with an epithelial or a mesenchymal cell state are found in a range of combinations and to different degrees in cells in different developmental contexts. The accumulated loss or gain of epithelial/mesenchymal (E/M) characteristics pushes a cell towards various intermediate states (bottom left and right) in a fluid and reversible manner, between a complete epithelial (middle left) and a complete mesenchymal (middle right) state. EMT, epithelial–mesenchymal transition. From (Yang et al. 2020).

1.2. Discovery of the EMT

Elizabeth Dexter Hay first described EMT while studying embryogenesis. To start with a historical anecdote, it is worth mentioning that Dr. Hay started to analyze the de-differentiation of cartilage cells from embryonic salamander's limbs, which can undergo re-differentiation to participate in limb regeneration (E. D. Hay 1958), a process which may include an EMT step (Bassat and Tanaka 2021)! Later, this project led her to study epithelial cells during the early development of chick embryo. Dr. Hay provided precise descriptions of the different cellular features in chick embryo tissues (Figure 20), showing mesenchymal cells arising from the epithelial ectoderm during gastrulation and neural tube formation (E. D. Hay 1968, 1995). She then introduced the term EMT for "epithelio-mesenchymal transformation". Together with her team, they later described EMT occurring *in vitro* in a culture of chick lens epithelial cells suspended in collagen gels (Greenburg and Hay 1982). In these conditions, invasive mesenchymal-like cells arise and move individually in the collagen matrix.

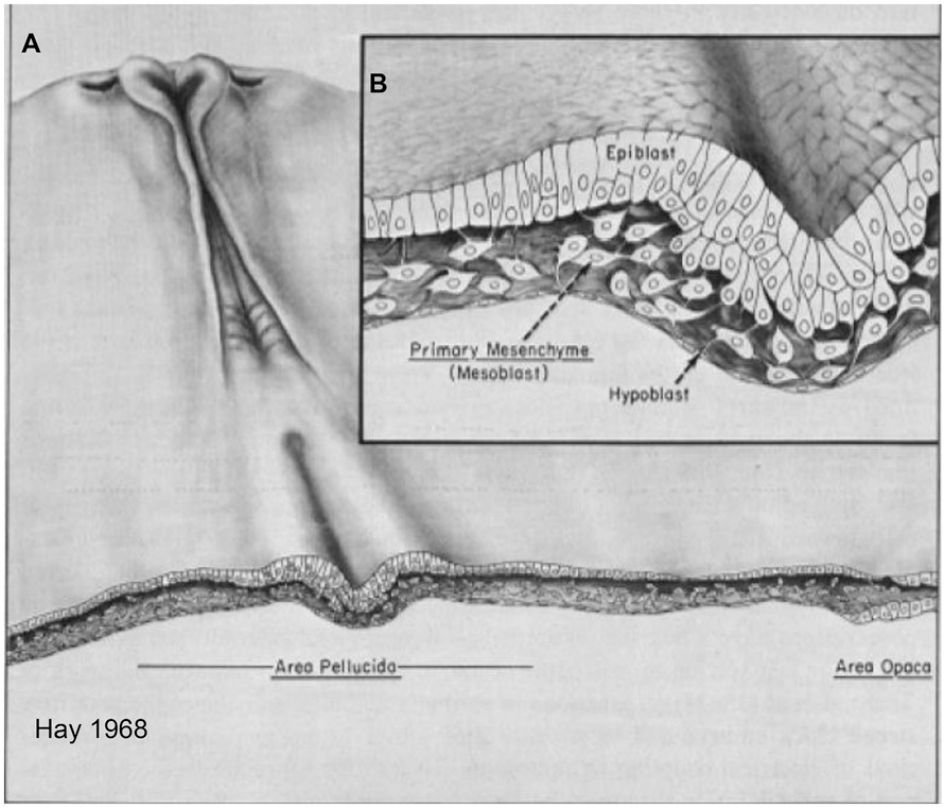


Figure 20. Betty Hay's original drawings illustrating EMT during chick mesendoderm formation. Illustration of EMT during chick gastrulation, reproduced from Hay 1968, showing epiblast, mesoblast and hypoblast labelled.

Of note, earlier studies had described EMT processes, such as cultured amnion cells that acquire fibroblast-like cells in response to a leukocyte medium (Nahmias et al. 1967). In addition, researchers had noted the co-existence of epithelial and mesenchymal cells in uterine sarcomas (Böcker and Stegner 1975; Ishikawa et al. 1979). This observation sparked a debate about the origins of these two cell

populations. At the time, researchers believed that epithelial cells could not acquire a mesenchymal phenotype, leading them to conclude that both cell types likely came from a common stem cell origin. Later, in the 1980s, researchers described a “cuboid-to-fusiform transition” during which rat epithelial tumor cells maintained in culture can turn into fusiform cells looking like fibroblasts (Bennett et al. 1978; Dulbecco et al. 1981). Another team studied the mesenchymal cells appearing from epithelial tissues during mice embryogenesis, showing they start to express vimentin while losing desmosome and cytokeratin expressions at the same time (Franke et al. 1982). Again, they did not use the term EMT introduced by Dr. Hay’s team, but instead the expression “rapid change from epithelial to mesenchymal character”. In the meantime, Hay’s team continued their research, providing descriptions of cell morphologies (Greenburg and Hay 1986, 1988) and cell-matrix interactions (E. D. Hay 1990) during EMT. Later on, many teams have started to uncover the mechanistic aspects of the EMT, and the research field has gained increasing prominence, notably with the observation that, beyond development, EMT is observed in wound healing and fibrosis processes, but also in cancer (**Part 3. Section 2. Different EMT types**). Following the first meeting of The Epithelial-Mesenchymal Transition International Association (TEMTIA), which brought the field together in 2003, the term “epithelial-mesenchymal transformation” was officially replaced by “epithelial-mesenchymal transition” in order to distinguish it from the process of neoplastic transformation.

1.3. Involvement of intermediate states

The change from epithelial-mesenchymal “transformation” to “transition” during the first TEMTIA meeting already conveyed the notions of plasticity and intermediate transition states. Instead of a binary switch between fully epithelial and fully mesenchymal states, cells progress through a continuum of diverse intermediate phenotypes.

This concept initially emerged from numerous studies that identified cells co-expressing both epithelial and mesenchymal markers, suggesting the existence of intermediate EMT states. In the literature, these intermediate phenotypes have been variably referred to as “intermediate”, “partial” or “incomplete” EMT, along with “hybrid epithelial/mesenchymal”, “intermediate mesenchymal” or “semi-mesenchymal”. Evidence for their existence was observed in different contexts, such as development (Blanco et al. 2007; Futterman, García, and Zamir 2011; Leroy and Mostov 2007; K. Watanabe et al. 2014) and wound healing (Arnoux et al. 2007, 2008), as well as fibrosis (Grande et al. 2015; Lovisa et al. 2015), more recently. However, most observations derived from the characterization of cell states among circulating tumor cells (Hou et al. 2011; Armstrong et al. 2011; M. Yu et al. 2013; S. Wu et al. 2015; Polioudaki et al. 2015; Murlidhar et al. 2017; Krol et al. 2018) of cancer patients. Additionally, intermediate E/M states have also been observed during immunohistochemistry (IHC) analysis of tumor tissues (Yagasaki et al. 1996; Kolijn, Verhoef, and van Leenders 2015) and in various cancer cell lines, including lung (Schliekelman et al. 2015; Jolly et al. 2016), breast (Bronsert et al. 2014; Hendrix et al.

1997), pancreatic (Bronsert et al. 2014), renal (Sampson et al. 2014), colorectal (Bronsert et al. 2014; Hiew et al. 2018), and ovarian (Strauss et al. 2009, 2011; R. Y.-J. Huang et al. 2013) cancer cell lines. However, most of the above studies were initially conducted at the cell population level rather than at the single-cell level, leading to confusion about the intermediate EMT state. This term has been used to describe (1) a mixed cell population of epithelial and mesenchymal cells, (2) a pure population of intermediate (hybrid epithelial/mesenchymal) cells, or (3) a mixed population of epithelial, intermediate, and mesenchymal cells. For instance, all cell lines mentioned above studied were either pure populations of intermediate cells or were analyzed at the population level by Western Blot and/or bulk RNA-sequencing. The stabilization of cancer cell lines at an intermediate stage indicates that cells can undergo a partial EMT program, reflecting the final intermediate state described during organ fibrosis (Grande et al. 2015; Lovisa et al. 2015).

Finally, recent work has provided direct evidence that EMT occurs in a stepwise manner, with cells gradually shifting from an epithelial to more mesenchymal states going through distinct intermediate stages (Pastushenko et al. 2018; Pastushenko and Blanpain 2019). Pastushenko et al. employed a mouse model of skin squamous cell carcinoma (SCC), driven by conditional oncogene expression and p53 deletion, which generates tumors that undergo spontaneous EMT. Through fluorescence-activated cell sorting (FACS) and immunofluorescence microscopy to analyze epithelial and mesenchymal markers, they identified distinct transition states during EMT. These findings open exciting avenues for research. The precise sequence of events (for example, vimentin expression is one of the first switches towards EMT in their model: does this apply to other models?) and the molecular mechanisms regulating cell progression through the various EMT states or stabilizing certain states remain open questions.

2. DIFFERENT EMT TYPES

2.1. Type 1 EMT: Development

Since EMT was first observed during the early development of chick embryos (E. D. Hay 1968, 1995), it is has been widely accepted that EMT occurs normally during early embryonic development, as well as later in development during organogenesis (reviewed in (Jean Paul Thiery et al. 2009)). In the context of development, cells of epithelial origin must migrate from their original position to a final destination; cells undergo an EMT to detach from their epithelial sheet and migrate to distant locations. In many cases, mesenchymal cells later undergo a reversal to an epithelial state through a mesenchymal-epithelial transition (MET). EMT and its converse MET are used repeatedly throughout embryogenesis to generate and remodel organs. These sequential rounds are generally referred to as primary, secondary, and tertiary EMTs.

In the following sections, I will discuss the critical role of the EMT in three key stages of animal development: gastrulation, neural tube formation, and embryonic palatal fusion. It is important to note

that EMT is also pivotal in numerous other developmental processes, including heart valve formation from the embryonic endocardium (Markwald, Fitzharris, and Manasek 1977), male Müllerian duct regression (Trelstad et al. 1982), and in the organogenesis and development of the liver (Si-Tayeb, Lemaigre, and Duncan 2010), ovaries (C.-F. Liu, Liu, and Yao 2010), and pancreas (F. C. Pan and Wright 2011), among others.

2.1.1. Gastrulation

"It's not birth, marriage or death, but gastrulation which is truly the most important time in your life" (Wolpert 2008). Gastrulation indeed represents a critical step of development; it ensures the arrangement of the three germ layers within the embryo (Haeckel 1874): the ectoderm, which will generate the epidermis and neural tissues, the endoderm, which will give rise to the digestive tube and most organs, and the mesoderm, which will form muscles, cardiovascular and skeletal elements (reviewed in (Solnica-Krezel 2005)). Before gastrulation, the embryo consists of an embryonic disk including two layers. These cellular layers are termed hypoblast (primitive endoderm) and epiblast (primitive ectoderm) in mammalian, reptilian and avian embryos. During gastrulation, some epiblast cells undergo an EMT in order to detach from the primitive ectoderm and move to form a third layer (the mesoderm) between the two primitive layers (P. P. Tam and Beddington 1987; P. P. Tam, Williams, and Chan 1993; Nakaya and Sheng 2008) (Figure 21A). Next, to form the mesoderm, cells from the primary mesenchyme undergo a MET to form a secondary epithelium. This epithelialization of the early mesoderm enables to form important structures like the somites (Barnes et al. 1997; Nakaya et al. 2004) and is later followed by secondary EMTs (Figure 21) enabling somite differentiation into, for example, dermomyotome, cartilage and bones (Noden 1988). Importantly, gastrulation concerns triploblastic organisms (all bilaterians), thus including all vertebrates, mollusks, insects and worms. *Xenopus* and zebrafish embryos are popular models of study due to the fact that they are easy to maintain and to manipulate (external development, rapid generation times). Avian and mouse embryos have also been extensively studied and allowed to generate most of data regarding developmental EMT. The set of developmental stages and patterns of cell movements are similar between triploblastic animals, despite some differences in terms of anatomy and embryonic cycle length, for example with gastrulation starting at ~14 days after fertilization and lasting one week in humans, starting ~2 days post-fertilization (just after laying) and completing in 2 days in chick, while it occurs between day 6.5 and 9.5 post-fertilization in mouse (reviewed in (Massé and Dale 2012; Nance and Priess 2002; Solnica-Krezel 2005)). Consistent with the fact that they undergo gastrulation during embryogenesis, the EMT is a conserved process in triploblastic animals, from *C. elegans* to humans (Sauka-Spengler and Bronner-Fraser 2008; Barriga et al. 2013; A. Zhang et al. 2021).

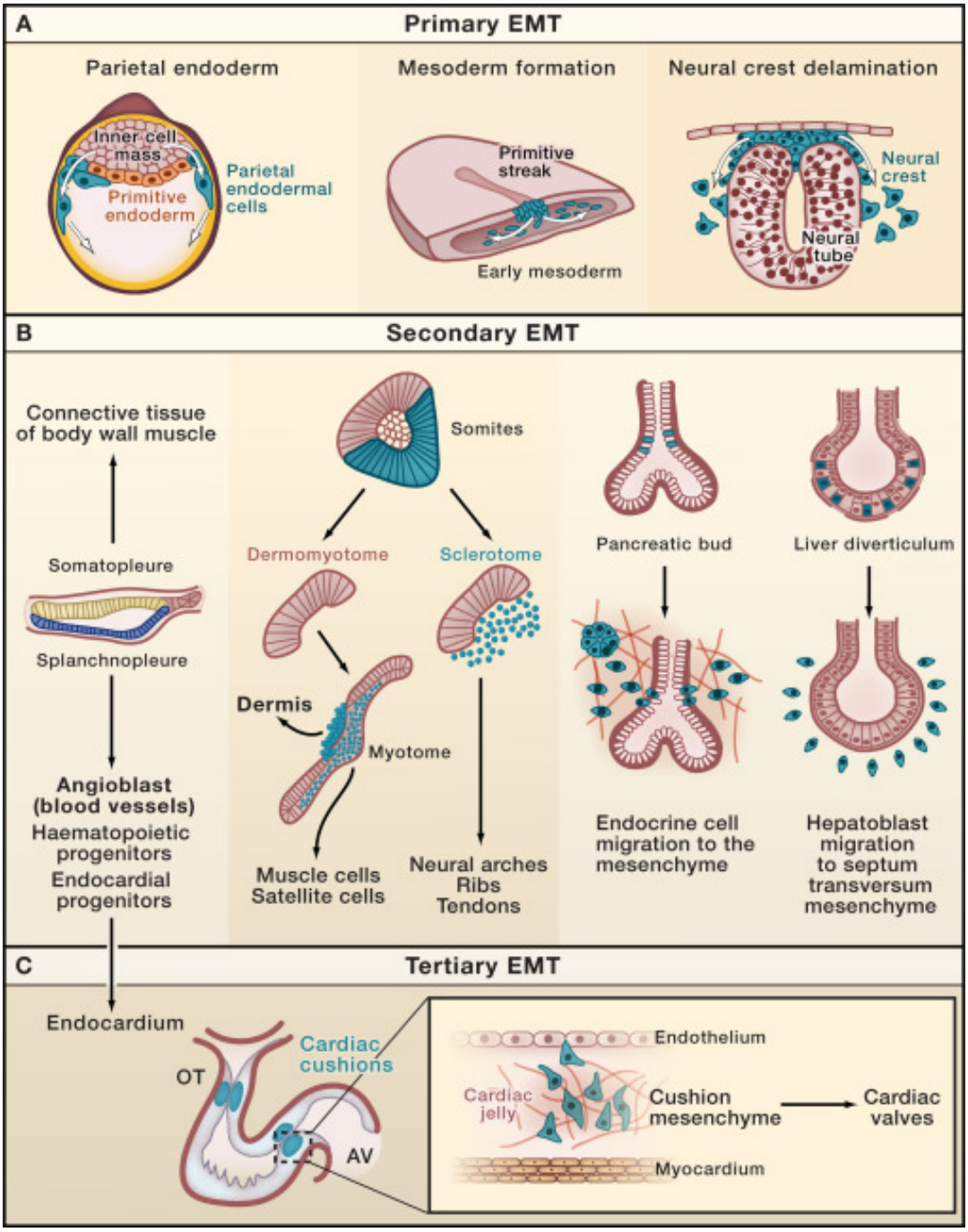


Figure 21. Successive EMTs during embryo development.
(A) Primary EMT occurs early during embryonic development, even before implantation such as during the formation of the parietal endoderm in mice. The first EMT after implantation is that undergone by the mesendodermal progenitors during gastrulation, whereas the delamination of neural crest cells from the dorsal neural tube is a later event. (B) Early mesodermal cells are subdivided into axial, paraxial, intermediate, and lateral plate mesodermal cells that will condense into transient epithelial structures: the notochord, the somites, and the somatopleure and splanchnopleure, respectively. These transient structures will undergo secondary EMT, leading to the generation of mesenchymal cells that differentiate into specific cell types. Endodermal tissues, including the pancreas bud and the liver diverticulum, exhibit morphological changes reminiscent of a secondary EMT to induce the dissociation of endocrine cells and hepatoblasts from their respective epithelial primordia. (C) An example of tertiary EMT arises during the formation of the cushion mesenchyme in the heart from the atrioventricular canal (AV) or the outflow tract (OT). The cushion mesenchyme is the precursor of the cardiac valves. (From Thiery et al 2009).

However, the cell mass can greatly differ (in terms of size/number of cells and shape) between species. For example, in *C. elegans*, EMT involves a few cells which move only small distances – generally single cell diameters – and the blastocoel space is small (reviewed in (Nance, Lee, and Goldstein 2005)). Despite this, gastrulation is essential in their development, internalizing endodermal, mesodermal, and germ-line precursors.

2.1.2. Neurulation

After gastrulation, the embryo comprises the three layers described above: the ectoderm, mesoderm, and endoderm. At this moment, a key process known as neurulation occurs in chordates, which establishes the internal positioning of the developing nervous system through the involution of the neuroectoderm (Gilbert, Opitz, and Raff 1996). The neural plate, a thick region of the ectoderm characterized by rapid cell division, is the starting point of this process. The edges of the neural plate grow to form the neural groove, with neural crests positioned on either side. In tetrapods, this process promotes the bending of the epithelial layer inward until it is fully internalized, forming of the neural tube (Harrington, Hong, and Brewster 2009; Nikolopoulou et al. 2017). Specifically, apical constriction generates a force within the neural epithelium that induces a change in cell shape to a wedge by shrinking the apical surface, leading to tissue bending (Sawyer et al. 2010). At the molecular level, force is generated via contraction of apical actomyosin, with E-cadherin (at adherens junctions) anchoring the contracting actomyosin and enabling the transmittance of force across the cell layer (Ilina and Friedl 2009; Adam Martin and Goldstein 2014). During neural tube formation, neural crest cells move to the medial edge, allowing the fusion of the neural crests. At this stage, neural crest cells within the dorsal neural epithelium undergo an EMT and individual mesenchymal cells migrate and scatter in the mesoderm (Newgreen, Ritterman, and Peters 1979; J. P. Thiery et al. 1982; Bronner-Fraser and Fraser 1988; Bronner 2012). The neural tube then splits from the ectoderm thanks to the scattering of the neural crest cells (Figure 21A). Mesenchymal neural crest cells will give rise to different derivatives such as craniofacial structures and most of the peripheral nervous system.

2.1.3. Embryonic Palatal Fusion: An example of secondary EMT

The palatal fusion is an important process during the craniofacial development. In mammals, the palate separates the oral from the nasal cavity and consists, anteriorly, of the bony hard palate (which serves for feeding and speech) and, posteriorly, of the muscular soft palate (which closes off the nasal airway during swallowing). Mammalian palatogenesis is the morphogenetic process that generates the intact palate. The embryonic primary and secondary palatal shelves develop as outgrowths; they must remodel and fuse to form the intact roof of the oral cavity. The embryonic palatal shelves (one each side) move to meet on the medial edge and fuse. First, the epithelia of both shelves stick to each other to form the medial edge epithelium of the embryonic palate. This epithelium then disappears when epithelial cells

undergo an EMT and scatter in the neighboring mesenchyme (Fitchett and Hay 1989; Gibbins et al. 1999). Of note, apoptosis may contribute to the disappearance of the medial edge epithelium of the palate (Martínez-Álvarez et al. 2000). The disappearance of the superficial layer of this epithelium enables the fusion of cells from basal layers, which undergo an EMT to migrate efficiently (Nawshad, LaGamba, and Hay 2004; Jalali et al. 2012). Thus, mesenchymal cells do not scatter but migrate together towards the oral cavity through a collective, unidirectional movement (Logan and Benson 2020). This observation suggests that cells might undergo a partial EMT, leading to the maintenance of some cell–cell junctions, while mesenchymal cells that completed the transition, among them, can lead the migration of the group of cells.

2.2. "Type 2" EMT: Wound healing and fibrosis

This second type of EMT is associated with tissue regeneration in adults. The wound healing EMT program begins as part of a repair-associated event that normally generates fibroblasts to reconstruct tissues following trauma and inflammation. In contrast to developmental EMT, inflammation is an essential inducer and positive regulator of wound healing EMT, which stops once the inflammatory signaling is attenuated. During wound healing, epithelial cells at the edge of the wound undergo EMT and move together into the damaged area before reverting to an epithelial phenotype to re-establish the epithelium in a process referred to as re-epithelialization (reviewed in (M. Angela Nieto et al. 2016)). This migration as a coordinated group of cells involves a partial EMT, with stable intermediate states (T. J. Shaw and Martin 2016; Vu et al. 2023). Wound healing is often investigated in animal models, such as the dorsal closure model in *Drosophila*, which involves the "closure" of a gap in its epidermis. In this model, cells from epidermal flanks undergo a partial EMT and migrate to occupy the hole in the epidermis (Bahri et al. 2010).

Fibrosis, or tissue scarring, characterized by excessive deposition of ECM, represents an "exaggerated" healing response due to prolonged inflammation upon repeated injuries (Qian et al. 2016), such as in kidney obstruction, glomerulonephritis or diabetes (which associates with fibrosis in various tissues). Fibrosis is a hallmark of many chronic degenerative disorders and is associated with reduced organ function and eventual organ failure in end-stage diseases. During organ fibrosis, persistent inflammation leads to maintenance of the EMT program (M. Zeisberg et al. 2003; Boutet et al. 2006). Normally, shortly after an initial inflammatory phase induced by the wound micro-environment, resident fibroblasts become myofibroblasts ("activated" fibroblasts), and produce ECM components – mainly collagen deposited as fibers – in damaged tissues, a process termed fibrogenesis (reviewed in (Plikus et al. 2021)). When inflammation is maintained for too long, myofibroblasts are continuously activated, accumulate and secrete excessive amounts of collagen, thus compromising organ function (Crosby and Waters 2010). The origin of these myofibroblasts has been debated for many years. When first described in 2002, EMT has initially been considered to drive of the transition of epithelial and endothelial cells

into myofibroblasts (Iwano et al. 2002; E. M. Zeisberg et al. 2007) in a kidney fibrosis model. Lineage-tracing experiments provided evidence of EMT (or endothelial-to-mesenchymal transition) to form fibroblast-like cells in liver or cardiac fibrosis (E. M. Zeisberg et al. 2007; M. Zeisberg et al. 2007). However, subsequent lineage-tracing analyses have not always provided compelling evidence of epithelial cells as precursors of fibrosis-associated myofibroblasts (Humphreys et al. 2010; Ling Li et al. 2010; LeBleu et al. 2013). Recently, new data in renal fibrosis indicated that renal epithelial cells can actually undergo a partial EMT, stably remaining at an intermediate state. These intermediate cells relay signals to recruit bone marrow-derived mesenchymal cells, resident fibroblasts and pericytes and promote myofibroblast differentiation, fibrogenesis and to sustain inflammation (Borges et al. 2013; Grande et al. 2015; Lovisa et al. 2015).

2.3. "Type 3" EMT: Cancer

The involvement of EMT in cancer has long been controversial, but growing evidence have supported its role in cancer progression, more so than in cancer initiation itself. Tumor aggressiveness is an important factor in mortality for cancer patients, characterized by metastasis, treatment resistance, immune escape, and cancer stem cell formation.

2.3.1. Cancer initiation

During the progression of carcinomas, epithelial cells acquire a few mesenchymal traits that confer the ability to locally invade adjacent tissues, a step that may be promoted by EMT. Interestingly, he EMT program may be engaged at premalignant stages, with essential EMT-TFs (**Part 3. Section. 3.1. EMT transcription programs**) being upregulated in both animal models (Hüsemann et al. 2008; Rhim et al. 2012) and human samples (Geradts et al. 2011; Mironchik et al. 2005; Montserrat et al. 2012; Morel et al. 2012) of non-invasive neoplastic lesions. This suggests that EMT may be a very early event in tumorigenesis. Remarkably, malignant cells maintain their epithelial phenotype despite overexpression of EMT-TFs (Hüsemann et al. 2008). Progressively during tumor development, these EMT factors are further upregulated, and cells progressively exhibit EMT features such as a switch from E-cadherin to N-cadherin expression (Montserrat et al. 2012). However, interestingly, in mouse spontaneous mammary tumors, certain EMT-TFs become overexpressed during local tissue invasion, but their levels are not further upregulated while they undergo bone marrow metastatic colonization (Xin Ye et al. 2015). In breast cancers, expression of EMT-TFs is commonly observed in claudin-low carcinoma that are aggressive, chemoresistant, of triple-negative subtype (negative for estrogen receptor, progesterone receptor and HER2) (Prat et al. 2010; Prat and Perou 2011). Intriguingly, this type of cancer is characterized by low expression of adherens and tight junctions proteins, a low level of epithelial differentiation, enrichment for EMT markers, stem-cell-like features, and a high frequency of metaplastic differentiation (cancer cells changing into another cell identity) (Hennessy et al. 2009).

They are believed to originate from stem-like cells located in the mammary glands and expressing high levels of EMT markers (Mani et al. 2008). The mechanisms underlying the expression of EMT-TFs in primary lesions remains unsolved. Of note, several phenomena associated with tumor initiation are known to trigger EMT: inflammation (reviewed in (López-Novoa and Nieto 2009)), physical constraints (Desprat et al. 2008), abnormal activation of signaling pathways such as Wnt/β-catenin, Notch, RAS–ERK1/2 and TGF-β signaling pathways (**Part 3. Section. 3.1. EMT transcription programs**) (reviewed in (J. Yang, Antin, Berx, Blanpain, Brabletz, Bronner, Campbell, Cano, Casanova, Christofori, Dedhar, Derynck, Ford, Fuxe, García de Herreros, et al. 2020)). It is tempting to hypothesize that EMT induction may be, to some extent, a natural consequence of oncogenic events. Furthermore, oncogene-induced senescence and apoptosis, which constrain cells in premalignant lesions, may be altered by certain EMT programs which can modulate p53 and retinoblastoma-dependent pathways by repressing the transcription of their targets (Ansieau et al. 2008; Maestro et al. 1999; Valsesia-Wittmann et al. 2004) and binding p53 to promote its MCM2-mediated degradation (Piccinin et al. 2012). Finally, EMT induction is associated with the acquisition of molecular and functional traits of cancer stem cells (CSCs) (Mani et al. 2008; Morel et al. 2008; Polyak and Weinberg 2009). This is an interesting connection since CSCs are defined as the source of tumor development and/or being capable of being so, due to their stem characteristics and high clonogenic potential. For example, CSCs are marked by high levels of CD44 and ALDH1 (aldehyde dehydrogenase 1), and low levels of CD24, all of these features being generated upon EMT in breast cancer cells (Mani et al. 2008; Ocaña et al. 2012; Xin Ye et al. 2015). In addition, main stem cell transcription factors (OCT4, NANOG, SOX2 and Notch1) are frequently expressed during EMT (Kong et al. 2010). In pancreas cancers, EMT is linked to stem cell properties because EMT-TFs repress the expression of miRNAs that normally inhibit their stem cell phenotype (Hwang et al. 2014; Wellner et al. 2009a). Therefore, stemness and cancer initiation could be two sides of the same coin for cells undergoing EMT, and the strong interconnection between EMT-inducing factors and oncogenesis factors forms a solid network that may drive tumor progression (reviewed in (De Craene and Berx 2013)).

2.3.2. The metastatic cascade

To date, it remains unclear whether primary carcinoma cells can undergo metastatic dissemination without activating, at least transiently and/or partially, the EMT program. EMT provides cells with migratory properties and resistance to anoikis, a type of cell death targeting anchorage-dependent cells when they detach from the ECM (Frisch, Schaller, and Cieply 2013). Various studies, based on tumor cell xenografts and/or overexpression of EMT-TFs (Mani et al. 2008), contributed to show the involvement of EMT during metastasis. In mouse models of breast cancer, inhibiting the expression of a key EMT-TF (Snail1; **Part 3. Section 3.1.1. EMT transcription factors**) prevents metastasis formation (Tran et al. 2014). However, the impact of the EMT in cancer progression is still not fully

understood. In the past years, the role of EMT in metastasis has been challenged by two publications using genetic mouse models for breast (K. R. Fischer et al. 2015) and pancreatic (Zheng et al. 2015) cancer, showing that the depletion of two important EMT-TFs (Snail1 or Twist1) had no effect on tumor invasion or metastasis in a pancreatic cancer driven by an inducible activation of oncogene and p53 loss. However, in the same mouse model, the depletion of another EMT-TF (ZEB1) strongly affected tumor formation, invasion, and metastasis. Thus, while EMT might not always be required for metastasis, there is considerable variability and tissue specificity in the impact of different EMT-TFs (Krebs et al. 2017). Due to this intrinsic heterogeneity in EMT programs and, more generally, in tumor cells, the impact of EMT in cancer diagnosis and treatment has remained limited. It is now widely accepted that EMT is involved in metastatic processes, directly or indirectly (reviewed in (Jean Paul Thiery et al. 2009; J. Yang, Antin, Berx, Blanpain, Brabletz, Bronner, Campbell, Cano, Casanova, Christofori, Dedhar, Derynck, Ford, Fuxe, García de Herreros, et al. 2020)). For instance, an alternative hypothesis could be that EMT facilitates invasion and intravasation of other cells that retain their epithelial character. To test this hypothesis, Beerling et al. followed metastasis formation by intravital fluorescence microscopy in mice; they detected a pool of breast tumor cells that spontaneously underwent EMT, became motile and disseminated in the blood, and finally reversed to a complete epithelial state upon metastatic outgrowth (Beerling et al. 2016). However, the different EMT states involved during the process were not characterized.

The metastatic cascade involving EMT is thought to consist of sequential steps: migration, invasion, intravasation and extravasation (reviewed in (J. Yang, Antin, Berx, Blanpain, Brabletz, Bronner, Campbell, Cano, Casanova, Christofori, Dedhar, Derynck, Ford, Fuxe, García de Herreros, et al. 2020)). Migration: Initial escape from the primary site (invasion) requires that epithelial tumor cells loosen their cell–cell interactions/junctions to become motile. Invasion: Cells release metalloproteases (MMPs), contributing to degrade the extracellular matrix (ECM). Breakdown of this physical barrier allows cells to migrate and invade nearby tissues. Of note, the involvement of several MMPs in tumor progression through EMT has been demonstrated in many cancer types including liver, gastric, pancreatic, colorectal, lung, ovarian, mammary and prostate (Lochter et al. 1997; W. Jiang et al. 2015; W. Li et al. 2015; Ding et al. 2016; Yusi Liu et al. 2016; Vos et al. 2016; C.-M. Chen et al. 2017). Intravasation: Tumor cells invade across the endothelial lamina, penetrate into the vascular or lymphatic vessels and thereby enter the systemic circulation. Extravasation: Subsequently, some cells may extravasate through the capillary endothelium of distant organs into their parenchyma. In this new environment, a subset of cells can proliferate, forming micrometastases that develop into secondary malignant tumors (metastases). Additionally, mesenchymal cells could revert to a more epithelial identity via MET to regain more proliferating abilities.

The EMT process involves various intermediate states which are detectable in CTCs (Hou et al. 2011; Armstrong et al. 2011; M. Yu et al. 2013; S. Wu et al. 2015; Polioudaki et al. 2015; Murlidhar et al.

2017; Krol et al. 2018) (Figure 22). This suggests that an active EMT process is likely to operate during the dissemination of carcinoma cells. Furthermore, the description of the tumor invasive front as being functionally distinct from the main tumor bulk (Brabletz et al. 2001) highlights this heterogeneous nature of the EMT in cancer. This data indicates that, at the tumor invasive front, cells have a mesenchymal phenotype. By contrast, the main tumor bulk remains largely epithelial. Thus, there is probably an EMT gradient from full, to partial, to no EMT (Brabletz et al. 2001). This gradient may be more or less steep depending on the tumor, reflecting the intrinsic molecular heterogeneity that arises from diverse driver mutation profiles or altered signaling networks. For example, the CTCs in breast cancers with a triple-negative molecular subtype tend to have a more mesenchymal phenotype than most other tumor types (reviewed in (M. Angela Nieto et al. 2016)). Interestingly, CTC clusters are more efficient at colonizing secondary sites than single mesenchymal CTCs (Aceto et al. 2014). These clusters comprise distinct intermediate states; this observation underlies the ability of intermediate cells to generate both epithelial and mesenchymal states, while mesenchymal cells are less efficient at reversing and forming intermediate and epithelial states for metastatic growth (Pastushenko et al. 2018).

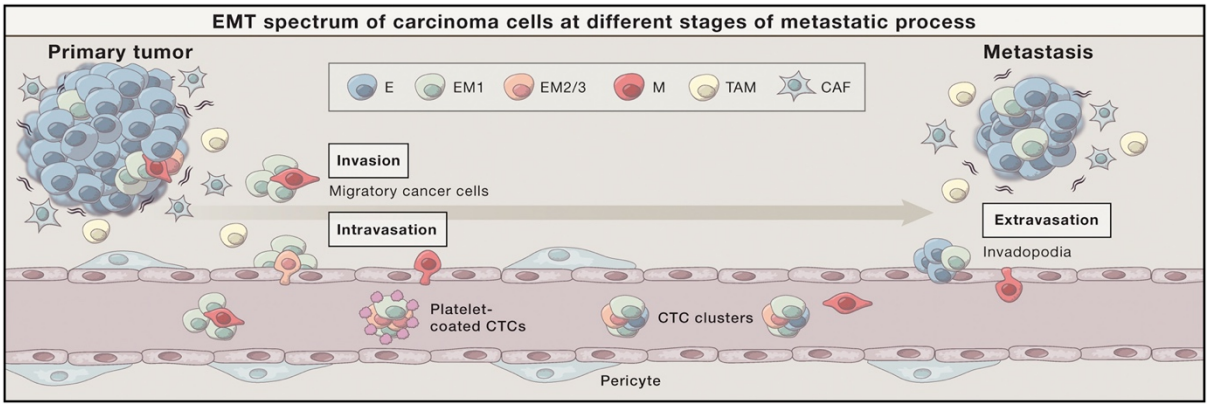


Figure 22. The metastatic cascade.
Scheme illustrating the complexity of the metastatic cascade from the point of view of cell plasticity, from carcinoma cell heterogeneity in the primary tumor to the different strategies that cancer cells adopt to survive in the bloodstream and colonize distant sites. E, epithelial; EM, intermediate; M, mesenchymal; TAM, tumor-associated macrophages; CAF, cancer-associated fibroblast. CTC, circulating tumor cells.

2.3.3. Resistance

Various experiments have shown that EMT can induce resistance to classical anticancer treatments. For example, breast cancer patients resistant to chemotherapies have more CTCs and more mesenchymal cells than patients with sensitive tumor (M. Yu et al. 2013a). Similarly, an increased, EMT-associated chemoresistance has been observed in various tumor types including breast (Cheng et al. 2007; K. R. Fischer et al. 2015), pancreas (Zheng et al. 2015), colorectal (A. D. Yang et al. 2006) and ovarian (Kajiyama et al. 2007) cancers, as well as in hepatocellular carcinoma (HCC), where the expression of most EMT-TFs correlates with poor prognosis (M.-H. Yang et al. 2009; Mima et al. 2013; Wan et al. 2017). At a molecular level, EMT-TFs can induce the expression of genes involved in DNA damage

response, which could potentially counterbalance the effects of chemotherapy and radiotherapy (Hsu et al. 2010; De Mattos-Arruda et al. 2015; Deng et al. 2016; Debaugnies et al. 2023). Furthermore, EMT-TFs have recently been associated with increased tolerance to DNA replication stress (Schuhwerk et al. 2022).

The EMT program is also associated with immune evasion, as suggested by the observation of tumor cells that spontaneously underwent EMT while undergoing immunoediting to escape immune surveillance (Knutson et al. 2006). Tumor cells can escape immune surveillance by (1) modifying their phenotype, so through immunoediting. EMT offers this possibility and can lead to a reduced expression of MHC class 1 (major histocompatibility complex) in cancer cells, and so to a diminution of the formation of immune synapses with cytotoxic T cells or NK (natural killer) cells (Akalay et al. 2013; Dongre et al. 2017). In non-small cell lung cancer (NSCLC) (Asgarova et al. 2018), as well as in MCF7 cells and mouse lung adenocarcinoma model (L. Chen et al. 2014; Noman et al. 2017), EMT can also induce an overexpression of PD-L1 (programmed death ligand 1), a cell surface inhibitory receptor which is normally involved in immunotolerance (to prevent excessive immune activity during pregnancy, for example). This allows cancer cells to suppress the activity of immune cells harboring the associated receptor PD1 (programmed death 1). Inducing EMT in mouse melanoma cells co-cultured with spleen cells promotes the activation of immunosuppressive cytokines and leads to increased proliferation of a specific cell subpopulation – regulatory T cells – corresponding to immunosuppressive cells, which normally modulate the immune system (Kudo-Saito et al. 2009). Regulatory T cells suppress or downregulate the proliferation of effector T cells to maintain the tolerance to self-antigens, in order to prevent autoimmune disease. In the context of the EMT, they promote immune evasion and metastasis. Interestingly, forced expression of a negative regulator of EMT, restores chemotherapeutic sensitivity (Cochrane et al. 2009). Interestingly, several studies point to inflammation as critical contributor to EMT-driven tumor progression and resistance (reviewed in (López-Novoa and Nieto 2009; Briede et al. 2021)). Both in the tumor microenvironment and during organ fibrosis, different mechanisms converge towards the induction of inflammatory signaling.

Finally, the activation of various EMT programs and the progression of individual cells to different states along the EMT spectrum can generate extensive phenotypic heterogeneity within tumors, as revealed in CTCs; this phenotypic heterogeneity may provide cancer cells with increased adaptability and resistance, enabling them to respond to a variety of external cues and physiological stresses (reviewed in (M. Angela Nieto et al. 2016; Lambert, Pattabiraman, and Weinberg 2017)).

2.3.4. Cancer EMT heterogeneity

Cells bearing an intermediate phenotype have been referred to as “metastable” (Jordan, Johnson, and Abell 2011; W. L. Tam and Weinberg 2013), referring to their flexibility to induce or reverse EMT. This particular plasticity of intermediate cells allows them to induce EMT heterogeneity by generating

multiple other distinct states, hence their higher metastatic potential. Indeed, when injected into immunodeficient mice, intermediate cells would give rise to various EMT transition states in the secondary by contrast with complete epithelial or mesenchymal cells (Pastushenko et al. 2018).

This idea also emerged due to the fact that, initially, circulating tumor cells were harvested using epithelial cell surface markers such as EpCAM (Riethdorf et al. 2007), as most cancers of interest were epithelial in origin. This method led to a misrepresentation of CTCs, since mesenchymal cells lose epithelial markers during EMT (Gorges et al. 2012). Although EpCAM-based methods are still commonly used for patient diagnostics (Eslami-S., Cortés-Hernández, and Alix-Panabières 2020), new microfluidics-based methods have been developed to capture all CTC states (S. Wu et al. 2015; Alix-Panabières and Pantel 2021). In this case, the populations of epithelial, intermediate, and mesenchymal CTCs defined by EMT markers – such as E-cadherin and vimentin – are, surprisingly, relatively equal in advanced diseases. Experimentally, multiple EMT states with distinct gene expression signatures have been reported in the same primary tumor derived from xenotransplantation into immunodeficient mice (PDX). These subpopulations localize within specific areas of the tumor in several cancer types (Pastushenko et al. 2018; Pastushenko and Blanpain 2019). Thus, in breast cancer, but also in lung and esophageal SCC, certain areas express only epithelial markers, some co-express both epithelial and mesenchymal markers and the others express exclusively mesenchymal markers. This spatial organization reflects the one observed in CTCs which organize as a "gradient", with mesenchymal cells at the leading front (Brabletz et al. 2001) (**Part 3. Section 2.3.2. Metastasis**). Thus, it is likely that metastatic progression, rather than relying solely or mostly on intermediate states, involves multiple transition states along the EMT spectrum.

Such heterogeneity (i.e., mesenchymal and intermediate cells migrating collectively, while they are partially held together by cell-cell contacts), is also similar to the observations in the endoderm and mesoderm cells of *D. melanogaster*, zebrafish, *X. laevis* and mouse (Montero et al. 2005; I. B. N. Clark et al. 2011; Dumortier et al. 2012; Campbell and Casanova 2015; Weber, Bjerke, and DeSimone 2012; Viotti, Nowotschin, and Hadjantonakis 2014), and in neural crest cells of zebrafish, chick and *X. laevis* (Theveneau and Mayor 2012; Scarpa et al. 2015). This observation highlights similarities between cancer-associated EMT and developmental EMT; this is consistent with the well-established idea that cancer cells actually hijack the EMT programs occurring in normal states such as during development.

The fact that cancer CTCs exhibit a full range of EMT phenotypes, along with the existence of pure intermediate cell lines that are stable over time, raise the following question: how are these intermediate states stabilized? To answer this question, researchers used computational modeling of mutual inhibitory loops existent in EMT signaling between several microRNAs (miRNAs) and EMT-TFs (**Section**). Overall, considering TF-promoter and miRNA-mRNA binding/unbinding dynamics, synthesis and degradation rates, the fact that miRNAs are more stable than mRNAs (Khanin and

Vinciotti 2008) and the capacity for ZEB to self-activate, their model results in a typical bifurcation diagram illustrating the range of *coexistence of* and of *transition between* three stable states. As it is inferred from the bifurcation curve, another role of the inhibitory feedback is to break the symmetry between the forward (EMT) and backward (MET) transitions: whereas EMT occurs through the hybrid phenotype, the backward transition (MET) rather proceeds directly from the mesenchymal phenotype to the epithelial one. This result could explain the lack of intermediate states observed during MET in previous studies (R. Li et al. 2010; Samavarchi-Tehrani et al. 2010). Furthermore, consistently with experimental data, their model predicts the existence of intermediate states; it also predicts the existence of "phenotypic stability factors" such as Ovo like zinc finger 2 (OVOL2) and grainyhead-like transcription factor 2 (GRHL2), which couple to core EMT circuits (involving mutual inhibitory loops between activators and inhibitors of EMT) to stabilize intermediate phenotypes that, therefore, are not necessarily metastable because they lack the plasticity to convert to other states (Lu, Jolly, Levine, et al. 2013; Lu, Jolly, Gomoto, et al. 2013; Hong et al. 2015; Jolly et al. 2016). Consistently, experimental inhibition of OVOL2 or GRHL2 in a pure intermediate cell line promoted its differentiation (Jolly et al. 2016).

Multiple studies have found a correlation between high levels of mesenchymal cells among CTCs and worsened patient prognosis (Khoo et al. 2015; Markiewicz et al. 2019; Revenco et al. 2019). Consistently, increased EMT heterogeneity in cancer correlates with aggressive advanced disease (Puram et al. 2017; Simeonov et al. 2021; M. S. Brown et al. 2022). Altogether, these data suggest that, overall, rather that promoting a linear transition towards mesenchymal, EMT processes in cancer tend to generate high heterogeneity, thus enhancing the ability of cancer cells to adapt together to diverse microenvironments and shear forces encountered during the metastatic spread. This idea is in line with the fact that no individual EMT state – isolated from an heterogeneous (mixed) EMT population – is capable of recapitulating the aggressive growth and decrease in survival of the mixed population (M. S. Brown et al. 2022). Furthermore, using isolated clonal derivatives of a breast cancer cell line, Brown et al. identified various EMT states, from epithelial to 3 intermediate states and 2 distinct mesenchymal phenotypes, thus suggesting multiple, nonlinear trajectories for EMT. Similarly, in a mouse model of pancreatic ductal adenocarcinoma combining oncogene activation and p53 loss, tumor cells exhibited spontaneously two distinct EMT programs, leading to different cells states (Aiello et al. 2018). Indeed, in addition to the heterogeneity in terms of states, there are numerous evidence support the model of a nonlinear EMT, with different transition states coming from multiple contexts, although the mechanism is unknown and may involve the combination between transcription programs and epigenetic determinants (van Dijk et al. 2018; Cook and Vanderhyden 2020). Thus, even when a mesenchymal trait is gained, there is still high heterogeneity in terms of the mesenchymal characteristic induced: in the analysis of 43 ovarian cancer cell lines, only 50% of mesenchymal cells expressed N-cadherin (R. Y.-J. Huang et al. 2013). This heterogeneity may reflect different biological consequences of the

intermediate states. The diversity of EMT-associated cancer cell phenotypes is reflected in the discrepancies in experimental and histopathological observations of human tumors that have fueled a long-standing debate regarding the roles of EMT in cancer progression. Indeed, such discrepancies can be attributed, in many cases, to the use of different EMT markers, but also to the different EMT programs operating, depending on the tissue. Intermediate states probably reflect the delicate balance of transcriptional drivers and suppressors of EMT, which is affected by epigenetic changes. This wider view of EMT offers a dynamic interpretation of the plasticity of the transition.

In summary, in cancer, EMT is characterized by a high heterogeneity in terms of EMT phenotypes and programs, demonstrated mostly in CTC clusters, which represent a "window" on cancer. Intermediate EMT states have long been considered metastable although they do not recapitulate the metastatic ability of the heterogeneous population. Injection on intermediate cells have a higher metastatic potential, compared to other states isolated, associated with their higher plasticity enabling to generate diversity, i.e. to give rise to different EMT states depending on the context. However, these intermediates cells are often stable, as suggested by the study of pure intermediate cell lines *in vitro* and require more plasticity to convert to other states. This might be dependent on factors present in the tumor micro-environment, which require more investigations.

3. REGULATING THE EPITHELIAL-MESENCHYMAL PLASTICITY: KEY PROGRAMS

3.1. EMT transcription programs

Dramatic changes in transcriptomic (Stemmler et al. 2019; Valcourt et al. 2005) and epigenetic programs (Dumont et al. 2008; Du et al. 2018; Sample et al. 2023) drive the EMT. In the context of its transcriptional activation, a large number of signaling pathways, which are interconnected, converge towards a small number of transcription factors that coordinate EMT at the cellular and molecular levels.

3.1.1. EMT transcription factors (EMT-TFs)

The first signal-transduction pathways leading to EMT were defined from genetic studies in *Drosophila* and in vertebrate embryos. *Drosophila* developmental genetic studies led to the identification of the transcription factors Snail and Twist, which act pleiotropically to orchestrate mesoderm formation during gastrulation (Leptin 1991). In vertebrates, the first described EMT-TFs were Snail and Slug (later called Snail1 and Snail2) (M. A. Nieto et al. 1992; D. E. Smith, Franco del Amo, and Gridley 1992). Dr. Nieto had identified a Zn++ finger homeobox-containing transcription factor, Slug (Snail2), ortholog of the *Drosophila Snail* gene that is expressed during the formation of the ventral furrow (Leptin and Grunewald 1990). Slug(Snail2) drives EMT during neural crest migration in chick embryos (Romano and Runyan 1999) and is critical to the formation of the primary

mesenchyme during gastrulation in the chicken embryo (M. A. Nieto et al. 1994). More recently, researchers uncovered Snail1/2's implication in EMT during fibrosis (Grande et al. 2015). Although Snail factors were considered purely as transcriptional repressors (Batlle et al. 2000; Cano et al. 2000; Perl et al. 1998), Snail is converted into an activator upon its binding to Twist or to CREB-binding protein (CBP) (Rembold et al. 2014). Interestingly, the blockade of Snail or Slug (Snail2) expression can inhibit EMT in cancer cells, suggesting a role in cancer cells (Carver et al. 2001; M. A. Nieto et al. 1994; Tran et al. 2014).

The Twist family (Twist1 and Twist2) of transcription factors was first described in 2004 during tumor metastasis in a mouse model (J. Yang et al. 2004). Like Snail, Twist proteins are highly conserved in bilaterians, e.g., from the sea urchin (reviewed in (D. Lyons, Kaltenbach, and McClay 2012)) to humans. In addition, immunofluorescence and reporter fusions experiments in *C. elegans* revealed the function of a Twist-related factor, CeTwist, during development; although is not active during mesoderm development, CeTwist later contributes to the transition of a number of mesodermal cells to nonstriated muscle fates by activating FGFR and NK-homeodomain target genes (Harfe et al. 1998). Twist1/2 belong to the super-family of bHLH (basic helix–loop–helix) proteins and exhibit bi-functional roles as both activators and repressors of gene transcription. They are expressed at low levels in adult tissues, except in the adipose tissue where Twist1 is abundantly expressed and may regulate tissue remodeling and inflammation. Twist1/2 often become aberrantly expressed in cells undergoing malignant transformation. Moreover, it is known that Twist1 plays an important role in EMT in various forms of malignant tumors, and high levels of Twist1 positively correlate with the metastatic potential (Alberto Martin and Cano 2010; Qin et al. 2012). In highly hypoxic tumoral environments, HIF proteins lead to Twist1 upregulation, contributing to EMT and tumor metastasis (M.-H. Yang et al. 2008). Twist1 contributes to EMT by regulating pathways involved in cell migration, cadherin and extracellular matrix remodeling (in particular of collagen fibers) (Alberto Martin and Cano 2010). Finally, Twist1 was showed to induce angiogenesis in hepatocellular carcinomas (Niu et al. 2007) and was correlated with VEGF expression in breast cancer tumors (Mironchik et al. 2005).

The last main family of EMT-TFs is the Zinc finger E-box-binding homeobox (ZEB) family, which was first described in 2001 (Comijn et al. 2001), when studying E-cadherin downregulation and the effect on tumoral invasion. ZEB family includes two members, ZEB1 and ZEB2, which can be both activators and repressors of transcription. In the context of their transcriptional repressor function, E-cadherin is one of their major targets along with members of the miR-200 family of microRNAs (which act as EMT repressors) (Brabletz and Brabletz 2010). This involves a ZEB/miR-200 negative feedback loop regulating EMT plasticity. ZEB1/2 are crucial during development; they are also expressed in adults by various immune cells, where they can mediate their differentiation and maintenance, and also regulate cytokine expression (reviewed in (Scott and Omilusik 2019)).

Other transcription factors have been shown to impact EMT in certain contexts, such as PRRX1. However, these transcription factors are also involved in other cellular processes such as proliferation, apoptosis and stemness and are not considered "core" EMT-TFs (reviewed in (J. Yang, Antin, Berx, Blanpain, Brabletz, Bronner, Campbell, Cano, Casanova, Christofori, Dedhar, Derynck, Ford, Fuxe, García de Herreros, et al. 2020)). Overall, all EMT-TFs can repress/activate epithelial/mesenchymal markers expression during EMT; early on, studies uncovered the loss of E-cadherin and the gain of vimentin expression as central events in the transition (reviewed in (Birchmeier, Birchmeier, and Brand-Saberi 1996; Pastushenko and Blanpain 2019)). Finally, core EMT-TFs are often co-expressed in various combinations in order to orchestrate complex EMT programs depending on the specific biological context (Stemmler et al. 2019). For instance, Snai1 and Twist1 are both important for metastasis in a specific oncogene-driven breast cancer model (Tran et al. 2014; Yixiang Xu et al. 2017) but dispensable for metastasis – although it promotes chemoresistance – in a pancreatic cancer model (Zheng et al. 2015), which instead depends on Zeb1 (Krebs et al. 2017).

3.1.2. EMT inducers and their signaling pathways

EMT can be induced by several intracellular signaling pathways that are activated when epithelial cells encounter specific signals released by the cells in their microenvironment (Figure 23).

a) TGF-β

This signaling pathway involves a large cohort of ligands comprising TGF-β isoforms and several bone morphogenic proteins (BMPs), among others. In the canonical pathway, TGF-β proteins bind to receptors, such as TGF-β receptor type 1 (TGFβR1), TGFβR2 and TGFβR3 at the plasma membrane; this leads to the phosphorylation of SMAD2 and SMAD3, which proceed to form complexes with SMAD4. Recent findings indicate that a combination of the two SMAD signaling pathways (SMAD2-SMAD3 and SMAD1-SMAD5) is essential for the activation of EMT across various carcinoma cell lines *in vitro* (Ramachandran et al. 2018). Once formed, these SMAD complexes migrate to the nucleus, where they function as transcription factors to regulate the expression of genes implicated in the acquisition of a mesenchymal state (reviewed in (Jian Xu, Lamouille, and Derynck 2009)). TGFβ-induced SMAD complexes directly stimulate the transcription of mesenchymal markers such as vimentin and fibronectin, while also inducing key EMT-TFs like Snail, Slug, ZEB1, and TWIST (reviewed in (Jian Xu, Lamouille, and Derynck 2009)). Once expressed, these EMT-TFs can upregulate TGFβ ligands, establishing an autocrine signaling loop that sustains EMT activation (Dhasarathy et al. 2011; Grande et al. 2015). Indeed, in Grande et al the EMT-TF Snail has been shown to promote TGFβ1 expression in renal epithelial cells. Moreover, co-expression of Snail1 and Snail2 enhances TGFβ pathway gene expression and leads to increased histone acetylation at the TGFBR2 locus in breast carcinoma cells 89. This autocrine production of TGFβ in response to EMT activation suggests a feedforward loop that enables cells to sustain EMT programs once initiated.

Since 1990, increasing amount of evidence have demonstrated the importance of transforming growth factor (TGF) family proteins during EMT. First, TGF-α expression has proven to induce an mesenchymal and invasive phenotype in rat prostate cancer cells (Gavrilović et al. 1990). Then, researchers identified a role for TGF-β family members in EMT in embryonic heart endothelial cells (Potts et al. 1991), in mammary epithelial cells (Miettinen et al. 1994) where it induces a reversible EMT associated with decreased cell proliferation, but also during the early chick embryo development, with the important involvement of TGF-β3 during EMT for palatal fusion (D. Sun et al. 1998). Early studies also showed that transgenic expression of TGF-β1 correlates with the conversion of squamous into more invasive spindle cell carcinomas (Cui et al. 1996). Later, TGF-β has been found to be a potent initiator of EMT associated with renal fibrosis (M. Zeisberg and Kalluri 2004), but also in cancer cells stimulating cell invasion and metastasis (Akhurst and Derynck 2001; Medici, Hay, and Olsen 2008). A recent study linked TGF-β with the generation of mesenchymal motile cancer cells residing in G1-phase (Takahashi et al. 2022), consistent with earlier findings (D. Sun et al. 1998). In TGF-β3 null mutant mice, defects in EMT lead to defects in palate fusion (Kaartinen et al. 1995; Proetzel et al. 1995). Indeed, TGF-β3 plays a critical role in processes such as palatal fusion and formation of endocardial cushions (Mercado-Pimentel and Runyan 2007; Nawshad, LaGamba, and Hay 2004). Additionally, TGFβ signaling is essential in wound healing and pulmonary, kidney and hepatic fibrosis (Gressner et al. 2002; Willis et al. 2005; Willis and Borok 2007) (section). In the context of carcinomas, TGF-β1 facilitates the transition to a mesenchymal phenotype, promoting cellular invasion and metastasis (reviewed in (Seoane and Gomis 2017)). Cancer cells often increase their production of active TGF-β, which not only triggers EMT and allows the cells to become invasive, but also enhances angiogenesis in close proximity to the tumor microenvironment, providing an exit route for migratory mesenchymal cells (reviewed in (R. Derynck, Akhurst, and Balmain 2001)).

b) Notch

In mammals, four isoforms of the Notch receptor can bind the Delta-like or Jagged family of ligands. This interaction triggers a cascade of proteolytic cleavages, ultimately releasing a free intracellular fragment of Notch, termed Notch ICD (Notch intracellular domain). Following nuclear translocation, Notch ICD associates with binding partners and transcriptional activators to induce the expression of target genes (Kopan 2002; B. A. Osborne and Minter 2007). For instance, upon binding to the RPB-Jκ protein complex, Notch ICD converts the complex from a repressor to an activator of Notch target gene transcription. Although the precise role of Notch in regulating developmental EMT is not fully elucidated evidence suggests its involvement: In zebrafish, Notch is expressed in embryonic regions where EMT occurs and Notch or RPB-Jκ depletion results in embryos that do not express Snail and cannot undergo endocardial EMT (Timmerman et al. 2004). In addition, a recent study revealed that Notch signaling during morphogenesis of the *C. elegans* digestive system is essential for the expression (or inhibition) of several target genes. This would promote the EMT of two adjacent epithelial cells in

the cyst (called pm8 and vpi1). This way, they could migrate through neighboring cells and self-fusion to form the digestive tract (Rasmussen et al. 2008). Furthermore, Notch signaling has been implicated in the regulation of EMT in several types of carcinomas, including breast, lung, pancreatic and squamous cell carcinomas (Anusewicz, Orzechowska, and Bednarek 2021; Y. Tang, Tang, and Cheng 2017). Interestingly, Notch and TGF-β pathways are interconnected at several levels. The major mode of crosstalk between these two pathways is via SMADs, which associate with Notch ICD to regulate the expression of several genes, including EMT genes (Blokzijl et al. 2003; Rik Derynck, Muthusamy, and Saeteurn 2014).

c) Wnt/β-catenin

Three Wnt signaling pathways can operate, in mammals, following the binding of 19 distinct Wnt ligands to the Frizzled family of cell surface receptors: the "canonical" Wnt signaling pathway, the non-canonical Wnt-calcium pathway and the non-canonical planar cell polarity pathway (reviewed in (Klaus and Birchmeier 2008)). The canonical pathway is initiated by the binding of a Wnt ligand to a Frizzled receptor. This triggers a series of signaling events leading to β-catenin stabilization (i.e., inhibition of the GSK3-mediated β-catenin phosphorylation that usually leads to its ubiquitylation and proteasomal degradation) followed by nuclear translocation (reviewed in (Anthony et al. 2020)). The resulting nuclear β-catenin, acting as a transcriptional cofactor, induces the expression of target genes involved in cellular fate specification, proliferation and tumorigenesis (reviewed in (Anthony et al. 2020; Clevers 2006)), but also angiogenesis (reviewed in (Olsen et al. 2017)), notably by interacting with T-cell factor/lymphoid enhancer factor (TCF/LEF). This signaling pathway is considered to be a key activator of EMT (Brembeck, Rosário, and Birchmeier 2006; van Genderen et al. 1994). In the context of developmental EMT, absence of the WNT3A ligand impairs the formation of the primitive streak, mesoderm and node (P. Liu et al. 1999). Additionally, canonical Wnt signaling is critical for the formation and the proliferation of neural crest precursors (García-Castro, Marcelle, and Bronner-Fraser 2002). In adults, β-catenin can trigger the activation of a wound healing EMT and it promotes malignant progression by regulating EMT and CSCs in multiple types of carcinoma where it drives proliferation potential and progression of cancer cells (Arwert, Hoste, and Watt 2012; Tammela et al. 2017). Of note, E-cadherin normally sequesters almost all the pool of β-catenin at the cell membrane of epithelial cells. The dissolution of adherens junctions liberates β-catenin into the cytosol, poising cell for nuclear translocation in response to Wnt signaling (reviewed in (Anthony et al. 2020)). The EMT-TF Snail directly improves the transcriptional ability of β- catenin via a direct interaction in the nucleus (Stemmer et al. 2008) while miR-200, which repress EMT by translationally inhibiting ZEB1, inhibits the expression of β-catenin (J. Liu et al. 2013; J. Su et al. 2011). When the Wnt/β-catenin signaling pathway is activated, nuclear β-catenin activates the expression of several genes including vascular endothelial growth factor (VEGF) (H. Sui et al. 2017), an angiogenic growth factor (reviewed in (Amini et al.

2012)) strongly associated with metastasis and poor prognosis in different cancers (Kallergi et al. 2009; Y. Yang and Cao 2022).

d) Integrins

Integrins are heterodimeric transmembrane glycoproteins consisting of α and β subunits. For example, β3 integrin can form a heterodimer with αv integrin to form the αvβ3 integrin, a cell-surface receptor for ECM proteins. αvβ3 is expressed at low levels in healthy epithelial tissues but is highly expressed in tumor tissues (reviewed in (Desgrosellier and Cheresh 2010)), correlating with tumor growth, cancer invasion, metastasis, and stemness (H. Liu et al. 2012; Parvani et al. 2015; Seguin et al. 2014). In addition, αvβ3 integrin can be part of TGF-β signaling-related EMT (Galliher and Schiemann 2006). Another integrin, α9β1, could promote VEGF-mediated angiogenesis and metastasis (S. K. Gupta et al. 2013). These data suggest a role for integrin-mediated EMT, potentially in relation with the microenvironment of the cell, in particular the ECM. However, activation of EMT signaling downstream of integrins concerns mostly major basement membrane receptors and has only been assessed *in vitro*. This may be the reason why, when activated in lung cancer cells independently of TGF-β signaling, αvβ3 induces a partial EMT (Kariya et al. 2021).

e) Mitogen growth factors: PI3K-AKT and MAPK axes

Growth factors including epidermal, fibroblast and hepatocyte growth factors (EGF, FGF, and HGF) bind to their respective receptors to activate Mitogen-activated protein kinases (MAPK) and PI3K-AKT signaling. Their interaction triggers receptor dimerization, followed by the activation of receptor-associated tyrosine kinases which phosphorylate the carboxyl-terminal domains of these receptors. This, in turn, enables the activation of the MAPK and/or PI3K-AKT pathway, which interconnects with β-catenin: AKT phosphorylates GSK3, thus inhibiting GSK3 activity (reviewed in (Hermida, Dinesh Kumar, and Leslie 2017)). Both PI3K-AKT and ERK-MAPK pathways promote cell growth and proliferation as well as EMT, thus, consistently, their inhibitors in HCC suppress proliferation and invasion as well as the expression of EMT markers (Di Domenico and Giordano 2017; Grotegut et al. 2006; S. Lee et al. 2020; Tashiro et al. 2016). Using a Ras mutant that specifically activates the RAF/MEK/ERK pathway or the PI3K/AKT pathway, researchers showed that the PI3K/AKT axis enables the protection from TGF-β-induced apoptosis, potentially through NFκB, while it is not the case for MAPK (Janda et al. 2002). Moreover, in several cancer types, EGF activates the Janus kinase 2 (JAK2)-signal transducer and activator of transcription 3 (STAT3) pathway. Recent reports have suggested that FGF2-mediated ERK signaling is required for the formation of cancer stem-like cells in esophageal squamous cell carcinoma. Thus, pharmacological inhibition of either FGFR or ERK induces MET *in vitro* and delays tumor growth *in vivo* (O. Maehara et al. 2017). In addition, the analysis of The Cancer Genome Atlas (TCGA) datasets has revealed that FGF2 overexpression in several carcinomas

correlates with a poor prognosis, reduced overall survival and EMT gene signature (McNiel and Tsichlis 2017).

f) IL-6/JAK/STAT

More than 50 cytokines and growth factors have been identified in the Janus kinase/signal transducer and activator of transcription (JAK/STAT) signaling pathway. This includes hormones, interferons (IFN), interleukins (ILs), and colony-stimulating factors (reviewed in (Darnell 1997)). There are four JAK family members in mammals: JAK1, JAK2, and TYK2, which are ubiquitously expressed, and JAK3, which is predominantly expressed in hematopoietic cells. When JAKs associate (noncovalently association) with cytokine receptors, they mediate the tyrosine phosphorylation of these receptors, that in turn recruit one or more STAT proteins. Tyrosine-phosphorylated STATs dimerize, leading to their nuclear translocation to regulate specific genes. JAK/STAT-mediated downstream events vary and include activation of various genes related to immune fitness, tissue repair, inflammation, apoptosis, and adipogenesis (Owen, Brockwell, and Parker 2019). STAT3 is the most well studied; it is an important transcription factor associated with EMT in cancer, and the activation of IL-6/JAK2/STAT3 signaling promotes metastasis (H. Yu, Pardoll, and Jove 2009). Constitutively active IL-6/JAK/STAT3 signaling drives cancer cell proliferation and invasiveness while suppressing apoptosis, and STAT3 enhances IL-6 signaling to promote an inflammatory-mediated positive feedback loop. Interestingly, multiple cell types in the tumor microenvironment produce IL-6; this may promote the activation of the JAK/STAT3 signaling in both tumor cells and tumor-infiltrating immune cells and, in turn, it could stimulate proliferation, survival, invasiveness, and metastasis.

g) Others/non-canonical

Uncontrolled proliferation within tumor tissue can create an oxygen-starved environment as the blood supply becomes insufficient. The Hypoxia inducible factor (HIF) is a transcription factor that regulates cellular adaption to low oxygen (i.e., hypoxic) conditions. HIF proteins are heterodimers formed from a constitutively expressed protein subunit, paired with an oxygen-regulated, hypoxia-inducible factor 1-α (HIF-1α) protein (Reyes, Reisz-Porszasz, and Hankinson 1992; G. L. Wang et al. 1995). In normal conditions, prolyl-hydroxylase domain (PHD) proteins hydroxylate HIF-1α, allowing the recruitment of an E3 ubiquitin ligase, targeting it for proteasomal degradation (Ivan et al. 2001). Conversely, under hypoxic conditions, hydroxylation of HIF-1α is inhibited, allowing its dimerization with HIF-1β to form the active HIF-1 transcription factor. HIF-1 has been demonstrated to trigger the TFs ZEB1/2 (Esteban et al. 2006; Krishnamachary et al. 2006), TWIST1 (M.-H. Yang et al. 2008) and Snail (Luo et al. 2011).

Finally, recent studies have started to uncover the link between EMT and DNA damage. First, EMT has been described to be a potent regulator of the DNA damage response (DDR) signaling and choice of repair pathways in human cells (reviewed in (Scully et al. 2019)). Overall, EMT is known to limit the establishment of high genomic instability (Morel et al. 2017; Prodhomme et al. 2021) by preventing the

use of a mutagenic repair pathway (Moyret-Lalle et al. 2022). Furthermore, DNA damage can promote the activation of the Three prime repair exonuclease 1 (TREX1), which leads to nuclear envelope rupture, promotes tumor cell invasion and upregulation of SNAIL1 (E. R. Gomes and de Almeida 2021).

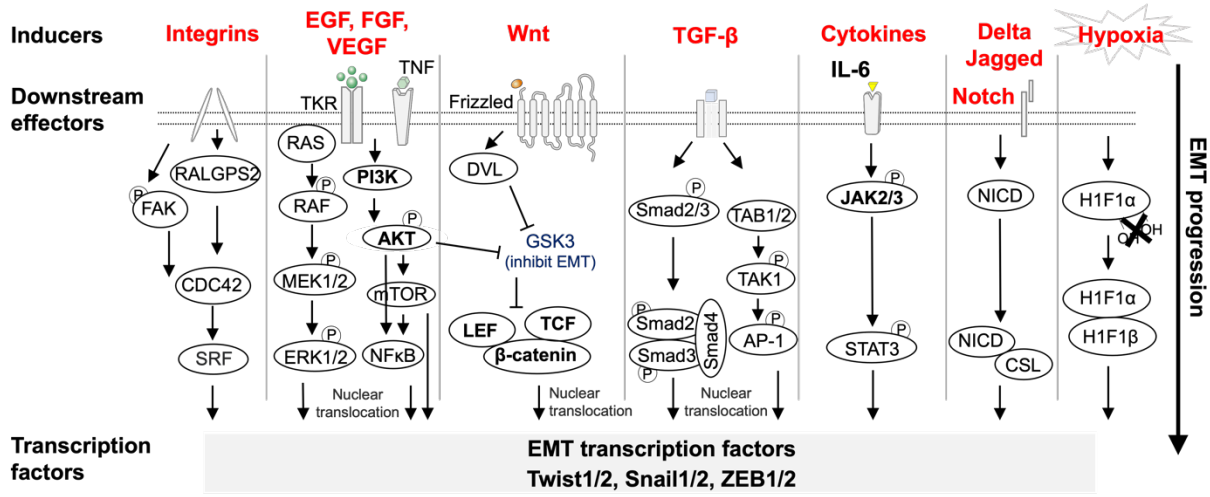


Figure 23. EMT signaling pathways.
Schematic representation of the different EMT pathways (simplified). From left to right: Integrins, mitogen factors, Wnt/β-catenin, TGF-β, Il-6/JAK/STAT, Notch and HIF-1 (Hypoxia inducible factor).

h) A known EMT inhibitor: p53

The well-known "tumor suppressor" and "guardian of the genome" p53 is a tumor-suppressor that modulates several signaling cascades to ensure genetic stability. Its gene *TP53* is mutated in about half of human cancers (reviewed in (Toledo and Wahl 2006)). p53 undergoes several PTMs to be stabilized and activated in response to cellular stress, such as DNA damage (Kastan et al. 1991; Maltzman and Czyzyk 1984) or oncogene expression (reviewed in (Lowe 1999)). In turn, p53 activates the transcription of important genes implicated in cell cycle arrest (*CDKN1A*/*p21*) (el-Deiry et al. 1993), DNA repair (*DDB2*, *XPC*, *GADD45A*) (Bieging, Mello, and Attardi 2014; Yoon et al. 2005; Zhan 2005), apoptosis (*BAX*, *BBC3/PUMA*, *NOXA*) (P. Shaw et al. 1992), and senescence (*CDKN1A*/*p21*, *PAI1*, *PML*) (Kortlever, Higgins, and Bernards 2006) (reviewed in (Riley et al. 2008)). By maintaining genome integrity and preventing the proliferation of cells with damaged DNA, p53 can prevent tumorigenesis (reviewed in (Lane 1992; Toledo and Wahl 2006)) and EMT (Chang et al. 2011; Parfenyev et al. 2021; Sharma et al. 2024).

3.1.3. Stabilizing transition states

At the molecular level, EMT activators suppress the transcription of all five members of microRNAs (miRNAs) from the miR-200 family (Bracken et al. 2008; Burk et al. 2008). miRNAs are short

noncoding RNAs that regulate gene expression post-transcriptionally. They are crucial players in regulating cell plasticity and EMT (reviewed in (Díaz-López, Moreno-Bueno, and Cano 2014)). Conversely, miR-200 members inhibit the translation of EMT-activators, in particular ZEB1/2, thereby promoting MET (Burk et al. 2008; Gregory et al. 2008; Korpal et al. 2008; Park et al. 2008). Thus, miR-200 and ZEB1 factors are linked in a reciprocal, mutual inhibitory feedback loop, which may explain the multi-step and reversible/bi-directional aspect of the EMT. Interestingly, miR-200 not only counteracts classical EMT activators, but also suppresses the translation of stem cells factors, such as BMI1 (Shimono et al. 2009; Wellner et al. 2009b). By measuring mRNA and protein levels of miRNAs and other core EMT regulators in non-tumoral MCF10A cells induced with different amounts of TGF-β for 7 days, Zhang et al. provided experimental confirmation for a model of cascading switches between EMT states involving the stepwise activation of, at least, two double-negative feedback loops of EMT activators and inhibitors: one between Snail1 and the miR-34 family and another between ZEB1 and the miR-200 family (Jingyu Zhang et al. 2014). Other studies provided evidence for additional negative feedback loops between ZEB1 and OVOL2 (Hong et al. 2015) or grainyhead-like transcription factor 2 (GRHL2) (Silveira and Mombach 2020).

Altogether, these data lead to a model with a core regulatory machinery: the miR34-Snail1 and miR200-ZEB1 double-negative feedback circuit in which miRNAs and EMT-TF repress each other. Other TFs, like OVOL1/2 and GRHL2, can feed into this core regulatory machinery to protect the epithelial phenotype. Importantly, disrupting the regulation of ZEB1 by miR-200c *in vivo* is sufficient to drive EMT (Title et al. 2018). Thus, miR34-Snail1 and miR200-ZEB1 loops contribute to the epigenetic control of epithelial-mesenchymal plasticity and represent key targets for epigenetic modifications. How other EMT-TFs affect the network and its epigenetic control requires further study. Finally, another gene regulatory network has been implicated in regulating EMT programs in development and disease; it involves a negative feedback loop between Snail1 and PRXX1 through the direct activation of miRNAs from the miR-15 family, which target Snail1. This is associated with a switch from Snail1-associated gain to Prrx1-associated loss of stem-like properties (Fazilaty et al. 2019).

3.1.4. The programs activated in type 1, 2 or 3 EMT

a) Development

Similar signaling pathways regulate the EMT during both gastrulation and neural crest delamination in the amniote embryo. During gastrulation, epiblast cells exit pluripotency and commit to one of the three germ layers: ectoderm, mesoderm, or endoderm. This ultimately gives rise to the progenitors of major organs (reviewed in (Zorn and Wells 2009)). In amniotes, such as chick and mouse, Wnt signaling plays a crucial role in rendering cells competent to respond to extracellular signals that initiate EMT (Skromne and Stern 2001). For instance, the primitive streak (a key structure at gastrulation) fails to form in Wnt3-deficient mice, consistently with the absence of EMT in the same context (P. Liu et al. 1999).

Conversely, Wnt8c overexpression in mouse embryos results in the formation of multiple primitive streaks (Pöpperl et al. 1997). Downstream of Wnt signaling the activity of proteins of the TGF-β family, such as Nodal and Vg1, induces gastrulation (reviewed in (Chea, Wright, and Swalla 2005)). Interestingly, while *Nodal* mutants fail to complete gastrulation, this phenotype can be rescued by transplantation of only a few Nodal-expressing cells from wild-type embryos, suggesting that low levels of secreted Nodal are sufficient for gastrulation (Varlet, Collignon, and Robertson 1997). The positioning of the primitive streak is regulated by inhibitors of Nodal secreted in the lower layer of the embryo (Bertocchini and Stern 2002; Perea-Gomez et al. 2002). In addition, FGF signaling, interacting through a positive regulatory loop with Nodal, is required to maintain the EMT regulatory network (Ciruna and Rossant 2001; Mathieu et al. 2004). Snail1/2 are key to complete gastrulation; embryos lacking Snail activity fail to gastrulate, leading to an accumulation of epithelial cells still expressing E-cadherin that are unable to migrate (M. A. Nieto et al. 1994; M. Angela Nieto 2002). Finally, studies in mouse embryos revealed other transcription factors contributing to regulate EMT at gastrulation, such as Eomesodermin, which increases the ability of Snail to repress E-cadherin through an unknown mechanism, perhaps involving the induction of partners of Snail or modulating the availability of Snail-binding sites (Arnold et al. 2008). In other organisms, the. Wnt or Toll-Dorsal pathways enable the activation of Snail and Twist to activate EMT.

A revised concept of germ layer formation during gastrulation involves epithelial-mesenchymal plasticity, i.e., intermediate transition states, for endoderm formation. This involves the Forkhead box A2 (FOXA2) protein, an EMT inhibitor targeting Wnt signaling in the endoderm. Mesoderm progenitors (arising from $FOXA2^{low}$ epiblast progenitors) undergo a complete EMT to commit to a mesenchymal fate, while $FOXA2^{high}$ transitory progenitors (arising from $FOXA2^{+}$ posterior epiblasts) leaves the posterior epiblast epithelium collectively as intermediate cells. Once they reach the endoderm layer (Burtscher, Barkey, and Lickert 2013; Burtscher and Lickert 2009); $FOXA2^{high}$ transitory progenitors quickly re-establish the apical-basal polarity as they intercalate into the layer (Scheibner et al. 2021).

Finally, p53 regulation is important for normal development. This has been demonstrated in *Xenopus laevis*, where p53-deficient embryos fail mesoderm formation and exhibit severe gastrulation defects (Wallingford et al. 1997). However, although p53 seems required, its stabilization and activation is lethal at the late blastula stage, just before gastrulation, and the inhibition of p53 activity rescues the phenotype. Indeed, normally, p53 activity is repressed post-transcriptionally during gastrulation. Following mesoderm development, p53 becomes essential for mesendoderm differentiation and is released from inhibition by Aurora-A kinase after gastrulation (D.-F. Lee et al. 2012). p53 is also a critical regulator of neurulation, coordinating neural crest cell growth and EMT (Rinon et al. 2011). Indeed, consistent with a role in EMT inhibition, expression of p53 is negatively correlated with neural crest EMT in the chick. Although p53 is expressed in neural crest cells in chick embryos, its expression

decreases when cells delaminate from the neural tube. Stabilization of p53 results in reduced expression of Snail2, fewer migrating neural crest cells and craniofacial defects. By contrast, electroporation of a dominant-negative p53 construct increased EMT of neural crest cells migrating from the neural tube.

b) Wound healing & fibrosis

During kidney fibrosis, damaged epithelial cells undergo a partial EMT driven by Snail1/2 and Twist TFs (Arnoux et al. 2008; Grande et al. 2015; Hudson et al. 2009). This activation may occur through EGF-mediated signaling, as proposed in mouse skin explants. Partial EMT is crucial for fibrotic progression (Grande et al. 2015; Lovisa et al. 2015). Interestingly, in this case, the stable intermediate cells lose their epithelial markers and apicobasal polarity but remain confined in the tubules, without engaging into the delamination and invasion programs, contrary to EMT in development and cancer. They release cytokines and TGF-β, which converts pre-existing fibroblasts in the microenvironment into myofibroblasts. Myofibroblasts then produce proinflammatory cytokines to strengthen the immune response, such as IL-6, and IL-12 (Correa-Gallegos, Jiang, and Rinkevich 2021), collagen fibers and migrate into wounds (Correa-Gallegos et al. 2019). Importantly, TGF-B appears to be the main critical regulator in fibrotic diseases, (Kim et al. 2006; Willis et al. 2005), not only to stimulate the transdifferentiation and the proliferation of myofibroblasts, but also to induce the partial EMT program, as demonstrated in lung fibrosis (Grande et al. 2015; Willis and Borok 2007). Therefore, inhibition of TGF-β signaling by targeting Smad7 (Saika et al. 2004) or Smad3 (Sato et al. 2003) prevents fibrosis. TGF-β is the main inducer of Snail1 in different contexts, and, interestingly, activation of Snail1 alone in the adult kidney is sufficient to induce renal fibrosis and renal failure (Boutet et al. 2006). Thus, TGF-B-mediated EMT may rely on Snail1.

In contrast with developmental EMT, which requires transient inhibition of p53 activity, increased p53 levels have been correlated with fibrotic diseases in several organs. In mice, hepatocyte-specific MDM2 knockout, accompanied by p53 accumulation in hepatocytes, led to spontaneous liver fibrosis (Kodama et al. 2011). p53-mediated cell senescence and apoptosis may be a pre-requisite for organ fibrosis signaling (reviewed in (Bao et al. 2024)). In the adult mammalian heart, cardiomyocyte senescence plays a crucial role in the development of cardiac fibrosis. The released SASP factors, including TGF-β and IL-6, promote chronic inflammation, myofibroblast activation and collagen deposition, thereby progressively resulting in cardiac fibrosis (reviewed in (Osorio et al. 2023)). Finally, another aspect to consider is the connection between p53 signaling and other signaling pathways. In this case, several studies suggest that p53 could be involved in mediating TGF-β signaling; indeed, in a model of renal fibrosis, TGF-β promotes the phosphorylation and acetylation of p53 to stimulate the p53-SMAD3 complexes assembly (Y.-Y. Gu et al. 2020; Higgins et al. 2018).

c) Cancer

In cancer, many extra-cellular factors in the tumor microenvironment can induce EMT. Main sources of origin are hypoxia (Eskiizmir et al. 2018), changes in extracellular matrix density and rigidity (Fattet et al. 2020; Provenzano et al. 2009; Wei et al. 2015) and inflammation (D. Gao and Mittal 2012). Inflammation at the tumor site is characterized by the presence of immune cells which secrete growth factors like TGF-β (D. Gao and Mittal 2012) and cytokines like TNF-α, IL-6, and IL-8, which promote EMT in cancer cells (Bonde et al. 2012; Ieda et al. 2019; Toh et al. 2011). Carcinoma-associated fibroblasts (CAFs), frequently observed at the invasive front of tumors, are also expected to contribute to the induction of EMT in nearby carcinoma cells by secreting various cytokines. Moreover, Snail1 promotes cytokine expression, which can induce a positive feedback loop (J. G. Lyons et al. 2008). Therefore, EMT can be induced by multiple molecular pathways in the context of cancer. Consistently, the mechanisms that govern the intermediate phases of EMT are non-linear. Despite the efforts to identify common regulatory networks in cancer, it is clear that no pathway is universal, some may be unique to a given EMT event in a particular tissue or tumor subset. The process of EMT in cancer generally involves the combination of different pathways and high cellular plasticity, both enabling cells to adapt to their environment. Interestingly in a mouse model involving two EMT programs simultaneously, adding a TGF-β treatment prompted a switch towards the same program; this result indicated that, contrary to spontaneous EMT models, the use of inducers might bias the EMT towards one program, which does not reflect the mechanism in cancer (Aiello et al. 2018).

Finally, in cancer, both p53 wild type (WT) and defective contexts can occur. A growing body of evidence demonstrates that WT p53 negatively regulates EMT (Parfenyev et al. 2021). For instance, when p53 gets activated, the formation of a complex between p53, the ubiquitin ligase MDM2, and Snail2 triggers the degradation of Snail2 (S.-P. Wang et al. 2009). p53 also contributes to maintain an epithelial identity by directly activating the miR-200 family (Parfenyev et al. 2021). Therefore, loss of p53 confers aggressive mesenchymal phenotypes upon EMT induction (Semenov et al. 2022).

3.2. Epigenetic mechanisms

EMT is modulated at different levels by integrating epigenetic modifications, transcriptional control, alternative splicing, protein stability, and subcellular localization. Lineage studies in carcinoma cells led to the conclusion that, in the context of partial EMT (intermediate state), cells reduce their epithelial phenotype through post-transcriptional mechanisms (Aiello et al. 2018). Indeed, while in early intermediate cells, the epithelial gene transcription (based on epithelial markers mRNA levels) was persisting while their protein levels decreased. This observation is interesting and would require further investigations; such aspect should be considered when interpreting transcriptomes. Furthermore, many epigenetic factors affect upstream and downstream miRNA-Snail-ZEB networks (reviewed in (Bedi et al. 2014)). Snail1 can recruit numerous chromatin modifiers at gene promoters, including histone deacetylases 1 and 2 (HDAC1/2) (Peinado et al. 2004), lysine-specific demethylase 1 (LSD1) (Y. Lin

et al. 2010), components of PRC2 (Herranz et al. 2008), and histone methyltransferases (HMTs) such as Suv39H1 (C. Dong et al. 2013). In addition, Snail1 can also regulate heterochromatin transcription (Millanes-Romero et al. 2013). ZEB1 shows a similar activity, repressing target genes by recruiting writers and erasers at gene promoters, such as the LSD1-containing co-repressor complex (Jianxun Wang et al. 2007) as well as HDAC1/2 (Aghdassi et al. 2012). Furthermore, ZEB1 itself is affected by the HMT-mediated recruitment of PRC2 during human stem cell reprogramming (Y.-S. Chan et al. 2013). Therefore, multiple epigenetic changes initiated by inducers and EMT-TFs could confer a dynamic control over chromatin information.

3.2.1. microRNAs

miRNAs are endogenously expressed non-coding RNAs of ~22-nt length that negatively regulate the expression of their targeted genes post-transcriptionally. They bind to perfect or imperfect complementary sequences on mRNAs, termed miRNA recognition elements (MREs), leading to the degradation of the target mRNAs and/or inhibition of their translation (reviewed in (Bartel 2004)). miRNAs that selectively bind mRNAs which contribute to regulate the epithelial phenotype and EMT (reviewed in (Lamouille et al. 2013)). Many miRNAs control the expression of EMT master transcription factors. For example, miR-29b and miR-30a repress Snail1 expression in normal and cancer cells (Ru et al. 2012; Jingcheng Zhang et al. 2012). Therefore, increased miR-29b expression can reverse EMT and decrease cell invasion. Another well-characterized example is miR-200 which induces ZEB1/2 and Snail1/2 mRNA degradation. Thus, the forced expression of miR-200 is sufficient to block TGF-β-induced EMT (Gregory et al. 2008; Korpal et al. 2008; Park et al. 2008; H.-F. Zhang, Xu, and Li 2014). Once they are expressed, ZEB1/2 and Snail1/2 are able to repress miR-200 expression, forming a regulatory loop (Burk et al. 2008). In the same way, miR-34 can also target Snail family mRNA and Snail1/2, which themselves directly decrease the expression of miR-34 and thus constitute a similar regulatory loop (Morizane et al. 2014). In addition to controlling the expression of EMT transcription factors, miRNAs also target epithelial and mesenchymal genes, such as genes encoding adhesion junction and polarity complex proteins. For example, increased miR-9 expression in mammary carcinomas has been associated with the repression of E-cadherin expression increased mesenchymal phenotype; cell migration and invasion (L. Ma et al. 2010). Finally, miRNAs can be epigenetically regulated. The expression of miR-200 family members is regulated by the histone demethylase KDM5B (Enkhbaatar et al. 2013) and DNA methylation (Chung et al. 2016; Lim et al. 2013). The epigenetic modulation of miR-200 RNAs is associated with distinct states in HMLE cells and their gene cluster is silenced by PRCs in the stem-cell-like state.

3.2.2. Alternative splicing

In eukaryotes, nuclear coding genes are composed of coding sequences (exons) interspaced with non-coding sequences (introns). Transcription of nuclear genes by RNA polymerase II generate a pre-messenger RNA (pre-mRNA) which requires maturation to be a "functional" mRNA. It is only after this processing that the mRNA is translocated into the cytoplasm for its translation. Three major steps are necessary for mRNA maturation: (1) The 5' capping of one extremity, which protects RNA from 5' ribonucleases and is essential for the binding of the RNA to ribosomes during protein synthesis (Furuichi 2015), (2) the 3'polyadenylation of the other extremity to protect the mRNA from 3' ribonucleases (J. Zhao, Hyman, and Moore 1999), and (3) the splicing of introns, a process in which the non-coding regions of the transcript, called introns, are removed by excision while remaining exons are connected to produce a mRNA. Intron excision and exon linking are performed by a large complex called spliceosome, composed of proteins and small nuclear RNAs (snRNA) (De Conti, Baralle, and Buratti 2013). RNA splicing can occur post-transcriptionally, after complete synthesis of the RNA transcript and 5' and 3' maturation, and co-transcriptionally (Bentley 2014).

Two types of splicing exist: (1) Constitutive splicing concerns exons that are systematically inserted into the mature transcript, and (2) alternative splicing is a process during which specific exons can be included or skipped from the mature transcript (reviewed in (Black 2003)). Alternative splicing increases the number of mRNA produced by the same gene and, consequently, increases the number of alternative proteins that can be translated. This process is mediated by splicing factors that can be altered in cancer; their mutations or level changes associate with a global reprogramming (Anczuków and Krainer 2016). Alternative splicing occurs mostly co-transcriptionally (Oesterreich et al. 2016) and the elongation rate of RNA polymerase II influences the outcome. The processivity of the RNA polymerase II depends on chromatin structure and composition (Saint-André et al. 2011). Another mechanism that impacts splicing is through the recruitment of specific proteins at histone modifications to, in turn, recruit splicing factors (Luco et al. 2011).

During EMT, the process of alternative splicing leads to various additional proteins that regulate the transition, such as such factors involved in cytoskeleton remodeling, regulation of cell-cell junction formation, and regulation of cell migration (Shapiro et al. 2011). This EMT-driven alternative splicing program leads to an "EMT alternative splicing signature" which can be classified into basal and luminal subtypes in human breast cancer cell lines. Furthermore, EMT is marked by changes in the splicing of many mRNAs involved in the mesenchymal identity, such as p120 catenin (Yanagisawa et al. 2008), the adhesion protein cluster of differentiation 44 (CD44) (R. L. Brown et al. 2011) and the FGF receptor 2 (FGFR2) involved in mitogen signaling (Shirakihara et al. 2011). In particular, FGFR2 harbors two mutually exclusive exons IIIb and IIIc, respectively included in epithelial and mesenchymal cells. These exons are differentially enriched in histone marks that can be deposited by SET2 or EZH2: H3K36me3 and H3K27me3. In mesenchymal cells, the enrichment in H3K36me3 correlates with exon IIIb exclusion. Consistently, H3K36me3 is an anchoring platform for the chromatin adaptor MGR15 that in

turn recruits the splicing factor PTB to exon IIIb to prevent its inclusion (Luco et al. 2011). In a similar way, changes in splicing for CD44 are associated with changes in H3K9me3 enrichment that is recognized by HP1γ (Saint-André et al. 2011).

Epithelial specific regulatory proteins 1 and 2 (ESRP1/2) are major EMT splicing regulators (Bebee et al. 2015). Many of the changes in splicing during EMT result from the rapid downregulation of their expression, which results in mesenchymal protein isoforms (Warzecha et al. 2010). For example, in breast cancer, the repression of ESRP results in a CD44 isoform switching that promotes EMT and cancer progression (R. L. Brown et al. 2011). Conversely, OVOL1/2, major MET inducers, upregulate the expression of ESRP1 (Roca et al. 2013). These changes in splicing impose another layer of complexity on the gene expression changes that occur during EMT.

Finally, using CRISPR epigenome editing to induce site-specific changes in H3K27 methyl or acetyl levels, Segelle et al. showed that a local change in H3K27ac or H3K27me3 levels at an alternatively spliced exon (*CTNND1* exon 2 or *FGFR2* exon IIIc) is necessary and sufficient to induce a splicing change. This change is mediated by the direct recruitment of the splicing regulator PTB to its RNA binding sites. These results support a role for H3K27 PTMs in inducing a change in cell identity by regulating alternative splicing (Segelle et al. 2022). Importantly, such chromatin-induced change in splicing were sufficient to induce an EMT in MCF10A cells.

3.2.3. The role of histone variants in EMT

Induction of EMT programs triggers a cascade of cellular signaling molecules which interact closely with chromatin-modifying factors such as DMTs, HATs/HDACs, and HMT/LSDs. This results in global changes in DNA methylation and histone marks (including, but not limited to, H3K4me3, H3K4Ac, H3K27me3, and H3K9me3). This diverse epigenetic reprogramming accommodates the required activation of mesenchymal genes and the inhibition of epithelial genes (reviewed in (Skrypek et al. 2017)). Of note, data about the epigenetic regulation of EMT are scarce, and the role of histone variants has been only partially uncovered. Yet, in cancer, alterations in the expression of histone variants and their regulators frequently occur due to transcription defects or mutations, thereby impacting genome regulation (reviewed in (Buschbeck and Hake 2017; Ghiraldini, Filipescu, and Bernstein 2021; Ray-Gallet and Almouzni 2022)). Alterations in histone variant levels, functions and localizations can impact chromatin structure directly, or indirectly by impacting other factors such as splicing or transcription factors. Indeed, histone variants shape the genome landscape of the cells, which, in turn, controls major cellular events. Adding a new dimension to EMT regulation, this general function of histone variants can be exemplified in the case of EMT.

For example, the histone variant H2A.X, typically recognized for its role as a DNA damage sensor of DSBs (Collins et al. 2020; Firsanov, Solovjeva, and Svetlova 2011), may also play a key role in

regulating EMT. Studies have demonstrated that silencing or removing H2A.X promotes EMT in both human colon cancer cells and non-tumoral breast cells (Weyemi, Redon, Choudhuri, et al. 2016; Weyemi, Redon, Sethi, et al. 2016). Notably, this loss of H2A.X leads to upregulation of the transcription factors Snail2 and ZEB1 in colon cancer cells, while in breast cells, it instead promotes Snail2 and Twist1. Of interest, this data indicates that the effect mediated by H2A.X loss could be tissue specific. Furthermore, an inverse correlation has been observed between H2A.X expression and Twist1 levels across various breast cancer cell lines. Finally, the re-expression of H2A.X in colon cancer cells induces partial EMT reversal, and *in vivo* studies using a mouse model show that this reversal enhances metastatic colonization in the lung.

In another study, the loss of H2A.Z in *Xenopus* was found to impair the cell movements necessary for mesoderm and neural crest formation (Ridgway et al. 2004), both of which are critically dependent on EMT. In liver cancer cells, H2A.Z has been linked to cell migration signatures, with its knockdown significantly suppressing migratory, invasive, and wound-healing responses (S. Tang et al. 2020). These observations suggest that H2A.Z may act as a chromatin regulator of EMT. Supporting this idea, H2A.Z deletion is lethal in mouse at the preimplantation stage of the blastocyst (Faast et al. 2001). Further research using Madin-Darby Canine Kidney (MDCK) cells revealed that +1 H2A.Z nucleosomes (relative to the TSS) could repress the expression of key epithelial genes while other H2A.Z promoter nucleosomes were correlated with gene activation of mesenchymal genes (Domaschenz et al. 2017). This correlates with gene expression changes during EMT. Thus, H2A.Z might serve as both an activator and a repressor of epithelial and mesenchymal genes, potentially depending on its re-organization.

Another H2A variant, macroH2A, has a unique tripartite structure composed of an amino-terminal histone fold, an unstructured and highly basic linker region and a globular macro domain that protrudes from the core nucleosome structure. This variant is known to represent an epigenetic barrier to cellular reprogramming (Gaspar-Maia et al. 2013). Genomic analyses have shown that macroH2A is often enriched at pluripotency genes marked by H3K27me3, which are reactivated early during induced pluripotent stem (iPS) cell reprogramming. Notably, macroH2A knockout allows iPS cells to differentiate properly both *in vitro* and *in vivo*. In agreement with this model, macroH2A1.2 expression has been found to inhibit EMT (Pliatska et al. 2018). Interestingly, mesoderm-derived human fibroblasts can be efficiently reprogrammed into iPSCs through the exogenous expression of Yamanaka transcription factors (OCT4, SOX2, KLF4, and c-MYC) when combined with macroH2A1 depletion. Furthermore, EMT induction via Snail1 or Twist1 overexpression in HMLE cells leads to a significant reduction of macroH2A1, while ectopic macroH2A1 expression prevents EMT in these cells (Hodge et al. 2018). Conversely, macroH2A1 knockout alone is sufficient to induce EMT. These findings suggest that although macroH2A1 loss alone may not drive EMT, it likely acts as a barrier to reprogramming in the presence of other EMT-inducing factors.

Finally, regarding H3 histone variants, a recent study revealed that the exchange of H3.1/H3.2 for H3.3 precedes EMT and is essential for the acquisition of aggressive traits driven by TGF-β and TNFα (A. P. Gomes et al. 2019). Metastatic/EMT inducers promote a decrease in total nucleosome abundance in chromatin and regulate histone chaperones to decrease, in particular, the incorporation of H3.1/H3.2, thereby promoting the deposition of the H3.3 variant as a "gap-filling" mechanism. This exchange is both necessary and sufficient for inducing the aggressive characteristics required for metastasis formation. Supporting this, experimental suppression of the CAF-1 complex in breast cancer cells reduced H3.1/H3.2 incorporation, leading to increased H3.3 deposition. This, in turn, triggered chromatin remodeling and the expression of genes associated with metastasis.

QUESTION

The centromeric variant of histone H3, called CENP-A (Centromere Protein A) in mammals, marks centromere and is deposited by the chaperone HJURP (Dunleavy et al. 2009; Foltz et al. 2009). CENP-A defines epigenetically the centromere position (Fachinetti et al. 2013) and provides the foundation for building the kinetochore (Ali-Ahmad and Sekulić 2020b), of critical importance for proper segregation of human chromosomes during cell division. Therefore, the maintenance of genome integrity depends on the proper regulation of CENP-A. Interestingly, at a transcriptional level, this regulation involves a p53-dependent transcriptional repression (Filipescu et al. 2017). However, when compared to healthy tissues, CENP-A expression levels increase in many cancers, an increase that strongly correlates with tumor aggressiveness in over 20 cancer types (Lacoste et al. 2014; Renaud-Pageot et al. 2022; X. Sun et al. 2016). Beyond the p53-transcriptional regulation, additional levels of control should be considered, which is underlined by TCGA PanCancer Atlas studies showing that both p53-defective and p53 wild type cancers can display high levels of CENP-A. Furthermore, studies in cell lines showed that overexpression or abnormal upregulation of endogenous CENP-A leads to its association with other H3 chaperones (in addition to HJURP) and ectopic localization of CENP-A at non-centromeric regions (Lacoste et al. 2014). Thus, to understand how CENP-A overexpression could contribute to cancer aggressiveness, a major objective that arises is to characterize how CENP-A overexpression and subsequent mislocalization impact cell fate. Thus, during my Ph.D., I aimed at elucidating how CENP-A overexpression participates in cell fate changes that may guide cancer evolution, considering the cellular context.

To this end, during the course of my Ph.D., I have tried to address these fundamental questions:

How does CENP-A overexpression impact cell fate and response to therapy?

Does p53 influence the way CENP-A overexpression impacts cell fate?

Does CENP-A overexpression impact resistance to a DNA damaging agent (X-irradiation)?

Does it impact cell state (cell cycle, proliferation) and/or cell identity (stemness, differentiation)?

How does CENP-A overexpression promote changes in cell identity?

Does CENP-A alter cell identity in any context?

Does it rely on changes at centromere and/or at chromosome arms?

Is it promoted by genetic and/or non-genetic modifications? Is it reversible?

RESULTS

GENERAL APPROACHES AND METHODOLOGY

In order to explore the impact of CENP-A expression levels on human cells, I capitalized on a tunable system which relies on a doxycycline-inducible CENP-A overexpression construct (Tet-On–CENPA–FLAG–HA), stably integrated into human cell lines by lentiviral transduction (Figure 24). This system enables to bypass p53 regulation of CENP-A expression, and to induce and reverse CENP-A overexpression at will by adding and removing doxycycline from the cell media. Doxycycline was renewed every 2-3 days in the growth media in order to maintain constant overexpression of CENP-A. Importantly, CENP-A overexpression levels are within the range of those found in patient tumors.

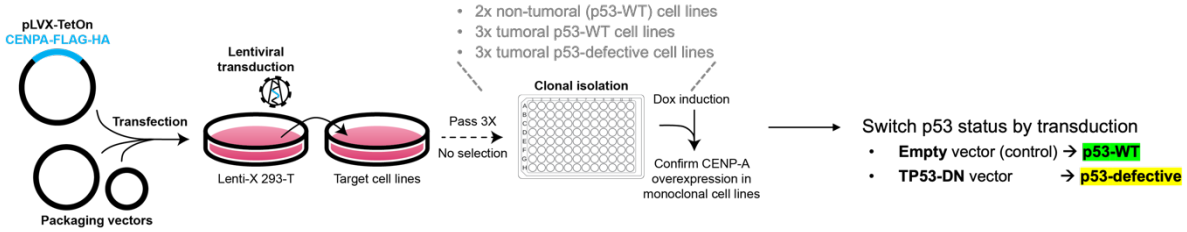


Figure 24. Doxycycline-inducible CENP-A overexpression in human cell lines.
Schematic representation of the methods used to generate a tunable CENP-A-overexpression system.

To assess the impact of CENP-A overexpression in various contexts, I used this system in several human epithelial cell lines. Additionally, to switch the p53 status in a same cell line, MCF10-2A and RPE-1 cell lines were stably transduced with either an empty vector (control, remains p53-WT) or a vector constitutively expressing a dominant negative TP53 construct that mimics p53 loss of function (DN, p53-defective). In the p53-DN context, p53 missense mutant proteins are constitutively expressed. They have a dominant negative effect by forming tetramers with wild type p53, thus interfering with their transcriptional activation function.

For a typical experiment, doxycycline is added at a 10 ng/ml concentration (considered 1X), thus increasing the total CENP-A protein levels by approximately 12-fold. Typical staining in CSK-extracted nuclei is presented below.

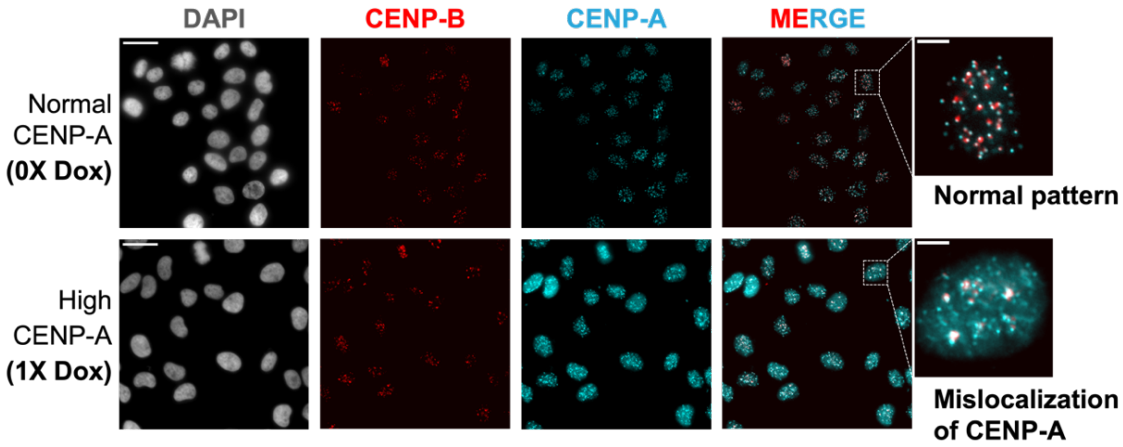


Figure 25. Induction of CENP-A overexpression in the MCF10-2A cell line (human breast epithelial). CENP-B (red) and CENP-A (blue) staining in CSK-T extracted cells, with DAPI counterstaining (grey). Scale bars = 20 µm (left), 10 µm (right, zooms).

PART 1. CENP-A OVEREXPRESSION PROMOTES DISTINCT FATES IN HUMAN CELLS, DEPENDING ON P53 STATUS

Published in Comm. Biol. (2021)

Daniel Jeffery [1], Alberto Gatto [1], Katrina Podsypanina [1], Charlène Renaud-Pageot [1], Rebeca Ponce Landete [1], Lorraine Bonneville [1], Marie Dumont [2], Daniele Fachinetti [2], Geneviève Almouzni [3]

1. RATIONALE AND CONTRIBUTION

During my Ph.D., I had the chance to participate in a collaborative work with team members, including my thesis co-supervisor Daniel Jeffery.

CENP-A overexpression in cancer correlates with tumor aggressiveness, invasiveness, and metastatic development. However, previous studies investigating the correlation of high CENP-A levels with response to cancer therapy had shown contrasting results, indicating that the level of CENP-A should be considered in a given context. The expression of CENP-A can evade p53 regulation and is found to be aberrant in both wild-type and p53-defective cancers. This distinction was not considered in early studies linking CENP-A and cancer but could be decisive for tumor evolution and therapeutic sensitivity. Thus, the objective of this project was to determine the impact of CENP-A overexpression on cell fate and resistance to therapy depending on the p53 status of the cells.

In order to explore the impact of CENP-A expression levels on human cells, I developed and characterized our CENP-A inducible system in five human epithelial cell lines to assess the impact of CENP-A overexpression in various contexts. I performed clonogenic survival assays after X-irradiation on the p53-WT cells. This way, we found that CENP-A overexpression strongly increases sensitivity to X-irradiation in p53-WT cell lines, whereas cells are tolerant to X-irradiation in a p53-defective context. Daniel Jeffery and collaborators used bulk and single-cell RNA-seq, performed in p53-WT and p53-DN MCF10-2A cells after 24 hours (acute) or 69 days (chronic) CENP-A overexpression. Their transcriptomic analysis showed that, upon CENP-A overexpression, p53-WT cells exit from cell cycle and arrest. In contrast, in p53-DN cells, this arrest was severely reduced, and CENP-A overexpression led to a strong increase in a distinct cell population with mesenchymal properties. I then performed FACS and immunofluorescence microscopy analyses to confirm the impact of CENP-A overexpression on cell cycle and identity. Taken together, our results demonstrate that CENP-A overexpression affects cell fate in a manner that is dependent on the p53 status in our system. Data discussion and manuscript corrections involved all authors. These results have been published in *Communications Biology* in 2021.

2. RESULTS

Results are detailed below. A copy of the full manuscript, including the abstract, introduction and references, is provided in the appendix.

Inducible and reversible CENP-A overexpression in cells with varied p53 status

In order to explore how CENP-A expression levels and p53 status impact cell fate and cell response to anti-cancer treatment, we first established a system where we could specifically alter CENP-A expression independent of its regulation by p53. For this, we added a doxycycline-inducible CENP-A overexpression construct (*TetOn-CENPA-FLAG-HA*) by lentiviral transduction into several cell lines with varied p53 status (Figure 1A, see also Methods). Importantly, we did not use antibiotic selection to obtain CENP-A overexpression. This enables us to investigate the unbiased effects of CENP-A overexpression over time, without provoking cell adaptations or secondary mutations that could arise from selective pressure. The TetOn system allows induction of CENP-A overexpression within 24h of adding doxycycline (Figure 1B-D, see also Figure S1A). This acute induced overexpression of CENP-A increases HJURP protein levels (Figure 1C), increases levels of CENP-A at centromeres and also causes mislocalization of CENP-A to the chromosome arms (Figure 1D), regardless of p53 status. These effects are similar to those observed with constitutive CENP-A overexpression in HeLa cells[44]. Here, however, we could reverse both CENP-A overexpression and mislocalization simply by washing out doxycycline (Figure 1C-D), consistent with the observation of rapid removal of ectopic CENP-A from chromosome arms with DNA replication[45]. Thus, we had at hand an efficient and reliable system to test therapeutic sensitivity in several cell lines with varied p53 status under conditions of tunable CENP-A overexpression.

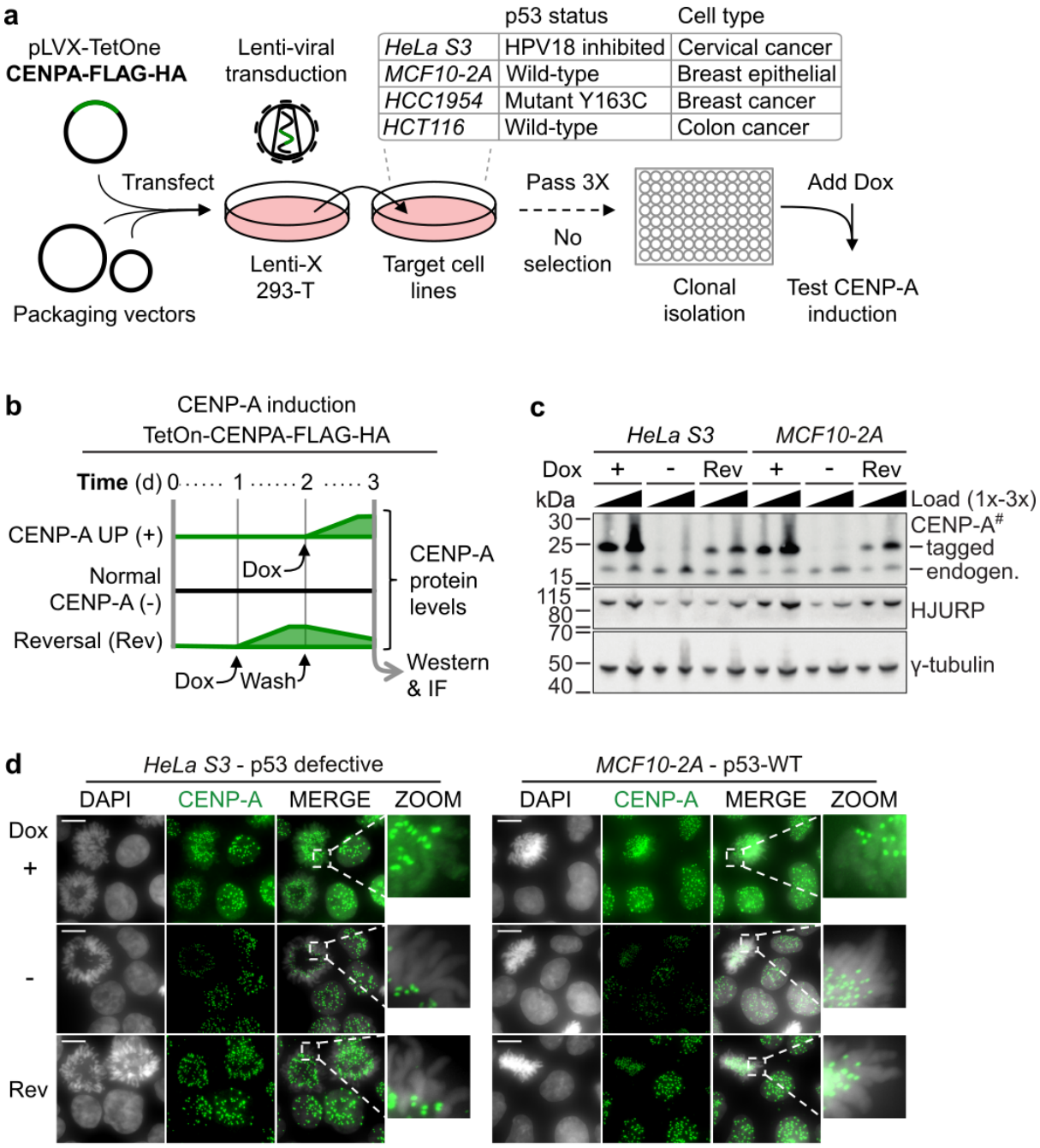

a
pLVX-TetOne
CENPA-FLAG-HA
Lenti-viral
transduction
Transfect
Packaging vectors
Lenti-X
293-T
Target cell
lines
p53 status
Cell type
HeLa S3
HPV18 inhibited
Cervical cancer
MCF10-2A
Wild-type
Breast epithelial
HCC1954
Mutant Y163C
Breast cancer
HCT116
Wild-type
Colon cancer
Pass 3X
No
selection
Clonal
isolation
Add Dox
Test CENP-A
induction
b
CENP-A induction
TetOn-CENPA-FLAG-HA
Time (d) 0 1 2 3
CENP-A UP (+)
Normal
CENP-A (-)
Reversal (Rev)
Dox
Dox
Wash
CENP-A
protein
levels
Western
& IF
c
HeLa S3
MCF10-2A
Dox
+
-
Rev
+
-
Rev
kDa
Load (1x-3x)
30
25
15
115
80
70
50
40
CENP-A#
tagged
endogen.
HJURP
γ-tubulin
d
HeLa S3 - p53 defective
MCF10-2A - p53-WT
DAPI
CENP-A
MERGE
ZOOM
DAPI
CENP-A
MERGE
ZOOM
Dox
+
-
Rev

Figure 1

Figure 1 – Inducible and reversible CENP-A overexpression in cells with varied p53 status
(A) Scheme for the generation of doxycycline (Dox) inducible CENP-A overexpression cell lines. *TetOn-CENPA-FLAG-HA* construct was randomly integrated into several indicated target cell lines by lentiviral transfection without selection. After clonal isolation, we tested cells for clear homogenous CENP-A and HA increase by IF in approximately all cells 24h after the addition of 80 ng/ml of Dox. Cells were also tested to ensure no detectable background HA signal by Western or IF, when no Dox was added. (B) Scheme representing relative CENP-A protein levels over time for *TetOn-CENPA-FLAG-HA* cell lines. Dox = 10 ng/ml. (C) Western blot of total cell extracts (TCEs) pertaining to scheme in B. Primary antibodies indicated on the right. Exogenous CENP-A (tagged) can be distinguished from endogenous CENP-A (endogen.) by its increased molecular weight. # = high sensitivity ECL. y-tubulin used as loading control. See also Figure S1A for Western blot analysis corresponding to all cell lines.
(D) Immunofluorescence of paraformaldehyde-fixed cells using anti-CENP-A antibody (green) and DAPI staining (grey). Conditions in parallel with C. Showing max projection images from a Z-series with zoom on a mitotic cell (DAPI/CENP-A merge) to highlight chromosome arms. Scale bars = 10 μm.

Induced CENP-A overexpression causes reversible radiosensitivity in p53-WT cells

To test therapeutic sensitivity in our cell lines, we chose X-irradiation as a representative DNA damaging agent that is commonly used in cancer therapy. Thus, we tested cell survival after X-irradiation with or without induction of CENP-A overexpression by colony formation assays (CFAs), a surrogate for self-renewal capacity (Figure 2A). For cell lines with wild-type (WT) p53 status, we used both non-tumoural (MCF10-2A) and tumoural (HCT116) lines. CENP-A overexpression in these cells led to a strong increase in sensitivity to X-irradiation, independent of tumoural status. Meanwhile, CENP-A overexpression in all cell lines with defective p53 (HeLa S3, HCC1954 and DLD1) did not significantly affect radiosensitivity – a distinctly radio-tolerant phenotype (Figure 2B, see also Figure S1B). To assess if these distinct CFA phenotypes could be explained by the different CENP-A levels associated with each cell line, we first compared by Western blotting the levels of endogenous CENP-A and CENP-A overexpression in all cell lines used (Figure S1A). Since our data do not show a correlation between CENP-A levels and radiosensitivity upon CENP-A overexpression, we can discard this explanation. Second, in order to determine if the differences in sensitivity that we observed upon CENP-A overexpression were due to secondary mutations from mitotic defects, we tested the reversibility of this sensitivity by tuning down CENP-A expression to near-endogenous levels in p53-WT cells (MCF10-2A) and p53 defective cells (HeLa S3) (Figure 2C). Remarkably, restoration of CENP-A expression to endogenous levels reversed the sensitivity phenotype in MCF10-2A, while HeLa cells, used here as a control line, remained tolerant (Figure 2D). Therefore, the radiosensitivity observed in MCF10-2A cells requires the continued overexpression of CENP-A and it cannot be explained by genetic effects (i.e. secondary mutations) that occur after induced CENP-A overexpression. Thus, CENP-A overexpression in both tumoural and non-tumoural cell lines leads to radiosensitivity in a manner that correlates with p53 status.

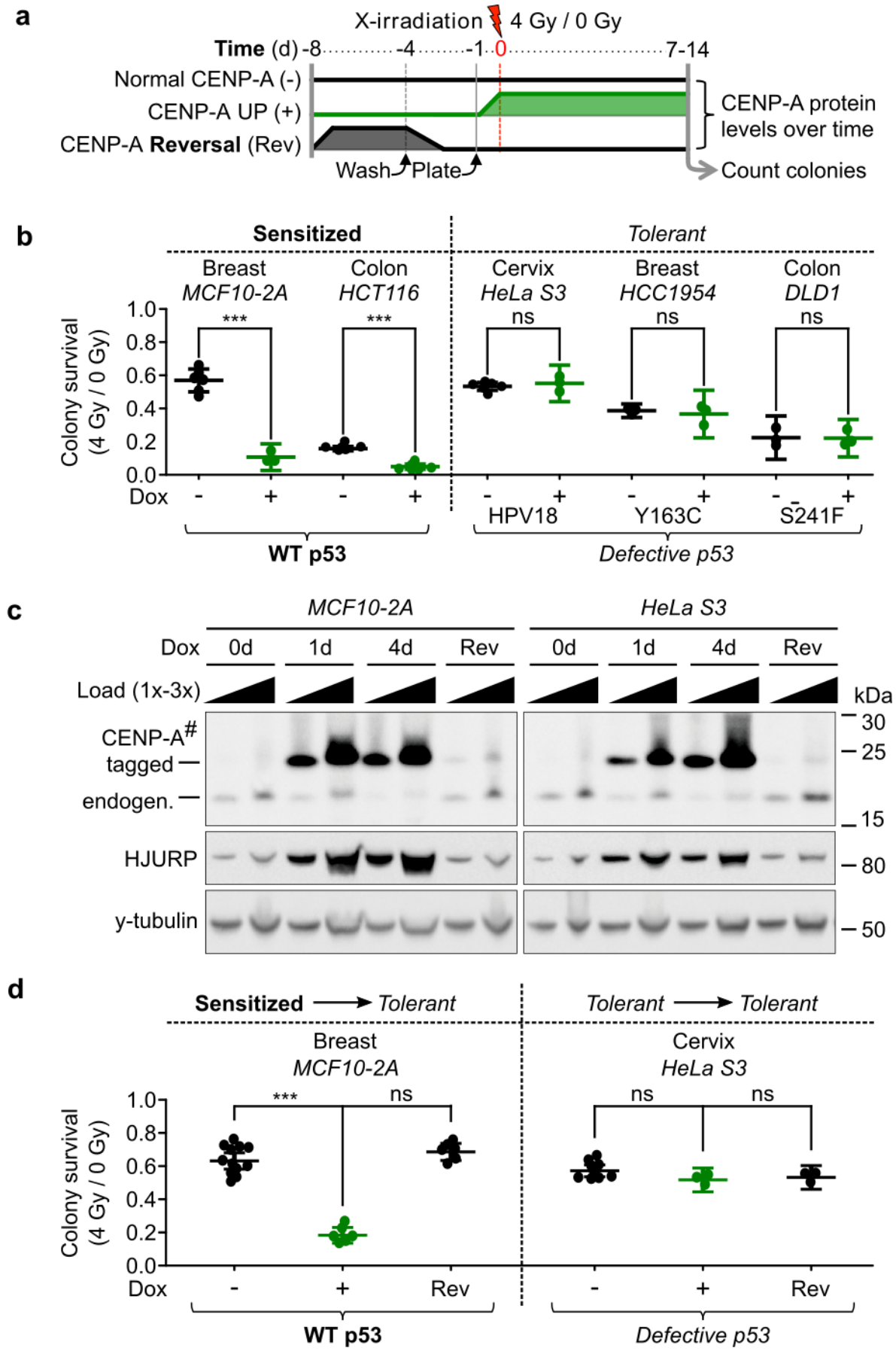

a
X-irradiation
4 Gy / 0 Gy
Time (d) -8
-4
-1
0
7-14
Normal CENP-A (-)
CENP-A UP (+)
CENP-A Reversal (Rev)
CENP-A protein levels over time
Wash
Plate
Count colonies
b
Sensitized
Tolerant
Breast
MCF10-2A
Colon
HCT116
Cervix
HeLa S3
Breast
HCC1954
Colon
DLD1
***
***
ns
ns
ns
Colony survival (4 Gy / 0 Gy)
1.0
0.8
0.6
0.4
0.2
0.0
Dox
-
+
-
+
-
+
-
+
-
+
HPV18
Y163C
S241F
WT p53
Defective p53
c
MCF10-2A
HeLa S3
Dox
0d
1d
4d
Rev
0d
1d
4d
Rev
Load (1x-3x)
kDa
CENP-A#
tagged
endogen.
30
25
15
HJURP
80
y-tubulin
50
d
Sensitized → Tolerant
Tolerant → Tolerant
Breast
MCF10-2A
Cervix
HeLa S3
***
ns
ns
ns
Colony survival (4 Gy / 0 Gy)
1.0
0.8
0.6
0.4
0.2
0.0
Dox
-
+
Rev
-
+
Rev
WT p53
Defective p53

Figure 2

Figure 2 – Induced CENP-A overexpression causes reversible radiosensitivity in p53 wild-type cells

(A) Scheme of colony formation assays (CFAs) with relative CENP-A protein levels over time for *TetOn-CENPA* cell lines. (B) CFA results corresponding to the scheme in A for five different cell lines of varied tissue origins and p53 status, as indicated. Each dot represents a single biological replicate. Plots show mean and 95% confidence interval. Statistical significance tested by two-tailed Welch's t-test with Bonferroni cutoff at a p-value of 0.01 ($\alpha = 0.05$). *** = p-value <0.0001. See also Figure S1B for survival ratios relative to untreated condition. (C) Western blot corresponding to scheme in A: TCEs after 1 day (1d) or 4d with 10 ng/ml Dox, no Dox control (0d), or 4d Dox followed by 4d without Dox (Rev). Primary antibodies indicated on the left. 1x load = ~30000 cells. # = high sensitivity ECL exposure. y-tubulin used as loading control. (D) CFA results corresponding to scheme in A for the indicated cell lines. Plots as in B. Statistical significance tested by two-tailed Welch's t-test, compared to non-induced control, with Bonferroni cutoff at a p-value of 0.0125 ($\alpha = 0.05$). *** = p-value <0.0001.

Sensitivity to X-irradiation upon CENP-A overexpression is dependent on functional p53

To assess if p53 plays a causal role in the radiosensitivity associated with CENP-A overexpression, we took advantage of the possibility to switch the p53 status in two of our inducible CENP-A overexpression cell lines: the tolerant HeLa cells and the sensitized MCF10-2A cells. We could thus carry out CFAs after CENP-A overexpression and X-irradiation in isogenic cell lines, but with altered p53 status (Figure 3A). For the change from p53-defective to p53-WT in the CENP-A inducible HeLa cells, we transiently activated WT p53 by incubation at 42°C for 1h immediately prior to X-irradiation. This treatment enables the temporarily release of p53 repression from the HPV18 E6 protein, permitting a functional p53 response[47]. We confirmed that after hyperthermia treatment, p53 levels increased, followed shortly after by increased p21 (Figure 3B-C). This short hyperthermia treatment in HeLa cells was sufficient to mildly, but significantly, increase sensitivity to X-irradiation after CENP-A overexpression (Figure 3D). The fact that we find an increase in sensitivity only when CENP-A is overexpressed is consistent with the hypothesis of an effect dependent on the transient reactivation of p53, however, we cannot exclude potential effects of hyperthermia independent of p53. In this regard, it was important to specifically alter only the p53 status in a controlled manner. For this, we stably transduced the p53-WT MCF10-2A *TetON-CENPA-FLAG-HA* cells with either an empty vector control or a constitutively expressed dominant negative (DN) *TP53* construct, in order to mimic p53 loss and p53 loss of function (LOF) mutations (p53DD construct[46]). The p53-DN peptide stabilizes the WT p53 protein, causing a clear increase in p53 protein level, but suppresses its activation of downstream targets (e.g. p21). Indeed, the indirect activator of p53 (Nutlin-3) caused clear increases in p53 and p21 in p53-WT cells, but not those expressing the p53-DN peptide (Figure 3E). By stably switching p53 status in this manner, we observed a major change in the radiosensitivity of the cells. The p53-DN peptide in MCF10-2A cells strongly counteracted the radiosensitivity phenotype associated with CENP-A overexpression (Figure 3F). Furthermore, we confirmed the radiosensitivity phenotype using a range of doxycycline concentrations and a range of X-irradiation doses in CFAs for the p53-WT and p53-DN MCF10-2A cells (Figure S1B-C). Taken together, the results demonstrate that induced CENP-A overexpression increases radiosensitivity in a p53-dependent manner.

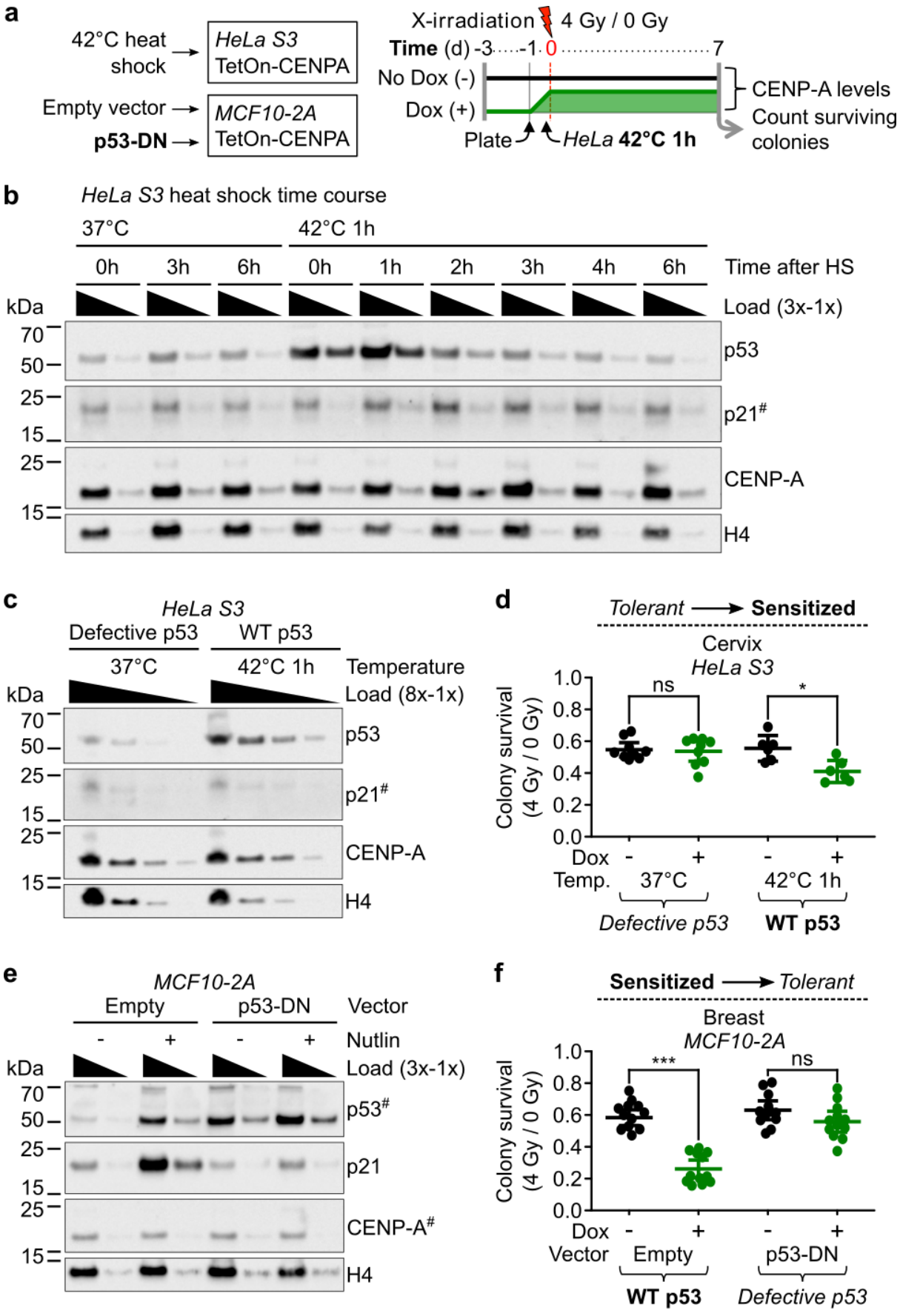

a
42°C heat shock
HeLa S3 TetOn-CENPA
Empty vector
p53-DN
MCF10-2A TetOn-CENPA
X-irradiation 4 Gy / 0 Gy
Time (d) -3 -1 0 7
No Dox (-)
Dox (+)
Plate
HeLa 42°C 1h
CENP-A levels
Count surviving colonies
b
HeLa S3 heat shock time course
37°C
42°C 1h
0h 3h 6h 0h 1h 2h 3h 4h 6h
Time after HS
kDa
Load (3x-1x)
70
50
25
15
25
15
p53
p21#
CENP-A
H4
c
HeLa S3
Defective p53
WT p53
37°C
42°C 1h
Temperature
kDa
Load (8x-1x)
70
50
25
15
25
15
p53
p21#
CENP-A
H4
d
Tolerant → Sensitized
Cervix
HeLa S3
Colony survival (4 Gy / 0 Gy)
1.0
0.8
0.6
0.4
0.2
0.0
ns
*
Dox - + - +
Temp. 37°C 42°C 1h
Defective p53
WT p53
e
MCF10-2A
Empty
p53-DN
Vector
- + - +
Nutlin
kDa
Load (3x-1x)
70
50
25
15
25
15
p53#
p21
CENP-A#
H4
f
Sensitized → Tolerant
Breast
MCF10-2A
Colony survival (4 Gy / 0 Gy)
1.0
0.8
0.6
0.4
0.2
0.0
***
ns
Dox - + - +
Vector Empty p53-DN
WT p53
Defective p53

Figure 3

Figure 3 – Sensitivity to X-irradiation upon CENP-A overexpression is dependent on functional p53

(A) Scheme of Colony Formation Assays (CFAs) and change of p53 status with relative CENP-A protein levels over time for *TetOn-CENPA-FLAG-HA* cell lines. WT p53 is transiently activated in HeLa cells by a short heat shock, while p53 is stably inactivated in MCF10-2A cells by expression of a p53 dominant-negative peptide (p53-DN). (B) Temporary change of p53 status in HeLa cells by 1h heat shock (HS). Western blot of HeLa cell TCEs at indicated time points following 1h at 42°C or 37°C control. Temporary increase of p53 and subsequently p21. 1x load = ~33000 cells. Primary antibodies are indicated on the right. $^{\#}$ = high sensitivity ECL exposure. H4 used as loading control. (C) Increase of p53 levels in HeLa cells by heat shock. Western blot of TCEs after 1h at 42°C or 37°C control. Loaded at 8x, 4x, 2x, 1x concentrations, where 1x load = ~12500 cells. Primary antibodies are indicated on the right. $^{\#}$ = high sensitivity ECL exposure. H4 used as loading control. Representative Western blot from three independent experiments is shown. (D) HeLa S3 CFAs pertaining to scheme in A. Each dot represents a single biological replicate. Plots show mean and 95% confidence interval. Statistical significance tested by two-tailed Welch's t-test with Bonferroni cutoff at a p-value of 0.0125 ($\alpha = 0.05$). * = p-value <0.01. (E) Change of p53 status in MCF10-2A TetOn-CENPA-FLAG-HA cells. Western blot of TCEs after 24h of 10 μM Nutlin-3 treatment or DMSO control, as indicated. Dominant negative p53 peptide stabilizes p53 and suppresses its activation of p21. 1x load corresponds to total protein extract from ~30000 cells. Primary antibodies are indicated on the right. $^{\#}$ = high sensitivity ECL exposure. H4 used as loading control. Representative Western blot from three independent experiments is shown. (F) MCF10-2A CFAs pertaining to scheme in A. Each dot represents a single biological replicate. Plots show mean and 95% confidence interval. Statistical significance tested by two-tailed Welch's t-test with Bonferroni cutoff at a p-value of 0.0125 ($\alpha = 0.05$). *** = p-value <0.0001. See also Figure S1B-C for CFAs following range of Dox and X-irradiation doses and Figure S1D for representative CFA images.

Induced CENP-A overexpression promotes radiosensitivity by impairing cell cycle progression

Given that the p53-dependent radiosensitivity was due to non-genetic (reversible) effects of CENP-A overexpression, we decided to assess changes at the transcriptional level. We first assessed global transcription by RNA-seq, analyzing the effects of acute CENP-A overexpression (at two different concentrations of Dox), switch of p53 status, and X-irradiation treatment in the MCF10-2A cells (Figure 4A). X-irradiation and inactivation of p53 affected the transcription of several genes (Figure 4B). Notably, CENP-A overexpression induced more extensive changes, with more than 8000 genes affected. According to Gene Set Enrichment Analysis (GSEA), CENP-A overexpression mainly led to the repression of genes involved in cell cycle progression, DNA repair and RNA metabolism (Figure 4C, details in Table S1). To more specifically identify the key cellular pathways involved in radiosensitivity and its reversal by inactivation of p53, we applied hierarchical clustering to identify co-regulated subsets of differentially expressed genes (DEGs). In particular, we wanted to identify genes for which p53-DN could counteract the effects of CENP-A overexpression. Out of ten clusters (Figure 4D, see also Figure S2C), there was only one that corresponded to these criteria (Cluster 8). This subset of genes is strongly downregulated by CENP-A overexpression and upregulated by p53-DN (Figure 4E). Importantly, this upregulation is further increased after X-irradiation (see Table S1 for significance testing). Importantly, we verified whether the effect of CENP-A overexpression on these genes also extends to cancer cell lines with different genetic backgrounds. We performed RT-qPCR of selected Cluster 8 genes after CENP-A overexpression in the p53-WT HCT116 and p53-defective DLD1 colon cancer cell lines for comparison. CENP-A overexpression decreased the relative expression of this group of genes in the p53-WT HCT116 cell line, and had a somewhat reduced effect in the p53-defective DLD1 cells (Figure S2D). The fact that these data are consistent with the effects observed in MCF10-2A p53-WT and p53-DN cells further emphasizes the importance of this core set of genes. Over-representation analysis shows that these genes are mainly involved in cell cycle control, followed by DNA repair (Figure 4E, bottom). We then used cellular assays to investigate the effects of CENP-A overexpression and p53 inactivation on these two pathways. Concerning DNA repair, we did not detect significant changes in either acute DNA damage or rate of DNA repair (Figure S3A-D). However, on a longer timescale, we observed an increase in mitotic stress associated with CENP-A overexpression that was similar in both p53-WT and p53-DN cells (micronuclei in Figure 4F, and CIN in Figure S3E, including numerical and structural aneuploidy by mFISH karyotypes). This is in agreement with previous studies[29,48]. In the p53-WT cells, this mitotic stress was associated with p53 activation, as shown by Western blot (Figure S3F). As for cell cycle control, CENP-A overexpression leads to prolonged growth inhibition, even in the absence of irradiation (Figure 4G). This is consistent with the reduced colony size and colony density visible in the CFA stains (Figure 1SD). Importantly, this growth inhibition is amplified with increased Dox and is partially counteracted by p53-DN (Figure 4G, see also Figure S3G for control). These findings enabled us to discard a major role for DNA damage or repair

in the radiosensitivity phenotype. Therefore, based on both the bulk RNA-seq data and cellular assays, we conclude that induced CENP-A overexpression leads to p53-dependent radiosensitivity mainly by impairing cell cycle progression. We then wished to understand how this was operating at the level of individual cells.

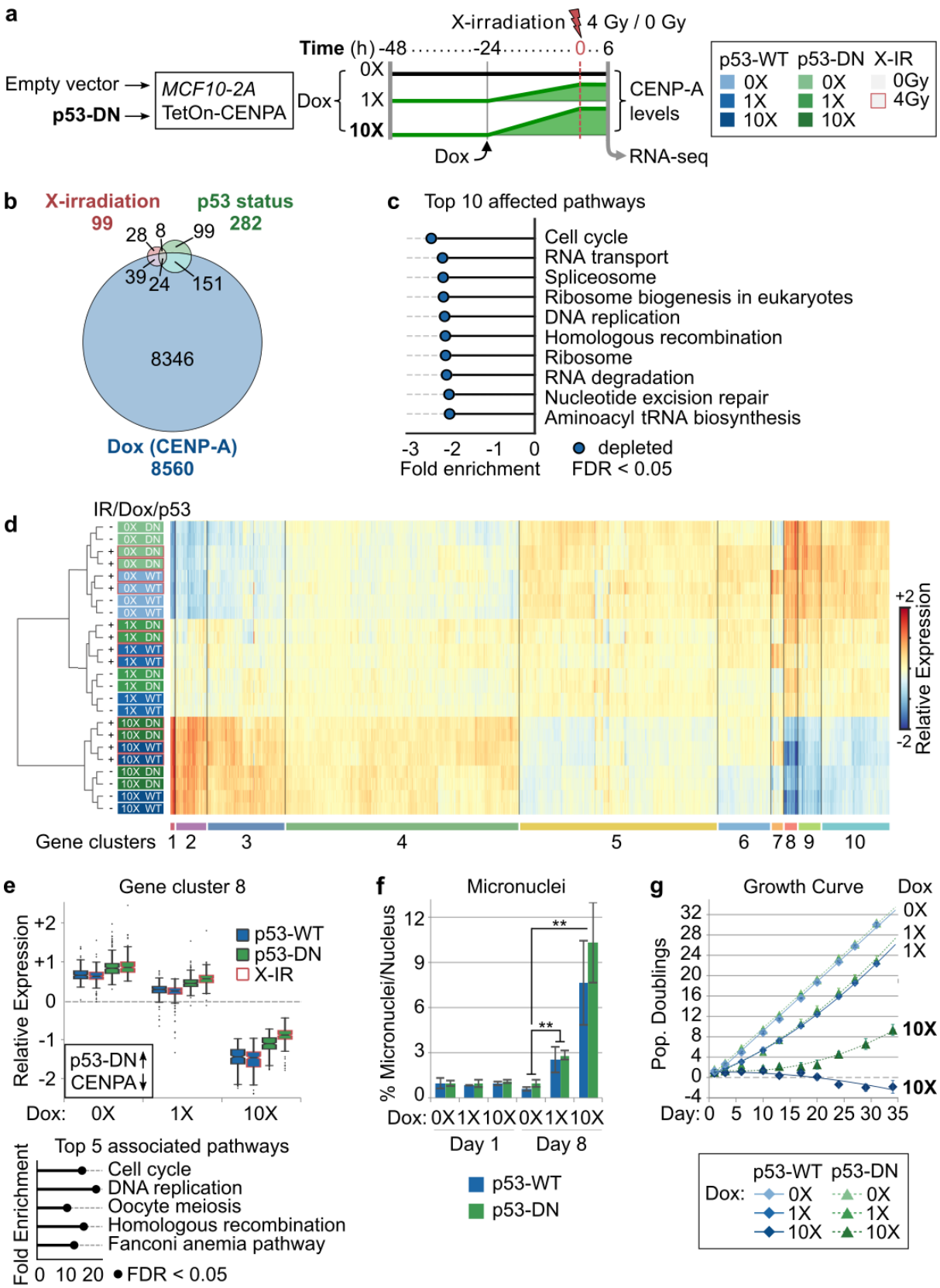

a
X-irradiation
4 Gy / 0 Gy
Time (h) -48 -24 0 6
Empty vector
p53-DN
MCF10-2A
TetOn-CENPA
Dox
0X
1X
10X
CENP-A
levels
RNA-seq
p53-WT p53-DN X-IR
0X 0X 0Gy
1X 1X 4Gy
10X 10X
b
X-irradiation
99
p53 status
282
28 8 99
39 24 151
8346
Dox (CENP-A)
8560
c
Top 10 affected pathways
Cell cycle
RNA transport
Spliceosome
Ribosome biogenesis in eukaryotes
DNA replication
Homologous recombination
Ribosome
RNA degradation
Nucleotide excision repair
Aminoacyl tRNA biosynthesis
-3 -2 -1 0
Fold enrichment
depleted
FDR < 0.05
d
IR/Dox/p53
0X DN
0X WT
1X DN
1X WT
10X DN
10X WT
Relative Expression
+2
-2
Gene clusters 1 2 3 4 5 6 7 8 9 10
e
Gene cluster 8
Relative Expression
p53-WT
p53-DN
X-IR
p53-DN↑
CENPA↓
Dox: 0X 1X 10X
Top 5 associated pathways
Fold Enrichment
Cell cycle
DNA replication
Oocyte meiosis
Homologous recombination
Fanconi anemia pathway
0 10 20
FDR < 0.05
f
Micronuclei
% Micronuclei/Nucleus
Dox: 0X 1X 10X 0X 1X 10X
Day 1 Day 8
p53-WT
p53-DN
g
Growth Curve
Dox
Pop. Doublings
Day: 0 5 10 15 20 25 30 35
0X
1X
1X
10X
10X
p53-WT p53-DN
Dox: 0X 0X
1X 1X
10X 10X

Figure 4

Figure 4 – Induced CENP-A overexpression promotes radiosensitivity by impairing cell cycle progression

(A) Scheme delineating conditions tested by RNA-sequencing showing relative CENP-A protein levels over time and corresponding legend (pertains to D). All conditions tested in duplicate. See Figure S1E for CENP-A protein levels corresponding to 0X, 1X (10 ng/ml) and 10X (100 ng/ml) Dox. The transcriptional impact of Dox treatment alone was tested in the non-inducible MCF10-2A parental control (See Figure S2A-B). (B) Proportional Venn diagram summarizing the number of differentially expressed genes (DEGs) upon X-irradiation (Red, 0 Gy vs 4 Gy); change of p53 status (Green, p53-WT vs p53-DN); and CENP-A overexpression (Blue, 0X Dox vs 1X Dox vs 10X Dox). Number of DEGs in each category and overlapping categories is indicated. (C) Gene Set Enrichment Analysis showing the top ten KEGG pathways affected by CENP-A overexpression (WebGestaltR v0.4.2) and normalized enrichment score. All ten pathways are downregulated with increasing levels of Dox (i.e. significant depletion, at FDR < 0.05). See Table S1 (GSEA) for all significantly depleted/enriched processes. (D) Heat map showing hierarchical clustering of samples (rows, coloured according to legend in A) and DEGs (columns), with the 10 main gene clusters annotated below. Relative expression: expression relative to the average for a given gene across all conditions (mean-centered counts, $\log_2$-transformed and TMM-normalized). See also Table S1 for normalized counts, differential expression analysis, and cluster assignment for all genes and conditions. (E) Top: Box plot showing the distribution of expression levels for DEGs in Cluster 8 according to experimental condition. See Figure S2C for all gene clusters. Black box: for genes in this cluster, p53-DN increases expression (up arrow) and CENP-A overexpression decreases expression (down arrow). Bottom: Top five enriched KEGG pathways (WebGestaltR v0.4.2) for genes within Cluster 8 based on over-representation analysis (ORA). All five terms are significantly over-represented (FDR < 0.05). See Table S1 (ORA) for top ten pathways for all clusters. (F) Accumulation of micronuclei pertaining to Day 1 and Day 8 of MCF10-2A *TetOn-CENPA-FLAG-HA* cells with either empty vector (p53-WT) or dominant-negative p53 (p53-DN) grown continuously with 0X Dox, 1X Dox (10 ng/ml), or 10X Dox (100 ng/l). Plots show mean ± standard deviation for three biological replicates from a single experiment. Statistical significance tested by two-tailed Welch's t-test with Bonferroni cutoff at a p-value of 0.01 ($\alpha = 0.05$). No significant differences between p53-WT and p53-DN samples with same Dox treatment. ** = p-value <0.001. N = >1000 nuclei per condition for each replicate. (G) Growth curve of MCF10-2A *TetOn-CENPA-FLAG-HA* cells with either empty vector (p53-WT) or dominant-negative p53 (p53-DN) grown continuously with 0X Dox, 1X Dox (10 ng/ml), or 10X Dox (100 ng/l). Growth curve shows number of population doublings relative to the initial seeding population at Day 0. Dots show mean ± standard deviation for three biological replicates at each time point where cells were counted. Lines show best-fit curves. Similar results were obtained for a second independent experiment. (See Figure S3G for growth curve of the non-inducible parental MCF10-2A cells after Dox exposure).

CENP-A overexpression promotes acute cell cycle arrest and senescence in p53-WT cells

To determine the effects of CENP-A overexpression and p53 status on individual cell fate and evolution of the cell population over time, we performed single-cell RNA sequencing (scRNA-seq), a powerful tool for characterizing cell state and identity[51]. Using our p53-WT and p53-DN MCF10-2A cells, we compared prolonged, continuous CENP-A overexpression (chronic induction for 69 days), to acute CENP-A overexpression (1 day) and non-overexpressing conditions, passaged in parallel (See scheme in Figure 5A). First, we confirmed the chronic overexpression of CENP-A by Western blot (Figure S4A) and verified that the scRNA-seq data agreed with the bulk RNA-seq data from comparable samples (Figure S4B). Principle component analysis of the single-cell expression profiles revealed that most of the cell-to-cell variability across conditions could be attributed to cell cycle differences (Figure 5B). Indeed, with the scRNA-seq data we could identify distinct sub-populations of cycling and non-cycling cells, and further distinguish G2/M and G1/S cells within the cycling cluster (Figure 5C). Both acute and chronic CENP-A overexpression in the p53-WT cells caused a clear shift in the proportion of cycling to non-cycling cells, a shift that was substantially reduced in the p53-DN cells (Figure 5D-E). We confirmed these findings by a direct classical analysis of cell cycle using propidium iodide FACS (Figure S4D). Interestingly, we found that the non-cycling populations in the scRNA-seq experiments displayed a striking downregulation of the genes corresponding to Cluster 8 in the bulk RNA-seq analysis (Figure S4C), the subset of genes identified as critical for the radiosensitivity phenotype. Given the well-documented role of p53 in senescence[53,54], we also confirmed that the non-cycling scRNA-seq cluster was consistent with a senescence gene expression signature (Figure 5F). We thus tested the impact of p53 status and prolonged CENP-A overexpression on cell senescence using Beta-galactosidase senescence assays (Figure 5G). p53-WT cells showed on average ~19% senescence after 13 days of chronic CENP-A overexpression, compared to less than 3% in the non-induced control. Meanwhile, p53-DN cells showed approximately half the levels of senescence (~9% and ~1%, respectively). This is consistent with the non-cycling ratios for p53-WT and p53-DN cells in the scRNA-seq data and shows a significant impact on senescence from p53 status. Taken together, our results reveal that CENP-A overexpression causes a clear shift in cell state, promoting acute cell cycle exit and senescence in p53-WT cells that is severely reduced when p53 is defective.

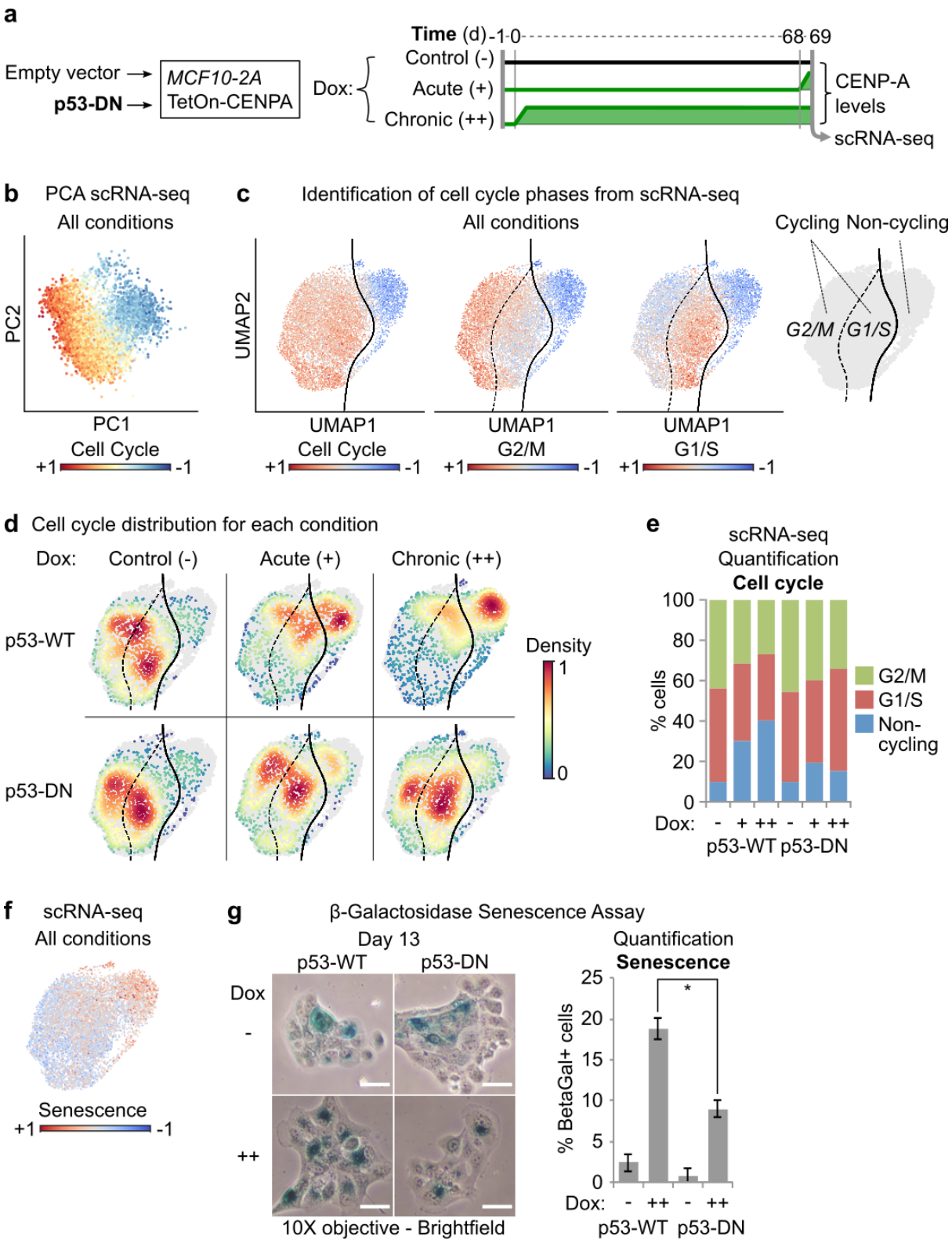

a
Empty vector
p53-DN
MCF10-2A
TetOn-CENPA
Dox:
Time (d)
-1
0
68
69
Control (-)
Acute (+)
Chronic (++)
CENP-A levels
scRNA-seq
b
PCA scRNA-seq
All conditions
PC2
PC1
Cell Cycle
+1
-1
c
Identification of cell cycle phases from scRNA-seq
All conditions
Cycling
Non-cycling
G2/M
G1/S
UMAP2
UMAP1
Cell Cycle
G2/M
G1/S
d
Cell cycle distribution for each condition
Dox:
Control (-)
Acute (+)
Chronic (++)
p53-WT
p53-DN
Density
1
0
e
scRNA-seq
Quantification
Cell cycle
% cells
100
80
60
40
20
0
G2/M
G1/S
Non-cycling
Dox:
- + ++ - + ++
p53-WT p53-DN
f
scRNA-seq
All conditions
Senescence
+1
-1
g
β-Galactosidase Senescence Assay
Day 13
p53-WT
p53-DN
Dox
-
++
10X objective - Brightfield
Quantification
Senescence
% BetaGal+ cells
25
20
15
10
5
0
*
Dox:
- ++ - ++
p53-WT p53-DN

Figure 5

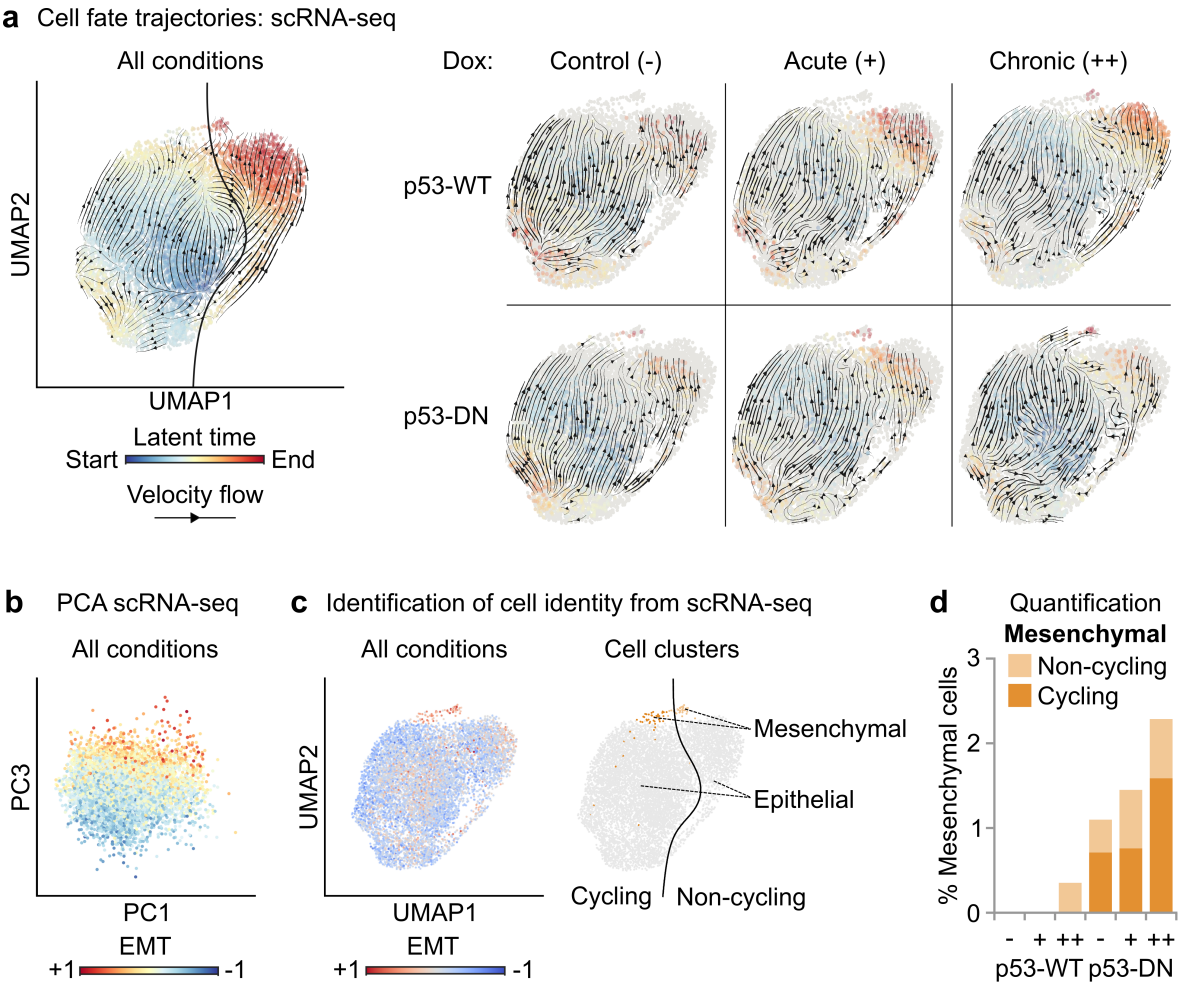
Figure 5 – CENP-A overexpression promotes acute cell cycle arrest and senescence in p53-WT cells

(A) Scheme delineating conditions tested by single-cell RNA-sequencing showing relative CENP-A protein levels over time (pertaining to Figures 5B-F, 6A-D, S4B-C and S5A-D, and Table S2). (B) Principal component analysis (PCA) of all scRNA-seq samples, illustrated in A. All conditions merged. Each dot represents a single cell on the first two principal components (PC1 and PC2), coloured by expression of cell cycle genes (Cell Cycle signature includes all genes from Cyclebase v3.0, *CENPA* excluded). (C) Uniform Manifold Approximation and Projection (UMAP) maps of scRNA-seq data, pertaining to scheme in A. All conditions combined. Each dot corresponds to an individual cell projected in a 2D space where the topology reflects global similarities in expression. The colour gradient is proportional to the expression of Cell Cycle, G2/M and G1/S genes (Cyclebase v3.0). Far right plot: boundary between cycling (G2/M or G1/S) and non-cycling cells in UMAP space computed by Support Vector Classification. (D) Cell density by condition (colour gradient) in UMAP space for each scRNA-seq experimental condition, pertaining to scheme in A. (E) Stacked bar plot showing the % of cells in G2/M, G1/S and non-cycling scRNA-seq clusters for each experimental condition. (F) UMAP of scRNA-seq data as in C for all conditions merged, coloured by expression gradient of senescence-associated genes (Fridman Senescence Up gene set from MSigDB v6.2). (G) Beta-galactosidase senescence assays. Left: Representative brightfield images after 13 days of growth without Dox (-) or with chronic Dox (10 ng/ml, ++), taken with a 10X objective. Scale bars = 20 µm. Only cells with dark blue staining were considered senescent. Right: quantification of frequency of senescence, showing mean ± standard deviation from two biological replicates of a single experiment. Similar results were obtained in a second independent experiment. * = two-tailed Welch's t-test comparing p53-WT to p53-DN after chronic CENP-A overexpression; p-value = 0.05.

CENP-A overexpression promotes epithelial-mesenchymal transition in p53-defective cells

Next, we explored if CENP-A overexpression also impacts cell identity in the different p53 contexts. To do this, we investigated cell fate trajectories across all conditions by estimating transcriptional kinetics based on RNA velocity[55]. In line with Figure 5, the main trajectory inferred from RNA velocities is the transition of cycling cells to a terminal non-cycling state (see velocity flow and latent time gradient in Figure 6A). At the same time, we noticed that a minority of cycling cells follows an alternative trajectory converging to a distinct terminal state. This corresponds to a smaller subpopulation comprising both cycling and non-cycling cells. By computing the RNA velocity separately for each condition, we revealed that the main directional flow upon CENP-A overexpression in p53-WT cells is associated with the cell cycle exit trajectory, whereas the alternative cell fate trajectory is mainly followed by p53-DN cells under prolonged CENP-A overexpression. This suggests that CENP-A overexpression in p53-DN cells leads to an alternative cell fate different from cell cycle exit, underlying the emergence of a distinct subpopulation of terminal cells. We thus identified the main clusters of cells after adjusting for cell cycle effects (Figure S5A) and characterized the specific markers associated to each cluster (Table S2). The largest clusters corresponded to distinct subpopulations of epithelial cells with differences in expression related to cell metabolism (Figure S5B-C). Interestingly, the alternative cell fate trajectory converged instead to a smaller cluster of cells that were negative for epithelial markers. This cluster showed high expression of mesenchymal genes and broad upregulation of genes involved in epithelial-mesenchymal transition (EMT)(Figure 6B-C, see also Table S2 and Figure S5D). This is consistent with highly advanced EMT or complete mesenchymal transition. The mesenchymal cluster was nearly exclusive to the p53-DN cells (Figure 6D), consistent with previous studies demonstrating that WT p53 counteracts EMT[56–61]. Remarkably, the highest proportion of mesenchymal cells in the p53-DN condition occurred after chronic CENP-A overexpression, in line with the alternative cell fate trajectory. Given that these cells represent a highly advanced stage of EMT, these findings led us to re-explore our cells for earlier EMT signatures by microscopy. We first noticed that large groups of cells with mesenchymal-like characteristics (reduced cell-cell contacts, distorted cell shape) could be observed in the p53-DN cells by simple brightfield microscopy as early as 10 days after continuous CENP-A overexpression (Figure S6A). At Day 34, we immunostained simultaneously for the classic epithelial marker E-cadherin and the mesenchymal marker vimentin (Figure 6E), to identify cells in a broad range of early to late stages of EMT[62]. The results revealed a major increase in the EMT population after prolonged CENP-A overexpression, which was again nearly exclusive to our p53-DN cells. Indeed, MCF10-2A cells are known to undergo low levels of spontaneous EMT[63], so it was unclear if this increase in EMT was result of a stimulation or if CENP-A overexpression—in a p53-defective context—would be sufficient to drive EMT on its own. To assess this, we tested chronic CENP-A overexpression in our p53-defective breast epithelial cancer cell line HCC1954, which does not undergo spontaneous EMT[64]. We did not observe the emergence of EMT in the time frame of our

investigation (Figure S6B), suggesting that the major increase in EMT observed in the p53-DN MCF10-2A cells was most likely a stimulation rather than an induction. Together, these assays reveal that chronic CENP-A overexpression promotes a reprogramming of cell identity in p53-defective cells, corresponding to a striking EMT in the p53-DN cell population.


a Cell fate trajectories: scRNA-seq
All conditions
UMAP2
UMAP1
Latent time
Start
End
Velocity flow
Dox:
Control (-)
Acute (+)
Chronic (++)
p53-WT
p53-DN
b PCA scRNA-seq
All conditions
PC3
PC1
EMT
+1
-1
c Identification of cell identity from scRNA-seq
All conditions
UMAP2
UMAP1
EMT
+1
-1
Cell clusters
Mesenchymal
Epithelial
Cycling
Non-cycling
d Quantification
Mesenchymal
Non-cycling
Cycling
% Mesenchymal cells
0
1
2
3
- + ++ - + ++
p53-WT p53-DN

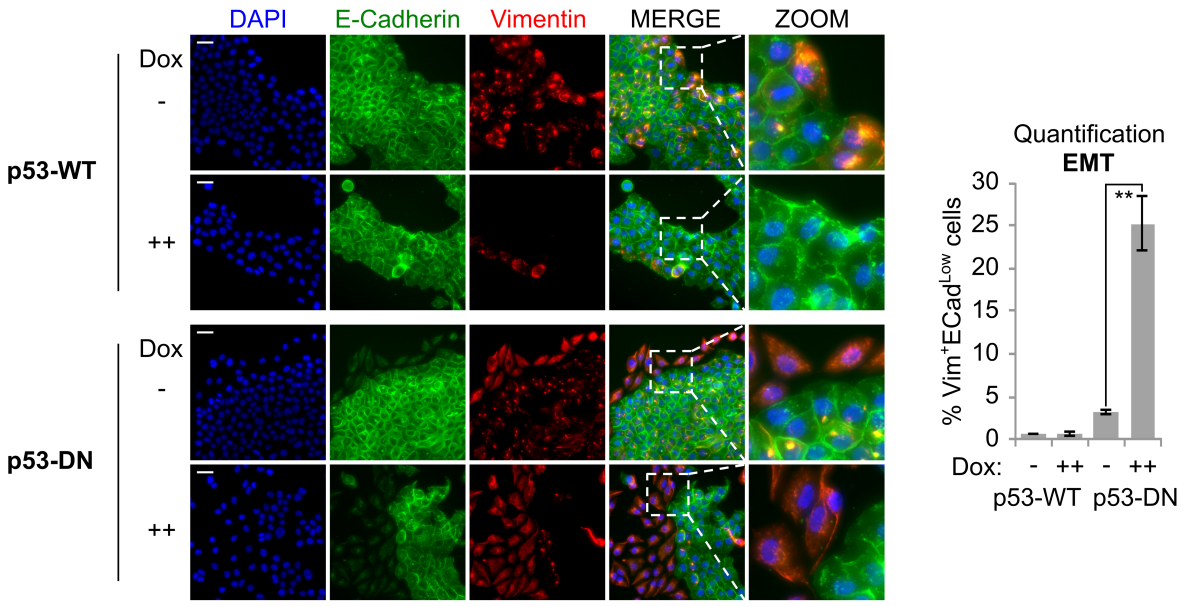

e Immunofluorescence - Day 34
DAPI
E-Cadherin
Vimentin
MERGE
ZOOM
p53-WT
Dox
-
++
p53-DN
Dox
-
++
Quantification
EMT
% Vim+ECadLow cells
0
5
10
15
20
25
30
**
Dox: - ++ - ++
p53-WT p53-DN

Figure 6

Figure 6 – CENP-A overexpression promotes epithelial-mesenchymal transition in p53-defective cells

(A) Cell fate trajectories inferred by RNA velocity analysis of scRNA-seq samples illustrated in Figure 5A. RNA velocities estimated by dynamical modelling across all samples are depicted in the left panel by a streamline plot (black arrows) showing the main directional flow across cells (gene-averaged velocity vector field in UMAP embedding from Figure 5). Each cell is coloured by the estimated latent time from initial (blue, start) to terminal states (red, end). Left: RNA velocities calculated across all conditions. Right: RNA velocities calculated separately for each condition by stochastic modelling in individual samples. (B) Principal component analysis (PCA) of scRNA-seq experiments. All conditions merged. Each dot represents a single cell on the first (PC1) and third (PC3) principal components, coloured by expression of epithelial-mesenchymal transition genes (EMT; Hallmark gene set, **MSigDB v6.2**). Cell-to-cell variability along the third principal component can be explained by differences in expression of EMT genes. (C) Classification of epithelial and mesenchymal subpopulations based on Leiden clustering after correcting for cell cycle effects. Left: The colour gradient shows, for each cell, the relative expression trend of genes involved in EMT (EMT; Hallmark gene set, **MSigDB v6.2**) in UMAP space. See also Figure S5D for additional EMT signatures. Right: Classification of cells as mesenchymal (EMT high cluster, orange) and epithelial (EMT low clusters, grey), divided as either Cycling (dark) or Non-cycling (pale), as determined in Figure 5. (D) Stacked bar plot showing the percentage of cells within the mesenchymal cluster per experimental condition. (E) Assessment of EMT by immunofluorescence after 34 days with (++) or without (-) continuous CENP-A overexpression (10 ng/ml Dox). Left: Representative max intensity projections: DAPI (blue), E-cadherin (green, epithelial marker), and Vimentin (red, mesenchymal marker). Scale bars = 40 μm. Right: Quantification of the frequency of cells with high Vimentin surrounding the nucleus and low/absent E-cadherin on the cell membrane for each condition. Plot shows mean ± standard deviation from three biological replicates. N = >1000 nuclei per condition per replicate. Similar results were obtained in a second independent experiment. ** = two-tailed Welch's t-test comparing control p53-DN to p53-DN after chronic CENP-A overexpression; p-value = 0.0002.

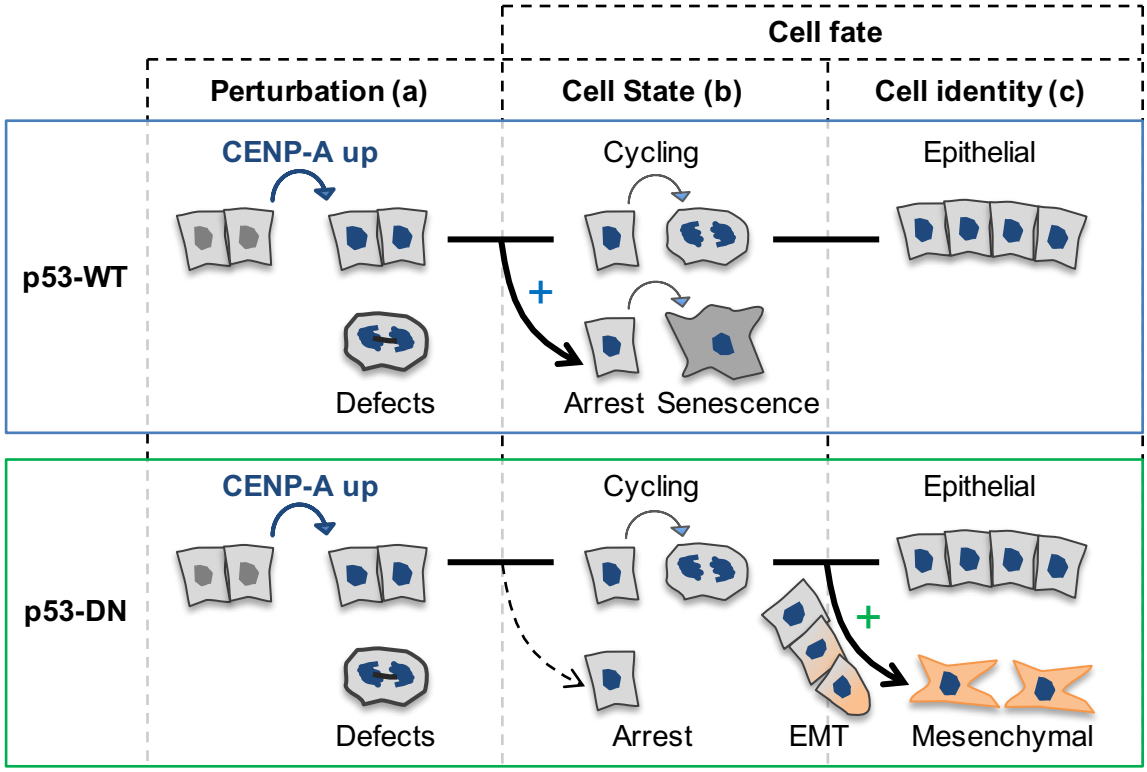

Cell fate
Perturbation (a)
Cell State (b)
Cell identity (c)
p53-WT
CENP-A up
Cycling
Epithelial
+
Defects
Arrest
Senescence
p53-DN
CENP-A up
Cycling
Epithelial
+
Defects
Arrest
EMT
Mesenchymal

Figure 7 – CENP-A overexpression promotes distinct cell fates depending on p53 status

CENP-A overexpression reprograms cell fate with distinct effects on cell state and cell identity that depend on p53 status. Perturbation (A) by CENP-A overexpression (in blue) induces mitotic defects in both wild-type p53 (p53-WT, top panel blue) and p53-defective cells (p53-DN, dominant negative, bottom panel green). These defects provoke distinct cell fate decisions according to p53 status, impacting cell state (B) or identity (C). When p53 is functional, cell state shifts towards acute cell cycle arrest and senescence, reducing self-renewal capacity. Additional stress, like DNA damage from X-irradiation, amplifies this response, resulting in radiosensitivity. Furthermore, functional p53 ensures the preservation of epithelial identity. In contrast, when p53 is defective, the cells evade arrest and continue cycling, allowing CENP-A overexpression to promote epithelial-mesenchymal transition (EMT). “+” symbol: reprogramming stimulated by CENP-A overexpression.

3. DISCUSSION

CENP-A overexpression promotes distinct cell fates depending on p53 status

In this study, we found that CENP-A overexpression promotes radiosensitivity through non-genetic, reversible effects. This is accompanied by major transcriptional reprogramming involving acute cell cycle shutdown and senescence when p53 is active. However, inactivation of p53 suppresses the cell shutdown response, enabling radio-tolerance. Strikingly, prolonged CENP-A overexpression also promotes EMT in our p53-DN MCF10-2A cells. Taken together, our findings demonstrate that CENP-A overexpression can promote two distinct cell fates that depend on p53 status: (i) loss of self-renewal capacity and radiosensitivity in p53-WT cells, and (ii) reprogramming of cell identity through stimulation of EMT when p53 is defective (Figure 7). Our work reveals an unanticipated link between a centromeric protein and genome reprogramming with clear implications for tumour evolution. These findings open up exciting avenues for future research and have broad implications for cancer treatment.

Induced CENP-A overexpression alters cell state and global transcription: implications for cancer treatment

Our work shows that at the time scale of one cell division or less, induced CENP-A overexpression in MCF10-2A cells results in major transcriptional reprogramming across the genome. Switching p53 status from wild-type to defective counteracted a subset of these transcriptional changes, corresponding to cell cycle genes. But, while our scRNA-seq analyses revealed that these effects on cell cycle genes at the population level can be explained by changes in the proportion of arresting cells, how CENP-A overexpression leads to such broad and rapid changes to gene expression across the genome remains an open question. Given that CENP-A overexpression results in its mislocalization and incorporation into chromatin across the chromosome arms, including numerous genic loci[44,45,48,65], we envisage two main scenarios for how CENP-A impacts global transcription: (i) the changes reflect a response to defects induced by CENP-A overexpression and/or, (ii) CENP-A incorporation into chromatin directly affects transcription at the sites where it is mislocalized. The idea that ectopic CENP-A could directly affect transcription at genic loci has recently been proposed[35], but remains to be formally assessed. Understanding the underlying mechanisms of these effects could provide important insights into alternative functions of CENP-A and its impact beyond the centromere. On a longer time-scale, our scRNA-seq results revealed that prolonged CENP-A overexpression promotes chronic cell cycle arrest in a major proportion of p53-WT cells. Thus, our findings support a model where CENP-A overexpression induces mitotic defects and increases CIN[29], which, in turn, lead to the activation of p53 and senescence[49,50]. In this way, CENP-A overexpression causes a p53-dependent loss of self-renewal capacity. Additional cell stress from DNA damaging agents, like X-irradiation, would add to the mitotic stress associated with CENP-A overexpression. This would then amplify the p53-dependent shutdown of self-renewal, promoting radiosensitivity. Thus, our findings suggest that differences in p53 status

may be able to explain why high CENP-A levels are associated with both sensitivity[33,36,38] and resistance[30] to cancer treatments in different patient cohorts. This could have important implications for patient prognosis and treatment strategies. Radiosensitivity associated with high CENP-A levels in p53-WT cancers could represent an opportunity to stratify patients or minimize radiotherapy dose for equal therapeutic outcome with reduced side-effects. Furthermore, alternative treatment options for patients with non-functional p53 could also be considered, as drugs combatting mutant p53 (including LOF mutations) are currently in development[66,67]. A number of these drugs are now in clinical trials, including direct re-activators of mutant p53 (e.g. PRIMA-1^{MET}/APR-246) and drugs designed to return functionality to WT p53 by inhibiting its upstream regulators (e.g. MDM2/X inhibitors)[68]. Here, we showed that transiently reactivating p53 in CENP-A overexpressing HeLa cells—by a transient, clinically relevant, heat shock—was able to significantly increase sensitivity to X-irradiation. Thus, by returning functional p53 status to tumours with high CENP-A, not only could this induce the anti-tumoural effects of activating p53 alone, but it may also promote radiosensitivity due to the effects of CENP-A overexpression on cell state.

Prolonged CENP-A overexpression and cell identity: implications for stimulating EMT

One of the most surprising findings from our study was the striking stimulation of EMT in p53-DN MCF10-2A cells after prolonged CENP-A overexpression. EMT is a multi-stage process where epithelial cells, characterized by strong cell-cell junctions and apical-basal polarity, undergo a series of changes to gene expression and morphology to gain a mesenchymal phenotype, including a reorganized cytoskeleton, altered cell shape, and increased cell motility[69]. These changes are highly context-dependent, varying substantially among epithelial cells and depending on the factor driving the EMT response[70]. Indeed, the transition to a mesenchymal identity is an essential process during mammalian development, but also occurs aberrantly in epithelial cancers. This can lead to the development of invasive and metastatic properties, with impacts on proliferation, cell plasticity, stemness, and therapeutic resistance[71,72]. In this context, different EMT responses can be driven by distinct signaling pathways, including TGF-β, hypoxia, WNT and others[73]. In MCF10-2A cells, that spontaneously undergo low levels of EMT[63], we found that CENP-A overexpression strongly favours the EMT response as an alternative fate to cell cycle exit when p53 is inactivated. However, CENP-A overexpression alone was not sufficient to initiate EMT in the p53-defective HCC1954 breast cancer cells, where EMT does not occur spontaneously but can be induced by TGF-β[64]. Investigating whether high levels of CENP-A favour a mesenchymal fate when the EMT response is induced by different pathways is an important avenue of investigation with critical implications for cancer care. Indeed, CENP-A overexpression has previously been linked to invasion and metastasis in human patients[30,32,33,35,36,38], but whether this could involve the stimulation of EMT was not known. Thus, the link with EMT provides a mechanism by which CENP-A overexpression could promote these outcomes in patient tumours that lack functional p53. Evidence linking EMT to the direct inhibition of

senescence[74,75], promotion of radioresistance[76–78], and cancer stemness[79], imply that EMT may also play an important role in the evasion of senescence, radio-tolerance, and increased clonogenic capacity that we observed in our p53-defective cells. Interestingly, the effect of CENP-A overexpression on EMT also suggests that high CENP-A levels could promote stemness, depending on p53 status. Indeed, human pluripotent stem cells naturally overexpress CENP-A[80,81], and maintain p53 in an inactive state through post-translational regulation[82]. Intriguingly, recent work in Drosophila showed that intestinal stem cells preferentially retain pre-existing CENP-A during asymmetric divisions[83], suggesting that CENP-A nucleosomes may epigenetically mark stem cell identity in this system. Furthermore, Drosophila germ line stem cells showed asymmetric distribution of CENP-A during differentiation and CENP-A overexpression could promote self-renewal[84]. Thus, in addition to its effect on EMT, how CENP-A overexpression contributes to stem cell renewal and pluripotency in human cells will be an important avenue for future research. Importantly, as with the effect of CENP-A overexpression on global transcription, which underlying mechanism is at play remains to be deciphered. Since the initiation of EMT is associated with several of the cell stresses that result from mitotic defects, including genotoxic stress[85], replication stress[86], and metabolic stress[87], amongst others[88–91], they are likely important in the process. Interestingly, a recent report by Gomes et al demonstrated that the perturbation of the histone H3 variants, H3.1/2 and H3.3, promotes or represses EMT[92]. In particular, knockdown of the H3.1/2-dedicated chaperone CAF-1 caused widespread opening of chromatin, with increased incorporation of H3.3 at the promoters of EMT-inducing transcription factors (e.g. *ZEB1*, *SNAI1*, and *SOX9*), which induced EMT and increased cell migration and invasion. Previously, we found that overexpressed CENP-A hijacks the H3.3-dedicated chaperone Daxx[44]. This results in the mis-incorporation of CENP-A-containing nucleosomes into regions of high histone turnover normally enriched for H3.3. Thus, CENP-A overexpression could have a direct impact on EMT, and transcription in general, through its perturbation of other H3 variants and their dedicated histone chaperones. Deciphering the mechanisms that link CENP-A, EMT, and possibly stemness, will expand our understanding of the direct and indirect molecular consequences of CENP-A overexpression and its impact on tumour evolution.

In conclusion, the interplay of CENP-A overexpression and p53 status alters cell fate, with distinct implications for the role of CENP-A in therapeutic sensitivity, resistance and metastasis.

4. MATERIAL AND METHODS

Cell lines

CELL LINE	P53 STATUS*	CELL TYPE	CONSTRUCT	COMMENTS
MCF10-2A	Functional wild-type	Immortal non-tumoural (fibrocystic disease) breast epithelial	*TetOn-CENP-A-FLAG-HA* (lentiviral)	Female origin
HCT116	Functional wild-type	Colon cancer	*TetOn-CENP-A-FLAG-HA* (lentiviral)	Male origin
HELA S3	Non-functional wild-type: HPV18 inactivated	Cervical cancer	*TetOn-CENP-A-FLAG-HA* (lentiviral)	Female origin
HCC1954	LOF p53 mutation at Y163C	Invasive ductal carcinoma, breast	*TetOn-CENP-A-FLAG-HA* (lentiviral)	Female origin; HER^+ ER^- PR^- luminal
DLD1	One functionally silent allele of p53 & LOF mutation at S241F	Colon cancer	*TetOn-CENPA-YFP-AID* (FlpIn)	Male origin; Kind gift from D. Fachinetti

*p53 status for missense mutations from the TP53 database[93].

Cell culture and CENP-A overexpression

HCT116, HeLa S3, and DLD-1 FRT Fbox (+OSTR1-Myc9)+CENP-A-YFP-AID were cultured with DMEM 10% Fetal Cow Serum (FCS) Pen/Strep 1%; MCF10-2A, 1:1 DMEM:Ham's F12, 20 ng/ml epidermal growth factor, 100 ng/ml cholera toxin, 0.01 mg/ml insulin and 500 ng/ml hydrocortisone, 5% horse serum; HCC1954, RPMI 10% FCS Pen/Strep 1%; Base media from Thermofisher Scientific. All cell lines tested and confirmed to be mycoplasma free using the Mycoplasma PCR ELISA kit (Sigma). CENP-A overexpression was induced by the addition of Dox to typical growth media at 10 ng/ml (considered 1X), unless otherwise indicated. To maintain overexpression, media and Dox was

replaced every one to three days. When applicable, the media in the non-induced control was replaced in parallel without Dox. For reversal of CENP-A overexpression, we removed media containing Dox and washed two times with warm PBS then replaced the media without Dox.

Generation of *TetOn-CENPA-FLAG-HA* cell lines

To obtain an inducible CENP-A overexpression system, we sub-cloned *CENPA-FLAG-HA* from the eCENP-A plasmid[44] by PCR (Forward primer containing EcoRI site: *CACAGTTAGAATTC**ATG**GGCCCGCGCCG*; Reverse primer containing AgeI site: *ATCGAATCACCGGT**CTA**GGCGTAGTCGGGCACGT*) and inserted it into the multiple cloning site of the pLVX-TetOne (ClonTech) plasmid by restriction enzyme digestion with EcoRI and AgeI, followed by ligation. To confirm proper integration and lack of mutation in the *CENPA* gene, we then sequenced the *CENPA-FLAG-HA* pLVX-TetOne plasmid around the insertion site. To encapsulate the construct for transduction we co-transfected Lenti-X 293T cells (ClonTech) with 10 µg *CENPA-FLAG-HA* pLVX-TetOne and packaging vectors 7.5 µg psPAX2 and 2.5 µg pMD2.G using PolyPlus JetPrime transfection reagent according to manufacturer instructions. Media was replaced 4h after transfection. For infection and stable integration of the construct without selection, we filtered (0.45 µm) supernatant from the transfected cell flask at 24h and 48h post-transfection, added 8 µg/ml of polybrene to the filtered virus-containing media, and added the media directly to the target cell lines. We removed the virus-containing media after 48h and grew the cells for at least three passages without virus. Then we tested the polyclonal cell lines for the induction of *CENPA-FLAG-HA* by Western and IF of CENP-A and HA following 24h of treatment with 80 ng/ml of doxycycline. We isolated clonal cell lines by serial dilution to single cells. Then tested 10-20 colonies arising from single cells for *CENPA-FLAG-HA* induction, as before. We selected cell lines for further experimentation if they showed a clear homogenous CENP-A and HA increase by IF in ~100% of cells after doxycycline treatment with no detectable background of HA signal by Western or IF when no doxycycline was added.

Change of p53 status

For the p53-WT and p53-DN MCF10-2A cells, we transduced empty vector pWZL Hygro (Scott Lowe, Addgene plasmid #18750) or vector containing the dominant negative *TP53* construct (pBABE-hygro p53 DD, Bob Weinberg, Addgene plasmid #9058) into the clonal MCF10-2A *TetOn-CENPA-FLAG-HA* cell line by lentiviral transduction, as above. Cells were selected with hygromycin for >14 days and then passaged in typical media. For heat shock of HeLa S3 *TetOn-CENPA-FLAG-HA cells*, we performed a 1h 42°C heat shock on non-induced HeLa *TetOn-CENPA-FLAG-HA* cells and examined total cell extracts by Western blotting at various time points following heat shock. Two parallel sets of cells were grown under normal conditions at 37°C. One set was moved to a 42°C incubator while the other remained at 37°C as a control. After 1h, we harvested cells for total cell extraction from each

condition (time 0h), then returned both sets to 37°C. We then harvested cells for total cell extraction at the indicated times after heat shock (1h, 2h, 3h, 4h, or 6h: Time after HS).

Total cell extracts

We harvested cells by trypsin, counted cells by Beckman Automated Cell Counter, and spun down at 300g, 5 min, washed 1X in PBS, spun again, aspirated PBS and froze pellets at -20°C. Cell pellets were incubated for 15min at room temperature with 300 µl per 1 million cells of 1.2X LDS Sample Buffer (NuPAGE) containing 1.2X Sample Reducing Agent (NuPAGE) and 125kU/ml Pierce Universal Nuclease Buffer for Cell Lysis, then heated at 95°C for 10min, vortexed, spun down, and cooled briefly on ice prior to Western blotting.

Western blotting

Total cell extracts were loaded at one to four different concentrations, as indicated, onto pre-made NuPAGE Bis-Tris 4-12% gradient gels in an XCell 4 Sure-Lock SDS-PAGE chamber with 1X NuPAGE MES SDS Running Buffer, with a PageRuler (Thermofisher scientific) molecular weight marker. Gels were run at 130-150v for 1h-1h15min. We transferred protein to a 0.2 µm nitrocellulose membrane by BioRad Trans-Blot Turbo, mixed-molecular weight setting, or semi-dry transfer (BioRad, 15v, 1.5h). Membranes were stained with Pierce reversible protein stain to detect bulk protein and assess quality of transfer, then cut, blocked in 5% milk-PBST (0.1% Tween-20) for 1h, RT, and incubated overnight with rocking at 4°C with primary antibodies in 5% milk-PBST containing 0.02% sodium azide. Membranes were washed 3X 10min in PBST, then incubated 1h (RT) with Horse Radish Peroxidase (HRP) secondary antibodies in 5% milk-PBST, washed 3X 10 min in PBST and exposed with SuperSignal West Pico Chemiluminescent Reagent or, for high sensitivity exposures, SuperSignal West Femto Maximum Sensitivity Reagent, and imaged using a ChemiDoc Touch system and ImageLab software. Primary antibodies: CENP-A 1:500 (2186 Cell Signaling Technology (CST)), H4-pan 1:2500 (05-858, Sigma-Aldrich), HJURP 1:300 (HPA008436 Sigma-Aldrich), γTubulin 1:10000 (T5326 Sigma-Aldrich), p53 (1C12) 1:1000 (2524 CST), p21 1:500 (556431 BD Pharmingen), phospho-p53 (Ser15) 1:500 (9284 CST). Secondary antibodies: Jackson ImmunoResearch, 1:10000, donkey anti-mouse or donkey anti-rabbit.

Immunofluorescence (IF)

Glass cover slips were coated with collagen (1 µg/ml) + fibronectin (1 µg/ml) in PBS, 30min, RT, washed in PBS and added to culture dishes prior to cell seeding. After at least 24h of growth, coverslips were washed 3X with PBS, fixed with 2% PFA, 20min, RT, washed 3X PBS, incubated 5 min with 0.3% Triton-X 100 in PBS, washed 3X PBS, blocked in filter-sterilized 5% BSA-PBST (0.1% Tween-20) for 20-30min, RT, and incubated 1-1.5h, RT, with primary antibodies in 5% BSA-PBST. Coverslips were then washed 3X 5min in 5% BSA-PBST, and incubated 30min with secondary antibody in 5% BSA-PBST, RT, in darkness. DAPI was added directly to secondary antibody solution (final

concentration 1/4000) and incubated in darkness, RT, 5min, followed by 3X PBS wash. Coverslips were inverted onto microscope slides with ~10 µl of VectaShield and imaged with a Zeiss Axiovert Z1 microscope or Inverted Widefield Deltavision Core Microscope (Applied Precision) with CoolSNAP HQ2 camera. Primary antibodies: CENP-A (3-19) 1:300 (ADI-KAM-CC006-E Enzo Life Sciences), E-cadherin (24E10) 1:200 (3195S CST), γH2AX 1:250 (2577 CST), Vimentin (N-term) 1:100 (5741S Progen). Secondary antibodies: 1:1000 Alexa Fluor donkey anti-mouse IgG (H+L) 488, 1:1000 Alexa Fluor goat anti-rabbit IgG (H+L) 488 or 594, 1:1000 Alexa Fluor goat anti-Guinea Pig IgG (H+L) 594.

Colony Formation Assays (CFAs)

At Day -1, cells are trypsinized and diluted to single-cell level (300-600 cells per well, in triplicate) in 6-well plates. At Day 0, one set of cells is irradiated by CIXD Dual Irradiator or Philips X-ray tube X-ray generator (4 Gy, unless otherwise indicated) while a control set remains un-irradiated (0 Gy). When the cells have had sufficient time to form visible colonies, depending on their typical speed of growth (7-14 days), they are washed gently with PBS, stained with 1% Crystal Violet 20% Ethanol solution for 15 min, washed with water, allowed to dry, scanned and counted by eye from the acquired images with the counter blinded to the conditions. Unless otherwise indicated, ratio of surviving colonies is calculated as the number of colonies formed after 4 Gy of X-irradiation divided by the number of colonies formed when not irradiated. Cells are considered sensitized to irradiation by CENP-A overexpression when the CENP-A overexpression condition has a significantly lower survival ratio compared to the non-induced control. Cells are considered tolerant to CENP-A overexpression if the survival ratio is not significantly affected by the CENP-A overexpression.

Bulk RNA-seq

Sample preparation: We grew MCF10-2A *TetOn-CENPA-FLAG-HA* cells expressing either empty vector (p53-WT) or dominant-negative p53 (p53-DN) with 0X Dox (no Dox), 1X Dox (10 ng/ml), or 10X Dox (100 ng/m) for 24h. At time 0, we irradiated one set of cells by X-ray generator (4 Gy) while a control set remained un-irradiated (0 Gy). 6h later, we extracted RNA for RNA-seq. All conditions tested in duplicate. We extracted RNA directly from culture dishes using the Qiagen RNeasy Mini kit according to the manufacturer's instructions and confirmed the quality and quantity of the RNA by TapeStation and NanoDrop. mRNA library preparation and sequencing were performed by the Next Generation Sequencing (NGS) platform, Institut Curie, using the Illumina TruSeq Stranded mRNA kit and NovaSeq 6000 sequencer. Library preparation and sequencing of irradiated and non-irradiated samples were performed on different dates, with a single repeat of one sample included for batch correction.

Bulk RNA-seq analysis

Reads were aligned to the human reference genome (GRCh38 assembly) based on Ensembl gene annotation (release 95) with hisat2 (version 2.1.0[94]), run in paired-end mode with default parameters.

Gene-level counts were computed from primary alignments with MAPQ > 2 using featureCounts (Subread package version 1.6.3[95]) in paired-end mode with the -s 2 option for reverse-stranded libraries. Raw counts were normalized for differences in library size (counts per million) and across samples (via trimmed mean of M-values normalization, TMM) using edgeR (version 3.28.0[96]). Differential expression analyses were performed with edgeR[97]. We assessed the stand-alone and combined response to each treatment (CENP-A overexpression at increasing Dox concentrations, p53-DN, and X-irradiation) by fitting a quasi-likelihood negative binomial generalized log-linear model (GLM), including both additive and synergistic effects for all treatment combinations. A batch coefficient was also included to account for potential batch effects. Full details about the variable encoding and GLM formulation are provided in Table S1 (sheet 1). The effect of each treatment, both stand-alone and combined, was evaluated via quasi-likelihood F-test on the respective GLM coefficient, followed by multiple testing correction via the Benjamini-Hochberg method (Table S1, sheet 2). A false discovery rate (FDR) cut-off of 0.05 was used to identify differentially expressed genes (DEGs). For proportional Venn diagrams, we only considered DEGs that change with CENP-A overexpression, p53 status or X-irradiation, since we could not detect significant interaction effects for most treatment combinations (Table S1, sheet 2). Mean-centered TMM-normalized counts were used for PCA and hierarchical clustering analyses via Ward's variance minimization method (Table S1, sheet 3 and 4). For hierarchical clustering, we tested the combined effect of all coefficients, excluding batch, and included any DEG showing significant differences relative to baseline at 0.05 FDR. Functional enrichment analyses for KEGG pathways were carried out using the WebGestaltR package (version 0.4.2[98]). Gene set enrichment analyses (GSEA) for CENP-A effects were performed on all expressed genes ranked by fold change and p-value upon overexpression i.e. $\log_2$ fold change * - $\log_{10}$ p-value of the Dox coefficient (Table S1, sheets 5 and 6). Pathways associated to specific gene clusters were identified by over-representation analysis (ORA) after hierarchical clustering of all DEGs via Ward's method (Table S1, sheets 7 and 8). Coordinated changes in expression within DEG clusters were evaluated by assessing the distribution of mean-centered expression values (averaged per condition) for all genes in a given cluster. For genes in Cluster 8, we fit a linear mixed model (LMM) to estimate the fixed effects of p53 inactivation and X-irradiation at each level of Dox (relative to non-irradiated p53-WT samples), with a varying intercept for each gene. The LMM formulation, model estimates and pairwise comparisons by F-test are reported in Table S1 (sheet 9), along with adjusted p-values after Bonferroni correction. Bulk RNA-seq analyses were carried out with custom Python scripts. pandas (version 0.24.2), NumPy (version 1.16.2), SciPy (version 1.3.1), statsmodels (version 0.10.1) and scikit-learn (version 0.21.3) libraries were used for data manipulation, statistical analysis and unsupervised learning. matplotlib (version 2.2.4), matplotlib-venn (version 0.11.5) and seaborn (version 0.9.0) were used for plotting and statistical data visualization. R packages were imported into Python using rpy2 (version 2.8.4).

Reverse transcription quantitative PCR (RT-qPCR)

We cultured two replicates for each cell type and condition in separate 60mm dishes for one day in typical media, then added 0, 10 or 100 ng/ml Dox for 24h. We extracted RNA directly from plates using the Qiagen RNeasy Mini kit with in-column DNase I treatment, according to the manufacturer's instructions. RNA concentrations were quantified by NanoDrop and diluted to 125 ng/µl and confirmed by NanoDrop. To obtain cDNA, we then performed reverse transcription PCR on 1000ng of RNA for each sample using the SuperScript III First-Strand Synthesis SuperMix kit, according to the manufacturer's instructions. We performed quantitative PCR using Power SYBR Green qPCR master mix with three technical replicates in 384-well plates using the QuantStudio 5 Real-Time PCR System. Relative expression was calculated subtracting Ct for each gene of interest from the Ct for *PPIA* for each technical replicate (ΔCt) and took the mean ΔCt. For normalization, we then subtracted the mean across biological replicates of the p53-WT 0X condition for each gene of interest (ΔΔCt). Relative expression was then calculated as the mean ± standard deviation of the fold change of ΔΔCt (2^ΔΔCt) across biological replicates.

Comet assays

Prior to irradiation, cells were harvested and submerged into media containing low-melting agarose on ice. When hardened, cells were exposed to the indicated dose of γ-irradiation (GSR D1 gamma ray). Either immediately, or at the indicated times post-irradiation, the cells in the gel were submerged in alkaline solution and run by gel electrophoresis to form comets to visualize the levels of DNA damage. Comet assays were performed by the RadExP platform, Institut Curie, according to the Trevigen Single Cell Electrophoresis Assay alkaline comet protocol. Automatic counting and measuring of comets on Trevigen slides (two wells used for each condition, per experiment), imaged using the Metafer system with the "comet" module from MetaSystems.

Micronuclei

We seeded cells into dishes containing collagen/fibronectin-coated glass coverslips 48h prior to fixation, added indicated concentrations of Dox and allowed the cells to grow for 24h (Day 1) or passed cells and replaced Dox every 2-3 days until Day 8. Cells were fixed, prepared for IF, and nuclei were imaged with a Zeiss Z1 inverted microscope using a 10X objective. We counted micronuclei using a custom ImageJ macro with at least three fields and >1000 nuclei counted per condition.

Multicolor fluorescence in situ hybridization (mFISH) karyotyping

Cells were grown with or without 10 ng/ml Dox (as in the growth curve assay) for 15 days, then treated with colcemid (100 ng/ml, Roche) for 1.5 hours and prepared as previously described for mFISH (MetaSystems) staining[99]. Briefly, mitotic cells were collected by mitotic shake-off after a short trypsin treatment and centrifuged at 1000 rpm for 10 min. Cell pellets were resuspended in 75 mM KCl and incubated for 15 min in a 37°C waterbath. Carnoy fixative solution (methanol/acetic acid, 3:1) was prepared and 1:10 volume added on the cells, before centrifugation at 1000 rpm for 15 min. Cells were

then fixed 30 min at room temperature in the Carnoy solution, centrifuged and washed once more with fixative. Minimum volume of fixative was left to resuspend the pellet and cells were dropped onto clean glass slides. Multicolor FISH (mFISH) staining was performed following manufacturer's instructions (MetaSystems). The Metafer imaging platform (MetaSystems) and the Isis software were used for automated acquisition of the chromosome spread and mFISH image analysis. Chromosome rearrangements and specific chromosome counts for each spread were assessed and counted by eye from the automated chromosome spread images, with the researchers blinded to the conditions. Losses and gains of chromosomes per cell were calculated as the sum of the absolute difference from the mean for each chromosome of the p53-WT no Dox control. New chromosome rearrangements per cell were determined as the total number of structural chromosomal anomalies observed per spread, excluding the ones that were common to all p53-WT no Dox spreads. Potential acrocentric fusions were not considered in our study.

Growth curve / Proliferation assays

Cells that had never been exposed to Dox were trypsinized, counted using a Beckman Automated Cell Counter, and seeded into nine culture dishes with equivalent cell numbers (Corresponds to MCF10-2A non-inducible control, plus the p53-WT and p53-DN TetOn-CENP-A-FLAG-HA cell lines, at three Dox concentrations each, all grown in parallel). The next day (Day 0), Dox was added in triplicate at the indicated concentrations (0, 10, or 100 ng/ml), corresponding to 0X, 1X or 10X Dox. At Day 1, we trypsinized and counted the cells from all conditions, and seeded equivalent numbers of cells into fresh media. We immediately added the corresponding concentrations of Dox to the culture dishes. From then on, every 2-6 days cells were trypsinized, counted and re-plated, as plotted, with media containing fresh Dox of corresponding concentrations replaced every 2-3 days. Biological replicates were maintained separately throughout the entirety of the experiment.

Single-cell RNA-seq

Sample preparation: We grew MCF10-2A *TetOn-CENPA-FLAG-HA* cells expressing either empty vector (p53-WT) or dominant-negative p53 (p53-DN) without Dox or with continuous exposure to Dox (10 ng/ml, ++, chronic) for 69 days in parallel. Cells in the no Dox condition were split into two dishes at day 67 and Dox was added to one set on day 68 for 24h of CENP-A overexpression (10 ng/ml, +, acute) while the other remained without Dox (-, control). We prepared samples in singlet according to the 10x Genomics Sample Preparation Demonstrated Protocol. In brief, we harvested cells by trypsinization, resuspended in typical media and mixed thoroughly by pipette, passed cells through a 40 µm cell strainer, and counted cells by Beckman Automated Cell Counter. We resuspended cells in 1x PBS + 0.04% BSA, mixed, centrifuged gently, aspired supernatant and repeated wash two times. We passed cells through another cell strainer (40 µm), counted again and diluted to a final concentration between 700 and 1200 cells/µl. We then proceeded directly to GEM generation and barcoding at the

NGS platform, Institut Curie, using the Single-cell 3' Reagent Kits v2 protocol with a targeted cell recovery of 2000 cells per sample, followed by post GEM-RT cleanup and cDNA amplification, then 3' Gene Expression Library Construction, according to the manufacturer's instructions. Sequencing was performed by the NGS platform with a NovaSeq 6000 sequencer.

Single-cell RNA-seq analysis

Reads were pseudoaligned to Ensembl transcripts (GRCh38, release 95) using kallisto (version 0.46.0[100]) with the -x 10x2 option for Chromium Single Cell 3' v2 chemistry. Count matrices were generated from sorted BUS files using bustools (version 0.39.2[101]), after barcode correction with the 10x v2 whitelist. For each sample, we selected cells via distance-based estimation of the knee in the cumulative distribution of distinct UMIs per barcode (unique molecular identifiers) using UMI-tools (version 1.0.0[102]). Sample matrices were thus converted to AnnData objects and concatenated for further quality control (QC) and analysis with Scanpy (version 1.4.6[103]). From the merged count matrix, we filtered out cells with abnormal levels of mitochondrial RNA, after adjusting for depth and total number of detected genes. Outliers were detected by covariance estimation (elliptic envelope with 5% contamination) using the number of genes, total counts (log-transformed) and mitochondrial counts (log-transformed) as features for outlier detection. Genes detected in less than 100 cells (after filtering) were also excluded. For comparison of scRNA-seq and bulk RNA-seq results, raw counts from matched samples were pooled across all cells, TMM-normalized and mean-centered.

For single-cell analyses, raw counts were normalized per cell, log-transformed, and adjusted for differences in sequencing depth via linear regression (using log-transformed total counts per cell). PCA was performed on the top 3000 highly variable genes (HVGs) after scaling. We computed a neighborhood graph using the first 20 principal components, adjusting for technical differences by batch alignment with BBKNN (version 1.3.9[104]). Uniform Manifold Approximation and Projection (UMAP) was used to visualize cell-to-cell variation in a low-dimensional (2D) space. Cell subpopulations were detected by Leiden clustering (at 0.5 resolution). Epithelial and mesenchymal cells were separately identified with the same procedure, but normalized counts were also adjusted for cell cycle differences (using the G1/S and G2/M signature) prior to scaling and PCA. For each cluster, genes were ranked by one-vs-all logistic regression to identify the top markers (See Table S2). Boundaries among clusters were computed via Support Vector Classification with a 3rd degree polynomial kernel. Gene sets for computing expression signatures were retrieved from Cyclebase v3.0 (Cell Cycle, G1/S and G2/M)[105] or MSigDB v6.2 (hallmark and curated gene sets related to senescence, EMT and cell metabolism)[106]. References for each of the signatures are provided in Table S2 (sheet 1). The scores (colour gradients) are a measure of the average expression of the given set of genes, relative to a set of randomly sampled genes at comparable expression levels. Log-transformed normalized counts (prior to scaling) were used for the calculation. The score is then rescaled across cells from -1 (lowest) to +1 (highest).

For RNA velocity analyses, an additional index including both cDNA and intron sequences was generated from Ensembl annotations (GRCh38, release 95) using the kb-python wrapper (version 0.24.4) for pseudoalignment and quantification with kallisto and bustools (La Manno workflow). Filtered count matrices for both spliced and unspliced transcripts were added to the preprocessed data and analyzed using the scVelo package (version 0.2.2). RNA velocity was first evaluated across all samples for the top 3000 highly variable genes by fitting a dynamical model estimating the kinetic rate parameters for each gene, as well as the latent time underlying the overall kinetics[55]. To check whether the velocity flow changes by condition, we further estimated RNA velocities in individual samples by stochastic modeling. The trajectories across all conditions, and for each sample, were visualized in the pre-computed UMAP embedding using a streamline plot that shows the directional flow across cells (considering velocities with a minimum mass of 3 and applying a smoothing factor of 0.8). In all UMAP plots, the latent time is represented by a color gradient ranging from 0 (initial state, blue) to 1 (terminal state, red).

Singe-cell RNA-seq analyses were carried out with custom Python scripts using Scanpy (version 1.4.6), scVelo (version 0.2.2), BBKNN (version 1.3.9), UMI-tools (version 1.0.0), pandas (version 0.25.0), NumPy (version 1.17.0), scikit-learn (version 0.21.3), matplotlib (version 3.3.0), and seaborn (version 0.9.0).

Beta-galactosidase senescence assay

We tested samples in duplicate for senescence using the Cell Signaling Technologies Senescence β-Galactosidase Staining Kit, according to the manufacturer's instructions. After 24h with the stain, we imaged at least three fields per sample by brightfield microscopy using a 10X objective on a Nikon Eclipse TS100 microscope. Cells were counted manually from the acquired images with the counter blinded to the conditions. Only cells with dark blue staining were considered senescent.

Propidium iodide FACS

To analyze cell cycle changes by FACS, we harvested cells with trypsin and fixed with cold 70% ethanol. We stained fixed cells with propidium iodide using FxCycle PI/RNase solution (ThermoFisher Scientific), according to the manufacturer's instructions. FACS was performed on three biological replicates with a FACS Accuri 6 machine and cell cycle was assessed on a minimum 10000 gated cells, excluding cell debris and doublets, using the Dean-Jett-Fox model with FlowJo software (V10.1r5).

PART 2. CENP-A OVEREXPRESSION IS AN EPIGENETIC REGULATOR OF CELL PLASTICITY AND HETEROGENEITY DURING EPITHELIAL-MESENCHYMAL TRANSITION IN HUMAN CELLS

In preparation

C. Renaud-Pageot [1], D. Capocefalo [2*], S. Lemaire [1*], A. Forest [1], J.-P. Quivy [1], L. Cantini [2] & G. Almouzni [1]

[1] Institut Curie, PSL University, Sorbonne Université, CNRS, UMR 3664 Nuclear Dynamics, Chromatin Dynamics lab, 75005 Paris, France

[2] Institut Pasteur, Université Paris Cité, CNRS, UMR 3738, Machine Learning for Integrative Genomics lab, 75015, Paris, France

* Equal contributions

1. RATIONALE AND CONTRIBUTION

To further understand the effects of CENP-A overexpression on cell fate regulation, in the context of EMT, I next wanted to expand the analysis to other models. I found that CENP-A overexpression on its own was not sufficient to induce EMT in every cell line, even p53-defective, that I tested. These data led me to consider that CENP-A overexpression likely stimulates or potentiates EMT in specific cellular contexts. Thus, for this second project, I aimed at (1) identifying the context in which CENP-A promotes EMT and (2) characterizing the transition in order to understand whether it relies on genetic or non-genetic and reversible mechanisms. Under the supervision of my thesis directors, I designed the experimental strategy, performed all cell biology, imaging and biochemistry analyses and wrote the following manuscript. Together with Audrey Forest, we performed cytometry and chromatin immunoprecipitation experiments. Daniele Capocefalo and Laura Cantini performed the integration of the multiomics dataset. Bioinformatics analyses, data discussion and manuscript corrections involved all authors.

2. ABSTRACT

The overexpression of the centromeric histone variant CENP-A, a common feature of aggressive cancers, can promote an epithelial-mesenchymal transition (EMT), a key driver of cancer progression and metastasis. Yet, the dynamics of this phenotypic plasticity and the underlying mechanisms remain poorly characterized. To address these issues, we used a reversible CENP-A induction system for a controlled overexpression in human cells. We find that chronic CENP-A overexpression, along with its ectopic incorporation, drives a progressive transition from intermediate towards mesenchymal states. Furthermore, CENP-A overexpression upregulates distinct EMT transcription programs, including a pro-survival program which is inhibited by active p53, thereby increasing EMT heterogeneity. Remarkably, by reversing CENP-A overexpression, we erase ectopic incorporation of CENP-A and reverse induced mesenchymal states, in line with non-genetic alterations. We propose that CENP-A overexpression regulates epithelial-mesenchymal plasticity and heterogeneity in an epigenetic manner. We discuss implications for tumor evolution and tailored therapeutic strategies.

3. INTRODUCTION

The centromere protein A (CENP-A) is a histone H3 variant specifically incorporated into centromeric chromatin and essential for the proper segregation of human chromosomes to daughter cells (Fukagawa and Earnshaw 2014; McKinley and Cheeseman 2014; Muller, Gil, and Drinnenberg 2019; Musacchio and Desai 2017). CENP-A combines both genetic and epigenetic features to provide the foundation of kinetochore assembly during cell division (Ali-Ahmad and Sekulić 2020), and to determine (Barnhart et al. 2011; Fachinetti et al. 2013) and maintain (Amor et al. 2004; Jansen et al. 2007; Smoak et al. 2016; Tyler-Smith et al. 1999) centromere position across mitotic and meiotic divisions. CENP-A restriction to the centromere depends on key parameters. First, the exclusive partnership between CENP-A and its dedicated histone chaperone, the holiday junction recognition protein (HJURP) directs the specific incorporation of newly synthetized CENP-A at centromeres in late mitosis (Dunleavy et al. 2009; Foltz et al. 2009). This ensures to both replenish CENP-A at centromeres to counteract dilution in S phase (Jansen et al. 2007), and parental CENP-A recycling at the replication fork (Zasadzińska et al. 2018). Second, chromatin replication acts as an error correction mechanism removing CENP-A from chromosome arms, keeping CENP-A nucleosomes specifically at centromeres (Nechemia-Arbely et al. 2019). Third, the partnership between CENP-A and HJURP is reinforced by co-regulating their levels during the cell cycle with a peak of expression in G2/M (Richard D. Shelby, Vafa, and Sullivan 1997). They both harbor in their promoters a CDE/CHR motif which is recognized by the DREAM complex (M. Fischer et al. 2016), enabling to mediate a p53-dependent transcriptional repression of *CENPA* and *HJURP* (Filipescu et al. 2017).

CENP-A is frequently overexpressed across many tumor types in both p53-WT and p53-defective cancers (Lacoste et al. 2014; Renaud-Pageot et al. 2022; X. Sun et al. 2016) since CENP-A can evade p53 control (Jeffery et al. 2021). This CENP-A overexpression could (i) simply reflect the increased mitotic activity of cancer states, but also (ii) represent an active process participating to cancer resistance and/or progression. Furthermore, CENP-A overexpression also leads to an imbalance in the proportions of histone H3 variants and the excess of CENP-A hijacks H3.3-dedicated chaperones DAXX (Lacoste et al. 2014) and HIRA (Nye et al. 2018). This situation enables the misincorporation of CENP-A in non-centromeric chromatin (Athwal et al. 2015; Balachandra et al. 2024; Lacoste et al. 2014; Nye et al. 2018; Renaud-Pageot and Almouzni 2024; Shrestha et al. 2023). Since ectopic CENP-A traps a series of kinetochore components away from native centromeres (Shrestha et al. 2017, 2021), this has been proposed to weaken centromere function thereby contributing to chromosomal instability and aneuploidy (Amato et al. 2009; Athwal et al. 2015; Shrestha et al. 2017, 2021). In addition, we previously reported that high CENP-A levels promotes an epithelial-mesenchymal transition (EMT) in p53-defective human cells (Jeffery et al. 2021). EMT represents a major cell fate, during which cells switch from an epithelial to a mesenchymal phenotype, which has been associated with cancer progression, resistance and metastasis (E. D. Hay 1995). In line with these observations, high CENP-A

levels correlate with cancer aggressiveness, invasion and metastasis in several tumor types (Renaud-Pageot et al. 2022). Distinct EMT programs are normally activated during early embryogenesis in vertebrates (E. D. Hay 1995; Elizabeth D. Hay 2005) and in adult wound healing and fibrosis (Youssef and Nieto 2024). In cancer, by hijacking EMT, tumor cells can acquire stem cell-like properties, tumor-initiating capabilities, increased resistance to therapy along with invasive and migratory properties that facilitate metastatic processes (Jean Paul Thiery et al. 2009). Increasing evidence from circulating tumor cells in blood (M. Yu et al. 2013) and mouse models (Pastushenko et al. 2018) points to the existence of intermediate states between epithelial and mesenchymal. Little is known about their dynamics, their contribution to tumor progression and, more broadly, about the molecular actors at play in cancer-associated EMT states. The emerging notion of epithelial-mesenchymal plasticity (EMP) describes the spectrum of transitions between epithelial and mesenchymal states in a given cellular context with the ability for cells to interconvert between different intermediate states (M. Angela Nieto et al. 2016; J. Yang, Antin, Berx, Blanpain, Brabletz, Bronner, Campbell, Cano, Casanova, Christofori, Dedhar, Derynck, Ford, Fuxe, García de Herreros, et al. 2020). This process, associated with high phenotypic plasticity (P. B. Gupta et al. 2019) and diversity (Pastushenko and Blanpain 2019), proceeds through multiple alternative paths to progress towards a mesenchymal state. Importantly, we previously showed that CENP-A overexpression increased the mesenchymal population in a given p53-defective human cell line (Jeffery et al. 2021). However, how CENP-A overexpression impacts the epithelial-mesenchymal plasticity, its context-dependency and whether this is operating through genetic or non-genetic properties remained an open question. Unravelling this issue is of major importance regarding cancer invasiveness and metastasis.

In this study, we investigated the impact of reversible CENP-A overexpression over time on EMT. We monitored the temporal dynamics of EMT states in a model of fibrocystic breast human cell line conditionally overexpressing CENP-A. We characterized specific transition states by combining microscopy and flow cytometry. We next identified transition by chromatin immunoprecipitation followed by sequencing (ChIP-seq) analyses along with single cell multiomics approaches combining ATAC and RNA sequencing. These analyses allowed to demonstrate that CENP-A overexpression drives the transition of intermediate cells by stimulating two distinct paths towards mesenchymal states. Finally, by reversing overexpression of CENP-A, we erase ectopic CENP-A from chromosome arms and show that induced mesenchymal states are reversed. Thus, while CENP-A has long been considered mainly for its key role in maintaining genome stability, we unveil here a non-genetic and reversible feature in regulating epithelial-mesenchymal plasticity. We discuss this unanticipated epigenetic role of CENP-A outside centromere for its impact on cancer progression, therapy and developmental biology.

4. RESULTS

CENP-A overexpression promotes EMT in cell lines displaying intermediate transition states

With a doxycycline-inducible overexpression of CENP-A (Tet-On-CENPA–FLAG–HA, see Material and Methods), we had previously observed that CENP-A overexpression increases the mesenchymal population in the MCF10-2A human cell line (Jeffery et al. 2021) (benign fibrocystic breast (Soule et al. 1990)). While we could also reproduce this observation in RPE-1 cells, other cell lines did not respond similarly to this stimulus (Fig S1). We thus decided to concentrate on the MCF10-2A cell line to understand what makes them "special". We immunostained cells simultaneously for epithelial markers (E-cadherin or β-Catenin, both forming a complex at the membrane of epithelial cells (Ozawa, Baribault, and Kemler 1989)) and the mesenchymal marker vimentin. This way, we revealed a population of cells with hybrid epithelial/mesenchymal (E/M) features, co-existing with epithelial and mesenchymal cells (Fig. 1a and 1b). While epithelial cells showed intercellular adherence and epithelial markers, by contrast, mesenchymal cells lost adhesion and epithelial markers at their membrane and showed a round or spindle shape with a vimentin-rich network assembled into extensive filaments. Strikingly, intermediate cells showed hybrid phenotypes, co-expressing both epithelial and mesenchymal markers in a spectrum ranging from (a) weak vimentin staining and high expression of epithelial markers to (b) intense speckle of vimentin at the nuclear periphery and high expression of epithelial markers to, more rarely, (c) extensive vimentin expression throughout the cytoplasm and lower expression of epithelial markers (Fig. 1a, 1b). These phenotypes exist in both p53 contexts: p53-WT (cells transduced with an empty vector) and p53-DN (p53-defective cells following transduction with a constitutively expressed dominant negative (DN) TP53 construct(Jeffery et al. 2021)). Since the culture medium of MCF10-2A cells is usually supplemented with epidermal growth factor (EGF), an EMT inducer. (Ackland et al. 2003; Gross et al. 2022; Pagan et al. 1997), we checked if different EGF concentrations promotes or potentiates EMT in this system. In the absence of EGF, which reduces cell proliferation(Bessette et al. 2015), the intermediate cell population decreased to less than 1% (Fig. S1e, left panel) and CENP-A overexpression had no effect on EMT (Fig. S1e, right panel). Relative to 1X, increasing EGF concentration up to 20X did not further increase the intermediate cell population and only modestly increased the mesenchymal cell population by 4% in p53-DN cells (Fig. S1e), indicating that EGF does not promote further the mesenchymal transition. Thus, CENP-A overexpression promotes EMT in proliferating cells already displaying intermediate cell states, such as MCF10-2A and RPE-1 cell lines, and this is unlikely operating via an enhanced EGF signaling.

Figure 1

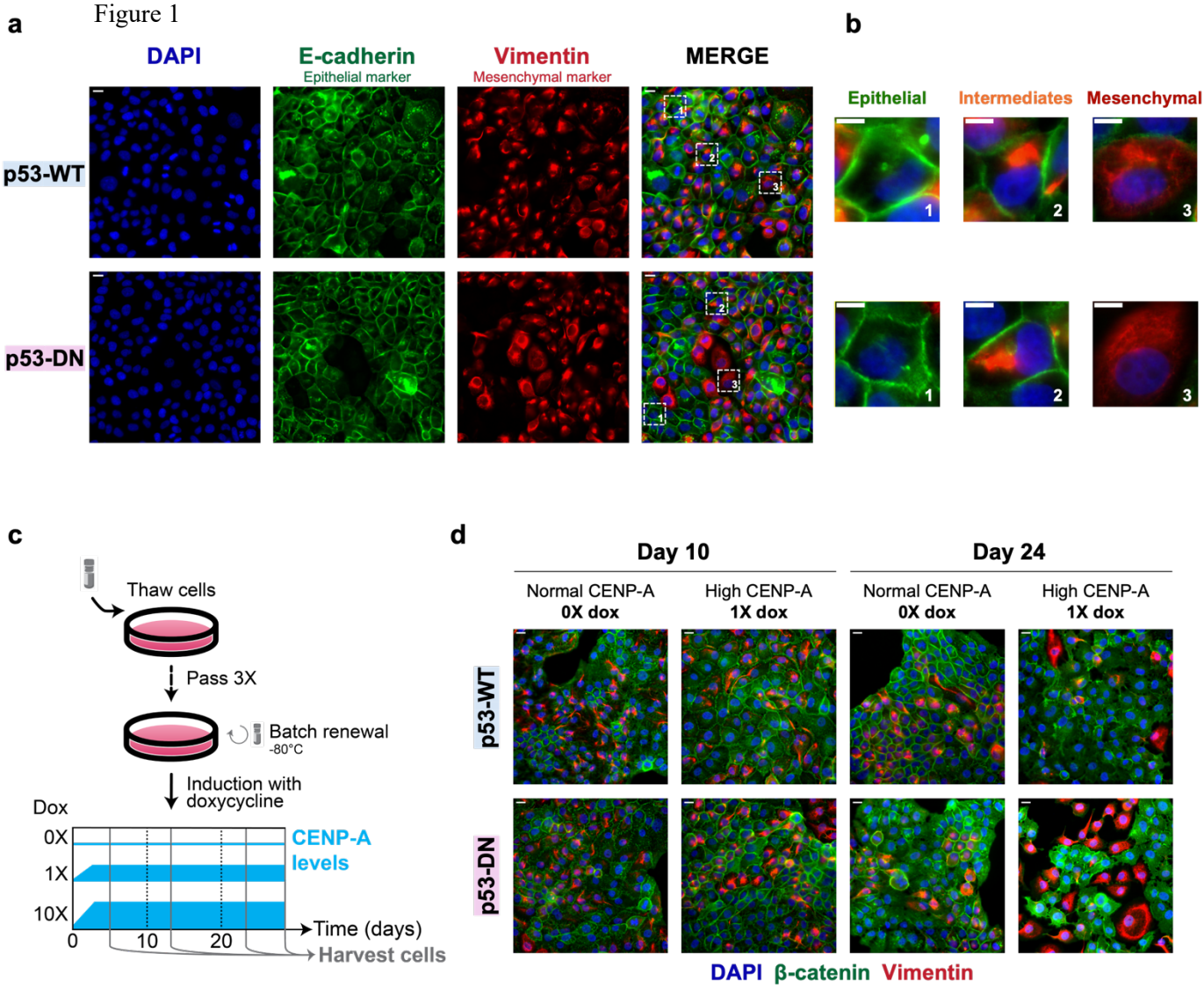

a
DAPI
E-cadherin
Epithelial marker
Vimentin
Mesenchymal marker
MERGE
p53-WT
p53-DN
b
Epithelial
Intermediates
Mesenchymal
c
Thaw cells
Pass 3X
Batch renewal
-80°C
Induction with
doxycycline
Dox
0X
1X
10X
CENP-A
levels
0
10
20
Time (days)
Harvest cells
d
Day 10
Day 24
Normal CENP-A
0X dox
High CENP-A
1X dox
p53-WT
p53-DN
DAPI β-catenin Vimentin
e
Quantification of EMT states across time
Normal CENP-A
0X dox
High CENP-A
1X dox
p53-WT
p53-DN
% cell states
Days
Epithelial
Intermediates
Mesenchymal

Figure 1. Mesenchymal states increase while intermediate states decrease upon CENP-A overexpression. (**a**) EMT states in the MCF10-2A cell line at start ("day 0") without induction of CENP-A overexpression. Representative wide-field epifluorescence images of cells immunostained for E-cadherin (green, epithelial marker) and vimentin (red, mesenchymal marker), with DNA counterstaining with DAPI (blue). Squared boxes indicate cells on panel (b). Same range of pixel values displayed between conditions. Scale bars = 20 μm. (**b**) Insets of representative EMT states. Definition of the three states observed based on green (epithelial marker E-cadherin or β-catenin) and red (mesenchymal marker vimentin) signals: (1) Epithelial: strong green signal at the membrane, little or no red signal in the cytoplasm, polygonal cell; (2) Intermediate: co-expression of both markers (green signal at the membrane with at least an intense red speckle which can spread out in the cytoplasm), polygonal or round cell; (3) Mesenchymal: red marker extending throughout the cytoplasm as a network of filaments, loss of green signal, round or spindle-shaped cell. Scale bars = 10 μm. (**c**) Experimental scheme of time course experiments. Cells are thawed and passed three times prior to renewing batch and starting the induction with 0X (1:100000 DMSO), 1X (10 ng/ml) or 10X (100 ng/ml) doxycycline (Dox). Samples are harvested at several time points across cell passages. (**d**) EMT states in the MCF10-2A cell line after 10 days and 24 days induction. Representative wide-field epifluorescence images of cells immunostained for β-catenin (green, epithelial marker) and vimentin (red, mesenchymal marker), with DNA counterstaining with DAPI (blue). Same range of displayed pixel values between conditions. Corresponding CENP-A signals are shown in Suppl. Fig. 1a. (**e**) Quantification of epithelial (green), intermediate (orange) and mesenchymal (red) cell states across time. For each condition, data show the trendline as polynomial of the fourth degree, data points and range between four highest and lowest values, for at least 4 biologically independent experiments. >200 cells counted per data point in at least three fields. Day 0 share same data points between and 0X and 1X conditions (same plate at start).

CENP-A overexpression drives the transition from intermediate towards mesenchymal states

We then tracked EMT states by immunostaining in cells with normal and high CENP-A levels in time course experiments, and monitored the proportions of epithelial, mesenchymal, and intermediate cells with at least an intense speckle of vimentin (Fig. 1c). After 24 days in culture, as expected, chronic CENP-A overexpression (1X Dox, Fig. 1d-e; 10X Dox, Fig. S1), led to the highest proportion of mesenchymal cells in the p53-DN condition. In p53-WT cells, in normal conditions, all cell states remained stable over time (mostly epithelial and 20% intermediates, see Fig. 1e, top left panel) and CENP-A overexpression only led to a limited increase in the mesenchymal population (from 10% to 20% on average), which decreased after 15 days while the epithelial population increased (Fig. 1e, top right panel). In p53-DN cells, in the control, intermediate states decreased over time from 40% to 20% while epithelial states increased up to 80% (Fig. 1e, bottom left panel). In contrast, CENP-A overexpression in p53-DN cells led to a strong increase in the mesenchymal population starting from day 10, from 5% to 30% on average (Fig. 1e, bottom right panel). Remarkably, the increase in mesenchymal cells correlated strongly with a decrease (from 40% to 15%) in the intermediate population, and the mesenchymal proportions stayed around 25-30% after 25 days. Thus, in p53-defective MCF10-2A cells, CENP-A overexpression promotes a robust and stable increase in the mesenchymal population after 10 days. This increase occurs while the intermediate states present at start in the model decrease to the same extent. To further assess whether CENP-A overexpression acts by pushing intermediate towards mesenchymal states, we searched for more advanced (late) intermediate states when CENP-A is overexpressed. For this, we monitored the mesenchymal marker vimentin in the intermediate cells. Indeed, upon CENP-A overexpression we detected high vimentin levels throughout the cytoplasm in the remaining intermediate cells (Fig. 2a), generally at the periphery of cell colonies. This is confirmed by quantifying the average vimentin intensity per cell in different areas of CENP-A-overexpressing cell cultures (relative to the intensity in cells with normal CENP-A levels) (Fig. 2b). Importantly, we also detected these transitions in intermediate states using cytometry based on E-cadherin and vimentin markers (Fig. 2c-d, S2a). Again, in normal conditions, cells shifted towards an epithelial state while, in contrast, upon CENP-A overexpression, the balance was rather towards more advanced (late) intermediate (I3) and mesenchymal (M) states. Remarkably, the proportions of epithelial, mid/late intermediates, and mesenchymal cells revealed by FACS corresponded to those detected by IF (Fig. S2b). Overall, this analysis revealed how intermediate cells can be pushed in different directions depending on the context. In normal conditions, they progressively revert to an epithelial state, while CENP-A overexpression pushes them towards mesenchymal.

Figure 2

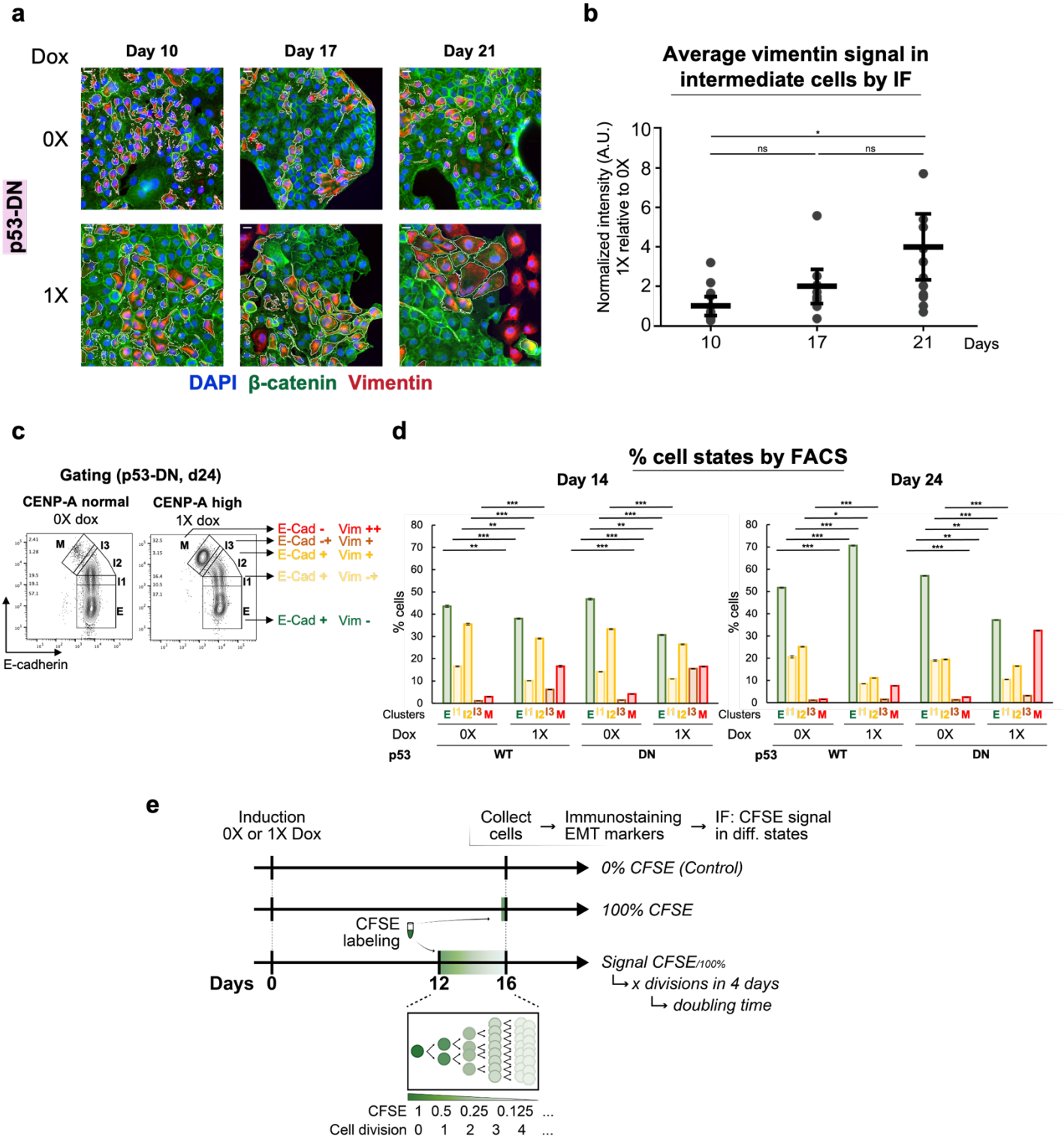

a
Dox
Day 10
Day 17
Day 21
0X
1X
p53-DN
DAPI β-catenin Vimentin
b
Average vimentin signal in intermediate cells by IF
Normalized intensity (A.U.) 1X relative to 0X
ns
ns
*
10
17
21
Days
c
Gating (p53-DN, d24)
CENP-A normal
0X dox
CENP-A high
1X dox
M
I3
I2
I1
E
E-Cad - Vim ++
E-Cad -/+ Vim +
E-Cad + Vim +
E-Cad + Vim -/+
E-Cad + Vim -
Vimentin
E-cadherin
d
% cell states by FACS
Day 14
Day 24
% cells
Clusters
E I1 I2 I3 M
Dox
0X
1X
p53
WT
DN
e
Induction
0X or 1X Dox
Collect cells
Immunostaining EMT markers
IF: CFSE signal in diff. states
0% CFSE (Control)
100% CFSE
CFSE labeling
Signal CFSE/100%
x divisions in 4 days
doubling time
Days 0
12
16
CFSE 1 0.5 0.25 0.125 ...
Cell division 0 1 2 3 4 ...
f
Cell doubling time between day 12 & 16
p53-WT
p53-DN
hrs
ns
*
0X 1X
Epithelial
Intermediate
Mesenchymal
Dox

Figure 2. CENP-A overexpression progressively promotes the transition of intermediate cells towards mesenchymal. (a) Epifluorescence images of cells immunostained for β-catenin (green) and vimentin (red), with DNA counterstaining with DAPI (blue). Intermediate cells, co-expressing β-catenin and vimentin at different levels, are segmented (white lines). This enables to monitor vimentin intensity across time in different regions of intermediate cells. Range of pixel values displayed are the same. Scale bars = 20 μm. (b) Average vimentin intensity per intermediate cell, based on IF image segmentation as shown in panel a. Plots show mean per (intermediate) cell and 95% confidence interval for two experiments. Each dot represent the mean per cell in a microscopic field. Statistical significance tested by two-tailed Welch's t test. * = p-value < 0.05. (c) Gating strategy for EMT state detection by Fluorescence-Activated Cell Sorting (FACS) based on E-cadherin and vimentin levels: Epithelial (E); Early Intermediate (I1); Mid-Intermediate (I2); Late Intermediate (I3); Mesenchymal (M). Representative example of MCF10-2A p53-DN cells at day 24 with 0X or 1X Dox. All cells passaged in parallel then fixed with ethanol. See Fig. Suppl. 2a for representative plots for all conditions. (d) EMT state quantification by FACS at day 14 and day 24. Bar plot shows mean and standard deviation for two experiments. Based on E-cadherin and vimentin levels: Green = Epithelial (E); Yellow = Early Intermediate (I1); Orange = Mid-Intermediate (I2); Dark orange = Late Intermediate (I3); Red = Mesenchymal (M). Statistical significance tested by two-tailed Welch's t test. * = p-value < 0.05; ** = p-value < 0.01; *** = p-value < 0.001. N.B. – Regarding p53-WT cells, note the early increase in the mesenchymal population, which is not maintained, similarly, to results by IF. (e) Experimental scheme of CFSE tracing experiment. Cells are cultivated for 16 days with 0X or 1X Dox in 3 plates per condition. At day 14, cells in one plate are pulse labelled with 5 μM CFSE solution, then cultivated for 4 days. At day 16, another plate is pulse labelled using the same solution (100% signal). All cells are then immediately harvested. Cells are immunostained for EMT markers β-catenin and vimentin. CFSE signal in different EMT states is tracked by IF microscopy. The relative signal (normalized to 100% signal) enables to calculate the number of divisions underwent by a cell between day 12 and 16, and to estimate their doubling time. (f) Average doubling time of different EMT states between day 12 and 16. Bar plot shows mean and standard deviation for two experiments. Statistical significance tested by two-tailed Welch's t test. * = p-value < 0.05.

Promotion of the mesenchymal population does not involve DNA damage or proliferation advantage

We then wanted to understand which mechanisms promoted the transition from intermediate to mesenchymal upon CENP-A overexpression. We previously showed, on a short time scale, increased mitotic stress in both p53-WT and p53-DN cells upon CENP-A overexpression, without increase in acute DNA damage or the rate of DNA repair assessed by detection of H2A.X phosphorylation (γ-H2A.X) levels and comet assay (Jeffery et al. 2021). Here, we checked γ-H2A.X levels on a longer timescale in our time course experiments and detected no significant change (Fig. S2g). In addition, our transcriptomic analysis did not reveal a significant impact on the DNA damage response pathway (Fig. 3a). These findings enabled us to discard a major role for DNA damage in the induction of the transition. Then, we examined whether cell proliferation could be advantageous to increase the mesenchymal population upon CENP-A overexpression. Thus, we tracked proliferating cells with carboxyfluorescein diacetate succinimidyl ester (CFSE), a widely used intracellular fluorescent dye that is divided equally between daughter cells, allowing discrimination of successive rounds of cell division. We followed cells between day 12 and day 16, a critical time window during which the mesenchymal cell population increase upon CENP-A overexpression. To estimate the average doubling time for each cell state, we harvested cells at day 16 and revealed EMT markers in parallel to CFSE levels (Fig. 2e). This way, we estimated the number of cell divisions and doubling time for each EMT state, in order to compare their proliferation rates between day 12 and day 16. We revealed that CENP-A overexpression has a negative impact on the proliferation rate of all subpopulations (Fig. 2f) in both p53 contexts. Notably, intermediate cells were the least impacted, their doubling time increasing by 1.5 hrs with CENP-A overexpression while it increased by 2 hrs for epithelial and mesenchymal populations in p53-DN cells. Furthermore, mesenchymal cells were proliferating slower than the other populations in all cases. While CFSE tracing can reveal cells that stop dividing, it does not reveal cell death. We thus monitored apoptotic cells with cleaved caspase-3 staining and revealed no major cell death or proliferation advantage between mesenchymal and non-mesenchymal cells (Fig. S2f). In addition, cell cycle analysis by FACS showed that the mesenchymal population have the highest proportions of G1 cells (and lowest proportions of S and G2/M cells) compared to other populations (Fig. S2c-d). Therefore, the increase in the mesenchymal population in the MCF10-2A cell line cannot merely result from a proliferation advantage. Thus, we conclude that CENP-A overexpression driving EMT cannot depend on DNA damage or any survival or proliferation advantage for mesenchymal cells compared to the other states and rather involves an increase in the transition from intermediate towards the mesenchymal state.

Figure 3

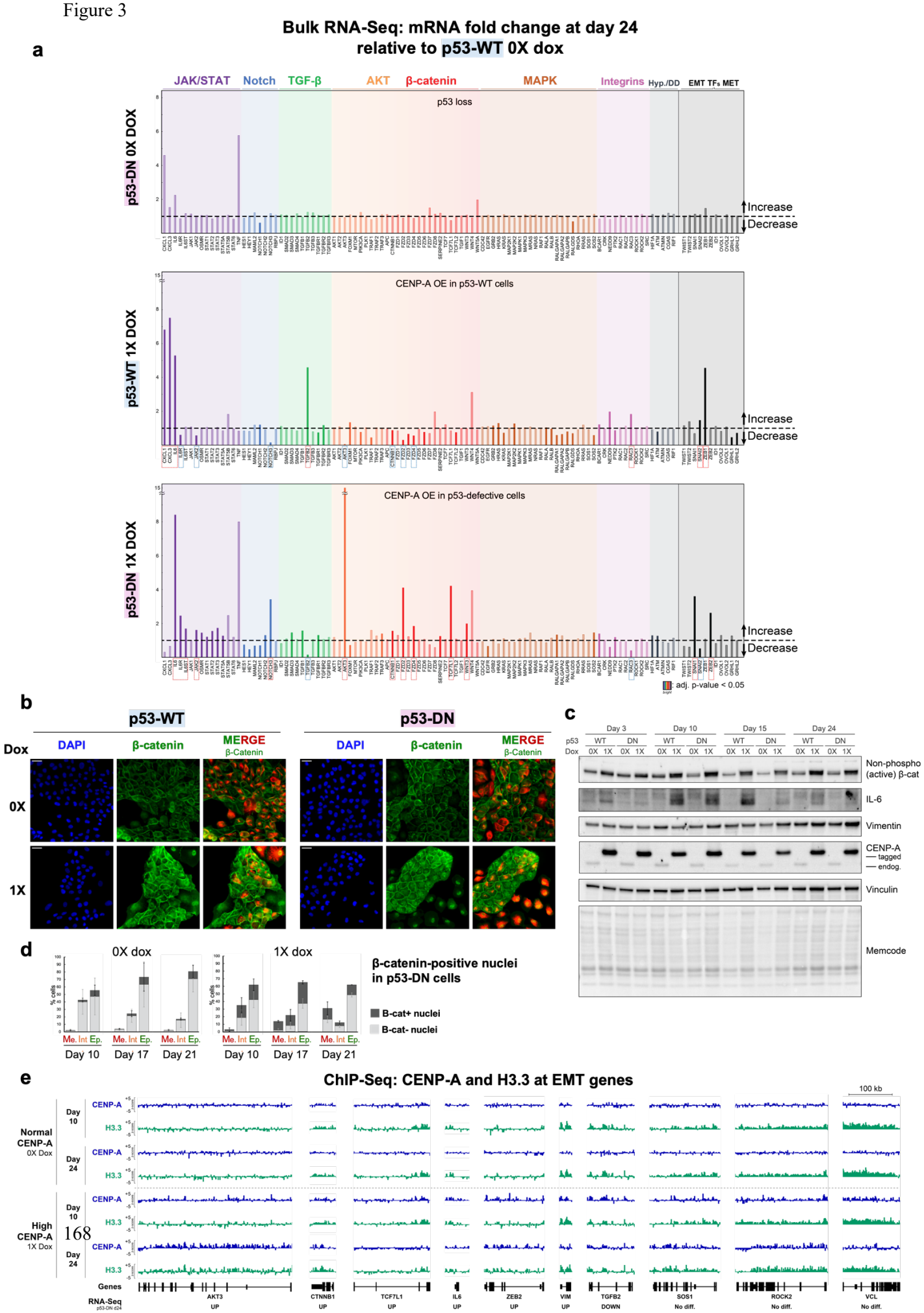

a
Bulk RNA-Seq: mRNA fold change at day 24
relative to p53-WT 0X dox
JAK/STAT
Notch
TGF-β
AKT
β-catenin
MAPK
Integrins
Hyp./DD
EMT TFs
MET
p53-DN 0X DOX
p53 loss
p53-WT 1X DOX
CENP-A OE in p53-WT cells
p53-DN 1X DOX
CENP-A OE in p53-defective cells
Increase
Decrease
adj. p-value < 0.05
b
p53-WT
p53-DN
Dox
DAPI
β-catenin
MERGE
β-Catenin
0X
1X
c
Day 3
Day 10
Day 15
Day 24
p53
WT
DN
Dox
0X 1X
Non-phospho (active) β-cat
IL-6
Vimentin
CENP-A
tagged
endog.
Vinculin
Memcode
d
0X dox
1X dox
% cells
Me. Int Ep.
Day 10
Day 17
Day 21
β-catenin-positive nuclei
in p53-DN cells
B-cat+ nuclei
B-cat- nuclei
e
ChIP-Seq: CENP-A and H3.3 at EMT genes
100 kb
Normal CENP-A
0X Dox
High CENP-A
1X Dox
Day 10
Day 24
CENP-A
H3.3
Genes
RNA-Seq
p53-DN d24
AKT3
CTNNB1
TCF7L1
IL6
ZEB2
VIM
TGFB2
SOS1
ROCK2
VCL
UP
DOWN
No diff.

Figure 3. CENP-A overexpression upregulates specific EMT pathways without specific local enrichment at DEGs. (**a**) Bar plot showing mRNA fold change at day 24 in MCF10-2A cells for EMT genes with their related pathways annotated above. Expression relative to the p53-WT 0X Dox condition (TMM normalized). (**b**) Western blot of MCF10-2A cells at four time points from the same time-course experiment. Loading corresponds to total protein extract from ~30000 cells. Primary antibodies are indicated on the right. Vinculin was used as loading control. (**c**) β-catenin localization in MCF10-2A cells at day 24. Epifluorescence images of cells immunostained for β-catenin (green) and vimentin (red) with DNA counterstaining with DAPI (blue). Range of pixel values displayed are the same. Scale bars = 40 μm. (**d**) Quantification of cells with positive and negative β-catenin nuclear signal in MCF10-2A cells at different time points. Complete nuclear translocation (i.e., loss at the membrane and positive signal in the nucleus) only occurred for mesenchymal cells (red). Figure shows proportions of β-catenin-negative and -positive nuclei in all populations. Stacked bar plots show mean and standard deviation for two experiments. >200 cells counted per condition in at least three fields. (**e**) CENP-A and H3.3 ChIP-Sequencing analysis at day 10 and day 24. Example of peak distribution and read density (z-score) of CENP-A and H3.3 mapping to gene sequences of differentially and non-differentially expressed genes in the bulk RNA-Seq analysis.

CENP-A overexpression upregulates specific EMT signaling pathways through global changes in chromatin organization

To explore the mechanisms guiding cell-fate changes, we analyzed how CENP-A overexpression impacts transcription considering the EMT signaling pathways. Indeed, considering that CENP-A overexpression likely stimulates EMT when already engaged, we reasoned that an amplification of distinct signaling pathways involved in the EMT could occur. Using bulk RNA-seq data set at day 24, we searched EMT effectors affected by CENP-A overexpression in the MCF10-2A cells. Firstly, p53 inactivation alone did not have a detectable impact on EMT pathways at the bulk transcriptional level (Fig. 3a, top panel). In contrast, CENP-A overexpression alone already resulted in a specific upregulation of IL-6 and TGF-β2, with a significant downregulation of AKT3 (Fig. 3a, middle panel). In a p53-defective context, CENP-A overexpression amplified IL-6 and, in addition, the pro-survival AKT3/β-catenin signaling pathways without engaging TGF-β2, which was rather significantly repressed (Fig. 3a, bottom panel). These results indicate that CENP-A overexpression promotes a p53 context-dependent EMT program. The same analysis at day 1 revealed no significant change, confirming that chronic CENP-A overexpression is required to activate these programs (Fig. S3a). To confirm these EMT effects at a protein level, upon CENP-A overexpression, we assessed β-catenin activation and IL-6 protein levels by Western Blot (Fig. 3b), along with β-catenin nuclear translocation by immunofluorescence (Fig. 3c-d). Both confirmed the impact of CENP-A on these programs at the protein level. Only mesenchymal cells showed complete β-catenin nuclear translocation (loss at the membrane, positive nuclear signal) and, when tracking β-catenin-positive nuclei, a large portion of induced mesenchymal cells showed nuclear accumulation in contrast with spontaneous mesenchymal cells (Fig. 3d). Next, we examined whether changes in CENP-A at the transcriptional level correlates with CENP-A enrichment at specific gene bodies and promoters. We combined transcriptomic information with CENP-A and H3.3 ChIP-Seq obtained at different time points to assess genome-wide distribution of CENP-A and H3.3. The analysis revealed an overall enrichment at turnover regions marked by H3.3, consistent with our previous data(Lacoste et al. 2014), but no specific enrichment at EMT genes whose transcription was significantly affected by CENP-A overexpression (Fig. 3e), or more generally at EMT transcription factor genes (Fig. S3c). Thus, CENP-A does not impact local chromatin organization at EMT genes, although its broad distribution at regulatory elements may enable a global plasticity. Interestingly, CENP-A overexpressing leads to H3.3 re-organization between day 10 and 24 into broader domains (Fig. S3b) accompanied by an increase in active histone marks H3K4me3 and K27Ac as detected by Western Blot, as opposed to K9me2, K27me3 or K36me3 marks (Fig. S3d). We conclude that CENP-A overexpressing cells promote distinct EMT gene expression programs without a local effect at EMT genes, but rather through a broad impact on chromatin structure, potentially increasing chromatin plasticity.

Figure 4

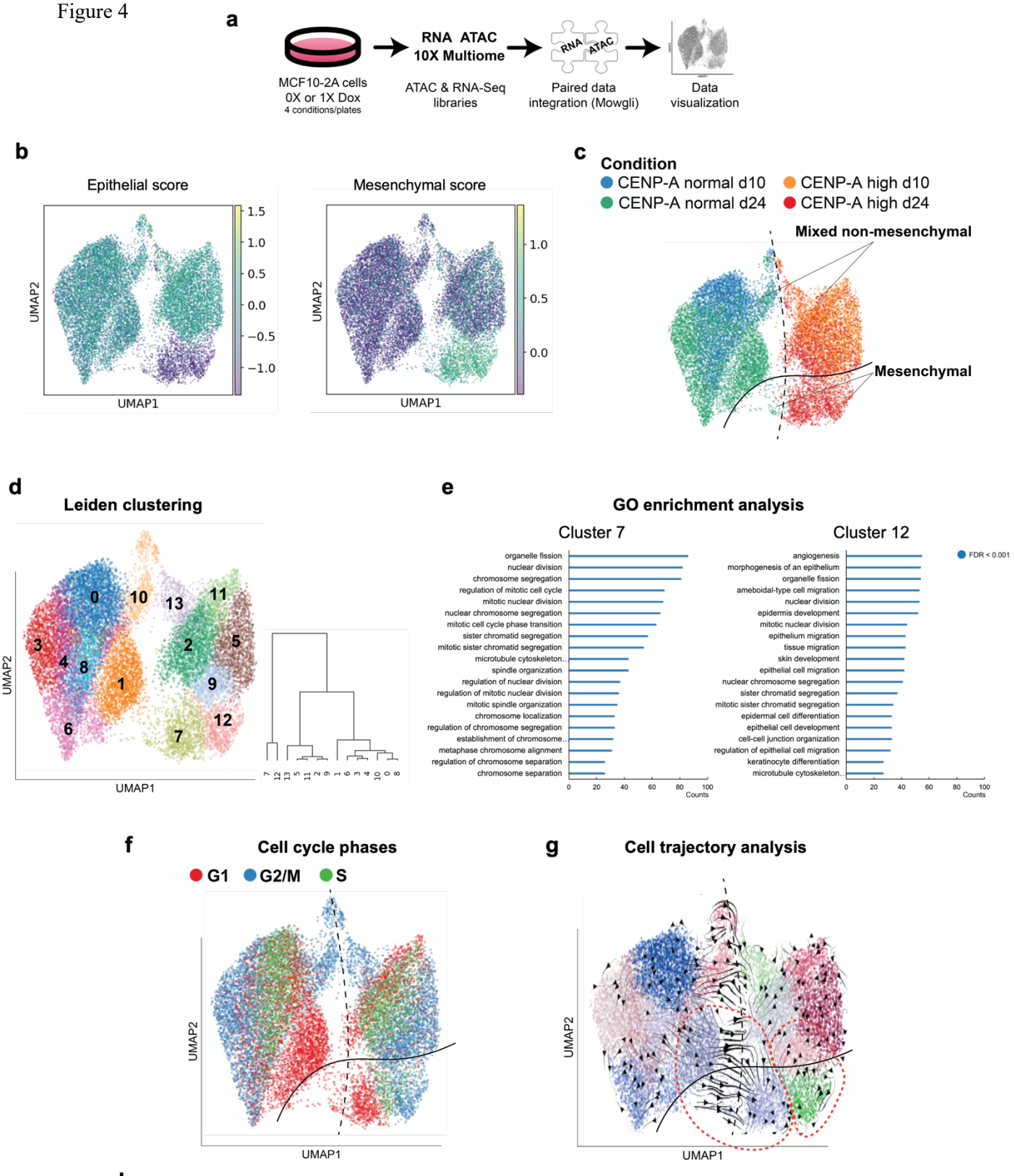

a
RNA ATAC
10X Multiome
MCF10-2A cells
0X or 1X Dox
4 conditions/plates
ATAC & RNA-Seq
libraries
Paired data
integration (Mowgli)
Data
visualization
b
Epithelial score
Mesenchymal score
UMAP1
UMAP2
c
Condition
CENP-A normal d10
CENP-A high d10
CENP-A normal d24
CENP-A high d24
Mixed non-mesenchymal
Mesenchymal
d
Leiden clustering
e
GO enrichment analysis
Cluster 7
Cluster 12
FDR < 0.001
Counts
f
Cell cycle phases
G1
G2/M
S
g
Cell trajectory analysis
h
Top 5 DEGs per cluster
Fraction of cells in group (%)
log fold change

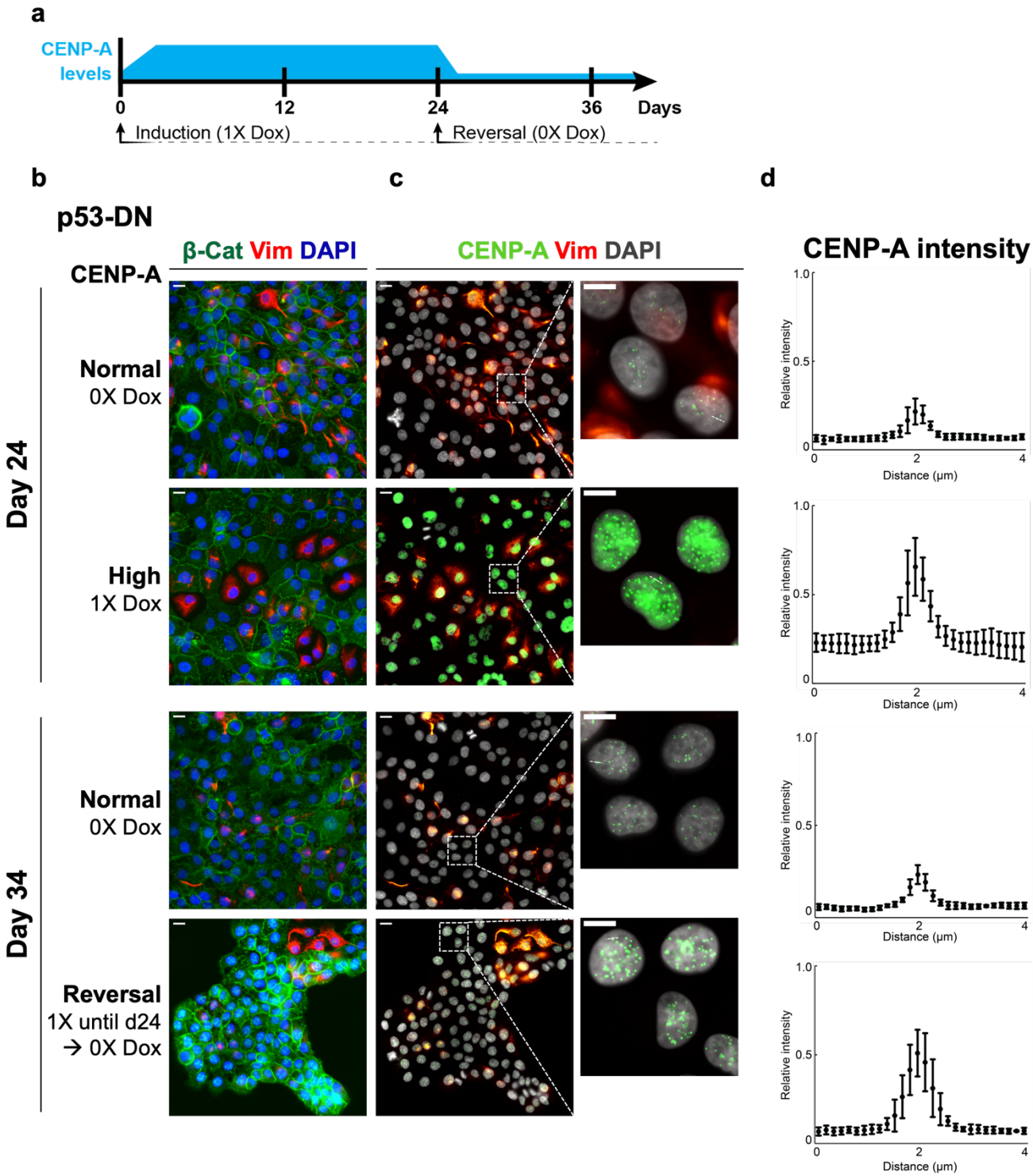
Figure 4. Single cell multi-omics analysis reveals two EMT programs promoted by CENP-A overexpression. (**a**) Schematic representation of the single cell multi-omics study of MCF10-2A p53-DN cells at two time points. (**b**) Uniform Manifold Approximation and Projection maps (UMAPs) of Mowgli's embedding with epithelial and mesenchymal scores based on the following markers: CDH1 and EPCAM (epithelial genes), VIM, FN1 and ZEB1 (mesenchymal genes). (**c**) UMAP plot of mesenchymal and non-mesenchymal subpopulations with focus on the different samples. Each dot corresponds to an individual cell projected in a 2D space where the topology reflects global similarities in expression. Four different colors correspond to the different samples analysed: 0X Dox and 1X Dox, both at days 10 and 24. (**d**) UMAP with Leiden hierarchical clustering labels, with corresponding dendrogram showing hierarchy of clustering. (**e**) GO enrichment analysis for DEGs in Biological Process (BP) terms. Bar plots shows top 20 BP terms significantly enriched in mesenchymal clusters 7 and 12 based on DEG counts (FDR > 0.05 for all). (**f**) UMAP visualization of cell cycle phases. (**g**) Cell fate trajectories inferred by RNA velocity analysis. Dynamical modelling depicted by a streamline plot (black arrows) showing the main directional flow across cells (gene-averaged velocity vector field in UMAP embedding). (**h**) Dot plot of scaled average expression and percentage of top 5 DEGs by annotated Leiden cluster.

CENP-A overexpression in p53-defective cells drives the activation of two distinct EMT trajectories, including a non-preexistant, developmental EMT program

We next investigated whether CENP-A overexpression stimulates either pre-existent EMT or new programs in the MCF10-2A cell line. Since our microscopy and cytometry analyses revealed a dynamic and heterogeneous cell population, we examined gene expression patterns and cell states in single cell analyses at two distinct time points. We combined single cell RNA and ATAC sequencing to profile both transcriptome and chromatin accessibility from the same cells in the p53-DN MCF10-2As (Fig. 4a). First, with our scMulti-omics data, we distinguished mesenchymal and non-mesenchymal populations (Fig. 4b). We also identified G2/M, S and G1 cells within each cluster (Fig. 4f). Remarkably, we noticed that the non-mesenchymal cluster gathers a mix of two sub-populations, both E-cadherin and EpCAM positive but vimentin positive or negative (Fig. 4b, S4c). This suggests that the cluster contains a mix of intermediate and epithelial cells, phenotypically close to each other. As expected, CENP-A overexpression caused a clear increase in the proportions of mesenchymal cells (Fig. 4c). Interestingly, while the spontaneously appearing mesenchymal cells reside in G1, the CENP-A-induced mesenchymal cells reside in all phases of the cell cycle (Fig. 4f). To further determine the key cellular pathways involved in the transition, we applied hierarchical clustering to identify co-regulated subsets of differentially expressed genes (DEGs). This revealed distinct clusters, including two mesenchymal clusters (Fig. 4d): **(i)** spontaneous and induced mesenchymal cells residing in G1 (cluster 7; Fig. 4c-d, 4f), **(ii)** induced mesenchymal cells only, in all phases of the cell cycle (cluster 12; Fig. 4e-f, S4f). To study cell dynamics and EMT trajectories, we inferred RNA velocity with scVelo (Bergen et al. 2020). With normal CENP-A levels, one EMT trajectory only led to mesenchymal cluster 7 (Fig. 4g). However, upon CENP-A overexpression, two non-connected trajectories led to the two mesenchymal clusters 7 and 12 (Fig. 4d, 4g). Thus, CENP-A overexpression stimulated both a pre-existing program leading to mesenchymal cells residing in G1 (leading to cluster 7), and a non-preexisting EMT trajectory (leading to cluster 12). According to gene set enrichment analysis (GSEA), cluster 7 was mainly associated with the upregulation of genes involved in cell division and chromosome segregation (Fig. 4e, left panel) while cluster 12 was mainly enriched in processes relating to angiogenesis and development (Fig. 4e, bottom panel). Top DEGs in cluster 7 mainly included drivers of EMT such as RBMS3, a RNA-binding protein involved in stabilization of PRRX1 mRNAs (Block et al. 2021), and well-known drivers of inflammation and fibrosis: HIPK2 (Garufi, Pistritto, and D'Orazi 2023), NEAT1 (X. Jiang 2023), IL-6 and IL6ST (Fig. 4h, S4d-f). Cluster 12 shared RBMS3 among its top DEGs and was marked by TOP2A (Fig. 4h) and, to a lesser extent, to other genes associated with proliferation and development such as AKT3 and VANGL1 (Fig. S4f, supplementary data 1). Thus, in normal conditions, EMT reaches an end point with cells residing in G1 phase of the cell cycle. In p53-defective cells, CENP-A overexpression promotes two transitions at different stages of the cell cycle and lead to different mesenchymal states: A pre-existing program associated with

inflammation and G1, and a new trajectory associated with cell cycle progression and activation of developmental signaling pathways. These data indicate that CENP-A overexpression enables to enrich the alternative trajectories available for intermediate cells to switch, thus increasing the heterogeneity of the final population, with distinct mesenchymal phenotypes in addition to different EMT states.

Figure 5


a
CENP-A levels
0
12
24
36
Days
Induction (1X Dox)
Reversal (0X Dox)
b
c
d
p53-DN
β-Cat Vim DAPI
CENP-A Vim DAPI
CENP-A intensity
CENP-A
Day 24
Normal
0X Dox
High
1X Dox
Day 34
Normal
0X Dox
Reversal
1X until d24
→ 0X Dox
Relative intensity
Distance (μm)

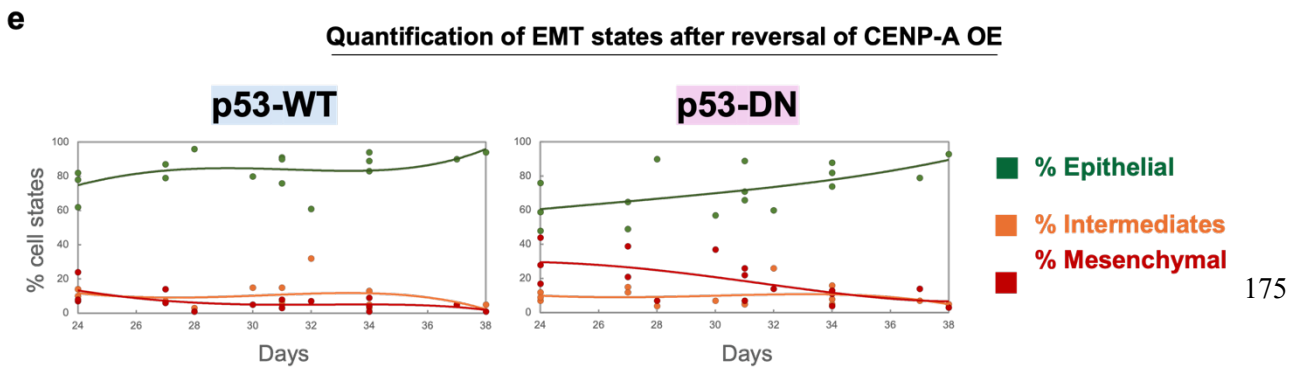

e
Quantification of EMT states after reversal of CENP-A OE
p53-WT
p53-DN
% cell states
Days
% Epithelial
% Intermediates
% Mesenchymal

Figure 5. Reversal of CENP-A overexpression reverses cell population phenotypes. (**a**) Experimental scheme of the reversal experiments. Cells are cultivated with continuous induction with 1X Dox until day 24. Then, cells are cultivated with 0X Dox for at least 10 more days to monitor CENP-A levels and localization along with EMT states. (**b**) Representative epifluorescence images of cells immunostained for β-catenin (green) and vimentin (red), with DNA counterstaining with DAPI (blue). Scale bars = 20 μm. (**c**) Epifluorescence images of cells immunostained for CENP-A (green) and vimentin (red), with DNA counterstaining with DAPI (grey). CENP-A dots correspond to centromeric localizations. Zooms on the right, with white dotted lines defining regions of interest to define CENP-A pattern at and outside centromeres. Scale bars = 20 μm, Zoom = 10 μm. (**d**) Dot-scan plots displaying the relative intensities of CENP-A IF signal intensity along a 4 μm dashed line traced above representative centromeric chromatin domains as shown in (c). (**e**) Quantification of epithelial (green), intermediate (orange) and mesenchymal (red) cell states across time starting from day 24, upon reversal of CENP-A overexpression. For each condition, data show the trendline as polynomial of the fourth degree, data points and range between four highest and lowest values, for 3 biologically independent experiments. >200 cells counted per data point in at least three fields.

CENP-A overexpression is a nongenetic driver of EMT requiring ectopic CENP-A localization

We next wondered if CENP-A overexpression induces genetic or nongenetic, reversible phenotypic changes. We took advantage of the possibility to reverse CENP-A overexpression in our doxycycline-inducible MCF10-2A system. In both p53-WT cells (associated with senescence, inflammation, and non-maintained mesenchymal states) and p53-DN cells (associated with mesenchymal transition through inflammation and proliferative EMT programs, and mesenchymal states maintained after 20 days), we induced CENP-A overexpression for 24 days, then reversed CENP-A back to normal levels by removing doxycycline from the media of our cells (Fig. 5a). Starting from this time point, we monitored the proportions of each cell state, considering that mesenchymal states remain stable when high CENP-A levels are maintained (Fig. 1), even on a long timescale. As previously documented (Jeffery et al. 2021; Nechemia-Arbely et al. 2019), reversal of CENP-A overexpression led to the removal of ectopic CENP-A from chromosome arms with DNA replication while centromeric CENP-A levels remain high, marking cell populations that previously underwent CENP-A overexpression (Fig. 5c-d). Under these conditions, the mesenchymal population decreased from 30% to less than 10% on average after 10 days of reversal of CENP-A overexpression (Fig. 5e, S5a-b) along with a change in mesenchymal cell morphology (Fig. 5b) and decreased levels of non-phosphorylated (active form) β-catenin (Fig. S5a). These results indicate that ectopic CENP-A, but not centromeric CENP-A, is key to maintain the mesenchymal states and programs induced by CENP-A overexpression. Furthermore, upon reversal, chromosomal instability (CIN) levels, assessed by micronuclei frequency, relative to normal conditions, were comparable to those observed when CENP-A is overexpressed (Fig. S5d). Thus, induced mesenchymal transition did not rely on genetic alterations or different CIN levels and, most importantly, erasing ectopic CENP-A was sufficient to revert mesenchymal states. Importantly, the decrease in the mesenchymal population did not lead to significant increase in the intermediate population, but rather by an increase in the epithelial population (Fig. 5e, S5b). This observation prompted us to consider whether the proliferation of mesenchymal cells was affected by the reversal of CENP-A overexpression. CFSE proliferation analysis showed that, following reversal, the proliferation of the mesenchymal cells is the most affected, with an average doubling time of 33 hrs in the p53-DN context upon reversal, while epithelial cells had the lowest doubling time (Fig. S5c). This strong decrease in mesenchymal proliferation is in line with a role for CENP-A in promoting a proliferative EMT program associated with cell cycle progression, which is reversed with CENP-A. We extended the analysis to the RPE-1 cell line with only intermediate cells. In line with the hypothesis that CENP-A overexpression promotes a reversible program in p53-defective cells, induced-mesenchymal states completely disappeared after 10 days reversal in p53-DN cells, while not completely in RPE-1 p53-WT cells (Fig. S5e). Altogether, these results suggest that CENP-A mislocalization enables the mesenchymal transition of intermediate cells through a reversible program in p53-DN cells associated with higher phenotypic plasticity. Based on these results, we conclude that ectopic CENP-A, but not

centromeric CENP-A, is an epigenetic driver promoting the transition of intermediate cells towards mesenchymal states.

Figure 6

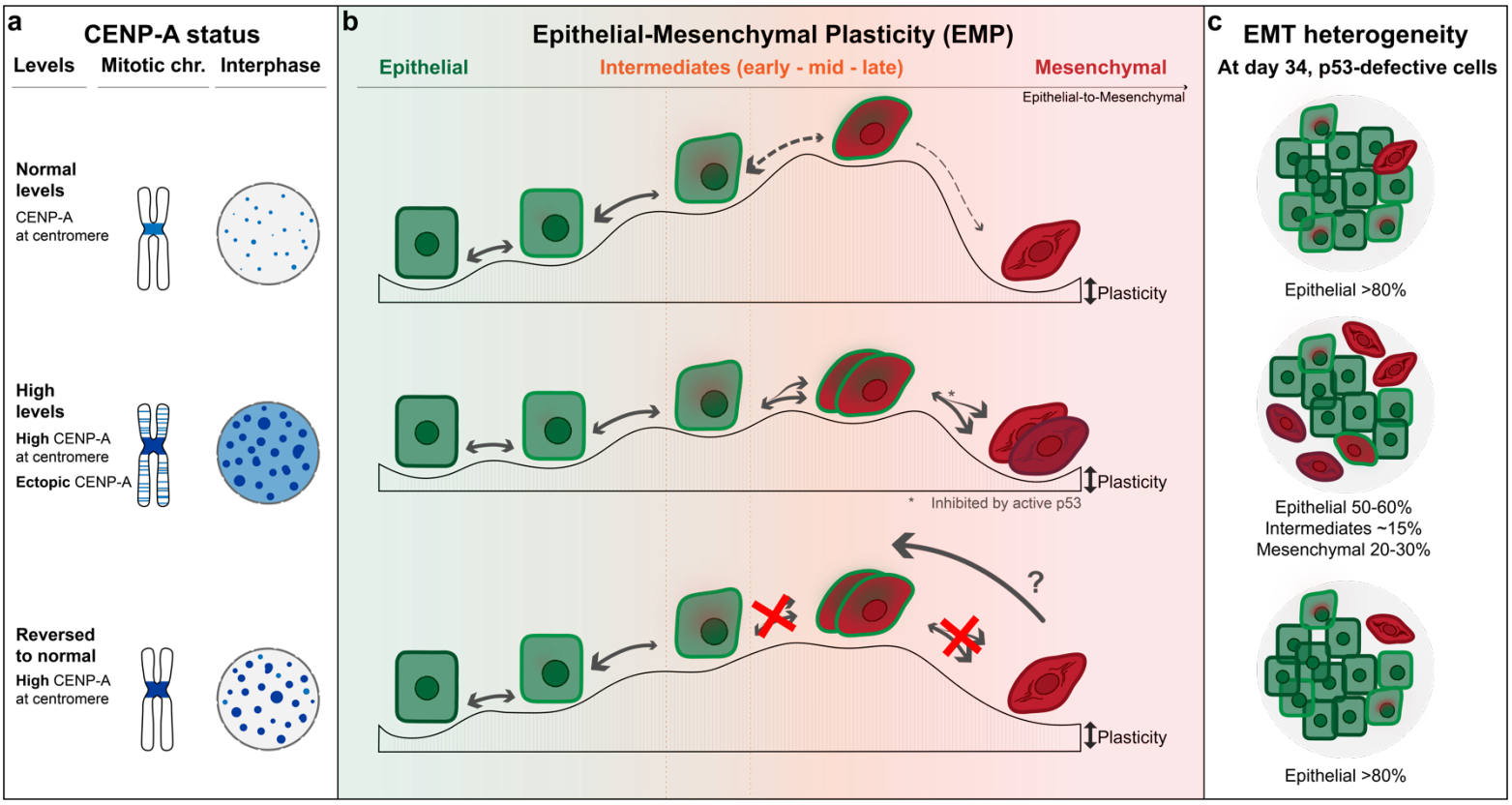

a
CENP-A status
Levels
Mitotic chr.
Interphase
Normal levels
CENP-A at centromere
High levels
High CENP-A at centromere
Ectopic CENP-A
Reversed to normal
High CENP-A at centromere
b
Epithelial-Mesenchymal Plasticity (EMP)
Epithelial
Intermediates (early - mid - late)
Mesenchymal
Epithelial-to-Mesenchymal
Plasticity
Plasticity
* Inhibited by active p53
?
Plasticity
c
EMT heterogeneity
At day 34, p53-defective cells
Epithelial >80%
Epithelial 50-60%
Intermediates ~15%
Mesenchymal 20-30%
Epithelial >80%

Figure 6. CENP-A overexpression is a reversible epigenetic driver of plasticity. (**a**) Scheme of CENP-A localization in mitotic chromosomes and in interphase nuclei depending on CENP-A levels. Normal CENP-A levels is associated with specific centromere localization of CENP-A, appearing as dots in interphase nuclei. CENP-A overexpression leads to increased levels at centromeres along with mislocalization at chromosome arms. Reversal of CENP-A overexpression reverses CENP-A mislocalization, while high centromeric levels of CENP-A are maintained. (**b**) Depiction of Epithelial-Mesenchymal-Plasticity (EMP) in different CENP-A levels. reflects the ability of cells to interconvert between epithelial and mesenchymal phenotypes. In normal conditions, intermediate cells tend to go back to an epithelial phenotype. CENP-A overexpression affects the EMP phenotype, intermediate cells being able to undergo mesenchymal transition. When CENP-A levels are back to normal, this is reversed. (**c**) Representation of cell populations observed after chronic CENP-A overexpression in p53-defective cells.

5. DISCUSSION

In this study, we found that CENP-A overexpression promotes the transition of intermediate towards mesenchymal states in a reversible manner, depending on ectopic CENP-A. As illustrated in figure 6, in normal conditions, most of the intermediate cells tend to reverse to an epithelial phenotype. Thus, in normal conditions, the population is enriched in epithelial and early intermediate states. However, CENP-A overexpression and mislocalization enables an alternative fate towards mesenchymal states in a nongenetic manner. CENP-A overexpression can promote two trajectories: (i) a pre-existant, pro-inflammatory EMT, (ii) a proliferative EMT program which is inhibited in p53-WT cells. This way, CENP-A overexpression promotes EMT heterogeneity with advanced transition states and different mesenchymal phenotypes. Remarkably, erasing ectopic CENP-A from chromosome arms is sufficient to reverse this phenotypic plasticity. These findings shed light on a new role for CENP-A, beyond its centromeric function, in remodeling epithelial-mesenchymal plasticity, with broad implications for cell identity reprogramming during development and cancer progression. Here, we discuss first the nature of the dynamics of the cell transitions driven by CENP-A overexpression and then the mechanistics underlying these dynamics. Finally, we consider the implications for tumor evolution and therapeutic strategies.

CENP-A overexpression promotes the transition towards mesenchymal

We found that CENP-A overexpression could promote EMT in cell lines harboring intermediate features. In a model of fibrocystic human breast cell line with a subpopulation of intermediate states at start, intermediate cells represent about 20% of the cells. Strikingly, when overexpressing CENP-A, these intermediate states decrease while the mesenchymal population increases up to 30%. The dynamics we uncovered suggest two hypothetical models: (i) the intermediate cells can potentially revert to an epithelial state in normal conditions, but the overexpression of CENP-A may promote their transition towards a more mesenchymal state, possibly by preventing the reversion, and/or (ii) CENP-A overexpression could affect the balance of cell proliferation rates between the different states, giving an advantage to mesenchymal states relatively to others. Our analysis of cell proliferation revealed that these dynamics are not driven by different proliferation rates of the co-existing EMT subpopulations. Thus, our results show that CENP-A overexpression stimulates the transition of E/M intermediate cell states towards mesenchymal. Furthermore, here we show that CENP-A overexpression can promote this transition in both p53 backgrounds. However, in p53-WT MCF10-2A cells, the mesenchymal states are not maintained after day 15. This is in line with the ability for active p53 to promote senescence in cells overexpressing CENP-A to prevent EMT (Jeffery et al. 2021). Here, we show that p53 (i) restricts the transition, as we detect less mesenchymal cells in p53-WT MCF10-2A cells, and (ii) targets the mesenchymal population in a second time.

The role of CENP-A in remodeling the epithelial-mesenchymal plasticity: Underlying mechanisms

Our work uncovers an unanticipated role for the histone variant CENP-A, beyond its centromere function, as an epigenetic factor regulating plasticity in the EMT context. This raises questions as to how ectopic CENP-A can mechanistically modulate EMT. How does ectopic CENP-A promote transition towards mesenchymal? Our findings enable to discard a major role for genetic alterations in driving the EMT of cells overexpressing CENP-A. First, we did not detect a change in the levels of acute DNA damage or DNA repair signaling at the mRNA and protein levels. Second, upon reversal of CENP-A overexpression, the population could be reversed to a normal phenotype with mostly epithelial states. This is in line with a plastic behavior driven by epigenetic alterations. Furthermore, the levels of CIN remained high during the reversal of CENP-A overexpression. This is consistent with previous data[18] and indicates that, in our model, CENP-A-driven mitotic stress and CIN are not drivers of EMT. Finally, upon reversal, CENP-A levels at centromeres remain high while ectopic CENP-A in chromosome arms is lost. This observation indicates that the increase in centromeric CENP-A does not drive the transition, in contrast with ectopic CENP-A which is required to promote and maintain the induced mesenchymal states. Then, a tempting hypothesis suggests that CENP-A mislocalization could increase the plasticity of the chromatin landscape. When overexpressed, the excess of CENP-A can associate with H3.3 chaperones and forms heterotypic nucleosomes with H3.3 at high histone turnover regions of the genome (Athwal et al. 2015; Lacoste et al. 2014). Our results confirmed these findings and further showed that EMT genes transcriptionally affected upon CENP-A overexpression did not present a significant enrichment in CENP-A relative to the rest of the genome. In addition, when overexpressing CENP-A, intermediate cells could switch to different mesenchymal states through distinct paths. These observations are in line with the idea that the EMT is not a linear process but is variable and context-dependent (Cook and Vanderhyden 2020), and requires increased plasticity for cells to change their ability to self-maintain or convert to mesenchymal states (Al-Radhawi et al. 2022). Other epigenetic factors are known to regulate the epithelial-mesenchymal plasticity, including chromatin remodelers like HMGA2, which promotes plasticity and transition towards advanced intermediate and mesenchymal states in prostate tumor cells (Ruscetti et al. 2016). This also includes histone variants such as H2A.X, whose depletion stimulates EMT in the HCTT116 (colon cancer) (Weyemi, Redon, Choudhuri, et al. 2016) and MCF10A (nontumoral breast) (Weyemi, Redon, Sethi, et al. 2016) cell lines. Finally, an important aspect to keep in mind is the ability, for ectopic CENP-A, to recruit some kinetochore proteins such as CENP-C, CENP-N and the Mis18 complex (Gascoigne et al. 2011; Lacoste et al. 2014; Van Hooser et al. 2001). At the centromere, such complexes result in compact, but dynamic chromatin structures (Ali-Ahmad et al. 2019; Melters et al. 2019). Such organization outside centromeres may impact chromatin structure and transcriptional regulation. Thus, altogether, the features of ectopic CENP-A nucleosomes may impact chromatin accessibility while also

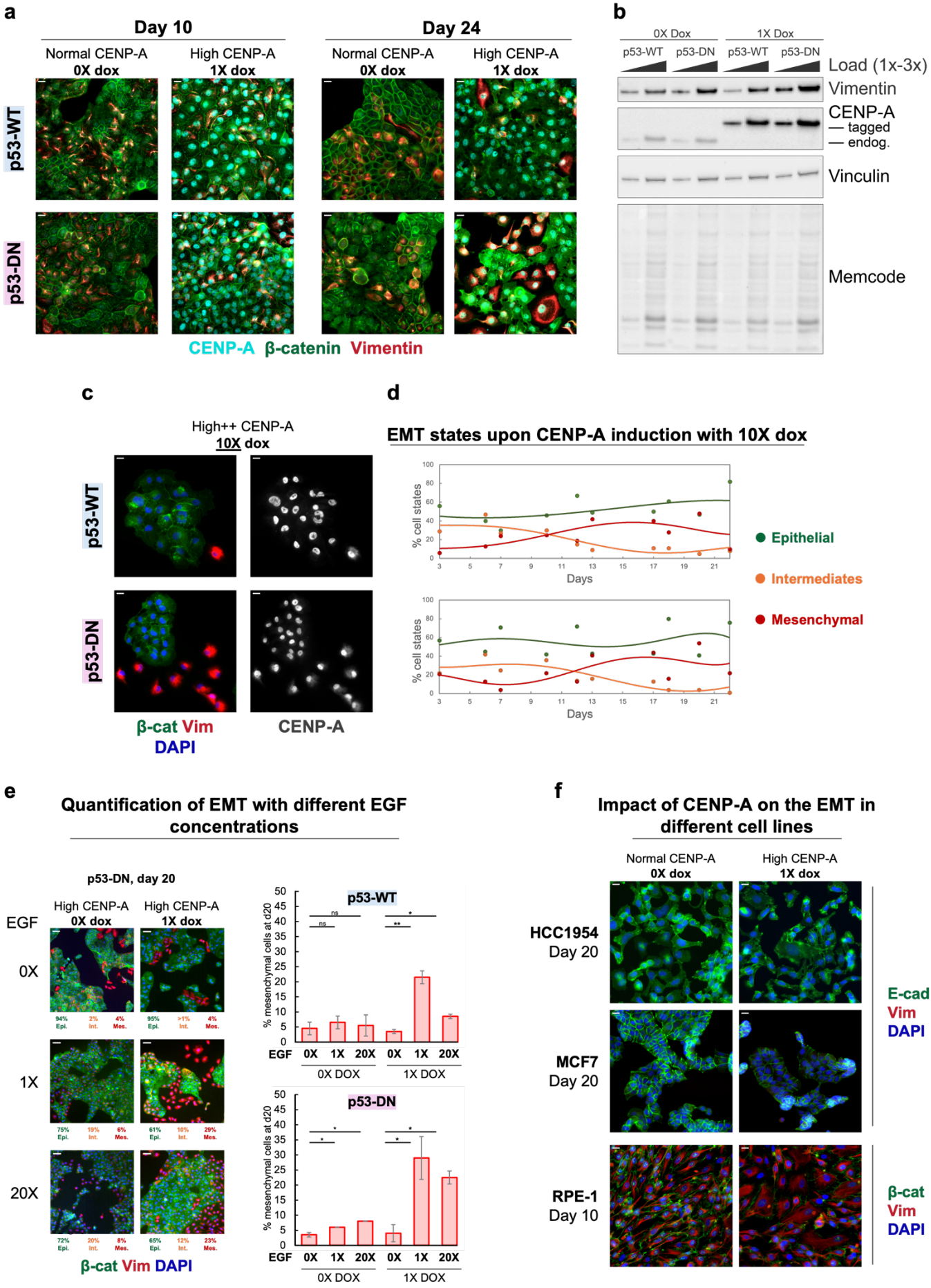
leading to increased dynamics and plasticity. This way, CENP-A may endow E/M intermediate cells with the ability to deviate from their trajectory to adopt alternative cell fates. Exploring these issues represents exciting avenues to better understand the control in nuclear organization and plasticity during cell fate decisions.

CENP-A promotes plasticity and heterogeneity: implications for cancer progression and therapy

We showed several intermediate transition states in the MCF10-2A fibrocystic model, most of them reverting to an epithelial state or keeping the same state across cell passages. These findings are consistent with the fact that during organ fibrosis, intermediate EMT states remain stable, do not undergo a full transition towards mesenchymal and do not become invasive (Grande et al. 2015). In contrast, when CENP-A is overexpressed, part of the intermediate population is pushed towards more mesenchymal states. This observation supports a role for CENP-A in endowing intermediate cells with higher cellular/phenotypic plasticity. Consistent with this idea, our combination of imaging and cell trajectory analysis revealed two different EMT trajectories in cells overexpressing CENP-A, in contrast with normal cells showing only one. Thus, CENP-A overexpression promotes EMT heterogeneity at two levels: (i) first, by promoting more advanced intermediate and mesenchymal states, which were almost inexistent in normal conditions, (ii) second, by giving rise to different EMTs and mesenchymal states in p53-defective conditions, including a proliferative EMT program marked by TOPA2, AKT and β-catenin and highly correlated with metastasis in various tumor types (Y. Dong et al. 2021.; Yi Liu et al. 2022; J. Wu et al. 2024; K. Zhang et al. 2024). High phenotypic plasticity correlates best with cancer aggressiveness and metastatic potential in mouse models and patient tumors (M. S. Brown et al. n.d.; Puram et al. 2017; Simeonov et al. 2021). Altogether, these findings indicate that metastasis could involve the synergy between several EMT states, providing cancer cells with increased adaptability and resistance to survive in different environments during their migration (Lambert, Pattabiraman, and Weinberg 2017). CENP-A overexpression might contribute to enhancing this feature. Our results thus represent exciting avenues to better comprehend the role of CENP-A in cancer progression and metastasis. In conclusion, our work reveals a role for non-centromeric CENP-A in modeling epithelial-mesenchymal plasticity to promote the transition of intermediate cell states towards mesenchymal in a reversible, nongenetic way, through distinct trajectories. This impacts EMT heterogeneity, with important implications for cancer.

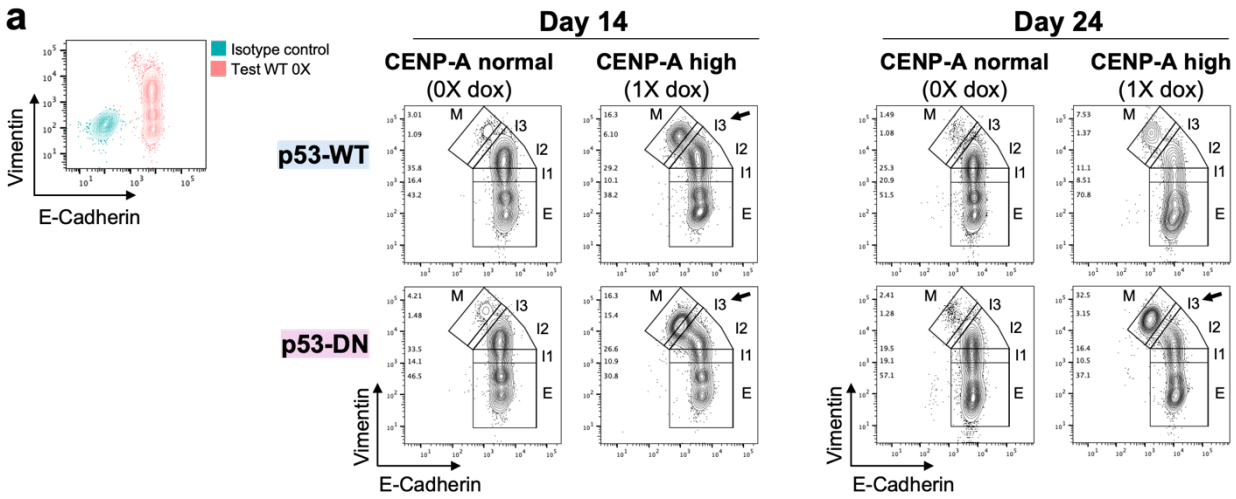
6. SUPPLEMENTARY FIGURES

Supplementary Figure 1



Supplementary Figure 1. CENP-A overexpression promotes EMT in proliferating cells harbouring intermediate states. (**a**) CENP-A signal in the MCF10-2A cell line with and without induction of CENP-A. Epifluorescence images of cells from figure 1d, immunostained for CENP-A (cyan), E-cadherin (green) and vimentin (red). Low aspecific vimentin signal detected in the cyan channel. Range of pixel values displayed are the same. Scale bars = 20 μm. (**b**) Western blot of MCF10-2A cells at day 22. 1x load corresponds to total protein extract from ~30000 cells. Primary antibodies are indicated on the right. Vinculin was used as loading control. (**c**) EMT states in the MCF10-2A cell line after 22 days induction with 10X (100ng/ml) Dox. Representative wide-field epifluorescence images of cells immunostained for β-catenin (green) and vimentin (red), with DNA counterstaining with DAPI (blue). Same range of pixel values displayed between conditions. Scale bars = 20 μm. (**d**) Quantification of epithelial (green), intermediate (orange) and mesenchymal (red) cell states across time upon induction with 10X Dox. For each condition, data show the trendline as polynomial of the fourth degree for 2 biologically independent experiments. >200 cells counted per data point in at least three fields. (**e**) Left panel: Representative wide-field epifluorescence images of MCF10-2A cells at day 20 immunostained for β-catenin (green) and vimentin (red), with DNA counterstaining with DAPI (blue). Same range of pixel values displayed between conditions. Scale bars = 80 μm. Corresponding percentages of EMT states indicated below each image. Right panel: Quantification of mesenchymal cells at day 20. Plots show mean and standard deviation for two biological replicates. >100 cells counted per data point in at least three fields. Statistical significance tested by two-tailed Welch's t test, compared to non-induced (0X) condition. ns = not significant (p-value > 0.05), * = p-value < 0.05, ** = p-value < 0.01. (**f**) Representative wide-field epifluorescence images of HCC1954, MC7 and RPE-1 cells at indicated time points. Immunostainings: Vimentin (red), E-cadherin or β-catenin (green) in HCC1954/MCF7 and RPE-1 cells, respectively. DNA counterstaining with DAPI (blue). Range of pixel values displayed are the same. Scale bars = 20 μm. *N.B. – Note the hybrid (intermediate) states at start in RPE-1 cells, switching to mesenchymal states after 10 days of CENP-A overexpression. By contrast, there is no EMT induction in HCC1954 (p53-defective) or MCF7 (p53-WT) cell lines, displaying a complete epithelial state.*

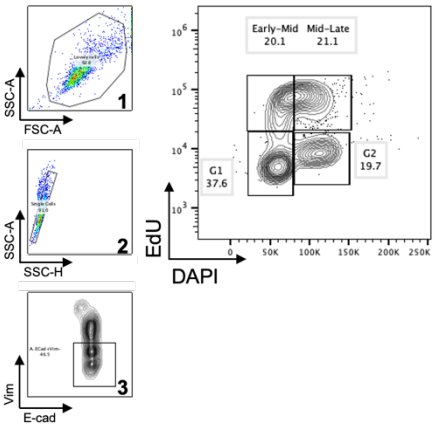
Supplementary Figure 2

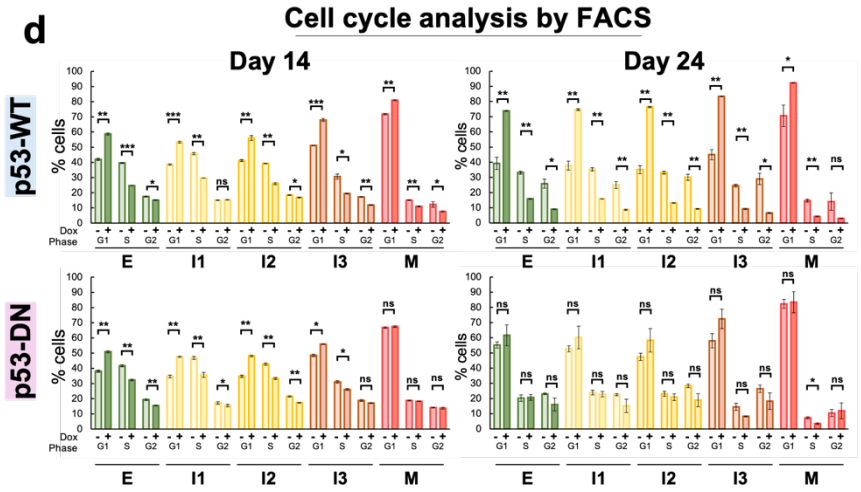


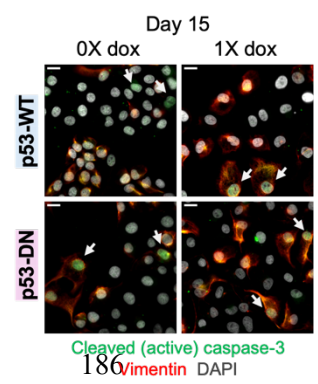
b

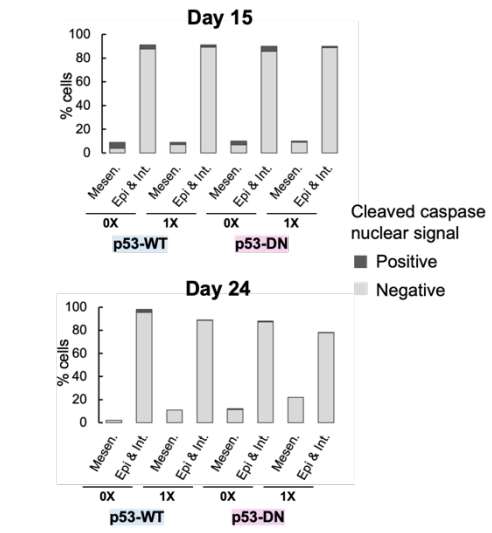
p53-WT cells %		Day	E Ecad+ Vim-	I1 Ecad+ Vim-+	I2 Ecad+ Vim+	I3 Ecad-+ Vim+	M Ecad- Vim++
FACS	0X Dox	14	60	Δ = +13	37	Δ = -11	3 Δ = -2
		24	73		26		1
	1X Dox	14	48	Δ = +32	35	Δ = -23	17 Δ = -9
		24	80		12		8
IF	0X Dox	12-16	61	Δ = +17	34	Δ = -14	5 Δ = -3
		24	78		20		2
	1X Dox	12-16	66	Δ = +11	23	Δ = -9	11 Δ = -2
		24	77		14		9

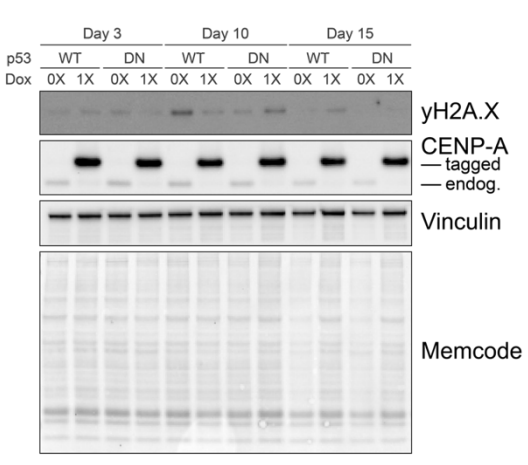
p53-DN cells %		Day	E Ecad+ Vim-	I1 Ecad+ Vim-+	I2 Ecad+ Vim+	I3 Ecad-+ Vim+	M Ecad- Vim++
FACS	0X Dox	14	61	Δ = +16	35	Δ = -14	4 Δ = -2
		24	77		21		2
	1X Dox	14	42	Δ = +5	42	Δ = -22	16 Δ = +17
		24	47		20		33
IF	0X Dox	12-16	59	Δ = +16	34	Δ = -11	7 Δ = -5
		24	75		23		2
	1X Dox	12-16	64	Δ = -1	22	Δ = -8	14 Δ = +9
		24	63		14		23





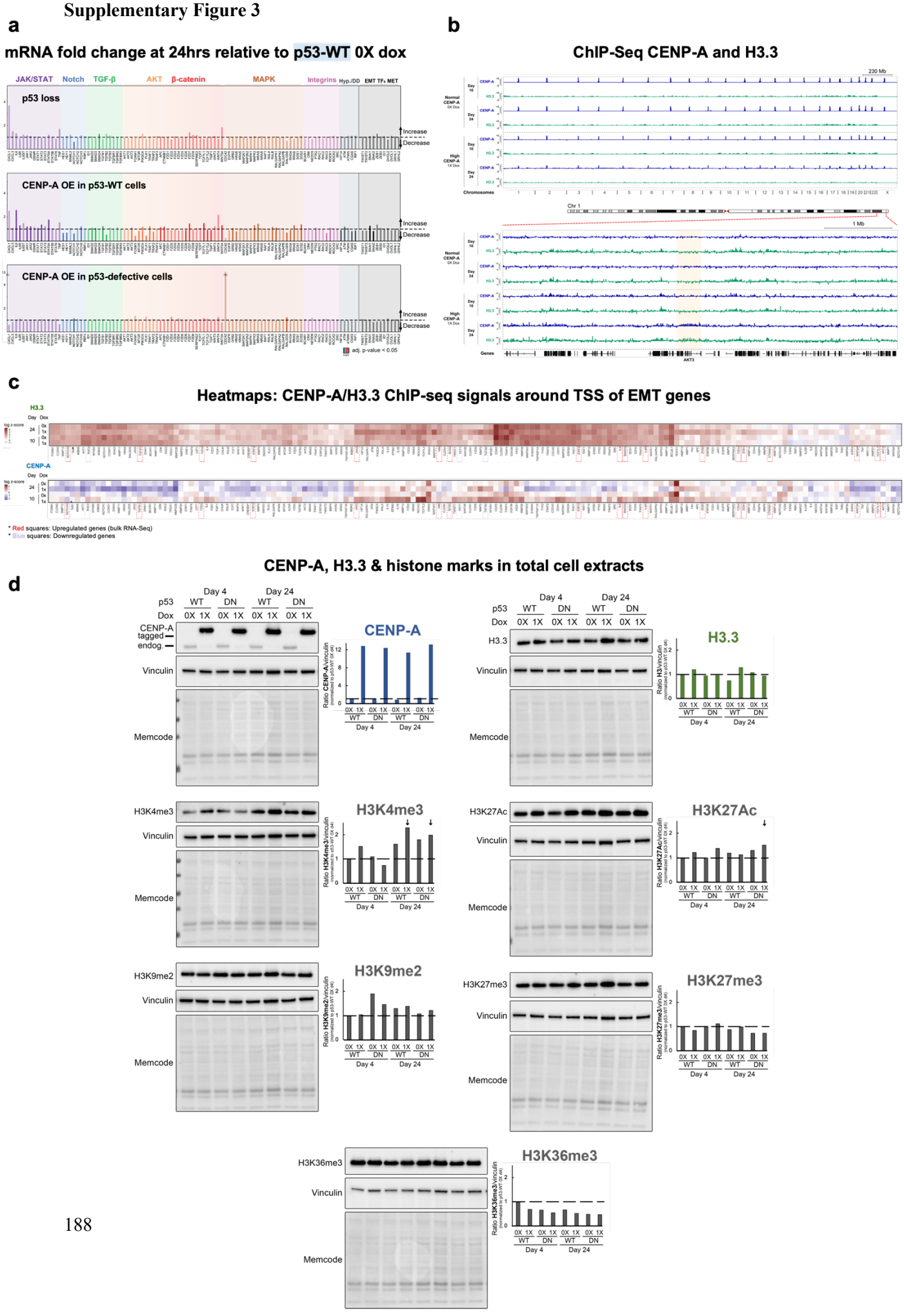






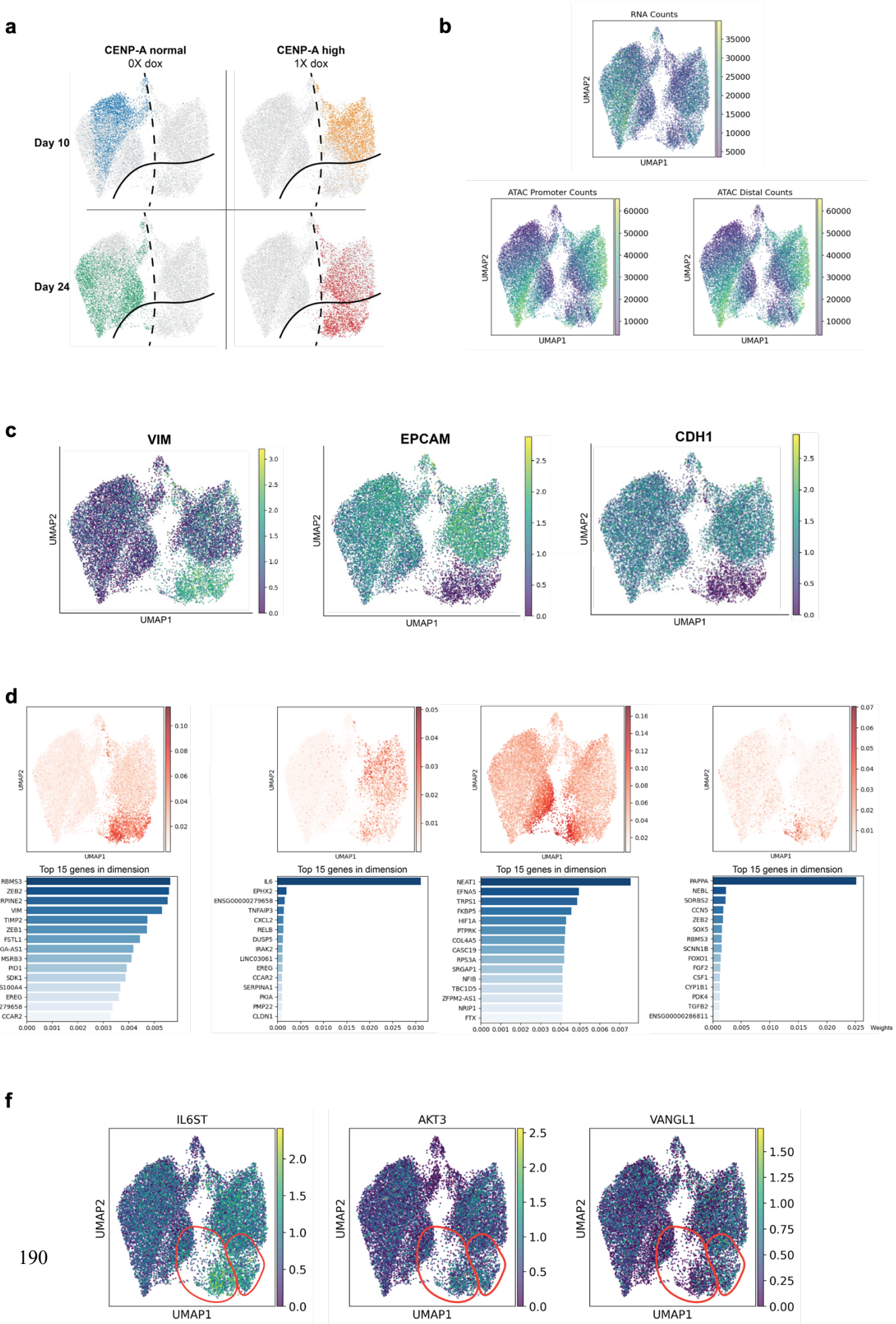
Supplementary Figure 2. CENP-A-induced EMT in p53-defective cells does not involve cell cycle changes, cell death or DNA damage. (**a**) EMT state detection by FACS based on E-cadherin and vimentin levels, in p53-WT and p53-DN MCF10-2A cells with 0X or 1X Dox: Epithelial (E); Early Intermediate (I1); Mid-Intermediate (I2); Late Intermediate (I3); Mesenchymal (M). All cells passaged and harvested in parallel. Increase in the Late Intermediate (I3) population upon CENP-A overexpression indicated with an arrow. (**b**) Comparison of EMT states percentages detected by FACS (in figure 2) and IF (in figure 1): Cells on the epithelial side of the EMT spectrum (epithelial and early intermediates merged) (green), intermediates (mid and late intermediates merged) (orange), mesenchymal states (red). Day 14 (FACS) compared with the average percentages between days 12-26 (IF). Day 24 (FACS) compared with day 24 (IF). (**c**) Gating strategy for cell cycle analysis by FACS based on EdU and DAPI signals. Representative example of MCF10-2A p53-DN cells with 0X Dox. (**d**) Analysis of cell cycle phases (G1, S, G2) by FACS. Green = Epithelial (E); Yellow = Early Intermediate (I1); Orange = Mid-Intermediate (I2); Dark orange = Late Intermediate (I3); Red = Mesenchymal (M). Bar plots shows mean and standard deviation for two experiments. Statistical significance tested by two-tailed Welch's t test. * = p-value < 0.05; ** = p-value < 0.01; *** = p-value < 0.001. (**e**) Detection of apoptotic cells. Epifluorescence images of cells immunostained for cleaved (active) effector caspase-3 (green) and vimentin (red), with DNA counterstaining with DAPI (grey). Example of positive nuclei indicated with an arrow. Scale bars = 20 μm. (**f**) Quantification of apoptotic nuclei, based on nuclear signal of cleaved caspase-3, at day 15 and day 24 in mesenchymal (vimentin filaments) and non-mesenchymal (speckle or no vimentin signal) cells. Stacked bar plots show mean percentages for >200 nuclei per condition in a single experiment. (**g**) Western blot of MCF10-2A cells at three time points. Load corresponds to total protein extract from ~30000 cells. Primary antibodies are indicated on the right. Vinculin was used as loading control.

Supplementary Figure 3



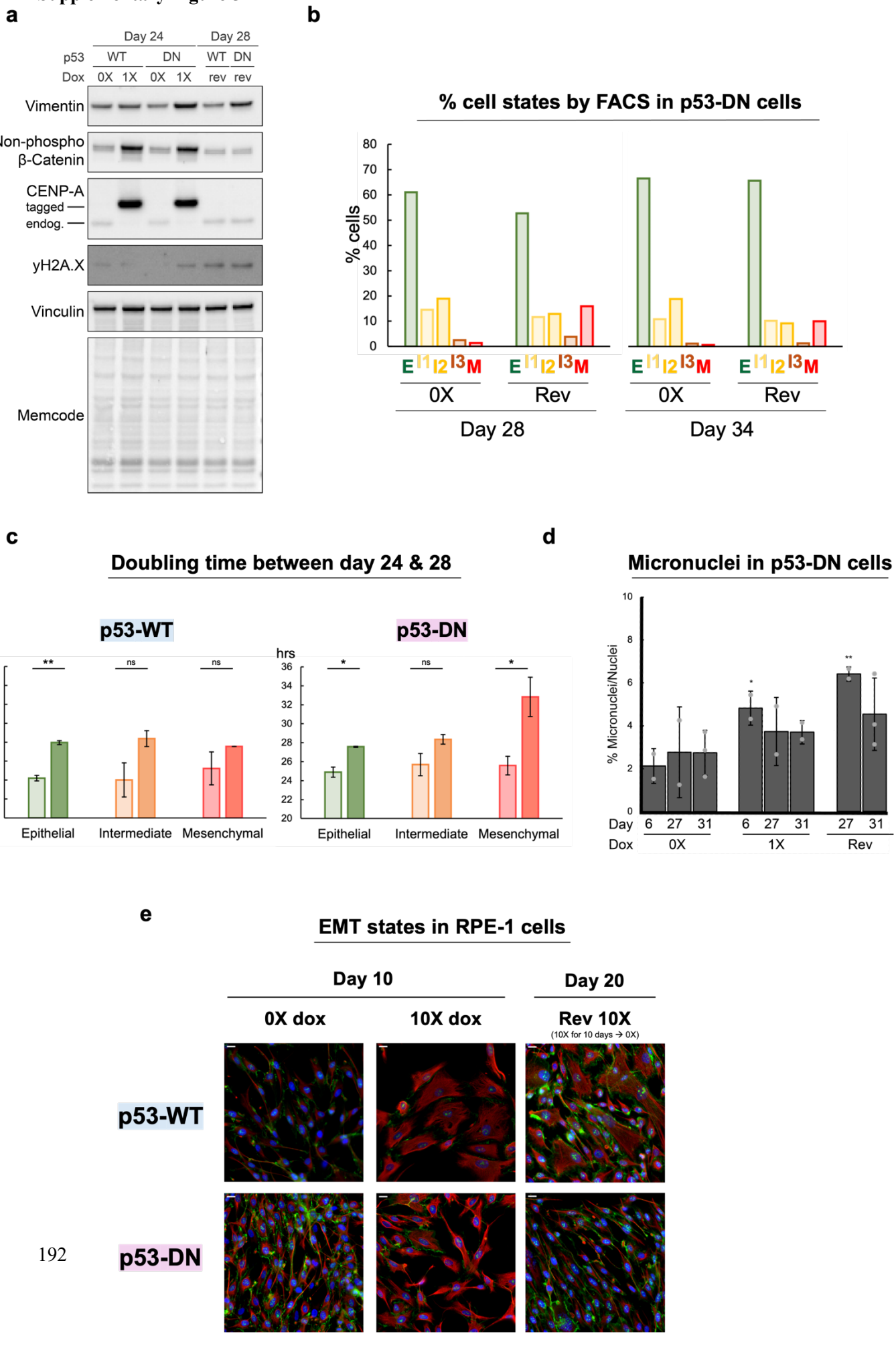
Supplementary Figure 3. CENP-A overexpression induces global changes of chromatin structure. (**a**) Bar plot showing mRNA fold change at 24 hours in MCF10-2A cells for EMT genes with their related pathways annotated above. Expression relative to the p53-WT 0X Dox condition. (**b**) CENP-A and H3.3 ChIP-Sequencing analysis at day 10 and day 24. Example of peak distribution and read density of CENP-A and H3.3 (z-score) mapping to nonrepetitive sequences including a portion of chromosome 1. The AKT3 gene locus (significantly upregulated upon CENP-A overexpression) is highlighted in yellow. (**c**) Heatmaps for CENP-A and H3.3 enrichment at TSS among EMT genes (log2 z-score). Upregulated genes are indicated in red and downregulated genes in blue. (**d**) Western blots of MCF10-2A cells, after 20 days with 0X or 1X Dox, for several histone variants and histone marks from the same time-course experiment. Load corresponds to total protein extract from ~30000 cells. Primary antibodies are indicated on the right. Vinculin was used as loading control for normalized values shown in bar plots.

Supplementary Figure 4



Supplementary Figure 4. Paired single cell multi-omics analysis of RNA and ATAC sequencing profiles at two time points. (**a**) UMAP visualization of each sample. (**b**) UMAP plots of total number of counts (based on Muon's filter_obs) for RNA and ATAC (at promoter and distal intergenic regions) datasets. (**c**) UMAP plots showing VIM, EPCAM and CDH1 enrichments. (**d**) Latent dimensions corresponding to the mesenchymal cluster (UMAP is parametrized by several latent dimensions)**.** Top panel: UMAPs with colour gradient proportional to the expression of genes for the indicated dimension, defined by DEGs below. Bottom panel: Top 15 genes defining each dimension and their RNA-specific weights, which can be used for biological characterization. (**e**) UMAP plots showing IL6ST, AKT3 and VANGL1 enrichments.

Supplementary Figure 5



Supplementary Figure 5. Reversal of CENP-A overexpression reverses cell population phenotypes in different cell lines. (**a**) Western blots of MCF10-2A cells at day 24 (0X and 1X Dox) and after 4 days reversal (from 1X to 0X Dox). Load corresponds to total protein extract from ~30000 cells. Primary antibodies are indicated on the right. Vinculin was used as loading control. (**b**) EMT state quantification in p53-DN MCF10-2A cells by FACS at day 28 and day 34 following reversal at day 24. Bar plot shows mean a single experiment. Based on E-cadherin and vimentin levels: Green = Epithelial (E); Yellow = Early Intermediate (I1); Orange = Mid-Intermediate (I2); Dark orange = Late Intermediate (I3); Red = Mesenchymal (M). (**c**) Average doubling time of different EMT states between day 24 and 28. Bar plot shows mean and standard deviation for two experiments. Statistical significance tested by two-tailed Welch's t test. * = p-value < 0.05, ** = p-value < 0.01. (**d**) Accumulation of micronuclei pertaining to days 6 and 27 (0X and 1X Dox) and after reversal at days 27 and 31 (Rev) in p53-DN MCF10-2A cells. Plots show mean and standard deviation for two or three experiments. n > 200 nuclei per condition for each condition. Statistical significance tested by two-tailed Welch's t test (relative to 0X Dox condition). No significant difference between samples with same Dox treatment. * = p-value < 0.05, ** = p-value < 0.01. (**e**) Representative epifluorescence images of RPE-1 cells immunostained for β-catenin (green) and vimentin (red), with DNA counterstaining with DAPI (blue). Three conditions per p53 status: No induction (0X Dox), Induction of CENP-A overexpression with 10X Dox for 10 days (10X), Induction of CENP-A for 10 days followed by reversal of CENP-A overexpression for 10 more days (Rev). Scale bars = 20 μm.

7. MATERIALS AND METHODS

Cell lines

All parental human cell lines originally from ATCC: MCF10-2A (CRL-10781), T47D (HTB-133), HCC1954 (CRL-2338), MCF7 (HTB-22), and hTERT RPE-1 (CRL-4000, kind gift from D. Fachinetti, Institut Curie). The MCF10-2A cell line was authenticated by STR profiling (Powerplex 16 HS). All cell lines were transduced with the inducible CENP-A overexpression construct TetOn-CENPA-FLAG-HA as in Jeffery et al. (2021). All cell lines were tested negative for mycoplasma contamination. No commonly misidentified cell lines were used in this study. For the p53-WT and p53-DN cells, we transduced cells with the empty vector pWZL Hygro (Scott Lowe, Addgene plasmid #18750) or a vector containing the DN TP53 construct (pBABE-hygro p53DD, Bob Weinberg, Addgene plasmid #9058) as in Jeffery et al. (2021).

Cell culture

We cultured all cells at 37°C in 5% CO_2. MCF10-2A cells were cultured with DMEM:Ham's F12 5% horse serum, 5 ng/ml epidermal growth factor, 100 ng/ml cholera toxin, 0.01 mg/ml insulin, 500 ng/ml hydrocortisone and 1% Pen/Strep; T47D with RPMI Medium 10% fetal cow serum (FCS), 0.01 mg/ml insulin and 1% Pen/Strep; HCC1954 and A549 with RPMI Medium 10% FCS and 1% Pen/Strep; MCF7 and HCT-116 with DMEM 10% FCS and Pen/Strep 1%; RPE-1 with DMEM:Ham's F12 10% FCS, 0.123% sodium bicarbonate and 1% Pen/Strep. All base media were purchased from ThermoFisher Scientific. We pulsed cells with 5μM carboxyfluorescein diacetate, succinimidyl ester (CFSE) according to the manufacturer's instructions to measure number of cell divisions. We pulsed cells with 10 μM 5-ethynyl-2′-deoxyuridine (EdU) for 20 min to monitor S-phase as described in Mendiratta et al. (2024).

Induction of CENP-A overexpression

CENP-A overexpression was induced by the addition of doxycycline (in DMSO) to typical growth media at 10 ng/ml (considered 1X), unless otherwise indicated. For 0X Dox (control condition), DMSO only was added. We seeded cells into dishes containing collagen/fibronectin-coated glass coverslips, added indicated concentrations of Dox 24 hrs later to start the induction (corresponds to day 0). Growth media with or without Dox were replaced every 2-3 days. For reversal of CENP-A overexpression, media containing Dox was removed, cells were washed two times with warm PBS and fresh media without Dox was added.

Cell extract preparation and western blotting

We prepared nuclear extract as previously described (Martini et al. 1998), except that 300 mM NaCl was used. We obtained chromatin fraction as described in -paper from Dominique or Daniel's ????. We performed Western bloting as in paper from Dominique od Daniels's ????, and images were

acquired with a ChemiDoc Touch system and ImageLab software. Primary antibodies: CENP-A 1:500 (#2186 Cell Signaling Technology), HJURP 1:300 (#HPA008436 Sigma-Aldrich), vimentin (R28) 1:1000 (#3932 Cell Signaling Technology), hIL-6 1:300 (#AF-206-NA, R&D Systems), active Beta-catenin (D13A1) 1:100 (#ab16051 Abcam), yH2A.X 1:1000 (# 05-636 Merck), H3.1/3.2 1:1000 (#61629 Active Motif), H2A1 1:1000 (#ABE215 Merck), H3.3 1:1000 (#09-838, Milipore), TBP 1:1000 (#ab818, Abcam), H3K27Ac 1:1000 (#ab4729, Abcam), H3K27me3 1:1000 (#39155 Active Motif), H3K4me3 1:1000 (#39915 Active Motif), H3K9me2 1:1000 (#39753 Active Motif), H3K36me3 1:1000 (#61021 Active Motif), Vinculin 1:10000 (#V9131 Sigma-Aldrich). Secondary antibodies: Jackson ImmunoResearch, 1:10000, donkey anti-mouse, donkey anti-rabbit donkey anti-goat.

Fluorescence microscopy

We performed immunofluorescence staining on cells grown on coverslips coated with collagen (1 µg/ml) + fibronectin (1 µg/ml) as described in, paper from the lab, or Daniels paper. Primary antibodies: CENP-A (3-19) 1:300 (#ADI-KAM-CC006-E Enzo Life Sciences), E-cadherin (24E10) 1:200 (#3195S CST), Beta-catenin 1:100 (#9562 Cell Signaling), Vimentin (N-term) 1:200 (#5741S Progen). Secondary antibodies: 1:1000 Alexa Fluor donkey anti-mouse IgG (H + L) 488 or 647, 1:1000 Alexa Fluor goat anti-rabbit IgG (H + L) 488 or 594, 1:1000 Alexa Fluor goat anti-Guinea Pig IgG (H + L) 594. We visualized CFSE after fixing the cells with 2% PFA. Nuclei were counterstained with DAPI. We combined CFSE with immunofluorescence staining by performing first immunodetection.

Quantification from microscopy images

For EMT states counting, we took several images in at least three fields for each coverslip. For each time point and condition, we counted 200-1000 nuclei, then the corresponding EMT states based on epithelial and mesenchymal marker stainings, with the ImageJ software.: For quantification of Vimentin intensity in intermediate cells, we generated Masks from at least three fields for the Red (Vimentin) and Green (E-cadherin or B-catenin) channels and used the "AND" command to combine Masks (the result corresponding to regions with co-expression of both markers). From the Red channel, we extracted the IntDen (sum of all pixel values divided by area size) in the corresponding Mask area and divided by the corresponding number of cells. We counted micronuclei using a custom ImageJ macro with at least three fields and >1000 nuclei counted per condition.

FACS analysis

After trypsinization, we counted cells using Vi-Cell XR Cell Viability Analyzer (Beckman coulter). We harvested around one million cells per condition using trypsin and fixed the cells with 70% cold ethanol. We washed cells with 1 ml PBS before mixing them with 100 µl PBS-Tween 5% BSA for blocking (45 min, RT). Then, we directly added 1 µl of each primary antibody (E-cadherin (24E10) (#3195S CST), Vimentin (VI-RE/1) conjugated with APC (#MA5-28601 ThermoFisher)) or isotype control (IgG1κ

conjugated with APC (#17-4714-42, ThermoFisher) and Alexa Fluor goat anti-rabbit IgG (H + L) 488) for 1 hr protected from light (RT). We added 1 µl of secondary antibody for E-cadherin detection (Alexa Fluor goat anti-rabbit IgG (H + L) 488) for 1 hr protected from light (RT). We washed cells with 1 ml PBS-Tween then with PBS. Finally, we added 0.5 µg/ml DAPI. For EdU-stained cells, we acquired data using an Aria III cytometer (BD Biosciences) at the Cytometry platform CYTPIC of Institut Curie. Otherwise, we acquired data with an Attune NxT cytometer (ThermoFisher Scientific). We performed analysis on a minimum 15,000 gated cells, excluding cell debris and doublets, with FlowJo software (10.9.0).

Bulk RNA-seq analysis

We grew MCF10-2A TetOn-CENPA-FLAG-HA cells expressing either empty vector (p53-WT) or dominant-negative p53 (p53-DN) with 0X Dox (no Dox, DMSO control), or with 1X Dox (10 ng/ml) for 24 days or 24 hours. All conditions were tested in duplicate. We extracted RNA directly from culture dishes (5 million cells) using the Qiagen RNeasy Mini kit according to the manufacturer's instructions and confirmed the quality and quantity of the RNA by TapeStation and NanoDrop. mRNA library preparation and sequencing were performed by the next-generation sequencing (NGS) platform, Institut Curie, using the Illumina TruSeq Stranded mRNA kit and NovaSeq 6000 sequencer.

Bulk ChIP sequencing and analysis

We performed CENP-A and H3.3 ChIP-seq from the MCF10-2A TetOn-CENP-A-FLAG-HA cell line. We used 4 million cells digested in 100 µL with MNase for 8 min at 37 °C (3 units/million cell) for mononucleosome purification. We performed ChIP by incubating chromatin (100 µL) supplemented with 500 µL incubation buffer (Tris-HCl 50 mM pH 7.5, NaCl 100 mM, BSA 0.5%, protease inhibitors tablet cocktail, Roche) with antibodies targeting H3.3 or CENP-A. We recovered immunoprecipitated DNA after proteinase K digestion (20 µg/µL) for 2 h at 37 °C. DNA was then purified with Agencourt AMPure XP Beads (Beckman Coulter) according to the manufacturer's recommendations in 20 µL water. Sequencing libraries (TruSeq ChIP) were prepared with 15 ng of DNA and paired-end sequenced on Illumina HiSeq 2500 at the Institut Curie Next Generation Sequencing (NGS) platform. Reads were aligned to the human genome version hg38/GRCh38 with Bowtie2, run in paired-end mode using the very-sensitive parameter. Genome-wide coverage in bedGraph format was obtained for each alignment using bedtools after sorting and indexing the corresponding BAM file with samtools. Custom Python scripts were used to compute the mean per-base coverage at consecutive 10 kb bins along each chromosome, after normalizing the read counts to the total sequencing depth for each sample. The log2 ratio to input at non-zero bins was used as a proxy for H3.3 and CENP-A enrichments.

Single cell multiomics

We grew MCF10-2A TetOn-CENPA-FLAG-HA cells either empty vector (p53-WT) or dominant-negative p53 (p53-DN) with 0X Dox (no Dox, DMSO control), or with 1X Dox (10 ng/ml) for 24 days.

We harvested samples at day 10 and at day 24. We prepared samples according to the Active Motif Single-Cell Multiome Sample Preparation Protocol. In brief, we harvested cells by trypsinization, resuspended in complete media and mixed thoroughly by pipette, centrifuged at 500g at 4°C to pellet the cells and remove supernatant, resuspended cells in the appropriate volume of ice-cold cryopreservation solution (50% horse serum, 40% growth media, 10% DMSO) to achieve a concentration of 4 million cells/mL, then transferred 500 uL (2 million cells) to a 1.5 mL Eppendorf tube on ice and froze cells by transferring the tubes to a pre-chilled container and placing at -80°C. The samples were then shipped in dry ice to Active Motif services, who proceeded to a cell viability test by Trypan blue and nuclei isolation with 5 minutes lysis as described in the Nuclei Isolation for Single Cell Multiome protocol. Nuclei concentration and quality were confirmed with PI and Acridine orange staining. ATAC and RNA libraries were generated using the Chromium Next GEM Single Cell Multiome ATAC + Gene Expression protocol from 10X Genomics, relying on microdroplet)based isolation of single nuclei.

Bioinformatics analysis

For bulk RNA-Seq analysis, we used Gene set enrichment analysis (GSEA): Custom sources GO:CC, GO: MF, GO: BP, Azimuth, and ImmuneSigDB were retrieved from the Enrichr website. Gene sets enriched with adjusted p-values under 0.05 (with Bonferroni correction) were selected for further analysis.

For single cell multiomics, paired data integration and visualization were performed with Multi-Omics Wasserstein inteGrative anaLysIs (Mowgli) as described in Huizing et al. 2023(Huizing et al. 2023). Briefly, we selected the number of latent dimensions displaying the overall best performances across evaluation metrics (Silhouette score, ARI, purity score). We computed kNN graphs with the euclidean distance between the cells' low-dimensional embeddings (using Scanpy's neighbors). We used these graphs to compute 2D UMAP projections (using Scanpy's umap). Then, we clustered datasets using the Leiden algorithm(Traag, Waltman, and van Eck 2019) with varying resolutions (using Scanpy's leiden). Similarly to UMAP visualization, the inputs of the Leiden algorithm were the previously computed kNN graphs.

Competing interests

The authors declare no competing interests.

Author contributions

G.A., J.-P.Q. and C.R.-P. conceived the strategy and wrote the manuscript. G.A and J.-P.Q. supervised the work. C.R.-P. designed and performed cell biology, imaging and biochemistry experiments and analyzed data. A.F. and C.R.-P. performed cytometry and chromatin immunoprecipitation experiments. S.L. and C.R.-P. analyzed data in Fig. 3A and 3D. D.C. and L.C. performed integration of multiomics data and analyzed the data with C.R.-P., S.L. and G.A. C.R.-P. and G.A. and J.-P.Q. acquired funding. Critical reading and data discussion involved all authors.

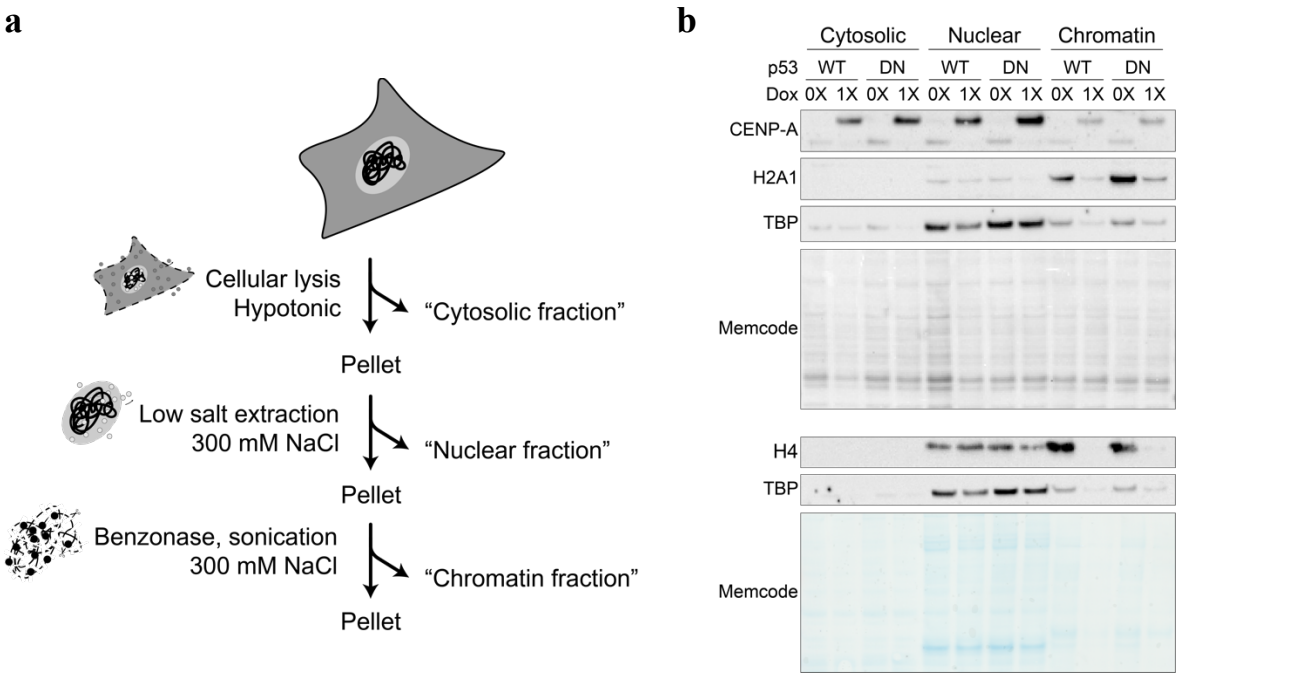
Acknowledgments

We sincerely thank Dr. Daniel Jeffery for helpful discussions and critical reading of the paper. We also thank Dr. Daniele Fachinetti and all team/unit members for stimulating discussions and for their advice. We thank the Cell and Tissue Imaging Platform PICT-IBiSA (member of France-Bioimaging ANR-10-INBS-04) in UMR3664, the NGS platform ICGex and the Cytometry platform CYTPIC of Institut Curie. This work was supported by La Ligue Nationale contre le Cancer (labellisation), Labex DEEP-PSL (ANR-11LABX-0044_DEEP, ANR-10-IDEX-0001-02) and the ERC (ERC-2015-ADG 694694 “ChromADICT”). The Ph.D. of C.R.-P. was funded by Sorbonne Université for 3 years and by the Fondation pour la Recherche Medicale (FRM) for 1 year (Grant No. FDT202304016871).

ADDITIONAL RESULTS (PRELIMINARY DATA)

An impact of CENP-A overexpression on chromatin plasticity, structure?

To uncover the underlying mechanisms guiding cell-fate changes, I started to explore the impact of CENP-A on chromatin structure. To see whether CENP-A overexpression impacts protein-chromatin interactions in MCF10-2A cells, I harvested cells and isolated proteins in cytosolic, nuclear and chromatin fractions by biochemical extraction, 15 days post-induction. In the chromatin fraction, CENP-A overexpression reduces the levels of H2A/H4 and CENP-A, along with the transcription factor TBP. This decrease is consistent with the fact that, in the overexpression condition, the levels of CENP-A are more abundant in both cytosolic/nuclear fractions than in the chromatin-bound fraction. This observation supports the model of histones and chromatin proteins which are hyperdynamic and bind loosely to chromatin when CENP-A is overexpressed.



(**a**) Scheme depicting the preparation of cytosolic, nuclear and chromatin fractions from MCF10-2A cells. Cytosolic extract: cytoplasmic membranes disrupted using Dounce glass homogenizer and hypotonic lysis buffer. Nuclear extract: proteins unbound or lowly bound to chromatin released at low salt concentrations (soluble) while chromatin-bound proteins (not soluble) fractionate to the pellet. Chromatin extract: pellet treated with benzonase and sonicated to release chromatin-bound proteins. (**b, c**) Western blot analysis of chromatin fraction, nuclear extract and cytosolic extract from MCF10-2A cells after 15 days of CENP-A overexpression (1X Dox) or not (0X Dox). 20 μg of protein extracts loaded. Two blots from the same experiment.

Methods

Protein extracts and Western blotting

The cytosolic and nuclear extracts were prepared from MCF10-2A cells using the protocol from (Martini et al., 1998), except that 300 mM NaCl was used. Briefly, cells were lysed with hypotonic buffer using Dounce homogenizer and then centrifuged. The supernatant (cytosolic extract) was collected, and the pellet was treated with lysis buffer containing 300 mM NaCl. After centrifugation, the supernatant (nuclear extract) was collected, and the pellet was treated with benzonase and sonicated. After centrifugation the supernatant containing the chromatin fraction was collected. We quantified protein content in the extracts using Pierce BCA protein assay kit. We performed Western blotting as in Jeffery et al., 2021 and acquired images using ChemiDoc Touch system and ImageLab software. Primary antibodies: CENP-A 1:500 (#2186 Cell Signaling Technology), H2A1 1:1000 (#ABE215 Merck), H4-pan 1:2500 (#05-858, Sigma-Aldrich), TBP 1:1000 (#ab818, Abcam). Secondary antibodies: Jackson ImmunoResearch, 1:10000, donkey anti-mouse, donkey anti-rabbit.

DISCUSSION

During the course of my Ph.D., I aimed to provide a better understanding of the impact of CENP-A overexpression in cancer. For this, I capitalized on a tunable CENP-A overexpression system in human cells to bypass p53 regulation of *CENPA* transcription.

First, I contributed to uncover the importance of the p53 status of cells in how CENP-A overexpression affects their fate, i.e., cell cycle and identity, and cell sensitivity to X-irradiation.

Second, I identified a cell population corresponding to an intermediate state between epithelial and mesenchymal in the human cell lines. I designed time course experiments to track EMT and revealed that these intermediate cells tend to revert to an epithelial state in normal conditions, while CENP-A overexpression promotes their progressive mesenchymal transition in both p53 contexts. I showed that mesenchymal states are maintained with CENP-A overexpression in p53-defective cells only. To identify the EMT programs activated by CENP-A overexpression, I generated a single cell multi-omics dataset combining ATAC and RNA-sequencing and I established a collaboration with specialists in integrative genomics at Institut Pasteur. We showed that CENP-A overexpression promotes two transitions, (1) by stimulating a pre-existent program associated with inflammation and G1 phase of the cell cycle, and (2) by initiating a new program associated with cell growth and proliferation. Their activation correlates with global changes in chromatin organization, with rearrangements of broad CENP-A/H3.3 domains. I further demonstrated that induced EMT programs and states are reversed back to normal when erasing ectopic CENP-A, in line with non-genetic changes. These findings support a model in which ectopic CENP-A can drive EMT epigenetically. These results have several biological implications for cancer and development and open up exciting avenues to investigate the role of ectopic CENP-A in regulating chromatin plasticity and gene expression.

In the following section, I will discuss the genetic and epigenetic facets of CENP-A overexpression. I will elaborate on the possible epigenetic mechanisms promoting cell fate changes, including how CENP-A can impact chromatin architecture and dynamics. I will then consider the possible implications in physiological processes. I will finally discuss the impact for cancer.

Genetic and epigenetic facets of CENP-A overexpression

CENP-A combines both genetic and non-genetic properties to direct kinetochore assembly during chromosome segregation and to determine and maintain centromere position. As a consequence, CENP-A overexpression and mislocalization could reflect both of these genetic and epigenetic features, with consequences for genome integrity and chromatin structure. In human cells, CENP-A overexpression and subsequent mislocalization to chromosome arms weakens the native kinetochore, causing mitotic defects which result in high incidence of micronuclei, copy number alterations (CNAs) and aneuploidy (Shrestha et al. 2017, 2021). In our inducible model, CENP-A overexpression similarly promotes micronuclei formation along with numerical and structural aneuploidy (Jeffery et al. 2021) (Fig S5d). However, in both p53 contexts, comet assay and γ-H2AX quantification show no change in acute DNA damage or repair upon CENP-A overexpression (Jeffery et al. 2021), even on longer time scales (Fig. S2g, S5a in **Results** – **Part 2**). Thus, chromosomal instability involving micronuclei, CNAs and genomic rearrangements could drive the cell state and identity changes induced by high CENP-A levels. Additional genetic alterations could be implicated. For example, micronuclei formation can lead to chromothripsis (chromosome shattering and reassembly), characterized by thousands of chromosomal rearrangements in a single or several chromosome(s) (C.-Z. Zhang et al. 2015). Of note, we did not detect such massive rearrangement by mFISH karyotype analysis after 15 days CENP-A overexpression (Jeffery et al. 2021, suppl. data), but the technique does not allow visual detection of inversions and small aberrations. Such genomic rearrangements promote gene expression changes (Cortés-Ciriano et al. 2020; Y.-F. Lin et al. 2023; Trivedi et al. 2023) and could impact cell fate upon CENP-A overexpression. Moreover, with the inducible and reversible cell reprogramming that is the EMT, we uncovered a non-genetic feature of CENP-A overexpression. CENP-A overexpression leads to mislocalization and higher levels at centromeres (Jeffery et al. 2021; Lacoste et al. 2014). Once CENP-A levels go back to normal, cells lose the ectopic CENP-A fraction while centromeric levels remain high. This is accompanied by the loss of β-catenin activation and CENP-A-induced mesenchymal states. Together, our findings show that ectopic incorporation of CENP-A drives cell identity changes independently from genetic alterations. Thus, our inducible system enabled to uncover an epigenetic feature of CENP-A overexpression that relies on reversible changes in the epigenome due to ectopic CENP-A. It is yet to be determined how its misincorporation along chromosome arms can perturb gene expression.

How can ectopic CENP-A promote cell fate transitions?

Re-organizing 3D genome architecture

A first aspect we can consider is the connection between CENP-A localization and 3D chromatin organization. Normally, CENP-A organizes as small foci, homogeneous in size and shape, dispersed throughout interphase nuclei of cycling human cells in culture (Ollion et al. 2015; Solovei et al. 2004). This organization reflects centromere clustering in the nucleus and influences genome organization (Muller, Gil, and Drinnenberg 2019). Dynamic centromere clustering is linked to cell type and differentiation state. For example, different centromeres cluster together depending on the hematopoietic differentiation stage (I. Alcobia, Dilão, and Parreira 2000b; Isabel Alcobia et al. 2003). In addition, CENP-A nuclear localization pattern in human tissue is impaired in tumor cells (in terms of foci size, shape and localization) and is even further altered with tumor grade (Verrelle et al. 2021). Although they could relate, these changes have not yet been linked to CENP-A levels in cancer and represent an interesting avenue to explore. Our CENP-A overexpression system in human cell lines enables to distinguish between (1) cells with normal CENP-A levels, (2) cells overexpressing CENP-A and (3) cells that previously underwent high CENP-A levels (Fig. 5 in **Results** – **Part 2**). Contrasting with the normal pattern, CENP-A overexpression causes a strong background corresponding to CENP-A ectopic localization, along with large/intense foci that tend to be heterogeneous in terms of size and shape (Fig. 5b in **Results** – **Part 2**). Once CENP-A levels are back to normal, nuclei lose the background signal, but foci intensity and heterogeneity are maintained (Fig. 5b in **Results** – **Part 2**). This observation suggests that CENP-A overexpression could induce changes in centromere and/or genome architecture, an impact that is not completely reversed upon CENP-A overexpression reversal. If these changes are associated with EMT in cells overexpressing CENP-A, they may facilitate a new "round" of EMT if CENP-A is re-overexpressed a second time. Such experiment may provide further insights into the link between CENP-A levels, subnuclear organization and EMT. Cell differentiation has previously been associated with changes in the subnuclear localization of centromeres (Jansz and Torres-Padilla 2019; Schlesinger and Meshorer 2019). Single-cell Hi-C and ChIP-Seq analysis of 3D genome organization during EMT revealed that A/B compartments are relatively stable between EMT states, with only a small fraction of EMT genes influenced by compartment switching. Among these genes, epithelial genes become enriched with H3K27me3 while mesenchymal genes progressively show increased contact frequency within mesenchymal TADs during EMT (Pang et al. 2022). In parallel, ectopic CENP-A is enriched at areas of high histone turnover, including CTCF binding sites and leading to CTCF occlusion from these sites (Lacoste et al. 2014). Decrease in CTCF binding has been associated with chromatin remodeling and promotion of AKT and inflammation-related EMT programs, that are both activated upon CENP-A overexpression (Fig. 3, S4d-e in **Results** – **Part 2**). For instance, single allele knockout of CTCF in MCF10A cells (reducing CTCF levels by approximately 50%) lead to upregulation of EMT genes involved in AKT/PI3K signaling (Lebeau et al. 2022). In this

case, most CTCF binding sites remain unaffected but a subset – enriched in AKT/PI3K and ECM-related gene loci – loses CTCF binding. A similar process occurs in p53-defective cells following whole genome doubling, causing a relative 50% reduction in CTCF levels (Lambuta et al. 2023). This is associated with reduced H3K9me3 and leads to a loss of insulation at boundaries (potentially due to stochastic loss of CTCF binding), which in turn results in reduced segregation of A/B compartments, compartment switches and transcription changes, with notably the upregulation of inflammation-related genes and the EMT transcription factor (EMT-TF) ZEB1. Therefore, several observations point to a possible effect of ectopic CENP-A on 3D chromatin architecture, potentially by affecting CTCF binding.

Modulating chromatin composition and gene expression

Chromatin composition regulates transcription programs (Yadav, Quivy, and Almouzni 2018) and pre-mRNA splicing outcomes (Luco and Misteli 2011), and is likely perturbed by CENP-A mislocalization. CENP-A could affect transcription or splicing processes directly (given that CENP-A displays distinct characteristics compared to other H3 variants) or indirectly (by impacting other histone variants). Ectopic CENP-A preferentially localizes at high histone turnover regions including active promoters and genes, where it can form heterotypic nucleosomes containing both H3.3 and CENP-A (Lacoste et al. 2014). First, evidence has been reported illustrating the impact of H3 variants on EMT. In several human cell lines, activation of EMT genes leads to the downregulation of the H3.1 histone chaperone CAF-1, causing a global decrease in chromatin-bound histone levels; this increases chromatin accessibility and H3.3 incorporation into chromatin through a gap-filling mechanism mediated by the chaperone HIRA (A. P. Gomes et al. 2019). In MCF10A cells, H3.3 overexpression alone does not promote EMT but the knockdown of CAF-1 subunits, which promotes H3.3 gap-filling, is sufficient to promote EMT after 10 days of treatment. ChIP-qPCR analysis shows H3.3 enrichment at the promoters of EMT-TFs SOX9, ZEB1 and SNAI1, but the study does not show where H3.3 gets redistributed genome-wide. Gene set enrichment analysis show that H3.3 gets mainly enriched at genes essential for metastasis, relative to morphogenesis/development and wound healing EMT programs. Thus, CAF-1 depletion may provide cells with increased plasticity, an essential characteristic for cellular transitions, through transient access of factors to the genome and/or changes in histone marks. A similar example exists in a model of myeloid lineage (R. Franklin et al. 2022). Here, CAF-1 knockdown in progenitor cells has been proposed to promote their rapid differentiation through increased chromatin accessibility at regulatory elements and subsequent binding of transcription factors. Interestingly, it also led to increased expression of H3 variants CENP-A and H3.3. However, CAF-1-depleted cells do not share the same morphology as mature neutrophils. The authors conclude that CAF-1 knockdown promotes either partial differentiation after 4 days or an alternative, mixed lineage fate. These examples share interesting similarities with the inducible CENP-A overexpression model: the transition starts after several days, different programs are (or may be) promoted simultaneously, and the process involves a

switch in H3 variants bound to chromatin. In our case, CENP-A overexpression promotes rearrangements of H3.3 peaks into broad domains in chromatin after 10 days. Furthermore, considering switches in histone marks, an increase in H3K4me3 and H3K36me3 levels has been associated with EMT induced by TGF-β treatment or E-cadherin knockdown (McDonald et al. 2011). EMT leads to switches between active H3K4me3 and repressive H3K27me3 marks that correlate with the expression of mesenchymal genes and the inhibition of epithelial genes in mesenchymal cells induced by TWIST1 in mammary epithelial cells (Malouf et al. 2013), by TGF-β in basal breast cancer cells (Chaffer et al. 2013), or in spontaneously mesenchymal cells selected among cells surviving contact inhibition at high confluence (Ke et al. 2010). In addition, overall, the number of gene promoters marked by H3K4me3 increase during EMT (Malouf et al. 2013). A fraction of targeted genes, pre-marked by H3K27me3, acquire a bivalent H3K4me3/H3K27me3 state. Newly bivalent genes are mostly development-related and overlap with the bivalent gene signature of ESCs. This indicates that EMT is associated with an epigenetic reprogramming that promotes stem cell properties, likely associated with greater plasticity. In addition to favoring the H3K4me3 modification to modulate the transcription program, the EMT-associated epigenetic reprogramming also includes dynamic changes in H3K27ac levels at mesenchymal genes, as shown upon TGF-β induction in lung cancer cells (Qiao et al. 2020). Recent evidence supports a model by which dynamic changes in H3K27ac and H3K27me3 locally modulate the splicing of common EMT genes, such as *FGFR2* and *CTNND1*, by regulating the recruitment of Polypyrimidine-tract-binding protein (PTB), a repressive regulator of alternative splicing (Segelle et al. 2022). Importantly, changes in chromatin modifications and alternative splicing are reversible upon MET. Thus, epigenetic reprogramming may also drive EMT by coordinating splicing events that are required to induce mesenchymal features in a reversible manner. Altogether, these studies indicate a major role for histone modifications H3K4me3, H3K27ac and H3K27me3 in the epigenetic reprogramming supporting EMT. Our results suggest a slight increase, upon CENP-A overexpression, in H3K27Ac levels, and even more in H3K4me3 levels (Fig. S3d in **Results** – **Part 2**). In this context, an exciting aspect to consider would be gene bivalency. CENP-A might drive a similar epigenetic reprogramming to what has been described, which may favor active marks, notably H3K4me3. Importantly, by comparison with other H3 variants, the CENP-A histone tail has very few lysine residues and its arginine residues are rarely modified (Srivastava and Foltz 2018). As a consequence, CENP-A is generally significantly less modified than H3 and is not marked by activating or repressing marks such as H3K4 methylation or H3K27 methylation/acetylation. Thus, it is likely that ectopic CENP-A does not directly harbor these marks, even at ectopic positions. However, heterotypic particles containing CENP-A and H3.3 (Lacoste et al. 2014) could contribute to modifying/enriching the epigenetic landscape. Alternatively, instead of being a direct consequence of ectopic CENP-A deposition, such changes could also simply follow the activation of EMT inducers. These aspects should be considered when studying the architecture of the epigenetic reprogramming upon CENP-A

overexpression, and the potential functional consequences on transcription and splicing processes, which are still open questions and will be an exciting avenue to explore. Exploring CENP-A overexpression in the context of the H3 variant-chaperone network would provide valuable insights into understanding how disrupting the balance in histone supply can contribute to transcription changes and cell fate transitions.

Disrupting the spatiotemporal DNA replication program

In addition to its role on transcription and splicing processes, chromatin composition contributes to shaping the DNA replication spatiotemporal program. The lack of a consensus DNA sequence defining replication origins in mammals further illustrates the importance of chromatin to define these regions (Fragkos et al. 2015). Indeed, H3.3 deposition is critical for preserving early replication origins, which are characterized by the boundaries of H3.1 and H3.3 (Gatto et al. 2022). By altering H3.3 enrichment at early-firing replication initiation zones, CENP-A overexpression may affect early initiation zone function. My first analyses of EdU patterns defining early, mid and late replicating nuclei show that CENP-A overexpression perturbs the relative pattern frequencies in asynchronous cells, showing higher "late replicating" patterns (data not shown). This observation indicates that, overall, the spatiotemporal organization of the replication program is indeed affected by CENP-A overexpression. In addition, preliminary results in synchronized cells show a slight delay in completing genome replication for cells which have been chronically overexpressing CENP-A (data not shown). Interestingly, the DNA replication program gets reorganized with changes in the transcription program during cell differentiation (Hiratani et al. 2008, 2010; Rivera-Mulia et al. 2015). In the context of the EMT, high levels of the EMT-TF ZEB1 is associated with premature entry into S-phase (Schuhwerk et al. 2022), along with global tolerance to DNA replication stress through MRE11 (Schuhwerk et al. 2022) and/or RHOJ which activates new origins of replication (Debaugnies et al. 2023). Recent publications have illustrated the association between the replication fork speed and cell fate reprogramming (Koch 2022; Nakatani et al. 2022), showing that replication speed increases as development proceeds in mouse embryos. Furthermore, experimentally reducing the replication fork speed with low doses of hydroxyurea contributes to cell reprogramming to totipotent-like cells resembling 2-cell-stage (2CLCs). In another model, the combination of G1 arrest, combined with the inhibition of DNA replication, promotes the differentiation of pancreatic progenitor cells. Further reducing the replication fork speed contributes to differentiation (L. Sui et al. 2021). We could envisage a model where ectopic CENP-A affects replication timing and/or fork speed, thus facilitating or potentiating cell fate reprogramming. Further studies should help to uncover (1) how CENP-A overexpression can interfere with early replication zones and (2) consider the association with cell fate reprogramming.

Remodeling chromatin structure and plasticity

CENP-A overexpression and ectopic localization leads to the remodeling of CENP-A/H3.3 domains between day 10 and 24 (Fig. 3, S3 in **Results** – **Part 2**) More precisely, after 10 days, H3.3 peaks are reorganized as larger domains genome-wide, and are accompanied by CENP-A. This observation suggests a global impact of CENP-A overexpression on chromatin structure, but the underlying mechanism remains unknown. The structure of CENP-A chromatin at centromeres may give insights into the impact of ectopic CENP-A incorporation at chromosome arms. CENP-A nucleosomes wrap 121 bp of DNA, compared to the 147 bp for H3 nucleosomes (Hasson et al. 2013; Tachiwana, Kagawa, and Kurumizaka 2012). At centromeres, they display looser DNA binding relative to H3 nucleosomes, along with flexible, dynamic nucleosomal DNA ends which may interfere with linker histone binding (Ali-Ahmad et al. 2019; Arimura et al. 2019; Panchenko et al. 2011; Sekulic et al. 2010; Tachiwana et al. 2011). These features, further exacerbated by CENP-C binding, locally promote chromatin flexibility and opening. This is likely related to the initial function of CENP-A in kinetochore assembly. At ectopic loci, heterotypic nucleosomes combining CENP-A and H3 (Lacoste et al. 2014) harbor a "hybrid structure" sharing structural characteristics of both CENP-A and H3.3, with asymmetric DNA wrapping (Arimura et al. 2014). Thus, ectopic CENP-A could promote a certain level of local flexibility/accessibility to transcription factors or chromatin remodelers. However, while CENP-A properties imply highly dynamic structures, CENP-A interactions with kinetochore proteins also involve more compact structures (Melters et al. 2019, 2023). Regarding this aspect, ectopic CENP-A only recruits a subset of kinetochore proteins – CENP-C, CENP-N and the Mis18 complex (Gascoigne et al. 2011; Lacoste et al. 2014; Van Hooser et al. 2001) – but also CENP-T and Nuf2 during chromosome segregation (Shrestha et al. 2017, 2021). As a consequence, when overexpressed, CENP-A punctate signal in the arms of mitotic chromosomes (Lacoste et al. 2014; Shrestha et al. 2017, 2021) suggests the ectopic formation of locally compact structures involving CENP-A and partners. These ectopic structures appear in condensed chromosomes but not in interphase nuclei. Importantly, core regions bound by CENP-A and CENP-C in human centromeres (Corless, Höcker, and Erhardt 2020) and neocentromeres (resulting from centromere repositioning) (Naughton et al. 2022) are actively transcribed. These results indicate that ectopic CENP-A should be at least permissive to transcription. Finally, CENP-A mislocalization may impact chromatin plasticity. Indeed, during centromere replication, CENP-A recycling by HJURP (Dunleavy et al. 2009) enables the equal distribution of parental CENP-A to each daughter strand. By contrast, at ectopic loci, replication normally evicts CENP-A particles without recycling (Nechemia-Arbely et al. 2019). This mechanism likely contributes to the loss of ectopic CENP-A once its levels go back to normal (Fig. 5b in **Results** – **Part 2**), as soon as 24 hours after the reversal (Jeffery et al. 2021), whereas high centromeric CENP-A levels are maintained (Fig. 5b in **Results** – **Part 2**). Thus, replication-coupled eviction of CENP-A normally prevents the accumulation of CENP-A in chromosome arms. However, upon continuous overexpression

of CENP-A, it may induce high turnover rates with CENP-A nucleosomes loaded into chromatin but not stably maintained/incorporated across the cell cycle. Such process would favor high chromatin plasticity. This is further suggested by preliminary analysis of cellular fractions, showing decreased amounts of chromatin-bound histones and TBP upon CENP-A overexpression (Fig. 5b in **Results – Part 2**). This observation support the hypothesis of chromatin proteins that are loosely/hyperdynamically bound to chromatin, very similarly to the dynamic plasticity of chromatin proteins observed in undifferentiated ES cells (Meshorer et al. 2006). In the context of EMT, such process may endow intermediate cell states with higher plasticity, thus providing them with alternative cell fate options and facilitating their mesenchymal transition through different trajectories.

A role for CENP-A in physiological contexts?

Our results suggest that CENP-A could play a role in physiological contexts that would require increased chromatin plasticity. Interestingly, CENP-A has been associated with response to DNA damage, which operates in the context of chromatin, requires important rearrangements involving incorporation of DNA damage-responsive modifications, histone variant exchange and deposition of newly synthesized histones (Adam, Dabin, and Polo 2015). In human cells, induction of DNA double strand breaks (DSB) by laser or site-specific endonuclease has been associated with CENP-A accumulation (Zeitlin et al. 2009). This observation could imply a role for CENP-A in DNA damage repair. Of note, the recruitment of CENP-A takes several minutes, which contrasts with most other repair proteins whose assembly occurs within a minute (Aleksandrov et al. 2018). However, the recruitment of CENP-A to DSBs has shown contrasting results (Helfricht et al. 2013) and may be context-dependent. Recently, HJURP has been proposed to mediate CENP-A deposition at DSBs (Serafim et al. 2024), contrasting with the H3 chaperone-mediated deposition of ectopic CENP-A in overexpressing cells (Lacoste et al. 2014; Nye et al. 2018). The HJURP-mediated accumulation of CENP-A specifically at DSBs would promote the turnover of H3K9me3 and HP1, thus facilitating DSB signalling and repair (Serafim et al. 2024). In mouse cells, accumulation of DNA damage through genotoxic stress has been associated with CENP-A delocalization from centromeres, accompanied by centromere disorganization (Hédouin et al. 2017). This requires the Ataxia-telangiectasia mutated (ATM) kinase (a DNA damage response effector), the histone chaperone FACT and active p53 triggering cell cycle arrest. Altogether, these data indicate that CENP-A deposition at DNA damage sites might favor DNA repair, while also potentially representing a defense mechanism to maintain genomic stability, when depleted from centromeres, by preventing centromere-defective cells from cycling and proliferating. Furthermore, as shown in *Drosophila*, certain factors such as Chromatin accessibility complex (CHRAC) prevent the targeting of CENPA (CID) to damage sites, avoiding ectopic kinetochore assembly of and accumulation of genetic instability (Mathew et al. 2014). Thus, overall, the role of CENP-A in DSB repair could involve chromatin accessibility and plasticity but still remains an open question.

Furthermore, transition of intermediate cells towards mesenchymal promoted by ectopic CENP-A deposition represents a process strongly associated with the acquisition of stem cell properties (Battula et al. 2010; Malouf et al. 2013; Mani et al. 2008). In addition, we show that CENP-A overexpression could induce similar chromatin properties to that of ES cells, in terms of histone modifications and chromatin plasticity. Compared to differentiated cells, pluripotent ESCs show high chromatin plasticity. This is supported by several mechanisms maintaining a bivalent H3K4me3/H3K27me3 chromatin (Bernstein et al. 2006) and an open/accessible chromatin state (Mattout and Meshorer 2010; Meshorer et al. 2006). Interestingly, CENP-A at centromeres may epigenetically mark stem cell identity, for instance in *Drosophila* intestinal stem cells, which preferentially retain pre-existing CENP-A histones during asymmetric divisions, when one daughter cell differentiates and the other maintains stemness (Arco, Edgar, and Erhardt 2018). In addition, asymmetry in CENP-A (CID) levels between sister centromeres promotes a centromere drive, the future stem cell having more CENP-A (CID) than the differentiated cyst cell in *Drosophila* male (Ranjan, Snedeker, and Chen 2019) and female (Dattoli et al. 2020) germ lines. Beyond this aspect focusing on centromeres, interestingly, high CENP-A levels may be implicated in ESC biology. Low p53 levels generally promote stem-cell formation and proliferation in vertebrates, whereas normal p53 levels and activity promote the commitment to a differentiation pathway (Levine et al. 2016). For example, both mouse and human ESCs keep p53 in an inactive state through post-translational regulation, p53 reactivation promoting their differentiation (Jain and Barton 2018). Given that p53 negatively regulates *CENPA* transcription (Filipescu et al. 2017), the levels of CENP-A should be considered in this context. Human ESCs and iPSCs maintain high CENP-A mRNA levels, up to two-fold of levels in fibroblasts (Ambartsumyan et al. 2010; Milagre et al. 2020). Despite increased expression, cell fractionation experiments show reduced amounts of chromatin-bound CENP-A in hESCs compared to differentiated cells, along with an increase in the soluble fraction (Milagre et al. 2020). In other systems, high CENP-A is also generally associated with stemness. For example, in mouse, CENP-A mRNA and protein levels in the heart are the highest in the embryo and decrease with aging (McGregor et al. 2014). Consistently with this observation, in the same study, cultured cardiac progenitor cells isolated from young mice show high CENP-A levels at start, which are progressively reduced as cells age. In the *Drosophila* female germ line, CENP-A (CID) overexpression promotes stem cell self-renewal (Dattoli et al. 2020). However, the localization of CENP-A (centromere-specific or with ectopic deposition) in this context remains unclear. Overall, recent publications indicate that CENP-A contributes to maintain stemness properties. This could involve changes in chromatin accessibility and plasticity, as suggested by the study of chromatin-bound CENP-A in hESCs. Further research investigating the role of CENP-A in stem cells should consider both centromeric and ectopic CENP-A pools. Moreover, EMT progression upon CENP-A overexpression in human cell lines may reflect an increased cellular plasticity which could be involved

in development and wound healing processes, which also undergo EMT programs, or in cellular functions requiring plasticity such as neuroplasticity (or brain plasticity).

In mammals, neuroplasticity refers to the ability for the nervous system to change its structure and activity in response to various stimuli (Herre and Korb 2019). This is exemplified in the hippocampus, a brain structure that relies on plastic features for lifelong neurogenesis (Toni and Schinder 2016) and memory formation (Alberini and Kandel 2014; Squire 1992). First, in the context of neurogenesis, the hippocampus contains neural stem cells that divide and generate glutamatergic granule cells (a type of differentiated neuron cells) throughout life (Toni and Schinder 2016). Although it has become evident that epigenetic regulators are key players in neural stem cell self-renewal and fate specification processes (Denoth-Lippuner and Jessberger 2021), the molecular mechanisms and how they translate into cell fate changes remain unknown. Given the link between CENP-A, stemness and cell fate specifications, a role for centromeric and ectopic CENP-A could be considered. Second, most interestingly, the formation of memories at the cellular level requires neuronal activation through the expression of specific genes termed immediate early genes (Zovkic 2021). This is mediated by epigenetic mechanisms, including DNA methylation (Day and Sweatt 2010; D. K. Ma et al. 2009), modulation of chromatin folding and compartmentalization (L. A. Watson and Tsai 2017), high histone turnover and histone variant exchanges (Maze et al. 2015; Yap and Greenberg 2018; Zovkic 2021). Importantly, analysis of gene expression in mouse hippocampus tissue before and after neuronal activation *in vivo* shows dynamic regulation of CENP-A levels with neuronal activity (Fernandez-Albert et al. 2019; Y. Su et al. 2017). These publications reveal that the activation of immediate early genes is accompanied with a gain of H3K4me1/3 and H3K27ac marks and chromatin accessibility at activity-regulated genes, along with an increase in CENP-A levels (supplementary information, RNA-seq analysis). A tempting hypothesis would be that ectopic CENP-A deposition occurs and contributes to chromatin plasticity in a similar way to what we uncovered with an EMT model. The molecular programs driving plasticity-related neuronal activation need further characterization to understand the principles of memory formation in the mammalian hippocampus and the mechanisms associated with loss of hippocampal function and severe memory dysfunction such as Alzheimer's disease. CENP-A localization at genomic regions that become actively transcribed in response to neuronal stimulation, and the connection with changes in chromatin structure, could be an interesting aspect to explore.

CENP-A in promoting EMT: Implications for cancer

Prolonged CENP-A overexpression promotes EMT in p53-defective cells. These findings support a role for CENP-A overexpression in promoting aggressive phenotypes in p53-defective cancers. Although EMT programs and inducers are quite well characterized in development and wound healing, the ones orchestrating EMT in cancer cells remain unclear. Our results thus give new insights into mechanisms that may be involved in aggressive cancers overexpressing CENP-A. First, overexpression of CENP-A

leading to its ectopic distribution induces CIN (section 1. *Genetic and epigenetic facets of CENP-A overexpression*). In p53-WT cells, this promotes p53 activation, senescence and sensitivity to X-irradiation. Indeed, additional stress, like DNA damage from X-irradiation, should amplify the response to DNA damage. By contrast, in p53-defective cells, CENP-A overexpression does not affect the sensitivity to X-irradiation and can promote EMT (Jeffery et al. 2021). In this context, CENP-A overexpression can also confer a DAXX-dependent tolerance to DNA damage, induced by either camptothecin (a topoisomerase inhibitor) or ionizing radiation, in HeLa cells (Lacoste et al. 2014). The contribution of CENP-A to DNA repair might be possible, although its enrichment at sites of DNA damage remains unclear.

As a major protein for chromosome segregation during cell division that is cell cycle regulated and expressed in G2/M, CENP-A is considered a marker of cell proliferation. However, CENP-A upregulation does not increase cell proliferation rate in mouse embryonic fibroblasts (MEFs). Our work in human cell lines shows that CENP-A overexpression actually induces a slight decrease in doubling rate that is only partially counteracted by p53 inactivation (Jeffery et al. 2021), and which happens in all EMT phenotypes (**Results** – **Part 2**) This observation probably reflects the fact that, while an increase in centromeric CENP-A could reinforce centromere function, excess of CENP-A leads to mislocalization and centromere weakening (Shrestha et al. 2017, 2021). Indeed, studies focusing on centromere drive suggest that increased CENP-A at centromere can reinforce centromere function. For instance, asymmetric CENP-A loading on sister chromatids in mouse (Iwata-Otsubo et al. 2017) and *Drosophila* (Dattoli et al. 2020; Ranjan, Snedeker, and Chen 2019) leads to an asymmetry in mitosis because the difference in CENP-A levels at sister centromeres associates with an asymmetry in microtubule binding and in levels of CENP-C (Carty, Dattoli, and Dunleavy 2021) and NDC80 (Ranjan, Snedeker, and Chen 2019). Our results thus highlight the importance of considering both centromeric and ectopic CENP-A functions distinctly. Consistent with this observation, HJURP overexpression, leading to increased levels of CENP-A at centromeres exclusively (Filipescu et al. 2017), promotes cell proliferation and tumor growth (Lin Li et al. 2018, 2023), by contrast with CENP-A overexpressing cells. HJURP overexpression thus enables to maintain a hyperproliferative state but represents an "Achille's heel" in addicted cells (Filipescu et al. 2017). Regarding tumorigenesis, neither CENP-A nor HJURP overexpression are sufficient for tumorigenic transformation of MEFs, even when combined with p53 loss (Filipescu et al. 2017). These results suggest that they would rather tend to become upregulated as a consequence of cellular transformation. However, this aspect remains unclear. Indeed, our findings indicate that CENP-A overexpression potentiates cell fate changes depending on the cellular context. This context-dependency could potentially apply to cellular transformation too. This is also suggested by glioblastoma initiating cells (GICs), which arise from the transformation of neural stem cells. Interestingly, CENP-A levels are upregulated at both mRNA and protein levels in GICs (Behnan et al. 2016; Stangeland et al. 2015). This is accompanied with ectopic incorporation of CENP-

A. In addition, CENP-A knockdown in GICs leads to reduced stemness, measured by sphere-forming ability and immunofluorescence of the stemness marker SOX2 (Behnan et al. 2016; Stangeland et al. 2015). Thus, CENP-A could potentiate cell transformation in particular contexts, potentially by favoring stemness properties.

Furthermore, CENP-A overexpression correlates with cancer aggressiveness. First, our results confirm a role for CENP-A mislocalization in CIN (Jeffery et al. 2021), which is a driving force in tumorigenesis by inducing high rates of mutagenesis, thus increasing the genetic diversification (Potapova, Zhu, and Li 2013). This feature is generally associated with cancer progression and resistance to therapy through clonal selection (Greaves and Maley 2012), although excessive CIN can be deleterious. Second, we reveal that CENP-A overexpression can promote EMT in p53-defective cells. More precisely, when p53 is defective, the cells evade cell cycle arrest, allowing CENP-A overexpression to promote EMT. By contrast, in p53-WT cells, the amounts of mesenchymal cells are limited, and induced mesenchymal states are not maintained after several days in the MCF10-2A cell line. In p53-WT RPE-1 cells, prolonged CENP-A overexpression promotes EMT, but cells progressively stop proliferating, consistently with the fact that CENP-A overexpression in p53-WT cells promotes cell cycle exit. This observation is coherent with previous publications, indicating that p53 inhibits EMT through a miRNA-dependent mechanism that targets key EMT regulators such as Zeb1/2 and Snail (Semenov et al. 2022). Thus, p53 plays a dual role: first, inhibiting the transition as much as possible and second, targeting cells that transitioned towards mesenchymal anyway by promoting cell cycle exit. In p53-defective cells however, the proportions of mesenchymal cells are maintained with CENP-A, even after more than 60 days in culture, as shown by our analyses at late time points (Jeffery et al. 2021).

CENP-A overexpression promotes EMT heterogeneity, by stimulating different transitions and promoting more advanced transition states in the population. These features are similar to those found in advanced cancers, with cells exhibiting heterogeneity at both gene expression and phenotype levels (D. Li et al. 2023). First, CENP-A overexpression and mislocalization promotes inflammation-associated mesenchymal states, a conserved feature in the progression of organ fibrosis and cancer that promotes the survival of injured or malignant cells and favors the generation of autoregulatory loops to reinforce the EMT program (López-Novoa and Nieto 2009). Second, CENP-A mislocalization promotes another trajectory which relies on proliferating cells and is associated with development and survival. Indeed, this second type of EMT is marked by AKT and TOP2A (Topoisomerase IIα) (**Results – Part 2**). Interestingly, TOP2A has been proposed to be an activator of AKT/β-catenin signaling, and its expression correlates in many cancers with bad prognosis and metastatic capability (Y. Dong et al. 2021; B. Wang et al. 2020; K. Wang et al. 2019; J. Wu et al. 2024). The mechanism by which TOP2A increases the activation of AKT/β-catenin signaling is unknown and could be indirect. TOP2A is critical for structural maintenance of chromosomes, including chromosome condensation, but also catalyzing cleavage and relegation of DNA DSBs in a physiological context (without involving DNA damage

response pathways) to resolve a wide variety of topological problems resulting from DNA-templated processes such as replication and transcription (Uusküla-Reimand and Wilson 2022). Therefore, TOP2A is highly expressed in mitosis and considered a cell proliferation marker.

EMT occurs through various intermediate states, which display distinct properties. For example, intermediate and mesenchymal states display enhanced stemness, tumor-initiating capacity and invasive properties compared with epithelial cells. Moreover, intermediate cells show increased proliferative and decreased invasive potential and resistance to therapy compared to mesenchymal cells (De Las Rivas et al. 2021; Pastushenko et al. 2018; Pastushenko and Blanpain 2019; Ruscetti et al. 2015). Intermediate cells don't have the advanced mesenchymal properties enabling to invade the underlying mesenchyme, but they proliferate almost as efficiently as epithelial cells and, importantly, they have increased ability to generate both mesenchymal and epithelial identities. Thus, when injected in mouse, early intermediate cells give rise to similar, epithelial-like cells, while advanced intermediate cells give rise to a highly heterogeneous population comprising various advanced transition states, including mesenchymal states (Pastushenko et al. 2018). This feature makes them more efficient at colonizing lungs and forming metastases; advanced intermediate states are thus associated with increased metastatic potential (De Las Rivas et al. 2021; Pastushenko et al. 2018; J. Yang, Antin, Berx, Blanpain, Brabletz, Bronner, Campbell, Cano, Casanova, Christofori, Dedhar, Derynck, Ford, Fuxe, García de Herreros, et al. 2020). It is important to highlight that this reflects what happens in advanced carcinoma developing spontaneous metastases: several EMT subpopulations co-exist, increasing the level of plasticity within the tumor (Pastushenko et al. 2018). Altogether, these studies imply that (1) advanced intermediate cells show the highest metastatic potential, likely due to their ability to generate a mixed population of epithelial, intermediate and mesenchymal cells, and (2) the EMT phenotypic heterogeneity is a driving force of the metastatic cascade (D. Li et al. 2023). However, the dynamics allowing conversions between epithelial, early and advanced intermediate, and mesenchymal states are unknown. Given that the transition relies on an important epigenetic reprogramming, the EMT community agrees on the fact that conversions towards more advanced mesenchymal states requires increased plasticity, hence the notion of Epithelial-Mesenchymal Plasticity . CENP-A overexpression may provide early intermediate cells with increased plasticity, enabling conversions to more advanced states. As a conclusion, CENP-A overexpression-induced EMT likely contributes to the aggressive phenotype of cancers overexpressing CENP-A. The potential of reversing CENP-A overexpression, or re-activating p53 offers promises for cancer treatment.

Limitations of the study

It is interesting to note that, upon reversal of CENP-A overexpression, we do not detect an increase in intermediate states, but directly an increase in the epithelial population (Fig. 5 in **Results** – **Part 2**), which is coherent with previous data. For example, when forming lung metastases, mesenchymal cells

mostly revert to an epithelial state, showing they are not locked into their mesenchymal state once in the lung microenvironment (Pastushenko, Brisebarre, Sifrim, Fioramonti, Revenco, Boumahdi, Van Keymeulen, et al. 2018). MET is fast and would require much less plasticity, proceeding directly from the mesenchymal phenotype to the epithelial one (Lu, Jolly, Levine, et al. 2013). But, since this process is not fully characterized or understood, results from the reversal experiment should be considered carefully. Although it is clear that the EMT programs are reversed with CENP-A (loss of activated (non-phosphorylated by GSK3) form of β-catenin is reversed, loss of advanced intermediates and mesenchymal cells), we cannot be sure that mesenchymal cells actually reverse back to an epithelial state. Alternatively, mesenchymal cells could die or stop proliferating following the inactivation of the developmental/survival program. The same experiment in RPE-1 cells gives interesting insights on this aspect, as the p53-defective RPE-1 seem to reverse back to their original phenotype without involving cell death (Fig. S5). Furthermore, our single cell multiomics could not distinguish between epithelial and intermediate phenotypes. Interestingly, classical epithelial and mesenchymal markers EpCAM and Vimentin indicate that the "non-mesenchymal" cluster includes both epithelial (EpCAM+, Vim-) and (early) intermediate (EpCAM+, Vim+) cells. This raises the possibility that epithelial and intermediate states are too phenotypically close, and/or that part of the regulation relies on post-transcriptional mechanisms. Exciting future perspectives could rely on lineage tracing or single cell live imaging at a defined time window (for example, between day 19 and 20) to follow the transition and, more interestingly, could include the characterization of mesenchymal markers located at the cell membrane (our current markers rely on Vimentin, which requires cell permeabilization) in order to isolate different EMT cell populations by FACS-sorting. In addition, a combination of mathematical modelling could contribute to gaining a mechanistic understanding of the EMT plasticity in our model. Finally, the study of EMT dynamics upon CENP-A overexpression mostly rely on one inducible model of non-tumoral, fibrocystic breast cultured cell line (MCF10-2A), with several implications for fibrotic diseases. Regarding cancer, several questions remain unanswered before translating this model to cancer biology and complementary models. Do cells in culture reflect the processes at play in cancer? There are indeed several discrepancies between centromere/CENP-A architecture in cultured cells *versus* tumor samples, as described above. Is CENP-A mislocalized in patient tumor cells overexpressing CENP-A? And is CENP-A continuously overexpressed along the cell cycle in cancer, similarly to our inducible system, or do cancer cells still maintain a certain level of cell cycle-dependent regulation? Although interesting insights regarding CENP-A localization suggest its perturbation in cancer (Verrelle et al. 2021), research will require technological innovations to enable the study of CENP-A in more physiological models, with implications for cancer research.

CONCLUSION

My Ph.D. research aimed to characterize the impact of CENP-A overexpression on human cell state and identity across different contexts, with a focus on the impact of p53.

Firstly, I collaborated with my team to explore the effects of CENP-A overexpression on cell fate and resistance to therapy in different p53 contexts. We engineered a tunable CENP-A overexpression system in multiple epithelial human cell lines, which allowed us to assess changes in cell state, identity and sensitivity to X-irradiation, serving as a model for radiotherapy. My contributions have helped clarify how elevated CENP-A levels can promote sensitivity or therapeutic resistance, depending on the p53 context. Additionally, our findings demonstrated that CENP-A overexpression can increase a distinct mesenchymal cell population likely through the promotion of an EMT.

Secondly, since EMT progresses through distinct cellular states, I designed time-course experiments to monitor their emergence depending on CENP-A levels. I identified a specific cell population, representing an early intermediate state between epithelial and mesenchymal, in which CENP-A overexpression promotes EMT. To investigate the transcription programs activated by CENP-A, I generated a single-cell multi-omics dataset and initiated a collaboration with experts in integrative genomics. We demonstrated that CENP-A overexpression drives two EMT programs: a pre-existing program linked to inflammation, and a new one associated with proliferation and development. Importantly, I showed that the programs and states induced by CENP-A are reversible upon the removal of ectopic CENP-A. These results support a model of epigenetic regulation. In conclusion, while CENP-A has long been known for its essential role in maintaining genome stability, my project revealed a novel epigenetic function in regulating epithelial-mesenchymal plasticity.

These findings carry important biological implications for both cancer and developmental processes. They also pave the way for exploring how ectopic CENP-A influences chromatin plasticity and gene expression. By unravelling the mechanisms that link CENP-A, EMT, and potentially cell plasticity and stemness, we will gain a deeper understanding of the molecular consequences of CENP-A overexpression and its role in tumor progression.

REFERENCES

Aceto, Nicola, Aditya Bardia, David T. Miyamoto, Maria C. Donaldson, Ben S. Wittner, Joel A. Spencer, Min Yu, et al. 2014. 'Circulating Tumor Cell Clusters Are Oligoclonal Precursors of Breast Cancer Metastasis'. Cell 158(5): 1110–22. doi:10.1016/j.cell.2014.07.013.

Ackland, Margaret L., Donald F. Newgreen, Masha Fridman, Mark C. Waltham, Angela Arvanitis, Joseph Minichiello, John T. Price, and Erik W. Thompson. 2003. 'Epidermal Growth Factor-Induced Epithelio-Mesenchymal Transition in Human Breast Carcinoma Cells'. Laboratory Investigation 83(3): 435–48. doi:10.1097/01.LAB.0000059927.97515.FD.

Adam, Salomé, Juliette Dabin, and Sophie E. Polo. 2015. 'Chromatin Plasticity in Response to DNA Damage: The Shape of Things to Come'. DNA repair 32: 120–26. doi:10.1016/j.dnarep.2015.04.022.

Adam, Salomé, Sophie E. Polo, and Geneviève Almouzni. 2013. 'Transcription Recovery after DNA Damage Requires Chromatin Priming by the H3.3 Histone Chaperone HIRA'. Cell 155(1): 94–106. doi:10.1016/j.cell.2013.08.029.

Aghdassi, Ali, Matthias Sendler, Annett Guenther, Julia Mayerle, Claas-Olsen Behn, Claus-Dieter Heidecke, Helmut Friess, et al. 2012. 'Recruitment of Histone Deacetylases HDAC1 and HDAC2 by the Transcriptional Repressor ZEB1 Downregulates E-Cadherin Expression in Pancreatic Cancer'. Gut 61(3): 439–48. doi:10.1136/gutjnl-2011-300060.

Aiello, Nicole M., Ravikanth Maddipati, Robert J. Norgard, David Balli, Jinyang Li, Salina Yuan, Taiji Yamazoe, et al. 2018. 'EMT Subtype Influences Epithelial Plasticity and Mode of Cell Migration'. Developmental Cell 45(6): 681-695.e4. doi:10.1016/j.devcel.2018.05.027.

Aitken, Sarah J., Ximena Ibarra-Soria, Elissavet Kentepozidou, Paul Flicek, Christine Feig, John C. Marioni, and Duncan T. Odom. 2018. 'CTCF Maintains Regulatory Homeostasis of Cancer Pathways | Genome Biology'. https://genomebiology.biomedcentral.com/articles/10.1186/s13059-018-1484-3 (January 19, 2022).

Akalay, Intissar, Bassam Janji, Meriem Hasmim, Muhammad Zaeem Noman, Fabrice André, Patricia De Cremoux, Philippe Bertheau, et al. 2013. 'Epithelial-to-Mesenchymal Transition and Autophagy Induction in Breast Carcinoma Promote Escape from T-Cell-Mediated Lysis'. Cancer Research 73(8): 2418–27. doi:10.1158/0008-5472.CAN-12-2432.

Akhurst, Rosemary J., and Rik Derynck. 2001. 'TGF-β Signaling in Cancer – a Double-Edged Sword'. Trends in Cell Biology 11(11): S44–51. doi:10.1016/S0962-8924(01)02130-4.

Alabert, Constance, Teresa K. Barth, Nazaret Reverón-Gómez, Simone Sidoli, Andreas Schmidt, Ole N. Jensen, Axel Imhof, and Anja Groth. 2015. 'Two Distinct Modes for Propagation of Histone PTMs across the Cell Cycle'. Genes & Development 29(6): 585–90. doi:10.1101/gad.256354.114.

Alberini, Cristina M., and Eric R. Kandel. 2014. 'The Regulation of Transcription in Memory Consolidation'. Cold Spring Harbor Perspectives in Biology 7(1): a021741. doi:10.1101/cshperspect.a021741.

Alcobia, I., R. Dilão, and L. Parreira. 2000. 'Spatial Associations of Centromeres in the Nuclei of Hematopoietic Cells: Evidence for Cell-Type-Specific Organizational Patterns'. Blood 95(5): 1608–15.

Alcobia, Isabel, Ana Sofia Quina, Hélia Neves, Nuno Clode, and Leonor Parreira. 2003. 'The Spatial Organization of Centromeric Heterochromatin during Normal Human Lymphopoiesis: Evidence for Ontogenically Determined Spatial Patterns'. Experimental Cell Research 290(2): 358–69. doi:10.1016/s0014-4827(03)00335-5.

Aldrup-MacDonald, Megan E., Molly E. Kuo, Lori L. Sullivan, Kimberline Chew, and Beth A. Sullivan. 2016. 'Genomic Variation within Alpha Satellite DNA Influences Centromere Location on Human Chromosomes with Metastable Epialleles'. Genome Research 26(10): 1301–11. doi:10.1101/gr.206706.116.

Aldrup-Macdonald, Megan E., and Beth A. Sullivan. 2014. 'The Past, Present, and Future of Human Centromere Genomics'. Genes 5(1): 33–50. doi:10.3390/genes5010033.

Aldwaik, Reem Kamal, Denen Shian, Roshina Thapa, Swetha Vasudevan, Mimi Abo-Ayoub Ashqar, Eli Reich, Nataly Kravchenko-Balasha, and Michael Klutstein. 2023. 'Overexpressed Kinetochore Genes Are Used by Cancer Cells as Genome Destabilizers and Transformation Catalysts'. Translational Oncology 34: 101703. doi:10.1016/j.tranon.2023.101703.

Aleksandrov, Radoslav, Anton Dotchev, Ina Poser, Dragomir Krastev, Georgi Georgiev, Greta Panova, Yordan Babukov, et al. 2018. 'Protein Dynamics in Complex DNA Lesions'. Molecular Cell 69(6): 1046-1061.e5. doi:10.1016/j.molcel.2018.02.016.

Alexandrow, Mark G., and Joyce L. Hamlin. 2005. 'Chromatin Decondensation in S-Phase Involves Recruitment of Cdk2 by Cdc45 and Histone H1 Phosphorylation'. The Journal of Cell Biology 168(6): 875–86. doi:10.1083/jcb.200409055.

Ali-Ahmad, Ahmad, Silvija Bilokapić, Ingmar B. Schäfer, Mario Halić, and Nikolina Sekulić. 2019. 'CENP-C Unwraps the Human CENP-A Nucleosome through the H2A C-Terminal Tail'. EMBO reports 20(10): e48913. doi:10.15252/embr.201948913.

Ali-Ahmad, Ahmad, and Nikolina Sekulić. 2020. 'CENP-A Nucleosome-a Chromatin-Embedded Pedestal for the Centromere: Lessons Learned from Structural Biology'. Essays in Biochemistry 64(2): 205–21. doi:10.1042/EBC20190074.

Alix-Panabières, C., and K. Pantel. 2021. 'Liquid Biopsy: From Discovery to Clinical Application | Cancer Discovery | American Association for Cancer Research'. In Cancer Discov,

https://aacrjournals.org/cancerdiscovery/article/11/4/858/665896/Liquid-Biopsy-From-Discovery-to-Clinical (September 4, 2024).

Alkan, Can, Maria Francesca Cardone, Claudia Rita Catacchio, Francesca Antonacci, Stephen J. O'Brien, Oliver A. Ryder, Stefania Purgato, et al. 2011. 'Genome-Wide Characterization of Centromeric Satellites from Multiple Mammalian Genomes'. Genome Research 21(1): 137–45. doi:10.1101/gr.111278.110.

Allan, J., P. G. Hartman, C. Crane-Robinson, and F. X. Aviles. 1980. 'The Structure of Histone H1 and Its Location in Chromatin'. Nature 288(5792): 675–79. doi:10.1038/288675a0.

Allfrey, V. G., R. Faulkner, and A. E. Mirsky. 1964. 'ACETYLATION AND METHYLATION OF HISTONES AND THEIR POSSIBLE ROLE IN THE REGULATION OF RNA SYNTHESIS'. Proceedings of the National Academy of Sciences of the United States of America 51(5): 786–94. doi:10.1073/pnas.51.5.786.

Allshire, Robin C., and Hiten D. Madhani. 2018. 'Ten Principles of Heterochromatin Formation and Function'. Nature Reviews. Molecular Cell Biology 19(4): 229–44. doi:10.1038/nrm.2017.119.

Allu, Praveen Kumar, Jennine M. Dawicki-McKenna, Trevor Van Eeuwen, Moriya Slavin, Merav Braitbard, Chen Xu, Nir Kalisman, Kenji Murakami, and Ben E. Black. 2019. 'Structure of the Human Core Centromeric Nucleosome Complex'. Current biology : CB 29(16): 2625-2639.e5. doi:10.1016/j.cub.2019.06.062.

Almouzni, G, D J Clark, M Méchali, and A P Wolffe. 1990. 'Chromatin Assembly on Replicating DNA in Vitro.' Nucleic Acids Research 18(19): 5767–74.

Al-Radhawi, M. Ali, Shubham Tripathi, Yun Zhang, Eduardo D. Sontag, and Herbert Levine. 2022. 'Epigenetic Factor Competition Reshapes the EMT Landscape'. Proceedings of the National Academy of Sciences of the United States of America 119(42): e2210844119. doi:10.1073/pnas.2210844119.

Altemose, N. 2022. 'Complete Genomic and Epigenetic Maps of Human Centromeres | Science'. https://www.science.org/doi/10.1126/science.abl4178 (September 1, 2024).

Amato, Angela, Tiziana Schillaci, Laura Lentini, and Aldo Di Leonardo. 2009. 'CENPA Overexpression Promotes Genome Instability in pRb-Depleted Human Cells'. Molecular Cancer 8: 119. doi:10.1186/1476-4598-8-119.

Ambartsumyan, Gayane, Rajbir K. Gill, Silvia Diaz Perez, Deirdre Conway, John Vincent, Yamini Dalal, and Amander T. Clark. 2010. 'Centromere Protein A Dynamics in Human Pluripotent Stem Cell Self-Renewal, Differentiation and DNA Damage'. Human Molecular Genetics 19(20): 3970–82. doi:10.1093/hmg/ddq312.

Amini, A., S. Masoumi Moghaddam, D. L. Morris, and M. H. Pourgholami. 2012. 'The Critical Role of Vascular Endothelial Growth Factor in Tumor Angiogenesis'. Current Cancer Drug Targets 12(1): 23–43. doi:10.2174/156800912798888956.

Amor, David J., Karen Bentley, Jacinta Ryan, Jo Perry, Lee Wong, Howard Slater, and K. H. Andy Choo. 2004. 'Human Centromere Repositioning "in Progress"'. Proceedings of the National Academy of Sciences of the United States of America 101(17): 6542–47. doi:10.1073/pnas.0308637101.

Amor, David J., and K. H. Andy Choo. 2002. 'Neocentromeres: Role in Human Disease, Evolution, and Centromere Study'. The American Journal of Human Genetics 71(4): 695–714. doi:10.1086/342730.

An, W., K. van Holde, and J. Zlatanova. 1998. 'Linker Histone Protection of Chromatosomes Reconstituted on 5S rDNA from Xenopus Borealis:A Reinvestigation'. Nucleic Acids Research 26(17): 4042–46. doi:10.1093/nar/26.17.4042.

An, W., S. H. Leuba, K. van Holde, and J. Zlatanova. 1998. 'Linker Histone Protects Linker DNA on Only One Side of the Core Particle and in a Sequence-Dependent Manner'. Proceedings of the National Academy of Sciences of the United States of America 95(7): 3396–3401. doi:10.1073/pnas.95.7.3396.

Anczuków, Olga, and Adrian R. Krainer. 2016. 'Splicing-Factor Alterations in Cancers'. RNA (New York, N.Y.) 22(9): 1285–1301. doi:10.1261/rna.057919.116.

Annunziato, A. T., R. K. Schindler, C. A. Thomas, and R. L. Seale. 1981. 'Dual Nature of Newly Replicated Chromatin. Evidence for Nucleosomal and Non-Nucleosomal DNA at the Site of Native Replication Forks.' Journal of Biological Chemistry 256(22): 11880–86. doi:10.1016/S0021-9258(19)68488-7.

Annunziato, Anthony T. 2015. 'The Fork in the Road: Histone Partitioning During DNA Replication'. Genes 6(2): 353–71. doi:10.3390/genes6020353.

Ansieau, S, J Bastid, A Doreau, Ap Morel, Bp Bouchet, C Thomas, F Fauvet, et al. 2008. 'Induction of EMT by Twist Proteins as a Collateral Effect of Tumor-Promoting Inactivation of Premature Senescence'. Cancer cell 14(1). doi:10.1016/j.ccr.2008.06.005.

Anthony, Christin C., David J. Robbins, Yashi Ahmed, and Ethan Lee. 2020. 'Nuclear Regulation of Wnt/β-Catenin Signaling: It's a Complex Situation'. Genes 11(8): 886. doi:10.3390/genes11080886.

Antonin, Wolfram, and Heinz Neumann. 2016. 'Chromosome Condensation and Decondensation during Mitosis'. Current Opinion in Cell Biology 40: 15–22. doi:10.1016/j.ceb.2016.01.013.

Anusewicz, Dorota, Magdalena Orzechowska, and Andrzej K. Bednarek. 2021. 'Notch Signaling Pathway in Cancer—Review with Bioinformatic Analysis'. Cancers 13(4): 768. doi:10.3390/cancers13040768.

Aranda, Sergi, Gloria Mas, and Luciano Di Croce. 2015. ‘Regulation of Gene Transcription by Polycomb Proteins’. Science Advances 1(11): e1500737. doi:10.1126/sciadv.1500737.

Arco, Ana García del, Bruce A. Edgar, and Sylvia Erhardt. 2018. ‘In Vivo Analysis of Centromeric Proteins Reveals a Stem Cell-Specific Asymmetry and an Essential Role in Differentiated, Non-Proliferating Cells’. Cell Reports 22(8): 1982–93. doi:10.1016/j.celrep.2018.01.079.

Arents, G., R. W. Burlingame, B. C. Wang, W. E. Love, and E. N. Moudrianakis. 1991. ‘The Nucleosomal Core Histone Octamer at 3.1 A Resolution: A Tripartite Protein Assembly and a Left-Handed Superhelix’. Proceedings of the National Academy of Sciences of the United States of America 88(22): 10148–52. doi:10.1073/pnas.88.22.10148.

Arents, G., and E. N. Moudrianakis. 1995. ‘The Histone Fold: A Ubiquitous Architectural Motif Utilized in DNA Compaction and Protein Dimerization’. Proceedings of the National Academy of Sciences of the United States of America 92(24): 11170–74. doi:10.1073/pnas.92.24.11170.

Arimura, Yasuhiro, Kazuyoshi Shirayama, Naoki Horikoshi, Risa Fujita, Hiroyuki Taguchi, Wataru Kagawa, Tatsuo Fukagawa, Geneviève Almouzni, and Hitoshi Kurumizaka. 2014. ‘Crystal Structure and Stable Property of the Cancer-Associated Heterotypic Nucleosome Containing CENP-A and H3.3’. Scientific Reports 4(1): 7115. doi:10.1038/srep07115.

Arimura, Yasuhiro, Hiroaki Tachiwana, Hiroki Takagi, Tetsuya Hori, Hiroshi Kimura, Tatsuo Fukagawa, and Hitoshi Kurumizaka. 2019. ‘The CENP-A Centromere Targeting Domain Facilitates H4K20 Monomethylation in the Nucleosome by Structural Polymorphism’. Nature Communications 10: 576. doi:10.1038/s41467-019-08314-x.

Ariyoshi, Mariko, Fumiaki Makino, Reito Watanabe, Reiko Nakagawa, Takayuki Kato, Keiichi Namba, Yasuhiro Arimura, et al. 2021. ‘Cryo-EM Structure of the CENP-A Nucleosome in Complex with Phosphorylated CENP-C’. The EMBO Journal 40(5): e105671. doi:10.15252/embj.2020105671.

Armache, Anja, Shuang Yang, Alexia Martínez de Paz, Lexi E. Robbins, Ceyda Durmaz, Jin Q. Cheong, Arjun Ravishankar, et al. 2020. ‘Histone H3.3 Phosphorylation Amplifies Stimulation-Induced Transcription’. Nature 583(7818): 852–57. doi:10.1038/s41586-020-2533-0.

Armstrong, Andrew J., Matthew S. Marengo, Sebastian Oltean, Gabor Kemeny, Rhonda L. Bitting, James D. Turnbull, Christina I. Herold, et al. 2011. ‘Circulating Tumor Cells from Patients with Advanced Prostate and Breast Cancer Display Both Epithelial and Mesenchymal Markers’. Molecular cancer research: MCR 9(8): 997–1007. doi:10.1158/1541-7786.MCR-10-0490.

Arnold, Sebastian J., Ulf K. Hofmann, Elizabeth K. Bikoff, and Elizabeth J. Robertson. 2008. ‘Pivotal Roles for Eomesodermin during Axis Formation, Epithelium-to-Mesenchyme Transition and Endoderm Specification in the Mouse’. Development (Cambridge, England) 135(3): 501–11. doi:10.1242/dev.014357.

Arnould, Coline, Vincent Rocher, Florian Saur, Aldo S. Bader, Fernando Muzzopappa, Sarah Collins, Emma Lesage, et al. 2023. 'Chromatin Compartmentalization Regulates the Response to DNA Damage'. Nature 623(7985): 183–92. doi:10.1038/s41586-023-06635-y.

Arnoux, Valerie, Christophe Côme, Donna F. Kusewitt, Laurie G. Hudson, and Pierre Savagner. 2007. 'Cutaneous Wound Reepithelialization | Request PDF'. In Rise and Fall of Epithelial Phenotype: Concepts of Epithelial-Mesenchymal Transition, Eurekah.com and Kluwer Academic/Plenum Publishers. www.researchgate.net/publication/227035315_Cutaneous_Wound_Reepithelialization (September 3, 2024).

Arnoux, Valerie, Mayssaa Nassour, Annie L'Helgoualc'h, Robert A. Hipskind, and Pierre Savagner. 2008. 'Erk5 Controls Slug Expression and Keratinocyte Activation during Wound Healing'. Molecular Biology of the Cell 19(11): 4738–49. doi:10.1091/mbc.e07-10-1078.

Arwert, Esther N., Esther Hoste, and Fiona M. Watt. 2012. 'Epithelial Stem Cells, Wound Healing and Cancer'. Nature Reviews. Cancer 12(3): 170–80. doi:10.1038/nrc3217.

Asgarova, A., K. Asgarov, Y. Godet, P. Peixoto, A. Nadaradjane, M. Boyer-Guittaut, J. Galaine, et al. 2018. 'PD-L1 Expression Is Regulated by Both DNA Methylation and NF-kB during EMT Signaling in Non-Small Cell Lung Carcinoma'. Oncoimmunology 7(5): e1423170. doi:10.1080/2162402X.2017.1423170.

Athwal, Rajbir K., Marcin P. Walkiewicz, Songjoon Baek, Song Fu, Minh Bui, Jordi Camps, Thomas Ried, Myong-Hee Sung, and Yamini Dalal. 2015. 'CENP-A Nucleosomes Localize to Transcription Factor Hotspots and Subtelomeric Sites in Human Cancer Cells'. Epigenetics & Chromatin 8. doi:10.1186/1756-8935-8-2.

Attali, Ilan, Michael R. Botchan, and James M. Berger. 2021. 'Structural Mechanisms for Replicating DNA in Eukaryotes'. Annual Review of Biochemistry 90: 77–106. doi:10.1146/annurev-biochem-090120-125407.

Au, Wei-Chun, Tianyi Zhang, Prashant K. Mishra, Jessica R. Eisenstatt, Robert L. Walker, Josefina Ocampo, Anthony Dawson, et al. 2020. 'Skp, Cullin, F-Box (SCF)-Met30 and SCF-Cdc4-Mediated Proteolysis of CENP-A Prevents Mislocalization of CENP-A for Chromosomal Stability in Budding Yeast'. PLoS genetics 16(2): e1008597. doi:10.1371/journal.pgen.1008597.

Avery, O. T., Macleod, C. M., and McCarty, M. 1944. Studies on the chemical nature of the substance inducing transformation of pneumococcal types : induction of transformation by a desoxyribonucleic acid fraction isolated from pneumococcus type III. The Journal of experimental medicine, 79(2), 137–158. Doi:10.1084/jem.79.2.137.

Bahri, Sami, Simon Wang, Ryan Conder, Juliana Choy, Stephanie Vlachos, Kevin Dong, Carlos Merino, et al. 2010. 'The Leading Edge during Dorsal Closure as a Model for Epithelial Plasticity: Pak

Is Required for Recruitment of the Scribble Complex and Septate Junction Formation'. Development (Cambridge, England) 137(12): 2023–32. doi:10.1242/dev.045088.

Balachandra, Vinutha, Roshan L Shrestha, Colin M Hammond, Shinjen Lin, Ivo A Hendriks, Subhash Chandra Sethi, Lu Chen, et al. 2024. 'DNAJC9 Prevents CENP-A Mislocalization and Chromosomal Instability by Maintaining the Fidelity of Histone Supply Chains'. The EMBO Journal 43(11): 2166–97. doi:10.1038/s44318-024-00093-6.

Ballaré, Cecilia, Giancarlo Castellano, Laura Gaveglia, Sonja Althammer, Juan González-Vallinas, Eduardo Eyras, Francois Le Dily, et al. 2013. 'Nucleosome-Driven Transcription Factor Binding and Gene Regulation'. Molecular Cell 49(1): 67–79. doi:10.1016/j.molcel.2012.10.019.

Balzano, Elisa, and Simona Giunta. 2020. 'Centromeres under Pressure: Evolutionary Innovation in Conflict with Conserved Function'. Genes 11(8): 912. doi:10.3390/genes11080912.

Banaszynski, Laura A., Duancheng Wen, Scott Dewell, Sarah J. Whitcomb, Mingyan Lin, Nichole Diaz, Simon J. Elsässer, et al. 2013. 'Hira-Dependent Histone H3.3 Deposition Facilitates PRC2 Recruitment at Developmental Loci in ES Cells'. Cell 155(1): 107–20. doi:10.1016/j.cell.2013.08.061.

Bantignies, Frédéric, Virginie Roure, Itys Comet, Benjamin Leblanc, Bernd Schuettengruber, Jérôme Bonnet, Vanessa Tixier, André Mas, and Giacomo Cavalli. 2011. 'Polycomb-Dependent Regulatory Contacts between Distant Hox Loci in Drosophila'. Cell 144(2): 214–26. doi:10.1016/j.cell.2010.12.026.

Bao, Yi-Ni, Qiao Yang, Xin-Lei Shen, Wen-Kai Yu, Li Zhou, Qing-Ru Zhu, Qi-Yuan Shan, Zhi-Chao Wang, and Gang Cao. 2024. 'Targeting Tumor Suppressor P53 for Organ Fibrosis Therapy'. Cell Death & Disease 15(5): 1–11. doi:10.1038/s41419-024-06702-w.

Barnes, G. L., P. G. Alexander, C. W. Hsu, B. D. Mariani, and R. S. Tuan. 1997. 'Cloning and Characterization of Chicken Paraxis: A Regulator of Paraxial Mesoderm Development and Somite Formation'. Developmental Biology 189(1): 95–111. doi:10.1006/dbio.1997.8663.

Barnhart, Meghan C., P. Henning J. L. Kuich, Madison E. Stellfox, Jared A. Ward, Emily A. Bassett, Ben E. Black, and Daniel R. Foltz. 2011. 'HJURP Is a CENP-A Chromatin Assembly Factor Sufficient to Form a Functional de Novo Kinetochore'. The Journal of Cell Biology 194(2): 229–43. doi:10.1083/jcb.201012017.

Barra, V., and D. Fachinetti. 2018. 'The Dark Side of Centromeres: Types, Causes and Consequences of Structural Abnormalities Implicating Centromeric DNA'. Nature Communications 9(1): 4340. doi:10.1038/s41467-018-06545-y.

Barriga, Elias H., Patrick H. Maxwell, Ariel E. Reyes, and Roberto Mayor. 2013. 'The Hypoxia Factor Hif-1α Controls Neural Crest Chemotaxis and Epithelial to Mesenchymal Transition'. The Journal of Cell Biology 201(5): 759–76. doi:10.1083/jcb.201212100.

Barry, Elizabeth R., and Stephen D. Bell. 2006. 'DNA Replication in the Archaea'. Microbiology and molecular biology reviews: MMBR 70(4): 876–87. doi:10.1128/MMBR.00029-06.

Barski, Artem, Suresh Cuddapah, Kairong Cui, Tae-Young Roh, Dustin E. Schones, Zhibin Wang, Gang Wei, Iouri Chepelev, and Keji Zhao. 2007. 'High-Resolution Profiling of Histone Methylations in the Human Genome'. Cell 129(4): 823–37. doi:10.1016/j.cell.2007.05.009.

Bartel, David P. 2004. 'MicroRNAs: Genomics, Biogenesis, Mechanism, and Function'. Cell 116(2): 281–97. doi:10.1016/s0092-8674(04)00045-5.

Bartke, Till, Michiel Vermeulen, Blerta Xhemalce, Samuel C. Robson, Matthias Mann, and Tony Kouzarides. 2010. 'Nucleosome-Interacting Proteins Regulated by DNA and Histone Methylation'. Cell 143(3): 470–84. doi:10.1016/j.cell.2010.10.012.

Bassat, Elad, and Elly M. Tanaka. 2021. 'The Cellular and Signaling Dynamics of Salamander Limb Regeneration'. Current Opinion in Cell Biology 73: 117–23. doi:10.1016/j.ceb.2021.07.010.

Bassett, Emily A., Jamie DeNizio, Meghan C. Barnhart-Dailey, Tanya Panchenko, Nikolina Sekulic, Danielle J. Rogers, Daniel R. Foltz, and Ben E. Black. 2012a. 'HJURP Uses Distinct CENP-A Surfaces to Recognize and to Stabilize CENP-A/Histone H4 for Centromere Assembly'. Developmental Cell 22(4): 749–62. doi:10.1016/j.devcel.2012.02.001.

Batlle, E., E. Sancho, C. Francí, D. Domínguez, M. Monfar, J. Baulida, and A. García De Herreros. 2000. 'The Transcription Factor Snail Is a Repressor of E-Cadherin Gene Expression in Epithelial Tumour Cells'. Nature Cell Biology 2(2): 84–89. doi:10.1038/35000034.

Battula, Venkata Lokesh, Kurt William Evans, Brett George Hollier, Yuexi Shi, Frank C. Marini, Ayyakkannu Ayyanan, Rui-Yu Wang, et al. 2010. 'Epithelial-Mesenchymal Transition-Derived Cells Exhibit Multilineage Differentiation Potential Similar to Mesenchymal Stem Cells'. Stem Cells (Dayton, Ohio) 28(8): 1435–45. doi:10.1002/stem.467.

Bauman, J. G., J. Wiegant, P. Borst, and P. van Duijn. 1980. 'A New Method for Fluorescence Microscopical Localization of Specific DNA Sequences by in Situ Hybridization of Fluorochromelabelled RNA'. Experimental Cell Research 128(2): 485–90. doi:10.1016/0014-4827(80)90087-7.

Bebee, Thomas W, Juw Won Park, Katherine I Sheridan, Claude C Warzecha, Benjamin W Cieply, Alex M Rohacek, Yi Xing, and Russ P Carstens. 2015. 'The Splicing Regulators Esrp1 and Esrp2 Direct an Epithelial Splicing Program Essential for Mammalian Development' ed. James L Manley. eLife 4: e08954. doi:10.7554/eLife.08954.

Becker, Peter B., and Jerry L. Workman. 2013. 'Nucleosome Remodeling and Epigenetics'. Cold Spring Harbor Perspectives in Biology 5(9): a017905. doi:10.1101/cshperspect.a017905.

Bedi, Upasana, Vivek Kumar Mishra, David Wasilewski, Christina Scheel, and Steven A. Johnsen. 2014. 'Epigenetic Plasticity: A Central Regulator of Epithelial-to-Mesenchymal Transition in Cancer'. Oncotarget 5(8): 2016–29. doi:10.18632/oncotarget.1875.

Beerling, Evelyne, Daniëlle Seinstra, Elzo de Wit, Lennart Kester, Daphne van der Velden, Carrie Maynard, Ronny Schäfer, et al. 2016. 'Plasticity between Epithelial and Mesenchymal States Unlinks EMT from Metastasis-Enhancing Stem Cell Capacity'. Cell Reports 14(10): 2281–88. doi:10.1016/j.celrep.2016.02.034.

Behjati, Sam, Patrick S. Tarpey, Nadège Presneau, Susanne Scheipl, Nischalan Pillay, Peter Van Loo, David C. Wedge, et al. 2013. 'Distinct H3F3A and H3F3B Driver Mutations Define Chondroblastoma and Giant Cell Tumor of Bone'. Nature Genetics 45(12): 1479–82. doi:10.1038/ng.2814.

Behnan, Jinan, Zanina Grieg, Mrinal Joel, Ingunn Ramsness, and Biljana Stangeland. 2016. 'Gene Knockdown of CENPA Reduces Sphere Forming Ability and Stemness of Glioblastoma Initiating Cells'. Neuroepigenetics 7: 6–18. doi:10.1016/j.nepig.2016.08.002.

Bellelli, Roberto, Ondrej Belan, Valerie E. Pye, Camille Clement, Sarah L. Maslen, J. Mark Skehel, Peter Cherepanov, Genevieve Almouzni, and Simon J. Boulton. 2018. 'POLE3-POLE4 Is a Histone H3-H4 Chaperone That Maintains Chromatin Integrity during DNA Replication'. Molecular Cell 72(1): 112-126.e5. doi:10.1016/j.molcel.2018.08.043.

Bender, Sebastian, Yujie Tang, Anders M. Lindroth, Volker Hovestadt, David T. W. Jones, Marcel Kool, Marc Zapatka, et al. 2013. 'Reduced H3K27me3 and DNA Hypomethylation Are Major Drivers of Gene Expression in K27M Mutant Pediatric High-Grade Gliomas'. Cancer Cell 24(5): 660–72. doi:10.1016/j.ccr.2013.10.006.

Bennett, D. C., L. A. Peachey, H. Durbin, and P. S. Rudland. 1978. 'A Possible Mammary Stem Cell Line'. Cell 15(1): 283–98. doi:10.1016/0092-8674(78)90104-6.

Bentley, David L. 2014. 'Coupling mRNA Processing with Transcription in Time and Space'. Nature Reviews. Genetics 15(3): 163–75. doi:10.1038/nrg3662.

Bergen, Volker, Marius Lange, Stefan Peidli, F. Alexander Wolf, and Fabian J. Theis. 2020. 'Generalizing RNA Velocity to Transient Cell States through Dynamical Modeling'. Nature Biotechnology 38(12): 1408–14. doi:10.1038/s41587-020-0591-3.

Bergmann, Jan H., Mariluz Gómez Rodríguez, Nuno M. C. Martins, Hiroshi Kimura, David A. Kelly, Hiroshi Masumoto, Vladimir Larionov, Lars E. T. Jansen, and William C. Earnshaw. 2011. 'Epigenetic Engineering Shows H3K4me2 Is Required for HJURP Targeting and CENP-A Assembly on a Synthetic Human Kinetochore'. The EMBO journal 30(2): 328–40. doi:10.1038/emboj.2010.329.

Bernstein, Bradley E., Michael Kamal, Kerstin Lindblad-Toh, Stefan Bekiranov, Dione K. Bailey, Dana J. Huebert, Scott McMahon, et al. 2005. 'Genomic Maps and Comparative Analysis of Histone Modifications in Human and Mouse'. Cell 120(2): 169–81. doi:10.1016/j.cell.2005.01.001.

Bernstein, Bradley E., Tarjei S. Mikkelsen, Xiaohui Xie, Michael Kamal, Dana J. Huebert, James Cuff, Ben Fry, et al. 2006. 'A Bivalent Chromatin Structure Marks Key Developmental Genes in Embryonic Stem Cells'. Cell 125(2): 315–26. doi:10.1016/j.cell.2006.02.041.

Bertocchini, Federica, and Claudio D. Stern. 2002. 'The Hypoblast of the Chick Embryo Positions the Primitive Streak by Antagonizing Nodal Signaling'. Developmental Cell 3(5): 735–44. doi:10.1016/s1534-5807(02)00318-0.

Bessette, Darrell C., Erik Tilch, Tatjana Seidens, Michael C. J. Quinn, Adrian P. Wiegmans, Wei Shi, Sibylle Cocciardi, et al. 2015. 'Using the MCF10A/MCF10CA1a Breast Cancer Progression Cell Line Model to Investigate the Effect of Active, Mutant Forms of EGFR in Breast Cancer Development and Treatment Using Gefitinib'. PLoS ONE 10(5): e0125232. doi:10.1371/journal.pone.0125232.

Bieging, Kathryn T., Stephano Spano Mello, and Laura D. Attardi. 2014. 'Unravelling Mechanisms of P53-Mediated Tumour Suppression'. Nature Reviews. Cancer 14(5): 359–70. doi:10.1038/nrc3711.

Birchmeier, C., W. Birchmeier, and B. Brand-Saberi. 1996. 'Epithelial-Mesenchymal Transitions in Cancer Progression'. Acta Anatomica 156(3): 217–26. doi:10.1159/000147848.

Bird, A. P. 1986. 'CpG-Rich Islands and the Function of DNA Methylation'. Nature 321(6067): 209–13. doi:10.1038/321209a0.

Bird, A., M. Taggart, M. Frommer, O. J. Miller, and D. Macleod. 1985. 'A Fraction of the Mouse Genome That Is Derived from Islands of Nonmethylated, CpG-Rich DNA'. Cell 40(1): 91–99. doi:10.1016/0092-8674(85)90312-5.

Bird, Adrian. 2007. 'Perceptions of Epigenetics'. Nature 447(7143): 396–98. doi:10.1038/nature05913.

Bjerke, Lynn, Alan Mackay, Meera Nandhabalan, Anna Burford, Alexa Jury, Sergey Popov, Dorine A. Bax, et al. 2013. 'Histone H3.3. Mutations Drive Pediatric Glioblastoma through Upregulation of MYCN'. Cancer Discovery 3(5): 512–19. doi:10.1158/2159-8290.CD-12-0426.

Black, Douglas L. 2003. 'Mechanisms of Alternative Pre-Messenger RNA Splicing'. Annual Review of Biochemistry 72: 291–336. doi:10.1146/annurev.biochem.72.121801.161720.

Blanco, María J., Alejandro Barrallo-Gimeno, Hervé Acloque, Ariel E. Reyes, Masazumi Tada, Miguel L. Allende, Roberto Mayor, and M. Angela Nieto. 2007. 'Snail1a and Snail1b Cooperate in the Anterior Migration of the Axial Mesendoderm in the Zebrafish Embryo'. Development (Cambridge, England) 134(22): 4073–81. doi:10.1242/dev.006858.

Blandino, Giovanni, and Silvia Di Agostino. 2018. 'New Therapeutic Strategies to Treat Human Cancers Expressing Mutant P53 Proteins'. Journal of Experimental & Clinical Cancer Research : CR 37: 30. doi:10.1186/s13046-018-0705-7.

Block, C. James, Allison V. Mitchell, Ling Wu, James Glassbrook, Douglas Craig, Wei Chen, Gregory Dyson, et al. 2021. 'RNA Binding Protein RBMS3 Is a Common EMT Effector That Modulates Triple-Negative Breast Cancer Progression via Stabilizing PRRX1 mRNA'. Oncogene 40(46): 6430–42. doi:10.1038/s41388-021-02030-x.

Blokzijl, Andries, Camilla Dahlqvist, Eva Reissmann, Anna Falk, Annalena Moliner, Urban Lendahl, and Carlos F. Ibáñez. 2003. 'Cross-Talk between the Notch and TGF-Beta Signaling Pathways Mediated by Interaction of the Notch Intracellular Domain with Smad3'. The Journal of Cell Biology 163(4): 723–28. doi:10.1083/jcb.200305112.

Blower, Michael D., Beth A. Sullivan, and Gary H. Karpen. 2002. 'Conserved Organization of Centromeric Chromatin in Flies and Humans'. Developmental Cell 2(3): 319–30. doi:10.1016/s1534-5807(02)00135-1.

Bobkov, Georg O. M., Nick Gilbert, and Patrick Heun. 2018. 'Centromere Transcription Allows CENP-A to Transit from Chromatin Association to Stable Incorporation'. Journal of Cell Biology 217(6): 1957–72. doi:10.1083/jcb.201611087.

Böcker, W., and H. E. Stegner. 1975. 'A Light and Electron Microscopic Study of Endometrial Sarcomas of the Uterus'. Virchows Archiv. A, Pathological Anatomy and Histology 368(2): 141–56. doi:10.1007/BF00432414.

Bodor, Dani L, João F Mata, Mikhail Sergeev, Ana Filipa David, Kevan J Salimian, Tanya Panchenko, Don W Cleveland, et al. 2014. 'The Quantitative Architecture of Centromeric Chromatin'. eLife 3. doi:10.7554/eLife.02137.

Bodor, Dani L., Luis P. Valente, João F. Mata, Ben E. Black, and Lars E. T. Jansen. 2013. 'Assembly in G1 Phase and Long-Term Stability Are Unique Intrinsic Features of CENP-A Nucleosomes'. Molecular Biology of the Cell 24(7): 923–32. doi:10.1091/mbc.E13-01-0034.

Boettiger, Alistair, and Sedona Murphy. 2020. 'Advances in Chromatin Imaging at Kilobase-Scale Resolution'. Trends in genetics: TIG 36(4): 273–87. doi:10.1016/j.tig.2019.12.010.

Bolduc. 2021. Préformation et épigenèse en développement. Naissance de l'embryologie expérimentale, Presses de l'Université de Montréal, 50(2) : 9–27.

Bolzer, Andreas, Gregor Kreth, Irina Solovei, Daniela Koehler, Kaan Saracoglu, Christine Fauth, Stefan Müller, et al. 2005. 'Three-Dimensional Maps of All Chromosomes in Human Male Fibroblast Nuclei and Prometaphase Rosettes'. PLoS biology 3(5): e157. doi:10.1371/journal.pbio.0030157.

Bonde, Anne-Katrine, Verena Tischler, Sushil Kumar, Alex Soltermann, and Reto A. Schwendener. 2012. 'Intratumoral Macrophages Contribute to Epithelial-Mesenchymal Transition in Solid Tumors'. BMC cancer 12: 35. doi:10.1186/1471-2407-12-35.

Bonev, Boyan, and Giacomo Cavalli. 2016. 'Organization and Function of the 3D Genome'. Nature Reviews. Genetics 17(11): 661–78. doi:10.1038/nrg.2016.112.

Boopathi, Ramachandran, Radostin Danev, Maryam Khoshouei, Seyit Kale, Sunil Nahata, Lorrie Ramos, Dimitar Angelov, et al. 2020. 'Phase-Plate Cryo-EM Structure of the Widom 601 CENP-A Nucleosome Core Particle Reveals Differential Flexibility of the DNA Ends'. Nucleic Acids Research 48(10): 5735–48. doi:10.1093/nar/gkaa246.

Borges, Fernanda, Sonia Melo, Berna Özdemir, Noritoshi Kato, Ignacio Revuelta, Caroline Miller, Vincent Gattone, Valerie LeBleu, and Raghu Kalluri. 2013. 'TGF-B1-Containing Exosomes from Injured Epithelial Cells Activate Fibroblasts to Initiate Tissue Regenerative Responses and Fibrosis'. Journal of the American Society of Nephrology : JASN 24(3). doi:10.1681/ASN.2012101031.

Boutet, Agnès, Cristina A. De Frutos, Patrick H. Maxwell, M. José Mayol, J. Romero, and M. Angela Nieto. 2006. 'Snail Activation Disrupts Tissue Homeostasis and Induces Fibrosis in the Adult Kidney'. The EMBO journal 25(23): 5603–13. doi:10.1038/sj.emboj.7601421.

Boveri, Theodor. 1902. 'Über mehrpolige Mitosen als Mittel zur Analyse des Zellkerns'. Verhandlungen der Physikalisch-Medizinischen Gesellschaft zu Würzburg 35: 67–90.

Bowman, Gregory D., and Michael G. Poirier. 2015. 'Post-Translational Modifications of Histones That Influence Nucleosome Dynamics'. Chemical Reviews 115(6): 2274–95. doi:10.1021/cr500350x.

Boyes, J., and A. Bird. 1991. 'DNA Methylation Inhibits Transcription Indirectly via a Methyl-CpG Binding Protein'. Cell 64(6): 1123–34. doi:10.1016/0092-8674(91)90267-3.

Boyes, J., and A. Bird. 1992. 'Repression of Genes by DNA Methylation Depends on CpG Density and Promoter Strength: Evidence for Involvement of a Methyl-CpG Binding Protein'. The EMBO journal 11(1): 327–33. doi:10.1002/j.1460-2075.1992.tb05055.x.

Boyle, S., S. Gilchrist, J. M. Bridger, N. L. Mahy, J. A. Ellis, and W. A. Bickmore. 2001. 'The Spatial Organization of Human Chromosomes within the Nuclei of Normal and Emerin-Mutant Cells'. Human Molecular Genetics 10(3): 211–19. doi:10.1093/hmg/10.3.211.

Brabletz, Jung, Reu, Porzner, Hlubek, Kunz-Schughart, Knuechel, and Kirchner. 2001. 'Variable Beta-Catenin Expression in Colorectal Cancers Indicates Tumor Progression Driven by the Tumor Environment'. Proceedings of the National Academy of Sciences of the United States of America 98(18). doi:10.1073/pnas.171610498.

Brabletz, Simone, and Thomas Brabletz. 2010. 'The ZEB/miR-200 Feedback Loop—a Motor of Cellular Plasticity in Development and Cancer?' EMBO Reports 11(9): 670–77. doi:10.1038/embor.2010.117.

Bracken, Cameron P., Philip A. Gregory, Natasha Kolesnikoff, Andrew G. Bert, Jun Wang, M. Frances Shannon, and Gregory J. Goodall. 2008. 'A Double-Negative Feedback Loop between ZEB1-SIP1 and the microRNA-200 Family Regulates Epithelial-Mesenchymal Transition'. Cancer Research 68(19): 7846–54. doi:10.1158/0008-5472.CAN-08-1942.

Branco, Miguel R., and Ana Pombo. 2006. 'Intermingling of Chromosome Territories in Interphase Suggests Role in Translocations and Transcription-Dependent Associations'. PLoS biology 4(5): e138. doi:10.1371/journal.pbio.0040138.

Branzei, Dana, and Marco Foiani. 2010. 'Maintaining Genome Stability at the Replication Fork'. Nature Reviews. Molecular Cell Biology 11(3): 208–19. doi:10.1038/nrm2852.

Brembeck, Felix H., Marta Rosário, and Walter Birchmeier. 2006. 'Balancing Cell Adhesion and Wnt Signaling, the Key Role of Beta-Catenin'. Current Opinion in Genetics & Development 16(1): 51–59. doi:10.1016/j.gde.2005.12.007.

Briede, Inese, Dainis Balodis, Janis Gardovskis, and Ilze Strumfa. 2021. 'Stemness, Inflammation and Epithelial–Mesenchymal Transition in Colorectal Carcinoma: The Intricate Network'. International Journal of Molecular Sciences 22(23). doi:10.3390/ijms222312891.

Bronner, Marianne E. 2012. 'Formation and Migration of Neural Crest Cells in the Vertebrate Embryo'. Histochemistry and cell biology 138(2): 179–86. doi:10.1007/s00418-012-0999-z.

Bronner-Fraser, M., and S. E. Fraser. 1988. 'Cell Lineage Analysis Reveals Multipotency of Some Avian Neural Crest Cells'. Nature 335(6186): 161–64. doi:10.1038/335161a0.

Bronsert, P, K Enderle-Ammour, M Bader, S Timme, M Kuehs, A Csanadi, G Kayser, et al. 2014. 'Cancer Cell Invasion and EMT Marker Expression: A Three-Dimensional Study of the Human Cancer–Host Interface'. The Journal of Pathology 234(3): 410–22. doi:10.1002/path.4416.

Brown. 1833. Observations on the Organs and Mode of Fecundation in *Orchideae* and *Asclepiadeae*. https://books.google.fr/books?hl=fr&lr=&id=iABLAAAAYAAJ&oi=fnd&pg=PA683&ots=w5YLjU7uR-&sig=CQa1jjqADCb0mSXyAm8xF6OWUIM&redir_esc=y#v=onepage&q&f=false (August 25, 2024).

Brown, Meredith S., Behnaz Abdollahi, Owen M. Wilkins, Hanxu Lu, Priyanka Chakraborty, Nevena B. Ognjenovic, Kristen E. Muller, et al. 2022. 'Phenotypic Heterogeneity Driven by Plasticity of the Intermediate EMT State Governs Disease Progression and Metastasis in Breast Cancer'. Science Advances 8(31): eabj8002. doi:10.1126/sciadv.abj8002.

Brown, Rhonda L., Lauren M. Reinke, Marin S. Damerow, Denise Perez, Lewis A. Chodosh, Jing Yang, and Chonghui Cheng. 2011. 'CD44 Splice Isoform Switching in Human and Mouse Epithelium Is Essential for Epithelial-Mesenchymal Transition and Breast Cancer Progression'. The Journal of Clinical Investigation 121(3): 1064–74. doi:10.1172/JCI44540.

Buitrago, Diana, Mireia Labrador, Juan Pablo Arcon, Rafael Lema, Oscar Flores, Anna Esteve-Codina, Julie Blanc, et al. 2021. 'Impact of DNA Methylation on 3D Genome Structure'. Nature Communications 12(1): 3243. doi:10.1038/s41467-021-23142-8.

Burgers, Peter M. J., and Thomas A. Kunkel. 2017. 'Eukaryotic DNA Replication Fork'. Annual Review of Biochemistry 86: 417–38. doi:10.1146/annurev-biochem-061516-044709.

Burgess, Rebecca J., and Zhiguo Zhang. 2013. 'Histone Chaperones in Nucleosome Assembly and Human Disease'. Nature Structural & Molecular Biology 20(1): 14–22. doi:10.1038/nsmb.2461.

Burk, Ulrike, Jörg Schubert, Ulrich Wellner, Otto Schmalhofer, Elizabeth Vincan, Simone Spaderna, and Thomas Brabletz. 2008. 'A Reciprocal Repression between ZEB1 and Members of the miR-200 Family Promotes EMT and Invasion in Cancer Cells'. EMBO reports 9(6): 582–89. doi:10.1038/embor.2008.74.

Burtscher, Ingo, Wenke Barkey, and Heiko Lickert. 2013. 'Foxa2-Venus Fusion Reporter Mouse Line Allows Live-Cell Analysis of Endoderm-Derived Organ Formation'. Genesis (New York, N.Y.: 2000) 51(8): 596–604. doi:10.1002/dvg.22404.

Burtscher, Ingo, and Heiko Lickert. 2009. 'Foxa2 Regulates Polarity and Epithelialization in the Endoderm Germ Layer of the Mouse Embryo'. Development (Cambridge, England) 136(6): 1029–38. doi:10.1242/dev.028415.

Bury, Leah, Brittania Moodie, Jimmy Ly, Liliana S. McKay, Karen Hh Miga, and Iain M. Cheeseman. 2020. 'Alpha-Satellite RNA Transcripts Are Repressed by Centromere-Nucleolus Associations'. eLife 9: e59770. doi:10.7554/eLife.59770.

Buschbeck, Marcus, and Sandra B. Hake. 2017. 'Variants of Core Histones and Their Roles in Cell Fate Decisions, Development and Cancer'. Nature Reviews. Molecular Cell Biology 18(5): 299–314. doi:10.1038/nrm.2016.166.

Bykov, Vladimir J. N., Sofi E. Eriksson, Julie Bianchi, and Klas G. Wiman. 2018. 'Targeting Mutant P53 for Efficient Cancer Therapy'. Nature Reviews Cancer 18(2): 89–102. doi:10.1038/nrc.2017.109.

Cairns, J. 1966. 'Autoradiography of HeLa Cell DNA'. Journal of Molecular Biology 15(1): 372–73. doi:10.1016/s0022-2836(66)80233-4.

Cajal, R. 1903. 'Cajal: Un Sencillo Metodo de Coloracione Del Reticulo... - Google Scholar'. https://scholar.google.com/scholar_lookup?hl=en&volume=2&publication_year=1903&pages=129-221&journal=Trab.+Lab.+Invest.+Biol.+%28Madrid%29&author=S.+Cajal&title=Un+sencillo+meto

do+de+coloracion+seletiva+del+reticulo+protoplasmatico+y+sus+efectos+en+los+diversos+organos+nerviosos+de+vertebrados+e+invertebrados. (September 6, 2024).

Camahort, Raymond, Manjunatha Shivaraju, Mark Mattingly, Bing Li, Shima Nakanishi, Dongxiao Zhu, Ali Shilatifard, Jerry L. Workman, and Jennifer L. Gerton. 2009. 'Cse4 Is Part of an Octameric Nucleosome in Budding Yeast'. Molecular Cell 35(6): 794–805. doi:10.1016/j.molcel.2009.07.022.

Campbell, Kyra, and Jordi Casanova. 2015. 'A Role for E-Cadherin in Ensuring Cohesive Migration of a Heterogeneous Population of Non-Epithelial Cells'. Nature Communications 6: 7998. doi:10.1038/ncomms8998.

Cano, A., M. A. Pérez-Moreno, I. Rodrigo, A. Locascio, M. J. Blanco, M. G. del Barrio, F. Portillo, and M. A. Nieto. 2000. 'The Transcription Factor Snail Controls Epithelial-Mesenchymal Transitions by Repressing E-Cadherin Expression'. Nature Cell Biology 2(2): 76–83. doi:10.1038/35000025.

Cappelletti, Eleonora, Francesca M. Piras, Lorenzo Sola, Marco Santagostino, Jessica L. Petersen, Rebecca R. Bellone, Carrie J. Finno, et al. 2023. 'The Localization of Centromere Protein A Is Conserved among Tissues'. Communications Biology 6: 963. doi:10.1038/s42003-023-05335-7.

Cardoso, M. C., H. Leonhardt, and B. Nadal-Ginard. 1993. 'Reversal of Terminal Differentiation and Control of DNA Replication: Cyclin A and Cdk2 Specifically Localize at Subnuclear Sites of DNA Replication'. Cell 74(6): 979–92. doi:10.1016/0092-8674(93)90721-2.

Carroll, Christopher W., Kirstin J. Milks, and Aaron F. Straight. 2010. 'Dual Recognition of CENP-A Nucleosomes Is Required for Centromere Assembly'. The Journal of Cell Biology 189(7): 1143–55. doi:10.1083/jcb.201001013.

Carty, Ben L., Anna A. Dattoli, and Elaine M. Dunleavy. 2021. 'CENP-C Functions in Centromere Assembly, the Maintenance of CENP-A Asymmetry and Epigenetic Age in Drosophila Germline Stem Cells'. PLOS Genetics 17(5): e1009247. doi:10.1371/journal.pgen.1009247.

Carty, Ben L., and Elaine M. Dunleavy. 2021. 'Truly Epigenetic: A Centromere Finds a "Neo" Home'. The Journal of Cell Biology 220(3): e202101027. doi:10.1083/jcb.202101027.

Carvalho, Célia, Henrique M. Pereira, João Ferreira, Cristina Pina, Denise Mendonça, Agostinho C. Rosa, and Maria Carmo-Fonseca. 2001. 'Chromosomal G-Dark Bands Determine the Spatial Organization of Centromeric Heterochromatin in the Nucleus'. Molecular Biology of the Cell 12(11): 3563–72.

Carver, E. A., R. Jiang, Y. Lan, K. F. Oram, and T. Gridley. 2001. 'The Mouse Snail Gene Encodes a Key Regulator of the Epithelial-Mesenchymal Transition'. Molecular and Cellular Biology 21(23): 8184–88. doi:10.1128/MCB.21.23.8184-8188.2001.

Cerami, Ethan, Jianjiong Gao, Ugur Dogrusoz, Benjamin E. Gross, Selcuk Onur Sumer, Bülent Arman Aksoy, Anders Jacobsen, et al. 2012. 'The cBio Cancer Genomics Portal: An Open Platform for

Exploring Multidimensional Cancer Genomics Data'. Cancer discovery 2(5): 401–4. doi:10.1158/2159-8290.CD-12-0095.

Chaffer, Christine L., Nemanja D. Marjanovic, Tony Lee, George Bell, Celina G. Kleer, Ferenc Reinhardt, Ana C. D'Alessio, Richard A. Young, and Robert A. Weinberg. 2013. 'Poised Chromatin at the ZEB1 Promoter Enables Breast Cancer Cell Plasticity and Enhances Tumorigenicity'. Cell 154(1): 61–74. doi:10.1016/j.cell.2013.06.005.

Chan, F. Lyn, Owen J. Marshall, Richard Saffery, Bo Won Kim, Elizabeth Earle, K. H. Andy Choo, and Lee H. Wong. 2012. 'Active Transcription and Essential Role of RNA Polymerase II at the Centromere during Mitosis'. Proceedings of the National Academy of Sciences of the United States of America 109(6): 1979–84. doi:10.1073/pnas.1108705109.

Chan, Yun-Shen, Jonathan Göke, Xinyi Lu, Nandini Venkatesan, Bo Feng, I.-Hsin Su, and Huck-Hui Ng. 2013. 'A PRC2-Dependent Repressive Role of PRDM14 in Human Embryonic Stem Cells and Induced Pluripotent Stem Cell Reprogramming'. Stem Cells (Dayton, Ohio) 31(4): 682–92. doi:10.1002/stem.1307.

Chang, Chun-Ju, Chi-Hong Chao, Weiya Xia, Jer-Yen Yang, Yan Xiong, Chia-Wei Li, Wen-Hsuan Yu, et al. 2011. 'P53 Regulates Epithelial-Mesenchymal Transition and Stem Cell Properties through Modulating miRNAs'. Nature Cell Biology 13(3): 317–23. doi:10.1038/ncb2173.

Chapman, G. E., P. G. Hartman, and E. M. Bradbury. 1976. 'Studies on the Role and Mode of Operation of the Very-Lysine-Rich Histone H1 in Eukaryote Chromatin. The Isolation of the Globular and Non-Globular Regions of the Histone H1 Molecule'. European Journal of Biochemistry 61(1): 69–75. doi:10.1111/j.1432-1033.1976.tb09998.x.

Chardon, Florian, Aleksandre Japaridze, Hannes Witt, Leonid Velikovsky, Camellia Chakraborty, Therese Wilhelm, Marie Dumont, et al. 2022. 'CENP-B-Mediated DNA Loops Regulate Activity and Stability of Human Centromeres'. Molecular Cell 82(9): 1751-1767.e8. doi:10.1016/j.molcel.2022.02.032.

Chargaff, E. 1950. 'Chemical Specificity of Nucleic Acids and Mechanism of Their Enzymatic Degradation'. Experientia 6(6): 201–9. doi:10.1007/BF02173653.

Chea, Helen K., Christopher V. Wright, and Billie J. Swalla. 2005. 'Nodal Signaling and the Evolution of Deuterostome Gastrulation'. Developmental Dynamics: An Official Publication of the American Association of Anatomists 234(2): 269–78. doi:10.1002/dvdy.20549.

Chen, Chien-Min, Chu-Liang Lin, Hui-Ling Chiou, Shu-Ching Hsieh, Chia-Liang Lin, Chun-Wen Cheng, Chia-Hung Hung, Jen-Pi Tsai, and Yi-Hsien Hsieh. 2017. 'Loss of Endothelial Cell-Specific Molecule 1 Promotes the Tumorigenicity and Metastasis of Prostate Cancer Cells through Regulation of the TIMP-1/MMP-9 Expression'. Oncotarget 8(8): 13886–97. doi:10.18632/oncotarget.14684.

Chen, Danqi, Qiao Yi Chen, Zhenjia Wang, Yusha Zhu, Thomas Kluz, Wuwei Tan, Jinquan Li, et al. 2020. 'Polyadenylation of Histone H3.1 mRNA Promotes Cell Transformation by Displacing H3.3 from Gene Regulatory Elements'. iScience 23(9): 101518. doi:10.1016/j.isci.2020.101518.

Chen, Limo, Don L. Gibbons, Sangeeta Goswami, Maria Angelica Cortez, Young-Ho Ahn, Lauren A. Byers, Xuejun Zhang, et al. 2014. 'Metastasis Is Regulated via microRNA-200/ZEB1 Axis Control of Tumour Cell PD-L1 Expression and Intratumoral Immunosuppression'. Nature Communications 5: 5241. doi:10.1038/ncomms6241.

Chen, Xi, Gerd A. Müller, Marianne Quaas, Martin Fischer, Namshik Han, Benjamin Stutchbury, Andrew D. Sharrocks, and Kurt Engeland. 2013. 'The Forkhead Transcription Factor FOXM1 Controls Cell Cycle-Dependent Gene Expression through an Atypical Chromatin Binding Mechanism'. Molecular and Cellular Biology 33(2): 227–36. doi:10.1128/MCB.00881-12.

Cheng, Chan, Wang, Zhang, Sun, and Wang. 2007. 'Twist Transcriptionally Up-Regulates AKT2 in Breast Cancer Cells Leading to Increased Migration, Invasion, and Resistance to Paclitaxel'. Cancer research 67(5). doi:10.1158/0008-5472.CAN-06-1479.

Cheng, Haili, Xin Bao, and Hai Rao. 2016. 'The F-Box Protein Rcy1 Is Involved in the Degradation of Histone H3 Variant Cse4 and Genome Maintenance'. The Journal of Biological Chemistry 291(19): 10372–77. doi:10.1074/jbc.M115.701813.

Chibazakura, Taku, Kazuhiro Kamachi, Mayu Ohara, Shoji Tane, Hirofumi Yoshikawa, and James M. Roberts. 2011. 'Cyclin A Promotes S-Phase Entry via Interaction with the Replication Licensing Factor Mcm7'. Molecular and Cellular Biology 31(2): 248–55. doi:10.1128/MCB.00630-10.

Chung, Vin Yee, Tuan Zea Tan, Ming Tan, Meng Kang Wong, Kuee Theng Kuay, Zhe Yang, Jieru Ye, et al. 2016. 'GRHL2-miR-200-ZEB1 Maintains the Epithelial Status of Ovarian Cancer through Transcriptional Regulation and Histone Modification'. Scientific Reports 6: 19943. doi:10.1038/srep19943.

Ciruna, B., and J. Rossant. 2001. 'FGF Signaling Regulates Mesoderm Cell Fate Specification and Morphogenetic Movement at the Primitive Streak'. Developmental Cell 1(1): 37–49. doi:10.1016/s1534-5807(01)00017-x.

Clark, D. J., and T. Kimura. 1990. 'Electrostatic Mechanism of Chromatin Folding'. Journal of Molecular Biology 211(4): 883–96. doi:10.1016/0022-2836(90)90081-V.

Clark, Ivan B. N., Villö Muha, Anna Klingseisen, Maria Leptin, and Hans-Arno J. Müller. 2011. 'Fibroblast Growth Factor Signalling Controls Successive Cell Behaviours during Mesoderm Layer Formation in Drosophila'. Development (Cambridge, England) 138(13): 2705–15. doi:10.1242/dev.060277.

Clarke, L., and J. Carbon. 1980. ‘Isolation of a Yeast Centromere and Construction of Functional Small Circular Chromosomes’. Nature 287(5782): 504–9. doi:10.1038/287504a0.

Clarke, L., and J. Carbon. 1985. ‘The Structure and Function of Yeast Centromeres’. Annual Review of Genetics 19: 29–55. doi:10.1146/annurev.ge.19.120185.000333.

Clément, Camille, Guillermo A. Orsi, Alberto Gatto, Ekaterina Boyarchuk, Audrey Forest, Bassam Hajj, Judith Miné-Hattab, et al. 2018. ‘High-Resolution Visualization of H3 Variants during Replication Reveals Their Controlled Recycling’. Nature Communications 9(1): 3181. doi:10.1038/s41467-018-05697-1.

Cleveland, Don W., Yinghui Mao, and Kevin F. Sullivan. 2003. ‘Centromeres and Kinetochores: From Epigenetics to Mitotic Checkpoint Signaling’. Cell 112(4): 407–21. doi:10.1016/s0092-8674(03)00115-6.

Clevers, Hans. 2006. ‘Wnt/Beta-Catenin Signaling in Development and Disease’. Cell 127(3): 469–80. doi:10.1016/j.cell.2006.10.018.

Cochrane, Dawn R., Nicole S. Spoelstra, Erin N. Howe, Steven K. Nordeen, and Jennifer K. Richer. 2009. ‘MicroRNA-200c Mitigates Invasiveness and Restores Sensitivity to Microtubule-Targeting Chemotherapeutic Agents’. Molecular Cancer Therapeutics 8(5): 1055–66. doi:10.1158/1535-7163.MCT-08-1046.

Collins, Patrick L., Caitlin Purman, Sofia I. Porter, Vincent Nganga, Ankita Saini, Katharina E. Hayer, Greer L. Gurewitz, et al. 2020. ‘DNA Double-Strand Breaks Induce H2Ax Phosphorylation Domains in a Contact-Dependent Manner’. Nature Communications 11(1): 3158. doi:10.1038/s41467-020-16926-x.

Comijn, J., G. Berx, P. Vermassen, K. Verschueren, L. van Grunsven, E. Bruyneel, M. Mareel, D. Huylebroeck, and F. van Roy. 2001. ‘The Two-Handed E Box Binding Zinc Finger Protein SIP1 Downregulates E-Cadherin and Induces Invasion’. Molecular Cell 7(6): 1267–78. doi:10.1016/s1097-2765(01)00260-x.

Conde e Silva, Natalia, Ben E. Black, Andrei Sivolob, Jan Filipski, Don W. Cleveland, and Ariel Prunell. 2007. ‘CENP-A-Containing Nucleosomes: Easier Disassembly versus Exclusive Centromeric Localization’. Journal of Molecular Biology 370(3): 555–73. doi:10.1016/j.jmb.2007.04.064.

Conti, Chiara, Barbara Saccà, John Herrick, Claude Lalou, Yves Pommier, and Aaron Bensimon. 2007. ‘Replication Fork Velocities at Adjacent Replication Origins Are Coordinately Modified during DNA Replication in Human Cells’. Molecular Biology of the Cell 18(8): 3059–67. doi:10.1091/mbc.E06-08-0689.

Contreras, Alejandro, Tracy K. Hale, David L. Stenoien, Jeffrey M. Rosen, Michael A. Mancini, and Rafael E. Herrera. 2003. ‘The Dynamic Mobility of Histone H1 Is Regulated by Cyclin/CDK

Phosphorylation'. Molecular and Cellular Biology 23(23): 8626–36. doi:10.1128/MCB.23.23.8626-8636.2003.

Cook, David P., and Barbara C. Vanderhyden. 2020. 'Context Specificity of the EMT Transcriptional Response'. Nature Communications 11(1): 2142. doi:10.1038/s41467-020-16066-2.

Cooper, Geoffrey M. 2000. 'The Eukaryotic Cell Cycle'. In The Cell: A Molecular Approach. 2nd Edition, Sinauer Associates. https://www.ncbi.nlm.nih.gov/books/NBK9876/ (September 6, 2024).

Cooper, Jennifer L., and Steven Henikoff. 2004. 'Adaptive Evolution of the Histone Fold Domain in Centromeric Histones'. Molecular Biology and Evolution 21(9): 1712–18. doi:10.1093/molbev/msh179.

Cole, . The Collected Letters of Antoni van Leeuwenhoek. Nature 163, 192–193 (1949). https://doi.org/10.1038/163192a0

Corless, Samuel, Saskia Höcker, and Sylvia Erhardt. 2020. 'Centromeric RNA and Its Function at and Beyond Centromeric Chromatin'. Journal of Molecular Biology. doi:10.1016/j.jmb.2020.03.027.

Corpet, Armelle, and Geneviève Almouzni. 2009. 'Making Copies of Chromatin: The Challenge of Nucleosomal Organization and Epigenetic Information'. Trends in Cell Biology 19(1): 29–41. doi:10.1016/j.tcb.2008.10.002.

Correa-Gallegos, Donovan, Dongsheng Jiang, Simon Christ, Pushkar Ramesh, Haifeng Ye, Juliane Wannemacher, Shruthi Kalgudde Gopal, et al. 2019. 'Patch Repair of Deep Wounds by Mobilized Fascia'. Nature 576(7786): 287–92. doi:10.1038/s41586-019-1794-y.

Correa-Gallegos, Donovan, Dongsheng Jiang, and Yuval Rinkevich. 2021. 'Fibroblasts as Confederates of the Immune System'. Immunological Reviews 302(1): 147–62. doi:10.1111/imr.12972.

Cortés-Ciriano, Isidro, Jake June-Koo Lee, Ruibin Xi, Dhawal Jain, Youngsook L. Jung, Lixing Yang, Dmitry Gordenin, et al. 2020. 'Comprehensive Analysis of Chromothripsis in 2,658 Human Cancers Using Whole-Genome Sequencing'. Nature Genetics 52(3): 331–41. doi:10.1038/s41588-019-0576-7.

Cosgrove, Michael S., Jef D. Boeke, and Cynthia Wolberger. 2004. 'Regulated Nucleosome Mobility and the Histone Code'. Nature Structural & Molecular Biology 11(11): 1037–43. doi:10.1038/nsmb851.

Costa, Alessandro, and John F. X. Diffley. 2022. 'The Initiation of Eukaryotic DNA Replication'. Annual Review of Biochemistry 91: 107–31. doi:10.1146/annurev-biochem-072321-110228.

Cousens, L. S., and B. M. Alberts. 1982. 'Accessibility of Newly Synthesized Chromatin to Histone Acetylase'. The Journal of Biological Chemistry 257(7): 3945–49.

Creyghton, Menno P., Albert W. Cheng, G. Grant Welstead, Tristan Kooistra, Bryce W. Carey, Eveline J. Steine, Jacob Hanna, et al. 2010. 'Histone H3K27ac Separates Active from Poised Enhancers and Predicts Developmental State'. Proceedings of the National Academy of Sciences of the United States of America 107(50): 21931–36. doi:10.1073/pnas.1016071107.

Croft, J. A., J. M. Bridger, S. Boyle, P. Perry, P. Teague, and W. A. Bickmore. 1999. 'Differences in the Localization and Morphology of Chromosomes in the Human Nucleus'. The Journal of Cell Biology 145(6): 1119–31. doi:10.1083/jcb.145.6.1119.

Crosby, Lynn M., and Christopher M. Waters. 2010. 'Epithelial Repair Mechanisms in the Lung'. American journal of physiology. Lung cellular and molecular physiology 298(6). doi:10.1152/ajplung.00361.2009.

Cui, W., D. J. Fowlis, S. Bryson, E. Duffie, H. Ireland, A. Balmain, and R. J. Akhurst. 1996. 'TGFbeta1 Inhibits the Formation of Benign Skin Tumors, but Enhances Progression to Invasive Spindle Carcinomas in Transgenic Mice'. Cell 86(4): 531–42. doi:10.1016/s0092-8674(00)80127-0.

Cvetic, Christin, and Johannes C. Walter. 2005. 'Eukaryotic Origins of DNA Replication: Could You Please Be More Specific?' Seminars in Cell & Developmental Biology 16(3): 343–53. doi:10.1016/j.semcdb.2005.02.009.

Dambacher, Silvia, Wen Deng, Matthias Hahn, Dennis Sadic, Jonathan Fröhlich, Alexander Nuber, Christian Hoischen, et al. 2012. 'CENP-C Facilitates the Recruitment of M18BP1 to Centromeric Chromatin'. Nucleus 3(1): 101–10. doi:10.4161/nucl.18955.

Darlington, Cyril D. 1936. 'The External Mechanics of the Chromosomes I—The Scope of Enquiry'. Proceedings of the Royal Society of London. Series B - Biological Sciences. doi:10.1098/rspb.1936.0064.

Darnell, J. E. 1997. 'STATs and Gene Regulation'. Science (New York, N.Y.) 277(5332): 1630–35. doi:10.1126/science.277.5332.1630.

Das, Arunika, Evan M. Smoak, Ricardo Linares-Saldana, Michael A. Lampson, and Ben E. Black. 2017. 'Centromere Inheritance through the Germline'. Chromosoma 126(5): 595–604. doi:10.1007/s00412-017-0640-y.

Dattoli, Anna Ada, Ben L. Carty, Antje M. Kochendoerfer, Conall Morgan, Annie E. Walshe, and Elaine M. Dunleavy. 2020. 'Asymmetric Assembly of Centromeres Epigenetically Regulates Stem Cell Fate'. The Journal of Cell Biology 219(4): e201910084. doi:10.1083/jcb.201910084.

Davey, Curt A., and Timothy J. Richmond. 2002. 'DNA-Dependent Divalent Cation Binding in the Nucleosome Core Particle'. Proceedings of the National Academy of Sciences of the United States of America 99(17): 11169–74. doi:10.1073/pnas.172271399.

Davey, Curt A., David F. Sargent, Karolin Luger, Armin W. Maeder, and Timothy J. Richmond. 2002. 'Solvent Mediated Interactions in the Structure of the Nucleosome Core Particle at 1.9 a Resolution'. Journal of Molecular Biology 319(5): 1097–1113. doi:10.1016/S0022-2836(02)00386-8.

Day, Jeremy J., and J. David Sweatt. 2010. 'DNA Methylation and Memory Formation'. Nature Neuroscience 13(11): 1319–23. doi:10.1038/nn.2666.

De Conti, Laura, Marco Baralle, and Emanuele Buratti. 2013. 'Exon and Intron Definition in Pre-mRNA Splicing'. Wiley interdisciplinary reviews. RNA 4(1): 49–60. doi:10.1002/wrna.1140.

De Craene, Bram, and Geert Berx. 2013. 'Regulatory Networks Defining EMT during Cancer Initiation and Progression'. Nature Reviews. Cancer 13(2): 97–110. doi:10.1038/nrc3447.

De Koning, Leanne, Armelle Corpet, James E. Haber, and Geneviève Almouzni. 2007. 'Histone Chaperones: An Escort Network Regulating Histone Traffic'. Nature Structural & Molecular Biology 14(11): 997–1007. doi:10.1038/nsmb1318.

De Las Rivas, Javier, Anamaria Brozovic, Sivan Izraely, Alba Casas-Pais, Isaac P. Witz, and Angélica Figueroa. 2021. 'Cancer Drug Resistance Induced by EMT: Novel Therapeutic Strategies'. Archives of Toxicology 95(7): 2279–97. doi:10.1007/s00204-021-03063-7.

De Mattos-Arruda, Leticia, Giulia Bottai, Paolo G. Nuciforo, Luca Di Tommaso, Elisa Giovannetti, Vicente Peg, Agnese Losurdo, et al. 2015. 'MicroRNA-21 Links Epithelial-to-Mesenchymal Transition and Inflammatory Signals to Confer Resistance to Neoadjuvant Trastuzumab and Chemotherapy in HER2-Positive Breast Cancer Patients'. Oncotarget 6(35): 37269–80. doi:10.18632/oncotarget.5495.

Debaugnies, Maud, Sara Rodríguez-Acebes, Jeremy Blondeau, Marie-Astrid Parent, Manuel Zocco, Yura Song, Viviane de Maertelaer, et al. 2023. 'RHOJ Controls EMT-Associated Resistance to Chemotherapy'. Nature 616(7955): 168–75. doi:10.1038/s41586-023-05838-7.

el-Deiry, W. S., T. Tokino, V. E. Velculescu, D. B. Levy, R. Parsons, J. M. Trent, D. Lin, et al. 1993. 'WAF1, a Potential Mediator of P53 Tumor Suppression'. Cell 75(4): 817–25. doi:10.1016/0092-8674(93)90500-p.

Delaney, Kamila, Jonathan Mailler, Joanna M. Wenda, Caroline Gabus, and Florian A. Steiner. 2018. 'Differential Expression of Histone H3.3 Genes and Their Role in Modulating Temperature Stress Response in Caenorhabditis Elegans'. Genetics 209(2): 551–65. doi:10.1534/genetics.118.300909.

Delaney, Kamila, Nicole Weiss, and Geneviève Almouzni. 2023. 'The Cell-Cycle Choreography of H3 Variants Shapes the Genome'. Molecular Cell 83(21): 3773–86. doi:10.1016/j.molcel.2023.08.030.

Deng, Wang, Chen, Hao, Ni, Chang, Duan, Graham, and Li. 2016. 'Targeting Epithelial-Mesenchymal Transition and Cancer Stem Cells for Chemoresistant Ovarian Cancer'. Oncotarget 7(34). doi:10.18632/oncotarget.9908.

Denoth-Lippuner, Annina, and Sebastian Jessberger. 2021. 'Formation and Integration of New Neurons in the Adult Hippocampus'. Nature Reviews. Neuroscience 22(4): 223–36. doi:10.1038/s41583-021-00433-z.

Derynck, R., R. J. Akhurst, and A. Balmain. 2001. 'TGF-Beta Signaling in Tumor Suppression and Cancer Progression'. Nature Genetics 29(2): 117–29. doi:10.1038/ng1001-117.

Derynck, Rik, Baby Periyanayaki Muthusamy, and Koy Y. Saeteurn. 2014. 'Signaling Pathway Cooperation in TGF-β-Induced Epithelial-Mesenchymal Transition'. Current Opinion in Cell Biology 31: 56–66. doi:10.1016/j.ceb.2014.09.001.

Desgrosellier, Jay S., and David A. Cheresh. 2010. 'Integrins in Cancer: Biological Implications and Therapeutic Opportunities'. Nature Reviews. Cancer 10(1): 9–22. doi:10.1038/nrc2748.

Desprat, Nicolas, Willy Supatto, Philippe-Alexandre Pouille, Emmanuel Beaurepaire, and Emmanuel Farge. 2008. 'Tissue Deformation Modulates Twist Expression to Determine Anterior Midgut Differentiation in Drosophila Embryos'. Developmental Cell 15(3): 470–77. doi:10.1016/j.devcel.2008.07.009.

Dhasarathy, Archana, Dhiral Phadke, Deepak Mav, Ruchir R. Shah, and Paul A. Wade. 2011. 'The Transcription Factors Snail and Slug Activate the Transforming Growth Factor-Beta Signaling Pathway in Breast Cancer'. PloS One 6(10): e26514. doi:10.1371/journal.pone.0026514.

Di Domenico, Marina, and Antonio Giordano. 2017. 'Signal Transduction Growth Factors: The Effective Governance of Transcription and Cellular Adhesion in Cancer Invasion'. Oncotarget 8(22): 36869–84. doi:10.18632/oncotarget.16300.

Di Pierro, Michele, Ryan R. Cheng, Erez Lieberman Aiden, Peter G. Wolynes, and José N. Onuchic. 2017. 'De Novo Prediction of Human Chromosome Structures: Epigenetic Marking Patterns Encode Genome Architecture'. Proceedings of the National Academy of Sciences of the United States of America 114(46): 12126–31. doi:10.1073/pnas.1714980114.

Díaz-López, Antonio, Gema Moreno-Bueno, and Amparo Cano. 2014. 'Role of microRNA in Epithelial to Mesenchymal Transition and Metastasis and Clinical Perspectives'. Cancer Management and Research 6: 205–16. doi:10.2147/CMAR.S38156.

van Dijk, David, Roshan Sharma, Juozas Nainys, Kristina Yim, Pooja Kathail, Ambrose J. Carr, Cassandra Burdziak, et al. 2018. 'Recovering Gene Interactions from Single-Cell Data Using Data Diffusion'. Cell 174(3): 716-729.e27. doi:10.1016/j.cell.2018.05.061.

Dillon, Shane C., and Charles J. Dorman. 2010. 'Bacterial Nucleoid-Associated Proteins, Nucleoid Structure and Gene Expression'. Nature Reviews. Microbiology 8(3): 185–95. doi:10.1038/nrmicro2261.

Diner, Rachel E., Chari M. Noddings, Nathan C. Lian, Anthony K. Kang, Jeffrey B. McQuaid, Jelena Jablanovic, Josh L. Espinoza, et al. 2017. 'Diatom Centromeres Suggest a Mechanism for Nuclear DNA Acquisition'. Proceedings of the National Academy of Sciences of the United States of America 114(29): E6015–24. doi:10.1073/pnas.1700764114.

Ding, Chenbo, Junmin Luo, Longmei Li, Shanshan Li, Liwen Yang, Hongfei Pan, Qianyi Liu, et al. 2016. 'Gab2 Facilitates Epithelial-to-Mesenchymal Transition via the MEK/ERK/MMP Signaling in

Colorectal Cancer'. Journal of experimental & clinical cancer research: CR 35: 5. doi:10.1186/s13046-015-0280-0.

Dixon, Jesse R., Inkyung Jung, Siddarth Selvaraj, Yin Shen, Jessica E. Antosiewicz-Bourget, Ah Young Lee, Zhen Ye, et al. 2015. 'Chromatin Architecture Reorganization during Stem Cell Differentiation'. Nature 518(7539): 331–36. doi:10.1038/nature14222.

Dolinoy, Dana C., Dale Huang, and Randy L. Jirtle. 2007. 'Maternal Nutrient Supplementation Counteracts Bisphenol A-Induced DNA Hypomethylation in Early Development'. Proceedings of the National Academy of Sciences of the United States of America 104(32): 13056–61. doi:10.1073/pnas.0703739104.

Domaschenz, Renae, Sebastian Kurscheid, Maxim Nekrasov, Shuyi Han, and David J. Tremethick. 2017. 'The Histone Variant H2A.Z Is a Master Regulator of the Epithelial-Mesenchymal Transition'. Cell Reports 21(4): 943–52. doi:10.1016/j.celrep.2017.09.086.

Donato, Justin J, Shau Chee C Chung, and Bik K Tye. 2006. 'Genome-Wide Hierarchy of Replication Origin Usage in Saccharomyces Cerevisiae'. PLoS Genetics 2(9): e141. doi:10.1371/journal.pgen.0020141.

Dong, C., Y. Wu, Y. Wang, C. Wang, T. Kang, P. G. Rychahou, Y.-I. Chi, B. M. Evers, and B. P. Zhou. 2013. 'Interaction with Suv39H1 Is Critical for Snail-Mediated E-Cadherin Repression in Breast Cancer'. Oncogene 32(11): 1351–62. doi:10.1038/onc.2012.169.

Dong, Qianhua, and Fei Li. 2022. 'Cell Cycle Control of Kinetochore Assembly'. Nucleus 13(1): 208–20. doi:10.1080/19491034.2022.2115246.

Dong, Yinying, Xiangyin Sun, Kong Zhang, Xinjia He, Qian Zhang, Hao Song, Mingjin Xu, Haijun Lu, and Ruimei Ren. 2021. 'Type IIA Topoisomerase (TOP2A) Triggers Epithelial-Mesenchymal Transition and Facilitates HCC Progression by Regulating Snail Expression'. Bioengineered 12(2): 12967–79. doi:10.1080/21655979.2021.2012069.

Dongre, Anushka, Mohammad Rashidian, Ferenc Reinhardt, Aaron Bagnato, Zuzana Keckesova, Hidde L. Ploegh, and Robert A. Weinberg. 2017. 'Epithelial-to-Mesenchymal Transition Contributes to Immunosuppression in Breast Carcinomas'. Cancer Research 77(15): 3982–89. doi:10.1158/0008-5472.CAN-16-3292.

Dorigo, Benedetta, Thomas Schalch, Kerstin Bystricky, and Timothy J. Richmond. 2003. 'Chromatin Fiber Folding: Requirement for the Histone H4 N-Terminal Tail'. Journal of Molecular Biology 327(1): 85–96. doi:10.1016/s0022-2836(03)00025-1.

Dorigo, Benedetta, Thomas Schalch, Alexandra Kulangara, Sylwia Duda, Rasmus R. Schroeder, and Timothy J. Richmond. 2004. 'Nucleosome Arrays Reveal the Two-Start Organization of the Chromatin Fiber'. Science (New York, N.Y.) 306(5701): 1571–73. doi:10.1126/science.1103124.

Drané, Pascal, Khalid Ouararhni, Arnaud Depaux, Muhammad Shuaib, and Ali Hamiche. 2010. 'The Death-Associated Protein DAXX Is a Novel Histone Chaperone Involved in the Replication-Independent Deposition of H3.3'. Genes & Development 24(12): 1253–65. doi:10.1101/gad.566910.

Du, Dan, Yoko Katsuno, Dominique Meyer, Erine H. Budi, Si-Han Chen, Hartmut Koeppen, Hongjun Wang, Rosemary J. Akhurst, and Rik Derynck. 2018. 'Smad3-Mediated Recruitment of the Methyltransferase SETDB1/ESET Controls Snail1 Expression and Epithelial-Mesenchymal Transition'. EMBO reports 19(1): 135–55. doi:10.15252/embr.201744250.

Duan, Zhijun, Mirela Andronescu, Kevin Schutz, Sean McIlwain, Yoo Jung Kim, Choli Lee, Jay Shendure, et al. 2010. 'A Three-Dimensional Model of the Yeast Genome'. Nature 465(7296): 363–67. doi:10.1038/nature08973.

Dueva, Rositsa, Karen Akopyan, Chiara Pederiva, Davide Trevisan, Soniya Dhanjal, Arne Lindqvist, and Marianne Farnebo. 2019. 'Neutralization of the Positive Charges on Histone Tails by RNA Promotes an Open Chromatin Structure'. Cell Chemical Biology 26(10): 1436-1449.e5. doi:10.1016/j.chembiol.2019.08.002.

Dulbecco, R., M. Henahan, M. Bowman, S. Okada, H. Battifora, and M. Unger. 1981. 'Generation of Fibroblast-like Cells from Cloned Epithelial Mammary Cells in Vitro: A Possible New Cell Type'. Proceedings of the National Academy of Sciences of the United States of America 78(4): 2345–49. doi:10.1073/pnas.78.4.2345.

Dumont, Nancy, Matthew B. Wilson, Yongping G. Crawford, Paul A. Reynolds, Mahvash Sigaroudinia, and Thea D. Tlsty. 2008. 'Sustained Induction of Epithelial to Mesenchymal Transition Activates DNA Methylation of Genes Silenced in Basal-like Breast Cancers'. Proceedings of the National Academy of Sciences of the United States of America 105(39): 14867–72. doi:10.1073/pnas.0807146105.

Dumortier, B. C. 1832. Recherches sur la structure comparée et le développement des animaux et des végétaux. doi:10.3406/marb.1832.2746.

Dumortier, Julien G., Sandro Martin, Dirk Meyer, Frederic M. Rosa, and Nicolas B. David. 2012. 'Collective Mesendoderm Migration Relies on an Intrinsic Directionality Signal Transmitted through Cell Contacts'. Proceedings of the National Academy of Sciences of the United States of America 109(42): 16945–50. doi:10.1073/pnas.1205870109.

Dunleavy, Elaine M., Geneviève Almouzni, and Gary H. Karpen. 2011. 'H3.3 Is Deposited at Centromeres in S Phase as a Placeholder for Newly Assembled CENP-A in G1 Phase'. Nucleus 2(2): 146. doi:10.4161/nucl.2.2.15211.

Dunleavy, Elaine M., Nicole L. Beier, Walter Gorgescu, Jonathan Tang, Sylvain V. Costes, and Gary H. Karpen. 2012. 'The Cell Cycle Timing of Centromeric Chromatin Assembly in Drosophila Meiosis

Is Distinct from Mitosis yet Requires CAL1 and CENP-C'. PLoS biology 10(12): e1001460. doi:10.1371/journal.pbio.1001460.

Dunleavy, Elaine M., Danièle Roche, Hideaki Tagami, Nicolas Lacoste, Dominique Ray-Gallet, Yusuke Nakamura, Yataro Daigo, Yoshihiro Nakatani, and Geneviève Almouzni-Pettinotti. 2009. 'HJURP Is a Cell-Cycle-Dependent Maintenance and Deposition Factor of CENP-A at Centromeres'. Cell 137(3): 485–97. doi:10.1016/j.cell.2009.02.040.

Earnshaw, W. C., and N. Rothfield. 1985. 'Identification of a Family of Human Centromere Proteins Using Autoimmune Sera from Patients with Scleroderma'. Chromosoma 91(3–4): 313–21. doi:10.1007/BF00328227.

Engeland, Kurt. 2018. 'Cell Cycle Arrest through Indirect Transcriptional Repression by P53: I Have a DREAM'. Cell Death & Differentiation 25(1): 114–32. doi:10.1038/cdd.2017.172.

English, Christine M., Melissa W. Adkins, Joshua J. Carson, Mair E.A. Churchill, and Jessica K. Tyler. 2006. 'Structural Basis for the Histone Chaperone Activity of Asf1'. Cell 127(3): 495–508. doi:10.1016/j.cell.2006.08.047.

Enkhbaatar, Zanabazar, Minoru Terashima, Dulamsuren Oktyabri, Shoichiro Tange, Akihiko Ishimura, Seiji Yano, and Takeshi Suzuki. 2013. 'KDM5B Histone Demethylase Controls Epithelial-Mesenchymal Transition of Cancer Cells by Regulating the Expression of the microRNA-200 Family'. Cell Cycle (Georgetown, Tex.) 12(13): 2100–2112. doi:10.4161/cc.25142.

Erdel, Fabian, and Karsten Rippe. 2018. 'Formation of Chromatin Subcompartments by Phase Separation'. Biophysical Journal 114(10): 2262–70. doi:10.1016/j.bpj.2018.03.011.

Escobar, Thelma M., Jia-Ray Yu, Sanxiong Liu, Kimberly Lucero, Nikita Vasilyev, Evgeny Nudler, and Danny Reinberg. 2022. 'Inheritance of Repressed Chromatin Domains during S Phase Requires the Histone Chaperone NPM1'. Science Advances. doi:10.1126/sciadv.abm3945.

Eskiizmir, Görkem, Erdoğan Özgür, Görkem Eskiizmir, and Erdoğan Özgür. 2018. 'Epithelial-Mesenchymal Transition in Tumor Microenvironment Induced by Hypoxia'. In Cancer Metastasis, IntechOpen. doi:10.5772/intechopen.78717.

Eslami-S., Z., L. Cortés-Hernández, and C. Alix-Panabières. 2020. 'Epithelial Cell Adhesion Molecule: An Anchor to Isolate Clinically Relevant Circulating Tumor Cells'. Cells 9(8). doi:10.3390/cells9081836.

Esteban, Miguel A., Maxine G. B. Tran, Sarah K. Harten, Peter Hill, Maria C. Castellanos, Ashish Chandra, Raju Raval, Tim S. O'brien, and Patrick H. Maxwell. 2006. 'Regulation of E-Cadherin Expression by VHL and Hypoxia-Inducible Factor'. Cancer Research 66(7): 3567–75. doi:10.1158/0008-5472.CAN-05-2670.

Evrin, Cecile, Pippa Clarke, Juergen Zech, Rudi Lurz, Jingchuan Sun, Stefan Uhle, Huilin Li, Bruce Stillman, and Christian Speck. 2009. 'A Double-Hexameric MCM2-7 Complex Is Loaded onto Origin DNA during Licensing of Eukaryotic DNA Replication'. Proceedings of the National Academy of Sciences of the United States of America 106(48): 20240–45. doi:10.1073/pnas.0911500106.

Faast, R., V. Thonglairoam, T. C. Schulz, J. Beall, J. R. Wells, H. Taylor, K. Matthaei, et al. 2001. 'Histone Variant H2A.Z Is Required for Early Mammalian Development'. Current biology: CB 11(15): 1183–87. doi:10.1016/s0960-9822(01)00329-3.

Fachinetti, Daniele, H. Diego Folco, Yael Nechemia-Arbely, Luis P. Valente, Kristen Nguyen, Alex J. Wong, Quan Zhu, et al. 2013. 'A Two-Step Mechanism for Epigenetic Specification of Centromere Identity and Function'. Nature Cell Biology 15(9): 1056–66. doi:10.1038/ncb2805.

Fachinetti, Daniele, Joo Seok Han, Moira A. McMahon, Peter Ly, Amira Abdullah, Alex J. Wong, and Don W. Cleveland. 2015. 'DNA Sequence-Specific Binding of CENP-B Enhances the Fidelity of Human Centromere Function'. Developmental cell 33(3): 314–27. doi:10.1016/j.devcel.2015.03.020.

Falk, Samantha J., Lucie Y. Guo, Nikolina Sekulic, Evan M. Smoak, Tomoyasu Mani, Glennis A. Logsdon, Kushol Gupta, et al. 2015. 'Chromosomes. CENP-C Reshapes and Stabilizes CENP-A Nucleosomes at the Centromere'. Science (New York, N.Y.) 348(6235): 699–703. doi:10.1126/science.1259308.

Falk, Samantha J., Jaehyoun Lee, Nikolina Sekulic, Michael A. Sennett, Tae-Hee Lee, and Ben E. Black. 2016. 'CENP-C Directs a Structural Transition of CENP-A Nucleosomes Mainly through Sliding of DNA Gyres'. Nature Structural & Molecular Biology 23(3): 204–8. doi:10.1038/nsmb.3175.

Farkash-Amar, Shlomit, Doron Lipson, Andreas Polten, Alon Goren, Charles Helmstetter, Zohar Yakhini, and Itamar Simon. 2008. 'Global Organization of Replication Time Zones of the Mouse Genome'. Genome Research 18(10): 1562–70. doi:10.1101/gr.079566.108.

Farley, J. and Geison, G. L. 1974. Science, politics and spontaneous generation in nineteenth-century France: the Pasteur-Pouchet debate. Bull Hist Med, 48(2): 161-198.

Fattet, Laurent, Hae-Yun Jung, Mike W. Matsumoto, Brandon E. Aubol, Aditya Kumar, Joseph A. Adams, Albert C. Chen, et al. 2020. 'Matrix Rigidity Controls Epithelial-Mesenchymal Plasticity and Tumor Metastasis via a Mechanoresponsive EPHA2/LYN Complex'. Developmental Cell 54(3): 302-316.e7. doi:10.1016/j.devcel.2020.05.031.

Fazilaty, Hassan, Luciano Rago, Khalil Kass Youssef, Oscar H. Ocaña, Francisco Garcia-Asencio, Aida Arcas, Juan Galceran, and M. Angela Nieto. 2019. 'A Gene Regulatory Network to Control EMT Programs in Development and Disease'. Nature Communications 10(1): 5115. doi:10.1038/s41467-019-13091-8.

Feinberg, A. P., and B. Vogelstein. 1983. ‘Hypomethylation Distinguishes Genes of Some Human Cancers from Their Normal Counterparts’. Nature 301(5895): 89–92. doi:10.1038/301089a0.

Felsenfeld, Gary, and Mark Groudine. 2003. ‘Controlling the Double Helix’. Nature 421(6921): 448–53. doi:10.1038/nature01411.

Feodorova, Yana, Martin Falk, Leonid A. Mirny, and Irina Solovei. 2020. ‘Viewing Nuclear Architecture through the Eyes of Nocturnal Mammals’. Trends in Cell Biology 30(4): 276–89. doi:10.1016/j.tcb.2019.12.008.

Fernandez-Albert, Jordi, Michal Lipinski, María T. Lopez-Cascales, M. Jordan Rowley, Ana M. Martin-Gonzalez, Beatriz Del Blanco, Victor G. Corces, and Angel Barco. 2019. ‘Immediate and Deferred Epigenomic Signatures of in Vivo Neuronal Activation in Mouse Hippocampus’. Nature Neuroscience 22(10): 1718–30. doi:10.1038/s41593-019-0476-2.

Ferreira, João, Giovanni Paolella, Carlos Ramos, and Angus I. Lamond. 1997. ‘Spatial Organization of Large-Scale Chromatin Domains in the Nucleus: A Magnified View of Single Chromosome Territories’. The Journal of Cell Biology 139(7): 1597–1610.

Filipescu, Dan, Sebastian Müller, and Geneviève Almouzni. 2014. ‘Histone H3 Variants and Their Chaperones during Development and Disease: Contributing to Epigenetic Control’. Annual Review of Cell and Developmental Biology 30: 615–46. doi:10.1146/annurev-cellbio-100913-013311.

Filipescu, Dan, Monica Naughtin, Katrina Podsypanina, Vincent Lejour, Laurence Wilson, Zachary A. Gurard-Levin, Guillermo A. Orsi, et al. 2017. ‘Essential Role for Centromeric Factors Following P53 Loss and Oncogenic Transformation’. Genes & Development 31(5): 463–80. doi:10.1101/gad.290924.116.

Finch, J. T., and A. Klug. 1976. ‘Solenoidal Model for Superstructure in Chromatin’. Proceedings of the National Academy of Sciences of the United States of America 73(6): 1897–1901. doi:10.1073/pnas.73.6.1897.

Finn, Elizabeth H., and Tom Misteli. 2019. ‘Molecular Basis and Biological Function of Variability in Spatial Genome Organization’. Science (New York, N.Y.) 365(6457): eaaw9498. doi:10.1126/science.aaw9498.

Firsanov, Denis V., Liudmila V. Solovjeva, and Maria P. Svetlova. 2011. ‘H2AX Phosphorylation at the Sites of DNA Double-Strand Breaks in Cultivated Mammalian Cells and Tissues’. Clinical Epigenetics 2(2): 283–97. doi:10.1007/s13148-011-0044-4.

Fischer, Kari R., Anna Durrans, Sharrell Lee, Jianting Sheng, Fuhai Li, Stephen T. C. Wong, Hyejin Choi, et al. 2015. ‘Epithelial-to-Mesenchymal Transition Is Not Required for Lung Metastasis but Contributes to Chemoresistance’. Nature 527(7579): 472–76. doi:10.1038/nature15748.

Fischer, Martin, Patrick Grossmann, Megha Padi, and James A. DeCaprio. 2016. 'Integration of TP53, DREAM, MMB-FOXM1 and RB-E2F Target Gene Analyses Identifies Cell Cycle Gene Regulatory Networks'. Nucleic Acids Research 44(13): 6070–86. doi:10.1093/nar/gkw523.

Fitchett, J. E., and E. D. Hay. 1989. 'Medial Edge Epithelium Transforms to Mesenchyme after Embryonic Palatal Shelves Fuse'. Developmental Biology 131(2): 455–74. doi:10.1016/s0012-1606(89)80017-x.

Flemming, Walther. 1882. Zellsubstanz, Kern Und Zelltheilung. Vogel. https://books.google.com/books?hl=fr&lr=&id=J4RIAAAAYAAJ&oi=fnd&pg=PA1&dq=Flemming+W.+Zellsubstanz,+kern+und+zelltheilung+1882+F.+C.+W.+Vogel+&ots=MxK5leAGVv&sig=gPHvIxg_kU9pKuNYh-lZKMngLqU (September 6, 2024).

Flury, Valentin, Nazaret Reverón-Gómez, Nicolas Alcaraz, Kathleen R. Stewart-Morgan, Alice Wenger, Robert J. Klose, and Anja Groth. 2023. 'Recycling of Modified H2A-H2B Provides Short-Term Memory of Chromatin States'. Cell 186(5): 1050-1065.e19. doi:10.1016/j.cell.2023.01.007.

Foltz, Daniel R., Lars E. T. Jansen, Ben E. Black, Aaron O. Bailey, John R. Yates, and Don W. Cleveland. 2006. 'The Human CENP-A Centromeric Nucleosome-Associated Complex'. Nature Cell Biology 8(5): 458–69. doi:10.1038/ncb1397.

Foltz, Daniel R., Lars E.T. Jansen, Aaron O. Bailey, John R. Yates, Emily A. Bassett, Stacey Wood, Ben E. Black, and Don W. Cleveland. 2009. 'Centromere Specific Assembly of CENP-A Nucleosomes Is Mediated by HJURP'. Cell 137(3): 472–84. doi:10.1016/j.cell.2009.02.039.

Fontebasso, Adam M., Tenzin Gayden, Hamid Nikbakht, Michael Neirinck, Simon Papillon-Cavanagh, Jacek Majewski, and Nada Jabado. 2014. 'Epigenetic Dysregulation: A Novel Pathway of Oncogenesis in Pediatric Brain Tumors'. Acta Neuropathologica 128(5): 615–27. doi:10.1007/s00401-014-1325-8.

Fragkos, Michalis, Olivier Ganier, Philippe Coulombe, and Marcel Méchali. 2015. 'DNA Replication Origin Activation in Space and Time'. Nature Reviews. Molecular Cell Biology 16(6): 360–74. doi:10.1038/nrm4002.

Franke, W. W., C. Grund, C. Kuhn, B. W. Jackson, and K. Illmensee. 1982. 'Formation of Cytoskeletal Elements during Mouse Embryogenesis. III. Primary Mesenchymal Cells and the First Appearance of Vimentin Filaments'. Differentiation; Research in Biological Diversity 23(1): 43–59. doi:10.1111/j.1432-0436.1982.tb01266.x.

Franklin, Reuben, Yiming Guo, Shiyang He, Meijuan Chen, Fei Ji, Xinyue Zhou, David Frankhouser, et al. 2022. 'Regulation of Chromatin Accessibility by the Histone Chaperone CAF-1 Sustains Lineage Fidelity'. Nature Communications 13(1): 2350. doi:10.1038/s41467-022-29730-6.

Franklin, Rosalind E., and R. G. Gosling. 1953. 'Molecular Configuration in Sodium Thymonucleate'. Nature 171(4356): 740–41. doi:10.1038/171740a0.

Franklin, S. G., and A. Zweidler. 1977. ‘Non-Allelic Variants of Histones 2a, 2b and 3 in Mammals’. Nature 266(5599): 273–75. doi:10.1038/266273a0.

Friedrich, Julian, Anna Bareis, Moritz Bross, Zoé Bürger, Álvaro Cortés Rodríguez, Nina Effenberger, Markus Kleinhansl, Fabienne Kremer, and Cornelius Schröder. 2023. ‘“How Is Your Thesis Going?”-Ph.D. Students’ Perspectives on Mental Health and Stress in Academia’. PloS One 18(7): e0288103. doi:10.1371/journal.pone.0288103.

Frisch, Steven M., Michael Schaller, and Benjamin Cieply. 2013. ‘Mechanisms That Link the Oncogenic Epithelial–Mesenchymal Transition to Suppression of Anoikis’. Journal of Cell Science 126(1): 21–29. doi:10.1242/jcs.120907.

Fritz, Andrew J., Nitasha Sehgal, Artem Pliss, Jinhui Xu, and Ronald Berezney. 2019. ‘Chromosome Territories and the Global Regulation of the Genome’. Genes, Chromosomes & Cancer 58(7): 407–26. doi:10.1002/gcc.22732.

Fujita, Yohta, Takeshi Hayashi, Tomomi Kiyomitsu, Yusuke Toyoda, Aya Kokubu, Chikashi Obuse, and Mitsuhiro Yanagida. 2007. ‘Priming of Centromere for CENP-A Recruitment by Human hMis18alpha, hMis18beta, and M18BP1’. Developmental Cell 12(1): 17–30. doi:10.1016/j.devcel.2006.11.002.

Fukagawa, Tatsuo, and William C. Earnshaw. 2014. ‘The Centromere: Chromatin Foundation for the Kinetochore Machinery’. Developmental Cell 30(5): 496–508. doi:10.1016/j.devcel.2014.08.016.

Furuichi, Yasuhiro. 2015. ‘Discovery of m(7)G-Cap in Eukaryotic mRNAs’. Proceedings of the Japan Academy. Series B, Physical and Biological Sciences 91(8): 394–409. doi:10.2183/pjab.91.394.

Furuyama, Suzanne, and Sue Biggins. 2007. ‘Centromere Identity Is Specified by a Single Centromeric Nucleosome in Budding Yeast’. Proceedings of the National Academy of Sciences of the United States of America 104(37): 14706–11. doi:10.1073/pnas.0706985104.

Futterman, Matt A., Andrés J. García, and Evan A. Zamir. 2011. ‘Evidence for Partial Epithelial-to-Mesenchymal Transition (pEMT) and Recruitment of Motile Blastoderm Edge Cells during Avian Epiboly’. Developmental Dynamics: An Official Publication of the American Association of Anatomists 240(6): 1502–11. doi:10.1002/dvdy.22607.

Galliher, Amy J., and William P. Schiemann. 2006. ‘Beta3 Integrin and Src Facilitate Transforming Growth Factor-Beta Mediated Induction of Epithelial-Mesenchymal Transition in Mammary Epithelial Cells’. Breast cancer research: BCR 8(4): R42. doi:10.1186/bcr1524.

Gamba, Riccardo, and Daniele Fachinetti. 2020. ‘From Evolution to Function: Two Sides of the Same CENP-B Coin?’ Experimental Cell Research 390(2): 111959. doi:10.1016/j.yexcr.2020.111959.

Gan, Haiyun, Albert Serra-Cardona, Xu Hua, Hui Zhou, Karim Labib, Chuanhe Yu, and Zhiguo Zhang. 2018. 'The Mcm2-Ctf4-Polα Axis Facilitates Parental Histone H3-H4 Transfer to Lagging Strands'. Molecular Cell 72(1): 140-151.e3. doi:10.1016/j.molcel.2018.09.001.

Ganier, Olivier, Paulina Prorok, Ildem Akerman, and Marcel Méchali. 2019. 'Metazoan DNA Replication Origins'. Current Opinion in Cell Biology 58: 134–41. doi:10.1016/j.ceb.2019.03.003.

Gao, Dingcheng, and Vivek Mittal. 2012. 'Tumor Microenvironment Regulates Epithelial-Mesenchymal Transitions in Metastasis'. Expert Review of Anticancer Therapy 12(7): 857–59. doi:10.1586/era.12.69.

Gao, Feng, and Chun-Ting Zhang. 2007. 'DoriC: A Database of oriC Regions in Bacterial Genomes'. Bioinformatics (Oxford, England) 23(14): 1866–67. doi:10.1093/bioinformatics/btm255.

García-Castro, Martín I., Christophe Marcelle, and Marianne Bronner-Fraser. 2002. 'Ectodermal Wnt Function as a Neural Crest Inducer'. Science (New York, N.Y.) 297(5582): 848–51. doi:10.1126/science.1070824.

Garufi, Alessia, Giuseppa Pistritto, and Gabriella D'Orazi. 2023. 'HIPK2 as a Novel Regulator of Fibrosis'. Cancers 15(4): 1059. doi:10.3390/cancers15041059.

Gascoigne, Karen E., Kozo Takeuchi, Aussie Suzuki, Tetsuya Hori, Tatsuo Fukagawa, and Iain M. Cheeseman. 2011. 'Induced Ectopic Kinetochore Assembly Bypasses the Requirement for CENP-A Nucleosomes'. Cell 145(3): 410–22. doi:10.1016/j.cell.2011.03.031.

Gaspar-Maia, Alexandre, Zulekha A. Qadeer, Dan Hasson, Kajan Ratnakumar, N. Adrian Leu, Gary Leroy, Shichong Liu, et al. 2013. 'MacroH2A Histone Variants Act as a Barrier upon Reprogramming towards Pluripotency'. Nature Communications 4(1): 1565. doi:10.1038/ncomms2582.

Gatto, Alberto, Audrey Forest, Jean-Pierre Quivy, and Geneviève Almouzni. 2022. 'HIRA-Dependent Boundaries between H3 Variants Shape Early Replication in Mammals'. Molecular Cell 82(10): 1909-1923.e5. doi:10.1016/j.molcel.2022.03.017.

Gavrilović, J., G. Moens, J. P. Thiery, and J. Jouanneau. 1990. 'Expression of Transfected Transforming Growth Factor Alpha Induces a Motile Fibroblast-like Phenotype with Extracellular Matrix-Degrading Potential in a Rat Bladder Carcinoma Cell Line'. Cell Regulation 1(13): 1003–14. doi:10.1091/mbc.1.13.1003.

Gemble, Simon, Anthony Simon, Carole Pennetier, Marie Dumont, Solène Hervé, Franz Meitinger, Karen Oegema, et al. 2019. 'Centromere Dysfunction Compromises Mitotic Spindle Pole Integrity'. Current biology: CB 29(18): 3072-3080.e5. doi:10.1016/j.cub.2019.07.052.

van Genderen, C., R. M. Okamura, I. Fariñas, R. G. Quo, T. G. Parslow, L. Bruhn, and R. Grosschedl. 1994. 'Development of Several Organs That Require Inductive Epithelial-Mesenchymal Interactions Is

Impaired in LEF-1-Deficient Mice'. Genes & Development 8(22): 2691–2703. doi:10.1101/gad.8.22.2691.

Geradts, Joseph, Antonio Garcia de Herreros, Zuowei Su, James Burchette, Gloria Broadwater, and Robin E. Bachelder. 2011. 'Nuclear Snail1 and Nuclear ZEB1 Protein Expression in Invasive and Intraductal Human Breast Carcinomas'. Human Pathology 42(8): 1125–31. doi:10.1016/j.humpath.2010.11.004.

Gershman, Ariel, Michael E. G. Sauria, Xavi Guitart, Mitchell R. Vollger, Paul W. Hook, Savannah J. Hoyt, Miten Jain, et al. 2022. 'Epigenetic Patterns in a Complete Human Genome'. Science (New York, N.Y.) 376(6588): eabj5089. doi:10.1126/science.abj5089.

Ghiraldini, Flávia G., Dan Filipescu, and Emily Bernstein. 2021. 'Solid Tumours Hijack the Histone Variant Network'. Nature Reviews. Cancer 21(4): 257–75. doi:10.1038/s41568-020-00330-0.

Gibbins, J. R., A. Manthey, Y. M. Tazawa, B. Scott, A. Bloch-Zupan, and N. Hunter. 1999. 'Midline Fusion in the Formation of the Secondary Palate Anticipated by Upregulation of Keratin K5/6 and Localized Expression of Vimentin mRNA in Medial Edge Epithelium'. The International Journal of Developmental Biology 43(3): 237–44.

Gibson, Bryan A., Lynda K. Doolittle, Maximillian W. G. Schneider, Liv E. Jensen, Nathan Gamarra, Lisa Henry, Daniel W. Gerlich, Sy Redding, and Michael K. Rosen. 2019. 'Organization of Chromatin by Intrinsic and Regulated Phase Separation'. Cell 179(2): 470-484.e21. doi:10.1016/j.cell.2019.08.037.

Gilbert, Scott F., John M. Opitz, and Rudolf A. Raff. 1996. 'Resynthesizing Evolutionary and Developmental Biology'. Developmental Biology 173(2): 357–72. doi:10.1006/dbio.1996.0032.

Giunta, Simona, Solène Hervé, Ryan R. White, Therese Wilhelm, Marie Dumont, Andrea Scelfo, Riccardo Gamba, et al. 2021. 'CENP-A Chromatin Prevents Replication Stress at Centromeres to Avoid Structural Aneuploidy'. Proceedings of the National Academy of Sciences of the United States of America 118(10): e2015634118. doi:10.1073/pnas.2015634118.

Gökbuget, Deniz, Ryan M. Boileau, Kayla Lenshoek, and Robert Blelloch. 2023. 'MLL3/MLL4 Enzymatic Activity Shapes DNA Replication Timing'. bioRxiv: The Preprint Server for Biology: 2023.12.07.569680. doi:10.1101/2023.12.07.569680.

Goldberg, Aaron D., Laura A. Banaszynski, Kyung-Min Noh, Peter W. Lewis, Simon J. Elsaesser, Sonja Stadler, Scott Dewell, et al. 2010. 'Distinct Factors Control Histone Variant H3.3 Localization at Specific Genomic Regions'. Cell 140(5): 678–91. doi:10.1016/j.cell.2010.01.003.

Gomes, Ana P., Didem Ilter, Vivien Low, Adam Rosenzweig, Zih-Jie Shen, Tanya Schild, Martin A. Rivas, et al. 2019. 'Dynamic Incorporation of Histone H3 Variants into Chromatin Is Essential for

Acquisition of Aggressive Traits and Metastatic Colonization'. Cancer Cell 36(4): 402-417.e13. doi:10.1016/j.ccell.2019.08.006.

Gomes, Edgar R., and Sérgio F. de Almeida. 2021. 'TREX1-Dependent DNA Damage Links Nuclear Rupture to Tumor Cell Invasion'. Developmental Cell 56(22): 3040–41. doi:10.1016/j.devcel.2021.11.003.

Gorges, Tobias M., Ingeborg Tinhofer, Michael Drosch, Lars Röse, Thomas M. Zollner, Thomas Krahn, and Oliver von Ahsen. 2012. 'Circulating Tumour Cells Escape from EpCAM-Based Detection Due to Epithelial-to-Mesenchymal Transition'. BMC cancer 12: 178. doi:10.1186/1471-2407-12-178.

Grande, M. Teresa, Berta Sánchez-Laorden, Cristina López-Blau, Cristina A. De Frutos, Agnès Boutet, Miguel Arévalo, R. Grant Rowe, et al. 2015. 'Snail1-Induced Partial Epithelial-to-Mesenchymal Transition Drives Renal Fibrosis in Mice and Can Be Targeted to Reverse Established Disease'. Nature Medicine 21(9): 989–97. doi:10.1038/nm.3901.

Graziano, V., S. E. Gerchman, A. J. Wonacott, R. M. Sweet, J. R. Wells, S. W. White, and V. Ramakrishnan. 1990. 'Crystallization of the Globular Domain of Histone H5'. Journal of Molecular Biology 212(2): 253–57. doi:10.1016/0022-2836(90)90122-3.

Greaves, Mel, and Carlo C. Maley. 2012. 'Clonal Evolution in Cancer'. Nature 481(7381): 306–13. doi:10.1038/nature10762.

Greenberg, Maxim V. C. 2020. 'Get Out and Stay Out: New Insights Into DNA Methylation Reprogramming in Mammals'. Frontiers in Cell and Developmental Biology 8: 629068. doi:10.3389/fcell.2020.629068.

Greenberg, Maxim V. C., and Deborah Bourc'his. 2019. 'The Diverse Roles of DNA Methylation in Mammalian Development and Disease'. Nature Reviews. Molecular Cell Biology 20(10): 590–607. doi:10.1038/s41580-019-0159-6.

Greenburg, G., and E. D. Hay. 1982. 'Epithelia Suspended in Collagen Gels Can Lose Polarity and Express Characteristics of Migrating Mesenchymal Cells'. The Journal of Cell Biology 95(1): 333–39. doi:10.1083/jcb.95.1.333.

Greenburg, G., and E. D. Hay. 1986. 'Cytodifferentiation and Tissue Phenotype Change during Transformation of Embryonic Lens Epithelium to Mesenchyme-like Cells in Vitro'. Developmental Biology 115(2): 363–79. doi:10.1016/0012-1606(86)90256-3.

Greenburg, G., and E. D. Hay. 1988. 'Cytoskeleton and Thyroglobulin Expression Change during Transformation of Thyroid Epithelium to Mesenchyme-like Cells'. Development (Cambridge, England) 102(3): 605–22. doi:10.1242/dev.102.3.605.

Gregory, Philip A., Andrew G. Bert, Emily L. Paterson, Simon C. Barry, Anna Tsykin, Gelareh Farshid, Mathew A. Vadas, Yeesim Khew-Goodall, and Gregory J. Goodall. 2008. 'The miR-200 Family and

miR-205 Regulate Epithelial to Mesenchymal Transition by Targeting ZEB1 and SIP1'. Nature Cell Biology 10(5): 593–601. doi:10.1038/ncb1722.

Gressner, Axel M., Ralf Weiskirchen, Katja Breitkopf, and Steven Dooley. 2002. 'Roles of TGF-Beta in Hepatic Fibrosis'. Frontiers in Bioscience: A Journal and Virtual Library 7: d793-807. doi:10.2741/A812.

Griffith, F. 1928. The Significance of Pneumococcal Types. The Journal of Hygiene 27(2): 113-159. doi: 10.1017/s0022172400031879.

Gross, Sean M., Mark A. Dane, Rebecca L. Smith, Kaylyn L. Devlin, Ian C. McLean, Daniel S. Derrick, Caitlin E. Mills, et al. 2022. 'A Multi-Omic Analysis of MCF10A Cells Provides a Resource for Integrative Assessment of Ligand-Mediated Molecular and Phenotypic Responses'. Communications Biology 5(1): 1–20. doi:10.1038/s42003-022-03975-9.

Grotegut, Stefan, Dietrich von Schweinitz, Gerhard Christofori, and François Lehembre. 2006. 'Hepatocyte Growth Factor Induces Cell Scattering through MAPK/Egr-1-Mediated Upregulation of Snail'. The EMBO journal 25(15): 3534–45. doi:10.1038/sj.emboj.7601213.

Groth, Anja. 2009. 'Replicating Chromatin: A Tale of Histones'. Biochemistry and Cell Biology = Biochimie Et Biologie Cellulaire 87(1): 51–63. doi:10.1139/O08-102.

Groth, Anja, Armelle Corpet, Adam J. L. Cook, Daniele Roche, Jiri Bartek, Jiri Lukas, and Geneviève Almouzni. 2007. 'Regulation of Replication Fork Progression through Histone Supply and Demand'. Science (New York, N.Y.) 318(5858): 1928–31. doi:10.1126/science.1148992.

Gu, Xiao-Min, Jie Fu, Xiao-Jun Feng, Xue Huang, Shou-Mei Wang, Xin-Feng Chen, Ming-Hua Zhu, and Shu-Hui Zhang. 2014. 'Expression and Prognostic Relevance of Centromere Protein A in Primary Osteosarcoma'. Pathology - Research and Practice 210(4): 228–33. doi:10.1016/j.prp.2013.12.007.

Gu, Yue-Yu, Xu-Sheng Liu, Xiao-Ru Huang, Xue-Qing Yu, and Hui-Yao Lan. 2020. 'Diverse Role of TGF-β in Kidney Disease'. Frontiers in Cell and Developmental Biology 8: 123. doi:10.3389/fcell.2020.00123.

Guenatri, Mounia, Delphine Bailly, Christèle Maison, and Geneviève Almouzni. 2004. 'Mouse Centric and Pericentric Satellite Repeats Form Distinct Functional Heterochromatin'. The Journal of Cell Biology 166(4): 493–505. doi:10.1083/jcb.200403109.

Gumbiner, Barry M. 2005. 'Regulation of Cadherin-Mediated Adhesion in Morphogenesis'. Nature Reviews. Molecular Cell Biology 6(8): 622–34. doi:10.1038/nrm1699.

Guo, Lucie Y., Praveen Kumar Allu, Levani Zandarashvili, Kara L. McKinley, Nikolina Sekulic, Jennine M. Dawicki-McKenna, Daniele Fachinetti, et al. 2017. 'Centromeres Are Maintained by Fastening CENP-A to DNA and Directing an Arginine Anchor-Dependent Nucleosome Transition'. Nature Communications 8: 15775. doi:10.1038/ncomms15775.

Gupta, Piyush B., Ievgenia Pastushenko, Adam Skibinski, Cedric Blanpain, and Charlotte Kuperwasser. 2019. 'Phenotypic Plasticity: Driver of Cancer Initiation, Progression, and Therapy Resistance'. Cell Stem Cell 24(1): 65–78. doi:10.1016/j.stem.2018.11.011.

Gupta, Shiv K, Saji Oommen, Marie-Christine Aubry, Brian P. Williams, and Nicholas E Vlahakis. 2013. 'Integrin A9β1 Promotes Malignant Tumor Growth and Metastasis by Potentiating Epithelial-Mesenchymal Transition'. Oncogene 32(2): 141–50. doi:10.1038/onc.2012.41.

Gurard-Levin, Zachary A., Jean-Pierre Quivy, and Geneviève Almouzni. 2014. 'Histone Chaperones: Assisting Histone Traffic and Nucleosome Dynamics'. Annual Review of Biochemistry 83(Volume 83, 2014): 487–517. doi:10.1146/annurev-biochem-060713-035536.

Guse, Annika, Christopher W. Carroll, Ben Moree, Colin J. Fuller, and Aaron F. Straight. 2011. 'In Vitro Centromere and Kinetochore Assembly on Defined Chromatin Templates'. Nature 477(7364): 354–58. doi:10.1038/nature10379.

Haeckel, Ernst. 1874. 'Die Gastraea-Theorie, die phylogenetische Classification des Thierreichs und die Homologie der Keimblätter'. Jen Ztts Naturwiss 8: 1–55.

Hake, Sandra B., and C. David Allis. 2006. 'Histone H3 Variants and Their Potential Role in Indexing Mammalian Genomes: The "H3 Barcode Hypothesis"'. Proceedings of the National Academy of Sciences of the United States of America 103(17): 6428–35. doi:10.1073/pnas.0600803103.

Hake, Sandra B., Benjamin A. Garcia, Elizabeth M. Duncan, Monika Kauer, Graham Dellaire, Jeffrey Shabanowitz, David P. Bazett-Jones, C. David Allis, and Donald F. Hunt. 2006. 'Expression Patterns and Post-Translational Modifications Associated with Mammalian Histone H3 Variants'. The Journal of Biological Chemistry 281(1): 559–68. doi:10.1074/jbc.M509266200.

Halazonetis, Thanos D., Vassilis G. Gorgoulis, and Jiri Bartek. 2008. 'An Oncogene-Induced DNA Damage Model for Cancer Development'. Science (New York, N.Y.) 319(5868): 1352–55. doi:10.1126/science.1140735.

Halliwell, Jason Alexander, Javier Martin-Gonzalez, Adnan Hashim, John Arne Dahl, Eva R. Hoffmann, and Mads Lerdrup. 2024. 'Sex-Specific DNA-Replication in the Early Mammalian Embryo'. Nature Communications 15(1): 6323. doi:10.1038/s41467-024-50727-w.

Hanahan, Douglas. 2022. 'Hallmarks of Cancer: New Dimensions'. Cancer Discovery 12(1): 31–46. doi:10.1158/2159-8290.CD-21-1059.

Hanna, Courtney W., Aaron Taudt, Jiahao Huang, Lenka Gahurova, Andrea Kranz, Simon Andrews, Wendy Dean, et al. 2018. 'MLL2 Conveys Transcription-Independent H3K4 Trimethylation in Oocytes'. Nature Structural & Molecular Biology 25(1): 73–82. doi:10.1038/s41594-017-0013-5.

Hansen, Anders S., Tsung-Han S. Hsieh, Claudia Cattoglio, Iryna Pustova, Ricardo Saldaña-Meyer, Danny Reinberg, Xavier Darzacq, and Robert Tjian. 2019. 'Distinct Classes of Chromatin Loops

Revealed by Deletion of an RNA-Binding Region in CTCF'. Molecular Cell 76(3): 395-411.e13. doi:10.1016/j.molcel.2019.07.039.

Harfe, Brian D., Ana Vaz Gomes, Cynthia Kenyon, Jun Liu, Michael Krause, and Andrew Fire. 1998. 'Analysis of a Caenorhabditis Elegans Twist Homolog Identifies Conserved and Divergent Aspects of Mesodermal Patterning'. Genes & Development 12(16): 2623–35.

Harrington, Michael J., Elim Hong, and Rachel Brewster. 2009. 'Comparative Analysis of Neurulation: First Impressions Do Not Count'. Molecular Reproduction and Development 76(10): 954–65. doi:10.1002/mrd.21085.

Harutyunyan, Ashot S., Brian Krug, Haifen Chen, Simon Papillon-Cavanagh, Michele Zeinieh, Nicolas De Jay, Shriya Deshmukh, et al. 2019. 'H3K27M Induces Defective Chromatin Spread of PRC2-Mediated Repressive H3K27me2/Me3 and Is Essential for Glioma Tumorigenesis'. Nature Communications 10(1): 1262. doi:10.1038/s41467-019-09140-x.

Hasson, Dan, Tanya Panchenko, Kevan J. Salimian, Mishah U. Salman, Nikolina Sekulic, Alicia Alonso, Peter E. Warburton, and Ben E. Black. 2013. 'The Octamer Is the Major Form of CENP-A Nucleosomes at Human Centromeres'. Nature Structural & Molecular Biology 20(6): 687–95. doi:10.1038/nsmb.2562.

Hay, E. D. 1958. 'The Fine Structure of Blastema Cells and Differentiating Cartilage Cells in Regenerating Limbs of Amblystoma Larvae'. The Journal of Biophysical and Biochemical Cytology 4(5): 583–91. doi:10.1083/jcb.4.5.583.

Hay, E. D. 1968. Epithelial–Mesenchymal Interactions: 18th Hahnemann Symposium (Eds R. Fleischmajer & Billingham, R. E.). Williams and Wilkins c°.

Hay, E. D. 1990. 'Role of Cell-Matrix Contacts in Cell Migration and Epithelial-Mesenchymal Transformation'. Cell Differentiation and Development: The Official Journal of the International Society of Developmental Biologists 32(3): 367–75. doi:10.1016/0922-3371(90)90052-x.

Hay, E. D. 1995. 'An Overview of Epithelio-Mesenchymal Transformation'. Acta Anatomica 154(1): 8–20. doi:10.1159/000147748.

Hay, Elizabeth D. 2005. 'The Mesenchymal Cell, Its Role in the Embryo, and the Remarkable Signaling Mechanisms That Create It'. Developmental Dynamics: An Official Publication of the American Association of Anatomists 233(3): 706–20. doi:10.1002/dvdy.20345.

Hayden, Karen E., Erin D. Strome, Stephanie L. Merrett, Hye-Ran Lee, M. Katharine Rudd, and Huntington F. Willard. 2013. 'Sequences Associated with Centromere Competency in the Human Genome'. Molecular and Cellular Biology 33(4): 763–72. doi:10.1128/MCB.01198-12.

Hédouin, Sabrine, Giacomo Grillo, Ivana Ivkovic, Guillaume Velasco, and Claire Francastel. 2017. 'CENP-A Chromatin Disassembly in Stressed and Senescent Murine Cells'. Scientific Reports 7(1): 42520. doi:10.1038/srep42520.

van der Heijden, Godfried W., Jürgen W. Dieker, Alwin A. H. A. Derijck, Sylviane Muller, Jo H. M. Berden, Didi D. M. Braat, Johan van der Vlag, and Peter de Boer. 2005. 'Asymmetry in Histone H3 Variants and Lysine Methylation between Paternal and Maternal Chromatin of the Early Mouse Zygote'. Mechanisms of Development 122(9): 1008–22. doi:10.1016/j.mod.2005.04.009.

Heintzman, Nathaniel D., Gary C. Hon, R. David Hawkins, Pouya Kheradpour, Alexander Stark, Lindsey F. Harp, Zhen Ye, et al. 2009. 'Histone Modifications at Human Enhancers Reflect Global Cell-Type-Specific Gene Expression'. Nature 459(7243): 108–12. doi:10.1038/nature07829.

Heitz, E. 1928. 'Heitz: "Das" Heterochromatin Der Moose - Google Scholar'. https://scholar.google.com/scholar_lookup?journal=Jahrb+Wiss+Botanik&title=Das+Heterochromatin+der+Moose&volume=69&publication_year=1928&pages=762-818& (September 6, 2024).

Helfricht, Angela, Wouter W. Wiegant, Peter E. Thijssen, Alfred C. Vertegaal, Martijn S. Luijsterburg, and Haico van Attikum. 2013. 'Remodeling and Spacing Factor 1 (RSF1) Deposits Centromere Proteins at DNA Double-Strand Breaks to Promote Non-Homologous End-Joining'. Cell Cycle (Georgetown, Tex.) 12(18): 3070–82. doi:10.4161/cc.26033.

Hendrix, M. J., E. A. Seftor, R. E. Seftor, and K. T. Trevor. 1997. 'Experimental Co-Expression of Vimentin and Keratin Intermediate Filaments in Human Breast Cancer Cells Results in Phenotypic Interconversion and Increased Invasive Behavior.' The American Journal of Pathology 150(2): 483–95.

Henikoff, Jorja G., Jitendra Thakur, Sivakanthan Kasinathan, and Steven Henikoff. 2015. 'A Unique Chromatin Complex Occupies Young α-Satellite Arrays of Human Centromeres'. Science Advances 1(1): e1400234. doi:10.1126/sciadv.1400234.

Henikoff, S., K. Ahmad, and H. S. Malik. 2001. 'The Centromere Paradox: Stable Inheritance with Rapidly Evolving DNA'. Science (New York, N.Y.) 293(5532): 1098–1102. doi:10.1126/science.1062939.

Hennessy, Bryan T., Ana-Maria Gonzalez-Angulo, Katherine Stemke-Hale, Michael Z. Gilcrease, Savitri Krishnamurthy, Ju-Seog Lee, Jane Fridlyand, et al. 2009. 'Characterization of a Naturally Occurring Breast Cancer Subset Enriched in Epithelial-to-Mesenchymal Transition and Stem Cell Characteristics'. Cancer Research 69(10): 4116–24. doi:10.1158/0008-5472.CAN-08-3441.

Hermida, Miguel A., J. Dinesh Kumar, and Nick R. Leslie. 2017. 'GSK3 and Its Interactions with the PI3K/AKT/mTOR Signalling Network'. Advances in Biological Regulation 65: 5–15. doi:10.1016/j.jbior.2017.06.003.

Herranz, Nicolás, Diego Pasini, Víctor M. Díaz, Clara Francí, Arantxa Gutierrez, Natàlia Dave, Maria Escrivà, et al. 2008. 'Polycomb Complex 2 Is Required for E-Cadherin Repression by the Snail1 Transcription Factor'. Molecular and Cellular Biology 28(15): 4772–81. doi:10.1128/MCB.00323-08.

Herre, Margaret, and Erica Korb. 2019. 'The Chromatin Landscape of Neuronal Plasticity'. Current Opinion in Neurobiology 59: 79–86. doi:10.1016/j.conb.2019.04.006.

Hewawasam, Geetha S., Mark Mattingly, Swaminathan Venkatesh, Ying Zhang, Laurence Florens, Jerry L. Workman, and Jennifer L. Gerton. 2014. 'Phosphorylation by Casein Kinase 2 Facilitates Psh1 Protein-Assisted Degradation of Cse4 Protein'. The Journal of Biological Chemistry 289(42): 29297–309. doi:10.1074/jbc.M114.580589.

Hewawasam, Geetha, Manjunatha Shivaraju, Mark Mattingly, Swaminathan Venkatesh, Skylar Martin-Brown, Laurence Florens, Jerry L. Workman, and Jennifer L. Gerton. 2010. 'Psh1 Is an E3 Ubiquitin Ligase That Targets the Centromeric Histone Variant Cse4'. Molecular Cell 40(3): 444–54. doi:10.1016/j.molcel.2010.10.014.

Hickman, Emma S, M. Cristina Moroni, and Kristian Helin. 2002. 'The Role of P53 and pRB in Apoptosis and Cancer'. Current Opinion in Genetics & Development 12(1): 60–66. doi:10.1016/S0959-437X(01)00265-9.

Hiew, Michele Sook Yuin, Han Ping Cheng, Chiu-Jung Huang, Kowit Yu Chong, Soon Keng Cheong, Kong Bung Choo, and Tunku Kamarul. 2018. 'Incomplete Cellular Reprogramming of Colorectal Cancer Cells Elicits an Epithelial/Mesenchymal Hybrid Phenotype'. Journal of Biomedical Science 25(1): 57. doi:10.1186/s12929-018-0461-1.

Higgins, Stephen P., Yi Tang, Craig E. Higgins, Badar Mian, Wenzheng Zhang, Ralf-Peter Czekay, Rohan Samarakoon, David J. Conti, and Paul J. Higgins. 2018. 'TGF-B1/P53 Signaling in Renal Fibrogenesis'. Cellular Signalling 43: 1–10. doi:10.1016/j.cellsig.2017.11.005.

Hiratani, Ichiro, Tyrone Ryba, Mari Itoh, Joy Rathjen, Michael Kulik, Bernadett Papp, Eden Fussner, et al. 2010. 'Genome-Wide Dynamics of Replication Timing Revealed by in Vitro Models of Mouse Embryogenesis'. Genome Research 20(2): 155–69. doi:10.1101/gr.099796.109.

Hiratani, Ichiro, Tyrone Ryba, Mari Itoh, Tomoki Yokochi, Michaela Schwaiger, Chia-Wei Chang, Yung Lyou, et al. 2008. 'Global Reorganization of Replication Domains during Embryonic Stem Cell Differentiation'. PLoS biology 6(10): e245. doi:10.1371/journal.pbio.0060245.

Hnisz, Denes, Daniel S. Day, and Richard A. Young. 2016. 'Insulated Neighborhoods: Structural and Functional Units of Mammalian Gene Control'. Cell 167(5): 1188–1200. doi:10.1016/j.cell.2016.10.024.

Hodge, Dayle Q., Jihong Cui, Matthew J. Gamble, and Wenjun Guo. 2018. 'Histone Variant MacroH2A1 Plays an Isoform-Specific Role in Suppressing Epithelial-Mesenchymal Transition'. Scientific Reports 8(1): 841. doi:10.1038/s41598-018-19364-4.

Hödl, Martina, and Konrad Basler. 2009. 'Transcription in the Absence of Histone H3.3'. Current biology: CB 19(14): 1221–26. doi:10.1016/j.cub.2009.05.048.

Hoencamp, Claire, Olga Dudchenko, Ahmed M.O. Elbatsh, Sumitabha Brahmachari, Jonne A. Raaijmakers, Tom van Schaik, Ángela Sedeño Cacciatore, et al. 2021. '3D Genomics across the Tree of Life Identifies Condensin II as a Determinant of Architecture Type'. Science (New York, N.Y.) 372(6545): 984–89. doi:10.1126/science.abe2218.

Hoffmann, Sebastian, Helena M. Izquierdo, Riccardo Gamba, Florian Chardon, Marie Dumont, Veer Keizer, Solène Hervé, et al. 2020. 'A Genetic Memory Initiates the Epigenetic Loop Necessary to Preserve Centromere Position'. The EMBO journal 39(20): e105505. doi:10.15252/embj.2020105505.

Hong, Tian, Kazuhide Watanabe, Catherine Ha Ta, Alvaro Villarreal-Ponce, Qing Nie, and Xing Dai. 2015. 'An Ovol2-Zeb1 Mutual Inhibitory Circuit Governs Bidirectional and Multi-Step Transition between Epithelial and Mesenchymal States'. PLOS Computational Biology 11(11): e1004569. doi:10.1371/journal.pcbi.1004569.

Hooke, R. 1665. Micrographia or Some physiological descriptions of minutes bodies made by magnifying glasses : with observations and inquiries thereupon. https://gallica.bnf.fr/ark:/12148/bpt6k98770v (September 5, 2024).

Horejs, Christine-Maria. 2016. 'Basement Membrane Fragments in the Context of the Epithelial-to-Mesenchymal Transition'. European Journal of Cell Biology 95(11): 427–40. doi:10.1016/j.ejcb.2016.06.002.

Hori, Tetsuya, Miho Amano, Aussie Suzuki, Chelsea B. Backer, Julie P. Welburn, Yimin Dong, Bruce F. McEwen, et al. 2008. 'CCAN Makes Multiple Contacts with Centromeric DNA to Provide Distinct Pathways to the Outer Kinetochore'. Cell 135(6): 1039–52. doi:10.1016/j.cell.2008.10.019.

Hotchkiss, R. D. 1948. 'The Quantitative Separation of Purines, Pyrimidines, and Nucleosides by Paper Chromatography'. The Journal of Biological Chemistry 175(1): 315–32.

Hou, Jian-Mei, Matthew Krebs, Tim Ward, Robert Sloane, Lynsey Priest, Andrew Hughes, Glen Clack, et al. 2011. 'Circulating Tumor Cells as a Window on Metastasis Biology in Lung Cancer'. The American Journal of Pathology 178(3): 989–96. doi:10.1016/j.ajpath.2010.12.003.

Howman, E. V., K. J. Fowler, A. J. Newson, S. Redward, A. C. MacDonald, P. Kalitsis, and K. H. Choo. 2000. 'Early Disruption of Centromeric Chromatin Organization in Centromere Protein A (Cenpa) Null Mice'. Proceedings of the National Academy of Sciences of the United States of America 97(3): 1148–53. doi:10.1073/pnas.97.3.1148.

Hoyt, Savannah J., Jessica M. Storer, Gabrielle A. Hartley, Patrick G. S. Grady, Ariel Gershman, Leonardo G. de Lima, Charles Limouse, et al. 2022. 'From Telomere to Telomere: The Transcriptional and Epigenetic State of Human Repeat Elements'. Science (New York, N.Y.) 376(6588): eabk3112. doi:10.1126/science.abk3112.

Hsu, Dennis Shin-Shian, Hsin-Yi Lan, Chi-Hung Huang, Shyh-Kuan Tai, Shyue-Yih Chang, Tung-Lung Tsai, Cheng-Chi Chang, et al. 2010. 'Regulation of Excision Repair Cross-Complementation Group 1 by Snail Contributes to Cisplatin Resistance in Head and Neck Cancer'. Clinical Cancer Research: An Official Journal of the American Association for Cancer Research 16(18): 4561–71. doi:10.1158/1078-0432.CCR-10-0593.

Hu, Yixin, and Bruce Stillman. 2023. 'Origins of DNA Replication in Eukaryotes'. Molecular Cell 83(3): 352–72. doi:10.1016/j.molcel.2022.12.024.

Huang, Hongda, Caroline B. Strømme, Giulia Saredi, Martina Hödl, Anne Strandsby, Cristina González-Aguilera, Shoudeng Chen, Anja Groth, and Dinshaw J. Patel. 2015. 'A Unique Binding Mode Enables MCM2 to Chaperone Histones H3-H4 at Replication Forks'. Nature Structural & Molecular Biology 22(8): 618–26. doi:10.1038/nsmb.3055.

Huang, R. Y.-J., M. K. Wong, T. Z. Tan, K. T. Kuay, A. H. C. Ng, V. Y. Chung, Y.-S. Chu, et al. 2013. 'An EMT Spectrum Defines an Anoikis-Resistant and Spheroidogenic Intermediate Mesenchymal State That Is Sensitive to e-Cadherin Restoration by a Src-Kinase Inhibitor, Saracatinib (AZD0530)'. Cell Death & Disease 4(11): e915. doi:10.1038/cddis.2013.442.

Huberman, J. A., and A. D. Riggs. 1968. 'On the Mechanism of DNA Replication in Mammalian Chromosomes'. Journal of Molecular Biology 32(2): 327–41. doi:10.1016/0022-2836(68)90013-2.

Hudson, Laurie G., Kimberly M. Newkirk, Heather L. Chandler, Changsun Choi, Stacey L. Fossey, Allison E. Parent, and Donna F. Kusewitt. 2009. 'Cutaneous Wound Reepithelialization Is Compromised in Mice Lacking Functional Slug (Snai2)'. Journal of dermatological science 56(1): 19–26. doi:10.1016/j.jdermsci.2009.06.009.

Huizing, Geert-Jan, Ina Maria Deutschmann, Gabriel Peyré, and Laura Cantini. 2023. 'Paired Single-Cell Multi-Omics Data Integration with Mowgli'. Nature Communications 14(1): 7711. doi:10.1038/s41467-023-43019-2.

Humphreys, Benjamin D., Shuei-Liong Lin, Akio Kobayashi, Thomas E. Hudson, Brian T. Nowlin, Joseph V. Bonventre, M. Todd Valerius, Andrew P. McMahon, and Jeremy S. Duffield. 2010. 'Fate Tracing Reveals the Pericyte and Not Epithelial Origin of Myofibroblasts in Kidney Fibrosis'. The American Journal of Pathology 176(1): 85–97. doi:10.2353/ajpath.2010.090517.

Hüsemann, Yves, Jochen B. Geigl, Falk Schubert, Piero Musiani, Manfred Meyer, Elke Burghart, Guido Forni, et al. 2008. 'Systemic Spread Is an Early Step in Breast Cancer'. Cancer Cell 13(1): 58–68. doi:10.1016/j.ccr.2007.12.003.

Hwang, Jiang, Yang, Huang, Lan, Teng, Yang, et al. 2014. 'MicroRNA-146a Directs the Symmetric Division of Snail-Dominant Colorectal Cancer Stem Cells'. Nature cell biology 16(3). doi:10.1038/ncb2910.

Ieda, Takeshi, Hiroshi Tazawa, Hiroki Okabayashi, Shuya Yano, Kunitoshi Shigeyasu, Shinji Kuroda, Toshiaki Ohara, et al. 2019. 'Visualization of Epithelial-Mesenchymal Transition in an Inflammatory Microenvironment-Colorectal Cancer Network'. Scientific Reports 9(1): 16378. doi:10.1038/s41598-019-52816-z.

Ilina, Olgae, and Peter Friedl. 2009. 'Mechanisms of Collective Cell Migration at a Glance'. Journal of cell science 122(Pt 18). doi:10.1242/jcs.036525.

Imre, László, Zoltán Simándi, Attila Horváth, György Fenyőfalvi, Péter Nánási, Erfaneh Firouzi Niaki, Éva Hegedüs, et al. 2017. 'Nucleosome Stability Measured in Situ by Automated Quantitative Imaging'. Scientific Reports 7(1): 12734. doi:10.1038/s41598-017-12608-9.

Ishikawa, S., H. Kaneko, T. Sumida, and M. Sekiya. 1979. 'Ultrastructure of Mesodermal Mixed Tumor of the Uterus'. Acta Pathologica Japonica 29(5): 801–9. doi:10.1111/j.1440-1827.1979.tb00945.x.

Ivan, M., K. Kondo, H. Yang, W. Kim, J. Valiando, M. Ohh, A. Salic, et al. 2001. 'HIFalpha Targeted for VHL-Mediated Destruction by Proline Hydroxylation: Implications for O2 Sensing'. Science (New York, N.Y.) 292(5516): 464–68. doi:10.1126/science.1059817.

Iwano, Masayuki, David Plieth, Theodore M. Danoff, Chengsen Xue, Hirokazu Okada, and Eric G. Neilson. 2002. 'Evidence That Fibroblasts Derive from Epithelium during Tissue Fibrosis'. The Journal of Clinical Investigation 110(3): 341–50. doi:10.1172/JCI15518.

Iwata-Otsubo, Aiko, Jennine M. Dawicki-McKenna, Takashi Akera, Samantha J. Falk, Lukáš Chmátal, Karren Yang, Beth A. Sullivan, et al. 2017. 'Expanded Satellite Repeats Amplify a Discrete CENP-A Nucleosome Assembly Site on Chromosomes That Drive in Female Meiosis'. Current biology: CB 27(15): 2365-2373.e8. doi:10.1016/j.cub.2017.06.069.

Jackson, V. 1988. 'Deposition of Newly Synthesized Histones: Hybrid Nucleosomes Are Not Tandemly Arranged on Daughter DNA Strands'. Biochemistry 27(6): 2109–20. doi:10.1021/bi00406a044.

Jackson, V., and R. Chalkley. 1985. 'Histone Segregation on Replicating Chromatin'. Biochemistry 24(24): 6930–38. doi:10.1021/bi00345a027.

Jackson, V., A. Shires, N. Tanphaichitr, and R. Chalkley. 1976. 'Modifications to Histones Immediately after Synthesis'. Journal of Molecular Biology 104(2): 471–83. doi:10.1016/0022-2836(76)90282-5.

Jain, Abhinav K., and Michelle Craig Barton. 2018. 'P53: Emerging Roles in Stem Cells, Development and Beyond'. Development (Cambridge, England) 145(8): dev158360. doi:10.1242/dev.158360.

Jalali, Azadeh, Xiujuan Zhu, ChangChih Liu, and Ali Nawshad. 2012. 'Induction of Palate Epithelial Mesenchymal Transition (EMT) by Transforming Growth Factor β (TGF) 3 Signaling'. Development, growth & differentiation 54(6): 633–48. doi:10.1111/j.1440-169X.2012.01364.x.

Janda, Elzbieta, Kerstin Lehmann, Iris Killisch, Martin Jechlinger, Michaela Herzig, Julian Downward, Hartmut Beug, and Stefan Grünert. 2002. 'Ras and TGF[Beta] Cooperatively Regulate Epithelial Cell Plasticity and Metastasis: Dissection of Ras Signaling Pathways'. The Journal of Cell Biology 156(2): 299–313. doi:10.1083/jcb.200109037.

Jang, Chuan-Wei, Yoichiro Shibata, Joshua Starmer, Della Yee, and Terry Magnuson. 2015. 'Histone H3.3 Maintains Genome Integrity during Mammalian Development'. Genes & Development 29(13): 1377–92. doi:10.1101/gad.264150.115.

Jansen, Lars E. T., Ben E. Black, Daniel R. Foltz, and Don W. Cleveland. 2007. 'Propagation of Centromeric Chromatin Requires Exit from Mitosis'. The Journal of Cell Biology 176(6): 795–805. doi:10.1083/jcb.200701066.

Jansz, Natasha, and Maria-Elena Torres-Padilla. 2019. 'Genome Activation and Architecture in the Early Mammalian Embryo'. Current Opinion in Genetics & Development 55: 52–58. doi:10.1016/j.gde.2019.04.011.

Jeffery, Daniel, Alberto Gatto, Katrina Podsypanina, Charlène Renaud-Pageot, Rebeca Ponce Landete, Lorraine Bonneville, Marie Dumont, Daniele Fachinetti, and Geneviève Almouzni. 2021. 'CENP-A Overexpression Promotes Distinct Fates in Human Cells, Depending on P53 Status'. Communications Biology 4(1): 1–18. doi:10.1038/s42003-021-01941-5.

Jenuwein, T., and C. D. Allis. 2001. 'Translating the Histone Code'. Science (New York, N.Y.) 293(5532): 1074–80. doi:10.1126/science.1063127.

Jessa, Selin, Abdulshakour Mohammadnia, Ashot S. Harutyunyan, Maud Hulswit, Srinidhi Varadharajan, Hussein Lakkis, Nisha Kabir, et al. 2022. 'K27M in Canonical and Noncanonical H3 Variants Occurs in Distinct Oligodendroglial Cell Lineages in Brain Midline Gliomas'. Nature Genetics 54(12): 1865–80. doi:10.1038/s41588-022-01205-w.

Jiang, Wei, Yaqing Zhang, Kevin T. Kane, Meredith A. Collins, Diane M. Simeone, Marina Pasca di Magliano, and Kevin Tri Nguyen. 2015. 'CD44 Regulates Pancreatic Cancer Invasion through MT1-MMP'. Molecular cancer research: MCR 13(1): 9–15. doi:10.1158/1541-7786.MCR-14-0076.

Jiang, Xiaoying. 2023. 'The Mechanisms and Therapeutic Potential of Long Noncoding RNA NEAT1 in Fibrosis'. Clinical and Experimental Medicine 23(7): 3339–47. doi:10.1007/s10238-023-01191-1.

Jiu, Yaming, Jaakko Lehtimäki, Sari Tojkander, Fang Cheng, Harri Jäälinoja, Xiaonan Liu, Markku Varjosalo, John E. Eriksson, and Pekka Lappalainen. 2015. 'Bidirectional Interplay between Vimentin

Intermediate Filaments and Contractile Actin Stress Fibers'. Cell Reports 11(10): 1511–18. doi:10.1016/j.celrep.2015.05.008.

Johannsen, W. 1909. Elemente der exakten Erblichkeitslehre. Cambridge University Press.

Jolly, Mohit Kumar, Satyendra C. Tripathi, Dongya Jia, Steven M. Mooney, Muge Celiktas, Samir M. Hanash, Sendurai A. Mani, et al. 2016. 'Stability of the Hybrid Epithelial/Mesenchymal Phenotype'. Oncotarget 7(19): 27067–84. doi:10.18632/oncotarget.8166.

Jordan, Nicole Vincent, Gary L Johnson, and Amy N Abell. 2011. 'Tracking the Intermediate Stages of Epithelial-Mesenchymal Transition in Epithelial Stem Cells and Cancer'. Cell Cycle 10(17): 2865–73. doi:10.4161/cc.10.17.17188.

Kaartinen, V., J. W. Voncken, C. Shuler, D. Warburton, D. Bu, N. Heisterkamp, and J. Groffen. 1995. 'Abnormal Lung Development and Cleft Palate in Mice Lacking TGF-Beta 3 Indicates Defects of Epithelial-Mesenchymal Interaction'. Nature Genetics 11(4): 415–21. doi:10.1038/ng1295-415.

Kajiyama, Shibata, Terauchi, Yamashita, Ino, Nawa, and Kikkawa. 2007. 'Chemoresistance to Paclitaxel Induces Epithelial-Mesenchymal Transition and Enhances Metastatic Potential for Epithelial Ovarian Carcinoma Cells'. International journal of oncology 31(2). https://pubmed.ncbi.nlm.nih.gov/17611683/ (September 4, 2024).

Kallergi, Galatea, Harris Markomanolaki, Vicky Giannoukaraki, Maria A. Papadaki, Areti Strati, Evi S. Lianidou, Vassilis Georgoulias, Dimitris Mavroudis, and Sofia Agelaki. 2009. 'Hypoxia-Inducible Factor-1alpha and Vascular Endothelial Growth Factor Expression in Circulating Tumor Cells of Breast Cancer Patients'. Breast cancer research: BCR 11(6): R84. doi:10.1186/bcr2452.

Kara, Nihan, Manzar Hossain, Supriya G. Prasanth, and Bruce Stillman. 2015. 'Orc1 Binding to Mitotic Chromosomes Precedes Spatial Patterning during G1 Phase and Assembly of the Origin Recognition Complex in Human Cells'. The Journal of Biological Chemistry 290(19): 12355–69. doi:10.1074/jbc.M114.625012.

Kariya, Yoshinobu, Midori Oyama, Takato Suzuki, and Yukiko Kariya. 2021. 'Avβ3 Integrin Induces Partial EMT Independent of TGF-β Signaling'. Communications Biology 4: 490. doi:10.1038/s42003-021-02003-6.

Karpen, G. H., and R. C. Allshire. 1997. 'The Case for Epigenetic Effects on Centromere Identity and Function'. Trends in genetics: TIG 13(12): 489–96. doi:10.1016/s0168-9525(97)01298-5.

Kastan, M. B., O. Onyekwere, D. Sidransky, B. Vogelstein, and R. W. Craig. 1991. 'Participation of P53 Protein in the Cellular Response to DNA Damage'. Cancer Research 51(23 Pt 1): 6304–11.

Katainen, Riku, Kashyap Dave, Esa Pitkänen, Kimmo Palin, Teemu Kivioja, Niko Välimäki, Alexandra E. Gylfe, et al. 2015. 'CTCF/Cohesin-Binding Sites Are Frequently Mutated in Cancer'. Nature Genetics 47(7): 818–21. doi:10.1038/ng.3335.

Kato, Hidenori, Jiansheng Jiang, Bing-Rui Zhou, Marieke Rozendaal, Hanqiao Feng, Rodolfo Ghirlando, T. Sam Xiao, Aaron F. Straight, and Yawen Bai. 2013. 'A Conserved Mechanism for Centromeric Nucleosome Recognition by Centromere Protein CENP-C'. Science (New York, N.Y.) 340(6136): 1110–13. doi:10.1126/science.1235532.

Katsuno, Yuko, Ayumi Suzuki, Kazuto Sugimura, Katsuzumi Okumura, Doaa H. Zineldeen, Midori Shimada, Hiroyuki Niida, et al. 2009. 'Cyclin A-Cdk1 Regulates the Origin Firing Program in Mammalian Cells'. Proceedings of the National Academy of Sciences of the United States of America 106(9): 3184–89. doi:10.1073/pnas.0809350106.

Ke, Xi-Song, Yi Qu, Yang Cheng, Wen-Cheng Li, Varda Rotter, Anne Margrete Øyan, and Karl-Henning Kalland. 2010. 'Global Profiling of Histone and DNA Methylation Reveals Epigenetic-Based Regulation of Gene Expression during Epithelial to Mesenchymal Transition in Prostate Cells'. BMC Genomics 11(1): 669. doi:10.1186/1471-2164-11-669.

Kemp, Christopher J., James M. Moore, Russell Moser, Brady Bernard, Matt Teater, Leslie E. Smith, Natalia Rabaia, et al. 2014. 'CTCF Haploinsufficiency Destabilizes DNA Methylation and Predisposes to Cancer'. Cell reports 7(4): 1020–29. doi:10.1016/j.celrep.2014.04.004.

Kempfer, Rieke, and Ana Pombo. 2020. 'Methods for Mapping 3D Chromosome Architecture'. Nature Reviews. Genetics 21(4): 207–26. doi:10.1038/s41576-019-0195-2.

Khanin, Raya, and Veronica Vinciotti. 2008. 'Computational Modeling of Post-Transcriptional Gene Regulation by microRNAs'. Journal of Computational Biology: A Journal of Computational Molecular Cell Biology 15(3): 305–16. doi:10.1089/cmb.2007.0184.

Khoo, Bee Luan, Soo Chin Lee, Prashant Kumar, Tuan Zea Tan, Majid Ebrahimi Warkiani, Samuel G. W. Ow, Sayantani Nandi, Chwee Teck Lim, and Jean Paul Thiery. 2015. 'Short-Term Expansion of Breast Circulating Cancer Cells Predicts Response to Anti-Cancer Therapy'. Oncotarget 6(17): 15578–93. doi:10.18632/oncotarget.3903.

Khuong-Quang, Dong-Anh, Pawel Buczkowicz, Patricia Rakopoulos, Xiao-Yang Liu, Adam M. Fontebasso, Eric Bouffet, Ute Bartels, et al. 2012. 'K27M Mutation in Histone H3.3 Defines Clinically and Biologically Distinct Subgroups of Pediatric Diffuse Intrinsic Pontine Gliomas'. Acta Neuropathologica 124(3): 439–47. doi:10.1007/s00401-012-0998-0.

Kim, Kevin K., Matthias C. Kugler, Paul J. Wolters, Liliane Robillard, Michael G. Galvez, Alexis N. Brumwell, Dean Sheppard, and Harold A. Chapman. 2006. 'Alveolar Epithelial Cell Mesenchymal Transition Develops in Vivo during Pulmonary Fibrosis and Is Regulated by the Extracellular Matrix'. Proceedings of the National Academy of Sciences of the United States of America 103(35): 13180–85. doi:10.1073/pnas.0605669103.

Kinkade, J.M., and R. David Cole. 1966. ‘A Structural Comparison of Different Lysine-Rich Histones of Calf Thymus’. Journal of Biological Chemistry 241(24): 5798–5805. doi:10.1016/S0021-9258(18)96343-X.

Kitagawa, Teppei, Kojiro Ishii, Kojiro Takeda, and Tomohiro Matsumoto. 2014. ‘The 19S Proteasome Subunit Rpt3 Regulates Distribution of CENP-A by Associating with Centromeric Chromatin’. Nature Communications 5: 3597. doi:10.1038/ncomms4597.

Klare, Kerstin, John R. Weir, Federica Basilico, Tomasz Zimniak, Lucia Massimiliano, Nina Ludwigs, Franz Herzog, and Andrea Musacchio. 2015. ‘CENP-C Is a Blueprint for Constitutive Centromere-Associated Network Assembly within Human Kinetochores’. The Journal of Cell Biology 210(1): 11–22. doi:10.1083/jcb.201412028.

Klaus, Alexandra, and Walter Birchmeier. 2008. ‘Wnt Signalling and Its Impact on Development and Cancer’. Nature Reviews. Cancer 8(5): 387–98. doi:10.1038/nrc2389.

Knutson, Keith L., Hailing Lu, Brad Stone, Jennifer M. Reiman, Marshall D. Behrens, Christine M. Prosperi, Ekram A. Gad, Arianna Smorlesi, and Mary L. Disis. 2006. ‘Immunoediting of Cancers May Lead to Epithelial to Mesenchymal Transition’. Journal of Immunology (Baltimore, Md.: 1950) 177(3): 1526–33. doi:10.4049/jimmunol.177.3.1526.

Koch, Linda. 2022. ‘DNA Replication in Cell Fate Reprogramming’. Nature Reviews. Genetics 23(5): 264. doi:10.1038/s41576-022-00474-9.

Kodama, Takahiro, Tetsuo Takehara, Hayato Hikita, Satoshi Shimizu, Minoru Shigekawa, Hinako Tsunematsu, Wei Li, et al. 2011. ‘Increases in P53 Expression Induce CTGF Synthesis by Mouse and Human Hepatocytes and Result in Liver Fibrosis in Mice’. The Journal of Clinical Investigation 121(8): 3343–56. doi:10.1172/JCI44957.

Köhler, G., and C. Milstein. 1975. ‘Continuous Cultures of Fused Cells Secreting Antibody of Predefined Specificity’. Nature 256(5517): 495–97. doi:10.1038/256495a0.

Kolijn, Kimberley, Esther I. Verhoef, and Geert J. L. H. van Leenders. 2015. ‘Morphological and Immunohistochemical Identification of Epithelial-to-Mesenchymal Transition in Clinical Prostate Cancer’. Oncotarget 6(27): 24488–98. doi:10.18632/oncotarget.4177.

Kong, Dejuan, Sanjeev Banerjee, Aamir Ahmad, Yiwei Li, Zhiwei Wang, Seema Sethi, and Fazlul Sarkar. 2010. ‘Epithelial to Mesenchymal Transition Is Mechanistically Linked with Stem Cell Signatures in Prostate Cancer Cells’. PloS one 5(8). doi:10.1371/journal.pone.0012445.

Kopan, Raphael. 2002. ‘Notch: A Membrane-Bound Transcription Factor’. Journal of Cell Science 115(Pt 6): 1095–97. doi:10.1242/jcs.115.6.1095.

Kornberg, R. D. 1974. ‘Chromatin Structure: A Repeating Unit of Histones and DNA’. Science (New York, N.Y.) 184(4139): 868–71. doi:10.1126/science.184.4139.868.

Korpal, Manav, Esther S. Lee, Guohong Hu, and Yibin Kang. 2008. 'The miR-200 Family Inhibits Epithelial-Mesenchymal Transition and Cancer Cell Migration by Direct Targeting of E-Cadherin Transcriptional Repressors ZEB1 and ZEB2'. The Journal of Biological Chemistry 283(22): 14910–14. doi:10.1074/jbc.C800074200.

Kortlever, Roderik M., Paul J. Higgins, and René Bernards. 2006. 'Plasminogen Activator Inhibitor-1 Is a Critical Downstream Target of P53 in the Induction of Replicative Senescence'. Nature Cell Biology 8(8): 877–84. doi:10.1038/ncb1448.

Kossel, A. 1884. The protamines and histones. https://scholar.google.com/scholar_lookup?journal=H-S.+Z.+Physiol.+Chem&title=On+protamines+and+histones&author=A+Kossel&author=H+Pringle&volume=49&publication_year=1906&pages=301-321& (August 10, 2024).

Koundrioukoff, S., Z. O. Jónsson, S. Hasan, R. N. de Jong, P. C. van der Vliet, M. O. Hottiger, and U. Hübscher. 2000. 'A Direct Interaction between Proliferating Cell Nuclear Antigen (PCNA) and Cdk2 Targets PCNA-Interacting Proteins for Phosphorylation'. The Journal of Biological Chemistry 275(30): 22882–87. doi:10.1074/jbc.M001850200.

Krebs, Angela M., Julia Mitschke, María Lasierra Losada, Otto Schmalhofer, Melanie Boerries, Hauke Busch, Martin Boettcher, et al. 2017. 'The EMT-Activator Zeb1 Is a Key Factor for Cell Plasticity and Promotes Metastasis in Pancreatic Cancer'. Nature Cell Biology 19(5): 518–29. doi:10.1038/ncb3513.

Krijger, Peter H. L., and Wouter de Laat. 2013. 'Identical Cells with Different 3D Genomes; Cause and Consequences?' Current Opinion in Genetics & Development 23(2): 191–96. doi:10.1016/j.gde.2012.12.010.

Krishnamachary, Balaji, David Zagzag, Hideko Nagasawa, Karin Rainey, Hiroaki Okuyama, Jin H. Baek, and Gregg L. Semenza. 2006. 'Hypoxia-Inducible Factor-1-Dependent Repression of E-Cadherin in von Hippel-Lindau Tumor Suppressor-Null Renal Cell Carcinoma Mediated by TCF3, ZFHX1A, and ZFHX1B'. Cancer Research 66(5): 2725–31. doi:10.1158/0008-5472.CAN-05-3719.

Krol, Ilona, Francesc Castro-Giner, Martina Maurer, Sofia Gkountela, Barbara Maria Szczerba, Ramona Scherrer, Niamh Coleman, et al. 2018. 'Detection of Circulating Tumour Cell Clusters in Human Glioblastoma'. British Journal of Cancer 119(4): 487–91. doi:10.1038/s41416-018-0186-7.

Kudo-Saito, Chie, Hiromi Shirako, Tadashi Takeuchi, and Yutaka Kawakami. 2009. 'Cancer Metastasis Is Accelerated through Immunosuppression during Snail-Induced EMT of Cancer Cells'. Cancer Cell 15(3): 195–206. doi:10.1016/j.ccr.2009.01.023.

Kursel, Lisa E, Hannah McConnell, Aida Flor A de la Cruz, and Harmit S Malik. 2021. 'Gametic Specialization of Centromeric Histone Paralogs in Drosophila Virilis'. Life Science Alliance 4(7): e202000992. doi:10.26508/lsa.202000992.

Kyriacou, Eftychia, and Patrick Heun. 2018. ‘High-Resolution Mapping of Centromeric Protein Association Using APEX-Chromatin Fibers’. Epigenetics & Chromatin 11(1): 68. doi:10.1186/s13072-018-0237-6.

Lachner, Monika, and Thomas Jenuwein. 2002. ‘The Many Faces of Histone Lysine Methylation’. Current Opinion in Cell Biology 14(3): 286–98. doi:10.1016/s0955-0674(02)00335-6.

Lacoste, Nicolas, Adam Woolfe, Hiroaki Tachiwana, Ana Villar Garea, Teresa Barth, Sylvain Cantaloube, Hitoshi Kurumizaka, Axel Imhof, and Geneviève Almouzni. 2014. ‘Mislocalization of the Centromeric Histone Variant CenH3/CENP-A in Human Cells Depends on the Chaperone DAXX’. Molecular Cell 53(4): 631–44. doi:10.1016/j.molcel.2014.01.018.

Lagana, Anaïck, Jonas F. Dorn, Valérie De Rop, Anne-Marie Ladouceur, Amy S. Maddox, and Paul S. Maddox. 2010. ‘A Small GTPase Molecular Switch Regulates Epigenetic Centromere Maintenance by Stabilizing Newly Incorporated CENP-A’. Nature Cell Biology 12(12): 1186–93. doi:10.1038/ncb2129.

Lam, Ai Leen, Christopher D. Boivin, Caitlin F. Bonney, M. Katharine Rudd, and Beth A. Sullivan. 2006. ‘Human Centromeric Chromatin Is a Dynamic Chromosomal Domain That Can Spread over Noncentromeric DNA’. Proceedings of the National Academy of Sciences of the United States of America 103(11): 4186–91. doi:10.1073/pnas.0507947103.

Lambert, Arthur W., Diwakar R. Pattabiraman, and Robert A. Weinberg. 2017. ‘Emerging Biological Principles of Metastasis’. Cell 168(4): 670–91. doi:10.1016/j.cell.2016.11.037.

Lambuta, Ruxandra A., Luca Nanni, Yuanlong Liu, Juan Diaz-Miyar, Arvind Iyer, Daniele Tavernari, Natalya Katanayeva, Giovanni Ciriello, and Elisa Oricchio. 2023. ‘Whole-Genome Doubling Drives Oncogenic Loss of Chromatin Segregation’. Nature 615(7954): 925–33. doi:10.1038/s41586-023-05794-2.

Lamouille, Samy, Deepa Subramanyam, Robert Blelloch, and Rik Derynck. 2013. ‘Regulation of Epithelial-Mesenchymal and Mesenchymal-Epithelial Transitions by microRNAs’. Current Opinion in Cell Biology 25(2): 200–207. doi:10.1016/j.ceb.2013.01.008.

Lamouille, Samy, Jian Xu, and Rik Derynck. 2014. ‘Molecular Mechanisms of Epithelial-Mesenchymal Transition’. Nature Reviews. Molecular Cell Biology 15(3): 178–96. doi:10.1038/nrm3758.

Lamm, E., Harman, O. 2020. Before Watson and Crick in 1953 Came Friedrich Miescher in 1869. Genetics 215(2): 291-296. doi:10.1534/genetics.120.303195.

Lando, David, Ulrike Endesfelder, Harald Berger, Lakxmi Subramanian, Paul D. Dunne, James McColl, David Klenerman, et al. 2012. ‘Quantitative Single-Molecule Microscopy Reveals That CENP-A(Cnp1) Deposition Occurs during G2 in Fission Yeast’. Open Biology 2(7): 120078. doi:10.1098/rsob.120078.

Lane, D. P. 1992. ‘Cancer. P53, Guardian of the Genome’. Nature 358(6381): 15–16. doi:10.1038/358015a0.

Langer, P. R., A. A. Waldrop, and D. C. Ward. 1981. ‘Enzymatic Synthesis of Biotin-Labeled Polynucleotides: Novel Nucleic Acid Affinity Probes’. Proceedings of the National Academy of Sciences of the United States of America 78(11): 6633–37. doi:10.1073/pnas.78.11.6633.

Lanier, M. Hunter, Taekyung Kim, and John A. Cooper. 2015. ‘CARMIL2 Is a Novel Molecular Connection between Vimentin and Actin Essential for Cell Migration and Invadopodia Formation’. Molecular Biology of the Cell 26(25): 4577–88. doi:10.1091/mbc.E15-08-0552.

Laskey, Ronald A., Anthony D. Mills, and N. Ronald Morris. 1977. ‘Assembly of SV40 Chromatin in a Cell-Free System from Xenopus Eggs’. Cell 10(2): 237–43. doi:10.1016/0092-8674(77)90217-3.

Laursen, Shawn P., Samuel Bowerman, and Karolin Luger. 2021. ‘Archaea: The Final Frontier of Chromatin’. Journal of Molecular Biology 433(6): 166791. doi:10.1016/j.jmb.2020.166791.

Lawrence, J. B., R. H. Singer, and L. M. Marselle. 1989. ‘Highly Localized Tracks of Specific Transcripts within Interphase Nuclei Visualized by in Situ Hybridization’. Cell 57(3): 493–502. doi:10.1016/0092-8674(89)90924-0.

Lawrence, J. B., R. H. Singer, C. A. Villnave, J. L. Stein, and G. S. Stein. 1988. ‘Intracellular Distribution of Histone mRNAs in Human Fibroblasts Studied by in Situ Hybridization’. Proceedings of the National Academy of Sciences of the United States of America 85(2): 463–67. doi:10.1073/pnas.85.2.463.

Lebeau, Benjamin, Maïka Jangal, Tiejun Zhao, Cheng Kit Wong, Nolan Wong, Eduardo Cepeda Cañedo, Steven Hébert, et al. 2022. ‘3D Chromatin Remodeling Potentiates Transcriptional Programs Driving Cell Invasion’. Proceedings of the National Academy of Sciences of the United States of America 119(36): e2203452119. doi:10.1073/pnas.2203452119.

LeBleu, Valerie S., Gangadhar Taduri, Joyce O’Connell, Yingqi Teng, Vesselina G. Cooke, Craig Woda, Hikaru Sugimoto, and Raghu Kalluri. 2013. ‘Origin and Function of Myofibroblasts in Kidney Fibrosis’. Nature Medicine 19(8): 1047–53. doi:10.1038/nm.3218.

Lee, Dung-Fang, Jie Su, Yen-Sin Ang, Xonia Carvajal-Vergara, Sonia Mulero-Navarro, Carlos F. Pereira, Julian Gingold, et al. 2012. ‘Regulation of Embryonic and Induced Pluripotency by Aurora Kinase-P53 Signaling’. Cell Stem Cell 11(2): 179–94. doi:10.1016/j.stem.2012.05.020.

Lee, Seulki, Eun Ji Choi, Eun Ju Cho, Yun Bin Lee, Jeong-Hoon Lee, Su Jong Yu, Jung-Hwan Yoon, and Yoon Jun Kim. 2020. ‘Inhibition of PI3K/Akt Signaling Suppresses Epithelial-to-Mesenchymal Transition in Hepatocellular Carcinoma through the Snail/GSK-3/Beta-Catenin Pathway’. Clinical and Molecular Hepatology 26(4): 529–39. doi:10.3350/cmh.2019.0056n.

Lehnertz, Bernhard, Yoshihide Ueda, Alwin A. H. A. Derijck, Ulrich Braunschweig, Laura Perez-Burgos, Stefan Kubicek, Taiping Chen, et al. 2003. 'Suv39h-Mediated Histone H3 Lysine 9 Methylation Directs DNA Methylation to Major Satellite Repeats at Pericentric Heterochromatin'. Current biology: CB 13(14): 1192–1200. doi:10.1016/s0960-9822(03)00432-9.

Leptin, M. 1991. 'Twist and Snail as Positive and Negative Regulators during Drosophila Mesoderm Development'. Genes & Development 5(9): 1568–76. doi:10.1101/gad.5.9.1568.

Leptin, M., and B. Grunewald. 1990. 'Cell Shape Changes during Gastrulation in Drosophila'. Development (Cambridge, England) 110(1): 73–84. doi:10.1242/dev.110.1.73.

Lermontova, Inna, Veit Schubert, Joerg Fuchs, Sabina Klatte, Jiri Macas, and Ingo Schubert. 2006. 'Loading of Arabidopsis Centromeric Histone CENH3 Occurs Mainly during G2 and Requires the Presence of the Histone Fold Domain'. The Plant Cell 18(10): 2443–51. doi:10.1105/tpc.106.043174.

Leroy, Pascale, and Keith E. Mostov. 2007. 'Slug Is Required for Cell Survival during Partial Epithelial-Mesenchymal Transition of HGF-Induced Tubulogenesis'. Molecular Biology of the Cell 18(5): 1943–52. doi:10.1091/mbc.e06-09-0823.

Lever, Elliott, and Denise Sheer. 2010. 'The Role of Nuclear Organization in Cancer'. The Journal of Pathology 220(2): 114–25. doi:10.1002/path.2651.

Levine, Arnold J., Anna M. Puzio-Kuter, Chang S. Chan, and Pierre Hainaut. 2016. 'The Role of the P53 Protein in Stem-Cell Biology and Epigenetic Regulation'. Cold Spring Harbor Perspectives in Medicine 6(9): a026153. doi:10.1101/cshperspect.a026153.

Lewis, Peter W., Simon J. Elsaesser, Kyung-Min Noh, Sonja C. Stadler, and C. David Allis. 2010. 'Daxx Is an H3.3-Specific Histone Chaperone and Cooperates with ATRX in Replication-Independent Chromatin Assembly at Telomeres'. Proceedings of the National Academy of Sciences of the United States of America 107(32): 14075–80. doi:10.1073/pnas.1008850107.

Lewis, Peter W., Manuel M. Müller, Matthew S. Koletsky, Francisco Cordero, Shu Lin, Laura A. Banaszynski, Benjamin A. Garcia, et al. 2013. 'Inhibition of PRC2 Activity by a Gain-of-Function H3 Mutation Found in Pediatric Glioblastoma'. Science (New York, N.Y.) 340(6134): 857–61. doi:10.1126/science.1232245.

Li, Bing, Michael Carey, and Jerry L. Workman. 2007. 'The Role of Chromatin during Transcription'. Cell 128(4): 707–19. doi:10.1016/j.cell.2007.01.015.

Li, Dandan, Lingyun Xia, Pan Huang, Zidi Wang, Qiwei Guo, Congcong Huang, Weidong Leng, and Shanshan Qin. 2023. 'Heterogeneity and Plasticity of Epithelial–Mesenchymal Transition (EMT) in Cancer Metastasis: Focusing on Partial EMT and Regulatory Mechanisms'. Cell Proliferation 56(6): e13423. doi:10.1111/cpr.13423.

Li, Lin, Xiaoli Li, Qin Meng, Abdul Qadir Khan, and Xiaomei Chen. 2018. 'Increased Expression of Holliday Junction-Recognizing Protein (HJURP) as an Independent Prognostic Biomarker in Advanced-Stage Serous Ovarian Carcinoma'. Medical Science Monitor : International Medical Journal of Experimental and Clinical Research 24: 3050–55. doi:10.12659/MSM.906647.

Li, Lin, Qiang Yuan, Yue-Ming Chu, Hang-Yu Jiang, Ju-Hua Zhao, Qiang Su, Dan-Qun Huo, and Xiao-Fen Zhang. 2023. 'Advances in Holliday Junction Recognition Protein (HJURP): Structure, Molecular Functions, and Roles in Cancer'. Frontiers in Cell and Developmental Biology 11: 1106638. doi:10.3389/fcell.2023.1106638.

Li, Ling, Diana Zepeda-Orozco, Rachel Black, and Fangming Lin. 2010. 'Autophagy Is a Component of Epithelial Cell Fate in Obstructive Uropathy'. The American Journal of Pathology 176(4): 1767–78. doi:10.2353/ajpath.2010.090345.

Li, Ronghui, Jialiang Liang, Su Ni, Ting Zhou, Xiaobing Qing, Huapeng Li, Wenzhi He, et al. 2010. 'A Mesenchymal-to-Epithelial Transition Initiates and Is Required for the Nuclear Reprogramming of Mouse Fibroblasts'. Cell Stem Cell 7(1): 51–63. doi:10.1016/j.stem.2010.04.014.

Li, Shuxiang, Yunhui Peng, and Anna R. Panchenko. 2022. 'DNA Methylation: Precise Modulation of Chromatin Structure and Dynamics'. Current Opinion in Structural Biology 75: 102430. doi:10.1016/j.sbi.2022.102430.

Li, Wenfeng, Shouzhi Li, Liang Deng, Shibin Yang, Mingzhe Li, Shuo Long, Sile Chen, Fuxiang Lin, and Longbin Xiao. 2015. 'Decreased MT1-MMP in Gastric Cancer Suppressed Cell Migration and Invasion via Regulating MMPs and EMT'. Tumour Biology: The Journal of the International Society for Oncodevelopmental Biology and Medicine 36(9): 6883–89. doi:10.1007/s13277-015-3381-7.

Li, Yongmei, Zhi Zhu, Shuhui Zhang, Danghui Yu, Hongyu Yu, Lina Liu, Xiaozhe Cao, et al. 2011. 'ShRNA-Targeted Centromere Protein A Inhibits Hepatocellular Carcinoma Growth'. PLOS ONE 6(3): e17794. doi:10.1371/journal.pone.0017794.

Li, Zhiming, Xu Hua, Albert Serra-Cardona, Xiaowei Xu, Songlin Gan, Hui Zhou, Wen-Si Yang, et al. 2020. 'DNA Polymerase α Interacts with H3-H4 and Facilitates the Transfer of Parental Histones to Lagging Strands'. Science Advances 6(35): eabb5820. doi:10.1126/sciadv.abb5820.

Lichter, P., T. Cremer, J. Borden, L. Manuelidis, and D. C. Ward. 1988. 'Delineation of Individual Human Chromosomes in Metaphase and Interphase Cells by in Situ Suppression Hybridization Using Recombinant DNA Libraries'. Human Genetics 80(3): 224–34. doi:10.1007/BF01790090.

Lieberman-Aiden, Erez, Nynke L. van Berkum, Louise Williams, Maxim Imakaev, Tobias Ragoczy, Agnes Telling, Ido Amit, et al. 2009. 'Comprehensive Mapping of Long Range Interactions Reveals Folding Principles of the Human Genome'. Science (New York, N.Y.) 326(5950): 289–93. doi:10.1126/science.1181369.

Lim, Yat-Yuen, Josephine A. Wright, Joanne L. Attema, Philip A. Gregory, Andrew G. Bert, Eric Smith, Daniel Thomas, et al. 2013. 'Epigenetic Modulation of the miR-200 Family Is Associated with Transition to a Breast Cancer Stem-Cell-like State'. Journal of Cell Science 126(Pt 10): 2256–66. doi:10.1242/jcs.122275.

Lin, Yiwei, Yadi Wu, Junlin Li, Chenfang Dong, Xiaofeng Ye, Young-In Chi, B. Mark Evers, and Binhua P. Zhou. 2010. 'The SNAG Domain of Snail1 Functions as a Molecular Hook for Recruiting Lysine-Specific Demethylase 1'. The EMBO journal 29(11): 1803–16. doi:10.1038/emboj.2010.63.

Lin, Yu-Fen, Qing Hu, Alice Mazzagatti, Jose Espejo Valle-Inclán, Elizabeth G. Maurais, Rashmi Dahiya, Alison Guyer, et al. 2023. 'Mitotic Clustering of Pulverized Chromosomes from Micronuclei'. Nature 618(7967): 1041–48. doi:10.1038/s41586-023-05974-0.

Lio, Chan-Wang J., Xiaojing Yue, Isaac F. López-Moyado, Mamta Tahiliani, L. Aravind, and Anjana Rao. 2020. 'TET Methylcytosine Oxidases: New Insights from a Decade of Research'. Journal of biosciences 45: 21.

Liu, Chia-Feng, Chang Liu, and Humphrey H.-C. Yao. 2010. 'Building Pathways for Ovary Organogenesis in the Mouse Embryo'. Current Topics in Developmental Biology 90: 263–90. doi:10.1016/S0070-2153(10)90007-0.

Liu, Guo, Joshua B. Stevens, Steven D. Horne, Batoul Y. Abdallah, Karen J. Ye, Steven W. Bremer, Christine J. Ye, David J. Chen, and Henry H. Heng. 2014. 'Genome Chaos: Survival Strategy during Crisis'. Cell Cycle (Georgetown, Tex.) 13(4): 528–37. doi:10.4161/cc.27378.

Liu, Hong, Derek C. Radisky, Dun Yang, Ren Xu, Evette S. Radisky, Mina J. Bissell, and J. Michael Bishop. 2012. 'MYC Suppresses Cancer Metastasis by Direct Transcriptional Silencing of Av and B3 Integrin Subunits'. Nature Cell Biology 14(6): 567–74. doi:10.1038/ncb2491.

Liu, Jie, Bai Ruan, Nan You, Qike Huang, Weihui Liu, Zheng Dang, Weihua Xu, et al. 2013. 'Downregulation of miR-200a Induces EMT Phenotypes and CSC-like Signatures through Targeting the β-Catenin Pathway in Hepatic Oval Cells'. PloS One 8(11): e79409. doi:10.1371/journal.pone.0079409.

Liu, P., M. Wakamiya, M. J. Shea, U. Albrecht, R. R. Behringer, and A. Bradley. 1999. 'Requirement for Wnt3 in Vertebrate Axis Formation'. Nature Genetics 22(4): 361–65. doi:10.1038/11932.

Liu, Song-Tao, Jerome B. Rattner, Sandra A. Jablonski, and Tim J. Yen. 2006. 'Mapping the Assembly Pathways That Specify Formation of the Trilaminar Kinetochore Plates in Human Cells'. The Journal of Cell Biology 175(1): 41–53. doi:10.1083/jcb.200606020.

Liu, Wan-Ting, Yang Wang, Jing Zhang, Fei Ye, Xiao-Hui Huang, Bin Li, and Qing-Yu He. 2018. 'A Novel Strategy of Integrated Microarray Analysis Identifies CENPA, CDK1 and CDC20 as a Cluster

of Diagnostic Biomarkers in Lung Adenocarcinoma'. Cancer Letters 425: 43–53. doi:10.1016/j.canlet.2018.03.043.

Liu, Yi, Jun Ma, Jiu-Shan Song, Hai-Ying Zhou, Jing-Hui Li, Cheng Luo, Xin Geng, and He-Xiang Zhao. 2022. 'DNA Topoisomerase II Alpha Promotes the Metastatic Characteristics of Glioma Cells by Transcriptionally Activating β-Catenin'. Bioengineered 13(2): 2207–16. doi:10.1080/21655979.2021.2023985.

Liu, Yusi, Xiaojiao Sun, Jinfa Feng, Li-Li Deng, Yihao Liu, Bokang Li, Mingyue Zhu, Changlian Lu, and Lingyun Zhou. 2016. 'MT2-MMP Induces Proteolysis and Leads to EMT in Carcinomas'. Oncotarget 7(30): 48193–205. doi:10.18632/oncotarget.10194.

Lochter, A., S. Galosy, J. Muschler, N. Freedman, Z. Werb, and M. J. Bissell. 1997. 'Matrix Metalloproteinase Stromelysin-1 Triggers a Cascade of Molecular Alterations That Leads to Stable Epithelial-to-Mesenchymal Conversion and a Premalignant Phenotype in Mammary Epithelial Cells'. The Journal of Cell Biology 139(7): 1861–72. doi:10.1083/jcb.139.7.1861.

Logan, Shaun M., and M. Douglas Benson. 2020. 'Medial Epithelial Seam Cell Migration during Palatal Fusion'. Journal of Cellular Physiology 235(2): 1417–24. doi:10.1002/jcp.29061.

Logsdon, Glennis A., Craig W. Gambogi, Mikhail A. Liskovykh, Evelyne J. Barrey, Vladimir Larionov, Karen H. Miga, Patrick Heun, and Ben E. Black. 2019. 'Human Artificial Chromosomes That Bypass Centromeric DNA'. Cell 178(3): 624-639.e19. doi:10.1016/j.cell.2019.06.006.

Logsdon, Glennis A., Allison N. Rozanski, Fedor Ryabov, Tamara Potapova, Valery A. Shepelev, Claudia R. Catacchio, David Porubsky, et al. 2024. 'The Variation and Evolution of Complete Human Centromeres'. Nature 629(8010): 136–45. doi:10.1038/s41586-024-07278-3.

Logsdon, Glennis A., Allison N. Rozanski, Fedor Ryabov, Tamara Potapova, Valery A. Shepelev, Yafei Mao, Mikko Rautiainen, et al. 2023. 'The Variation and Evolution of Complete Human Centromeres'. bioRxiv: The Preprint Server for Biology: 2023.05.30.542849. doi:10.1101/2023.05.30.542849.

Logsdon, Glennis A., Mitchell R. Vollger, PingHsun Hsieh, Yafei Mao, Mikhail A. Liskovykh, Sergey Koren, Sergey Nurk, et al. 2021. 'The Structure, Function and Evolution of a Complete Human Chromosome 8'. Nature 593(7857): 101–7. doi:10.1038/s41586-021-03420-7.

López-Novoa, Jose Miguel, and M. Angela Nieto. 2009. 'Inflammation and EMT: An Alliance towards Organ Fibrosis and Cancer Progression'. EMBO molecular medicine 1(6–7): 303–14. doi:10.1002/emmm.200900043.

Loppin, Benjamin, Emilie Bonnefoy, Caroline Anselme, Anne Laurençon, Timothy L. Karr, and Pierre Couble. 2005. 'The Histone H3.3 Chaperone HIRA Is Essential for Chromatin Assembly in the Male Pronucleus'. Nature 437(7063): 1386–90. doi:10.1038/nature04059.

Lorch, Yahli, Roger D Kornberg, and Barbara Maier-Davis. 2023. 'Role of the Histone Tails in Histone Octamer Transfer'. Nucleic Acids Research 51(8): 3671–78. doi:10.1093/nar/gkad079.

Lovisa, Sara, Valerie S. LeBleu, Björn Tampe, Hikaru Sugimoto, Komal Vadnagara, Julienne L. Carstens, Chia-Chin Wu, et al. 2015. 'Epithelial-to-Mesenchymal Transition Induces Cell Cycle Arrest and Parenchymal Damage in Renal Fibrosis'. Nature Medicine 21(9): 998–1009. doi:10.1038/nm.3902.

Lowe, S. W. 1999. 'Activation of P53 by Oncogenes'. Endocrine-Related Cancer 6(1): 45–48. doi:10.1677/erc.0.0060045.

Loyola, Alejandra, Tiziana Bonaldi, Danièle Roche, Axel Imhof, and Geneviève Almouzni. 2006. 'PTMs on H3 Variants before Chromatin Assembly Potentiate Their Final Epigenetic State'. Molecular Cell 24(2): 309–16. doi:10.1016/j.molcel.2006.08.019.

Lu, Mingyang, Mohit Kumar Jolly, Ryan Gomoto, Bin Huang, José Onuchic, and Eshel Ben-Jacob. 2013. 'Tristability in Cancer-Associated microRNA-TF Chimera Toggle Switch'. The Journal of Physical Chemistry. B 117(42): 13164–74. doi:10.1021/jp403156m.

Lu, Mingyang, Mohit Kumar Jolly, Herbert Levine, José N. Onuchic, and Eshel Ben-Jacob. 2013. 'MicroRNA-Based Regulation of Epithelial-Hybrid-Mesenchymal Fate Determination'. Proceedings of the National Academy of Sciences of the United States of America 110(45): 18144–49. doi:10.1073/pnas.1318192110.

Lucchini, R., and J. M. Sogo. 1995. 'Replication of Transcriptionally Active Chromatin'. Nature 374(6519): 276–80. doi:10.1038/374276a0.

Luco, Reini F., Mariano Allo, Ignacio E. Schor, Alberto R. Kornblihtt, and Tom Misteli. 2011. 'Epigenetics in Alternative Pre-mRNA Splicing'. Cell 144(1): 16–26. doi:10.1016/j.cell.2010.11.056.

Luco, Reini F, and Tom Misteli. 2011. 'More than a Splicing Code: Integrating the Role of RNA, Chromatin and Non-Coding RNA in Alternative Splicing Regulation'. Current opinion in genetics & development 21(4): 366–72. doi:10.1016/j.gde.2011.03.004.

Luger, K., A. W. Mäder, R. K. Richmond, D. F. Sargent, and T. J. Richmond. 1997. 'Crystal Structure of the Nucleosome Core Particle at 2.8 A Resolution'. Nature 389(6648): 251–60. doi:10.1038/38444.

Luo, Daochun, Jinxia Wang, Jeff Li, and Martin Post. 2011. 'Mouse Snail Is a Target Gene for HIF'. Molecular cancer research: MCR 9(2): 234–45. doi:10.1158/1541-7786.MCR-10-0214.

Lyons, Deidre, Stacy Kaltenbach, and David R. McClay. 2012. 'Morphogenesis in Sea Urchin Embryos: Linking Cellular Events to Gene Regulatory Network States'. Wiley interdisciplinary reviews. Developmental biology 1(2): 231–52. doi:10.1002/wdev.18.

Lyons, J. Guy, Vyomesh Patel, Naomi C. Roue, Sandra Y. Fok, Lilian L. Soon, Gary M. Halliday, and J. Silvio Gutkind. 2008. 'Snail Up-Regulates Proinflammatory Mediators and Inhibits Differentiation in Oral Keratinocytes'. Cancer Research 68(12): 4525–30. doi:10.1158/1078-0432.CCR-07-6735.

Ma, Dengke K., Mi-Hyeon Jang, Junjie U. Guo, Yasuji Kitabatake, Min-Lin Chang, Nattapol Pow-Anpongkul, Richard A. Flavell, et al. 2009. 'Neuronal Activity-Induced Gadd45b Promotes Epigenetic DNA Demethylation and Adult Neurogenesis'. Science (New York, N.Y.) 323(5917): 1074–77. doi:10.1126/science.1166859.

Ma, Li, Jennifer Young, Harsha Prabhala, Elizabeth Pan, Pieter Mestdagh, Daniel Muth, Julie Teruya-Feldstein, et al. 2010. 'miR-9, a MYC/MYCN-Activated microRNA, Regulates E-Cadherin and Cancer Metastasis'. Nature cell biology 12(3): 247–56. doi:10.1038/ncb2024.

Ma, Xiao-Jun, Ranelle Salunga, J. Todd Tuggle, Justin Gaudet, Edward Enright, Philip McQuary, Terry Payette, et al. 2003. 'Gene Expression Profiles of Human Breast Cancer Progression'. Proceedings of the National Academy of Sciences of the United States of America 100(10): 5974–79. doi:10.1073/pnas.0931261100.

Macas, Jiří, Laura Ávila Robledillo, Jonathan Kreplak, Petr Novák, Andrea Koblížková, Iva Vrbová, Judith Burstin, and Pavel Neumann. 2023. 'Assembly of the 81.6 Mb Centromere of Pea Chromosome 6 Elucidates the Structure and Evolution of Metapolycentric Chromosomes'. PLoS genetics 19(2): e1010633. doi:10.1371/journal.pgen.1010633.

Mackay, Alan, Anna Burford, Diana Carvalho, Elisa Izquierdo, Janat Fazal-Salom, Kathryn R. Taylor, Lynn Bjerke, et al. 2017. 'Integrated Molecular Meta-Analysis of 1,000 Pediatric High-Grade and Diffuse Intrinsic Pontine Glioma'. Cancer Cell 32(4): 520-537.e5. doi:10.1016/j.ccell.2017.08.017.

Maehara, Kayoko, Kohta Takahashi, and Shigeaki Saitoh. 2010. 'CENP-A Reduction Induces a P53-Dependent Cellular Senescence Response To Protect Cells from Executing Defective Mitoses'. Molecular and Cellular Biology 30(9): 2090–2104. doi:10.1128/MCB.01318-09.

Maehara, Osamu, Goki Suda, Mitsuteru Natsuizaka, Shunsuke Ohnishi, Yoshito Komatsu, Fumiyuki Sato, Masato Nakai, et al. 2017. 'Fibroblast Growth Factor-2–Mediated FGFR/Erk Signaling Supports Maintenance of Cancer Stem-like Cells in Esophageal Squamous Cell Carcinoma'. Carcinogenesis 38(11): 1073–83. doi:10.1093/carcin/bgx095.

Maestro, Roberta, Angelo P. Dei Tos, Yasuo Hamamori, Svetlana Krasnokutsky, Vittorio Sartorelli, Larry Kedes, Claudio Doglioni, David H. Beach, and Gregory J. Hannon. 1999. 'Twist Is a Potential Oncogene That Inhibits Apoptosis'. Genes & Development 13(17): 2207–17.

Mahlke, Megan A., and Yael Nechemia-Arbely. 2020. 'Guarding the Genome: CENP-A-Chromatin in Health and Cancer'. Genes 11(7): 810. doi:10.3390/genes11070810.

Mai, Sabine. 2019. 'The Three-Dimensional Cancer Nucleus'. Genes, Chromosomes & Cancer 58(7): 462–73. doi:10.1002/gcc.22720.

Maison, C., J.-P. Quivy, A. V. Probst, and G. Almouzni. 2010. 'Heterochromatin at Mouse Pericentromeres: A Model for de Novo Heterochromatin Formation and Duplication during

Replication'. Cold Spring Harbor Symposia on Quantitative Biology 75: 155–65. doi:10.1101/sqb.2010.75.013.

Malik, H. S., and S. Henikoff. 2001. 'Adaptive Evolution of Cid, a Centromere-Specific Histone in Drosophila'. Genetics 157(3): 1293–98. doi:10.1093/genetics/157.3.1293.

Malouf, Gabriel G., Joseph H. Taube, Yue Lu, Tapasree Roysarkar, Shoghag Panjarian, Marcos RH Estecio, Jaroslav Jelinek, et al. 2013. 'Architecture of Epigenetic Reprogramming Following Twist1-Mediated Epithelial-Mesenchymal Transition'. Genome Biology 14(12): R144. doi:10.1186/gb-2013-14-12-r144.

Maltzman, W., and L. Czyzyk. 1984. 'UV Irradiation Stimulates Levels of P53 Cellular Tumor Antigen in Nontransformed Mouse Cells'. Molecular and Cellular Biology 4(9): 1689–94. doi:10.1128/mcb.4.9.1689-1694.1984.

Malvezzi, Francesca, Gabriele Litos, Alexander Schleiffer, Alexander Heuck, Karl Mechtler, Tim Clausen, and Stefan Westermann. 2013. 'A Structural Basis for Kinetochore Recruitment of the Ndc80 Complex via Two Distinct Centromere Receptors'. The EMBO journal 32(3): 409–23. doi:10.1038/emboj.2012.356.

Mani, Sendurai A., Wenjun Guo, Mai-Jing Liao, Elinor Ng Eaton, Ayyakkannu Ayyanan, Alicia Y. Zhou, Mary Brooks, et al. 2008. 'The Epithelial-Mesenchymal Transition Generates Cells with Properties of Stem Cells'. Cell 133(4): 704–15. doi:10.1016/j.cell.2008.03.027.

Markiewicz, Aleksandra, Justyna Topa, Anna Nagel, Jaroslaw Skokowski, Barbara Seroczynska, Tomasz Stokowy, Marzena Welnicka-Jaskiewicz, and Anna J. Zaczek. 2019. 'Spectrum of Epithelial-Mesenchymal Transition Phenotypes in Circulating Tumour Cells from Early Breast Cancer Patients'. Cancers 11(1): 59. doi:10.3390/cancers11010059.

Markwald, R. R., T. P. Fitzharris, and F. J. Manasek. 1977. 'Structural Development of Endocardial Cushions'. The American Journal of Anatomy 148(1): 85–119. doi:10.1002/aja.1001480108.

Marshall, A D, C G Bailey, K Champ, M Vellozzi, P O'Young, C Metierre, Y Feng, et al. 2017. 'CTCF Genetic Alterations in Endometrial Carcinoma Are Pro-Tumorigenic'. Oncogene 36(29): 4100–4110. doi:10.1038/onc.2017.25.

Marshall, Owen J., Anderly C. Chueh, Lee H. Wong, and K. H. Andy Choo. 2008. 'Neocentromeres: New Insights into Centromere Structure, Disease Development, and Karyotype Evolution'. American Journal of Human Genetics 82(2): 261–82. doi:10.1016/j.ajhg.2007.11.009.

Martin, Adam, and Bob Goldstein. 2014. 'Apical Constriction: Themes and Variations on a Cellular Mechanism Driving Morphogenesis - PMC'. //www.ncbi.nlm.nih.gov/pmc/articles/PMC4011084/ (September 3, 2024).

Martin, Alberto, and Amparo Cano. 2010. ‘Tumorigenesis: Twist1 Links EMT to Self-Renewal’. Nature Cell Biology 12(10): 924–25. doi:10.1038/ncb1010-924.

Martin, Melvenia M., Michael Ryan, RyangGuk Kim, Anna L. Zakas, Haiqing Fu, Chii Mei Lin, William C. Reinhold, et al. 2011. ‘Genome-Wide Depletion of Replication Initiation Events in Highly Transcribed Regions’. Genome Research 21(11): 1822–32. doi:10.1101/gr.124644.111.

Martire, Sara, Aishwarya A. Gogate, Amanda Whitmill, Amanuel Tafessu, Jennifer Nguyen, Yu-Ching Teng, Melodi Tastemel, and Laura A. Banaszynski. 2019. ‘Phosphorylation of Histone H3.3 at Serine 31 Promotes P300 Activity and Enhancer Acetylation’. Nature Genetics 51(6): 941–46. doi:10.1038/s41588-019-0428-5.

Martínez-Álvarez, C., C. Tudela, J. Pérez-Miguelsanz, S. O’Kane, J. Puerta, and M. W. J. Ferguson. 2000. ‘Medial Edge Epithelial Cell Fate during Palatal Fusion’. Developmental Biology 220(2): 343–57. doi:10.1006/dbio.2000.9644.

Maruyama, Shinichiro, Haruko Kuroiwa, Shin-ya Miyagishima, Kan Tanaka, and Tsuneyoshi Kuroiwa. 2007. ‘Centromere Dynamics in the Primitive Red Alga Cyanidioschyzon Merolae’. The Plant Journal: For Cell and Molecular Biology 49(6): 1122–29. doi:10.1111/j.1365-313X.2006.03024.x.

Marzluff, William F. 2005. ‘Metazoan Replication-Dependent Histone mRNAs: A Distinct Set of RNA Polymerase II Transcripts’. Current Opinion in Cell Biology 17(3): 274–80. doi:10.1016/j.ceb.2005.04.010.

Massé, Karine, and Nicholas Dale. 2012. ‘Purines as Potential Morphogens during Embryonic Development’. Purinergic Signalling 8(3): 503–21. doi:10.1007/s11302-012-9290-y.

Mathew, Veena, Anne-Laure Pauleau, Natascha Steffen, Andrea Bergner, Peter B. Becker, and Sylvia Erhardt. 2014. ‘The Histone-Fold Protein CHRAC14 Influences Chromatin Composition in Response to DNA Damage’. Cell Reports 7(2): 321–30. doi:10.1016/j.celrep.2014.03.008.

Mathieu, Juliette, Kevin Griffin, Philippe Herbomel, Thomas Dickmeis, Uwe Strähle, David Kimelman, Frédéric M. Rosa, and Nadine Peyriéras. 2004. ‘Nodal and Fgf Pathways Interact through a Positive Regulatory Loop and Synergize to Maintain Mesodermal Cell Populations’. Development (Cambridge, England) 131(3): 629–41. doi:10.1242/dev.00964.

Mattout, Anna, and Eran Meshorer. 2010. ‘Chromatin Plasticity and Genome Organization in Pluripotent Embryonic Stem Cells’. Current Opinion in Cell Biology 22(3): 334–41. doi:10.1016/j.ceb.2010.02.001.

Maze, Ian, Wendy Wenderski, Kyung-Min Noh, Rosemary C. Bagot, Nikos Tzavaras, Immanuel Purushothaman, Simon J. Elsässer, et al. 2015. ‘Critical Role of Histone Turnover in Neuronal Transcription and Plasticity’. Neuron 87(1): 77–94. doi:10.1016/j.neuron.2015.06.014.

McDonald, Oliver G., Hao Wu, Winston Timp, Akiko Doi, and Andrew P. Feinberg. 2011. 'Genome-Scale Epigenetic Reprogramming during Epithelial to Mesenchymal Transition'. Nature structural & molecular biology 18(8): 867–74. doi:10.1038/nsmb.2084.

McGhee, J. D., and G. Felsenfeld. 1980. 'Nucleosome Structure'. Annual Review of Biochemistry 49: 1115–56. doi:10.1146/annurev.bi.49.070180.005343.

McGovern, Susan L, Yuan Qi, Lajos Pusztai, William F Symmans, and Thomas A Buchholz. 2012. 'Centromere Protein-A, an Essential Centromere Protein, Is a Prognostic Marker for Relapse in Estrogen Receptor-Positive Breast Cancer'. Breast Cancer Research : BCR 14(3): R72. doi:10.1186/bcr3181.

McGregor, Michael, Nirmala Hariharan, Anya Y Joyo, Robert L Margolis, and Mark A Sussman. 2014. 'CENP-A Is Essential for Cardiac Progenitor Cell Proliferation'. Cell Cycle 13(5): 739–48. doi:10.4161/cc.27549.

McKinley, Kara L., and Iain M. Cheeseman. 2014. 'Polo-like Kinase 1 Licenses CENP-A Deposition at Centromeres'. Cell 158(2): 397–411. doi:10.1016/j.cell.2014.06.016.

McKinley, Kara L., and Iain M. Cheeseman. 2016. 'The Molecular Basis for Centromere Identity and Function'. Nature Reviews. Molecular Cell Biology 17(1): 16–29. doi:10.1038/nrm.2015.5.

McKnight, S. L., and O. L. Miller. 1977. 'Electron Microscopic Analysis of Chromatin Replication in the Cellular Blastoderm Drosophila Melanogaster Embryo'. Cell 12(3): 795–804. doi:10.1016/0092-8674(77)90278-1.

McNiel, Elizabeth A., and Philip N. Tsichlis. 2017. 'Analyses of Publicly Available Genomics Resources Define FGF-2-Expressing Bladder Carcinomas as EMT-Prone, Proliferative Tumors with Low Mutation Rates and High Expression of CTLA-4, PD-1 and PD-L1'. Signal Transduction and Targeted Therapy 2: 16045-. doi:10.1038/sigtrans.2016.45.

McNulty, Shannon M., Lori L. Sullivan, and Beth A. Sullivan. 2017. 'Human Centromeres Produce Chromosome-Specific and Array-Specific Alpha Satellite Transcripts That Are Complexed with CENP-A and CENP-C'. Developmental Cell 42(3): 226-240.e6. doi:10.1016/j.devcel.2017.07.001.

McSwiggen, David Trombley, Anders S. Hansen, Sheila S. Teves, Hervé Marie-Nelly, Yvonne Hao, Alec Basil Heckert, Kayla K. Umemoto, et al. 2019. 'Evidence for DNA-Mediated Nuclear Compartmentalization Distinct from Phase Separation'. eLife 8: e47098. doi:10.7554/eLife.47098.

Méchali, Marcel. 2010. 'Eukaryotic DNA Replication Origins: Many Choices for Appropriate Answers'. Nature Reviews. Molecular Cell Biology 11(10): 728–38. doi:10.1038/nrm2976.

Medici, Damian, Elizabeth D. Hay, and Bjorn R. Olsen. 2008. 'Snail and Slug Promote Epithelial-Mesenchymal Transition through Beta-Catenin-T-Cell Factor-4-Dependent Expression of

Transforming Growth Factor-Beta3'. Molecular Biology of the Cell 19(11): 4875–87. doi:10.1091/mbc.e08-05-0506.

Mekhail, Karim, and Danesh Moazed. 2010. 'The Nuclear Envelope in Genome Organization, Expression and Stability'. Nature Reviews Molecular Cell Biology 11(5): 317–28. doi:10.1038/nrm2894.

Mellone, Barbara G., Kathryn J. Grive, Vladimir Shteyn, Sarion R. Bowers, Isaac Oderberg, and Gary H. Karpen. 2011. 'Assembly of Drosophila Centromeric Chromatin Proteins during Mitosis'. PLoS genetics 7(5): e1002068. doi:10.1371/journal.pgen.1002068.

Melters, Daniël P., Keith R. Bradnam, Hugh A. Young, Natalie Telis, Michael R. May, J. Graham Ruby, Robert Sebra, et al. 2013. 'Comparative Analysis of Tandem Repeats from Hundreds of Species Reveals Unique Insights into Centromere Evolution'. Genome Biology 14(1): R10. doi:10.1186/gb-2013-14-1-r10.

Melters, Daniël P., Keir C. Neuman, Reda S. Bentahar, Tatini Rakshit, and Yamini Dalal. 2023. 'Single Molecule Analysis of CENP-A Chromatin by High-Speed Atomic Force Microscopy'. eLife 12: e86709. doi:10.7554/eLife.86709.

Melters, Daniël P., Mary Pitman, Tatini Rakshit, Emilios K. Dimitriadis, Minh Bui, Garegin A. Papoian, and Yamini Dalal. 2019. 'Intrinsic Elasticity of Nucleosomes Is Encoded by Histone Variants and Calibrated by Their Binding Partners'. Proceedings of the National Academy of Sciences of the United States of America 116(48): 24066–74. doi:10.1073/pnas.1911880116.

Mendel, G. 1866. Versuche über Pflanzenhybriden. Ostwalds Klassiker der Exakten Wissenschaften. doi:10.1007/978-3-663-19714-0_4.

Mendiburo, María José, Jan Padeken, Stefanie Fülöp, Aloys Schepers, and Patrick Heun. 2011. 'Drosophila CENH3 Is Sufficient for Centromere Formation'. Science (New York, N.Y.) 334(6056): 686–90. doi:10.1126/science.1206880.

Mendiratta, Shweta, Alberto Gatto, and Genevieve Almouzni. 2019. 'Histone Supply: Multitiered Regulation Ensures Chromatin Dynamics throughout the Cell Cycle'. The Journal of Cell Biology 218(1): 39–54. doi:10.1083/jcb.201807179.

Mendiratta, Shweta, Dominique Ray-Gallet, Sébastien Lemaire, Alberto Gatto, Audrey Forest, Maciej A. Kerlin, and Geneviève Almouzni. 2024. 'Regulation of Replicative Histone RNA Metabolism by the Histone Chaperone ASF1'. Molecular Cell 84(4): 791-801.e6. doi:10.1016/j.molcel.2023.12.038.

Mercado-Pimentel, Melania E., and Raymond B. Runyan. 2007. 'Multiple Transforming Growth Factor-Beta Isoforms and Receptors Function during Epithelial-Mesenchymal Cell Transformation in the Embryonic Heart'. Cells, Tissues, Organs 185(1–3): 146–56. doi:10.1159/000101315.

Mersfelder, Erica L., and Mark R. Parthun. 2006. 'The Tale beyond the Tail: Histone Core Domain Modifications and the Regulation of Chromatin Structure'. Nucleic Acids Research 34(9): 2653–62. doi:10.1093/nar/gkl338.

Meshorer, Eran, Dhananjay Yellajoshula, Eric George, Peter J. Scambler, David T. Brown, and Tom Misteli. 2006. 'Hyperdynamic Plasticity of Chromatin Proteins in Pluripotent Embryonic Stem Cells'. Developmental Cell 10(1): 105–16. doi:10.1016/j.devcel.2005.10.017.

Messner, Simon, and Michael O. Hottiger. 2011. 'Histone ADP-Ribosylation in DNA Repair, Replication and Transcription'. Trends in Cell Biology 21(9): 534–42. doi:10.1016/j.tcb.2011.06.001.

Miettinen, Païvi, Reinhard Ebner, Alfredo R. Lopez, and Rik Derynck. 1994. 'TGF-Beta Induced Transdifferentiation of Mammary Epithelial Cells to Mesenchymal Cells: Involvement of Type I Receptors'. The Journal of Cell Biology 127(6): 2021–36.

Miga, Karen H., Sergey Koren, Arang Rhie, Mitchell R. Vollger, Ariel Gershman, Andrey Bzikadze, Shelise Brooks, et al. 2020. 'Telomere-to-Telomere Assembly of a Complete Human X Chromosome'. Nature 585(7823): 79–84. doi:10.1038/s41586-020-2547-7.

Mikkelsen, Tarjei S., Manching Ku, David B. Jaffe, Biju Issac, Erez Lieberman, Georgia Giannoukos, Pablo Alvarez, et al. 2007. 'Genome-Wide Maps of Chromatin State in Pluripotent and Lineage-Committed Cells'. Nature 448(7153): 553–60. doi:10.1038/nature06008.

Milagre, Inês, Carolina Pereira, Raquel A. Oliveira, and Lars E. T. Jansen. 2020. 'Reprogramming of Human Cells to Pluripotency Induces CENP-A Chromatin Depletion'. Open Biology 10(10): 200227. doi:10.1098/rsob.200227.

Milks, Kirstin J., Ben Moree, and Aaron F. Straight. 2009. 'Dissection of CENP-C-Directed Centromere and Kinetochore Assembly'. Molecular Biology of the Cell 20(19): 4246–55. doi:10.1091/mbc.e09-05-0378.

Millán-Ariño, Lluís, Andrea Izquierdo-Bouldstridge, and Albert Jordan. 2016. 'Specificities and Genomic Distribution of Somatic Mammalian Histone H1 Subtypes'. Biochimica Et Biophysica Acta 1859(3): 510–19. doi:10.1016/j.bbagrm.2015.10.013.

Millanes-Romero, Alba, Nicolás Herranz, Valentina Perrera, Ane Iturbide, Jordina Loubat-Casanovas, Jesús Gil, Thomas Jenuwein, Antonio García de Herreros, and Sandra Peiró. 2013. 'Regulation of Heterochromatin Transcription by Snail1/LOXL2 during Epithelial-to-Mesenchymal Transition'. Molecular Cell 52(5): 746–57. doi:10.1016/j.molcel.2013.10.015.

Millán-Zambrano, Gonzalo, Adam Burton, Andrew J. Bannister, and Robert Schneider. 2022. 'Histone Post-Translational Modifications - Cause and Consequence of Genome Function'. Nature Reviews. Genetics 23(9): 563–80. doi:10.1038/s41576-022-00468-7.

Mima, Kosuke, Hiromitsu Hayashi, Hideyuki Kuroki, Shigeki Nakagawa, Hirohisa Okabe, Akira Chikamoto, Masayuki Watanabe, Toru Beppu, and Hideo Baba. 2013. 'Epithelial-Mesenchymal Transition Expression Profiles as a Prognostic Factor for Disease-Free Survival in Hepatocellular Carcinoma: Clinical Significance of Transforming Growth Factor-β Signaling'. Oncology Letters 5(1): 149–54. doi:10.3892/ol.2012.954.

Mironchik, Yelena, Paul T. Winnard, Farhad Vesuna, Yoshinori Kato, Flonne Wildes, Arvind P. Pathak, Scott Kominsky, et al. 2005. 'Twist Overexpression Induces In Vivo Angiogenesis and Correlates with Chromosomal Instability in Breast Cancer'. Cancer research 65(23): 10801–9. doi:10.1158/0008-5472.CAN-05-0712.

Miyazawa-Onami, Mayumi, Hiroyuki Araki, and Seiji Tanaka. 2017. 'Pre-Initiation Complex Assembly Functions as a Molecular Switch That Splits the Mcm2-7 Double Hexamer'. EMBO reports 18(10): 1752–61. doi:10.15252/embr.201744206.

Moggs, J. G., P. Grandi, J. P. Quivy, Z. O. Jónsson, U. Hübscher, P. B. Becker, and G. Almouzni. 2000. 'A CAF-1-PCNA-Mediated Chromatin Assembly Pathway Triggered by Sensing DNA Damage'. Molecular and Cellular Biology 20(4): 1206–18. doi:10.1128/MCB.20.4.1206-1218.2000.

Mohammad, Faizaan, Simon Weissmann, Benjamin Leblanc, Deo P. Pandey, Jonas W. Højfeldt, Itys Comet, Chunqin Zheng, et al. 2017. 'EZH2 Is a Potential Therapeutic Target for H3K27M-Mutant Pediatric Gliomas'. Nature Medicine 23(4): 483–92. doi:10.1038/nm.4293.

Mohandas, T., R. S. Sparkes, and L. J. Shapiro. 1981. 'Reactivation of an Inactive Human X Chromosome: Evidence for X Inactivation by DNA Methylation'. Science (New York, N.Y.) 211(4480): 393–96. doi:10.1126/science.6164095.

Molina, Oscar, Giulia Vargiu, Maria Alba Abad, Alisa Zhiteneva, A. Arockia Jeyaprakash, Hiroshi Masumoto, Natalay Kouprina, Vladimir Larionov, and William C. Earnshaw. 2016. 'Epigenetic Engineering Reveals a Balance between Histone Modifications and Transcription in Kinetochore Maintenance'. Nature Communications 7: 13334. doi:10.1038/ncomms13334.

Monk, M. 1987. 'Genomic Imprinting. Memories of Mother and Father'. Nature 328(6127): 203–4. doi:10.1038/328203a0.

Monk, M., M. Boubelik, and S. Lehnert. 1987. 'Temporal and Regional Changes in DNA Methylation in the Embryonic, Extraembryonic and Germ Cell Lineages during Mouse Embryo Development'. Development (Cambridge, England) 99(3): 371–82. doi:10.1242/dev.99.3.371.

Monneron, A., and W. Bernhard. 1969. 'Fine Structural Organization of the Interphase Nucleus in Some Mammalian Cells'. Journal of Ultrastructure Research 27(3): 266–88. doi:10.1016/s0022-5320(69)80017-1.

Montero, Carvalho, Wilsch-Bräuninger, Kilian, Mustafa, and Heisenberg. 2005. 'Shield Formation at the Onset of Zebrafish Gastrulation'. Development (Cambridge, England) 132(6). doi:10.1242/dev.01667.

Montes de Oca, Rocío, Zachary A. Gurard-Levin, Frédérique Berger, Haniya Rehman, Elise Martel, Armelle Corpet, Leanne de Koning, et al. 2015. 'The Histone Chaperone HJURP Is a New Independent Prognostic Marker for Luminal A Breast Carcinoma'. Molecular Oncology 9(3): 657–74. doi:10.1016/j.molonc.2014.11.002.

Montserrat, Nuria, Ana Mozos, David Llobet, Xavier Dolcet, Cristina Pons, Antonio García de Herreros, Xavier Matias-Guiu, and Jaime Prat. 2012. 'Epithelial to Mesenchymal Transition in Early Stage Endometrioid Endometrial Carcinoma'. Human Pathology 43(5): 632–43. doi:10.1016/j.humpath.2011.06.021.

Moree, Ben, Corey B. Meyer, Colin J. Fuller, and Aaron F. Straight. 2011. 'CENP-C Recruits M18BP1 to Centromeres to Promote CENP-A Chromatin Assembly'. The Journal of Cell Biology 194(6): 855–71. doi:10.1083/jcb.201106079.

Morel, Anne-Pierre, Christophe Ginestier, Roxane M. Pommier, Olivier Cabaud, Emmanuelle Ruiz, Julien Wicinski, Mojgan Devouassoux-Shisheboran, et al. 2017. 'A Stemness-Related ZEB1-MSRB3 Axis Governs Cellular Pliancy and Breast Cancer Genome Stability'. Nature Medicine 23(5): 568–78. doi:10.1038/nm.4323.

Morel, Anne-Pierre, George W. Hinkal, Clémence Thomas, Frédérique Fauvet, Stéphanie Courtois-Cox, Anne Wierinckx, Mojgan Devouassoux-Shisheboran, et al. 2012. 'EMT Inducers Catalyze Malignant Transformation of Mammary Epithelial Cells and Drive Tumorigenesis towards Claudin-Low Tumors in Transgenic Mice'. PLoS genetics 8(5): e1002723. doi:10.1371/journal.pgen.1002723.

Morel, Anne-Pierre, Marjory Lièvre, Clémence Thomas, George Hinkal, Stéphane Ansieau, and Alain Puisieux. 2008. 'Generation of Breast Cancer Stem Cells through Epithelial-Mesenchymal Transition'. PloS One 3(8): e2888. doi:10.1371/journal.pone.0002888.

Moreno-Moreno, Olga, Sònia Medina-Giró, Mònica Torras-Llort, and Fernando Azorín. 2011. 'The F Box Protein Partner of Paired Regulates Stability of Drosophila Centromeric Histone H3, CenH3(CID)'. Current biology: CB 21(17): 1488–93. doi:10.1016/j.cub.2011.07.041.

Moreno-Moreno, Olga, Mònica Torras-Llort, and Fernando Azorín. 2006. 'Proteolysis Restricts Localization of CID, the Centromere-Specific Histone H3 Variant of Drosophila, to Centromeres'. Nucleic Acids Research 34(21): 6247–55. doi:10.1093/nar/gkl902.

Morgan, T. H. 1910. Chromosomes and Heredity. The American Naturalist 44(524): 449-496. https://www.jstor.org/stable/2455783 (August 10, 2024).

Morizane, Ryuji, Shizuka Fujii, Toshiaki Monkawa, Ken Hiratsuka, Shintaro Yamaguchi, Koichiro Homma, and Hiroshi Itoh. 2014. 'miR-34c Attenuates Epithelial-Mesenchymal Transition and Kidney Fibrosis with Ureteral Obstruction'. Scientific Reports 4: 4578. doi:10.1038/srep04578.

Moroi, Y., C. Peebles, M. J. Fritzler, J. Steigerwald, and E. M. Tan. 1980. 'Autoantibody to Centromere (Kinetochore) in Scleroderma Sera'. Proceedings of the National Academy of Sciences of the United States of America 77(3): 1627–31. doi:10.1073/pnas.77.3.1627.

Moyret-Lalle, Caroline, Mélanie K. Prodhomme, Delphine Burlet, Ayaka Kashiwagi, Virginie Petrilli, Alain Puisieux, Hiroyuki Seimiya, and Agnès Tissier. 2022. 'Role of EMT in the DNA Damage Response, Double-strand Break Repair Pathway Choice and Its Implications in Cancer Treatment'. Cancer Science 113(7): 2214–23. doi:10.1111/cas.15389.

Muller, Héloïse, José Gil, and Ines Anna Drinnenberg. 2019. 'The Impact of Centromeres on Spatial Genome Architecture'. Trends in genetics: TIG 35(8): 565–78. doi:10.1016/j.tig.2019.05.003.

Müller, Sebastian, and Geneviève Almouzni. 2017. 'Chromatin Dynamics during the Cell Cycle at Centromeres'. Nature Reviews Genetics 18(3): 192–208. doi:10.1038/nrg.2016.157.

Müller-Wille, S. 2010. Cell Theory, Specificity, and Reproduction, 1837–1870. Studies in history and philosophy of biological and biomedical sciences 41(3): 225-231. doi:10.1016/j.shpsc.2010.07.008.

Murillo-Pineda, Marina, Luis P. Valente, Marie Dumont, João F. Mata, Daniele Fachinetti, and Lars E. T. Jansen. 2021. 'Induction of Spontaneous Human Neocentromere Formation and Long-Term Maturation'. The Journal of Cell Biology 220(3): e202007210. doi:10.1083/jcb.202007210.

Murlidhar, Vasudha, Rishindra M. Reddy, Shamileh Fouladdel, Lili Zhao, Martin K. Ishikawa, Svetlana Grabauskiene, Zhuo Zhang, et al. 2017. 'Poor Prognosis Indicated by Venous Circulating Tumor Cell Clusters in Early-Stage Lung Cancers'. Cancer Research 77(18): 5194–5206. doi:10.1158/0008-5472.CAN-16-2072.

Musacchio, Andrea, and Arshad Desai. 2017. 'A Molecular View of Kinetochore Assembly and Function'. Biology 6(1): 5. doi:10.3390/biology6010005.

Nacev, Benjamin A., Lijuan Feng, John D. Bagert, Agata E. Lemiesz, JianJiong Gao, Alexey A. Soshnev, Ritika Kundra, et al. 2019. 'The Expanding Landscape of "oncohistone" Mutations in Human Cancers'. Nature 567(7749): 473–78. doi:10.1038/s41586-019-1038-1.

Nagarajan, Prabakaran, Zhongqi Ge, Bianca Sirbu, Cheryl Doughty, Paula A. Agudelo Garcia, Michaela Schlederer, Anthony T. Annunziato, et al. 2013. 'Histone Acetyl Transferase 1 Is Essential for Mammalian Development, Genome Stability, and the Processing of Newly Synthesized Histones H3 and H4'. PLoS genetics 9(6): e1003518. doi:10.1371/journal.pgen.1003518.

Nagpal, Harsh, Ahmad Ali-Ahmad, Yasuhiro Hirano, Wei Cai, Mario Halic, Tatsuo Fukagawa, Nikolina Sekulić, and Beat Fierz. 2023. 'CENP-A and CENP-B Collaborate to Create an Open

Centromeric Chromatin State'. Nature Communications 14(1): 8227. doi:10.1038/s41467-023-43739-5.

Nahmias, A. J., S. R. Cooperband, J. A. Green, and S. Kibrick. 1967. 'Transformation of Epithelial Cells in Vitro'. Nature 216(5122): 1349–50. doi:10.1038/2161349a0.

Nakano, Megumi, Stefano Cardinale, Vladimir N. Noskov, Reto Gassmann, Paola Vagnarelli, Stefanie Kandels-Lewis, Vladimir Larionov, William C. Earnshaw, and Hiroshi Masumoto. 2008. 'Inactivation of a Human Kinetochore by Specific Targeting of Chromatin Modifiers'. Developmental Cell 14(4): 507–22. doi:10.1016/j.devcel.2008.02.001.

Nakatani, Tsunetoshi, Jiangwei Lin, Fei Ji, Andreas Ettinger, Julien Pontabry, Mikiko Tokoro, Luis Altamirano-Pacheco, et al. 2022. 'DNA Replication Fork Speed Underlies Cell Fate Changes and Promotes Reprogramming'. Nature Genetics 54(3): 318–27. doi:10.1038/s41588-022-01023-0.

Nakatani, Tsunetoshi, Tamas Schauer, Luis Altamirano-Pacheco, Kyle N. Klein, Andreas Ettinger, Mrinmoy Pal, David M. Gilbert, and Maria-Elena Torres-Padilla. 2024. 'Emergence of Replication Timing during Early Mammalian Development'. Nature 625(7994): 401–9. doi:10.1038/s41586-023-06872-1.

Nakaya, Yukiko, Shinya Kuroda, Yuji T. Katagiri, Kozo Kaibuchi, and Yoshiko Takahashi. 2004. 'Mesenchymal-Epithelial Transition during Somitic Segmentation Is Regulated by Differential Roles of Cdc42 and Rac1'. Developmental Cell 7(3): 425–38. doi:10.1016/j.devcel.2004.08.003.

Nakaya, Yukiko, and Guojun Sheng. 2008. 'Epithelial to Mesenchymal Transition during Gastrulation: An Embryological View'. Development, Growth & Differentiation 50(9): 755–66. doi:10.1111/j.1440-169X.2008.01070.x.

Nance, Jeremy, Jen-Yi Lee, and Bob Goldstein. 2005. 'Gastrulation in C. Elegans'. WormBook: The Online Review of C. Elegans Biology: 1–13. doi:10.1895/wormbook.1.23.1.

Nance, Jeremy, and James R. Priess. 2002. 'Cell Polarity and Gastrulation in C. Elegans'. Development (Cambridge, England) 129(2): 387–97. doi:10.1242/dev.129.2.387.

Nardi, Isaac K., Ewelina Zasadzińska, Madison E. Stellfox, Christina M. Knippler, and Daniel R. Foltz. 2016. 'Licensing of Centromeric Chromatin Assembly through the Mis18α-Mis18β Heterotetramer'. Molecular cell 61(5): 774–87. doi:10.1016/j.molcel.2016.02.014.

Nassar, Rim, Lily Thompson, and Elise Fouquerel. 2023. 'Molecular Mechanisms Protecting Centromeres from Self-Sabotage and Implications for Cancer Therapy'. NAR Cancer 5(2): zcad019. doi:10.1093/narcan/zcad019.

Naughton, Catherine, Covadonga Huidobro, Claudia R. Catacchio, Adam Buckle, Graeme R. Grimes, Ryu-Suke Nozawa, Stefania Purgato, Mariano Rocchi, and Nick Gilbert. 2022. 'Human Centromere

Repositioning Activates Transcription and Opens Chromatin Fibre Structure'. Nature Communications 13(1): 5609. doi:10.1038/s41467-022-33426-2.

Nawshad, A., D. LaGamba, and E. D. Hay. 2004. 'Transforming Growth Factor Beta (TGFbeta) Signalling in Palatal Growth, Apoptosis and Epithelial Mesenchymal Transformation (EMT)'. Archives of Oral Biology 49(9): 675–89. doi:10.1016/j.archoralbio.2004.05.007.

Nechemia-Arbely, Yael, Daniele Fachinetti, and Don W. Cleveland. 2012. 'Replicating Centromeric Chromatin: Spatial and Temporal Control of CENP-A Assembly'. Experimental Cell Research 318(12): 1353–60. doi:10.1016/j.yexcr.2012.04.007.

Nechemia-Arbely, Yael, Daniele Fachinetti, Karen H. Miga, Nikolina Sekulic, Gautam V. Soni, Dong Hyun Kim, Adeline K. Wong, et al. 2017. 'Human Centromeric CENP-A Chromatin Is a Homotypic, Octameric Nucleosome at All Cell Cycle Points'. The Journal of Cell Biology 216(3): 607–21. doi:10.1083/jcb.201608083.

Nechemia-Arbely, Yael, Karen H. Miga, Ofer Shoshani, Aaron Aslanian, Moira A. McMahon, Ah Young Lee, Daniele Fachinetti, et al. 2019. 'DNA Replication Acts as an Error Correction Mechanism to Maintain Centromere Identity by Restricting CENP-A to Centromeres'. Nature cell biology 21(6): 743–54. doi:10.1038/s41556-019-0331-4.

Newgreen, D. F., M. Ritterman, and E. A. Peters. 1979. 'Morphology and Behaviour of Neural Crest Cells of Chick Embryo in Vitro'. Cell and Tissue Research 203(1): 115–40. doi:10.1007/BF00234333.

Nicetto, Dario, and Kenneth S. Zaret. 2019. 'Role of H3K9me3 Heterochromatin in Cell Identity Establishment and Maintenance'. Current Opinion in Genetics & Development 55: 1–10. doi:10.1016/j.gde.2019.04.013.

Nieduszynski, Conrad A., J. Julian Blow, and Anne D. Donaldson. 2005. 'The Requirement of Yeast Replication Origins for Pre-Replication Complex Proteins Is Modulated by Transcription'. Nucleic Acids Research 33(8): 2410–20. doi:10.1093/nar/gki539.

Nieto, M. A., M. F. Bennett, M. G. Sargent, and D. G. Wilkinson. 1992. 'Cloning and Developmental Expression of Sna, a Murine Homologue of the Drosophila Snail Gene'. Development (Cambridge, England) 116(1): 227–37. doi:10.1242/dev.116.1.227.

Nieto, M. A., M. G. Sargent, D. G. Wilkinson, and J. Cooke. 1994. 'Control of Cell Behavior during Vertebrate Development by Slug, a Zinc Finger Gene'. Science (New York, N.Y.) 264(5160): 835–39. doi:10.1126/science.7513443.

Nieto, M. Angela. 2002. 'The Snail Superfamily of Zinc-Finger Transcription Factors'. Nature Reviews. Molecular Cell Biology 3(3): 155–66. doi:10.1038/nrm757.

Nieto, M. Angela, Ruby Yun-Ju Huang, Rebecca A. Jackson, and Jean Paul Thiery. 2016. 'EMT: 2016'. Cell 166(1): 21–45. doi:10.1016/j.cell.2016.06.028.

Nikbakht, Hamid, Eshini Panditharatna, Leonie G. Mikael, Rui Li, Tenzin Gayden, Matthew Osmond, Cheng-Ying Ho, et al. 2016. 'Spatial and Temporal Homogeneity of Driver Mutations in Diffuse Intrinsic Pontine Glioma'. Nature Communications 7: 11185. doi:10.1038/ncomms11185.

Nikolopoulou, Evanthia, Gabriel L. Galea, Ana Rolo, Nicholas D. E. Greene, and Andrew J. Copp. 2017. 'Neural Tube Closure: Cellular, Molecular and Biomechanical Mechanisms'. Development (Cambridge, England) 144(4): 552–66. doi:10.1242/dev.145904.

Niu, R. F., L. Zhang, G. M. Xi, X. Y. Wei, Y. Yang, Y. R. Shi, and X. S. Hao. 2007. 'Up-Regulation of Twist Induces Angiogenesis and Correlates with Metastasis in Hepatocellular Carcinoma'. Journal of experimental & clinical cancer research: CR 26(3): 385–94.

Noden, D. M. 1988. 'Interactions and Fates of Avian Craniofacial Mesenchyme'. Development (Cambridge, England) 103 Suppl: 121–40. doi:10.1242/dev.103.Supplement.121.

Noll, M., and R. D. Kornberg. 1977. 'Action of Micrococcal Nuclease on Chromatin and the Location of Histone H1'. Journal of Molecular Biology 109(3): 393–404. doi:10.1016/s0022-2836(77)80019-3.

Noman, Muhammad Zaeem, Bassam Janji, Abderemane Abdou, Meriem Hasmim, Stéphane Terry, Tuan Zea Tan, Fathia Mami-Chouaib, Jean Paul Thiery, and Salem Chouaib. 2017. 'The Immune Checkpoint Ligand PD-L1 Is Upregulated in EMT-Activated Human Breast Cancer Cells by a Mechanism Involving ZEB-1 and miR-200'. Oncoimmunology 6(1): e1263412. doi:10.1080/2162402X.2016.1263412.

Nora, Elphège P., Bryan R. Lajoie, Edda G. Schulz, Luca Giorgetti, Ikuhiro Okamoto, Nicolas Servant, Tristan Piolot, et al. 2012. 'Spatial Partitioning of the Regulatory Landscape of the X-Inactivation Centre'. Nature 485(7398): 381–85. doi:10.1038/nature11049.

Nurk, Sergey, Sergey Koren, Arang Rhie, Mikko Rautiainen, Andrey V. Bzikadze, Alla Mikheenko, Mitchell R. Vollger, et al. 2022. 'The Complete Sequence of a Human Genome'. Science (New York, N.Y.) 376(6588): 44–53. doi:10.1126/science.abj6987.

Nye, Jonathan, David Sturgill, Rajbir Athwal, and Yamini Dalal. 2018. 'HJURP Antagonizes CENP-A Mislocalization Driven by the H3.3 Chaperones HIRA and DAXX'. PLoS ONE 13(10): e0205948. doi:10.1371/journal.pone.0205948.

Nyhart, L. K. 1995. Biology Takes Form: Animal Morphology and the German Universities, 1800-1900. University of Chicago Press.

Ocaña, Oscar H., Rebeca Córcoles, Angels Fabra, Gema Moreno-Bueno, Hervé Acloque, Sonia Vega, Alejandro Barrallo-Gimeno, Amparo Cano, and M. Angela Nieto. 2012. 'Metastatic Colonization Requires the Repression of the Epithelial-Mesenchymal Transition Inducer Prrx1'. Cancer Cell 22(6): 709–24. doi:10.1016/j.ccr.2012.10.012.

Oesterreich, Fernando Carrillo, Lydia Herzel, Korinna Straube, Katja Hujer, Jonathon Howard, and Karla M. Neugebauer. 2016. 'Splicing of Nascent RNA Coincides with Intron Exit from RNA Polymerase II'. Cell 165(2): 372–81. doi:10.1016/j.cell.2016.02.045.

Ogiyama, Yuki, Bernd Schuettengruber, Giorgio L. Papadopoulos, Jia-Ming Chang, and Giacomo Cavalli. 2018. 'Polycomb-Dependent Chromatin Looping Contributes to Gene Silencing during Drosophila Development'. Molecular Cell 71(1): 73-88.e5. doi:10.1016/j.molcel.2018.05.032.

Ohkuni, Kentaro, Yoshimitsu Takahashi, Alyona Fulp, Josh Lawrimore, Wei-Chun Au, Nagesh Pasupala, Reuben Levy-Myers, et al. 2016. 'SUMO-Targeted Ubiquitin Ligase (STUbL) Slx5 Regulates Proteolysis of Centromeric Histone H3 Variant Cse4 and Prevents Its Mislocalization to Euchromatin'. Molecular Biology of the Cell 27(9): 1500–1510. doi:10.1091/mbc.E15-12-0827.

Okada, Masahiro, Iain M. Cheeseman, Tetsuya Hori, Katsuya Okawa, Ian X. McLeod, John R. Yates, Arshad Desai, and Tatsuo Fukagawa. 2006. 'The CENP-H-I Complex Is Required for the Efficient Incorporation of Newly Synthesized CENP-A into Centromeres'. Nature Cell Biology 8(5): 446–57. doi:10.1038/ncb1396.

Okano, M., D. W. Bell, D. A. Haber, and E. Li. 1999. 'DNA Methyltransferases Dnmt3a and Dnmt3b Are Essential for de Novo Methylation and Mammalian Development'. Cell 99(3): 247–57. doi:10.1016/s0092-8674(00)81656-6.

Olins, A. L., and D. E. Olins. 1974. 'Spheroid Chromatin Units (v Bodies)'. Science (New York, N.Y.) 183(4122): 330–32. doi:10.1126/science.183.4122.330.

Ollion, Jean, François Loll, Julien Cochennec, Thomas Boudier, and Christophe Escudé. 2015. 'Proliferation-Dependent Positioning of Individual Centromeres in the Interphase Nucleus of Human Lymphoblastoid Cell Lines'. Molecular Biology of the Cell 26(13): 2550–60. doi:10.1091/mbc.E14-05-1002.

Olsen, Jun Jun, Sebastian Öther-Gee Pohl, Abhijeet Deshmukh, Malini Visweswaran, Natalie C Ward, Frank Arfuso, Mark Agostino, and Arun Dharmarajan. 2017. 'The Role of Wnt Signalling in Angiogenesis'. The Clinical Biochemist Reviews 38(3): 131–42.

Ooi, Steen K. T., Chen Qiu, Emily Bernstein, Keqin Li, Da Jia, Zhe Yang, Hediye Erdjument-Bromage, et al. 2007. 'DNMT3L Connects Unmethylated Lysine 4 of Histone H3 to de Novo Methylation of DNA'. Nature 448(7154): 714–17. doi:10.1038/nature05987.

Osborne, Barbara A., and Lisa M. Minter. 2007. 'Notch Signalling during Peripheral T-Cell Activation and Differentiation'. Nature Reviews. Immunology 7(1): 64–75. doi:10.1038/nri1998.

Osborne, Cameron S., Lyubomira Chakalova, Karen E. Brown, David Carter, Alice Horton, Emmanuel Debrand, Beatriz Goyenechea, et al. 2004. 'Active Genes Dynamically Colocalize to Shared Sites of Ongoing Transcription'. Nature Genetics 36(10): 1065–71. doi:10.1038/ng1423.

Osorio, José Miguel, Claudio Espinoza-Pérez, Constanza Rimassa-Taré, Víctor Machuca, Juan Ortega Bustos, Matías Vallejos, Héctor Vargas, and Guillermo Díaz-Araya. 2023. 'Senescent Cardiac Fibroblasts: A Key Role in Cardiac Fibrosis'. Biochimica Et Biophysica Acta. Molecular Basis of Disease 1869(4): 166642. doi:10.1016/j.bbadis.2023.166642.

Owen, Katie L., Natasha K. Brockwell, and Belinda S. Parker. 2019. 'JAK-STAT Signaling: A Double-Edged Sword of Immune Regulation and Cancer Progression'. Cancers 11(12): 2002. doi:10.3390/cancers11122002.

Ozawa, M, H Baribault, and R Kemler. 1989. 'The Cytoplasmic Domain of the Cell Adhesion Molecule Uvomorulin Associates with Three Independent Proteins Structurally Related in Different Species.' The EMBO Journal 8(6): 1711–17.

Padeganeh, Abbas, Joël Ryan, Jacques Boisvert, Anne-Marie Ladouceur, Jonas F. Dorn, and Paul S. Maddox. 2013. 'Octameric CENP-A Nucleosomes Are Present at Human Centromeres throughout the Cell Cycle'. Current biology: CB 23(9): 764–69. doi:10.1016/j.cub.2013.03.037.

Pagan, R., I. Martín, M. Llobera, and S. Vilaró. 1997. 'Epithelial-Mesenchymal Transition of Cultured Rat Neonatal Hepatocytes Is Differentially Regulated in Response to Epidermal Growth Factor and Dimethyl Sulfoxide'. Hepatology (Baltimore, Md.) 25(3): 598–606. doi:10.1002/hep.510250318.

Palladino, Jason, Ankita Chavan, Anthony Sposato, Timothy D. Mason, and Barbara G. Mellone. 2020. 'Targeted De Novo Centromere Formation in Drosophila Reveals Plasticity and Maintenance Potential of CENP-A Chromatin'. Developmental Cell 52(3): 379-394.e7. doi:10.1016/j.devcel.2020.01.005.

Palmer, D K, K O'Day, H L Trong, H Charbonneau, and R L Margolis. 1991. 'Purification of the Centromere-Specific Protein CENP-A and Demonstration That It Is a Distinctive Histone.' Proceedings of the National Academy of Sciences of the United States of America 88(9): 3734–38.

Palmer, D. K., K. O'Day, M. H. Wener, B. S. Andrews, and R. L. Margolis. 1987. 'A 17-kD Centromere Protein (CENP-A) Copurifies with Nucleosome Core Particles and with Histones'. The Journal of Cell Biology 104(4): 805–15. doi:10.1083/jcb.104.4.805.

Pan, Chenyi, and Yuhong Fan. 2016. 'Role of H1 Linker Histones in Mammalian Development and Stem Cell Differentiation'. Biochimica Et Biophysica Acta 1859(3): 496–509. doi:10.1016/j.bbagrm.2015.12.002.

Pan, Dongqing, Kerstin Klare, Arsen Petrovic, Annika Take, Kai Walstein, Priyanka Singh, Arnaud Rondelet, Alexander W Bird, and Andrea Musacchio. 2017. 'CDK-Regulated Dimerization of M18BP1 on a Mis18 Hexamer Is Necessary for CENP-A Loading' ed. Asifa Akhtar. eLife 6: e23352. doi:10.7554/eLife.23352.

Pan, Dongqing, Kai Walstein, Annika Take, David Bier, Nadine Kaiser, and Andrea Musacchio. 2019. 'Mechanism of Centromere Recruitment of the CENP-A Chaperone HJURP and Its Implications for Centromere Licensing'. Nature Communications 10: 4046. doi:10.1038/s41467-019-12019-6.

Pan, Fong Cheng, and Chris Wright. 2011. 'Pancreas Organogenesis: From Bud to Plexus to Gland'. Developmental Dynamics: An Official Publication of the American Association of Anatomists 240(3): 530–65. doi:10.1002/dvdy.22584.

Panchenko, Tanya, Troy C. Sorensen, Christopher L. Woodcock, Zhong-Yuan Kan, Stacey Wood, Michael G. Resch, Karolin Luger, et al. 2011. 'Replacement of Histone H3 with CENP-A Directs Global Nucleosome Array Condensation and Loosening of Nucleosome Superhelical Termini'. Proceedings of the National Academy of Sciences of the United States of America 108(40): 16588–93. doi:10.1073/pnas.1113621108.

Pang, Qing You, Tuan Zea Tan, Vignesh Sundararajan, Yi-Chia Chiu, Edward Yu Wing Chee, Vin Yee Chung, Mahesh A. Choolani, and Ruby Yun-Ju Huang. 2022. '3D Genome Organization in the Epithelial-Mesenchymal Transition Spectrum'. Genome Biology 23(1): 121. doi:10.1186/s13059-022-02687-x.

Pappalardo, Xena Giada, and Viviana Barra. 2021. 'Losing DNA Methylation at Repetitive Elements and Breaking Bad'. Epigenetics & Chromatin 14(1): 25. doi:10.1186/s13072-021-00400-z.

Parfenyev, Sergey, Aastha Singh, Olga Fedorova, Alexandra Daks, Ritu Kulshreshtha, and Nickolai A. Barlev. 2021. 'Interplay between P53 and Non-Coding RNAs in the Regulation of EMT in Breast Cancer'. Cell Death & Disease 12(1): 17. doi:10.1038/s41419-020-03327-7.

Park, Sun-Mi, Arti B. Gaur, Ernst Lengyel, and Marcus E. Peter. 2008. 'The miR-200 Family Determines the Epithelial Phenotype of Cancer Cells by Targeting the E-Cadherin Repressors ZEB1 and ZEB2'. Genes & Development 22(7): 894–907. doi:10.1101/gad.1640608.

Parvani, Jenny G., Maneesh D. Gujrati, Margaret A. Mack, William P. Schiemann, and Zheng-Rong Lu. 2015. 'Silencing B3 Integrin by Targeted ECO/siRNA Nanoparticles Inhibits EMT and Metastasis of Triple Negative Breast Cancer'. Cancer research 75(11): 2316–25. doi:10.1158/0008-5472.CAN-14-3485.

Pastushenko, Ievgenia, and Cédric Blanpain. 2019. 'EMT Transition States during Tumor Progression and Metastasis'. Trends in Cell Biology 29(3): 212–26. doi:10.1016/j.tcb.2018.12.001.

Pastushenko, Ievgenia, Audrey Brisebarre, Alejandro Sifrim, Marco Fioramonti, Tatiana Revenco, Soufiane Boumahdi, Alexandra Van Keymeulen, et al. 2018. 'Identification of the Tumour Transition States Occurring during EMT'. Nature 556(7702): 463–68. doi:10.1038/s41586-018-0040-3.

Pattabiraman, Sundararaghavan, Gajendra Kumar Azad, Triana Amen, Shlomi Brielle, Jung Eun Park, Siu Kwan Sze, Eran Meshorer, and Daniel Kaganovich. 2020. 'Vimentin Protects Differentiating Stem Cells from Stress'. Scientific Reports 10(1): 19525. doi:10.1038/s41598-020-76076-4.

Patteson, Alison E., Amir Vahabikashi, Katarzyna Pogoda, Stephen A. Adam, Kalpana Mandal, Mark Kittisopikul, Suganya Sivagurunathan, et al. 2019. 'Vimentin Protects Cells against Nuclear Rupture and DNA Damage during Migration'. The Journal of Cell Biology 218(12): 4079–92. doi:10.1083/jcb.201902046.

Peinado, Hector, Esteban Ballestar, Manel Esteller, and Amparo Cano. 2004. 'Snail Mediates E-Cadherin Repression by the Recruitment of the Sin3A/Histone Deacetylase 1 (HDAC1)/HDAC2 Complex'. Molecular and Cellular Biology 24(1): 306–19. doi:10.1128/MCB.24.1.306-319.2004.

Perea-Gomez, Aitana, Francis D. J. Vella, William Shawlot, Mustapha Oulad-Abdelghani, Claire Chazaud, Chikara Meno, Veronique Pfister, et al. 2002. 'Nodal Antagonists in the Anterior Visceral Endoderm Prevent the Formation of Multiple Primitive Streaks'. Developmental Cell 3(5): 745–56. doi:10.1016/s1534-5807(02)00321-0.

Pérez, Alberto, Chiara Lara Castellazzi, Federica Battistini, Kathryn Collinet, Oscar Flores, Ozgen Deniz, Maria Luz Ruiz, et al. 2012. 'Impact of Methylation on the Physical Properties of DNA'. Biophysical Journal 102(9): 2140–48. doi:10.1016/j.bpj.2012.03.056.

Pérez-Montero, Salvador, Albert Carbonell, and Fernando Azorín. 2016. 'Germline-Specific H1 Variants: The "Sexy" Linker Histones'. Chromosoma 125(1): 1–13. doi:10.1007/s00412-015-0517-x.

Perl, A. K., P. Wilgenbus, U. Dahl, H. Semb, and G. Christofori. 1998. 'A Causal Role for E-Cadherin in the Transition from Adenoma to Carcinoma'. Nature 392(6672): 190–93. doi:10.1038/32433.

Perpelescu, Marinela, Naohito Nozaki, Chikashi Obuse, Hua Yang, and Kinya Yoda. 2009. 'Active Establishment of Centromeric CENP-A Chromatin by RSF Complex'. The Journal of Cell Biology 185(3): 397–407. doi:10.1083/jcb.200903088.

Peters, A. H., D. O'Carroll, H. Scherthan, K. Mechtler, S. Sauer, C. Schöfer, K. Weipoltshammer, et al. 2001. 'Loss of the Suv39h Histone Methyltransferases Impairs Mammalian Heterochromatin and Genome Stability'. Cell 107(3): 323–37. doi:10.1016/s0092-8674(01)00542-6.

Peters, Antoine H. F. M., Stefan Kubicek, Karl Mechtler, Roderick J. O'Sullivan, Alwin A. H. A. Derijck, Laura Perez-Burgos, Alexander Kohlmaier, et al. 2003. 'Partitioning and Plasticity of Repressive Histone Methylation States in Mammalian Chromatin'. Molecular Cell 12(6): 1577–89. doi:10.1016/s1097-2765(03)00477-5.

Petryk, Nataliya, Maria Dalby, Alice Wenger, Caroline B. Stromme, Anne Strandsby, Robin Andersson, and Anja Groth. 2018. 'MCM2 Promotes Symmetric Inheritance of Modified Histones

during DNA Replication'. Science (New York, N.Y.) 361(6409): 1389–92. doi:10.1126/science.aau0294.

Phansalkar, Ragini, Pascal Lapierre, and Barbara G. Mellone. 2012. 'Evolutionary Insights into the Role of the Essential Centromere Protein CAL1 in Drosophila'. Chromosome Research: An International Journal on the Molecular, Supramolecular and Evolutionary Aspects of Chromosome Biology 20(5): 493–504. doi:10.1007/s10577-012-9299-7.

Piccinin, Sara, Elena Tonin, Sara Sessa, Silvia Demontis, Sabrina Rossi, Lorenza Pecciarini, Lucia Zanatta, et al. 2012. 'A "Twist Box" Code of P53 Inactivation: Twist Box: P53 Interaction Promotes P53 Degradation'. Cancer Cell 22(3): 404–15. doi:10.1016/j.ccr.2012.08.003.

Piña, B., and P. Suau. 1987. 'Changes in Histones H2A and H3 Variant Composition in Differentiating and Mature Rat Brain Cortical Neurons'. Developmental Biology 123(1): 51–58. doi:10.1016/0012-1606(87)90426-x.

Piras, Francesca M., Solomon G. Nergadze, Elisa Magnani, Livia Bertoni, Carmen Attolini, Lela Khoriauli, Elena Raimondi, and Elena Giulotto. 2010. 'Uncoupling of Satellite DNA and Centromeric Function in the Genus Equus'. PLOS Genetics 6(2): e1000845. doi:10.1371/journal.pgen.1000845.

Pliatska, Maria, Maria Kapasa, Antonis Kokkalis, Alexander Polyzos, and Dimitris Thanos. 2018. 'The Histone Variant MacroH2A Blocks Cellular Reprogramming by Inhibiting Mesenchymal-to-Epithelial Transition'. Molecular and Cellular Biology 38(10): e00669-17. doi:10.1128/MCB.00669-17.

Plikus, Maksim V., Xiaojie Wang, Sarthak Sinha, Elvira Forte, Sean M. Thompson, Erica L. Herzog, Ryan R. Driskell, et al. 2021. 'Fibroblasts: Origins, Definitions, and Functions in Health and Disease'. Cell 184(15). doi:10.1016/j.cell.2021.06.024.

Plohl, Miroslav, Nevenka Meštrović, and Brankica Mravinac. 2014. 'Centromere Identity from the DNA Point of View'. Chromosoma 123(4): 313–25. doi:10.1007/s00412-014-0462-0.

Pluta, A. F., A. M. Mackay, A. M. Ainsztein, I. G. Goldberg, and W. C. Earnshaw. 1995. 'The Centromere: Hub of Chromosomal Activities'. Science (New York, N.Y.) 270(5242): 1591–94. doi:10.1126/science.270.5242.1591.

Pokholok, Dmitry K., Christopher T. Harbison, Stuart Levine, Megan Cole, Nancy M. Hannett, Tong Ihn Lee, George W. Bell, et al. 2005. 'Genome-Wide Map of Nucleosome Acetylation and Methylation in Yeast'. Cell 122(4): 517–27. doi:10.1016/j.cell.2005.06.026.

Polioudaki, Hara, Sofia Agelaki, Rena Chiotaki, Eleni Politaki, Dimitris Mavroudis, Alexios Matikas, Vassilis Georgoulias, and Panayiotis A. Theodoropoulos. 2015. 'Variable Expression Levels of Keratin and Vimentin Reveal Differential EMT Status of Circulating Tumor Cells and Correlation with Clinical Characteristics and Outcome of Patients with Metastatic Breast Cancer'. BMC cancer 15: 399. doi:10.1186/s12885-015-1386-7.

Polizzi, C., and L. Clarke. 1991. ‘The Chromatin Structure of Centromeres from Fission Yeast: Differentiation of the Central Core That Correlates with Function’. The Journal of Cell Biology 112(2): 191–201. doi:10.1083/jcb.112.2.191.

Polyak, Kornelia, and Robert A. Weinberg. 2009. ‘Transitions between Epithelial and Mesenchymal States: Acquisition of Malignant and Stem Cell Traits’. Nature Reviews. Cancer 9(4): 265–73. doi:10.1038/nrc2620.

Pöpperl, H., C. Schmidt, V. Wilson, C. R. Hume, J. Dodd, R. Krumlauf, and R. S. Beddington. 1997. ‘Misexpression of Cwnt8C in the Mouse Induces an Ectopic Embryonic Axis and Causes a Truncation of the Anterior Neuroectoderm’. Development (Cambridge, England) 124(15): 2997–3005. doi:10.1242/dev.124.15.2997.

Potapova, Tamara A, Jin Zhu, and Rong Li. 2013. ‘Aneuploidy and Chromosomal Instability: A Vicious Cycle Driving Cellular Evolution and Cancer Genome Chaos’. Cancer metastasis reviews 32(0): 10.1007/s10555-013-9436–6. doi:10.1007/s10555-013-9436-6.

Potts, J. D., J. M. Dagle, J. A. Walder, D. L. Weeks, and R. B. Runyan. 1991. ‘Epithelial-Mesenchymal Transformation of Embryonic Cardiac Endothelial Cells Is Inhibited by a Modified Antisense Oligodeoxynucleotide to Transforming Growth Factor Beta 3’. Proceedings of the National Academy of Sciences of the United States of America 88(4): 1516–20. doi:10.1073/pnas.88.4.1516.

Prat, Aleix, Joel S. Parker, Olga Karginova, Cheng Fan, Chad Livasy, Jason I. Herschkowitz, Xiaping He, and Charles M. Perou. 2010. ‘Phenotypic and Molecular Characterization of the Claudin-Low Intrinsic Subtype of Breast Cancer’. Breast cancer research: BCR 12(5): R68. doi:10.1186/bcr2635.

Prat, Aleix, and Charles M. Perou. 2011. ‘Deconstructing the Molecular Portraits of Breast Cancer’. Molecular Oncology 5(1): 5–23. doi:10.1016/j.molonc.2010.11.003.

Prendergast, Laura, and Danny Reinberg. 2021. ‘The Missing Linker: Emerging Trends for H1 Variant-Specific Functions’. Genes & Development 35(1–2): 40–58. doi:10.1101/gad.344531.120.

Prodhomme, Mélanie K., Roxane M. Pommier, Camille Franchet, Frédérique Fauvet, Valérie Bergoglio, Pierre Brousset, Anne-Pierre Morel, et al. 2021. ‘EMT Transcription Factor ZEB1 Represses the Mutagenic POLθ-Mediated End-Joining Pathway in Breast Cancers’. Cancer Research 81(6): 1595–1606. doi:10.1158/0008-5472.CAN-20-2626.

Proetzel, G., S. A. Pawlowski, M. V. Wiles, M. Yin, G. P. Boivin, P. N. Howles, J. Ding, M. W. Ferguson, and T. Doetschman. 1995. ‘Transforming Growth Factor-Beta 3 Is Required for Secondary Palate Fusion’. Nature Genetics 11(4): 409–14. doi:10.1038/ng1295-409.

Provenzano, P. P., D. R. Inman, K. W. Eliceiri, and P. J. Keely. 2009. ‘Matrix Density-Induced Mechanoregulation of Breast Cell Phenotype, Signaling and Gene Expression through a FAK-ERK Linkage’. Oncogene 28(49): 4326–43. doi:10.1038/onc.2009.299.

Przewloka, Marcin R., Zsolt Venkei, Victor M. Bolanos-Garcia, Janusz Debski, Michal Dadlez, and David M. Glover. 2011. 'CENP-C Is a Structural Platform for Kinetochore Assembly'. Current biology: CB 21(5): 399–405. doi:10.1016/j.cub.2011.02.005.

Pueschel, Ringo, Francesca Coraggio, and Peter Meister. 2016. 'From Single Genes to Entire Genomes: The Search for a Function of Nuclear Organization'. Development (Cambridge, England) 143(6): 910–23. doi:10.1242/dev.129007.

Puram, Sidharth V., Itay Tirosh, Anuraag S. Parikh, Anoop P. Patel, Keren Yizhak, Shawn Gillespie, Christopher Rodman, et al. 2017. 'Single-Cell Transcriptomic Analysis of Primary and Metastatic Tumor Ecosystems in Head and Neck Cancer'. Cell 171(7): 1611-1624.e24. doi:10.1016/j.cell.2017.10.044.

Qian, Li-Wu, Andrea B. Fourcaudot, Kazuyoshi Yamane, Tao You, Rodney K. Chan, and Kai P. Leung. 2016. 'Exacerbated and Prolonged Inflammation Impairs Wound Healing and Increases Scarring'. Wound Repair and Regeneration: Official Publication of the Wound Healing Society [and] the European Tissue Repair Society 24(1): 26–34. doi:10.1111/wrr.12381.

Qiao, Yunbo, Zejian Wang, Fangzhi Tan, Jun Chen, Jianxiang Lin, Jie Yang, Hui Li, et al. 2020. 'Enhancer Reprogramming within Pre-Existing Topologically Associated Domains Promotes TGF-β-Induced EMT and Cancer Metastasis'. Molecular Therapy: The Journal of the American Society of Gene Therapy 28(9): 2083–95. doi:10.1016/j.ymthe.2020.05.026.

Qin, Qian, Young Xu, Tao He, Chunlin Qin, and Jianming Xu. 2012. 'Normal and Disease-Related Biological Functions of Twist1 and Underlying Molecular Mechanisms'. Cell Research 22(1): 90–106. doi:10.1038/cr.2011.144.

Qiu, Jun-Jun, Jun-Jie Guo, Tian-Jiao Lv, Hong-Yan Jin, Jing-Xin Ding, Wei-Wei Feng, Ying Zhang, and Ke-Qin Hua. 2013. 'Prognostic Value of Centromere Protein-A Expression in Patients with Epithelial Ovarian Cancer'. Tumor Biology 34(5): 2971–75. doi:10.1007/s13277-013-0860-6.

Rada-Iglesias, Alvaro, Ruchi Bajpai, Tomek Swigut, Samantha A. Brugmann, Ryan A. Flynn, and Joanna Wysocka. 2011. 'A Unique Chromatin Signature Uncovers Early Developmental Enhancers in Humans'. Nature 470(7333): 279–83. doi:10.1038/nature09692.

Ramachandran, Anassuya, Pedro Vizán, Debipriya Das, Probir Chakravarty, Janis Vogt, Katherine W. Rogers, Patrick Müller, et al. 2018. 'TGF-β Uses a Novel Mode of Receptor Activation to Phosphorylate SMAD1/5 and Induce Epithelial-to-Mesenchymal Transition'. eLife 7: e31756. doi:10.7554/eLife.31756.

Ranjan, Rajesh, Jonathan Snedeker, and Xin Chen. 2019. 'Asymmetric Centromeres Differentially Coordinate with Mitotic Machinery to Ensure Biased Sister Chromatid Segregation in Germline Stem Cells'. Cell stem cell 25(5): 666. doi:10.1016/j.stem.2019.08.014.

Ranjitkar, Prerana, Maximilian O. Press, Xianhua Yi, Richard Baker, Michael J. MacCoss, and Sue Biggins. 2010. 'An E3 Ubiquitin Ligase Prevents Ectopic Localization of the Centromeric Histone H3 Variant via the Centromere Targeting Domain'. Molecular Cell 40(3): 455–64. doi:10.1016/j.molcel.2010.09.025.

Rasmussen, Jeffrey P., Kathryn English, Jennifer Tenlen, and James R. Priess. 2008. 'Notch Signaling and Morphogenesis of Single-Cell Tubes in the C. Elegans Digestive Tract'. Developmental cell 14(4): 559–69. doi:10.1016/j.devcel.2008.01.019.

Rattner, J. B., and B. A. Hamkalo. 1978. 'Higher Order Structure in Metaphase Chromosomes. II. The Relationship between the 250 A Fiber, Superbeads and Beads-on-a-String'. Chromosoma 69(3): 373–79. doi:10.1007/BF00332140.

Rattner, J. B., and B. A. Hamkalo. 1979. 'Nucleosome Packing in Interphase Chromatin'. The Journal of Cell Biology 81(2): 453–57. doi:10.1083/jcb.81.2.453.

Ray-Gallet, Dominique, and Geneviève Almouzni. 2021. 'The Histone H3 Family and Its Deposition Pathways'. Advances in Experimental Medicine and Biology 1283: 17–42. doi:10.1007/978-981-15-8104-5_2.

Ray-Gallet, Dominique, and Geneviève Almouzni. 2021. 'The Histone H3 Family and Its Deposition Pathways'. In Histone Mutations and Cancer, Advances in Experimental Medicine and Biology, eds. Dong Fang and Junhong Han. Singapore: Springer, 17–42. doi:10.1007/978-981-15-8104-5_2.

Ray-Gallet, Dominique, and Geneviève Almouzni. 2022. 'H3-H4 Histone Chaperones and Cancer'. Current Opinion in Genetics & Development 73: 101900. doi:10.1016/j.gde.2022.101900.

Ray-Gallet, Dominique, Adam Woolfe, Isabelle Vassias, Céline Pellentz, Nicolas Lacoste, Aastha Puri, David C. Schultz, et al. 2011. 'Dynamics of Histone H3 Deposition in Vivo Reveal a Nucleosome Gap-Filling Mechanism for H3.3 to Maintain Chromatin Integrity'. Molecular Cell 44(6): 928–41. doi:10.1016/j.molcel.2011.12.006.

Razin, A., and H. Cedar. 1977. 'Distribution of 5-Methylcytosine in Chromatin'. Proceedings of the National Academy of Sciences of the United States of America 74(7): 2725–28. doi:10.1073/pnas.74.7.2725.

Régnier, Vinciane, Paola Vagnarelli, Tatsuo Fukagawa, Tatiana Zerjal, Elizabeth Burns, Didier Trouche, William Earnshaw, and William Brown. 2005. 'CENP-A Is Required for Accurate Chromosome Segregation and Sustained Kinetochore Association of BubR1'. Molecular and Cellular Biology 25(10): 3967–81. doi:10.1128/MCB.25.10.3967-3981.2005.

Rembold, Martina, Lucia Ciglar, J. Omar Yáñez-Cuna, Robert P. Zinzen, Charles Girardot, Ankit Jain, Michael A. Welte, et al. 2014. 'A Conserved Role for Snail as a Potentiator of Active Transcription'. Genes & Development 28(2): 167–81. doi:10.1101/gad.230953.113.

Renaud-Pageot, Charlène, and Geneviève Almouzni. 2024. ‘Tipping the Balance in Histone Supply Puts Genome Stability at Stake’. The EMBO journal 43(11): 2091–93. doi:10.1038/s44318-024-00112-6.

Renaud-Pageot, Charlène, Jean-Pierre Quivy, Marina Lochhead, and Geneviève Almouzni. 2022. ‘CENP-A Regulation and Cancer’. Frontiers in Cell and Developmental Biology 10: 907120. doi:10.3389/fcell.2022.907120.

Revenco, Tatiana, Adeline Nicodème, Ievgenia Pastushenko, Magdalena K. Sznurkowska, Mathilde Latil, Panagiota A. Sotiropoulou, Christine Dubois, et al. 2019. ‘Context Dependency of Epithelial-to-Mesenchymal Transition for Metastasis’. Cell Reports 29(6): 1458-1468.e3. doi:10.1016/j.celrep.2019.09.081.

Reyes, H., S. Reisz-Porszasz, and O. Hankinson. 1992. ‘Identification of the Ah Receptor Nuclear Translocator Protein (Arnt) as a Component of the DNA Binding Form of the Ah Receptor’. Science (New York, N.Y.) 256(5060): 1193–95. doi:10.1126/science.256.5060.1193.

Rhim, Andrew D., Emily T. Mirek, Nicole M. Aiello, Anirban Maitra, Jennifer M. Bailey, Florencia McCallister, Maximilian Reichert, et al. 2012. ‘EMT and Dissemination Precede Pancreatic Tumor Formation’. Cell 148(1–2): 349–61. doi:10.1016/j.cell.2011.11.025.

Rhind, Nicholas, Scott Cheng-Hsin Yang, and John Bechhoefer. 2010. ‘Reconciling Stochastic Origin Firing with Defined Replication Timing’. Chromosome Research: An International Journal on the Molecular, Supramolecular and Evolutionary Aspects of Chromosome Biology 18(1): 35–43. doi:10.1007/s10577-009-9093-3.

Ricci, Maria Aurelia, Carlo Manzo, María Filomena García-Parajo, Melike Lakadamyali, and Maria Pia Cosma. 2015. ‘Chromatin Fibers Are Formed by Heterogeneous Groups of Nucleosomes in Vivo’. Cell 160(6): 1145–58. doi:10.1016/j.cell.2015.01.054.

Richards, Eric J., and Sarah C. R. Elgin. 2002. ‘Epigenetic Codes for Heterochromatin Formation and Silencing: Rounding up the Usual Suspects’. Cell 108(4): 489–500. doi:10.1016/s0092-8674(02)00644-x.

Richmond, T. J., M. A. Searles, and R. T. Simpson. 1988. ‘Crystals of a Nucleosome Core Particle Containing Defined Sequence DNA’. Journal of Molecular Biology 199(1): 161–70. doi:10.1016/0022-2836(88)90386-5.

Ricketts, M. Daniel, and Ronen Marmorstein. 2017. ‘A Molecular Prospective for HIRA Complex Assembly and H3.3-Specific Histone Chaperone Function’. Journal of Molecular Biology 429(13): 1924–33. doi:10.1016/j.jmb.2016.11.010.

Ridgway, Patricia, Karl D. Brown, Danny Rangasamy, Ulrica Svensson, and David J. Tremethick. 2004. ‘Unique Residues on the H2A.Z Containing Nucleosome Surface Are Important for Xenopus

Laevis Development'. The Journal of Biological Chemistry 279(42): 43815–20. doi:10.1074/jbc.M408409200.

Riethdorf, Sabine, Herbert Fritsche, Volkmar Müller, Thomas Rau, Christian Schindlbeck, Brigitte Rack, Wolfgang Janni, et al. 2007. 'Detection of Circulating Tumor Cells in Peripheral Blood of Patients with Metastatic Breast Cancer: A Validation Study of the CellSearch System'. Clinical Cancer Research: An Official Journal of the American Association for Cancer Research 13(3): 920–28. doi:10.1158/1078-0432.CCR-06-1695.

Riley, Todd, Eduardo Sontag, Patricia Chen, and Arnold Levine. 2008. 'Transcriptional Control of Human P53-Regulated Genes'. Nature Reviews. Molecular Cell Biology 9(5): 402–12. doi:10.1038/nrm2395.

Rinon, Ariel, Alina Molchadsky, Elisha Nathan, Gili Yovel, Varda Rotter, Rachel Sarig, and Eldad Tzahor. 2011. 'P53 Coordinates Cranial Neural Crest Cell Growth and Epithelial-Mesenchymal Transition/Delamination Processes'. Development (Cambridge, England) 138(9): 1827–38. doi:10.1242/dev.053645.

Rivera-Mulia, Juan Carlos, Quinton Buckley, Takayo Sasaki, Jared Zimmerman, Ruth A. Didier, Kristopher Nazor, Jeanne F. Loring, et al. 2015. 'Dynamic Changes in Replication Timing and Gene Expression during Lineage Specification of Human Pluripotent Stem Cells'. Genome Research 25(8): 1091–1103. doi:10.1101/gr.187989.114.

Robinson, Philip J. J., and Daniela Rhodes. 2006. 'Structure of the "30 Nm" Chromatin Fibre: A Key Role for the Linker Histone'. Current Opinion in Structural Biology 16(3): 336–43. doi:10.1016/j.sbi.2006.05.007.

Roca, Hernan, James Hernandez, Savannah Weidner, Richard C. McEachin, David Fuller, Sudha Sud, Taibriana Schumann, et al. 2013. 'Transcription Factors OVOL1 and OVOL2 Induce the Mesenchymal to Epithelial Transition in Human Cancer'. PLOS ONE 8(10): e76773. doi:10.1371/journal.pone.0076773.

Romano, L. A., and R. B. Runyan. 1999. 'Slug Is a Mediator of Epithelial-Mesenchymal Cell Transformation in the Developing Chicken Heart'. Developmental Biology 212(1): 243–54. doi:10.1006/dbio.1999.9339.

Ross, Justyne E., Kaitlin Stimpson Woodlief, and Beth A. Sullivan. 2016. 'Inheritance of the CENP-A Chromatin Domain Is Spatially and Temporally Constrained at Human Centromeres'. Epigenetics & Chromatin 9: 20. doi:10.1186/s13072-016-0071-7.

Roulland, Yohan, Khalid Ouararhni, Mladen Naidenov, Lorrie Ramos, Muhammad Shuaib, Sajad Hussain Syed, Imtiaz Nizar Lone, et al. 2016. 'The Flexible Ends of CENP-A Nucleosome Are Required for Mitotic Fidelity'. Molecular Cell 63(4): 674–85. doi:10.1016/j.molcel.2016.06.023.

Rowley, M. Jordan, and Victor G. Corces. 2018. ‘Organizational Principles of 3D Genome Architecture’. Nature Reviews. Genetics 19(12): 789–800. doi:10.1038/s41576-018-0060-8.

Ru, Peng, Robert Steele, Philip Newhall, Nancy J. Phillips, Karoly Toth, and Ratna B. Ray. 2012. ‘miRNA-29b Suppresses Prostate Cancer Metastasis by Regulating Epithelial-Mesenchymal Transition Signaling’. Molecular Cancer Therapeutics 11(5): 1166–73. doi:10.1158/1535-7163.MCT-12-0100.

Ruiz-Carrillo, A., L. J. Wangh, and V. G. Allfrey. 1975. ‘Processing of Newly Synthesized Histone Molecules’. Science (New York, N.Y.) 190(4210): 117–28. doi:10.1126/science.1166303.

Ruscetti, Marcus, Eman L. Dadashian, Weilong Guo, Bill Quach, David J. Mulholland, Juw Won Park, Linh M. Tran, et al. 2016. ‘HDAC Inhibition Impedes Epithelial-Mesenchymal Plasticity and Suppresses Metastatic, Castration-Resistant Prostate Cancer’. Oncogene 35(29): 3781–95. doi:10.1038/onc.2015.444.

Ruscetti, Marcus, Bill Quach, Eman L. Dadashian, David J. Mulholland, and Hong Wu. 2015. ‘Tracking and Functional Characterization of Epithelial-Mesenchymal Transition and Mesenchymal Tumor Cells during Prostate Cancer Metastasis’. Cancer Research 75(13): 2749–59. doi:10.1158/0008-5472.CAN-14-3476.

Russev, G, and R Hancock. 1982. ‘Assembly of New Histones into Nucleosomes and Their Distribution in Replicating Chromatin.’ Proceedings of the Nat. Aca. of Sciences of the USA 79(10): 3143–47.

Russo, V., Martienssen, R., and Riggs, A. D. 1996. Epigenetic mechanisms of gene regulation. Cold Spring Harbor Laboratory Press.

Rust, Michael J., Mark Bates, and Xiaowei Zhuang. 2006. ‘Sub-Diffraction-Limit Imaging by Stochastic Optical Reconstruction Microscopy (STORM)’. Nature Methods 3(10): 793–95. doi:10.1038/nmeth929.

Sacristan, Carlos, Kumiko Samejima, Lorena Andrade Ruiz, Moonmoon Deb, Maaike L.A. Lambers, Adam Buckle, Chris A. Brackley, et al. 2024. ‘Vertebrate Centromeres in Mitosis Are Functionally Bipartite Structures Stabilized by Cohesin’. Cell 187(12): 3006-3023.e26. doi:10.1016/j.cell.2024.04.014.

Saha, Anjan K., Rafael Contreras-Galindo, Yashar S. Niknafs, Matthew Iyer, Tingting Qin, Karthik Padmanabhan, Javed Siddiqui, et al. 2020. ‘The Role of the Histone H3 Variant CENPA in Prostate Cancer’. The Journal of Biological Chemistry 295(25): 8537–49. doi:10.1074/jbc.RA119.010080.

Saika, Shizuya, Kazuo Ikeda, Osamu Yamanaka, Misako Sato, Yasuteru Muragaki, Yoshitaka Ohnishi, Akira Ooshima, et al. 2004. ‘Transient Adenoviral Gene Transfer of Smad7 Prevents Injury-Induced Epithelial-Mesenchymal Transition of Lens Epithelium in Mice’. Laboratory Investigation; a Journal of Technical Methods and Pathology 84(10): 1259–70. doi:10.1038/labinvest.3700151.

Saint-André, Violaine, Eric Batsché, Christophe Rachez, and Christian Muchardt. 2011. 'Histone H3 Lysine 9 Trimethylation and HP1γ Favor Inclusion of Alternative Exons'. Nature Structural & Molecular Biology 18(3): 337–44. doi:10.1038/nsmb.1995.

Sakai, Akiko, Brian E. Schwartz, Sara Goldstein, and Kami Ahmad. 2009. 'Transcriptional and Developmental Functions of the H3.3 Histone Variant in Drosophila'. Current biology: CB 19(21): 1816–20. doi:10.1016/j.cub.2009.09.021.

Saldaña-Meyer, Ricardo, Edgar González-Buendía, Georgina Guerrero, Varun Narendra, Roberto Bonasio, Félix Recillas-Targa, and Danny Reinberg. 2014. 'CTCF Regulates the Human P53 Gene through Direct Interaction with Its Natural Antisense Transcript, Wrap53'. Genes & Development 28(7): 723–34. doi:10.1101/gad.236869.113.

Saldaña-Meyer, Ricardo, Javier Rodriguez-Hernaez, Thelma Escobar, Mayilaadumveettil Nishana, Karina Jácome-López, Elphege P. Nora, Benoit G. Bruneau, et al. 2019. 'RNA Interactions Are Essential for CTCF-Mediated Genome Organization'. Molecular cell 76(3): 412-422.e5. doi:10.1016/j.molcel.2019.08.015.

Samavarchi-Tehrani, Payman, Azadeh Golipour, Laurent David, Hoon-Ki Sung, Tobias A. Beyer, Alessandro Datti, Knut Woltjen, Andras Nagy, and Jeffrey L. Wrana. 2010. 'Functional Genomics Reveals a BMP-Driven Mesenchymal-to-Epithelial Transition in the Initiation of Somatic Cell Reprogramming'. Cell Stem Cell 7(1): 64–77. doi:10.1016/j.stem.2010.04.015.

Sample, Reilly A., Marina F. Nogueira, Robi D. Mitra, and Sidharth V. Puram. 2023. 'Epigenetic Regulation of Hybrid Epithelial-Mesenchymal Cell States in Cancer'. Oncogene 42(29): 2237–48. doi:10.1038/s41388-023-02749-9.

Sampson, Valerie B., Justin M. David, Isabel Puig, Pratima U. Patil, Antonio García de Herreros, George V. Thomas, and Ayyappan K. Rajasekaran. 2014. 'Wilms' Tumor Protein Induces an Epithelial-Mesenchymal Hybrid Differentiation State in Clear Cell Renal Cell Carcinoma'. PloS One 9(7): e102041. doi:10.1371/journal.pone.0102041.

Sànchez, Ricardo, and William F. Marzluff. 2002. 'The Stem-Loop Binding Protein Is Required for Efficient Translation of Histone mRNA in Vivo and in Vitro'. Molecular and Cellular Biology 22(20): 7093–7104. doi:10.1128/MCB.22.20.7093-7104.2002.

Sanchez-Pulido, Luis, Alison L. Pidoux, Chris P. Ponting, and Robin C. Allshire. 2009. 'Common Ancestry of the CENP-A Chaperones Scm3 and HJURP'. Cell 137(7): 1173–74. doi:10.1016/j.cell.2009.06.010.

Sanford, J. P., H. J. Clark, V. M. Chapman, and J. Rossant. 1987. 'Differences in DNA Methylation during Oogenesis and Spermatogenesis and Their Persistence during Early Embryogenesis in the Mouse'. Genes & Development 1(10): 1039–46. doi:10.1101/gad.1.10.1039.

Sanz, Gema, Madhurendra Singh, Sylvain Peuget, and Galina Selivanova. 2019. ‘Inhibition of P53 Inhibitors: Progress, Challenges and Perspectives’. Journal of Molecular Cell Biology 11(7): 586–99. doi:10.1093/jmcb/mjz075.

Sarthy, Jay F, Michael P Meers, Derek H Janssens, Jorja G Henikoff, Heather Feldman, Patrick J Paddison, Christina M Lockwood, et al. 2020. ‘Histone Deposition Pathways Determine the Chromatin Landscapes of H3.1 and H3.3 K27M Oncohistones’ eds. Jerry L Workman, Jessica K Tyler, Jerry L Workman, and Jonathan Licht. eLife 9: e61090. doi:10.7554/eLife.61090.

Sato, Misako, Yasuteru Muragaki, Shizuya Saika, Anita B. Roberts, and Akira Ooshima. 2003. ‘Targeted Disruption of TGF-Beta1/Smad3 Signaling Protects against Renal Tubulointerstitial Fibrosis Induced by Unilateral Ureteral Obstruction’. The Journal of Clinical Investigation 112(10): 1486–94. doi:10.1172/JCI19270.

Sauka-Spengler, Tatjana, and Marianne Bronner-Fraser. 2008. ‘Evolution of the Neural Crest Viewed from a Gene Regulatory Perspective’. Genesis (New York, N.Y.: 2000) 46(11): 673–82. doi:10.1002/dvg.20436.

Sawyer, Jacob M., Jessica R. Harrell, Gidi Shemer, Jessica Sullivan-Brown, Minna Roh-Johnson, and Goldstein Goldstein. 2010. ‘Apical Constriction: A Cell Shape Change That Can Drive Morphogenesis’. Developmental biology 341(1). doi:10.1016/j.ydbio.2009.09.009.

Scarpa, Elena, András Szabó, Anne Bibonne, Eric Theveneau, Maddy Parsons, and Roberto Mayor. 2015. ‘Cadherin Switch during EMT in Neural Crest Cells Leads to Contact Inhibition of Locomotion via Repolarization of Forces’. Developmental Cell 34(4): 421–34. doi:10.1016/j.devcel.2015.06.012.

Scelfo, Andrea, Annapaola Angrisani, Marco Grillo, Bethany M. Barnes, Francesc Muyas, Carolin M. Sauer, Chin Wei Brian Leung, et al. 2024. ‘Specialized Replication Mechanisms Maintain Genome Stability at Human Centromeres’. Molecular Cell 84(6): 1003-1020.e10. doi:10.1016/j.molcel.2024.01.018.

Scheibner, Katharina, Silvia Schirge, Ingo Burtscher, Maren Büttner, Michael Sterr, Dapeng Yang, Anika Böttcher, et al. 2021. ‘Epithelial Cell Plasticity Drives Endoderm Formation during Gastrulation’. Nature Cell Biology 23(7): 692–703. doi:10.1038/s41556-021-00694-x.

Schermelleh, Lothar, Peter M. Carlton, Sebastian Haase, Lin Shao, Lukman Winoto, Peter Kner, Brian Burke, et al. 2008. ‘Subdiffraction Multicolor Imaging of the Nuclear Periphery with 3D Structured Illumination Microscopy’. Science (New York, N.Y.) 320(5881): 1332–36. doi:10.1126/science.1156947.

Schlesinger, Sharon, and Eran Meshorer. 2019. ‘Open Chromatin, Epigenetic Plasticity, and Nuclear Organization in Pluripotency’. Developmental Cell 48(2): 135–50. doi:10.1016/j.devcel.2019.01.003.

Schliekelman, Mark J., Ayumu Taguchi, Jun Zhu, Xudong Dai, Jaime Rodriguez, Muge Celiktas, Qing Zhang, et al. 2015. 'Molecular Portraits of Epithelial, Mesenchymal, and Hybrid States in Lung Adenocarcinoma and Their Relevance to Survival'. Cancer Research 75(9): 1789–1800. doi:10.1158/0008-5472.CAN-14-2535.

Schoenfelder, Stefan, Tom Sexton, Lyubomira Chakalova, Nathan F. Cope, Alice Horton, Simon Andrews, Sreenivasulu Kurukuti, et al. 2010. 'Preferential Associations between Co-Regulated Genes Reveal a Transcriptional Interactome in Erythroid Cells'. Nature Genetics 42(1): 53–61. doi:10.1038/ng.496.

Schoenfelder, Stefan, Robert Sugar, Andrew Dimond, Biola-Maria Javierre, Harry Armstrong, Borbala Mifsud, Emilia Dimitrova, et al. 2015. 'Polycomb Repressive Complex PRC1 Spatially Constrains the Mouse Embryonic Stem Cell Genome'. Nature Genetics 47(10): 1179–86. doi:10.1038/ng.3393.

Schueler, Mary G., Willie Swanson, Pamela J. Thomas, and Eric D. Green. 2010. 'Adaptive Evolution of Foundation Kinetochore Proteins in Primates'. Molecular Biology and Evolution 27(7): 1585–97. doi:10.1093/molbev/msq043.

Schuettengruber, Bernd, Henri-Marc Bourbon, Luciano Di Croce, and Giacomo Cavalli. 2017. 'Genome Regulation by Polycomb and Trithorax: 70 Years and Counting'. Cell 171(1): 34–57. doi:10.1016/j.cell.2017.08.002.

Schuh, Melina, Christian F. Lehner, and Stefan Heidmann. 2007. 'Incorporation of Drosophila CID/CENP-A and CENP-C into Centromeres during Early Embryonic Anaphase'. Current biology: CB 17(3): 237–43. doi:10.1016/j.cub.2006.11.051.

Schuhwerk, Harald, Julia Kleemann, Pooja Gupta, Ruthger van Roey, Isabell Armstark, Martina Kreileder, Nora Feldker, et al. 2022. 'The EMT Transcription Factor ZEB1 Governs a Fitness-Promoting but Vulnerable DNA Replication Stress Response'. Cell Reports 41(11). doi:10.1016/j.celrep.2022.111819.

Schwartzentruber, Jeremy, Andrey Korshunov, Xiao-Yang Liu, David T. W. Jones, Elke Pfaff, Karine Jacob, Dominik Sturm, et al. 2012. 'Driver Mutations in Histone H3.3 and Chromatin Remodelling Genes in Paediatric Glioblastoma'. Nature 482(7384): 226–31. doi:10.1038/nature10833.

Scott, Charlotte L., and Kyla D. Omilusik. 2019. 'ZEBs: Novel Players in Immune Cell Development and Function'. Trends in Immunology 40(5): 431–46. doi:10.1016/j.it.2019.03.001.

Screpanti, Emanuela, Anna De Antoni, Gregory M. Alushin, Arsen Petrovic, Tiziana Melis, Eva Nogales, and Andrea Musacchio. 2011. 'Direct Binding of Cenp-C to the Mis12 Complex Joins the Inner and Outer Kinetochore'. Current biology : CB 21(5): 391–98. doi:10.1016/j.cub.2010.12.039.

Scully, Ralph, Arvind Panday, Rajula Elango, and Nicholas A. Willis. 2019. ‘DNA Double-Strand Break Repair-Pathway Choice in Somatic Mammalian Cells’. Nature Reviews. Molecular Cell Biology 20(11): 698–714. doi:10.1038/s41580-019-0152-0.

Segelle, Alexandre, Yaiza Núñez-Álvarez, Andrew J. Oldfield, Kimberly M. Webb, Philipp Voigt, and Reini F. Luco. 2022. ‘Histone Marks Regulate the Epithelial-to-Mesenchymal Transition via Alternative Splicing’. Cell Reports 38(7): 110357. doi:10.1016/j.celrep.2022.110357.

Seguin, Laetitia, Shumei Kato, Aleksandra Franovic, M. Fernanda Camargo, Jacqueline Lesperance, Kathryn C. Elliott, Mayra Yebra, et al. 2014. ‘An Integrin B_3-KRAS-RalB Complex Drives Tumour Stemness and Resistance to EGFR Inhibition’. Nature Cell Biology 16(5): 457–68. doi:10.1038/ncb2953.

Sekulic, Nikolina, Emily A. Bassett, Danielle J. Rogers, and Ben E. Black. 2010. ‘The Structure of (CENP-A-H4)(2) Reveals Physical Features That Mark Centromeres’. Nature 467(7313): 347–51. doi:10.1038/nature09323.

Semenov, Oleg, Alexandra Daks, Olga Fedorova, Oleg Shuvalov, and Nickolai A. Barlev. 2022. ‘Opposing Roles of Wild-Type and Mutant P53 in the Process of Epithelial to Mesenchymal Transition’. Frontiers in Molecular Biosciences 9: 928399. doi:10.3389/fmolb.2022.928399.

Senaratne, Aruni P., Héloïse Muller, Kelsey A. Fryer, Munetaka Kawamoto, Susumu Katsuma, and Ines A. Drinnenberg. 2021. ‘Formation of the CenH3-Deficient Holocentromere in Lepidoptera Avoids Active Chromatin’. Current biology: CB 31(1): 173-181.e7. doi:10.1016/j.cub.2020.09.078.

Seoane, Joan, and Roger R. Gomis. 2017. ‘TGF-β Family Signaling in Tumor Suppression and Cancer Progression’. Cold Spring Harbor Perspectives in Biology 9(12): a022277. doi:10.1101/cshperspect.a022277.

Seong, Hoon Je, Sang-Wook Han, and Woo Jun Sul. 2021. ‘Prokaryotic DNA Methylation and Its Functional Roles’. Journal of Microbiology (Seoul, Korea) 59(3): 242–48. doi:10.1007/s12275-021-0674-y.

Serafim, Rodolfo B., Cibele Cardoso, Camila B. Storti, Patrick da Silva, Hongyun Qi, Ramya Parasuram, Geovana Navegante, et al. 2024. ‘HJURP Is Recruited to Double-Strand Break Sites and Facilitates DNA Repair by Promoting Chromatin Reorganization’. Oncogene 43(11): 804–20. doi:10.1038/s41388-024-02937-1.

Sexton, Tom, Eitan Yaffe, Ephraim Kenigsberg, Frédéric Bantignies, Benjamin Leblanc, Michael Hoichman, Hugues Parrinello, Amos Tanay, and Giacomo Cavalli. 2012. ‘Three-Dimensional Folding and Functional Organization Principles of the Drosophila Genome’. Cell 148(3): 458–72. doi:10.1016/j.cell.2012.01.010.

Shahbazian, Mona D., and Michael Grunstein. 2007. ‘Functions of Site-Specific Histone Acetylation and Deacetylation’. Annual Review of Biochemistry 76: 75–100. doi:10.1146/annurev.biochem.76.052705.162114.

Shang, Wei-Hao, Tetsuya Hori, Nuno M. C. Martins, Atsushi Toyoda, Sadahiko Misu, Norikazu Monma, Ichiro Hiratani, et al. 2013. ‘Chromosome Engineering Allows the Efficient Isolation of Vertebrate Neocentromeres’. Developmental Cell 24(6): 635–48. doi:10.1016/j.devcel.2013.02.009.

Shang, Wei-Hao, Tetsuya Hori, Atsushi Toyoda, Jun Kato, Kris Popendorf, Yasubumi Sakakibara, Asao Fujiyama, and Tatsuo Fukagawa. 2010. ‘Chickens Possess Centromeres with Both Extended Tandem Repeats and Short Non-Tandem-Repetitive Sequences’. Genome Research 20(9): 1219–28. doi:10.1101/gr.106245.110.

Shapiro, Irina M., Albert W. Cheng, Nicholas C. Flytzanis, Michele Balsamo, John S. Condeelis, Maja H. Oktay, Christopher B. Burge, and Frank B. Gertler. 2011. ‘An EMT-Driven Alternative Splicing Program Occurs in Human Breast Cancer and Modulates Cellular Phenotype’. PLoS genetics 7(8): e1002218. doi:10.1371/journal.pgen.1002218.

Sharma, Shreya, Harsha Rani, Yeshwanth Mahesh, Mohit Kumar Jolly, Jagannath Dixit, and Vijayalakshmi Mahadevan. 2024. ‘Loss of P53 Epigenetically Modulates Epithelial to Mesenchymal Transition in Colorectal Cancer’. Translational Oncology 43: 101848. doi:10.1016/j.tranon.2023.101848.

Shaw, P., R. Bovey, S. Tardy, R. Sahli, B. Sordat, and J. Costa. 1992. ‘Induction of Apoptosis by Wild-Type P53 in a Human Colon Tumor-Derived Cell Line’. Proceedings of the National Academy of Sciences of the United States of America 89(10): 4495–99. doi:10.1073/pnas.89.10.4495.

Shaw, Tanya J., and Paul Martin. 2016. ‘Wound Repair: A Showcase for Cell Plasticity and Migration’. Current Opinion in Cell Biology 42: 29–37. doi:10.1016/j.ceb.2016.04.001.

Shelby, R. D., O. Vafa, and K. F. Sullivan. 1997. ‘Assembly of CENP-A into Centromeric Chromatin Requires a Cooperative Array of Nucleosomal DNA Contact Sites’. The Journal of Cell Biology 136(3): 501–13. doi:10.1083/jcb.136.3.501.

Shi, Yuan-Xiang, Peng-Hui Dai, Yu-Fei Jiang, Yan-Qing Wang, and Wen Liu. 2023. ‘A Pan-Cancer Landscape of Centromere Proteins in Tumorigenesis and Anticancer Drug Sensitivity’. Translational Oncology 31: 101658. doi:10.1016/j.tranon.2023.101658.

Shibahara, K., and B. Stillman. 1999. ‘Replication-Dependent Marking of DNA by PCNA Facilitates CAF-1-Coupled Inheritance of Chromatin’. Cell 96(4): 575–85. doi:10.1016/s0092-8674(00)80661-3.

Shimono, Yohei, Maider Zabala, Robert W. Cho, Neethan Lobo, Piero Dalerba, Dalong Qian, Maximilian Diehn, et al. 2009. ‘Downregulation of miRNA-200c Links Breast Cancer Stem Cells with Normal Stem Cells’. Cell 138(3): 592–603. doi:10.1016/j.cell.2009.07.011.

Shirakihara, Takuya, Kana Horiguchi, Keiji Miyazawa, Shogo Ehata, Tatsuhiro Shibata, Ikuo Morita, Kohei Miyazono, and Masao Saitoh. 2011. 'TGF-β Regulates Isoform Switching of FGF Receptors and Epithelial-Mesenchymal Transition'. The EMBO journal 30(4): 783–95. doi:10.1038/emboj.2010.351.

Shono, Nobuaki, Jun-ichirou Ohzeki, Koichiro Otake, Nuno M. C. Martins, Takahiro Nagase, Hiroshi Kimura, Vladimir Larionov, William C. Earnshaw, and Hiroshi Masumoto. 2015. 'CENP-C and CENP-I Are Key Connecting Factors for Kinetochore and CENP-A Assembly'. Journal of Cell Science 128(24): 4572–87. doi:10.1242/jcs.180786.

Shrestha, Roshan L., Grace S. Ahn, Mae I. Staples, Kizhakke M. Sathyan, Tatiana S. Karpova, Daniel R. Foltz, and Munira A. Basrai. 2017. 'Mislocalization of Centromeric Histone H3 Variant CENP-A Contributes to Chromosomal Instability (CIN) in Human Cells'. Oncotarget 8(29): 46781–800. doi:10.18632/oncotarget.18108.

Shrestha, Roshan L., Vinutha Balachandra, Jee Hun Kim, Austin Rossi, Pranathi Vadlamani, Subhash Chandra Sethi, Laurent Ozbun, et al. 2023. 'The Histone H3/H4 Chaperone CHAF1B Prevents the Mislocalization of CENP-A for Chromosomal Stability'. Journal of Cell Science 136(10): jcs260944. doi:10.1242/jcs.260944.

Shrestha, Roshan L., Austin Rossi, Darawalee Wangsa, Ann K. Hogan, Kimberly S. Zaldana, Evelyn Suva, Yang Jo Chung, et al. 2021. 'CENP-A Overexpression Promotes Aneuploidy with Karyotypic Heterogeneity'. The Journal of Cell Biology 220(4): e202007195. doi:10.1083/jcb.202007195.

Shuaib, Muhammad, Khalid Ouararhni, Stefan Dimitrov, and Ali Hamiche. 2010. 'HJURP Binds CENP-A via a Highly Conserved N-Terminal Domain and Mediates Its Deposition at Centromeres'. Proceedings of the National Academy of Sciences of the United States of America 107(4): 1349–54. doi:10.1073/pnas.0913709107.

Shukla, Manu, Pin Tong, Sharon A. White, Puneet P. Singh, Angus M. Reid, Sandra Catania, Alison L. Pidoux, and Robin C. Allshire. 2018. 'Centromere DNA Destabilizes H3 Nucleosomes to Promote CENP-A Deposition during the Cell Cycle'. Current biology: CB 28(24): 3924-3936.e4. doi:10.1016/j.cub.2018.10.049.

Silva, Mariana C. C., Dani L. Bodor, Madison E. Stellfox, Nuno M. C. Martins, Helfrid Hochegger, Daniel R. Foltz, and Lars E. T. Jansen. 2012. 'Cdk Activity Couples Epigenetic Centromere Inheritance to Cell Cycle Progression'. Developmental Cell 22(1): 52–63. doi:10.1016/j.devcel.2011.10.014.

Silveira, Daner A., and José Carlos M. Mombach. 2020. 'Dynamics of the Feedback Loops Required for the Phenotypic Stabilization in the Epithelial-Mesenchymal Transition'. The FEBS journal 287(3): 578–88. doi:10.1111/febs.15062.

Simeonov, Kamen P., China N. Byrns, Megan L. Clark, Robert J. Norgard, Beth Martin, Ben Z. Stanger, Jay Shendure, Aaron McKenna, and Christopher J. Lengner. 2021. 'Single-Cell Lineage Tracing of

Metastatic Cancer Reveals Selection of Hybrid EMT States'. Cancer cell 39(8): 1150-1162.e9. doi:10.1016/j.ccell.2021.05.005.

Si-Tayeb, Karim, Frédéric P. Lemaigre, and Stephen A. Duncan. 2010. 'Organogenesis and Development of the Liver'. Developmental Cell 18(2): 175–89. doi:10.1016/j.devcel.2010.01.011.

Sitbon, David, Ekaterina Boyarchuk, Florent Dingli, Damarys Loew, and Geneviève Almouzni. 2020. 'Histone Variant H3.3 Residue S31 Is Essential for Xenopus Gastrulation Regardless of the Deposition Pathway'. Nature Communications 11(1): 1256. doi:10.1038/s41467-020-15084-4.

Sitbon, David, Katrina Podsypanina, Tejas Yadav, and Geneviève Almouzni. 2017. 'Shaping Chromatin in the Nucleus: The Bricks and the Architects'. Cold Spring Harbor Symposia on Quantitative Biology 82: 1–14. doi:10.1101/sqb.2017.82.033753.

Skalníková, M., S. Kozubek, E. Lukásová, E. Bártová, P. Jirsová, A. Cafourková, I. Koutná, and M. Kozubek. 2000. 'Spatial Arrangement of Genes, Centromeres and Chromosomes in Human Blood Cell Nuclei and Its Changes during the Cell Cycle, Differentiation and after Irradiation'. Chromosome Research: An International Journal on the Molecular, Supramolecular and Evolutionary Aspects of Chromosome Biology 8(6): 487–99. doi:10.1023/a:1009267605580.

Skromne, I., and C. D. Stern. 2001. 'Interactions between Wnt and Vg1 Signalling Pathways Initiate Primitive Streak Formation in the Chick Embryo'. Development (Cambridge, England) 128(15): 2915–27. doi:10.1242/dev.128.15.2915.

Skrypek, Nicolas, Steven Goossens, Eva De Smedt, Niels Vandamme, and Geert Berx. 2017. 'Epithelial-to-Mesenchymal Transition: Epigenetic Reprogramming Driving Cellular Plasticity'. Trends in genetics: TIG 33(12): 943–59. doi:10.1016/j.tig.2017.08.004.

Smith, D. E., F. Franco del Amo, and T. Gridley. 1992. 'Isolation of Sna, a Mouse Gene Homologous to the Drosophila Genes Snail and Escargot: Its Expression Pattern Suggests Multiple Roles during Postimplantation Development'. Development (Cambridge, England) 116(4): 1033–39. doi:10.1242/dev.116.4.1033.

Smith, S., and B. Stillman. 1989. 'Purification and Characterization of CAF-I, a Human Cell Factor Required for Chromatin Assembly during DNA Replication in Vitro'. Cell 58(1): 15–25. doi:10.1016/0092-8674(89)90398-x.

Smith, S., and B. Stillman. 1991. 'Stepwise Assembly of Chromatin during DNA Replication in Vitro'. The EMBO journal 10(4): 971–80. doi:10.1002/j.1460-2075.1991.tb08031.x.

Smoak, Evan M., Paula Stein, Richard M. Schultz, Michael A. Lampson, and Ben E. Black. 2016. 'Long-Term Retention of CENP-A Nucleosomes in Mammalian Oocytes Underpins Transgenerational Inheritance of Centromere Identity'. Current biology : CB 26(8): 1110–16. doi:10.1016/j.cub.2016.02.061.

Sogo, J. M., H. Stahl, T. Koller, and R. Knippers. 1986. ‘Structure of Replicating Simian Virus 40 Minichromosomes. The Replication Fork, Core Histone Segregation and Terminal Structures’. Journal of Molecular Biology 189(1): 189–204. doi:10.1016/0022-2836(86)90390-6.

Solnica-Krezel, Lilianna. 2005. ‘Conserved Patterns of Cell Movements during Vertebrate Gastrulation’. Current biology: CB 15(6): R213-228. doi:10.1016/j.cub.2005.03.016.

Solomon, M. J., P. L. Larsen, and A. Varshavsky. 1988. ‘Mapping Protein-DNA Interactions in Vivo with Formaldehyde: Evidence That Histone H4 Is Retained on a Highly Transcribed Gene’. Cell 53(6): 937–47. doi:10.1016/s0092-8674(88)90469-2.

Solovei, Irina, Lothar Schermelleh, Klaus Düring, Andrea Engelhardt, Stefan Stein, Christoph Cremer, and Thomas Cremer. 2004. ‘Differences in Centromere Positioning of Cycling and Postmitotic Human Cell Types’. Chromosoma 112(8): 410–23. doi:10.1007/s00412-004-0287-3.

Song, Feng, Ping Chen, Dapeng Sun, Mingzhu Wang, Liping Dong, Dan Liang, Rui-Ming Xu, Ping Zhu, and Guohong Li. 2014. ‘Cryo-EM Study of the Chromatin Fiber Reveals a Double Helix Twisted by Tetranucleosomal Units’. Science (New York, N.Y.) 344(6182): 376–80. doi:10.1126/science.1251413.

Soufi, Abdenour, Meilin Fernandez Garcia, Artur Jaroszewicz, Nebiyu Osman, Matteo Pellegrini, and Kenneth S. Zaret. 2015. ‘Pioneer Transcription Factors Target Partial DNA Motifs on Nucleosomes to Initiate Reprogramming’. Cell 161(3): 555–68. doi:10.1016/j.cell.2015.03.017.

Soule, H. D., T. M. Maloney, S. R. Wolman, W. D. Peterson, R. Brenz, C. M. McGrath, J. Russo, et al. 1990. ‘Isolation and Characterization of a Spontaneously Immortalized Human Breast Epithelial Cell Line, MCF-10’. Cancer Research 50(18): 6075–86.

Soyfer, V. N. "The consequences of political dictatorship for Russian science". Nature Reviews Genetics. 2 (9): 723–729. doi:10.1038/35088598.

Spiller, Frances, Bethan Medina-Pritchard, Maria Alba Abad, Martin A Wear, Oscar Molina, William C Earnshaw, and A Arockia Jeyaprakash. 2017. ‘Molecular Basis for Cdk1-regulated Timing of Mis18 Complex Assembly and CENP-A Deposition’. EMBO Reports 18(6): 894–905. doi:10.15252/embr.201643564.

Squire, L. R. 1992. ‘Memory and the Hippocampus: A Synthesis from Findings with Rats, Monkeys, and Humans’. Psychological Review 99(2): 195–231. doi:10.1037/0033-295x.99.2.195.

Srivastava, Shashank, and Daniel R. Foltz. 2018. ‘Posttranslational Modifications of CENP-A: Marks of Distinction’. Chromosoma 127(3): 279–90. doi:10.1007/s00412-018-0665-x.

Stangeland, Biljana, Awais A. Mughal, Zanina Grieg, Cecilie Jonsgar Sandberg, Mrinal Joel, Ståle Nygård, Torstein Meling, et al. 2015. ‘Combined Expressional Analysis, Bioinformatics and Targeted

Proteomics Identify New Potential Therapeutic Targets in Glioblastoma Stem Cells'. Oncotarget 6(28): 26192–215.

Stankovic, Ana, Lucie Y. Guo, João F. Mata, Dani L. Bodor, Xing-Jun Cao, Aaron O. Bailey, Jeffrey Shabanowitz, et al. 2017. 'A Dual Inhibitory Mechanism Sufficient to Maintain Cell Cycle Restricted CENP-A Assembly'. Molecular cell 65(2): 231–46. doi:10.1016/j.molcel.2016.11.021.

Steiner, Florian A, and Steven Henikoff. 2014. 'Holocentromeres Are Dispersed Point Centromeres Localized at Transcription Factor Hotspots'. eLife 3: e02025. doi:10.7554/eLife.02025.

Steiner, Florian A., and Steven Henikoff. 2015. 'Diversity in the Organization of Centromeric Chromatin'. Current Opinion in Genetics & Development 31: 28–35. doi:10.1016/j.gde.2015.03.010.

Stemmer, V., B. de Craene, G. Berx, and J. Behrens. 2008. 'Snail Promotes Wnt Target Gene Expression and Interacts with Beta-Catenin'. Oncogene 27(37): 5075–80. doi:10.1038/onc.2008.140.

Stemmler, Marc P., Rebecca L. Eccles, Simone Brabletz, and Thomas Brabletz. 2019. 'Non-Redundant Functions of EMT Transcription Factors'. Nature Cell Biology 21(1): 102–12. doi:10.1038/s41556-018-0196-y.

Stewart-Morgan, Kathleen R., Nataliya Petryk, and Anja Groth. 2020. 'Chromatin Replication and Epigenetic Cell Memory'. Nature Cell Biology 22(4): 361–71. doi:10.1038/s41556-020-0487-y.

Stimpson, Kaitlin M., and Beth A. Sullivan. 2010. 'Epigenomics of Centromere Assembly and Function'. Current Opinion in Cell Biology 22(6): 772–80. doi:10.1016/j.ceb.2010.07.002.

Strauss, Robert, Zong-Yi Li, Ying Liu, Ines Beyer, Jonas Persson, Pavel Sova, Thomas Möller, et al. 2011. 'Analysis of Epithelial and Mesenchymal Markers in Ovarian Cancer Reveals Phenotypic Heterogeneity and Plasticity'. PloS One 6(1): e16186. doi:10.1371/journal.pone.0016186.

Strauss, Robert, Pavel Sova, Ying Liu, Zong Yi Li, Sebastian Tuve, David Pritchard, Paul Brinkkoetter, et al. 2009. 'Epithelial Phenotype Confers Resistance of Ovarian Cancer Cells to Oncolytic Adenoviruses'. Cancer Research 69(12): 5115–25. doi:10.1158/0008-5472.CAN-09-0645.

Su, Juan, ANLING Zhang, Zhendong Shi, Feifei Ma, Peiyu Pu, Tao Wang, Jie Zhang, Chunsheng Kang, and Qingyu Zhang. 2011. 'MicroRNA-200a Suppresses the Wnt/β-Catenin Signaling Pathway by Interacting with β-Catenin'. International Journal of Oncology 40(4): 1162–70. doi:10.3892/ijo.2011.1322.

Su, Yijing, Jaehoon Shin, Chun Zhong, Sabrina Wang, Prith Roychowdhury, Jongseuk Lim, David Kim, Guo-li Ming, and Hongjun Song. 2017. 'Neuronal Activity Modifies the Chromatin Accessibility Landscape in the Adult Brain'. Nature neuroscience 20(3): 476–83. doi:10.1038/nn.4494.

Sui, Hua, Jihui Zhao, Lihong Zhou, Haotian Wen, Wanli Deng, Chunpu Li, Qing Ji, et al. 2017. 'Tanshinone IIA Inhibits β-Catenin/VEGF-Mediated Angiogenesis by Targeting TGF-B1 in Normoxic

and HIF-1α in Hypoxic Microenvironments in Human Colorectal Cancer'. Cancer Letters 403: 86–97. doi:10.1016/j.canlet.2017.05.013.

Sui, Lina, Yurong Xin, Qian Du, Daniela Georgieva, Giacomo Diedenhofen, Leena Haataja, Qi Su, et al. 2021. 'Reduced Replication Fork Speed Promotes Pancreatic Endocrine Differentiation and Controls Graft Size'. JCI Insight 6(5): e141553. doi:10.1172/jci.insight.141553.

Sullivan, Beth A., and Gary H. Karpen. 2004. 'Centromeric Chromatin Exhibits a Histone Modification Pattern That Is Distinct from Both Euchromatin and Heterochromatin'. Nature Structural & Molecular Biology 11(11): 1076–83. doi:10.1038/nsmb845.

Sullivan, K. F., M. Hechenberger, and K. Masri. 1994. 'Human CENP-A Contains a Histone H3 Related Histone Fold Domain That Is Required for Targeting to the Centromere'. The Journal of Cell Biology 127(3): 581–92. doi:10.1083/jcb.127.3.581.

Sun, D., C. R. Vanderburg, G. S. Odierna, and E. D. Hay. 1998. 'TGFbeta3 Promotes Transformation of Chicken Palate Medial Edge Epithelium to Mesenchyme in Vitro'. Development (Cambridge, England) 125(1): 95–105. doi:10.1242/dev.125.1.95.

Sun, Xia, Pier-Luc Clermont, Wenlin Jiao, Cheryl D. Helgason, Peter W. Gout, Yuzhuo Wang, and Sifeng Qu. 2016. 'Elevated Expression of the Centromere Protein-A(CENP-A)-Encoding Gene as a Prognostic and Predictive Biomarker in Human Cancers'. International Journal of Cancer 139(4): 899–907. doi:10.1002/ijc.30133.

Suzuki, Nobutaka, Megumi Nakano, Naohito Nozaki, Shin-ichiro Egashira, Tuneko Okazaki, and Hiroshi Masumoto. 2004. 'CENP-B Interacts with CENP-C Domains Containing Mif2 Regions Responsible for Centromere Localization'. The Journal of Biological Chemistry 279(7): 5934–46. doi:10.1074/jbc.M306477200.

Szenker, Emmanuelle, Nicolas Lacoste, and Geneviève Almouzni. 2012. 'A Developmental Requirement for HIRA-Dependent H3.3 Deposition Revealed at Gastrulation in Xenopus'. Cell Reports 1(6): 730–40. doi:10.1016/j.celrep.2012.05.006.

Tachiwana, Hiroaki, Wataru Kagawa, and Hitoshi Kurumizaka. 2012. 'Comparison between the CENP-A and Histone H3 Structures in Nucleosomes'. Nucleus (Austin, Tex.) 3(1): 6–11. doi:10.4161/nucl.18372.

Tachiwana, Hiroaki, Wataru Kagawa, Tatsuya Shiga, Akihisa Osakabe, Yuta Miya, Kengo Saito, Yoko Hayashi-Takanaka, et al. 2011. 'Crystal Structure of the Human Centromeric Nucleosome Containing CENP-A'. Nature 476(7359): 232–35. doi:10.1038/nature10258.

Tachiwana, Hiroaki, Sebastian Müller, Julia Blümer, Kerstin Klare, Andrea Musacchio, and Geneviève Almouzni. 2015. 'HJURP Involvement in de Novo CenH3(CENP-A) and CENP-C Recruitment'. Cell Reports 11(1): 22–32. doi:10.1016/j.celrep.2015.03.013.

Taddei, A., C. Maison, D. Roche, and G. Almouzni. 2001. ‘Reversible Disruption of Pericentric Heterochromatin and Centromere Function by Inhibiting Deacetylases’. Nature Cell Biology 3(2): 114–20. doi:10.1038/35055010.

Tagami, Hideaki, Dominique Ray-Gallet, Geneviève Almouzni, and Yoshihiro Nakatani. 2004. ‘Histone H3.1 and H3.3 Complexes Mediate Nucleosome Assembly Pathways Dependent or Independent of DNA Synthesis’. Cell 116(1): 51–61. doi:10.1016/s0092-8674(03)01064-x.

Takahashi, Kazuki, Katarzyna A. Podyma-Inoue, Maki Saito, Shintaro Sakakitani, Akinari Sugauchi, Keita Iida, Sadahiro Iwabuchi, et al. 2022. ‘TGF-β Generates a Population of Cancer Cells Residing in G1 Phase with High Motility and Metastatic Potential via KRTAP2-3’. Cell Reports 40(13): 111411. doi:10.1016/j.celrep.2022.111411.

Takizawa, Takumi, Prabhakar R. Gudla, Liying Guo, Stephan Lockett, and Tom Misteli. 2008. ‘Allele-Specific Nuclear Positioning of the Monoallelically Expressed Astrocyte Marker GFAP’. Genes & Development 22(4): 489–98. doi:10.1101/gad.1634608.

Takizawa, Yoshimasa, Cheng-Han Ho, Hiroaki Tachiwana, Hideyuki Matsunami, Wataru Kobayashi, Midori Suzuki, Yasuhiro Arimura, et al. 2020. ‘Cryo-EM Structures of Centromeric Tri-Nucleosomes Containing a Central CENP-A Nucleosome’. Structure (London, England: 1993) 28(1): 44-53.e4. doi:10.1016/j.str.2019.10.016.

Talbert, Paul B., and Steven Henikoff. 2022. ‘The Genetics and Epigenetics of Satellite Centromeres’. Genome Research 32(4): 608–15. doi:10.1101/gr.275351.121.

Talbert, Paul, and Steven Henikoff. 2022. ‘Centromere Drive: Chromatin Conflict in Meiosis’. Current Opinion in Genetics & Development 77: 102005. doi:10.1016/j.gde.2022.102005.

Tam, P. P., and R. S. Beddington. 1987. ‘The Formation of Mesodermal Tissues in the Mouse Embryo during Gastrulation and Early Organogenesis’. Development (Cambridge, England) 99(1): 109–26. doi:10.1242/dev.99.1.109.

Tam, P. P., E. A. Williams, and W. Y. Chan. 1993. ‘Gastrulation in the Mouse Embryo: Ultrastructural and Molecular Aspects of Germ Layer Morphogenesis’. Microscopy Research and Technique 26(4): 301–28. doi:10.1002/jemt.1070260405.

Tam, Wai Leong, and Robert A. Weinberg. 2013. ‘The Epigenetics of Epithelial-Mesenchymal Plasticity in Cancer’. Nature Medicine 19(11): 1438–49. doi:10.1038/nm.3336.

Tammela, Tuomas, Francisco J. Sanchez-Rivera, Naniye Malli Cetinbas, Katherine Wu, Nikhil S. Joshi, Katja Helenius, Yoona Park, et al. 2017. ‘A Wnt-Producing Niche Drives Proliferative Potential and Progression in Lung Adenocarcinoma’. Nature 545(7654): 355–59. doi:10.1038/nature22334.

Tan, Minjia, Hao Luo, Sangkyu Lee, Fulai Jin, Jeong Soo Yang, Emilie Montellier, Thierry Buchou, et al. 2011. 'Identification of 67 Histone Marks and Histone Lysine Crotonylation as a New Type of Histone Modification'. Cell 146(6): 1016–28. doi:10.1016/j.cell.2011.08.008.

Tanaka, Seiji, and Hiroyuki Araki. 2013. 'Helicase Activation and Establishment of Replication Forks at Chromosomal Origins of Replication'. Cold Spring Harbor Perspectives in Biology 5(12): a010371. doi:10.1101/cshperspect.a010371.

Tang, Shaomei, Xiaoliang Huang, Xi Wang, Xianguo Zhou, Huan Huang, Liwen Qin, Hongyu Tao, Qiuyan Wang, and Yuting Tao. 2020. 'Vital and Distinct Roles of H2A.Z Isoforms in Hepatocellular Carcinoma'. OncoTargets and Therapy 13: 4319–37. doi:10.2147/OTT.S243823.

Tang, Yan, Yong Tang, and Ying-sheng Cheng. 2017. 'miR-34a Inhibits Pancreatic Cancer Progression through Snail1-Mediated Epithelial–Mesenchymal Transition and the Notch Signaling Pathway'. Scientific Reports 7: 38232. doi:10.1038/srep38232.

Tashiro, Etsu, Shizuka Henmi, Hiroyuki Odake, Seitaro Ino, and Masaya Imoto. 2016. 'Involvement of the MEK/ERK Pathway in EGF-Induced E-Cadherin down-Regulation'. Biochemical and Biophysical Research Communications 477(4): 801–6. doi:10.1016/j.bbrc.2016.06.138.

Taverna, Sean D., Haitao Li, Alexander J. Ruthenburg, C. David Allis, and Dinshaw J. Patel. 2007. 'How Chromatin-Binding Modules Interpret Histone Modifications: Lessons from Professional Pocket Pickers'. Nature Structural & Molecular Biology 14(11): 1025–40. doi:10.1038/nsmb1338.

Theveneau, Eric, and Roberto Mayor. 2012. 'Neural Crest Delamination and Migration: From Epithelium-to-Mesenchyme Transition to Collective Cell Migration'. Developmental Biology 366(1): 34–54. doi:10.1016/j.ydbio.2011.12.041.

Thiery, J. P., J. L. Duband, U. Rutishauser, and G. M. Edelman. 1982. 'Cell Adhesion Molecules in Early Chicken Embryogenesis'. Proceedings of the National Academy of Sciences of the United States of America 79(21): 6737–41. doi:10.1073/pnas.79.21.6737.

Thiery, Jean Paul, Hervé Acloque, Ruby Y. J. Huang, and M. Angela Nieto. 2009. 'Epithelial-Mesenchymal Transitions in Development and Disease'. Cell 139(5): 871–90. doi:10.1016/j.cell.2009.11.007.

Thiru, Prathapan, David M. Kern, Kara L. McKinley, Julie K. Monda, Florencia Rago, Kuan-Chung Su, Tonia Tsinman, et al. 2014. 'Kinetochore Genes Are Coordinately Up-Regulated in Human Tumors as Part of a FoxM1-Related Cell Division Program'. Molecular Biology of the Cell 25(13): 1983–94. doi:10.1091/mbc.E14-03-0837.

Thomson, Alexander M., Peter J. Gillespie, and J. Julian Blow. 2010. 'Replication Factory Activation Can Be Decoupled from the Replication Timing Program by Modulating Cdk Levels'. The Journal of Cell Biology 188(2): 209–21. doi:10.1083/jcb.200911037.

Tian, Mengxue, Zhenjia Wang, Zhangli Su, Etsuko Shibata, Yoshiyuki Shibata, Anindya Dutta, and Chongzhi Zang. 2023. 'Integrative Analysis of DNA Replication Origins and ORC/MCM Binding Sites in Human Cells Reveals a Lack of Overlap'. bioRxiv: The Preprint Server for Biology: 2023.07.25.550556. doi:10.1101/2023.07.25.550556.

Timmerman, Luika A., Joaquín Grego-Bessa, Angel Raya, Esther Bertrán, José María Pérez-Pomares, Juan Díez, Sergi Aranda, et al. 2004. 'Notch Promotes Epithelial-Mesenchymal Transition during Cardiac Development and Oncogenic Transformation'. Genes & Development 18(1): 99–115. doi:10.1101/gad.276304.

Title, Alexandra C., Sue-Jean Hong, Nuno D. Pires, Lynn Hasenöhrl, Svenja Godbersen, Nadine Stokar-Regenscheit, David P. Bartel, and Markus Stoffel. 2018. 'Genetic Dissection of the miR-200–Zeb1 Axis Reveals Its Importance in Tumor Differentiation and Invasion'. Nature Communications 9(1): 4671. doi:10.1038/s41467-018-07130-z.

Tjio, Joe Hin, and Albert Levan. 1956. 'The Chromosome Number of Man'. Hereditas 42(1–2): 1–6. doi:10.1111/j.1601-5223.1956.tb03010.x.

Toh, Benjamin, Xiaojie Wang, Jo Keeble, Wen Jing Sim, Karen Khoo, Wing-Cheong Wong, Masashi Kato, et al. 2011. 'Mesenchymal Transition and Dissemination of Cancer Cells Is Driven by Myeloid-Derived Suppressor Cells Infiltrating the Primary Tumor'. PLoS biology 9(9): e1001162. doi:10.1371/journal.pbio.1001162.

Toledo, Franck, and Geoffrey M. Wahl. 2006. 'Regulating the P53 Pathway: In Vitro Hypotheses, in Vivo Veritas'. Nature Reviews. Cancer 6(12): 909–23. doi:10.1038/nrc2012.

Tomonaga, Takeshi, Kazuyuki Matsushita, Seiko Yamaguchi, Tatsuya Oohashi, Hideaki Shimada, Takenori Ochiai, Kinya Yoda, and Fumio Nomura. 2003. 'Overexpression and Mistargeting of Centromere Protein-A in Human Primary Colorectal Cancer'. Cancer Research 63(13): 3511–16.

Toni, Nicolas, and Alejandro F. Schinder. 2016. 'Maturation and Functional Integration of New Granule Cells into the Adult Hippocampus'. Cold Spring Harbor Perspectives in Biology 8(1): a018903. doi:10.1101/cshperspect.a018903.

Torres-Padilla, Maria-Elena, Andrew J. Bannister, Paul J. Hurd, Tony Kouzarides, and Magdalena Zernicka-Goetz. 2006. 'Dynamic Distribution of the Replacement Histone Variant H3.3 in the Mouse Oocyte and Preimplantation Embryos'. The International Journal of Developmental Biology 50(5): 455–61. doi:10.1387/ijdb.052073mt.

Traag, V. A., L. Waltman, and N. J. van Eck. 2019. 'From Louvain to Leiden: Guaranteeing Well-Connected Communities'. Scientific Reports 9(1): 5233. doi:10.1038/s41598-019-41695-z.

Tran, Hung D., Krishna Luitel, Michael Kim, Kun Zhang, Gregory D. Longmore, and David D. Tran. 2014. 'Transient SNAIL1 Expression Is Necessary for Metastatic Competence in Breast Cancer'. Cancer Research 74(21): 6330–40. doi:10.1158/0008-5472.CAN-14-0923.

Trelstad, R. L., A. Hayashi, K. Hayashi, and P. K. Donahoe. 1982. 'The Epithelial-Mesenchymal Interface of the Male Rate Mullerian Duct: Loss of Basement Membrane Integrity and Ductal Regression'. Developmental Biology 92(1): 27–40. doi:10.1016/0012-1606(82)90147-6.

Trivedi, Prasad, Christopher D. Steele, Franco K. C. Au, Ludmil B. Alexandrov, and Don W. Cleveland. 2023. 'Mitotic Tethering Enables Inheritance of Shattered Micronuclear Chromosomes'. Nature 618(7967): 1049–56. doi:10.1038/s41586-023-06216-z.

Tromer, Eelco C., Jolien J. E. van Hooff, Geert J. P. L. Kops, and Berend Snel. 2019. 'Mosaic Origin of the Eukaryotic Kinetochore'. Proceedings of the National Academy of Sciences 116(26): 12873–82. doi:10.1073/pnas.1821945116.

Tyler-Smith, C, G Gimelli, S Giglio, G Floridia, A Pandya, G Terzoli, P E Warburton, W C Earnshaw, and O Zuffardi. 1999. 'Transmission of a Fully Functional Human Neocentromere through Three Generations.' American Journal of Human Genetics 64(5): 1440–44.

Uhlén, Mathias, Linn Fagerberg, Björn M. Hallström, Cecilia Lindskog, Per Oksvold, Adil Mardinoglu, Åsa Sivertsson, et al. 2015. 'Tissue-Based Map of the Human Proteome'. Science. doi:10.1126/science.1260419.

Uusküla-Reimand, Liis, and Michael D. Wilson. 2022. 'Untangling the Roles of TOP2A and TOP2B in Transcription and Cancer'. Science Advances 8(44): eadd4920. doi:10.1126/sciadv.add4920.

Valcourt, Ulrich, Marcin Kowanetz, Hideki Niimi, Carl-Henrik Heldin, and Aristidis Moustakas. 2005. 'TGF-Beta and the Smad Signaling Pathway Support Transcriptomic Reprogramming during Epithelial-Mesenchymal Cell Transition'. Molecular Biology of the Cell 16(4): 1987–2002. doi:10.1091/mbc.e04-08-0658.

Valsesia-Wittmann, Sandrine, Maud Magdeleine, Sébastien Dupasquier, Elisabeth Garin, Anne-Catherine Jallas, Valérie Combaret, Alexander Krause, Philippe Leissner, and Alain Puisieux. 2004. 'Oncogenic Cooperation between H-Twist and N-Myc Overrides Failsafe Programs in Cancer Cells'. Cancer Cell 6(6): 625–30. doi:10.1016/j.ccr.2004.09.033.

Van Hooser, A. A., I. I. Ouspenski, H. C. Gregson, D. A. Starr, T. J. Yen, M. L. Goldberg, K. Yokomori, et al. 2001. 'Specification of Kinetochore-Forming Chromatin by the Histone H3 Variant CENP-A'. Journal of Cell Science 114(Pt 19): 3529–42.

Van Rechem, Capucine, Fei Ji, Damayanti Chakraborty, Joshua C. Black, Ruslan I. Sadreyev, and Johnathan R. Whetstine. 2021. 'Collective Regulation of Chromatin Modifications Predicts Replication Timing during Cell Cycle'. Cell Reports 37(1): 109799. doi:10.1016/j.celrep.2021.109799.

Varlet, I., J. Collignon, and E. J. Robertson. 1997. 'Nodal Expression in the Primitive Endoderm Is Required for Specification of the Anterior Axis during Mouse Gastrulation'. Development (Cambridge, England) 124(5): 1033–44. doi:10.1242/dev.124.5.1033.

Varshavsky, A. J., O. H. Sundin, and M. J. Bohn. 1978. 'SV40 Viral Minichromosome: Preferential Exposure of the Origin of Replication as Probed by Restriction Endonucleases'. Nucleic Acids Research 5(10): 3469–77. doi:10.1093/nar/5.10.3469.

Vermeulen, Michiel, H. Christian Eberl, Filomena Matarese, Hendrik Marks, Sergei Denissov, Falk Butter, Kenneth K. Lee, et al. 2010. 'Quantitative Interaction Proteomics and Genome-Wide Profiling of Epigenetic Histone Marks and Their Readers'. Cell 142(6): 967–80. doi:10.1016/j.cell.2010.08.020.

Verrelle, Pierre, Didier Meseure, Frédérique Berger, Audrey Forest, Renaud Leclère, André Nicolas, Emilie Fortas, et al. 2021. 'CENP-A Subnuclear Localization Pattern as Marker Predicting Curability by Chemoradiation Therapy for Locally Advanced Head and Neck Cancer Patients'. Cancers 13(16): 3928. doi:10.3390/cancers13163928.

Viotti, Manuel, Sonja Nowotschin, and Anna-Katerina Hadjantonakis. 2014. 'SOX17 Links Gut Endoderm Morphogenesis and Germ Layer Segregation'. Nature Cell Biology 16(12): 1146–56. doi:10.1038/ncb3070.

Virchow, R. 1858. Die Cellularpathologie in ihrer Begründung auf physiologische und pathologische Gewebelehre. https://www.digitale-sammlungen.de/de/view/bsb10926743?page=9 (August 13, 2024).

Vos, Maria Caroline, Eva Hollemans, Nicole Ezendam, Harry Feijen, Dorry Boll, Brenda Pijlman, Hans van der Putten, et al. 2016. 'MMP-14 and CD44 in Epithelial-to-Mesenchymal Transition (EMT) in Ovarian Cancer'. Journal of Ovarian Research 9(1): 53. doi:10.1186/s13048-016-0262-7.

Vu, Remy, Morgan Dragan, Peng Sun, Sabine Werner, and Xing Dai. 2023. 'Epithelial-Mesenchymal Plasticity and Endothelial-Mesenchymal Transition in Cutaneous Wound Healing'. Cold Spring Harbor Perspectives in Biology 15(8): a041237. doi:10.1101/cshperspect.a041237.

Waddington, C. H. 1942. The epigenotype. International Journal of Epidemiology 41(1): 10-13. doi:10.1093/ije/dyr184.

Waddington, C. H. 1957. The strategy of the genes: A Discussion of Some Aspects of Theoretical Biology. George Allen and Unwin, London.

Wallingford, J. B., D. W. Seufert, V. C. Virta, and P. D. Vize. 1997. 'P53 Activity Is Essential for Normal Development in Xenopus'. Current biology: CB 7(10): 747–57. doi:10.1016/s0960-9822(06)00333-2.

Walther, Nike, M. Julius Hossain, Antonio Z. Politi, Birgit Koch, Moritz Kueblbeck, Øyvind Ødegård-Fougner, Marko Lampe, and Jan Ellenberg. 2018. 'A Quantitative Map of Human Condensins Provides

New Insights into Mitotic Chromosome Architecture'. The Journal of Cell Biology 217(7): 2309–28. doi:10.1083/jcb.201801048.

Wan, Tao, Tianwei Zhang, Xiaoying Si, and Yanming Zhou. 2017. 'Overexpression of EMT-Inducing Transcription Factors as a Potential Poor Prognostic Factor for Hepatocellular Carcinoma in Asian Populations: A Meta-Analysis'. Oncotarget 8(35): 59500–508. doi:10.18632/oncotarget.18352.

Wang, Bi, Yaping Shen, Yin Zou, Zhengjun Qi, Guijia Huang, Shan Xia, Rui Gao, Fenghu Li, and Zhi Huang. 2020. 'TOP2A Promotes Cell Migration, Invasion and Epithelial–Mesenchymal Transition in Cervical Cancer via Activating the PI3K/AKT Signaling'. Cancer Management and Research 12: 3807–14. doi:10.2147/CMAR.S240577.

Wang, G. L., B. H. Jiang, E. A. Rue, and G. L. Semenza. 1995. 'Hypoxia-Inducible Factor 1 Is a Basic-Helix-Loop-Helix-PAS Heterodimer Regulated by Cellular O2 Tension'. Proceedings of the National Academy of Sciences of the United States of America 92(12): 5510–14. doi:10.1073/pnas.92.12.5510.

Wang, I-Ching, Yi-Ju Chen, Douglas Hughes, Vladimir Petrovic, Michael L. Major, Hyung Jung Park, Yongjun Tan, Timothy Ackerson, and Robert H. Costa. 2005. 'Forkhead Box M1 Regulates the Transcriptional Network of Genes Essential for Mitotic Progression and Genes Encoding the SCF (Skp2-Cks1) Ubiquitin Ligase'. Molecular and Cellular Biology 25(24): 10875–94. doi:10.1128/MCB.25.24.10875-10894.2005.

Wang, Jianxun, Kathleen Scully, Xiaoyan Zhu, Ling Cai, Jie Zhang, Gratien G. Prefontaine, Anna Krones, et al. 2007. 'Opposing LSD1 Complexes Function in Developmental Gene Activation and Repression Programmes'. Nature 446(7138): 882–87. doi:10.1038/nature05671.

Wang, Jianyu, Xing Liu, Zhen Dou, Liang Chen, Hao Jiang, Chuanhai Fu, Guosheng Fu, et al. 2014. 'Mitotic Regulator Mis18β Interacts with and Specifies the Centromeric Assembly of Molecular Chaperone Holliday Junction Recognition Protein (HJURP)'. The Journal of Biological Chemistry 289(12): 8326–36. doi:10.1074/jbc.M113.529958.

Wang, Kai, Yun Chen, Zhihong Zhao, Meiying Feng, and Shouquan Zhang. 2019. 'Identification of Potential Core Genes and miRNAs in Testicular Seminoma via Bioinformatics Analysis'. Molecular Medicine Reports 20(5): 4013–22. doi:10.3892/mmr.2019.10684.

Wang, Qi, Jiaju Xu, Zhiyong Xiong, Tianbo Xu, Jingchong Liu, Yuenan Liu, Jiaping Chen, et al. 2021. 'CENPA Promotes Clear Cell Renal Cell Carcinoma Progression and Metastasis via Wnt/β-Catenin Signaling Pathway'. Journal of Translational Medicine 19(1): 417. doi:10.1186/s12967-021-03087-8.

Wang, Shu-Ping, Wen-Lung Wang, Yih-Leong Chang, Chen-Tu Wu, Yu-Chih Chao, Shih-Han Kao, Ang Yuan, et al. 2009. 'P53 Controls Cancer Cell Invasion by Inducing the MDM2-Mediated Degradation of Slug'. Nature Cell Biology 11(6): 694–704. doi:10.1038/ncb1875.

Wang, Weitao, Kyle N. Klein, Karel Proesmans, Hongbo Yang, Claire Marchal, Xiaopeng Zhu, Tyler Borrman, et al. 2021. 'Genome-Wide Mapping of Human DNA Replication by Optical Replication Mapping Supports a Stochastic Model of Eukaryotic Replication'. Molecular Cell 81(14): 2975-2988.e6. doi:10.1016/j.molcel.2021.05.024.

Warzecha, Claude C, Peng Jiang, Karine Amirikian, Kimberly A Dittmar, Hezhe Lu, Shihao Shen, Wei Guo, Yi Xing, and Russ P Carstens. 2010. 'An ESRP-regulated Splicing Programme Is Abrogated during the Epithelial–Mesenchymal Transition'. The EMBO Journal 29(19): 3286–3300. doi:10.1038/emboj.2010.195.

Watanabe, Kazuhide, Alvaro Villarreal-Ponce, Peng Sun, Michael L. Salmans, Magid Fallahi, Bogi Andersen, and Xing Dai. 2014. 'Mammary Morphogenesis and Regeneration Require the Inhibition of EMT at Terminal End Buds by Ovol2 Transcriptional Repressor'. Developmental Cell 29(1): 59–74. doi:10.1016/j.devcel.2014.03.006.

Watanabe, Reito, Masatoshi Hara, Ei-Ichi Okumura, Solène Hervé, Daniele Fachinetti, Mariko Ariyoshi, and Tatsuo Fukagawa. 2019. 'CDK1-Mediated CENP-C Phosphorylation Modulates CENP-A Binding and Mitotic Kinetochore Localization'. The Journal of Cell Biology 218(12): 4042–62. doi:10.1083/jcb.201907006.

Waterland, Robert A., and Randy L. Jirtle. 2003. 'Transposable Elements: Targets for Early Nutritional Effects on Epigenetic Gene Regulation'. Molecular and Cellular Biology 23(15): 5293–5300. doi:10.1128/MCB.23.15.5293-5300.2003.

Watson, J. D., and F. H. Crick. 1953. 'Molecular Structure of Nucleic Acids; a Structure for Deoxyribose Nucleic Acid'. Nature 171(4356): 737–38. doi:10.1038/171737a0.

Watson, L. Ashley, and Li-Huei Tsai. 2017. 'In the Loop: How Chromatin Topology Links Genome Structure to Function in Mechanisms Underlying Learning and Memory'. Current Opinion in Neurobiology 43: 48–55. doi:10.1016/j.conb.2016.12.002.

Watt, F., and P. L. Molloy. 1988. 'Cytosine Methylation Prevents Binding to DNA of a HeLa Cell Transcription Factor Required for Optimal Expression of the Adenovirus Major Late Promoter'. Genes & Development 2(9): 1136–43. doi:10.1101/gad.2.9.1136.

Waye, J. S., S. J. Durfy, D. Pinkel, S. Kenwrick, M. Patterson, K. E. Davies, and H. F. Willard. 1987. 'Chromosome-Specific Alpha Satellite DNA from Human Chromosome 1: Hierarchical Structure and Genomic Organization of a Polymorphic Domain Spanning Several Hundred Kilobase Pairs of Centromeric DNA'. Genomics 1(1): 43–51. doi:10.1016/0888-7543(87)90103-0.

Weber, Bjerke, and DeSimone. 2012. 'A Mechanoresponsive Cadherin-Keratin Complex Directs Polarized Protrusive Behavior and Collective Cell Migration'. Developmental cell 22(1). doi:10.1016/j.devcel.2011.10.013.

Wei, Spencer C., Laurent Fattet, Jeff H. Tsai, Yurong Guo, Vincent H. Pai, Hannah E. Majeski, Albert C. Chen, et al. 2015. 'Matrix Stiffness Drives Epithelial-Mesenchymal Transition and Tumour Metastasis through a TWIST1-G3BP2 Mechanotransduction Pathway'. Nature Cell Biology 17(5): 678–88. doi:10.1038/ncb3157.

Weierich, Claudia, Alessandro Brero, Stefan Stein, Johann von Hase, Christoph Cremer, Thomas Cremer, and Irina Solovei. 2003. 'Three-Dimensional Arrangements of Centromeres and Telomeres in Nuclei of Human and Murine Lymphocytes'. Chromosome Research: An International Journal on the Molecular, Supramolecular and Evolutionary Aspects of Chromosome Biology 11(5): 485–502. doi:10.1023/a:1025016828544.

Weimer, R., T. Haaf, J. Krüger, M. Poot, and M. Schmid. 1992. 'Characterization of Centromere Arrangements and Test for Random Distribution in G0, G1, S, G2, G1, and Early S' Phase in Human Lymphocytes'. Human Genetics 88(6): 673–82. doi:10.1007/BF02265296.

Weir, John R., Alex C. Faesen, Kerstin Klare, Arsen Petrovic, Federica Basilico, Josef Fischböck, Satyakrishna Pentakota, et al. 2016. 'Insights from Biochemical Reconstitution into the Architecture of Human Kinetochores'. Nature 537(7619): 249–53. doi:10.1038/nature19333.

Wellner, Schubert, Burk, Schmalhofer, Zhu, Sonntag, Waldvogel, et al. 2009a. 'The EMT-Activator ZEB1 Promotes Tumorigenicity by Repressing Stemness-Inhibiting microRNAs'. Nature cell biology 11(12). doi:10.1038/ncb1998.

Wellner, Ulrich, Jörg Schubert, Ulrike C. Burk, Otto Schmalhofer, Feng Zhu, Annika Sonntag, Bettina Waldvogel, et al. 2009b. 'The EMT-Activator ZEB1 Promotes Tumorigenicity by Repressing Stemness-Inhibiting microRNAs'. Nature Cell Biology 11(12): 1487–95. doi:10.1038/ncb1998.

Wen, Qing, Jiaqi Zhou, Congcong Tian, Xinran Li, Guibing Song, Yuan Gao, Yaping Sun, et al. 2023. 'Symmetric Inheritance of Parental Histones Contributes to Safeguarding the Fate of Mouse Embryonic Stem Cells during Differentiation'. Nature Genetics 55(9): 1555–66. doi:10.1038/s41588-023-01477-w.

Wenger, Alice, Alva Biran, Nicolas Alcaraz, Alba Redó-Riveiro, Annika Charlotte Sell, Robert Krautz, Valentin Flury, et al. 2023. 'Symmetric Inheritance of Parental Histones Governs Epigenome Maintenance and Embryonic Stem Cell Identity'. Nature Genetics 55(9): 1567–78. doi:10.1038/s41588-023-01476-x.

Weyemi, Urbain, Christophe E. Redon, Rohini Choudhuri, Towqir Aziz, Daisuke Maeda, Myriem Boufraqech, Palak R. Parekh, et al. 2016. 'The Histone Variant H2A.X Is a Regulator of the Epithelial-Mesenchymal Transition'. Nature Communications 7: 10711. doi:10.1038/ncomms10711.

Weyemi, Urbain, Christophe E. Redon, Taresh K. Sethi, Allison S. Burrell, Parthav Jailwala, Manjula Kasoji, Natalie Abrams, Anand Merchant, and William M. Bonner. 2016. 'Twist1 and Slug Mediate

H2AX-Regulated Epithelial-Mesenchymal Transition in Breast Cells'. Cell Cycle (Georgetown, Tex.) 15(18): 2398–2404. doi:10.1080/15384101.2016.1198864.

Wilkins, M. H., W. E. Seeds, A. R. Stokes, and H. R. Wilson. 1953. 'Helical Structure of Crystalline Deoxypentose Nucleic Acid'. Nature 172(4382): 759–62. doi:10.1038/172759b0.

Willard, H. F. 1989. 'The Genomics of Long Tandem Arrays of Satellite DNA in the Human Genome'. Genome 31(2): 737–44. doi:10.1139/g89-132.

William, H. 1651. Exercitationes de generatione animalium (On Animal Generation).

Willis, Brigham C., and Zea Borok. 2007. 'TGF-Beta-Induced EMT: Mechanisms and Implications for Fibrotic Lung Disease'. American Journal of Physiology. Lung Cellular and Molecular Physiology 293(3): L525-534. doi:10.1152/ajplung.00163.2007.

Willis, Brigham C., Janice M. Liebler, Katherine Luby-Phelps, Andrew G. Nicholson, Edward D. Crandall, Roland M. du Bois, and Zea Borok. 2005. 'Induction of Epithelial-Mesenchymal Transition in Alveolar Epithelial Cells by Transforming Growth Factor-Beta1: Potential Role in Idiopathic Pulmonary Fibrosis'. The American Journal of Pathology 166(5): 1321–32. doi:10.1016/s0002-9440(10)62351-6.

Wollmann, Heike, Hume Stroud, Ramesh Yelagandula, Yoshiaki Tarutani, Danhua Jiang, Li Jing, Bhagyshree Jamge, et al. 2017. 'The Histone H3 Variant H3.3 Regulates Gene Body DNA Methylation in Arabidopsis Thaliana'. Genome Biology 18(1): 94. doi:10.1186/s13059-017-1221-3.

Wong, Lee H., Hua Ren, Evan Williams, James McGhie, Soyeon Ahn, Marcus Sim, Angela Tam, et al. 2009. 'Histone H3.3 Incorporation Provides a Unique and Functionally Essential Telomeric Chromatin in Embryonic Stem Cells'. Genome Research 19(3): 404–14. doi:10.1101/gr.084947.108.

Worcel, A., S. Han, and M. L. Wong. 1978. 'Assembly of Newly Replicated Chromatin'. Cell 15(3): 969–77. doi:10.1016/0092-8674(78)90280-5.

Wu, C. 1980. 'The 5′ Ends of Drosophila Heat Shock Genes in Chromatin Are Hypersensitive to DNase I'. Nature 286(5776): 854–60. doi:10.1038/286854a0.

Wu, C. 1984. 'Activating Protein Factor Binds in Vitro to Upstream Control Sequences in Heat Shock Gene Chromatin'. Nature 311(5981): 81–84. doi:10.1038/311081a0.

Wu, Gang, Alberto Broniscer, Troy A. McEachron, Charles Lu, Barbara S. Paugh, Jared Becksfort, Chunxu Qu, et al. 2012. 'Somatic Histone H3 Alterations in Pediatric Diffuse Intrinsic Pontine Gliomas and Non-Brainstem Glioblastomas'. Nature Genetics 44(3): 251–53. doi:10.1038/ng.1102.

Wu, Jiatao, Wenjuan Li, Xueying Zhang, Fan Shi, Qianhao Jia, Yufei Wang, Yuqi Shi, Shiwu Wu, and Xiaojing Wang. 2024. 'Expression and Potential Molecular Mechanism of TOP2A in Metastasis of Non-Small Cell Lung Cancer'. Scientific Reports 14(1): 12228. doi:10.1038/s41598-024-63055-2.

Wu, LiHong, Yang Liu, and DaoChun Kong. 2014. ‘Mechanism of Chromosomal DNA Replication Initiation and Replication Fork Stabilization in Eukaryotes’. Science China. Life Sciences 57(5): 482–87. doi:10.1007/s11427-014-4631-4.

Wu, Q., Y. M. Qian, X. L. Zhao, S. M. Wang, X. J. Feng, X. F. Chen, and S. H. Zhang. 2012. ‘Expression and prognostic significance of centromere protein A in human lung adenocarcinoma’. Lung cancer : Journal of the International Association for the Study of Lung Cancer 77(2): 407–14.

Wu, Qing, Yong-Feng Chen, Jie Fu, Qi-Han You, Shou-Mei Wang, Xue Huang, Xiao-Jun Feng, and Shu-Hui Zhang. 2014. ‘Short Hairpin RNA-Mediated down-Regulation of CENP-A Attenuates the Aggressive Phenotype of Lung Adenocarcinoma Cells’. Cellular Oncology (Dordrecht) 37(6): 399–407. doi:10.1007/s13402-014-0199-z.

Wu, R. S., S. Tsai, and W. M. Bonner. 1982. ‘Patterns of Histone Variant Synthesis Can Distinguish G0 from G1 Cells’. Cell 31(2 Pt 1): 367–74. doi:10.1016/0092-8674(82)90130-1.

Wu, Shiyang, Suyan Liu, Zhiming Liu, Jiefeng Huang, Xiaoyu Pu, Jing Li, Dinghua Yang, et al. 2015. ‘Classification of Circulating Tumor Cells by Epithelial-Mesenchymal Transition Markers’. PloS One 10(4): e0123976. doi:10.1371/journal.pone.0123976.

Xu, G. L., T. H. Bestor, D. Bourc’his, C. L. Hsieh, N. Tommerup, M. Bugge, M. Hulten, et al. 1999. ‘Chromosome Instability and Immunodeficiency Syndrome Caused by Mutations in a DNA Methyltransferase Gene’. Nature 402(6758): 187–91. doi:10.1038/46052.

Xu, Jian, Samy Lamouille, and Rik Derynck. 2009. ‘TGF-Beta-Induced Epithelial to Mesenchymal Transition’. Cell Research 19(2): 156–72. doi:10.1038/cr.2009.5.

Xu, Jianquan, Hongqiang Ma, Jingyi Jin, Shikhar Uttam, Rao Fu, Yi Huang, and Yang Liu. 2018. ‘Super-Resolution Imaging of Higher-Order Chromatin Structures at Different Epigenomic States in Single Mammalian Cells’. Cell Reports 24(4): 873–82. doi:10.1016/j.celrep.2018.06.085.

Xu, Mo, Chengzu Long, Xiuzhen Chen, Chang Huang, She Chen, and Bing Zhu. 2010. ‘Partitioning of Histone H3-H4 Tetramers during DNA Replication-Dependent Chromatin Assembly’. Science (New York, N.Y.) 328(5974): 94–98. doi:10.1126/science.1178994.

Xu, Shuangyi, Ning Wang, Michael V. Zuccaro, Jeannine Gerhardt, Rajan Iyyappan, Giovanna Nascimento Scatolin, Zongliang Jiang, et al. 2024. ‘DNA Replication in Early Mammalian Embryos Is Patterned, Predisposing Lamina-Associated Regions to Fragility’. Nature Communications 15(1): 5247. doi:10.1038/s41467-024-49565-7.

Xu, Xiaowei, Xu Hua, Kyle Brown, Xiaojun Ren, and Zhiguo Zhang. 2022. ‘Mcm2 Promotes Stem Cell Differentiation via Its Ability to Bind H3-H4’. eLife 11: e80917. doi:10.7554/eLife.80917.

Xu, Yixiang, Dong-Kee Lee, Zhen Feng, Yan Xu, Wen Bu, Yi Li, Lan Liao, and Jianming Xu. 2017. ‘Breast Tumor Cell-Specific Knockout of Twist1 Inhibits Cancer Cell Plasticity, Dissemination, and

Lung Metastasis in Mice'. Proceedings of the National Academy of Sciences of the United States of America 114(43): 11494–99. doi:10.1073/pnas.1618091114.

Xu, Yuan, Chao Liang, Xianlei Cai, Miaozun Zhang, Weiming Yu, and Qinshu Shao. 2020. 'High Centromere Protein-A (CENP-A) Expression Correlates with Progression and Prognosis in Gastric Cancer'. OncoTargets and therapy 13: 13237–46. doi:10.2147/OTT.S263512.

Yadav, Tejas, Jean-Pierre Quivy, and Geneviève Almouzni. 2018. 'Chromatin Plasticity: A Versatile Landscape That Underlies Cell Fate and Identity'. Science (New York, N.Y.) 361(6409): 1332–36. doi:10.1126/science.aat8950.

Yagasaki, R., M. Noguchi, M. Minami, and M. Earashi. 1996. 'Clinical Significance of E-Cadherin and Vimentin Co-Expression in Breast Cancer'. International Journal of Oncology 9(4): 755–61. doi:10.3892/ijo.9.4.755.

Yamasu, K., and T. Senshu. 1990. 'Conservative Segregation of Tetrameric Units of H3 and H4 Histones during Nucleosome Replication'. Journal of Biochemistry 107(1): 15–20. doi:10.1093/oxfordjournals.jbchem.a122999.

Yanagisawa, Masahiro, Deborah Huveldt, Pamela Kreinest, Christine M. Lohse, John C. Cheville, Alexander S. Parker, John A. Copland, and Panos Z. Anastasiadis. 2008. 'A P120 Catenin Isoform Switch Affects Rho Activity, Induces Tumor Cell Invasion, and Predicts Metastatic Disease'. The Journal of Biological Chemistry 283(26): 18344–54. doi:10.1074/jbc.M801192200.

Yang, Anthony D., Fan Fan, E. Ramsay Camp, George van Buren, Wenbiao Liu, Ray Somcio, Michael J. Gray, et al. 2006. 'Chronic Oxaliplatin Resistance Induces Epithelial-to-Mesenchymal Transition in Colorectal Cancer Cell Lines'. Clinical Cancer Research: An Official Journal of the American Association for Cancer Research 12(14 Pt 1): 4147–53. doi:10.1158/1078-0432.CCR-06-0038.

Yang, Jing, Parker Antin, Geert Berx, Cédric Blanpain, Thomas Brabletz, Marianne Bronner, Kyra Campbell, Amparo Cano, Jordi Casanova, Gerhard Christofori, Shoukat Dedhar, Rik Derynck, Heide L. Ford, Jonas Fuxe, Antonio García de Herreros, et al. 2020. 'Guidelines and Definitions for Research on Epithelial–Mesenchymal Transition'. Nature Reviews Molecular Cell Biology 21(6): 341–52. doi:10.1038/s41580-020-0237-9.

Yang, Jing, Sendurai A. Mani, Joana Liu Donaher, Sridhar Ramaswamy, Raphael A. Itzykson, Christophe Come, Pierre Savagner, et al. 2004. 'Twist, a Master Regulator of Morphogenesis, Plays an Essential Role in Tumor Metastasis'. Cell 117(7): 927–39. doi:10.1016/j.cell.2004.06.006.

Yang, Muh-Hwa, Chih-Li Chen, Gar-Yang Chau, Shih-Hwa Chiou, Chien-Wei Su, Teh-Ying Chou, Wei-Li Peng, and Jaw-Ching Wu. 2009. 'Comprehensive Analysis of the Independent Effect of Twist and Snail in Promoting Metastasis of Hepatocellular Carcinoma'. Hepatology (Baltimore, Md.) 50(5): 1464–74. doi:10.1002/hep.23221.

Yang, Muh-Hwa, Min-Zu Wu, Shih-Hwa Chiou, Po-Min Chen, Shyue-Yih Chang, Chung-Ji Liu, Shu-Chun Teng, and Kou-Juey Wu. 2008. 'Direct Regulation of TWIST by HIF-1alpha Promotes Metastasis'. Nature Cell Biology 10(3): 295–305. doi:10.1038/ncb1691.

Yang, Yunlong, and Yihai Cao. 2022. 'The Impact of VEGF on Cancer Metastasis and Systemic Disease'. Seminars in Cancer Biology 86(Pt 3): 251–61. doi:10.1016/j.semcancer.2022.03.011.

Yap, Ee-Lynn, and Michael E. Greenberg. 2018. 'Activity-Regulated Transcription: Bridging the Gap between Neural Activity and Behavior'. Neuron 100(2): 330–48. doi:10.1016/j.neuron.2018.10.013.

Ye, Xiaofen, Alexa A. Franco, Hidelita Santos, David M. Nelson, Paul D. Kaufman, and Peter D. Adams. 2003. 'Defective S Phase Chromatin Assembly Causes DNA Damage, Activation of the S Phase Checkpoint, and S Phase Arrest'. Molecular Cell 11(2): 341–51. doi:10.1016/s1097-2765(03)00037-6.

Ye, Xin, Thomas Brabletz, Yibin Kang, Gregory D. Longmore, M. Angela Nieto, Ben Z. Stanger, Jing Yang, and Robert A. Weinberg. 2017. 'Upholding a Role for EMT in Breast Cancer Metastasis'. Nature 547(7661): E1–3. doi:10.1038/nature22816.

Ye, Xin, Wai Leong Tam, Tsukasa Shibue, Yasemin Kaygusuz, Ferenc Reinhardt, Elinor Ng Eaton, and Robert A. Weinberg. 2015. 'Distinct EMT Programs Control Normal Mammary Stem Cells and Tumour-Initiating Cells'. Nature 525(7568): 256–60. doi:10.1038/nature14897.

Yeeles, Joseph T. P., Tom D. Deegan, Agnieszka Janska, Anne Early, and John F. X. Diffley. 2015. 'Regulated Eukaryotic DNA Replication Origin Firing with Purified Proteins'. Nature 519(7544): 431–35. doi:10.1038/nature14285.

Yoon, Taewon, Amit Chakrabortty, Roberta Franks, Ted Valli, Hiroaki Kiyokawa, and Pradip Raychaudhuri. 2005. 'Tumor-Prone Phenotype of the DDB2-Deficient Mice'. Oncogene 24(3): 469–78. doi:10.1038/sj.onc.1208211.

Youssef, Khalil Kass, and M. Angela Nieto. 2024. 'Epithelial–Mesenchymal Transition in Tissue Repair and Degeneration'. Nature Reviews Mol Cell Biol: 1–20. doi:10.1038/s41580-024-00733-z.

Yu, Chuanhe, Haiyun Gan, Albert Serra-Cardona, Lin Zhang, Songlin Gan, Sushma Sharma, Erik Johansson, et al. 2018. 'A Mechanism for Preventing Asymmetric Histone Segregation onto Replicating DNA Strands'. Science (New York, N.Y.) 361(6409): 1386–89. doi:10.1126/science.aat8849.

Yu, Hua, Drew Pardoll, and Richard Jove. 2009. 'STATs in Cancer Inflammation and Immunity: A Leading Role for STAT3'. Nature Reviews. Cancer 9(11): 798–809. doi:10.1038/nrc2734.

Yu, Min, Aditya Bardia, Ben S. Wittner, Shannon L. Stott, Malgorzata E. Smas, David T. Ting, Steven J. Isakoff, et al. 2013. 'Circulating Breast Tumor Cells Exhibit Dynamic Changes in Epithelial and Mesenchymal Composition'. Science (New York, N.Y.) 339(6119): 580–84. doi:10.1126/science.1228522.

Zaichuk, Tetiana, and John F. Marko. 2021. 'Single-Molecule Micromanipulation Studies of Methylated DNA'. Biophysical Journal 120(11): 2148–55. doi:10.1016/j.bpj.2021.03.039.

Zaidi, Sayyed K., Andrew J. Fritz, Kirsten M. Tracy, Jonathan A. Gordon, Coralee E. Tye, Joseph Boyd, Andre J. Van Wijnen, et al. 2018. 'Nuclear Organization Mediates Cancer-Compromised Genetic and Epigenetic Control'. Advances in Biological Regulation 69: 1–10. doi:10.1016/j.jbior.2018.05.001.

Zasadzińska, Ewelina, Meghan C Barnhart-Dailey, P Henning J L Kuich, and Daniel R Foltz. 2013. 'Dimerization of the CENP-A Assembly Factor HJURP Is Required for Centromeric Nucleosome Deposition'. The EMBO Journal 32(15): 2113–24. doi:10.1038/emboj.2013.142.

Zasadzińska, Ewelina, Jiehuan Huang, Aaron O. Bailey, Lucie Y. Guo, Nancy S. Lee, Shashank Srivastava, Kelvin A. Wong, et al. 2018. 'Inheritance of CENP-A Nucleosomes during DNA Replication Requires HJURP'. Developmental Cell 47(3): 348-362.e7. doi:10.1016/j.devcel.2018.09.003.

Zeisberg, Elisabeth M., Oleg Tarnavski, Michael Zeisberg, Adam L. Dorfman, Julie R. McMullen, Erika Gustafsson, Anil Chandraker, et al. 2007. 'Endothelial-to-Mesenchymal Transition Contributes to Cardiac Fibrosis'. Nature Medicine 13(8): 952–61. doi:10.1038/nm1613.

Zeisberg, Michael, Jun-ichi Hanai, Hikaru Sugimoto, Tadanori Mammoto, David Charytan, Frank Strutz, and Raghu Kalluri. 2003. 'BMP-7 Counteracts TGF-Beta1-Induced Epithelial-to-Mesenchymal Transition and Reverses Chronic Renal Injury'. Nature Medicine 9(7): 964–68. doi:10.1038/nm888.

Zeisberg, Michael, and Raghu Kalluri. 2004. 'The Role of Epithelial-to-Mesenchymal Transition in Renal Fibrosis'. Journal of Molecular Medicine (Berlin, Germany) 82(3): 175–81. doi:10.1007/s00109-003-0517-9.

Zeisberg, Michael, Changqing Yang, Margot Martino, Michael B. Duncan, Florian Rieder, Harikrishna Tanjore, and Raghu Kalluri. 2007. 'Fibroblasts Derive from Hepatocytes in Liver Fibrosis via Epithelial to Mesenchymal Transition'. The Journal of biological chemistry 282(32). doi:10.1074/jbc.M700194200.

Zeitlin, Samantha G., Norman M. Baker, Brian R. Chapados, Evi Soutoglou, Jean Y. J. Wang, Michael W. Berns, and Don W. Cleveland. 2009. 'Double-Strand DNA Breaks Recruit the Centromeric Histone CENP-A'. Proceedings of the National Academy of Sciences of the United States of America 106(37): 15762–67. doi:10.1073/pnas.0908233106.

Zhan, Qimin. 2005. 'Gadd45a, a P53- and BRCA1-Regulated Stress Protein, in Cellular Response to DNA Damage'. Mutation Research 569(1–2): 133–43. doi:10.1016/j.mrfmmm.2004.06.055.

Zhang, April, Hira Aslam, Neha Sharma, Aryeh Warmflash, and Walid D. Fakhouri. 2021. 'Conservation of Epithelial-to-Mesenchymal Transition Process in Neural Crest Cells and Metastatic Cancer'. Cells, tissues, organs 210(3): 151–72. doi:10.1159/000516466.

Zhang, Bingjie, Hui Zheng, Bo Huang, Wenzhi Li, Yunlong Xiang, Xu Peng, Jia Ming, et al. 2016. 'Allelic Reprogramming of the Histone Modification H3K4me3 in Early Mammalian Development'. Nature 537(7621): 553–57. doi:10.1038/nature19361.

Zhang, Cheng-Zhong, Alexander Spektor, Hauke Cornils, Joshua M. Francis, Emily K. Jackson, Shiwei Liu, Matthew Meyerson, and David Pellman. 2015. 'Chromothripsis from DNA Damage in Micronuclei'. Nature 522(7555): 179–84. doi:10.1038/nature14493.

Zhang, Hai-Feng, Li-Yan Xu, and En-Min Li. 2014. 'A Family of Pleiotropically Acting microRNAs in Cancer Progression, miR-200: Potential Cancer Therapeutic Targets'. Current Pharmaceutical Design 20(11): 1896–1903. doi:10.2174/13816128113199990519.

Zhang, Jingcheng, Haiyan Zhang, Junyu Liu, Xiaolong Tu, Yuhui Zang, Jie Zhu, Jiangning Chen, Lei Dong, and Junfeng Zhang. 2012. 'miR-30 Inhibits TGF-B1-Induced Epithelial-to-Mesenchymal Transition in Hepatocyte by Targeting Snail1'. Biochemical and Biophysical Research Communications 417(3): 1100–1105. doi:10.1016/j.bbrc.2011.12.121.

Zhang, Jingyu, Xiao-Jun Tian, Hang Zhang, Yue Teng, Ruoyan Li, Fan Bai, Subbiah Elankumaran, and Jianhua Xing. 2014. 'TGF-β-Induced Epithelial-to-Mesenchymal Transition Proceeds through Stepwise Activation of Multiple Feedback Loops'. Science Signaling 7(345): ra91. doi:10.1126/scisignal.2005304.

Zhang, Kaiwen, Xingyu Zheng, Yiqing Sun, Xinyu Feng, Xirong Wu, Wenlu Liu, Chao Gao, et al. 'TOP2A Modulates Signaling via the AKT/mTOR Pathway to Promote Ovarian Cancer Cell Proliferation'. Cancer Biology & Therapy 25(1): 2325126. doi:10.1080/15384047.2024.2325126.

Zhang, Weiguo, Jian-Hua Mao, Wei Zhu, Anshu K. Jain, Ke Liu, James B. Brown, and Gary H. Karpen. 2016. 'Centromere and Kinetochore Gene Misexpression Predicts Cancer Patient Survival and Response to Radiotherapy and Chemotherapy'. Nature Communications 7: 12619. doi:10.1038/ncomms12619.

Zhao, Haiqing, David Winogradoff, Minh Bui, Yamini Dalal, and Garegin A. Papoian. 2016. 'Promiscuous Histone Mis-Assembly Is Actively Prevented by Chaperones'. Journal of the American Chemical Society 138(40): 13207–18. doi:10.1021/jacs.6b05355.

Zhao, J., L. Hyman, and C. Moore. 1999. 'Formation of mRNA 3' Ends in Eukaryotes: Mechanism, Regulation, and Interrelationships with Other Steps in mRNA Synthesis'. Microbiology and molecular biology reviews: MMBR 63(2): 405–45. doi:10.1128/MMBR.63.2.405-445.1999.

Zheng, Xiaofeng, Julienne L. Carstens, Jiha Kim, Matthew Scheible, Judith Kaye, Hikaru Sugimoto, Chia-Chin Wu, Valerie S. LeBleu, and Raghu Kalluri. 2015. 'Epithelial-to-Mesenchymal Transition Is Dispensable for Metastasis but Induces Chemoresistance in Pancreatic Cancer'. Nature 527(7579): 525–30. doi:10.1038/nature16064.

Zhou, Bing-Rui, K. N. Sathish Yadav, Mario Borgnia, Jingjun Hong, Baohua Cao, Ada L. Olins, Donald E. Olins, Yawen Bai, and Ping Zhang. 2019. 'Atomic Resolution Cryo-EM Structure of a Native-like CENP-A Nucleosome Aided by an Antibody Fragment'. Nature Communications 10(1): 2301. doi:10.1038/s41467-019-10247-4.

Zhu, Fangjie, Lucas Farnung, Eevi Kaasinen, Biswajyoti Sahu, Yimeng Yin, Bei Wei, Svetlana O. Dodonova, et al. 2018. 'The Interaction Landscape between Transcription Factors and the Nucleosome'. Nature 562(7725): 76–81. doi:10.1038/s41586-018-0549-5.

Zorn, Aaron M., and James M. Wells. 2009. 'Vertebrate Endoderm Development and Organ Formation'. Annual Review of Cell and Developmental Biology 25: 221–51. doi:10.1146/annurev.cellbio.042308.113344.

Zovkic, Iva B. 2021. 'Epigenetics and Memory: An Expanded Role for Chromatin Dynamics'. Current Opinion in Neurobiology 67: 58–65. doi:10.1016/j.conb.2020.08.007.

SUMMARY

Abstract

CENP-A (Centromere protein A) is a histone H3 variant incorporated into centromeric chromatin and essential for the proper segregation of human chromosomes to daughter cells during cell division. CENP-A overexpression, which promotes its mislocalization, is commonly observed in many cancers and correlates with aggressiveness of the disease. Interestingly, CENP-A transcription, while negatively regulated by the "tumor suppressor" p53, can evade this control. Thus, both p53-defective and p53 wild type cancers can display high levels of CENP-A. My goal was to understand how CENP-A overexpression and its ectopic localization participate in tumor evolution, considering the cellular context. Thus, I established a series of human cell lines with a tunable and reversible system to control CENP-A overexpression in various p53 contexts, that I analyzed under different conditions over time. Firstly, my work contributed to reveal how CENP-A overexpression affects cell cycle and identity in a manner that depends on the p53 status of the cells. Secondly, I identified a cell sub-population which, upon CENP-A overexpression, transitions towards mesenchymal states over time. This process, termed epithelial-mesenchymal transition (EMT), is a key driver of cancer progression and metastasis. Notably, by reversing CENP-A overexpression and erasing its ectopic localization, I could reverse the induced mesenchymal states. Furthermore, I found that CENP-A mislocalization promotes distinct EMT transcription programs. Altogether, these results suggest that CENP-A overexpression regulates cell plasticity in an epigenetic manner with important implications for cancer research.

Résumé

CENP-A (Centromere protein A) est un variant d'histone H3 dont l'incorporation dans la chromatine centromérique est essentielle à la ségrégation des chromosomes humains lors de la division cellulaire. La surexpression de CENP-A, qui conduit à sa localisation ectopique en dehors des centromères, est observée dans de nombreux cancers et est corrélée à l'agressivité de la maladie. Il est intéressant de noter que la régulation transcriptionnelle des niveaux de CENP-A dépend de la protéine « suppresseur de tumeur » p53. Pour autant, CENP-A peut échapper au contrôle de p53. Par conséquent, les cancers déficients en p53 et de type p53 sauvage peuvent tous les deux présenter des niveaux élevés de CENP-A. Mon objectif était de comprendre comment la surexpression et la localisation aberrante de CENP-A participent à l'évolution tumorale en tenant compte du contexte cellulaire et de son évolution au cours du temps. J'ai établi une série de lignées cellulaires humaines avec un système permettant d'induire et d'inverser la surexpression de CENP-A dans différents contextes p53 afin de suivre les destins cellulaires au cours du temps. Ainsi, en premier lieu, mon travail a contribué à révéler comment la surexpression de CENP-A affecte le cycle et l'identité cellulaires d'une manière qui dépend de p53. J'ai ensuite mis en évidence l'existence d'une sous-population cellulaire, qui, lorsqu'elle surexprime CENP-A, effectue une transition épithélio-mésenchymateuse (TEM), un facteur clé de la progression du cancer et du développement métastatique. En inversant la surexpression de CENP-A, ce qui supprime sa localisation ectopique, j'ai pu inverser les états mésenchymateux induits. Enfin, j'ai également montré que la localisation aberrante de CENP-A favorise différents programmes de transcription de l'EMT. En conclusion, ces résultats indiquent un rôle, pour la surexpression de CENP-A, dans la plasticité cellulaire s'exerçant de manière épigénétique.

Lay abstract

Our genome is organized as a complex named chromatin. Its building block, the nucleosome, enables to wrap DNA around proteins named histones (H2A, H2B, H3, H4). Histones exist as variants with distinct properties. CENP-A (Centromere Protein A) is a variant of histone H3, present at the centromere of our chromosomes to ensure their segregation to daughter cells during cell division. High CENP-A levels are frequent in aggressive cancers. During my PhD thesis, I aimed to understand how CENP-A overexpression contribute to the acquisition of features associated with aggressive cancers. I induced experimentally high levels of CENP-A in human cells. My results contributed to show that the consequences of CENP-A overexpression depend on p53, known as the “guardian of the genome” and mutated in half of cancers. Then, I identified a cell population undergoing a change in identity termed epithelial-mesenchymal transition, which can promote invasiveness and metastases. Finally, by reversing CENP-A overexpression, I could reverse the induced mesenchymal states. Thus, I revealed a new function of CENP-A in cell plasticity, i.e., the ability for cells to change identity.

Résumé grand public

Dans le noyau de nos cellules, l'ADN est enroulé autour de protéines appelées histones (H2A, H2B, H3, H4). Elles existent sous forme de variants aux propriétés distinctes. CENP-A (Centromere Protein A) est un variant de l'histone H3 présent au centromère des chromosomes pour assurer leur ségrégation lors de la division cellulaire. Des niveaux élevés de CENP-A sont fréquents dans les cancers agressifs. Au cours de ma thèse, j'ai cherché à comprendre comment la surexpression de CENP-A contribue à l'acquisition de caractéristiques des cancers agressifs. J'ai induit expérimentalement des taux élevés de CENP-A dans des cellules humaines. Mes résultats ont montré que les conséquences de la surexpression de CENP-A dépendent de p53, le « gardien du génome », muté dans la moitié des cancers. J'ai aussi identifié une population cellulaire subissant un changement d'identité appelé transition épithélio-mésenchymateuse, qui favorise l'invasion tumorale. En inversant la surexpression de CENP-A, j'ai supprimé les états mésenchymateux, révélant ainsi une nouvelle fonction de CENP-A dans la plasticité cellulaire, la capacité des cellules à changer d'identité.

APPENDIX

communications biology

ARTICLE

https://doi.org/10.1038/s42003-021-01941-5 OPEN

CENP-A overexpression promotes distinct fates in human cells, depending on p53 status

Daniel Jeffery [1], Alberto Gatto [1], Katrina Podsypanina[1], Charlène Renaud-Pageot [1], Rebeca Ponce Landete [1], Lorraine Bonneville[1], Marie Dumont[2], Daniele Fachinetti [2] & Geneviève Almouzni [1✉]

Tumour evolution is driven by both genetic and epigenetic changes. CENP-A, the centromeric histone H3 variant, is an epigenetic mark that directly perturbs genetic stability and chromatin when overexpressed. Although CENP-A overexpression is a common feature of many cancers, how this impacts cell fate and response to therapy remains unclear. Here, we established a tunable system of inducible and reversible CENP-A overexpression combined with a switch in p53 status in human cell lines. Through clonogenic survival assays, single-cell RNA-sequencing and cell trajectory analysis, we uncover the tumour suppressor p53 as a key determinant of how CENP-A impacts cell state, cell identity and therapeutic response. If p53 is functional, CENP-A overexpression promotes senescence and radiosensitivity. Surprisingly, when we inactivate p53, CENP-A overexpression instead promotes epithelial-mesenchymal transition, an essential process in mammalian development but also a precursor for tumour cell invasion and metastasis. Thus, we uncover an unanticipated function of CENP-A overexpression to promote cell fate reprogramming, with important implications for development and tumour evolution.

[1] Institut Curie, PSL Research University, CNRS, Sorbonne Université, Nuclear Dynamics Unit, Equipe Labellisée Ligue contre le Cancer, Paris, France. [2] Institut Curie, PSL Research University, Centre de Recherche, Sorbonne Université, Cell Biology and Cancer Unit, Paris, France. ✉email: genevieve.almouzni@curie.fr

Tumor evolution is driven by both genetic and nongenetic changes from tumourigenesis to therapeutic resistance[1,2]. The fate of a given cell depends on how these changes impact both cell state (e.g., proliferation or death) and cell identity (e.g., stemness or differentiation). On the genetic side, tumor evolution is strongly linked to chromosomal instability (CIN)[3–5]. This subcategory of genome instability is characterized by an increased rate of mutagenesis through losses or gains of chromosomes, partial chromosomes, or chromosomal rearrangements. While extreme CIN is generally deleterious to cells, low or intermediate CIN increases the heterogeneity of the cell population[6]. These changes can promote the selection of advantageous clones through Darwinian evolution[7] a hypothesis put forward more than a century ago in cancer biology[8]. On the nongenetic side, environmental and metabolic insults can induce changes to epigenetic landscapes that perturb genome regulation[9]. This can further contribute to tumor heterogeneity[10] enabling cell plasticity[11], acquisition and maintenance of stemness properties[12], and the ability to counteract cell shutdown mechanisms[9]. All of these aspects can promote tumor development and reduce therapeutic response. But, in contrast to genetic changes, epigenetic changes are reversible[13]. This reversibility makes epigenetic marks and their regulatory factors interesting targets for cancer treatment, especially in combination with other anticancer therapies[14].

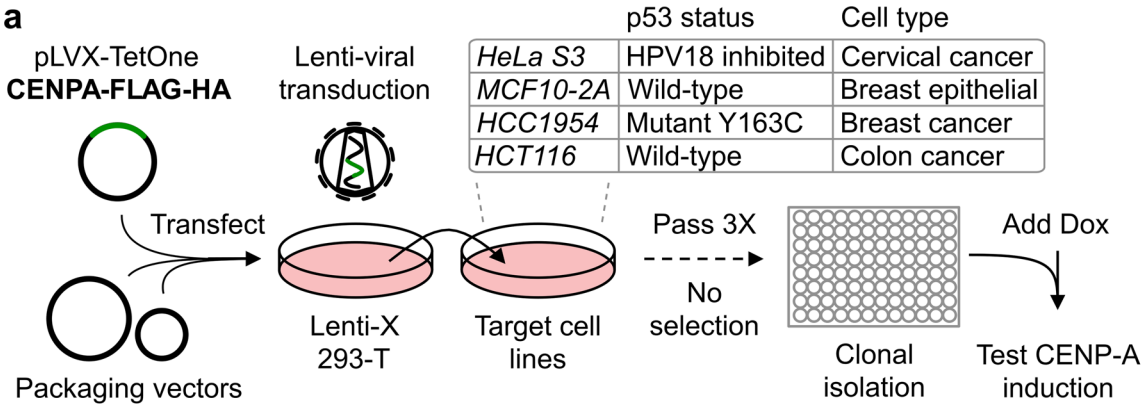
Furthermore, genetic and epigenetic parameters are tightly interconnected. As an illustration, the centromeric histone H3 variant, centromere protein A (CENP-A), is an epigenetic mark with direct effects on CIN[15]. In mammals, CENP-A is considered as a prime example of a bona fide transgenerational epigenetic mark[16]. Indeed, its deposition determines the location of the centromere[17,18] and it is transmitted across cell divisions and even organismal generations[19,20]. CENP-A is deposited[21,22] and maintained[23] at centric chromatin by its dedicated histone chaperone HJURP. CENP-A acts as the foundation for kinetochore assembly during cell division, where it is essential for efficient chromosome segregation (reviewed in[24–27]). Therefore, the maintenance of genome integrity depends on the proper regulation of CENP-A[28]. This is demonstrated by CENP-A depletion[29] and overexpression[30] experiments, which both promote mitotic defects and CIN in human cells. Importantly, high CENP-A levels correlate strongly with increased tumor aggressiveness in patients[31–39], including an intriguing connection with increased invasiveness/metastasis[31,33,34,36,37,39]. Examining the regulation of *CENPA* gene expression, we demonstrated that the tumor suppressor p53 (reviewed in[40,41]) negatively regulates CENP-A transcription through its downstream effector p21[42]. Thus, CENP-A levels are held in check by active p53. But CENP-A overexpression occurs in many cancers[36,37], and although *TP53* mutation correlates with higher CENP-A levels in patient tumors[42], many tumors overexpress CENP-A despite having wild-type (WT) *TP53* (cBioPortal[43]), indicating that p53 regulation is not the sole mechanism that controls CENP-A expression. Notably, correlation of high CENP-A levels with therapeutic response to DNA damaging agents is a matter of debate, with studies arguing for reduced[31] or improved response[37,39]. However, p53 status was not assessed in these studies. This is even more important, given that the p53 pathway responds differentially to distinct cell cycle defects[44]. Thus, understanding how CENP-A overexpression impacts cell fate in different p53 contexts is an important question that could shed light on how CENP-A influences tumor evolution, including tumor invasiveness and metastasis as well as cell response to cancer treatment.

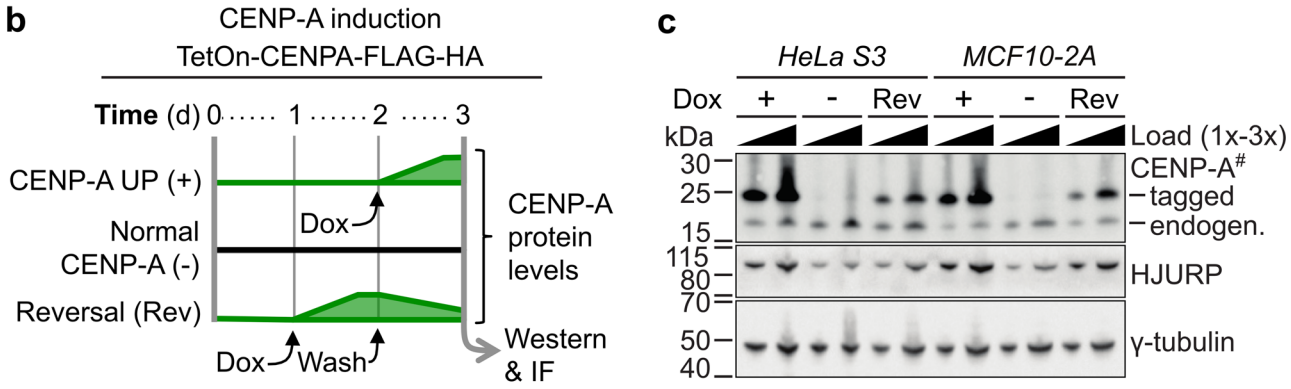
To address these issues, we set up a system to turn on and off the overexpression of CENP-A in various p53 contexts and switch p53 status in selected cell lines. Using this tunable system, we demonstrate that CENP-A overexpression alters cell fate in a manner dependent on p53 status. When p53 is functional, CENP-A overexpression alters cell state, promoting cell cycle arrest, senescence, and radiosensitivity. But when we inactivate p53 the cells evade arrest. Instead, CENP-A overexpression stimulates a change in cell identity, promoting epithelial–mesenchymal transition (EMT). Thus, our findings reveal an unanticipated function of CENP-A overexpression to promote the reprogramming of cell fate in distinct ways that depend on p53 status, with important implications for the role of CENP-A in tumor evolution.

Results

Inducible and reversible CENP-A overexpression in cells with varied p53 status. In order to explore how CENP-A expression levels and p53 status impact cell fate and cell response to anticancer treatment, we first established a system where we could specifically alter CENP-A expression independent of its regulation by p53. For this, we added a doxycycline-inducible CENP-A overexpression construct (*TetOn-CENPA-FLAG-HA*) by lentiviral transduction into several cell lines with varied p53 status (Fig. 1a, see also Table 1). Importantly, we did not use antibiotic selection to obtain CENP-A overexpression. This enables us to investigate the unbiased effects of CENP-A overexpression over time, without provoking cell adaptations or secondary mutations that could arise from selective pressure. The TetOn system allows induction of CENP-A overexpression within 24 h of adding doxycycline (Fig. 1b–d). This induction is within the range of CENP-A levels found in patient tumors, which can go over 1000-fold relative to healthy tissue (Supplementary Fig. 1A, B; cBioPortal[43]). Even in healthy tissues, there is a high degree of variability in CENP-A expression, where differences up to 50-fold can be observed (cf. CENP-A tissue expression in www.proteinatlas.org[45]). This acute-induced overexpression of CENP-A increases HJURP protein levels (Fig. 1c), increases levels of CENP-A at centromeres, and also causes mislocalization of CENP-A to the chromosome arms (Fig. 1d), regardless of p53 status. These effects are similar to those observed with constitutive CENP-A overexpression in HeLa cells[46]. Here, however, we could reverse both CENP-A overexpression and mislocalization simply by washing out doxycycline (Fig. 1c, d), consistent with the observation of rapid removal of ectopic CENP-A from chromosome arms with DNA replication[47]. Thus, while artificial, our controlled system is a powerful tool to test therapeutic sensitivity in several cell lines with varied p53 status under conditions of tunable CENP-A overexpression within the range of expression found in tumors.

Induced CENP-A overexpression causes reversible radiosensitivity in p53-WT cells. To test therapeutic sensitivity in our cell lines, we chose X-irradiation as a representative DNA damaging agent that is commonly used in cancer therapy. Thus, we tested cell survival after X-irradiation with or without induction of CENP-A overexpression by colony formation assays (CFAs), a surrogate for self-renewal capacity (Fig. 2a). For cell lines with WT p53 status, we used both non-tumoral (MCF10-2A) and tumoral (HCT116) lines. CENP-A overexpression in both cell lines led to a strong increase in sensitivity to X-irradiation, independent of tumoral status (Fig. 2b, left). Meanwhile, CENP-A overexpression in all cell lines with defective p53 (HeLa S3, HCC1954, and DLD1) did not significantly affect radiosensitivity—a distinctly radio-tolerant phenotype (Fig. 2b, right, see also Supplementary Fig. 1C). To assess if these distinct CFA phenotypes could be explained by the different CENP-A levels associated with each cell line, we first compared by western blotting the levels of endogenous CENP-A and CENP-A





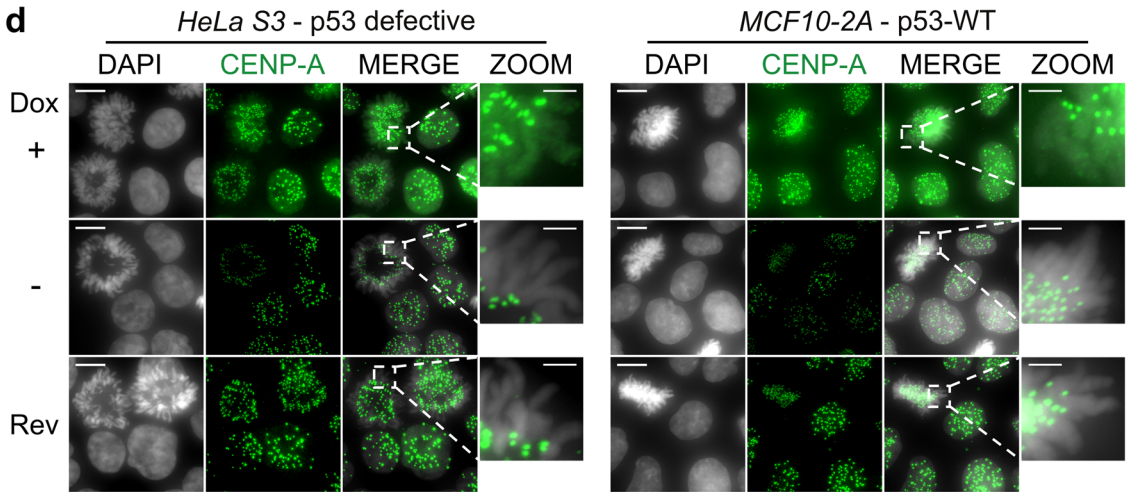


Fig. 1 Inducible and reversible CENP-A overexpression in cells with varied p53 status. a Scheme for the generation of doxycycline (Dox) inducible CENP-A overexpression cell lines. *TetOn-CENPA-FLAG-HA* construct was randomly integrated into several indicated target cell lines by lentiviral transfection without selection. After clonal isolation, we tested cells for clear homogenous CENP-A and HA increase by IF in approximately all cells 24 h after the addition of 80 ng/ml of Dox. Cells were also tested to ensure no detectable background HA signal by western or IF, when no Dox was added. **b** Scheme representing relative CENP-A protein levels over time for *TetOn-CENPA-FLAG-HA* cell lines. Dox = 10 ng/ml. **c** Western blot of total cell extracts (TCEs) pertaining to scheme in (**b**). Primary antibodies indicated on the right. Exogenous CENP-A (tagged) can be distinguished from endogenous CENP-A (endogen.) by its increased molecular weight. # = high sensitivity ECL. γ-tubulin used as loading control. See also Supplementary Fig. 1B for western blot analysis corresponding to all cell lines. **d** Immunofluorescence of paraformaldehyde-fixed cells using anti-CENP-A antibody (green) and DAPI staining (gray). Conditions in parallel with (**c**). Showing max projection images from a Z-series with zoom on a mitotic cell (DAPI/CENP-A merge) to highlight chromosome arms. Scale bars = 10 μm, Zoom = 2.5 μm.

Table 1 Description of cell lines used and their p53 status.

Cell line	p53 status[a]	Cell type	Construct	Comments
MCF10-2A	Functional wildtype	Immortal non-tumoral (fibrocystic disease) breast epithelial	*TetOn-CENP-A-FLAG-HA* (lentiviral)	Female origin
HCT116	Functional wildtype	Colon cancer	*TetOn-CENP-A-FLAG-HA* (lentiviral)	Male origin
HeLa S3	Nonfunctional wildtype: HPV18 inactivated	Cervical cancer	*TetOn-CENP-A-FLAG-HA* (lentiviral)	Female origin
HCC1954	LOF p53 mutation at Y163C	Invasive ductal carcinoma, breast	*TetOn-CENP-A-FLAG-HA* (lentiviral)	Female origin; HER^+ ER^- PR^- luminal
DLD1	One functionally silent allele of p53 and LOF mutation at S241F	Colon cancer	*TetOn-CENPA-YFP-AID* (FlpIn)	Male origin; kind gift from D. Fachinetti

[a]p53 status for missense mutations from the TP53 database[107].

overexpression in all cell lines used (Supplementary Fig. 1B). Since our data do not show a correlation between CENP-A levels and radiosensitivity upon CENP-A overexpression, we can discard this explanation. Second, in order to determine if the differences in sensitivity that we observed upon CENP-A overexpression were due to secondary mutations from mitotic defects, we tested the reversibility of this sensitivity by tuning down CENP-A expression to near-endogenous levels in p53-WT cells (MCF10-2A) and p53-defective cells (HeLa S3) (Fig. 2c). Remarkably, restoration of CENP-A expression to endogenous levels reversed the sensitivity phenotype in MCF10-2A, while HeLa cells, used here as a control line, remained tolerant (Fig. 2d). Therefore, the radiosensitivity observed in MCF10-2A cells requires the continued overexpression of CENP-A and it cannot be explained by genetic effects (i.e., secondary mutations) that occur after induced CENP-A overexpression. Thus, CENP-A overexpression in both tumoral and non-tumoral cell lines leads to radiosensitivity in a manner that correlates with p53 status.

Sensitivity to X-irradiation upon CENP-A overexpression is dependent on functional p53. To assess if p53 plays a causal role in the radiosensitivity associated with CENP-A overexpression, we took advantage of the possibility to switch the p53 status in two of our inducible CENP-A overexpression cell lines: the tolerant HeLa cells and the sensitized MCF10-2A cells. We could thus carry out CFAs after CENP-A overexpression and X-irradiation in isogenic cell lines, but with altered p53 status (Fig. 3a). For the change from p53-defective to p53-WT in the CENP-A inducible HeLa cells, we transiently activated WT p53 by incubation at 42 °C for 1 h immediately prior to X-irradiation. This treatment enables the temporary release of p53 repression from the HPV18 E6 protein, permitting a functional p53 response[48]. We confirmed that after hyperthermia treatment, p53 levels increased, followed shortly after by increased p21 (Fig. 3b, c). This short hyperthermia treatment in HeLa cells was sufficient to mildly, but significantly, increase sensitivity to X-irradiation after CENP-A overexpression (Fig. 3d). The fact that we find an increase in sensitivity only when CENP-A is overexpressed is consistent with the hypothesis of an effect dependent on the transient reactivation of p53, however, we cannot exclude potential effects of hyperthermia independent of p53. In this regard, it was important to specifically alter only the p53 status in a controlled manner. For this, we stably transduced the p53-WT MCF10-2A *TetON-CENPA-FLAG-HA* cells with either an empty vector control or a constitutively expressed dominant negative (DN) *TP53* construct, in order to mimic p53 loss and p53 loss of function (LOF) mutations (p53DD construct[49]). The p53-DN peptide stabilizes the WT p53 protein, causing a clear increase in p53 protein level, but suppresses its activation of downstream targets (e.g., p21). Indeed, the indirect activator of p53 (Nutlin-3) caused clear increases in p53 and p21 in p53-WT cells, but not those expressing the p53-DN peptide (Fig. 3e). By stably switching p53 status in this manner, we observed a major change in the radiosensitivity of the cells. The p53-DN peptide in MCF10-2A cells strongly counteracted the radiosensitivity phenotype associated with CENP-A overexpression (Fig. 3f). Furthermore, we confirmed the radiosensitivity phenotype using a range of doxycycline concentrations and a range of X-irradiation doses in CFAs for the p53-WT and p53-DN MCF10-2A cells (Supplementary Fig. 1C, D). Taken together, the results demonstrate that induced CENP-A overexpression increases radiosensitivity in a p53-dependent manner.

Induced CENP-A overexpression promotes radiosensitivity by impairing cell cycle progression. Given that the p53-dependent radiosensitivity was due to nongenetic (reversible) effects of CENP-A overexpression, we decided to assess changes at the transcriptional level. We first assessed global transcription by RNA-seq, analyzing the effects of acute CENP-A overexpression (at two different concentrations of Dox), switch of p53 status, and X-irradiation treatment in the MCF10-2A cells (Fig. 4a). X-irradiation and inactivation of p53 affected the transcription of several genes (Fig. 4b). Notably, CENP-A overexpression induced more extensive changes, with more than 8000 genes affected. According to gene set enrichment analysis (GSEA), CENP-A overexpression mainly led to the repression of genes involved in cell cycle progression, DNA repair, and RNA metabolism (Fig. 4c, details in Supplementary Data 2). To more specifically identify the key cellular pathways involved in radiosensitivity and its reversal by inactivation of p53, we applied hierarchical clustering to identify co-regulated subsets of differentially expressed genes (DEGs). In particular, we wanted to identify genes for which p53-DN could counteract the effects of CENP-A overexpression. Out of ten clusters (Fig. 4d, see also Supplementary Fig. 2C), there was only one that corresponded to these criteria (cluster 8). This subset of genes is strongly downregulated by CENP-A overexpression and upregulated by p53-DN (Fig. 4e). Importantly, this upregulation is further increased after X-irradiation and these effects are significant even at the lower dose of CENP-A overexpression (see Supplementary Data 2 for significance testing). Furthermore, we verified whether the effect of CENP-A overexpression on these genes also extends to cancer cell lines with different genetic backgrounds. We performed reverse transcription quantitative PCR of selected cluster 8 genes after CENP-A overexpression in the p53-WT HCT116 and p53-defective DLD1 colon cancer cell lines for comparison. CENP-A overexpression decreased the relative expression of this group of genes in the p53-WT HCT116 cell line, and had a

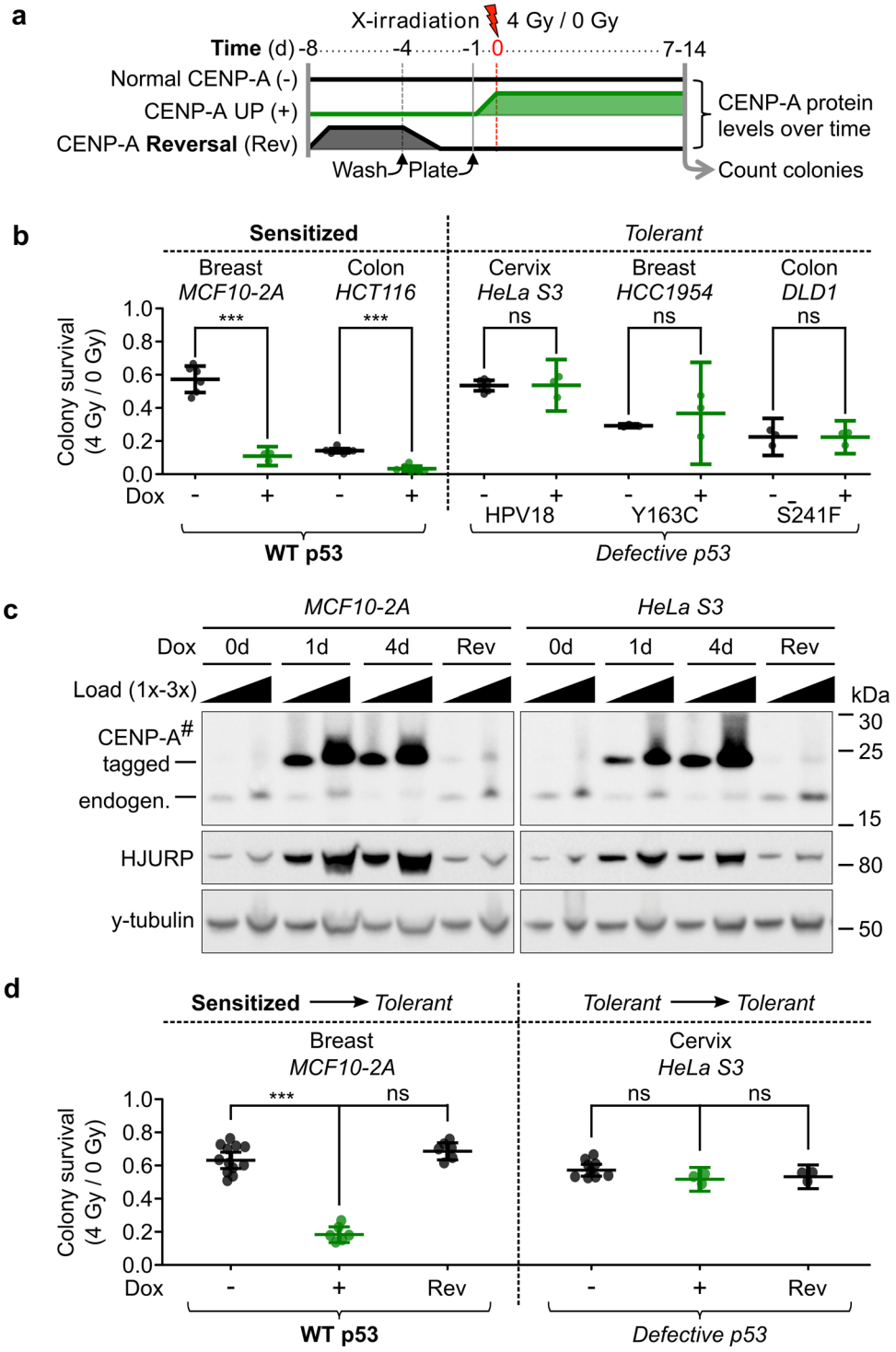
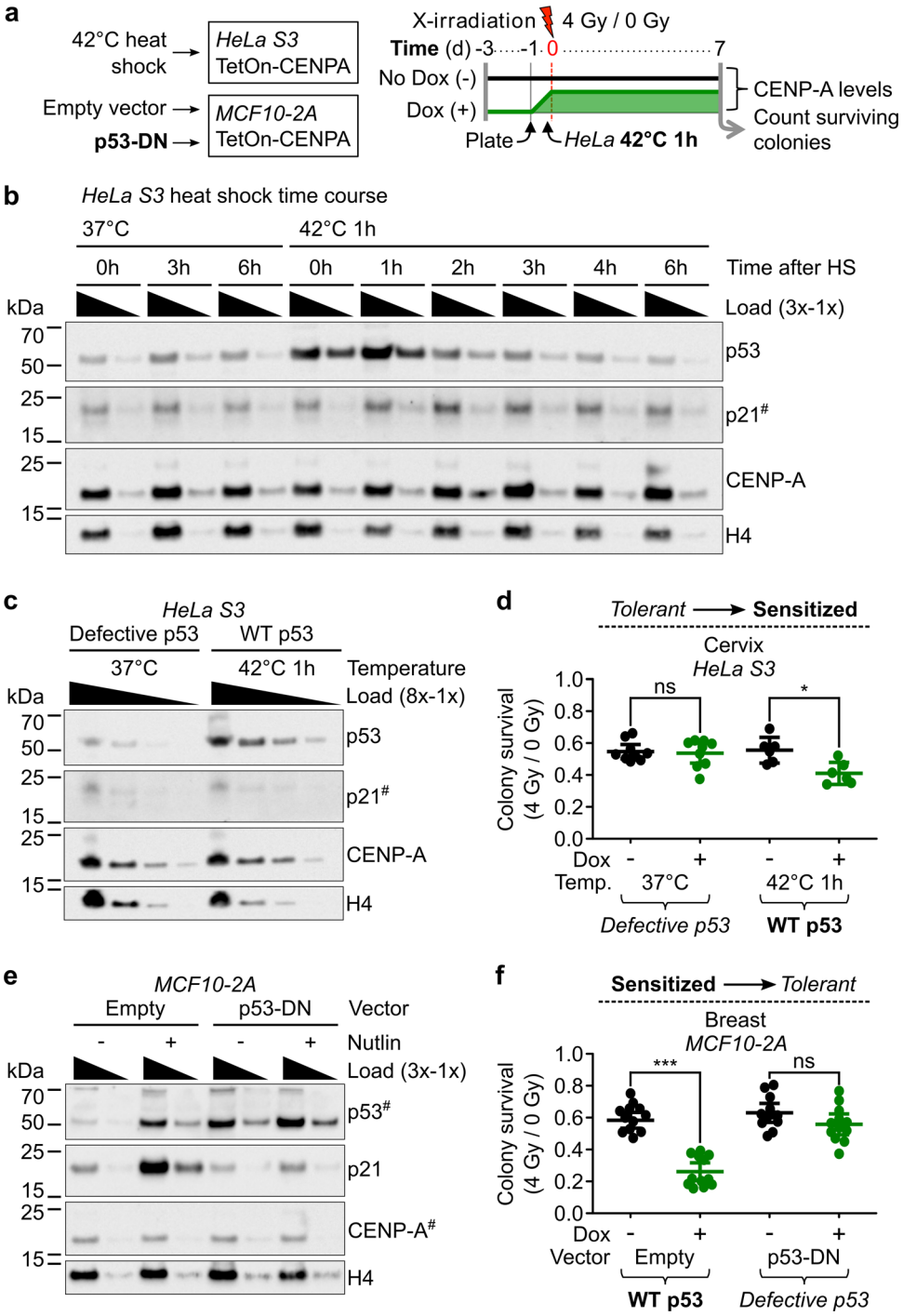


Fig. 2 Induced CENP-A overexpression causes reversible radiosensitivity in p53 wild-type cells. a Scheme of colony formation assays (CFAs) with relative CENP-A protein levels over time for *TetOn-CENPA* cell lines. **b** CFA results corresponding to the scheme in (**a**) for five different cell lines of varied tissue origins and p53 status, as indicated. Each dot represents a single biological replicate. Plots show mean and 95% confidence interval. Statistical significance tested by two-tailed Welch's *t* test with Bonferroni cutoff at a *p* value of 0.01 ($\alpha = 0.05$). *** = *p* value < 0.0001. See also Supplementary Fig. 1C for survival ratios relative to untreated condition. **c** Western blot corresponding to scheme in (**a**): TCEs after 1 day (1d) or 4d with 10 ng/ml Dox, no Dox control (0d), or 4d Dox followed by 4d without Dox (Rev). Primary antibodies indicated on the left. 1x load = ~30,000 cells. # = high sensitivity ECL exposure. y-tubulin used as loading control. **d** CFA results corresponding to scheme in (**a**) for the indicated cell lines. Plots as in (**b**). Statistical significance tested by two-tailed Welch's *t* test, compared to non-induced control, with Bonferroni cutoff at a *p* value of 0.0125 ($\alpha = 0.05$). *** = *p* value < 0.0001.



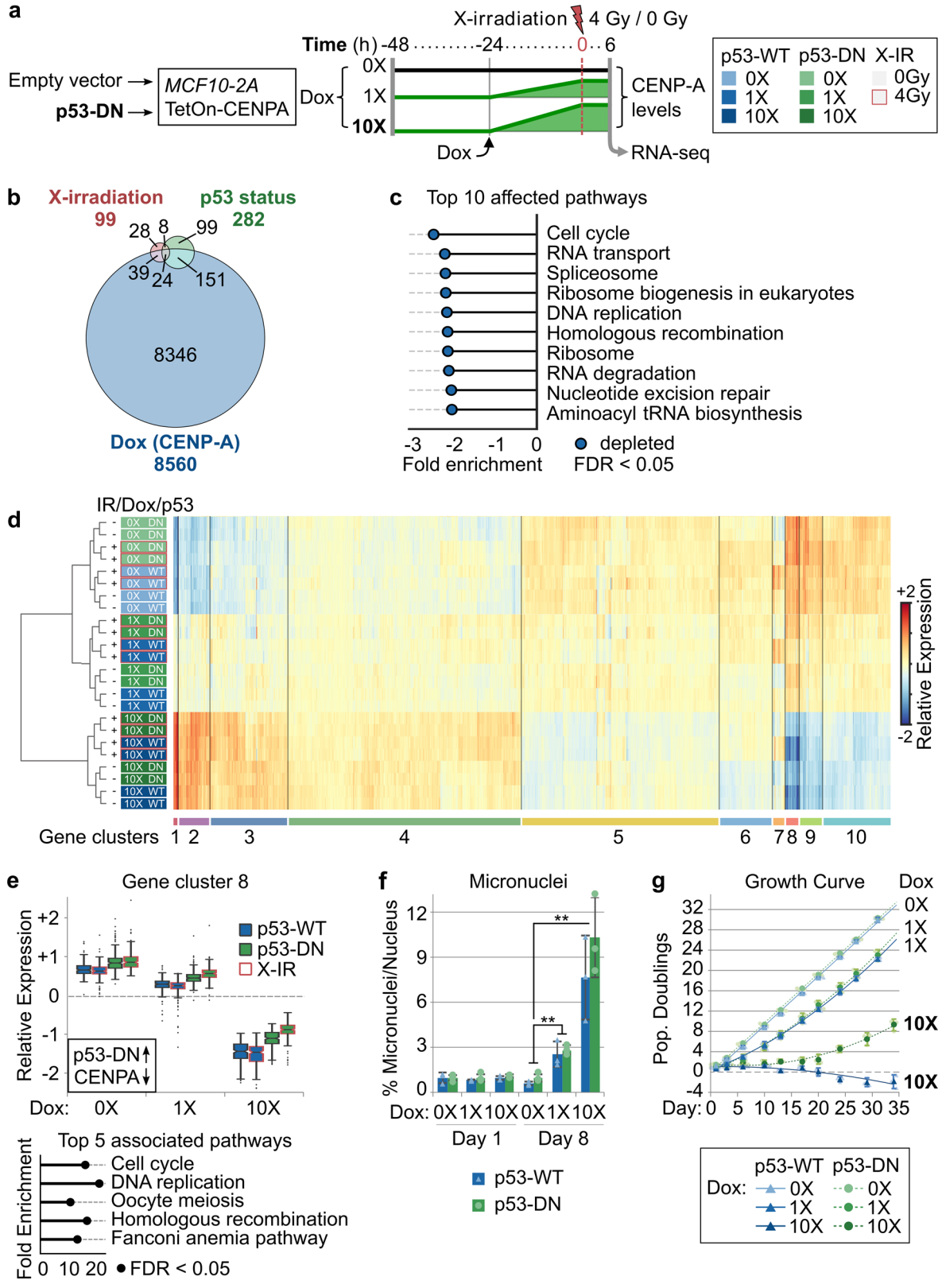
somewhat reduced effect in the p53-defective DLD1 cells (Supplementary Fig. 2D). The fact that these data are consistent with the effects observed in MCF10-2A p53-WT and p53-DN cells further emphasizes the importance of this core set of genes. Overrepresentation analysis (ORA) shows that these genes are mainly involved in cell cycle control, followed by DNA repair (Fig. 4e, bottom). We then used cellular assays to investigate the effects of CENP-A overexpression and p53 inactivation on these two pathways. Concerning DNA repair, we did not detect significant changes in either acute DNA damage or rate of DNA repair (Supplementary Fig. 3A–D). However, on a longer timescale, we observed an increase in mitotic stress associated with CENP-A overexpression that was similar in both p53-WT and p53-DN cells (micronuclei in Fig. 4f, and CIN in Supplementary Fig. 3E, including numerical and structural aneuploidy by multicolor fluorescence in situ hybridization (mFISH) karyotypes). This is in agreement with previous studies[30,50]. In the p53-WT cells, this mitotic stress was associated with p53 activation, as shown by western blot (Supplementary Fig. 3F). As for cell cycle control, CENP-A overexpression leads to prolonged growth inhibition, even in the absence of irradiation (Fig. 4g). This is consistent with the reduced colony size and colony density visible in the CFA stains (Supplementary Fig. 1D). Importantly, this growth inhibition is amplified with increased Dox and is partially counteracted by p53-DN (Fig. 4g, see also Supplementary Fig. 3G for control). These findings enabled us to discard a major role for DNA damage or repair in the radiosensitivity phenotype. Therefore, based on both the bulk RNA-seq data and cellular

Fig. 3 Sensitivity to X-irradiation upon CENP-A overexpression is dependent on functional p53. a Scheme of colony formation assays (CFAs) and change of p53 status with relative CENP-A protein levels over time for *TetOn-CENPA-FLAG-HA* cell lines. WT p53 is transiently activated in HeLa cells by a short heat shock, while p53 is stably inactivated in MCF10-2A cells by expression of a p53 dominant-negative peptide (p53-DN). **b** Temporary change of p53 status in HeLa cells by 1 h heat shock (HS). Western blot of HeLa cell TCEs at indicated time points following 1 h at 42 or 37 °C control. Temporary increase of p53 and subsequently p21. 1x load = ~33,000 cells. Primary antibodies are indicated on the right. # = high sensitivity ECL exposure. H4 used as loading control. **c** Increase of p53 levels in HeLa cells by heat shock. Western blot of TCEs after 1 h at 42 or 37 °C control. Loaded at 8x, 4x, 2x, 1x concentrations, where 1x load = ~12,500 cells. Primary antibodies are indicated on the right. # = high sensitivity ECL exposure. H4 used as loading control. Representative western blot from three independent experiments is shown. **d** HeLa S3 CFAs pertaining to scheme in (**a**). Each dot represents a single biological replicate. Plots show mean and 95% confidence interval. Statistical significance tested by two-tailed Welch's *t* test with Bonferroni cutoff at a *p* value of 0.0125 ($\alpha = 0.05$). * = *p* value < 0.01. **e** Change of p53 status in *MCF10-2A TetOn-CENPA-FLAG-HA* cells. Western blot of TCEs after 24 h of 10 μM Nutlin-3 treatment or DMSO control, as indicated. Dominant negative p53 peptide stabilizes p53 and suppresses its activation of p21. 1x load corresponds to total protein extract from ~30,000 cells. Primary antibodies are indicated on the right. # = high sensitivity ECL exposure. H4 used as loading control. Representative western blot from three independent experiments is shown. **f** MCF10-2A CFAs pertaining to scheme in (**a**). Each dot represents a single biological replicate. Plots show mean and 95% confidence interval. Statistical significance tested by two-tailed Welch's *t* test with Bonferroni cutoff at a *p* value of 0.0125 ($\alpha = 0.05$). *** = *p* value < 0.0001. See also Supplementary Fig. 1C, D for CFAs following range of Dox and X-irradiation doses and Supplementary Fig. 1E for representative CFA images.

assays, we conclude that induced CENP-A overexpression leads to p53-dependent radiosensitivity mainly by impairing cell cycle progression. We then wished to understand how this was operating at the level of individual cells.

CENP-A overexpression promotes acute cell cycle arrest and senescence in p53-WT cells. To determine the effects of CENP-A overexpression and p53 status on individual cell fate and evolution of the cell population over time, we performed single-cell RNA-sequencing (scRNA-seq), a powerful tool for characterizing cell state and identity[51]. Using our p53-WT and p53-DN MCF10-2A cells, we compared prolonged, continuous CENP-A overexpression (chronic induction for 69 days), to acute CENP-A overexpression (1 day) and non-overexpressing conditions, passaged in parallel (see scheme in Fig. 5a). Given that gene expression changes were detectable even at low doses of Dox (Fig. 4d and Supplementary Data 2), we chose this condition to avoid the cytotoxic effects of higher doses (Fig. 4f and Supplementary Fig. 1D). First, we confirmed the chronic overexpression of CENP-A by western blot (Supplementary Fig. 4A) and verified that the scRNA-seq data agreed with the bulk RNA-seq data from comparable samples (Supplementary Fig. 4B). Principle component analysis of the single-cell expression profiles revealed that most of the cell-to-cell variability across conditions could be attributed to cell cycle differences (Fig. 5b). Indeed, with the scRNA-seq data we could identify distinct subpopulations of cycling and non-cycling cells, and further distinguish G2/M and G1/S cells within the cycling cluster (Fig. 5c). Both acute and chronic CENP-A overexpression in the p53-WT cells caused a clear shift in the proportion of cycling to non-cycling cells, a shift that was substantially reduced in the p53-DN cells (Fig. 5d, e). We confirmed these findings by a direct classical analysis of cell cycle using propidium iodide FACS (Supplementary Fig. 4D). Interestingly, we found that the non-cycling populations in the scRNA-seq experiments displayed a striking downregulation of the genes corresponding to cluster 8 in the bulk RNA-seq analysis (Supplementary Fig. 4C), the subset of genes identified as critical for the radiosensitivity phenotype. Given the well-documented role of p53 in senescence[52,53], we also confirmed that the non-cycling scRNA-seq cluster was consistent with a senescence gene expression signature (Fig. 5f). We thus tested the impact of p53 status and prolonged CENP-A overexpression on cell senescence using Beta-galactosidase senescence assays (Fig. 5g). p53-WT cells showed on average ~19% senescence after 13 days of chronic CENP-A overexpression, compared to <3% in the non-induced control. Meanwhile, p53-DN cells showed approximately half the levels of senescence (~8% and ~1%, respectively). This is consistent with the non-cycling ratios for p53-WT and p53-DN cells in the scRNA-seq data and shows a significant impact on senescence from p53 status. Taken together, our results reveal that CENP-A overexpression causes a clear shift in cell state, promoting acute cell cycle exit and senescence in p53-WT cells that is severely reduced when p53 is defective.

CENP-A overexpression promotes epithelial–mesenchymal transition in p53-defective cells. Next, we explored if CENP-A overexpression also impacts cell identity in the different p53 contexts. To do this, we investigated cell fate trajectories across all conditions by estimating transcriptional kinetics based on RNA velocity[54]. In line with Fig. 5, the main trajectory inferred from RNA velocities is the transition of cycling cells to a terminal non-cycling state (see velocity flow and latent time gradient in Fig. 6a). At the same time, we noticed that a minority of cycling cells follows an alternative trajectory converging to a distinct terminal state. This corresponds to a smaller subpopulation comprising both cycling and non-cycling cells. By computing the RNA velocity separately for each condition, we revealed that the main directional flow upon CENP-A overexpression in p53-WT cells is associated with the cell cycle exit trajectory, whereas the alternative cell fate trajectory is mainly followed by p53-DN cells under prolonged CENP-A overexpression. This suggests that CENP-A overexpression in p53-DN cells leads to an alternative cell fate different from cell cycle exit, underlying the emergence of a distinct subpopulation of terminal cells. We thus identified the main clusters of cells after adjusting for cell cycle effects (Supplementary Fig. 5A) and characterized the specific markers associated to each cluster (Supplementary Data 3). The largest clusters corresponded to distinct subpopulations of epithelial cells with differences in expression related to cell metabolism (Supplementary Fig. 5B, C). Interestingly, the alternative cell fate trajectory converged instead to a smaller cluster of cells that were negative for epithelial markers. This cluster showed high expression of mesenchymal genes and broad upregulation of genes involved in EMT (Fig. 6b, c, see also Supplementary Data 3 and Supplementary Fig. 5D). This is consistent with highly advanced EMT or complete mesenchymal transition. The mesenchymal cluster was nearly exclusive to the p53-DN cells (Fig. 6d), consistent with previous studies demonstrating that WT p53 counteracts EMT[55–60]. Remarkably, the highest proportion of mesenchymal cells in the p53-DN condition occurred after chronic CENP-A overexpression, in line with the alternative cell fate trajectory. Given that these cells represent a highly advanced stage of EMT, these findings led us to reexplore our cells for earlier EMT signatures by microscopy. We first noticed that large



groups of cells with mesenchymal-like characteristics (reduced cell–cell contacts, distorted cell shape) could be observed in the p53-DN cells by simple brightfield microscopy as early as 10 days after continuous CENP-A overexpression (Supplementary Fig. 6A). At day 34, we immunostained simultaneously for the classic epithelial marker E-cadherin and the mesenchymal marker vimentin (Fig. 6e), to identify cells in a broad range of early to late stages of EMT[61]. The results revealed a major increase in the EMT population after prolonged CENP-A overexpression, which was again nearly exclusive to our p53-DN cells. Indeed, MCF10-2A cells are known to undergo low levels of spontaneous EMT[62], so it was unclear if this increase in EMT was the result of a stimulation or if CENP-A overexpression—in a p53-defective context—would be sufficient to drive EMT on its

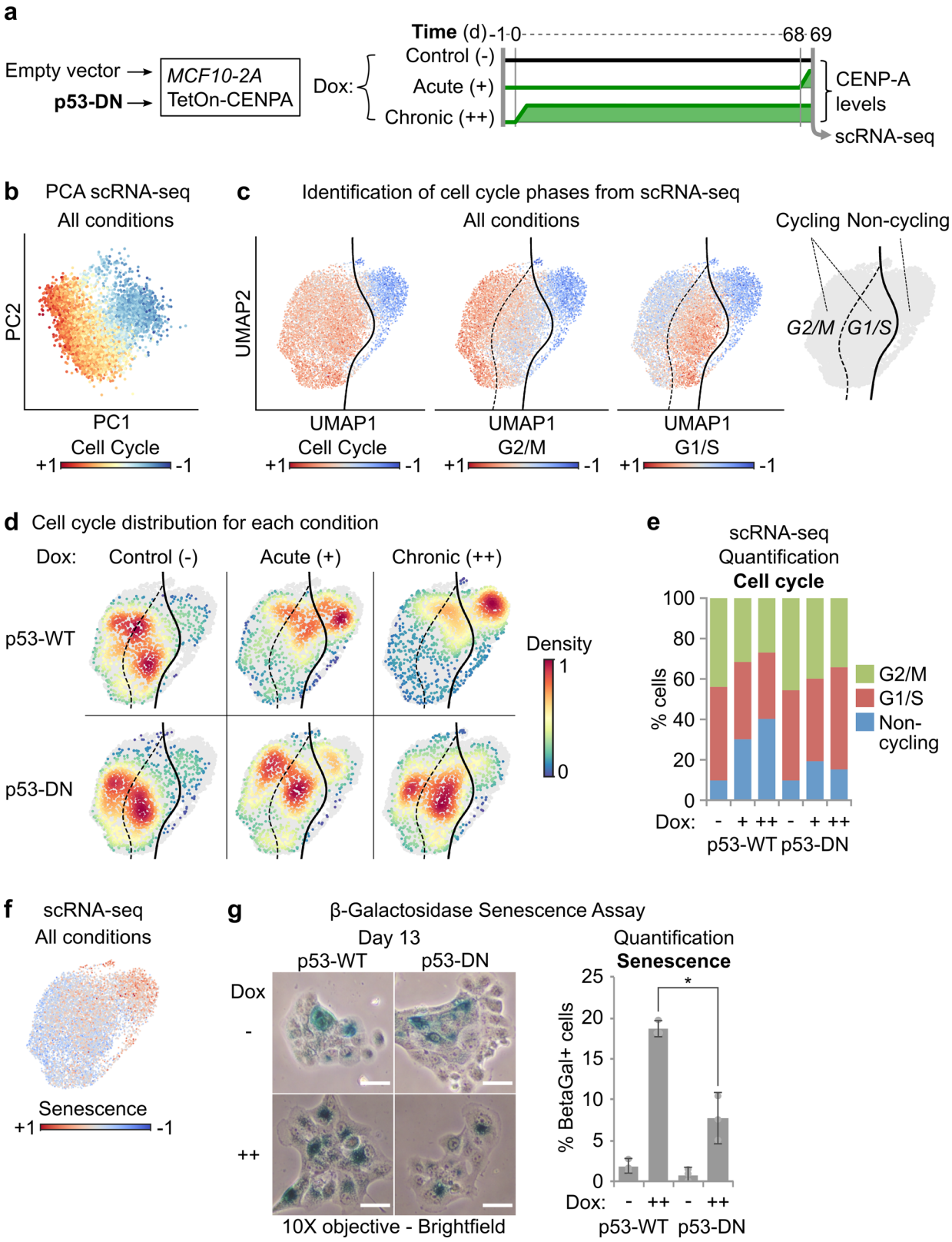
Fig. 4 Induced CENP-A overexpression promotes radiosensitivity by impairing cell cycle progression. a Scheme delineating conditions tested by RNA-sequencing showing relative CENP-A protein levels over time and corresponding legend (pertains to (**d**)). All conditions tested in duplicate. See Supplementary Fig. 1F for CENP-A protein levels corresponding to 0X, 1X (10 ng/ml), and 10X (100 ng/ml) Dox. The transcriptional impact of Dox treatment alone was tested in the non-inducible MCF10-2A parental control (see Supplementary Fig. 2A, B). **b** Proportional Venn diagram summarizing the number of differentially expressed genes (DEGs) upon X-irradiation (red, 0 vs 4 Gy); change of p53 status (green, p53-WT vs p53-DN); and CENP-A overexpression (blue, 0X Dox vs 1X Dox vs 10X Dox). Number of DEGs in each category and overlapping categories is indicated. **c** Gene set enrichment analysis showing the top 10 KEGG pathways affected by CENP-A overexpression (WebGestaltR v0.4.2) and normalized enrichment score. All ten pathways are downregulated with increasing levels of Dox (i.e., significant depletion, at FDR < 0.05). See Supplementary Data 2 (GSEA) for all significantly depleted/enriched processes. **d** Heat map showing hierarchical clustering of samples (rows, colored according to legend in (**a**)) and DEGs (columns), with the ten main gene clusters annotated below. Relative expression: expression relative to the average for a given gene across all conditions (mean-centered counts, $\log_2$ transformed, and TMM normalized). See also Supplementary Data 2 for normalized counts, differential expression analysis, and cluster assignment for all genes and conditions. **e** Top: box plot showing the distribution of expression levels for DEGs in cluster 8 according to experimental condition. Center lines show the medians; box limits indicate the 25th and 75th percentiles; whiskers extend 1.5 times the interquartile range from the 25th and 75th percentiles; outliers represented by dots. See Supplementary Fig. 2C for all gene clusters. Black box: for genes in this cluster, p53-DN increases expression (up arrow) and CENP-A overexpression decreases expression (down arrow). Bottom: top 5 enriched KEGG pathways (WebGestaltR v0.4.2) for genes within cluster 8 based on overrepresentation analysis (ORA). All five terms are significantly overrepresented (FDR < 0.05). See Supplementary Data 2 (ORA) for top 10 pathways for all clusters. **f** Accumulation of micronuclei pertaining to days 1 and 8 of MCF10-2A *TetOn-CENPA-FLAG-HA* cells with either empty vector (p53-WT) or dominant-negative p53 (p53-DN) grown continuously with 0X Dox, 1X Dox (10 ng/ml), or 10X Dox (100 ng/ml). Plots show mean and 95% confidence interval for three biological replicates (triangles/circles) from a single experiment. Statistical significance tested by two-tailed Welch's *t* test with Bonferroni cutoff at a *p* value of 0.01 ($\alpha = 0.05$). No significant differences between p53-WT and p53-DN samples with same Dox treatment. ** = *p* value < 0.001. *N* = > 1000 nuclei per condition for each replicate. **g** Growth curve of MCF10-2A *TetOn-CENPA-FLAG-HA* cells with either empty vector (p53-WT) or dominant-negative p53 (p53-DN) grown continuously with 0X Dox, 1X Dox (10 ng/ml), or 10X Dox (100 ng/ml). Growth curve shows number of population doublings relative to the initial seeding population at day −1. Circles/triangles show mean and 95% confidence interval for three biological replicates (smaller circles/triangles) at each time point where cells were counted. Lines show best-fit curves. Similar results were obtained for a second independent experiment (see Supplementary Fig. 3G for growth curve of the non-inducible parental MCF10-2A cells after Dox exposure).

own. To assess this, we tested chronic CENP-A overexpression in our p53-defective breast epithelial cancer cell line HCC1954, which does not undergo spontaneous EMT[63]. We did not observe the emergence of EMT in the time frame of our investigation (Supplementary Fig. 6B), suggesting that the major increase in EMT observed in the p53-DN MCF10-2A cells was most likely a stimulation rather than an induction. Together, these assays reveal that chronic CENP-A overexpression promotes a reprogramming of cell identity in p53-defective cells, corresponding to a striking EMT in the p53-DN cell population.

Discussion

CENP-A overexpression promotes distinct cell fates depending on p53 status. In this study, we found that CENP-A overexpression promotes radiosensitivity through nongenetic, reversible effects. This is accompanied by major transcriptional reprogramming involving acute cell cycle shutdown and senescence when p53 is active. However, inactivation of p53 suppresses the cell shutdown response, enabling radiotolerance. Strikingly, prolonged CENP-A overexpression also promotes EMT in our p53-DN MCF10-2A cells. Taken together, our findings demonstrate that CENP-A overexpression can promote two distinct cell fates that depend on p53 status: (1) loss of self-renewal capacity and radiosensitivity in p53-WT cells, and (2) reprogramming of cell identity through stimulation of EMT when p53 is defective (Fig. 7). Our work reveals an unanticipated link between a centromeric protein and genome reprogramming with clear implications for tumor evolution. These findings open up exciting avenues for future research and have broad implications for cancer treatment.

Induced CENP-A overexpression alters cell state and global transcription: implications for cancer treatment. Our work shows that at the timescale of one cell division or less, induced CENP-A overexpression in MCF10-2A cells results in major transcriptional reprogramming across the genome. Switching p53 status from WT to defective counteracted a subset of these transcriptional changes, corresponding to cell cycle genes. But, while our scRNA-seq analyses revealed that these effects on cell cycle genes at the population level can be explained by changes in the proportion of arresting cells, how CENP-A overexpression leads to such broad and rapid changes to gene expression across the genome remains an open question. Given that CENP-A overexpression results in its mislocalization and incorporation into chromatin across the chromosome arms, including numerous genic loci[46,47,50,64], we envisage two main scenarios for how CENP-A impacts global transcription: (1) the changes reflect a response to defects induced by CENP-A overexpression and/or, (2) CENP-A incorporation into chromatin directly affects transcription at the sites where it is mislocalized. The idea that ectopic CENP-A could directly affect transcription at genic loci has recently been proposed[36], but remains to be formally assessed. Understanding the underlying mechanisms of these effects could provide important insights into alternative functions of CENP-A and its impact beyond the centromere. On a longer timescale, our scRNA-seq results revealed that prolonged CENP-A overexpression promotes chronic cell cycle arrest in a major proportion of p53-WT cells. Thus, our findings support a model where CENP-A overexpression induces mitotic defects and increases CIN[30], which, in turn, lead to the activation of p53 and senescence[65,66]. In this way, CENP-A overexpression causes a p53-dependent loss of self-renewal capacity. Additional cell stress from DNA damaging agents, like X-irradiation, would add to the mitotic stress associated with CENP-A overexpression. This would then amplify the p53-dependent shutdown of self-renewal, promoting radiosensitivity. Thus, our findings suggest that differences in p53 status may be able to explain why high CENP-A levels are associated with both sensitivity[34,37,39] and resistance[31] to cancer treatments in different patient cohorts. This could have important implications for patient prognosis and treatment strategies. Radiosensitivity associated with high CENP-A levels in p53-WT cancers could represent an opportunity to stratify



patients or minimize radiotherapy dose for equal therapeutic outcome with reduced side effects. Furthermore, alternative treatment options for patients with nonfunctional p53 could also be considered, as drugs combatting mutant p53 (including LOF mutations) are currently in development[67,68]. A number of these drugs are now in clinical trials, including direct reactivators of mutant p53 (e.g., PRIMA-1^{MET}/APR-246) and drugs designed to return functionality to WT p53 by inhibiting its upstream regulators (e.g., MDM2/X inhibitors)[69]. Here, we showed that transiently reactivating p53 in CENP-A overexpressing HeLa cells

Fig. 5 CENP-A overexpression promotes acute cell cycle arrest and senescence in p53-WT cells. a Scheme delineating conditions tested by single-cell RNA-sequencing showing relative CENP-A protein levels over time (pertaining to **b**–**f**, Fig. 6a–d, Supplementary Figs. 4B, C and 5A–D, and Supplementary Data 3). **b** Principal component analysis (PCA) of all scRNA-seq samples, illustrated in (**a**). All conditions merged. Each dot represents a single cell on the first two principal components (PC1 and PC2), colored by expression of cell cycle genes (cell cycle signature includes all genes from Cyclebase v3.0, *CENPA* excluded). **c** Uniform Manifold Approximation and Projection (UMAP) maps of scRNA-seq data, pertaining to scheme in (**a**). All conditions combined. Each dot corresponds to an individual cell projected in a 2D space where the topology reflects global similarities in expression. The color gradient is proportional to the expression of cell cycle, G2/M, and G1/S genes (Cyclebase v3.0). Far right plot: boundary between cycling (G2/M or G1/S) and non-cycling cells in UMAP space computed by support vector classification. **d** Cell density by condition (color gradient) in UMAP space for each scRNA-seq experimental condition, pertaining to scheme in (**a**). **e** Stacked bar plot showing the % of cells in G2/M, G1/S, and non-cycling scRNA-seq clusters for each experimental condition. **f** UMAP of scRNA-seq data as in (**c**) for all conditions merged, colored by expression gradient of senescence-associated genes (Fridman Senescence Up gene set from MSigDB v6.2). **g** Beta-galactosidase senescence assays. Left: representative brightfield images after 13 days of growth without Dox (−) or with chronic Dox (10 ng/ml, ++), taken with a 10X objective. Scale bars = 20 μm. Only cells with dark blue staining were considered senescent. Right: quantification of frequency of senescence, showing mean and 95% confidence interval from a total of three biological replicates (gray circles) across two independent experiments. $N = >100$ cells per condition per replicate. * = two-tailed Welch's *t* test comparing p53-WT to p53-DN after chronic CENP-A overexpression; p value = 0.014.

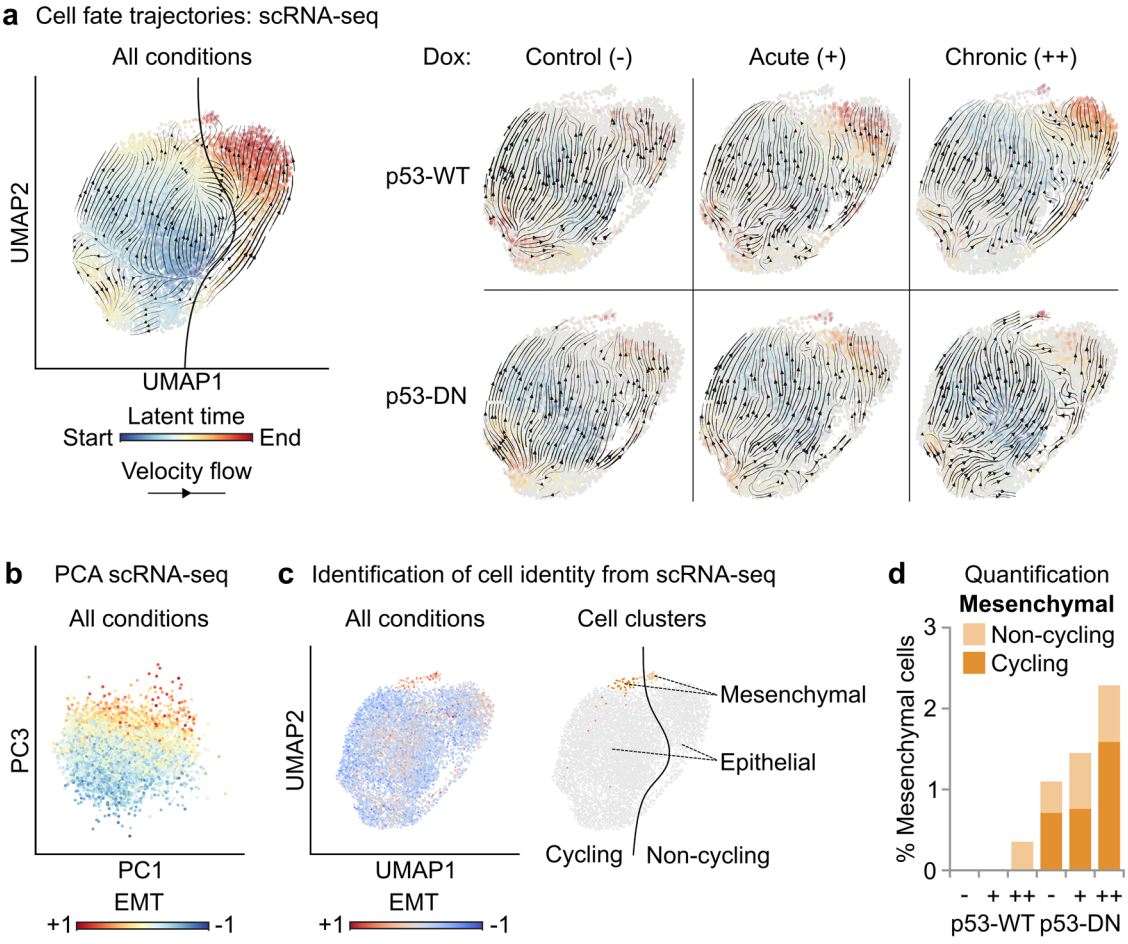
—by a transient, clinically relevant, heat shock—was able to significantly increase sensitivity to X-irradiation. Thus, by returning functional p53 status to tumors with high CENP-A, not only could this induce the anti-tumoral effects of activating p53 alone, but it may also promote radiosensitivity due to the effects of CENP-A overexpression on cell state.

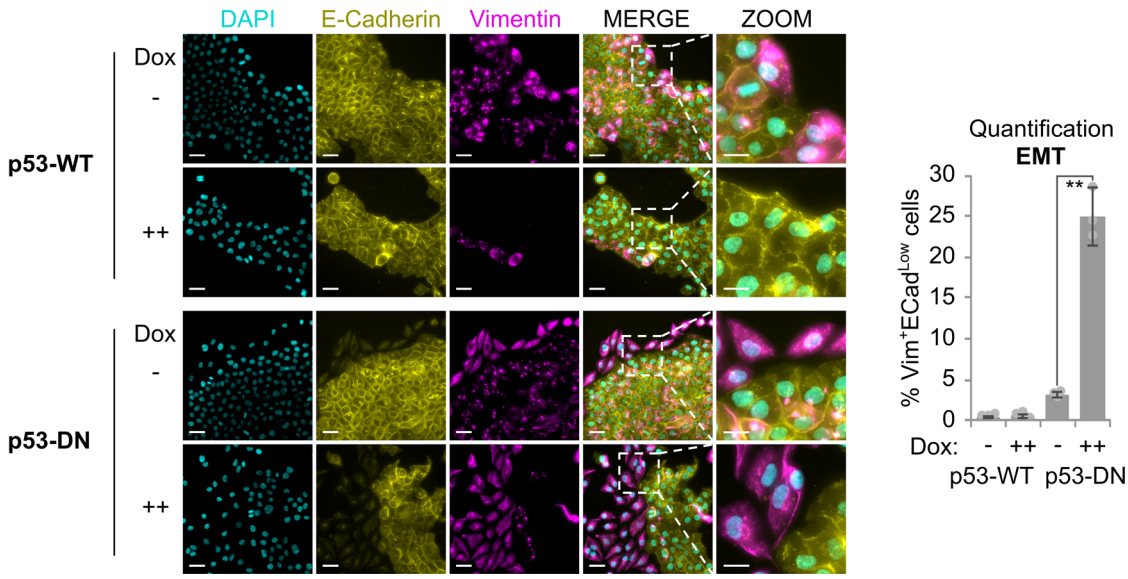
Prolonged CENP-A overexpression and cell identity: implications for stimulating EMT. One of the most surprising findings from our study was the striking stimulation of EMT in p53-DN MCF10-2A cells after prolonged CENP-A overexpression. EMT is a multistage process where epithelial cells, characterized by strong cell–cell junctions and apical–basal polarity, undergo a series of changes to gene expression and morphology to gain a mesenchymal phenotype, including a reorganized cytoskeleton, altered cell shape, and increased cell motility[70]. These changes are highly context dependent, varying substantially among epithelial cells and depending on the factor driving the EMT response[71]. Indeed, the transition to a mesenchymal identity is an essential process during mammalian development, but also occurs aberrantly in epithelial cancers. This can lead to the development of invasive and metastatic properties, with impacts on proliferation, cell plasticity, stemness, and therapeutic resistance[72,73]. In this context, different EMT responses can be driven by distinct signaling pathways, including TGF-β, hypoxia, WNT, and others[74]. In MCF10-2A cells, that spontaneously undergo low levels of EMT[62], we found that CENP-A overexpression strongly favors the EMT response as an alternative fate to cell cycle exit when p53 is inactivated. However, CENP-A overexpression alone was not sufficient to initiate EMT in the p53-defective HCC1954 breast cancer cells, where EMT does not occur spontaneously but can be induced by TGF-β[63]. Investigating whether high levels of CENP-A favor a mesenchymal fate when the EMT response is induced by different pathways is an important avenue of investigation with critical implications for cancer care. Indeed, CENP-A overexpression has previously been linked to invasion and metastasis in human patients[31,33,34,36,37,39], but whether this could involve the stimulation of EMT was not known. Thus, the link with EMT provides a mechanism by which CENP-A overexpression could promote these outcomes in patient tumors that lack functional p53. Evidence linking EMT to the direct inhibition of senescence[75,76], promotion of radioresistance[77–79], and cancer stemness[80] imply that EMT may also play an important role in the evasion of senescence, radiotolerance, and increased clonogenic capacity that we observed in our p53-defective cells. Interestingly, the effect of CENP-A overexpression on EMT also suggests that high CENP-A levels could promote stemness, depending on p53 status. Indeed, human pluripotent stem cells naturally overexpress CENP-A[81,82], and maintain p53 in an inactive state through post-translational regulation[83]. Intriguingly, recent work in Drosophila showed that intestinal stem cells preferentially retain preexisting CENP-A during asymmetric divisions[84], suggesting that CENP-A nucleosomes may epigenetically mark stem cell identity in this system. Furthermore, Drosophila germ line stem cells showed asymmetric distribution of CENP-A during differentiation and CENP-A overexpression could promote self-renewal[85]. Thus, in addition to its effect on EMT, how CENP-A overexpression contributes to stem cell renewal and pluripotency in human cells will be an important avenue for future research. Importantly, as with the effect of CENP-A overexpression on global transcription, which underlying mechanism is at play remains to be deciphered. Since the initiation of EMT is associated with several of the cell stresses that result from mitotic defects, including genotoxic stress[86], replication stress[87], and metabolic stress[88], among others[89–92], they are likely important in the process. Interestingly, a recent report by Gomes et al.[93] demonstrated that the perturbation of the histone H3 variants, H3.1/2 and H3.3, promotes or represses EMT. In particular, knockdown of the H3.1/2-dedicated chaperone CAF-1 caused widespread opening of chromatin, with increased incorporation of H3.3 at the promoters of EMT-inducing transcription factors (e.g., *ZEB1*, *SNAI1*, and *SOX9*), which induced EMT and increased cell migration and invasion. Previously, we found that overexpressed CENP-A hijacks the H3.3-dedicated chaperone Daxx[46]. This results in the mis-incorporation of CENP-A-containing nucleosomes into regions of high histone turnover normally enriched for H3.3. Thus, CENP-A overexpression could have a direct impact on EMT, and transcription in general, through its perturbation of other H3 variants and their dedicated histone chaperones. Deciphering the mechanisms that link CENP-A, EMT, and possibly stemness, will expand our understanding of the direct and indirect molecular consequences of CENP-A overexpression and its impact on tumor evolution.

In conclusion, the interplay of CENP-A overexpression and p53 status alters cell fate, with distinct implications for the role of CENP-A in therapeutic sensitivity, resistance and metastasis.

Methods

Cell lines. See Table 1 for cell lines used. Lenti-X 293T cells (632180) were purchased from Clontech. All other parental human cell lines originally from ATCC: HeLa S3 (CCL-2.2), MCF10-2A (CRL-10781), T47D (HTB-133), HCC1954 (CRL-2338). Inducible CENP-A overexpression DLD1 cells obtained from Daniele Fachinetti (Institut Curie). HeLa S3 and MCF10-2A cell lines were authenticated by STR profiling (Powerplex 16 HS). The other cell lines were not authenticated. All





cell lines tested negative for mycoplasma contamination. No commonly misidentified cell lines were used in this study.

Cell culture and CENP-A overexpression. HCT116, HeLa S3, and DLD1 FRT Fbox (+OSTR1-Myc9)+CENP-A-YFP-AID were cultured with DMEM 10% fetal cow serum (FCS) Pen/Strep 1%; MCF10-2A, 1:1 DMEM:Ham's F12, 20 ng/ml epidermal growth factor, 100 ng/ml cholera toxin, 0.01 mg/ml insulin and 500 ng/ml hydrocortisone, 5% horse serum; HCC1954, RPMI 10% FCS Pen/Strep 1%; Base media from ThermoFisher Scientific. All cell lines tested and confirmed to be mycoplasma free using the Mycoplasma PCR ELISA kit (Sigma). CENP-A overexpression was induced by the addition of Dox to typical growth media at 10 ng/ml (considered 1X), unless otherwise indicated. To maintain overexpression, media and Dox were replaced every 1–3 days. When applicable, the media in the non-induced control was replaced in parallel without Dox. For reversal of CENP-A overexpression, we removed media containing Dox and washed two times with warm PBS then replaced the media without Dox.

Fig. 6 CENP-A overexpression promotes epithelial–mesenchymal transition in p53-defective cells. a Cell fate trajectories inferred by RNA velocity analysis of scRNA-seq samples illustrated in Fig. 5a. RNA velocities estimated by dynamical modeling across all samples are depicted in the left panel by a streamline plot (black arrows) showing the main directional flow across cells (gene-averaged velocity vector field in UMAP embedding from Fig. 5). Each cell is colored by the estimated latent time from initial (blue, start) to terminal states (red, end). Left: RNA velocities calculated across all conditions. Right: RNA velocities calculated separately for each condition by stochastic modeling in individual samples. **b** Principal component analysis (PCA) of scRNA-seq experiments. All conditions merged. Each dot represents a single cell on the first (PC1) and third (PC3) principal components, colored by expression of epithelial–mesenchymal transition genes (EMT; Hallmark gene set, MSigDB v6.2). Cell-to-cell variability along the third principal component can be explained by differences in expression of EMT genes. **c** Classification of epithelial and mesenchymal subpopulations based on Leiden clustering after correcting for cell cycle effects. Left: the color gradient shows, for each cell, the relative expression trend of genes involved in EMT (EMT; Hallmark gene set, MSigDB v6.2) in UMAP space. See also Supplementary Fig. 5D for additional EMT signatures. Right: classification of cells as mesenchymal (EMT high cluster, orange) and epithelial (EMT low clusters, gray), divided as either cycling (dark) or non-cycling (pale), as determined in Fig. 5. **d** Stacked bar plot showing the percentage of cells within the mesenchymal cluster per experimental condition. **e** Assessment of EMT by immunofluorescence after 34 days with (++) or without (−) continuous CENP-A overexpression (10 ng/ml Dox). Left: representative max intensity projections: DAPI (cyan), E-cadherin (yellow, epithelial marker), and vimentin (magenta, mesenchymal marker). Scale bars = 40 µm, Zoom = 20 µm. Right: quantification of the frequency of cells with high vimentin surrounding the nucleus and low/absent E-cadherin on the cell membrane for each condition. Plot shows mean and 95% confidence interval from three biological replicates (gray circles). $N = > 1000$ nuclei per condition per replicate. Similar results were obtained in a second independent experiment. ** = two-tailed Welch's t test comparing control p53-DN to p53-DN after chronic CENP-A overexpression; p value = 0.0002.

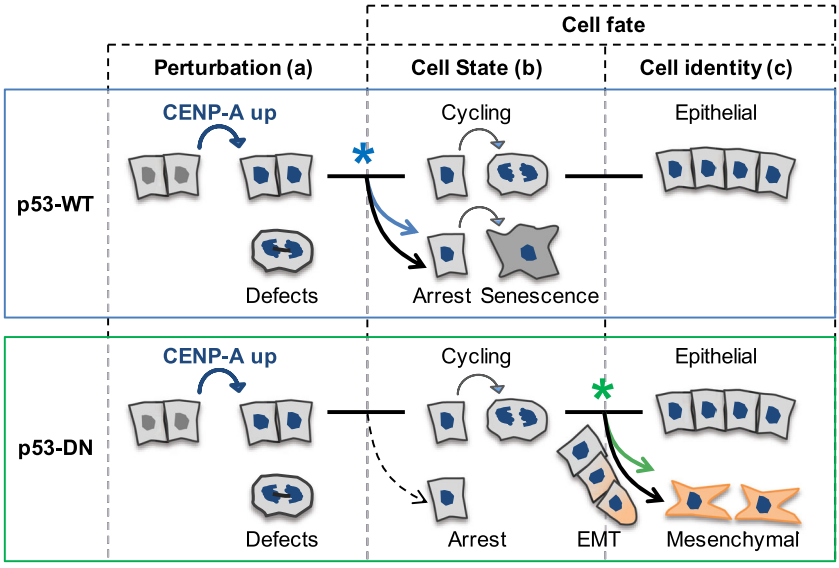


Fig. 7 CENP-A overexpression promotes distinct cell fates depending on p53 status. CENP-A overexpression reprograms cell fate with distinct effects on cell state and cell identity that depend on p53 status. Perturbation (**a**) by CENP-A overexpression (in blue) induces mitotic defects in both wild-type p53 (p53-WT, top panel blue) and p53-defective cells (p53-DN, dominant negative, bottom panel green). These defects provoke distinct cell fate decisions according to p53 status, impacting cell state (**b**) or identity (**c**). When p53 is functional, cell state shifts toward acute cell cycle arrest and senescence, reducing self-renewal capacity. Additional stress, like DNA damage from X-irradiation, amplifies this response, resulting in radiosensitivity. Furthermore, functional p53 ensures the preservation of epithelial identity. In contrast, when p53 is defective, the cells evade arrest and continue cycling, allowing CENP-A overexpression to promote epithelial–mesenchymal transition (EMT). * symbol: reprogramming stimulated by CENP-A overexpression.

Generation of *TetOn-CENPA-FLAG-HA* cell lines. To obtain an inducible CENP-A overexpression system, we sub-cloned *CENPA-FLAG-HA* from the eCENP-A plasmid[46] by PCR (forward primer containing EcoRI site: *CACAGTTAGAATTC**ATG**GGCCCGCGCCG*; reverse primer containing AgeI site: *ATCGAATCACCGGT**CTA**GGCGTAGTCGGGCACGT*) and inserted it into the multiple cloning site of the pLVX-TetOne (ClonTech) plasmid by restriction enzyme digestion with EcoRI and AgeI, followed by ligation. To confirm proper integration and lack of mutation in the *CENPA* gene, we then sequenced the *CENPA-FLAG-HA* pLVX-TetOne plasmid around the insertion site. To encapsulate the construct for transduction, we co-transfected Lenti-X 293T cells (ClonTech) with 10 µg *CENPA-FLAG-HA* pLVX-TetOne and packaging vectors 7.5 µg psPAX2 and 2.5 µg pMD2.G using PolyPlus JetPrime transfection reagent according to manufacturer instructions. Media was replaced 4 h after transfection. For infection and stable integration of the construct without selection, we filtered (0.45 µm) supernatant from the transfected cell flask at 24 and 48 h post transfection, added 8 µg/ml of polybrene to the filtered virus-containing media, and added the media directly to the target cell lines. We removed the virus-containing media after 48 h and grew the cells for at least three passages without virus. Then we tested the polyclonal cell lines for the induction of *CENPA-FLAG-HA* by western and immunofluorescence (IF) of CENP-A and HA following 24 h of treatment with 80 ng/ml of doxycycline. We isolated clonal cell lines by serial dilution to single cells. Then tested 10–20 colonies arising from single cells for *CENPA-FLAG-HA* induction, as before. We selected cell lines for further experimentation if they showed a clear homogenous CENP-A and HA increase by IF in ~100% of cells after doxycycline treatment with no detectable background of HA signal by western or IF when no doxycycline was added.

Change of p53 status. For the p53-WT and p53-DN MCF10-2A cells, we transduced empty vector pWZL Hygro (Scott Lowe, Addgene plasmid #18750) or vector containing the DN *TP53* construct (pBABE-hygro p53DD, Bob Weinberg, Addgene plasmid #9058) into the clonal MCF10-2A *TetOn-CENPA-FLAG-HA* cell line by lentiviral transduction, as above. Cells were selected with hygromycin for >14 days and then passaged in typical media. For heat shock of HeLa S3 *TetOn-CENPA-FLAG-HA cells*, we performed a 1 h 42 °C heat shock on non-induced HeLa *TetOn-CENPA-FLAG-HA* cells and examined total cell extracts by western blotting at various time points following heat shock. Two parallel sets of cells were grown under normal conditions at 37 °C. One set was moved to a 42 °C incubator, while the other remained at 37 °C as a control. After 1 h, we harvested cells for total cell extraction from each condition (time 0 h), then returned both sets to 37 °C.

We then harvested cells for total cell extraction at the indicated times after heat shock (1–4 or 6 h: time after HS).

Total cell extracts (TCEs). We harvested cells by trypsin, counted cells by Beckman Automated Cell Counter, and spun down at 300 g, 5 min, washed 1X in PBS, spun again, aspirated PBS, and froze pellets at −20 °C. Cell pellets were incubated for 15 min at room temperature with 300 µl per 1 million cells of 1.2X LDS Sample Buffer (NuPAGE) containing 1.2X Sample Reducing Agent (NuPAGE) and 125 kU/ml Pierce Universal Nuclease Buffer for Cell Lysis, then heated at 95 °C for 10 min, vortexed, spun down, and cooled briefly on ice prior to western blotting.

Western blotting. Total cell extracts were loaded at one to four different concentrations, as indicated, onto premade NuPAGE Bis-Tris 4–12% gradient gels in an XCell 4 Sure-Lock SDS-PAGE chamber with 1X NuPAGE MES SDS Running Buffer, with a PageRuler (ThermoFisher Scientific) molecular weight marker. Gels were run at 130–150 v for 1 h to 1 h15 min. We transferred protein to a 0.2 µm nitrocellulose membrane by BioRad Trans-Blot Turbo, mixed-molecular weight setting, or semi-dry transfer (BioRad, 15 v, 1.5 h). Membranes were stained with Pierce reversible protein stain to detect bulk protein and assess quality of transfer, then cut, blocked in 5% milk-PBST (0.1% Tween-20) for 1 h, RT, and incubated overnight with rocking at 4 °C with primary antibodies in 5% milk-PBST containing 0.02% sodium azide. Membranes were washed 3X 10 min in PBST, then incubated 1 h (RT) with horseradish peroxidase secondary antibodies in 5% milk-PBST, washed 3 × 10 min in PBST and exposed with SuperSignal West Pico Chemiluminescent Reagent or, for high sensitivity exposures, SuperSignal West Femto Maximum Sensitivity Reagent, and imaged using a ChemiDoc Touch system and ImageLab software. See Supplementary Figs. 7–10 for all uncropped blots. Primary antibodies: CENP-A 1:500 (2186 Cell Signaling Technology (CST)), H4-pan 1:2500 (05-858, Sigma-Aldrich), HJURP 1:300 (HPA008436 Sigma-Aldrich), γTubulin 1:10000 (T5326 Sigma-Aldrich), p53 (1C12) 1:1000 (2524 CST), p21 1:500 (556431 BD Pharmingen), phospho-p53 (Ser15) 1:500 (9284 CST). Secondary antibodies:Jackson ImmunoResearch, 1:10000, donkey anti-mouse or donkey anti-rabbit.

Immunofluorescence (IF). Glass coverslips were coated with collagen (1 µg/ml) + fibronectin (1 µg/ml) in PBS, 30 min, RT, washed in PBS and added to culture dishes prior to cell seeding. After at least 24 h of growth, coverslips were washed 3X with PBS, fixed with 2% PFA, 20 min, RT, washed 3X PBS, incubated 5 min with 0.3% Triton-X 100 in PBS, washed 3X PBS, blocked in filter-sterilized 5% BSA-PBST (0.1% Tween-20) for 20–30 min, RT, and incubated 1–1.5 h, RT, with primary antibodies in 5% BSA-PBST. Coverslips were then washed 3X 5 min in 5% BSA-PBST, and incubated 30 min with secondary antibody in 5% BSA-PBST, RT, in darkness. DAPI was added directly to secondary antibody solution (final concentration 1/4000) and incubated in darkness, RT, 5 min, followed by 3X PBS wash. Coverslips were inverted onto microscope slides with ~10 µl of VectaShield and imaged with a Zeiss Axiovert Z1 microscope or Inverted Widefield Deltavision Core Microscope (Applied Precision) with CoolSNAP HQ2 camera, using MetaMorph (Zeiss microscope) or Softworx (Deltavision microscope) software. Sample sizes for microscopy quantifications were determined according to the number of countable cells within at least three different fields per replicate. More fields were imaged if fewer cells were present than average. Image analysis performed with ImageJ software. Primary antibodies: CENP-A (3-19) 1:300 (ADI-KAM-CC006-E Enzo Life Sciences), E-cadherin (24E10) 1:200 (3195S CST), γH2AX 1:250 (2577 CST), vimentin (N-term) 1:100 (5741S Progen). Secondary antibodies: 1:1000 Alexa Fluor donkey anti-mouse IgG (H + L) 488, 1:1000 Alexa Fluor goat anti-rabbit IgG (H + L) 488 or 594, 1:1000 Alexa Fluor goat anti-Guinea Pig IgG (H + L) 594.

Colony formation assays (CFAs). At day −1, cells are trypsinized and diluted to single-cell level (300–600 cells per well, in triplicate) in six-well plates. At day 0, one set of cells is irradiated by CIXD Dual Irradiator or Philips X-ray tube X-ray generator (4 Gy, unless otherwise indicated), while a control set remains unirradiated (0 Gy). When the cells have had sufficient time to form visible colonies, depending on their typical speed of growth (7–14 days), they are washed gently with PBS, stained with 1% Crystal Violet 20% Ethanol solution for 15 min, washed with water, allowed to dry, scanned and counted by eye from the acquired images with the counter blinded to the conditions. Unless otherwise indicated, ratio of surviving colonies is calculated as the number of colonies formed after 4 Gy of X-irradiation divided by the number of colonies formed when not irradiated. Cells are considered sensitized to irradiation by CENP-A overexpression when the CENP-A overexpression condition has a significantly lower survival ratio compared to the non-induced control. Cells are considered tolerant to CENP-A overexpression if the survival ratio is not significantly affected by the CENP-A overexpression. See Supplementary Data 1 for all counts and calculations.

Bulk RNA-seq. Sample preparation: we grew MCF10-2A *TetOn-CENPA-FLAG-HA* cells expressing either empty vector (p53-WT) or dominant-negative p53 (p53-DN) with 0X Dox (no Dox), 1X Dox (10 ng/ml), or 10X Dox (100 ng/m) for 24 h. At time 0, we irradiated one set of cells by X-ray generator (4 Gy), while a control set remained unirradiated (0 Gy). Six hours later, we extracted RNA for RNA-seq. All conditions tested in duplicate. We extracted RNA directly from culture dishes using the Qiagen RNeasy Mini kit according to the manufacturer's instructions and confirmed the quality and quantity of the RNA by TapeStation and NanoDrop. mRNA library preparation and sequencing were performed by the next-generation sequencing (NGS) platform, Institut Curie, using the Illumina TruSeq Stranded mRNA kit and NovaSeq 6000 sequencer. Library preparation and sequencing of irradiated and nonirradiated samples were performed on different dates, with a single repeat of one sample included for batch correction.

Bulk RNA-seq analysis. Reads were aligned to the human reference genome (GRCh38 assembly) based on Ensembl gene annotation (release 95) with hisat2 (version 2.1.0[94]), run in paired-end mode with default parameters. Gene-level counts were computed from primary alignments with MAPQ > 2 using featureCounts (Subread package version 1.6.3[95]) in paired-end mode with the -s 2 option for reverse-stranded libraries. Raw counts were normalized for differences in library size (counts per million) and across samples (via trimmed mean of *M* values normalization, TMM) using edgeR (version 3.28.0[96]). Differential expression analyses were performed with edgeR[97]. We assessed the stand-alone and combined response to each treatment (CENP-A overexpression at increasing Dox concentrations, p53-DN, and X-irradiation) by fitting a quasi-likelihood negative binomial generalized log-linear model (GLM), including both additive and synergistic effects for all treatment combinations. A batch coefficient was also included to account for potential batch effects. Full details about the variable encoding and GLM formulation are provided in Supplementary Data 2 (sheet 1). The effect of each treatment, both stand-alone and combined, was evaluated via quasi-likelihood *F*-test on the respective GLM coefficient, followed by multiple testing correction via the Benjamini–Hochberg method (Supplementary Data 2, sheet 2). A false discovery rate (FDR) cut-off of 0.05 was used to identify DEGs. For proportional Venn diagrams, we only considered DEGs that change with CENP-A overexpression, p53 status or X-irradiation, since we could not detect significant interaction effects for most treatment combinations (Supplementary Data 2, sheet 2). Mean-centered TMM-normalized counts were used for PCA and hierarchical clustering analyses via Ward's variance minimization method (Supplementary Data 2, sheets 3 and 4). For hierarchical clustering, we tested the combined effect of all coefficients, excluding batch, and included any DEG showing significant differences relative to baseline at 0.05 FDR. Functional enrichment analyses for KEGG pathways were carried out using the WebGestaltR package (version 0.4.2[98]). GSEA for CENP-A effects were performed on all expressed genes ranked by fold change and *p* value upon overexpression, i.e., $\log_2$ fold change $*-\log_{10}$ *p* value of the Dox coefficient (Supplementary Data 2, sheets 5 and 6). Pathways associated to specific gene clusters were identified by ORA after hierarchical clustering of all DEGs via Ward's method (Supplementary Data 2, sheets 7 and 8). Coordinated changes in expression within DEG clusters were evaluated by assessing the distribution of mean-centered expression values (averaged per condition) for all genes in a given cluster. For genes in cluster 8, we fit a linear mixed model (LMM) to estimate the fixed effects of p53 inactivation and X-irradiation at each level of Dox (relative to nonirradiated p53-WT samples), with a varying intercept for each gene. We similarly estimated the effect of CENP-A overexpression at increasing levels of Dox by fitting a separate LMM across all conditions. The LMM formulation, model estimates, and pairwise comparisons by *F*-test are reported in Supplementary Data 2 (sheets 9 and 10), along with adjusted *p* values after Bonferroni correction. Bulk RNA-seq analyses were carried out with custom Python scripts. pandas (version 0.24.2), NumPy (version 1.16.2), SciPy (version 1.3.1), statsmodels (version 0.10.1) and scikit-learn (version 0.21.3) libraries were used for data manipulation, statistical analysis, and unsupervised learning. matplotlib (version 2.2.4), matplotlib-venn (version 0.11.5), and seaborn (version 0.9.0) were used for plotting and statistical data visualization. R packages were imported into Python using rpy2 (version 2.8.4).

Reverse transcription quantitative PCR (RT-qPCR). We cultured two replicates for each cell type and condition in separate 60 mm dishes for 1 day in typical media, then added 0, 10, or 100 ng/ml Dox for 24 h. We extracted RNA directly from plates using the Qiagen RNeasy Mini kit with in-column DNase I treatment, according to the manufacturer's instructions. RNA concentrations were quantified by NanoDrop and diluted to 125 ng/µl and confirmed by NanoDrop. To obtain cDNA, we then performed reverse transcription PCR on 1000 ng of RNA for each sample using the SuperScript III First-Strand Synthesis SuperMix kit, according to the manufacturer's instructions. We performed quantitative PCR using Power SYBR Green qPCR master mix with three technical replicates in 384-well plates using the QuantStudio 5 Real-Time PCR System. Relative expression was calculated subtracting Ct for each gene of interest from the Ct for *PPIA* for each technical replicate (ΔCt) and took the mean ΔCt. For normalization, we then subtracted the mean across biological replicates of the p53-WT 0X condition for each gene of interest (ΔΔCt). Relative expression was then calculated as the fold change of ΔΔCt ($2^{\Delta\Delta Ct}$) for each biological replicate. See Supplementary Data 1 for Cts and calculations. Primers used were as follows (desalt): CDC20 F e8/9 *GGGCTGTCAAGGCCGTAG*, CDC20 R e10 *GACCAGAGGATGGAGCACAC*; MCM2 F e8/9 *TTGACAAGATGAATGACCAGGAC*, MCM2 R e10 *GAGAAAGTC*

AGCGAGGGGTC; AURKB F e1/2 *TTGGACCCCAGCTCTCCTC*, AURKB R e3 *GACAAGTGCAGATGGGGTGA*; NDC80 F e4 *GTGCCGACAGCTTTGATGAG*, NDC80 R e5/6 *ACGACTCTAGACGATTCGGTTC*; PLK1 F e6/7 *GTCAGGCAAG AGGAGGCTG*, PLK1 R e8 *TCATTGAAGAGCACCCCCAC*.

Comet assays. Prior to irradiation, cells were harvested and submerged into media containing low-melting agarose on ice. When hardened, cells were exposed to the indicated dose of γ-irradiation (GSR D1 gamma ray). Either immediately, or at the indicated times postirradiation, the cells in the gel were submerged in alkaline solution and run by gel electrophoresis to form comets to visualize the levels of DNA damage. Comet assays were performed by the RadExP platform, Institut Curie, according to the Trevigen Single Cell Electrophoresis Assay alkaline comet protocol. Automatic counting and measuring of comets on Trevigen slides (two wells used for each condition, per experiment), imaged using the Metafer system with the "comet" module from MetaSystems. See Supplementary Data 1 for mean Olive Tail Moment per condition for each experiment and calculations.

Micronuclei. We seeded cells into dishes containing collagen/fibronectin-coated glass coverslips 48 h prior to fixation, added indicated concentrations of Dox, and allowed the cells to grow for 24 h (day 1) or passed cells and replaced Dox every 2–3 days until day 8. Cells were fixed, prepared for IF, and nuclei were imaged with a Zeiss Z1 inverted microscope using a 10X objective. We counted micronuclei using a custom ImageJ macro with at least three fields and >1000 nuclei counted per condition. See Supplementary Data 1 for all counts and calculations.

Multicolor fluorescence in situ hybridization (mFISH) karyotyping. Cells were grown with or without 10 ng/ml Dox for 15 days, then treated with colcemid (100 ng/ml, Roche) for 1.5 h and prepared as previously described for mFISH (MetaSystems) staining[99]. Briefly, mitotic cells were collected by mitotic shake-off after a short trypsin treatment and centrifuged at 1000 rpm for 10 min. Cell pellets were resuspended in 75 mM KCl and incubated for 15 min in a 37 °C waterbath. Carnoy fixative solution (methanol/acetic acid, 3:1) was prepared and 1:10 volume added on the cells, before centrifugation at 1000 rpm for 15 min. Cells were then fixed 30 min at room temperature in the Carnoy solution, centrifuged and washed once more with fixative. Minimum volume of fixative was left to resuspend the pellet and cells were dropped onto clean glass slides. mFISH staining was performed following manufacturer's instructions (MetaSystems). The Metafer imaging platform (MetaSystems) and the Isis software were used for automated acquisition of the chromosome spread and mFISH image analysis. Chromosome rearrangements and specific chromosome counts for each spread were assessed and counted by eye from the automated chromosome spread images, with the researchers blinded to the conditions. Losses and gains of chromosomes per cell were calculated as the sum of the absolute difference from the mode for each chromosome of the p53-WT no Dox control. New chromosome rearrangements per cell were determined as the total number of structural chromosomal anomalies observed per spread, excluding the ones that were common to most or all p53-WT no Dox spreads. Potential acrocentric fusions were not considered in our study. See Supplementary Data 1 for all counts and calculations.

Growth curve/proliferation assays. Cells that had never been exposed to Dox were trypsinized, counted using a Beckman Automated Cell Counter, and seeded into nine culture dishes with equivalent cell numbers (corresponds to MCF10-2A non-inducible control, plus the p53-WT and p53-DN TetOn-CENP-A-FLAG-HA cell lines, at three Dox concentrations each, all grown in parallel). The next day (day 0), Dox was added in triplicate at the indicated concentrations (0, 10, or 100 ng/ml), corresponding to 0X, 1X, or 10X Dox. At day 1, we trypsinized and counted the cells from all conditions, and seeded equivalent numbers of cells into fresh media. We immediately added the corresponding concentrations of Dox to the culture dishes. From then on, every 2–6 days cells were trypsinized, counted, and replated, as plotted, with media containing fresh Dox of corresponding concentrations replaced every 2–3 days. Biological replicates were maintained separately throughout the entirety of the experiment. See Supplementary Data 1 for all counts and calculations.

Single-cell RNA-seq. Sample preparation: we grew MCF10-2A *TetOn-CENPA-FLAG-HA* cells expressing either empty vector (p53-WT) or dominant-negative p53 (p53-DN) without Dox or with continuous exposure to Dox (10 ng/ml, ++, chronic) for 69 days in parallel. Cells in the no Dox condition were split into two dishes at day 67 and Dox was added to one set on day 68 for 24 h of CENP-A overexpression (10 ng/ml, +, acute), while the other remained without Dox (−, control). We prepared samples in singlet according to the 10x Genomics Sample Preparation Demonstrated Protocol. In brief, we harvested cells by trypsinization, resuspended in typical media and mixed thoroughly by pipette, passed cells through a 40 µm cell strainer, and counted cells by Beckman Automated Cell Counter. We resuspended cells in 1x PBS + 0.04% BSA, mixed, centrifuged gently, aspired supernatant, and repeated wash two times. We passed cells through another cell strainer (40 µm), counted again and diluted to a final concentration between 700 and 1200 cells/µl. We then proceeded directly to GEM generation and barcoding at the NGS platform, Institut Curie, using the Single-cell 3′ Reagent Kits v2 protocol with a targeted cell recovery of 2000 cells per sample, followed by post GEM-RT cleanup and cDNA amplification, then 3′ Gene Expression Library Construction, according to the manufacturer's instructions. Sequencing was performed by the NGS platform with a NovaSeq 6000 sequencer.

Single-cell RNA-seq analysis. Reads were pseudoaligned to Ensembl transcripts (GRCh38, release 95) using kallisto (version 0.46.0[100]) with the -x 10 × 2 option for Chromium Single Cell 3′ v2 chemistry. Count matrices were generated from sorted BUS files using bustools (version 0.39.2[101]), after barcode correction with the 10x v2 whitelist. For each sample, we selected cells via distance-based estimation of the knee in the cumulative distribution of distinct UMIs per barcode (unique molecular identifiers) using UMI-tools (version 1.0.0[102]). Sample matrices were thus converted to AnnData objects and concatenated for further quality control (QC) and analysis with Scanpy (version 1.4.6[103]). From the merged count matrix, we filtered out cells with abnormal levels of mitochondrial RNA, after adjusting for depth and total number of detected genes. Outliers were detected by covariance estimation (elliptic envelope with 5% contamination) using the number of genes, total counts (log-transformed), and mitochondrial counts (log-transformed) as features for outlier detection. Genes detected in <100 cells (after filtering) were also excluded. For comparison of scRNA-seq and bulk RNA-seq results, raw counts from matched samples were pooled across all cells, TMM normalized and mean centered.

For single-cell analyses, raw counts were normalized per cell, log-transformed, and adjusted for differences in sequencing depth via linear regression (using log-transformed total counts per cell). PCA was performed on the top 3000 highly variable genes (HVGs) after scaling. We computed a neighborhood graph using the first 20 principal components, adjusting for technical differences by batch alignment with BBKNN (version 1.3.9[104]). Uniform Manifold Approximation and Projection (UMAP) was used to visualize cell-to-cell variation in a low-dimensional (2D) space. Cell subpopulations were detected by Leiden clustering (at 0.5 resolution). Epithelial and mesenchymal cells were separately identified with the same procedure, but normalized counts were also adjusted for cell cycle differences (using the G1/S and G2/M signature) prior to scaling and PCA. For each cluster, genes were ranked by one-vs-all logistic regression to identify the top markers (see Supplementary Data 3). Boundaries among clusters were computed via Support Vector Classification with a third degree polynomial kernel. Gene sets for computing expression signatures were retrieved from Cyclebase v3.0 (cell cycle, G1/S and G2/M)[105] or MSigDB v6.2 (hallmark and curated gene sets related to senescence, EMT, and cell metabolism)[106]. References for each of the signatures are provided in Supplementary Data 3 (sheet 1). The scores (color gradients) are a measure of the average expression of the given set of genes, relative to a set of randomly sampled genes at comparable expression levels. Log-transformed normalized counts (prior to scaling) were used for the calculation. The score is then rescaled across cells from −1 (lowest) to +1 (highest).

For RNA velocity analyses, an additional index including both cDNA and intron sequences was generated from Ensembl annotations (GRCh38, release 95) using the kb-python wrapper (version 0.24.4) for pseudoalignment and quantification with kallisto and bustools (La Manno workflow). Filtered count matrices for both spliced and unspliced transcripts were added to the preprocessed data and analyzed using the scVelo package (version 0.2.2). RNA velocity was first evaluated across all samples for the top 3000 HVGs by fitting a dynamical model estimating the kinetic rate parameters for each gene, as well as the latent time underlying the overall kinetics[54]. To check whether the velocity flow changes by condition, we further estimated RNA velocities in individual samples by stochastic modeling. The trajectories across all conditions, and for each sample, were visualized in the precomputed UMAP embedding using a streamline plot that shows the directional flow across cells (considering velocities with a minimum mass of 3 and applying a smoothing factor of 0.8). In all UMAP plots, the latent time is represented by a color gradient ranging from 0 (initial state, blue) to 1 (terminal state, red).

Singe-cell RNA-seq analyses were carried out with custom Python scripts using Scanpy (version 1.4.6), scVelo (version 0.2.2), BBKNN (version 1.3.9), UMI-tools (version 1.0.0), pandas (version 0.25.0), NumPy (version 1.17.0), scikit-learn (version 0.21.3), matplotlib (version 3.3.0), and seaborn (version 0.9.0).

Beta-galactosidase senescence assay. We tested samples in singlet and duplicate for senescence using the Cell Signaling Technologies Senescence β-Galactosidase Staining Kit, according to the manufacturer's instructions. After 24 h with the stain, we imaged at least three fields per sample by brightfield microscopy using a 10X objective on a Nikon Eclipse TS100 microscope. Cells were counted manually from the acquired images with the counter blinded to the conditions. Only cells with dark blue staining were considered senescent. See Supplementary Data 1 for all counts and calculations.

Propidium iodide FACS. To analyze cell cycle changes by FACS, we harvested cells with trypsin and fixed with cold 70% ethanol. We stained fixed cells with propidium iodide using FxCycle PI/RNase solution (ThermoFisher Scientific), according to the manufacturer's instructions. FACS was performed on three biological replicates with a FACS Accuri 6 machine and cell cycle was assessed on a minimum

15,000 gated cells, excluding cell debris and doublets, with FlowJo software (V10.1r5). See Supplementary Fig. 4D for example of gating strategy and Supplementary Data 1 for all counts and calculations.

Statistics and reproducibility. Specific statistical tests, sample sizes, number of replicates, and information on the reproducibility of experiments are indicated in the figure legends and/or methods for each experiment. See Supplementary Data 1 for all source data pertaining to main figures and supplementary figures, including specific *N* values and *p* values from statistical tests. Biological replicates are defined as different sets of cells cultured under the same experimental conditions, processed separately but in parallel (at the same time). Independent experiments are defined as different sets of cells cultured under the same experimental conditions that were cultured (and processed) at different times. No statistics were derived from technical replicates (repeats/replicates of processed samples). No data were excluded from the analyses. For QCof scRNA-seq data, cells with abnormal levels of mitochondrial RNA, after adjusting for depth and total number of detected genes, were filtered out via outlier detection. Outliers were detected by covariance estimation (elliptic envelope with 5% contamination) using the number of genes, total counts (log-transformed) and mitochondrial counts (log-transformed) as features for outlier detection. Genes detected in <100 cells (after filtering) were also excluded. All experiments, with the exception of sequencing and mFISH experiments, were repeated independently at least once, as indicated in the figure legends. All repeats were consistent with the data reported. Number of biological replicates tested are also indicated for each experiment in the figure legends: typically 3 or 6 biological replicates were used for CFA experiments, 2 or 3 for IF and senescence quantifications, 1 for western blots, 3 for proliferation assays, and 2 for bulk RNA-seq. Single-cell RNA-seq was performed in singlet, but were validated by comparison to bulk RNA-seq. For all manual quantifications (CFAs, IF, senescence, micronuclei, mFISH), associated images were randomized and de-labeled prior to analysis to aid in blinding the researchers to the experimental conditions.

Reporting summary. Further information on research design is available in the Nature Research Reporting Summary linked to this article.

Data availability

Bulk- and single-cell RNA-seq data have been deposited in ArrayExpress under accession numbers E-MTAB-9867 and E-MTAB-9861, respectively. All other relevant data can be found in Supplementary Data 1 or are available from the authors upon request.

Received: 25 August 2020; Accepted: 25 February 2021;
Published online: 26 March 2021

References

1. Easwaran, H., Tsai, H. C. & Baylin, S. B. Cancer epigenetics: tumor heterogeneity, plasticity of stem-like states, and drug resistance. *Mol. Cell* **54**, 716–727 (2014).
2. Shen, H. & Laird, P. W. Interplay between the cancer genome and epigenome. *Cell* **153**, 38–55 (2013).
3. Gerstung, M. et al. The evolutionary history of 2,658 cancers. *Nature* **578**, 122–128 (2020).
4. Tijhuis, A. E., Johnson, S. C. & McClelland, S. E. The emerging links between chromosomal instability (CIN), metastasis, inflammation and tumour immunity. *Mol. Cytogenet.* **12**, 17 (2019).
5. Ye, C. J., Regan, S., Liu, G., Alemara, S. & Heng, H. H. Understanding aneuploidy in cancer through the lens of system inheritance, fuzzy inheritance and emergence of new genome systems. *Mol. Cytogenet.* **11**, 31 (2018).
6. Potapova, T. A., Zhu, J. & Li, R. Aneuploidy and chromosomal instability: a vicious cycle driving cellular evolution and cancer genome chaos. *Cancer Metastasis Rev.* **32**, 377–389 (2013).
7. Gerlinger, M. & Swanton, C. How Darwinian models inform therapeutic failure initiated by clonal heterogeneity in cancer medicine. *Br. J. Cancer* **103**, 1139–1143 (2010).
8. Boveri, T. Concerning the origin of malignant tumours by Theodor Boveri. Translated and annotated by Henry Harris. *J. Cell. Sci.* **121**, 1–84 (2008).
9. Flavahan, W. A., Gaskell, E. & Bernstein, B. E. Epigenetic plasticity and the hallmarks of cancer. *Science* **357**, eaal2380 (2017).
10. Guo, M., Peng, Y., Gao, A., Du, C. & Herman, J. G. Epigenetic heterogeneity in cancer. *Biomark. Res.* **7**, 23 (2019).
11. Wainwright, E. N. & Scaffidi, P. Epigenetics and cancer stem cells: unleashing, hijacking, and restricting cellular plasticity. *Trends Cancer* **3**, 372–386 (2017).
12. Lytle, N. K., Barber, A. G. & Reya, T. Stem cell fate in cancer growth, progression and therapy resistance. *Nat. Rev. Cancer* **18**, 669–680 (2018).
13. Feinberg, A. P. & Fallin, M. D. Epigenetics at the crossroads of genes and the environment. *JAMA* **314**, 1129–1130 (2015).
14. Morel, D., Jeffery, D., Aspeslagh, S., Almouzni, G. & Postel-Vinay, S. Combining epigenetic drugs with other therapies for solid tumours—past lessons and future promise. *Nat. Rev. Clin. Oncol.* https://doi.org/10.1038/s41571-019-0267-4 (2019).
15. Sharma, A. B., Dimitrov, S., Hamiche, A. & Van Dyck, E. Centromeric and ectopic assembly of CENP-A chromatin in health and cancer: old marks and new tracks. *Nucleic Acids Res.* **47**, 1051–1069 (2019).
16. Das, A., Smoak, E. M., Linares-Saldana, R., Lampson, M. A. & Black, B. E. Centromere inheritance through the germline. *Chromosoma* **126**, 595–604 (2017).
17. Barnhart, M. C. et al. HJURP is a CENP-A chromatin assembly factor sufficient to form a functional de novo kinetochore. *J. Cell Biol.* **194**, 229–243 (2011).
18. Fachinetti, D. et al. A two-step mechanism for epigenetic specification of centromere identity and function. *Nat. Cell Biol.* **15**, 1056–1066 (2013).
19. Amor, D. J. et al. Human centromere repositioning 'in progress'. *Proc. Natl Acad. Sci. USA* **101**, 6542–6547 (2004).
20. Tyler-Smith, C. et al. Transmission of a fully functional human neocentromere through three generations. *Am. J. Hum. Genet.* **64**, 1440–1444 (1999).
21. Dunleavy, E. M. et al. HJURP is a cell-cycle-dependent maintenance and deposition factor of CENP-A at centromeres. *Cell* **137**, 485–497 (2009).
22. Foltz, D. R. et al. Centromere-specific assembly of CENP-a nucleosomes is mediated by HJURP. *Cell* **137**, 472–484 (2009).
23. Zasadzińska, E. et al. Inheritance of CENP-A nucleosomes during DNA replication requires HJURP. *Dev. Cell* **47**, 348–362.e7 (2018).
24. Fukagawa, T. & Earnshaw, W. C. The centromere: chromatin foundation for the kinetochore machinery. *Dev. Cell* **30**, 496–508 (2014).
25. McKinley, K. L. & Cheeseman, I. M. The molecular basis for centromere identity and function. *Nat. Rev. Mol. Cell Biol.* **17**, 16–29 (2016).
26. Musacchio, A. & Desai, A. A molecular view of kinetochore assembly and function. *Biology* **6**, 5 (2017).
27. Muller, S. & Almouzni, G. Chromatin dynamics during the cell cycle at centromeres. *Nat. Rev. Genet.* **18**, 192–208 (2017).
28. Mahlke, M. A. & Nechemia-Arbely, Y. Guarding the genome: CENP-A-chromatin in health and cancer. *Genes* **11**, 810 (2020).
29. Maehara, K., Takahashi, K. & Saitoh, S. CENP-A reduction induces a p53-dependent cellular senescence response to protect cells from executing defective mitoses. *Mol. Cell Biol.* **30**, 2090–2104 (2010).
30. Shrestha, R. L. et al. Mislocalization of centromeric histone H3 variant CENP-A contributes to chromosomal instability (CIN) in human cells. *Oncotarget* **8**, 46781–46800 (2017).
31. Gu, X. M. et al. Expression and prognostic relevance of centromere protein A in primary osteosarcoma. *Pathol. Res. Pract.* **210**, 228–233 (2014).
32. Li, Y. et al. ShRNA-targeted centromere protein A inhibits hepatocellular carcinoma growth. *PLoS ONE* **6**, e17794 (2011).
33. Ma, X. J. et al. Gene expression profiles of human breast cancer progression. *Proc. Natl Acad. Sci. USA* **100**, 5974–5979 (2003).
34. McGovern, S. L., Qi, Y., Pusztai, L., Symmans, W. F. & Buchholz, T. A. Centromere protein-A, an essential centromere protein, is a prognostic marker for relapse in estrogen receptor-positive breast cancer. *Breast Cancer Res.* **14**, R72 (2012).
35. Qiu, J. J. et al. Prognostic value of centromere protein-A expression in patients with epithelial ovarian cancer. *Tumour Biol.* **34**, 2971–2975 (2013).
36. Saha, A. K. et al. The role of the histone H3 variant CENPA in prostate cancer. *J. Biol. Chem.* jbc.RA119.010080 https://doi.org/10.1074/jbc.RA119.010080 (2020).
37. Sun, X. et al. Elevated expression of the centromere protein-A(CENP-A)-encoding gene as a prognostic and predictive biomarker in human cancers. *Int J. Cancer* **139**, 899–907 (2016).
38. Wu, Q. et al. Expression and prognostic significance of centromere protein A in human lung adenocarcinoma. *Lung Cancer* **77**, 407–414 (2012).
39. Zhang, W. et al. Centromere and kinetochore gene misexpression predicts cancer patient survival and response to radiotherapy and chemotherapy. *Nat. Commun.* **7**, 12619 (2016).
40. Levine, A. J. p53: 800 million years of evolution and 40 years of discovery. *Nat. Rev. Cancer* 1–10 https://doi.org/10.1038/s41568-020-0262-1 (2020).
41. Toufektchan, E. & Toledo, F. The guardian of the genome revisited: p53 downregulates genes required for telomere maintenance, DNA repair, and centromere structure. *Cancers* **10**, 135 (2018).
42. Filipescu, D. et al. Essential role for centromeric factors following p53 loss and oncogenic transformation. *Genes Dev.* **31**, 463–480 (2017).
43. Cerami, E. et al. The cBio cancer genomics portal: an open platform for exploring multidimensional cancer genomics data. *Cancer Discov.* **2**, 401–404 (2012).
44. McKinley, K. L. & Cheeseman, I. M. Large-scale analysis of CRISPR/Cas9 cell-cycle knockouts reveals the diversity of p53-dependent responses to cell-cycle defects. *Deve. Cell* **40**, 405–420.e2 (2017).

45. Uhlén, M. et al. Tissue-based map of the human proteome. *Science* **347** https://www.proteinatlas.org/ENSG00000115163-CENPA/tissue (2015).
46. Lacoste, N. et al. Mislocalization of the centromeric histone variant CenH3/CENP-A in human cells depends on the chaperone DAXX. *Mol. Cell* **53**, 631–644 (2014).
47. Nechemia-Arbely, Y. et al. DNA replication acts as an error correction mechanism to maintain centromere identity by restricting CENP-A to centromeres. *Nat. Cell Biol.* **21**, 743–754 (2019).
48. Oei, A. L. et al. Hyperthermia selectively targets human papillomavirus in cervical tumors via p53-dependent apoptosis. *Cancer Res.* **75**, 5120–5129 (2015).
49. Hahn, W. C. et al. Enumeration of the simian virus 40 early region elements necessary for human cell transformation. *Mol. Cell Biol.* **22**, 2111–2123 (2002).
50. Athwal, R. K. et al. CENP-A nucleosomes localize to transcription factor hotspots and subtelomeric sites in human cancer cells. *Epigenet Chromatin* **8**, 2 (2015).
51. Tanay, A. & Regev, A. Single cell genomics: from phenomenology to mechanism. *Nature* **541**, 331–338 (2017).
52. Abbadie, C., Pluquet, O. & Pourtier, A. Epithelial cell senescence: an adaptive response to pre-carcinogenic stresses? *Cell. Mol. Life Sci.* **74**, 4471–4509 (2017).
53. Tonnessen-Murray, C. A., Lozano, G. & Jackson, J. G. The regulation of cellular functions by the p53 protein: cellular senescence. *Cold Spring Harb. Perspect. Med.* **7**, a026112 (2017).
54. Bergen, V., Lange, M., Peidli, S., Wolf, F. A. & Theis, F. J. Generalizing RNA velocity to transient cell states through dynamical modeling. *Nat. Biotechnol.* **38**, 1408–1414 (2020).
55. Brosh, R. et al. p53 counteracts reprogramming by inhibiting mesenchymal-to-epithelial transition. *Cell Death Differ.* **20**, 312–320 (2013).
56. Kim, N. H. et al. p53 regulates nuclear GSK-3 levels through miR-34-mediated Axin2 suppression in colorectal cancer cells. *Cell Cycle* **12**, 1578–1587 (2013).
57. Pinho, A. V., Rooman, I. & Real, F. X. p53-dependent regulation of growth, epithelial-mesenchymal transition and stemness in normal pancreatic epithelial cells. *Cell Cycle* **10**, 1312–1321 (2011).
58. Senoo, M., Pinto, F., Crum, C. P. & McKeon, F. p63 Is essential for the proliferative potential of stem cells in stratified epithelia. *Cell* **129**, 523–536 (2007).
59. Singh, S. K. et al. Antithetical NFATc1-Sox2 and p53-miR200 signaling networks govern pancreatic cancer cell plasticity. *EMBO J.* **34**, 517–530 (2015).
60. Wang, S. P. et al. p53 controls cancer cell invasion by inducing the MDM2-mediated degradation of Slug. *Nat. Cell Biol.* **11**, 694–704 (2009).
61. Pastushenko, I. et al. Identification of the tumour transition states occurring during EMT. *Nature* **556**, 463–468 (2018).
62. Sarrio, D., Franklin, C. K., Mackay, A., Reis-Filho, J. S. & Isacke, C. M. Epithelial and mesenchymal subpopulations within normal basal breast cell lines exhibit distinct stem cell/progenitor properties. *Stem Cells* **30**, 292–303 (2012).
63. Bruna, A. et al. TGFβ induces the formation of tumour-initiating cells in claudinlow breast cancer. *Nat. Commun.* **3**, 1055 (2012).
64. Nye, J., Sturgill, D., Athwal, R. & Dalal, Y. HJURP antagonizes CENP-A mislocalization driven by the H3.3 chaperones HIRA and DAXX. *PLoS ONE* **13**, e0205948 (2018).
65. Hinchcliffe, E. H. et al. Chromosome missegregation during anaphase triggers p53 cell cycle arrest through histoneH3.3 Ser31 phosphorylation. *Nat. Cell Biol.* **18**, 668–675 (2016).
66. Soto, M. et al. p53 prohibits propagation of chromosome segregation errors that produce structural aneuploidies. *Cell Rep.* **19**, 2423–2431 (2017).
67. Blandino, G. & Di Agostino, S. New therapeutic strategies to treat human cancers expressing mutant p53 proteins. *J. Exp. Clin. Cancer Res.* **37**, 30 (2018).
68. Bykov, V. J. N., Eriksson, S. E., Bianchi, J. & Wiman, K. G. Targeting mutant p53 for efficient cancer therapy. *Nat. Rev. Cancer* **18**, 89–102 (2018).
69. Sanz, G., Singh, M., Peuget, S. & Selivanova, G. Inhibition of p53 inhibitors: progress, challenges and perspectives. *J. Mol. Cell Biol.* **11**, 586–599 (2019).
70. Lamouille, S., Xu, J. & Derynck, R. Molecular mechanisms of epithelial-mesenchymal transition. *Nat. Rev. Mol. Cell Biol.* **15**, 178–196 (2014).
71. Cook, D. P. & Vanderhyden, B. C. Context specificity of the EMT transcriptional response. *Nat. Commun.* **11**, 2142 (2020).
72. Pastushenko, I. & Blanpain, C. EMT transition states during tumor progression and metastasis. *Trends Cell Biol.* **29**, 212–226 (2019).
73. Puisieux, A., Pommier, R. M., Morel, A. P. & Lavial, F. Cellular pliancy and the multistep process of tumorigenesis. *Cancer Cell* **33**, 164–172 (2018).
74. Craene, B. D. & Berx, G. Regulatory networks defining EMT during cancer initiation and progression. *Nat. Rev. Cancer* **13**, 97–110 (2013).
75. Ansieau, S. et al. Induction of EMT by twist proteins as a collateral effect of tumor-promoting inactivation of premature senescence. *Cancer Cell* **14**, 79–89 (2008).
76. Liu, Y., El-Naggar, S., Darling, D. S., Higashi, Y. & Dean, D. C. Zeb1 links epithelial-mesenchymal transition and cellular senescence. *Development* **135**, 579–588 (2008).
77. de Jong, M. C. et al. Pretreatment microRNA expression impacting on epithelial-to-mesenchymal transition predicts intrinsic radiosensitivity in head and neck cancer cell lines and patients. *Clin. Cancer Res.* **21**, 5630–5638 (2015).
78. Steinbichler, T. B. et al. Epithelial-mesenchymal crosstalk induces radioresistance in HNSCC cells. *Oncotarget* **9**, 3641–3652 (2018).
79. Theys, J. et al. E-Cadherin loss associated with EMT promotes radioresistance in human tumor cells. *Radiother. Oncol.* **99**, 392–397 (2011).
80. Shibue, T. & Weinberg, R. A. EMT, CSCs, and drug resistance: the mechanistic link and clinical implications. *Nat. Rev. Clin. Oncol.* **14**, 611–629 (2017).
81. Ambartsumyan, G. et al. Centromere protein A dynamics in human pluripotent stem cell self-renewal, differentiation and DNA damage. *Hum. Mol. Genet* **19**, 3970–3982 (2010).
82. Milagre, I., Pereira, C., Oliveira, R. & Jansen, L. E. T. Reprogramming of human cells to pluripotency induces CENP-A chromatin depletion. *bioRxiv* 2020.02.21.960252 https://doi.org/10.1101/2020.02.21.960252 (2020).
83. Jain, A. K. & Barton, M. C. p53: emerging roles in stem cells, development and beyond. *Development* **145**, dev158360 (2018).
84. García del Arco, A., Edgar, B. A. & Erhardt, S. In vivo analysis of centromeric proteins reveals a stem cell-specific asymmetry and an essential role in differentiated, non-proliferating cells. *Cell Rep.* **22**, 1982–1993 (2018).
85. Dattoli, A. A. et al. Asymmetric assembly of centromeres epigenetically regulates stem cell fate. *J. Cell Biol.* **219**, e201910084 (2020).
86. Wu, Q. et al. Chemoresistance to gemcitabine in hepatoma cells induces epithelial-mesenchymal transition and involves activation of PDGF-D pathway. *Oncotarget* **4**, 1999–2009 (2013).
87. McGrail, D. J. et al. Defective replication stress response is inherently linked to the cancer stem cell phenotype. *Cell Rep.* **23**, 2095–2106 (2018).
88. Cha, Y. H., Yook, J. I., Kim, H. S. & Kim, N. H. Catabolic metabolism during cancer EMT. *Arch. Pharm. Res.* **38**, 313–320 (2015).
89. Chen, Q. et al. Growth-induced stress enhances epithelial-mesenchymal transition induced by IL-6 in clear cell renal cell carcinoma via the Akt/GSK-3beta/beta-catenin signaling pathway. *Oncogenesis* **6**, e375 (2017).
90. Jiang, J. et al. Redox regulation in tumor cell epithelial-mesenchymal transition: molecular basis and therapeutic strategy. *Signal Transduct. Target Ther.* **2**, 17036 (2017).
91. Marcucci, F. & Rumio, C. How tumor cells choose between epithelial-mesenchymal transition and autophagy to resist stress-therapeutic implications. *Front. Pharm.* **9**, 714 (2018).
92. Shah, P. P. & Beverly, L. J. Regulation of VCP/p97 demonstrates the critical balance between cell death and epithelial-mesenchymal transition (EMT) downstream of ER stress. *Oncotarget* **6**, 17725–17737 (2015).
93. Gomes, A. P. et al. Dynamic incorporation of histone h3 variants into chromatin is essential for acquisition of aggressive traits and metastatic colonization. *Cancer Cell* **36**, 402–417.e13 (2019).
94. Kim, D., Paggi, J. M., Park, C., Bennett, C. & Salzberg, S. L. Graph-based genome alignment and genotyping with HISAT2 and HISAT-genotype. *Nat. Biotechnol.* **37**, 907–915 (2019).
95. Liao, Y., Smyth, G. K. & Shi, W. featureCounts: an efficient general purpose program for assigning sequence reads to genomic features. *Bioinformatics* **30**, 923–930 (2014).
96. Robinson, M. D., McCarthy, D. J. & Smyth, G. K. edgeR: a Bioconductor package for differential expression analysis of digital gene expression data. *Bioinformatics* **26**, 139–140 (2010).
97. McCarthy, D. J., Chen, Y. & Smyth, G. K. Differential expression analysis of multifactor RNA-Seq experiments with respect to biological variation. *Nucleic Acids Res* **40**, 4288–4297 (2012).
98. Liao, Y., Wang, J., Jaehnig, E. J., Shi, Z. & Zhang, B. WebGestalt 2019: gene set analysis toolkit with revamped UIs and APIs. *Nucleic Acids Res.* **47**, W199–W205 (2019).
99. Trott, J. et al. Long-term culture of self-renewing pancreatic progenitors derived from human pluripotent stem cells. *Stem Cell Rep.* **8**, 1675–1688 (2017).
100. Bray, N. L., Pimentel, H., Melsted, P. & Pachter, L. Near-optimal probabilistic RNA-seq quantification. *Nat. Biotechnol.* **34**, 525–527 (2016).
101. Melsted, P., Ntranos, V. & Pachter, L. The barcode, UMI, set format and BUStools. *Bioinformatics* **35**, 4472–4473 (2019).
102. Smith, T. S., Heger, A. & Sudbery, I. UMI-tools: Modelling sequencing errors in Unique Molecular Identifiers to improve quantification accuracy. *Genome Res.* gr.209601.116 https://doi.org/10.1101/gr.209601.116 (2017).
103. Wolf, F. A., Angerer, P. & Theis, F. J. SCANPY: large-scale single-cell gene expression data analysis. *Genome Biol.* **19**, 15 (2018).
104. Polanski, K. et al. BBKNN: fast batch alignment of single cell transcriptomes. *Bioinformatics* https://doi.org/10.1093/bioinformatics/btz625 (2019).

105. Santos, A., Wernersson, R. & Jensen, L. J. Cyclebase 3.0: a multi-organism database on cell-cycle regulation and phenotypes. *Nucleic Acids Res.* **43**, D1140–D1144 (2015).
106. Liberzon, A. et al. The Molecular Signatures Database (MSigDB) hallmark gene set collection. *Cell Syst.* **1**, 417–425 (2015).
107. Bouaoun, L. et al. TP53 variations in human cancers: new lessons from the IARC TP53 database and genomics data. *Hum. Mutat.* **37**, 865–876 (2016).

Acknowledgements

We sincerely thank Jean-Pierre Quivy and Leanne De Koning for critical reading of the paper. We also thank Patricia Le Baccon, Mickaël Garnier, and the Cell and Tissue Imaging Platform—PICT-IBiSA (member of France–Bioimaging—ANR-10-INBS-04) of the UMR3664, Institut Curie, for help with light microscopy, as well as Sophie Heinrich and the Experimental Radiobiology platform of Institut Curie for help with X-irradiation. High-throughput sequencing was performed by the ICGex NGS platform of the Institut Curie supported by the grants ANR-10-EQPX-03 (Equipex) and ANR-10-INBS-09-08 (France Génomique Consortium) from the Agence Nationale de la Recherche ("Investissements d'Avenir" program), by the Canceropole Ile-de-France and by the SiRIC-Curie program—SiRIC Grant "INCa-DGOS-4654." D.F. receives salary support from the Centre Nationale de Recherche Scientifique (CNRS). M.D. receives salary support from the City of Paris via Emergence(s) 2018 of D.F. A.G., C.R.P., D.J., K.P., L.B., R.P.L., and G.A. were supported by la Ligue Nationale contre le Cancer (Equipe labellisée Ligue), Labex DEEP (ANR-11-LABX-0044_DEEP, ANR-10-IDEX-0001-02), PSL, ERC-2015-ADG-694694 ChromADICT, and ANR-16-CE12-0024 CHIFT. Funding for R.P.L. provided by Horizon 2020 Marie Skłodowska-Curie Actions Initial Training Network "EpiSyStem" (grant number 765966). Individual funding was also provided to D.J. from la Fondation ARC pour la recherche sur le cancer ("Aides individuelles" 3 years, post-doc), and to AG from the Horizon 2020 Framework Programme for Research and Innovation (H2020 Marie Skłodowska-Curie Actions grant agreement 798106 "REPLICHROM4D").

Author contributions

Conceptualization: D.J. and G.A.; methodology: D.J., K.P., and G.A.; software: A.G.; validation: A.G., C.R.P., D.J., K.P., L.B., and R.P.L.; formal analysis: D.J. and A.G.; investigation: A.G., C.R.P., D.J., K.P., L.B., M.D., and R.P.L.; resources: D.F. and G.A.; data curation: A.G.; writing—original draft: D.J., A.G., and G.A.; writing—review and editing: A.G., C.R.P., D.J., K.P., L.B., R.P.L., M.D., D.F., and G.A.; visualization: A.G., C.R.P., D.J., K.P., M.D., and G.A.; supervision: D.F., K.P., and G.A.; project administration: G.A.; funding acquisition: G.A.

Competing interests

The authors declare no competing interests.

Additional information

Supplementary information The online version contains supplementary material available at https://doi.org/10.1038/s42003-021-01941-5.

Correspondence and requests for materials should be addressed to G.A.

Reprints and permission information is available at http://www.nature.com/reprints

Publisher's note Springer Nature remains neutral with regard to jurisdictional claims in published maps and institutional affiliations.

Open Access This article is licensed under a Creative Commons Attribution 4.0 International License, which permits use, sharing, adaptation, distribution and reproduction in any medium or format, as long as you give appropriate credit to the original author(s) and the source, provide a link to the Creative Commons license, and indicate if changes were made. The images or other third party material in this article are included in the article's Creative Commons license, unless indicated otherwise in a credit line to the material. If material is not included in the article's Creative Commons license and your intended use is not permitted by statutory regulation or exceeds the permitted use, you will need to obtain permission directly from the copyright holder. To view a copy of this license, visit http://creativecommons.org/licenses/by/4.0/.

© The Author(s) 2021

frontiers | Frontiers in Cell and Developmental Biology

REVIEW
published: 02 June 2022
doi: 10.3389/fcell.2022.907120

CENP-A Regulation and Cancer

*Charlène Renaud-Pageot, Jean-Pierre Quivy, Marina Lochhead and Geneviève Almouzni**

Institut Curie, PSL Research University, CNRS, Sorbonne Université, Nuclear Dynamics Unit, Équipe Labellisée Ligue contre le Cancer, Paris, France

In mammals, CENP-A, a histone H3 variant found in the centromeric chromatin, is critical for faithful chromosome segregation and genome integrity maintenance through cell divisions. Specifically, it has dual functions, enabling to define epigenetically the centromere position and providing the foundation for building up the kinetochore. Regulation of its dynamics of synthesis and deposition ensures to propagate proper centromeres on each chromosome across mitosis and meiosis. However, CENP-A overexpression is a feature identified in many cancers. Importantly, high levels of CENP-A lead to its mislocalization outside the centromere. Recent studies in mammals have begun to uncover how CENP-A overexpression can affect genome integrity, reprogram cell fate and impact 3D nuclear organization in cancer. Here, we summarize the mechanisms that orchestrate CENP-A regulation. Then we review how, beyond its centromeric function, CENP-A overexpression is linked to cancer state in mammalian cells, with a focus on the perturbations that ensue at the level of chromatin organization. Finally, we review the clinical interest for CENP-A in cancer treatment.

Keywords: CENP-A histone variant, centromere, cancer, chromosome instability, chromatin organization

OPEN ACCESS

Edited by:
Karen Wing Yee Yuen, The University of Hong Kong, Hong Kong SAR, China

Reviewed by:
Daniël Patrick Melters, National Cancer Institute (NIH), United States
A. Arockia Jeyaprakash, University of Edinburgh, United Kingdom

****Correspondence:***
Geneviève Almouzni
genevieve.almouzni@curie.fr

Specialty section:
This article was submitted to Cell Growth and Division, a section of the journal Frontiers in Cell and Developmental Biology

Received: *29 March 2022*
Accepted: *11 May 2022*
Published: *02 June 2022*

Citation:
Renaud-Pageot C, Quivy J-P, Lochhead M and Almouzni G (2022) CENP-A Regulation and Cancer. Front. Cell Dev. Biol. 10:907120. doi: 10.3389/fcell.2022.907120

INTRODUCTION

The first kinetochore proteins were described in 1985 using the sera of patients with an autoimmune disease called scleroderma (Moroi et al., 1980). William Earnshaw and Naomi Rothfield purified the autoantibodies targeting the centromeres of the patients and identified three proteins, including the Centromere Protein A: CENP-A (Earnshaw and Rothfield, 1985). Since then, biochemical approaches demonstrated that CENP-A is a variant of histone H3 (Palmer et al., 1987, 1991; Sullivan et al., 1994), which is one of the four major classes of histones (H2A, H2B, H3, H4) contributing to the basic unit of chromatin, the nucleosome. It is the only histone variant that is centromere-specific, its presence characterizing centromeric chromatin in most eukaryotes (Tromer et al., 2019). Within nucleosomes, CENP-A displays distinct features contributing to looser DNA binding and increased dynamics of the DNA ends in the nucleosome core particle (Sekulic et al., 2010; Panchenko et al., 2011; Tachiwana et al., 2011; Ali-Ahmad et al., 2019; Arimura et al., 2019). In addition, CENP-A-containing nucleosomes wrap only 121 bp of DNA, compared to the 147 bp in nucleosomes containing other H3 variants (Tachiwana et al., 2012; Hasson et al., 2013; Lacoste et al., 2014). These characteristics enable CENP-A to contribute to both the identity and function of centromeres. Centromeres are the loci where kinetochores assemble and dock to direct chromosome segregation during mitosis. Beyond this function during cell division, centromeres contribute to genome architecture as robust nuclear domains in interphase nuclei of mammalian cells (Dunleavy et al., 2009; Lacoste et al., 2014). Importantly, CENP-A has been involved as a key epigenetic determinant in defining the position of the centromere (Barnhart et al., 2011; Fachinetti et al., 2013). Furthermore, CENP-A is stably inherited across cell divisions, thereby helping to maintain centromere identity during cell proliferation (Jansen et al., 2007). Its inheritance through

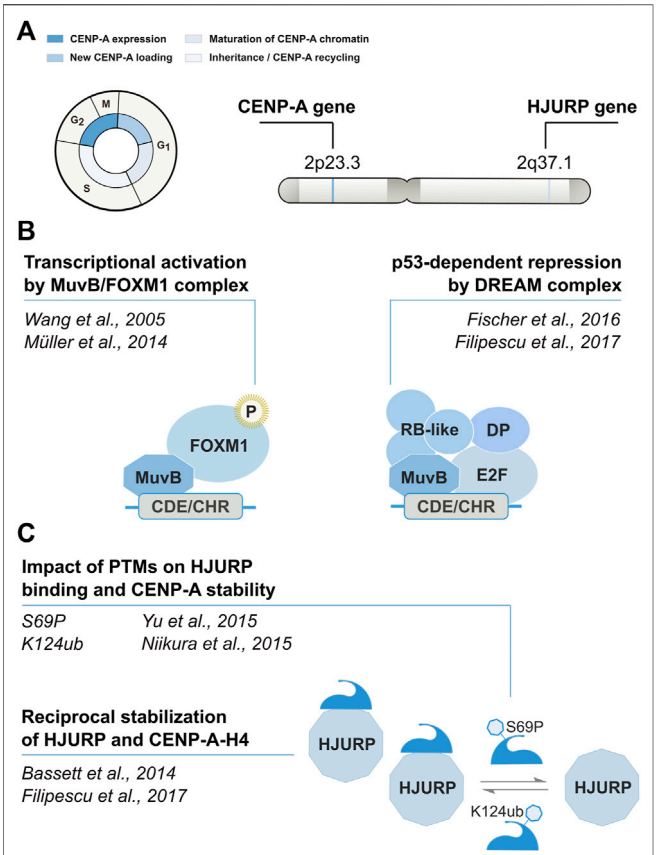


FIGURE 1 | Cell cycle timing and regulation of CENP-A. Modified from Mendiratta et al., 2019. **(A)** CENP-A and its chaperone HJURP are regulated in a cell cycle–dependent manner. **(B)** Transcription is regulated in cis by the CHR/CDE motif in their promoter region. The recruitment of the DREAM complex at the CHR is thought to promote transcriptional repression during G1. At the beginning of S phase, the MuvB core of the DREAM complex remains bound to the CHR/CDE while other components dissociate and are replaced by B-MYB. The B-MYB-MuvB (MMB) complex recruits FOXM1 in late S phase. B-MYB is degraded upon phosphorylation, whereas the progressive phosphorylation of FOXM1 leads to its activation in G2/M. **(C)** CENP-A and HJURP mutually stabilize each other at the protein level. The reciprocal stabilization is affected by posttranslational modifications of CENP-A.

meiosis ensures a maintenance over organismal generations in mammals (Tyler-Smith et al., 1999; Amor et al., 2004; Smoak et al., 2016). CENP-A is also key for centromere function, establishing the interface necessary for the binding of components of the CCAN (constitutive centromere associated network) complex, such as CENP-C and CENP-N (Ali-Ahmad et al., 2019; Allu et al., 2019). At a chromatin level, CENP-A nucleosomes are interspersed with H3 nucleosomes along the arrays of repetitive DNA of the centromere (Dunleavy et al., 2011). Additional kinetochore components, CENP-T and CENP-W, associate with H3 nucleosomes (Hori et al., 2008). Both CENP-C and CENP-T interact with Mis12 and the Ndc80 complex, which are components of the KMN network linking the kinetochore to microtubules (Przewloka et al., 2011; Screpanti et al., 2011; Malvezzi et al., 2013). The level of CENP-A is thus key to maintain genome integrity, as shown by experimental alterations in CENP-A levels where both depletion (Maehara et al., 2010) and overexpression (Shrestha et al., 2017) promote mitotic defects and chromosomal instability (CIN) in human cells. Since alteration in CENP-A availability can alter both the formation of CENP-A-containing nucleosomes and centromere function, a link with cancer states is expected. Therefore, the control of CENP-A transcription, its turn-over/stability and its deposition into chromatin is central to ensure genome stability.

REGULATION OF CENP-A

Histone chaperones escort non-nucleosomal (free) histones and ensure their deposition into chromatin (reviewed in (Ray-Gallet and Almouzni, 2021)). The timing of CENP-A deposition varies in different species. In mammals, the Holliday Junction Recognition Protein (HJURP) has been identified as the dedicated histone chaperone promoting CENP-A specific incorporation into centromeric chromatin, which in human occurs in late mitosis (outside S phase), to compensate for the replication-coupled dilution of CENP-A (Dunleavy et al., 2009; Foltz et al., 2009). Interestingly, in human cells, replication has been proposed as an error correction mechanism ensuring that CENP-A nucleosomes are retained at the centromere (Nechemia-Arbely et al., 2019). In addition, HJURP is involved in dealing with parental CENP-A displaced by the replication fork to ensure its recycling (Zasadzińska et al., 2018). This exclusive partnership is driven by the CENP-A targeting domain (CATD) in HJURP (Shuaib et al., 2010; Bassett et al., 2012). Furthermore, the presence of two C-terminal domains (HCTD1 and HCTD2) in HJURP is required for CENP-A deposition (Zasadzińska et al., 2013; Zhao et al., 2016; Pan et al., 2019).

CENP-A is encoded by a single multi-exon gene located outside of the histone gene clusters (**Figure 1**). The CENP-A gene (CENPA) undergoes conventional pre-mRNA processing *via* splicing and polyadenylation. Expression levels of CENP-A and its chaperone HJURP are cell cycle regulated, with a peak of expression in G2/M (Shelby et al., 1997) (**Figure 1A**). CENPA and HJURP transcription involves a CDE/CHR motif in their promoters recognized by the transcriptional regulator FOXM1 (Wang et al., 2005; Chen et al., 2013) and by the DREAM complex (Fischer et al., 2016). The DREAM complex is a transcriptional regulator binding to CDE/CHR sites to mediate indirect p53-p21-dependent repression, which can switch to an activator notably by recruitment of FOXM1 (reviewed in (Engeland, 2018)). These regulatory mechanisms provide means to keep these genes under a p53-dependent transcriptional repression (Filipescu et al., 2017) (**Figure 1B**). CENP-A expression levels vary depending on the tissue, in a range up to 50-fold changes, with the highest CENP-A expression scores found in lymphoid, skin and gastrointestinal tissues according to the Human Protein Atlas (Uhlén et al., 2015). In addition to transcriptional regulation, CENP-A amounts are also controlled at the protein level and CENP-A and its chaperone HJURP mutually stabilize each other (Bassett et al., 2012; Filipescu et al., 2017). Their reciprocal stabilization is affected by posttranslational modifications on the N-terminal tail of CENP-A, which can further regulate the

timing of deposition. CENP-A S69 phosphorylation prevents interaction with HJURP and premature loading, while K124 ubiquitylation favors HJURP binding and contributes to their stabilization (**Figure 1C**). Thus, the overexpression of either CENP-A or HJURP leads to an increase in the levels of their binding partner (Filipescu et al., 2017). Conversely, HJURP loss results in CENP-A depletion, and CENP-A knockdown leads to the proteasome-mediated degradation of HJURP. Specific enrichment of CENP-A at the centromere is achieved in telophase/early G1 by HJURP (Dunleavy et al., 2009; Foltz et al., 2009), which is recruited at the centromere during this critical time window by the Mis18 complex [composed of two subunits, Mis18α and Mis18β, and the Mis18-binding protein 1 (Mis18BP1)] (Jansen et al., 2007; Dunleavy et al., 2009; Foltz et al., 2009; Zasadzińska et al., 2013; Nardi et al., 2016). Specifically, during M phase, CDK1 phosphorylates CENP-C, which stabilizes its interaction with CENP-A nucleosomes (Watanabe et al., 2019; Ariyoshi et al., 2021). CENP-A-bound CENP-C can recruit Mis18 to centromeres (Moree et al., 2011; Dambacher et al., 2012; McKinley and Cheeseman, 2014). Following this step, during anaphase, reduced CDK1/2 activity results in the dephosphorylation of HJURP, which in turn promotes its binding to Mis18 (Wang et al., 2014; Stankovic et al., 2017). Finally, in the second part of the G1 phase, the RSF (remodeling and spacing factor) complex (Perpelescu et al., 2009) and MgcRacGap (a Rho family GTPase activating protein) (Lagana et al., 2010) interact transiently with centromeres via HsKNL2, a G1-specific CENP-A licensing factor, to stabilize newly deposited CENP-A nucleosomes and generate mature centromeric chromatin. When the cell transitions to S-phase, CDK1/2 activity levels increase, Mis18BP1 is phosphorylated, released from centromeric chromatin, and CENP-A deposition is inhibited (Silva et al., 2012; McKinley and Cheeseman, 2014; Pan et al., 2017; Spiller et al., 2017). Thus, under normal conditions, a combination of mechanisms, some of which exploit the partnership between CENP-A and its dedicated chaperone HJURP, ensure that CENP-A levels and deposition are restricted to the centromere to promote faithful chromosome segregation.

CENP-A LEVELS INCREASE IN CANCER

Interestingly, by comparison with healthy tissues, elevated CENP-A expression levels are documented in many cancer types in humans, including breast (Ma et al., 2003; McGovern et al., 2012), colon (Tomonaga et al., 2003), liver (Li et al., 2011), lung (Wu et al., 2012), ovarian (Qiu et al., 2013), bone (Gu et al., 2014), gastric (Xu et al., 2020), and prostate (Saha et al., 2020). Indeed, the analysis of matched normal-tumor transcriptomes from 101 datasets demonstrated that the overexpression of CENP-A is a common feature of more than 44% of human cancers (Lacoste et al., 2014). Additionally, Oncomine analysis of 51 studies showed that CENP-A expression is significantly upregulated in 20 types of solid tumors compared with healthy tissues (Sun et al., 2016). Among these studies, the most common cancer types showing CENP-A overexpression were breast, central nervous system, ovary, and lung cancers. By contrast, down-regulation of CENP-A expression has never been observed in cancer tissues. More recently, analysis using TCGA PanCancer Atlas confirmed the global increase in CENP-A levels in patient tumors relative to healthy tissues, which reaches over 1000-fold in the case of cholangiocarcinoma (Jeffery et al., 2021) (**Figure 2**). In line with their co-regulation (see above), the unusual level of CENP-A often occurs in parallel with upregulation of its chaperone HJURP (Dunleavy et al., 2009; Jeffery et al., 2021). Thus, on average CENP-A mRNA levels are significantly and positively correlated with those of HJURP in several cancer types as assessed based on gene expression profiling interactive analysis (Zhang et al., 2016).

The negative regulation of CENPA and HJURP transcription under a p53 control (Fischer et al., 2016) is aligned with observations in mouse tumor cell line models where TP53 loss-of-function mutations lead to high CENP-A and HJURP levels (Filipescu et al., 2017). However, according to TCGA PanCancer Atlas studies visualized on CBioPortal, CENP-A overexpression can be observed in many tumors displaying TP53 loss of function mutation or wild-type (WT) TP53 (Cerami et al., 2012). Notably, early studies did not consider the p53 status of the tumors when assessing CENP-A levels. As a result, two distinct situations (p53-WT or p53-defective) were combined in the data concerning CENP-A levels and its link with cancer, thereby masking potentially important distinctions. Thus, beside the direct loss of p53 function, other mechanisms underly aberrant expression levels of CENP-A in cancer. Genetic analysis indicated that the elevated CENP-A expression was not due to alterations in the sequence or an increased copy number of the CENPA gene (Sun et al., 2016) and other factors, apart from a direct impairment in p53, deserve to be explored to explain CENP-A overexpression in human cancers. Several hypotheses can be considered. First, the tumor suppressor protein pRb (retinoblastoma protein), whose inactivation leads to CENP-A upregulation (Amato et al., 2009), is frequently mutated or disabled in cancer [reviewed in (Hickman et al., 2002)]. Secondly, CENP-A and HJURP overexpression could be the result of a deregulation of FOXM1, a known oncogenic transcription factor and activator of CENPA and HJURP transcription (Wang et al., 2005; Thiru et al., 2014). Indeed, the upregulation of CENP-A strongly correlates with the expression of FOXM1 across many cancers and FOXM1 displays at least 100-fold relative enrichment at the CENPA promoter in cancer tissues compared with normal tissues (Thiru et al., 2014). Finally, E2F8 and E2F2 are also potential transcriptional regulators of CENPA with critical roles in tumorigenesis (Sun et al., 2016). Importantly, whichever underlying mechanism leads to CENP-A upregulation, an excess of this particular histone H3 variant leads to an unbalanced situation in histones with effects onto chromatin organization as we will now discuss.

CENP-A OVEREXPRESSION LEADS TO MISLOCALIZATION AND HETEROTYPIC NUCLEOSOMES

The localization of CENP-A at the centromere is normally controlled by HJURP. Thus, consistently, when HJURP is overexpressed, the increased levels of CENP-A that ensue result in an exclusive accumulation at the centromere, without ectopic localization (Filipescu et al., 2017). Strikingly though,

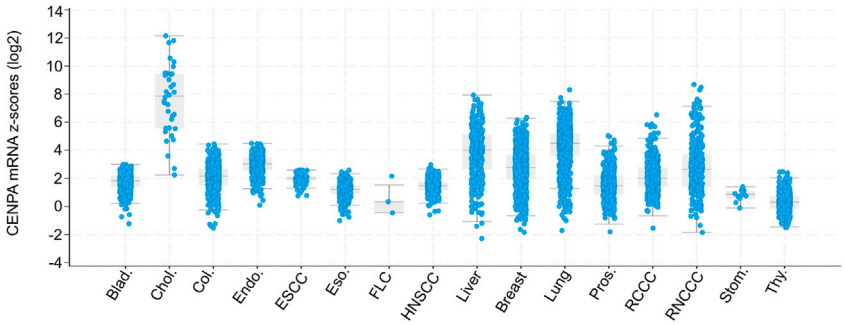


FIGURE 2 | Box and dot plots indicating CENPA expression in patient tumors relative to normal samples (z-score, log2 RNA SeqV2 RSEM). Modified from Jeffery et al., 2021. Box and dot plots indicating CENPA mRNA expression levels in patient tumors relative to normal samples (z-score, log2 RNA SeqV2 RSEM) from cBioPortal (TCGA PanCancer Atlas studies) (Cerami et al., 2012; Gao et al., 2013). The plot was generated using the cBioPortal web interface. X-axis indicates Cancer Type: Bladder Urothelial Carcinoma (Blad.), Cholangiocarcinoma (Chol.), Colorectal Adenocarcinoma (Col.), Endometrial Carcinoma (Endo.), Esophageal Squamous Cell Carcinoma (ESCC), Esophagogastric Adenocarcinoma (Eso.), Fibrolamellar Carcinoma (FLC), Head and Neck Squamous Cell Carcinoma (HNSCC), Hepatocellular Carcinoma (Liver), Invasive Breast Carcinoma (Breast), Non-Small Cell Lung Cancer (Lung), Prostate Adenocarcinoma (Pros.), Renal Clear Cell Carcinoma (RCCC), Renal Non-Clear Cell Carcinoma (RNCCC), Undifferentiated Stomach Adenocarcinoma (Stom.), Well-Differentiated Thyroid Carcinoma (Thy.). TCGA: The Cancer Genome Atlas.

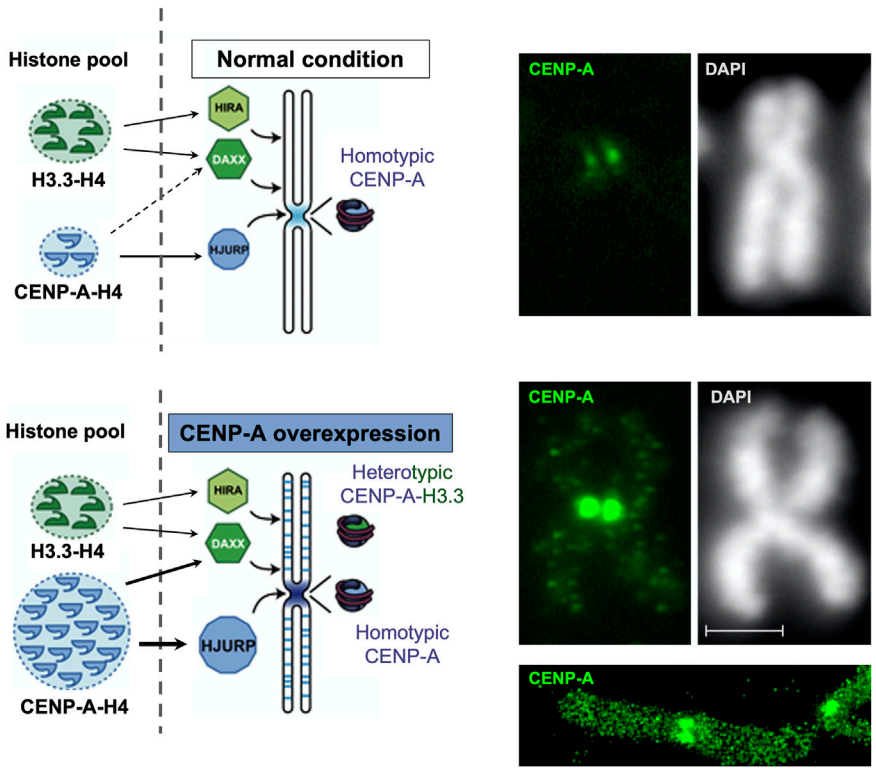


FIGURE 3 | CENP-A overexpression leads to a mislocalization to chromosome arms with formation of heterotypic nucleosomes. Modified from Lacoste et al., 2014. Left, scheme: in the normal situation (top), CENP-A is deposited specifically at the centromere by its dedicated chaperone HJURP and forms homotypic particles. Upon overexpression (bottom), CENP-A get mislocalized in the chromosome arms in a manner that depends on a H3.3 chaperone, DAXX. In these loci, the CENP-A particle is heterotypic. Right, immunofluorescence images for CENP-A detection on a mitotic chromosome compare normal (top) and CENP-A overexpressing (bottom) HeLa cells along with a DAPI staining. Scale bar = 2 μM. Below, a super-resolution image (courtesy of Tristan Piolot and Nicolas Lacoste) further illustrates the mislocalized CENP-A in chromosome arms.

exogenous overexpression or abnormal upregulation of endogenous CENP-A leads to its mislocalization at non-centromeric regions (Van Hooser et al., 2001; Gascoigne et al., 2011; Lacoste et al., 2014; Athwal et al., 2015) (**Figure 3**). This is observed for overexpression of CENP-A either constitutive (Lacoste et al., 2014; Athwal et al., 2015; Shrestha et al., 2017,

2021) or inducible (Van Hooser et al., 2001; Gascoigne et al., 2011; Shrestha et al., 2017, 2021; Jeffery et al., 2021). Interestingly, the ectopic incorporation of CENP-A is abrogated when both CENP-A and HJURP are overexpressed in a coordinated fashion, as found following p53 inactivation by the oncogene E1A (adenovirus oncoprotein) and/or HRas-V12 (Ras oncogenic mutant). In this case, while CENP-A levels increase, its localization remains exclusive to the centromere (Filipescu et al., 2017). It is tempting, based on these findings, to propose that it could be when CENP-A overexpression exceeds the one of HJURP, that its mislocalization occurs (Lacoste et al., 2014; Athwal et al., 2015; Jeffery et al., 2021). This interdependence thus illustrates the functional importance of CENP-A and HJURP partnership to restrict CENP-A localization at the centromere. In CENP-A overexpressing cells, when HJURP capacity to chaperone CENP-A gets saturated, the excess of CENP-A tends to associate with other histone H3 chaperones. Under these conditions, while HJURP still ensures a deposition of CENP-A at the centromere, the excess pool of CENP-A gets ectopically deposited within chromosome arms through a DAXX-dependent histone deposition pathway (Lacoste et al., 2014). Thus, in this case the DAXX-ATRX complex, normally responsible for depositing H3.3 at other chromatin sites [reviewed in (Ray-Gallet and Almouzni, 2021)], is diverted to compensate for a saturation of HJURP. Other H3 chaperones like the HIRA complex have also been proposed to act as a means to compensate for CENP-A overexpression (Nye et al., 2018). The strict selectivity of histone-chaperone partners is thus weakened with unbalanced levels of CENP-A. Thus, reestablishing a correct balance between levels of HJURP and CENP-A can preclude ectopic assembly of CENP-A by H3.3 chaperones (Nye et al., 2018).

In addition to mislocalization, the excess of CENP-A which is ectopically incorporated show distinct properties in the corresponding nucleosomal core particles. Whereas at centromeric loci, homotypic particles with two CENP-A-H4 dimers form as $(CENP\text{-}A\text{-}H4)_2$ tetramers, at ectopic loci, heterotypic nucleosomes combining both CENP-A and H3 variant are observed (CENP-A-H4,H3.3-H4) (Lacoste et al., 2014). Accumulation of ectopic CENP-A particles is mainly observed at sites of high histone turnover (Lacoste et al., 2014; Mahlke and Nechemia-Arbely, 2020) such as active promoters and enhancers (Lacoste et al., 2014), as well as subtelomeric and pericentromeric regions (Athwal et al., 2015; Nye et al., 2018). Moreover, ectopic CENP-A has also be found over CTCF binding sites, precluding proper CTCF localization at these sites (Lacoste et al., 2014). Given the importance of CTCF in 3D genome organization, how these CTCF displacements may impact chromatin architecture in the nucleus should be explored.

IMPACT OF CENP-A OVEREXPRESSION ON KINETOCHORE AND CHROMOSOME SEGREGATION

Assembling all components of the kinetochore is an important property of CENP-A to ensure a proper centromere function (Liu et al., 2006; Fachinetti et al., 2013). A major issue is thus to determine what happens at sites where CENP-A is mislocalized when overexpressed, since, in theory, this could potentially lead to the formation of neocentromeres competing with the original centromere. In fact, in human cells, ectopic CENP-A recruits only a subset of kinetochore proteins, namely CENP-C, CENP-N and the Mis18 complex (Van Hooser et al., 2001; Gascoigne et al., 2011; Lacoste et al., 2014), whereas the NDC80 complex has not been found. Therefore, overexpressing CENP-A is not sufficient to form stable neocentromeres in human cells. Since active neocentromere formation only occurs following inactivation of an endogenous centromere (Marshall et al., 2008), as long as the endogenous centromere is functional it may prevent the possibility for neocentromere to form. Indeed, following inactivation of endogenous centromere, ectopic CENP-A is capable of seeding stable neocentromere formation (Shang et al., 2013). Recently, Murillo-Pineda et al., using a CRISPR-Cas9 approach to remove the initial centromeric region from a copy of chromosome 4 in human retinal pigment epithelium cells, observed the spontaneous formation of a neocentromere correlating with CENP-A seeding and eviction of H3K9me3 (Carty and Dunleavy, 2021; Murillo-Pineda et al., 2021). These data support an important role of non-centromeric CENP-A deposition in neocentromere formation. However, conversely, the ectopic CENP-A traps a series of kinetochore components such as CENP-C, CENP-T and Nuf2 (a member of the Ndc80 complex) away from native centromeres, resulting in their weakening (Shrestha et al., 2017, 2021). Thus, these human cells exhibit mitotic defects such as lagging chromosomes, micronuclei formation, abnormal mitotic exit, and overall aneuploidy with karyotypic heterogeneity (Amato et al., 2009; Athwal et al., 2015; Shrestha et al., 2017, 2021). Of note, many of these chromosome segregation defects are suppressed when DAXX is depleted from CENP-A overexpressing cells (Shrestha et al., 2017, 2021). Altogether, these data indicate that ectopic incorporation of CENP-A into chromosome arms due to CENP-A overexpression represents a major source of mitotic stress that results in chromosomal instability (CIN) and aneuploidy. This in turn can lead to a large heterogeneity in the derived cell populations.

CENP-A OVEREXPRESSION AND CELL FATE REPROGRAMMING

Since chromatin states have been associated with transcription regulation and cell fate, it is important to understand how CENP-A overexpression and its impact on chromatin could impact transcription and cell fate. Cancer cells generally activate transcriptional programs that ensure an upregulation of both core kinetochore components and genes required for cell cycle progression and DNA replication (Thiru et al., 2014). Analysis of gene expression dynamics associated with CENP-A overexpression showed major changes in most genes involved in cell-cycle progression, apoptosis, DNA repair and RNA metabolism (Li et al., 2011; Sun et al., 2016; Jeffery et al., 2021). Interestingly, hotspots of ectopic CENP-A genomic localization had documented

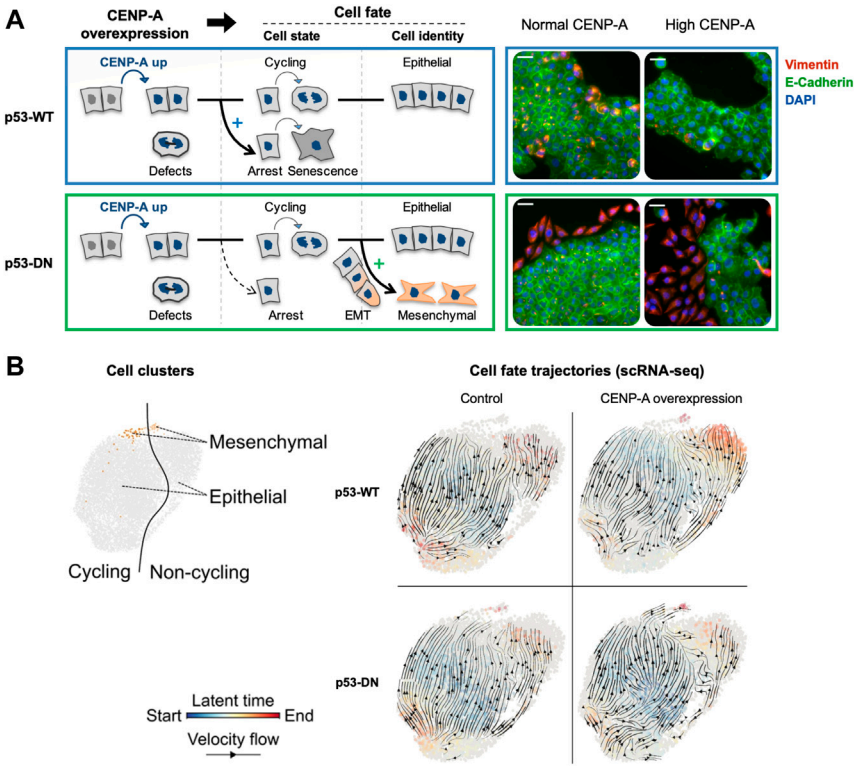


FIGURE 4 | CENP-A overexpression promotes distinct cell fates depending on p53 status. Modified from Jeffery et al., 2021. **(A)** Scheme summarizing the consequences of CENP-A overexpression (in blue) on cell state and identity, in wild-type p53 (p53-WT, top panel blue) and p53-defective cells (p53-DN, dominant negative, bottom panel green). IF images show representative max intensity projections after 34 days with or without continuous CENP-A overexpression. DAPI (blue), E-cadherin (green, epithelial marker), and vimentin (red, mesenchymal marker). Scale bars = 40 μM. **(B)** Cell fate trajectories inferred by RNA velocity analysis of scRNA-seq samples. RNA velocities (black arrows) were calculated for each condition by stochastic modeling in individual samples. Each cell is colored by the estimated latent time from initial (blue, start) to terminal states (red, end).

transcriptional start sites of genes, like CDC25C (Saha et al., 2020) and the oncogene MYC (Athwal et al., 2015). Furthermore, CENP-A mislocalization to the MYCN locus showed strong correlation with the amplification and overexpression of MYC (Nye et al., 2018). In addition, as mentioned above, aberrant CENP-A nucleosomes can occlude CTCF binding sites (Lacoste et al., 2014). This is particularly relevant when considering that the binding of CTCF is frequently altered in cancer and associated with tumorigenicity (Kemp et al., 2014; Katainen et al., 2015; Marshall et al., 2017; Aitken et al., 2018). However, while CENP-A overexpression could push/facilitate a transition for cells to progress towards cancer, alone, its overexpression does not affect proliferation rate and is not sufficient for tumorigenic transformation, even with a loss of p53 function (Filipescu et al., 2017). Thus, the impact of CENP-A overexpression is likely to operate in combination with other events occurring during oncogenesis and be dependent on the cellular context. A first context to consider is the difference in p53 status, and recent work examining various cellular contexts underlined the importance of the p53 status in the transcriptional reprogramming induced by CENP-A. This was achieved by comparing side by side, p53-WT cells and a counterpart where p53 status is altered with a dominant negative p53 (p53-DN). In the p53-WT cells, CENP-A upregulation could promote cell cycle exit and senescence whereas, in p53-defective cells, the shift from cycling to non-cycling cells was reduced and CENP-A overexpression lead to the emergence of a subpopulation of cells with downregulated epithelial genes but upregulated mesenchymal genes (Jeffery et al., 2021) (**Figure 4**). Thus, CENP-A, in a p53 dependent manner, can impact cell fate in two major ways: first with respect to cell cycle by evading from a senescence program, and second by promoting a cellular reprogramming favoring a change of cell identity, namely the epithelial-mesenchymal transition (EMT). EMT is an essential process during mammalian embryonic development and in wound healing [reviewed in (Yang et al., 2020)]. However, tumor cells hijack this process to migrate more efficiently and invade the underlying mesenchyme (Ye et al., 2017; Yang et al., 2020). Thus, in cancer, EMT has been associated with invasion, metastasis, and resistance to therapy [reviewed in (Yang et al., 2020)]. Similarly, high CENP-A levels correlate strongly with tumor aggressiveness, increased invasiveness and metastasis in cancer patient data (Ma et al., 2003; McGovern et al., 2012; Gu et al., 2014; Sun et al., 2016; Zhang et al., 2016; Saha et al., 2020). Of note, a recent study also linked CENP-A overexpression to invasion and metastasis via activation of the β-catenin pathway in clear cell renal cell

carcinoma (Wang et al., 2021). In cell culture, CENP-A overexpression has been associated with reduced expression of cell adhesion genes and higher cell invasion (Shrestha et al., 2021). Thus, the induction of EMT could explain the invasiveness and metastasis capacity of particular tumors overexpressing CENP-A. It will be important in the future to elucidate the exact mechanisms and pathways underlying EMT activation promoted by CENP-A. Indeed, CENP-A overexpression alone is not sufficient to induce EMT in any p53-defective cell line (Jeffery et al., 2021), only certain cells can undergo these transitions. Whether the effect on gene expression requires a certain threshold of CENP-A overexpression or is cell-type specific remains to be established. An attractive hypothesis to test is that CENP-A overexpression would function in the context of cells already in transition (e.g., cells in tumorigenic progression). Indeed, its targeting in active regions could particularly alter gene expression where both CTCF and the presence or absence of specific histone variants play a critical role (Goldberg et al., 2010; Szenker et al., 2012). The current emerging view is that CENP-A would help to maintain/stabilize the population of cells transitioning. How this is actually operating mechanistically remains to be determined. It is tempting to consider as well how CENP-A changes could impact the organization of the genome within the nucleus to possibly contribute to changes in gene expression and function, thus affecting cell fate (Krijger and de Laat, 2013; Bonev and Cavalli, 2016; Fritz et al., 2019). However, this latter aspect has not yet been examined.

CENP-A NUCLEAR DISTRIBUTION IN HEALTH AND CANCER

In the interphase nucleus, chromosomes are non-randomly arranged within the nuclear space. They are structurally and functionally organized into territories, and this nuclear organization is generally altered in cancer (Lever and Sheer, 2010; Zaidi et al., 2018; Mai, 2019). Notably, centromeres occupy particular subnuclear domains in interphase nuclei [review in (Muller et al., 2019)]. Within this organization, the DNA-binding protein CENP-B favors loops between DNA repeats (Chardon et al., 2022). These subnuclear localization of centromeres provide information that can be followed according to the cell fate and differentiation (Jansz and Torres-Padilla, 2019; Schlesinger and Meshorer, 2019; Feodorova et al., 2020). To date, however, much of our knowledge comes from data collected in mammalian cultured cells. In these proliferating cells, CENP-A marks the centromere of the mitotic chromosomes and, during interphase, these marks are detected as numerous foci dispersed throughout the nucleus (Dunleavy et al., 2009; Lacoste et al., 2014; Verrelle et al., 2021). Importantly, these cultured cells derived from tumors provide a CENP-A localization in interphase that cannot necessarily reflect the situation in normal cells. Indeed, in normal human primary lymphocytes, the visualization of centromeres both by FISH (Skalníková et al., 2000; Weierich et al., 2003) and CENP-A staining (Weimer et al., 1992; Alcobia et al., 2000) provided very defined nuclear patterns quite distinct from the tumoral cells. Furthermore, in the cell nuclei of human normal solid tissues, CENP-A is detected in 9–18 foci corresponding to the clustering of the centromeres from 2 to 5 distinct chromosomes. These foci, homogenous in size and shape, localize equidistantly at the nuclear periphery and, in fewer cases, at the periphery of the nucleolus (**Figure 5**) (Verrelle et al., 2021). This very distinct organization represents a general feature shared by distinct cell types originating from various progenitors and along various different differentiation pathways irrespective of the fact that cells could be circulating or in tissues. Thus, in line with the hypothesis that centromeric regions are robust and stable chromosomal loci (Krijger and de Laat, 2013), CENP-A labelling as foci at the nuclear periphery reflects a fundamental feature of centromeres organization and distribution in healthy cells. By contrast, in human tumor tissues, this discrete CENP-A subnuclear localization is drastically altered and, for invasive neoplastic lesions, similar to that detected in the cultured cell lines of tumoral origin (Verrelle et al., 2021). Interestingly, CENP-A subnuclear localization in breast lesions reveals distinct information. In healthy tissues, the normal reference pattern compares to benign lesions (Verrelle et al., 2021). By contrast, in neoplastic lesions, CENP-A foci localization in a regular distribution at the nuclear periphery is disrupted and clustering is altered or lost (smaller and many more foci) (**Figure 5**). Furthermore, the loss of CENP-A foci localization at the nuclear periphery with a high heterogeneity in terms of number, size, and shape within the nuclear volume can readily discriminate invasive from non-invasive neoplastic lesions. These major global change of centromere and nuclear organization in cancer reported recently (Verrelle et al., 2021) have not yet been related to ectopic localization of CENP-A in cancer (Lacoste et al., 2014). How these changes during oncogenic transformation and progression could possibly relate thus remains to be assessed. Notably, tumor grade is reported to combine major perturbations that can lead to genome chaos (Liu et al., 2014). This destabilizing context might reach a threshold above which normal centromeric loci and CENP-A nuclear organization cannot be maintained. Whether the change of CENP-A subnuclear localization in tumor cells/tissues is a cause or a consequence of oncogenesis remains an open question (Maison et al., 2010; Finn and Misteli, 2019; Muller et al., 2019). Given that the mechanisms involved in the clustering of centromeres and their link with the control of nuclear organization are yet to be discovered, the mechanisms contributing to the maintenance loss of CENP-A nuclear organization during tumorigenesis represent an exciting avenue to explore.

CLINICAL INTEREST FOR CENP-A IN CANCER TREATMENT

Elevated CENP-A levels correlate with cancer progression (Ma et al., 2003; Li et al., 2011; Qiu et al., 2013; Sun et al., 2016) and poor patient outcome (Ma et al., 2003; Li et al., 2011; McGovern et al., 2012; Wu

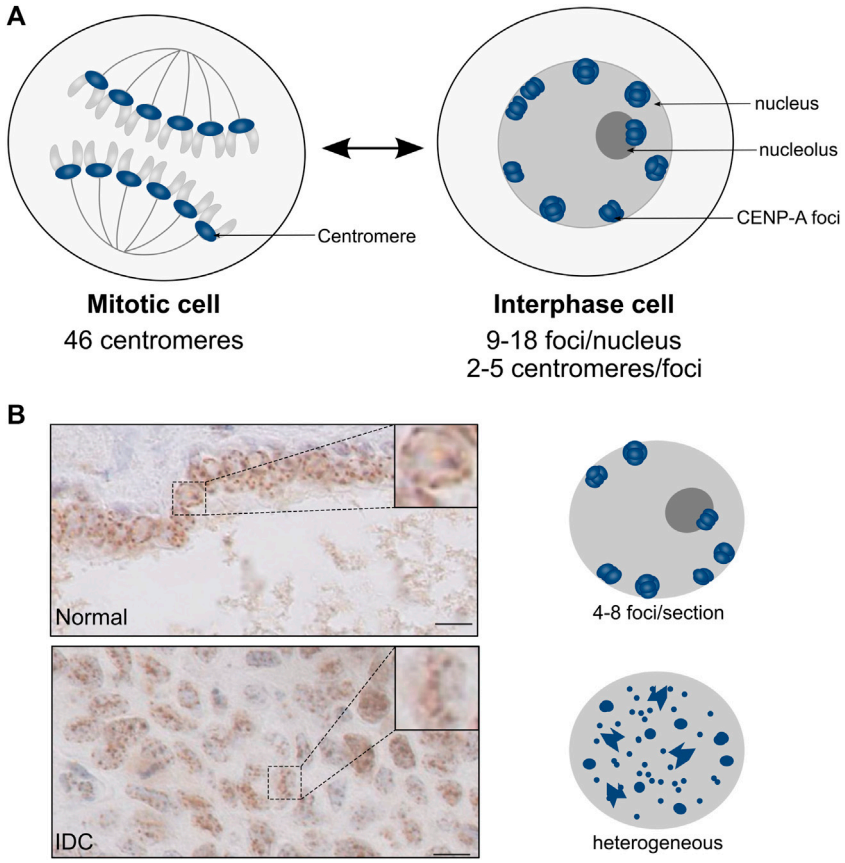


FIGURE 5 | CENP-A localization patterns in normal tissues and neoplastic lesions. Modified from Verrelle et al., 2021. **(A)** Schematic representation of nuclei from mitosis (left) and interphase (right) cells. In interphase cells, the clustering of centromeric CENP-A-enriched regions (blue) gives rise to CENP-A foci at the periphery of the nucleus and, in fewer cases, of the nucleolus. **(B)** CENP-A localization patterns visualized by IHC in breast tissues. Top: Normal duct; Bottom: Invasive Ductal Carcinoma (IDC). The boxed area shows the magnification of a representative nucleus. Scale bar = 10 μM. On the right is shown a schematic representation of the CENP-A localization pattern, with CENP-A foci (blue) within the nucleus (grey).

et al., 2012; Qiu et al., 2013; Gu et al., 2014; Sun et al., 2016; Zhang et al., 2016; Saha et al., 2020). This correlation could reflect the CENP-A-induced CIN that leads to an increase in chromosomal rearrangements and mutagenesis rate, which both increase the heterogeneity of the cell population, thereby promoting the selection of advantageous clones. An alternative explanation could relate to the essential role of CENP-A in mitotic progression (Dunleavy et al., 2009; Foltz et al., 2009; Fachinetti et al., 2013; Filipescu et al., 2017). Following malignant transformation, hyperproliferative cells require sufficient expression of CENP-A along with its chaperone HJURP to ensure a proper CENP-A deposition enabling accurate chromosome segregation (Filipescu et al., 2017). This has led to the hypothesis according which such cells become "addicted" to CENP-A (Filipescu et al., 2017). In line with this hypothesis, in cancer cells overexpressing CENP-A, its depletion suppresses cell growth both *in vitro* and *in vivo*, blocks cell-cycle progression, and promotes apoptosis (Li et al., 2011). Similarly, CENP-A partial depletion (Li et al., 2011; Wu et al., 2014) reduces proliferation, growth, migration, and invasiveness of cancer cells. Thus, CENP-A is required for tumor progression and its depletion may have anticancer effects which are likely mediated by genes involved in cell cycle control and apoptosis (Li et al., 2011; Wu et al., 2014). These two reports using cancer cell models show promising potential for targeting CENP-A as a cancer therapeutic, as an Achille's heel in addicted cells.

While CENP-A is generally associated with tumor aggressiveness, the correlation of high CENP-A levels with clear therapeutic response is not simple. Indeed, while a reduced therapeutic response is reported when CENP-A is overexpressed in osteosarcoma (Gu et al., 2014), some reports in breast (McGovern et al., 2012; Sun et al., 2016; Zhang et al., 2016) and lung (Zhang et al., 2016) cancers indicate a better clinical outcome. These discrepancies might reflect different cancer types/sub-types, various population of cells, possible heterogeneity in the samples and the methods of analyzing the therapeutic response. Considering the importance of the cellular context upon CENP-A overexpression, the p53 status clearly represented an important parameter to consider specifically (see discussion above). Indeed, CENP-A overexpression impacts cellular response to genotoxic stress, increasing the survival of p53-defective cells in the presence of DNA damage induced by a topoisomerase inhibitor (Lacoste et al., 2014). In addition, CENP-A overexpression strongly increases sensitivity to X-ray irradiation

of several p53-WT cell lines but not of p53-defective cell lines (Jeffery et al., 2021). Importantly, the inactivation of p53 is sufficient to counteract the CENP-A induced radio-sensitivity phenotype (Jeffery et al., 2021). Thus, CENP-A acts as a double-edged sword: its overexpression enhances radio-sensitivity in cells with wild type p53, however, p53-defective cells show a more tolerant state to X-ray irradiation. This exemplifies how CENP-A overexpression could lead to either sensitivity or resistance to treatment depending on the p53 status. These findings highlight the importance of integrating the p53 status when considering CENP-A for cancer treatment. Indeed, while tumors displaying high CENP-A levels in a wild-type p53 context would respond to radiotherapy, to treat tumors with defective p53 alternative options should be considered. These could include drugs that can recover an active p53 in combination with radiotherapy, and/or other DNA damaging agents. Importantly, a number of p53-targeted drugs are now being tested in clinical trials (Blandino and Di Agostino, 2018; Bykov et al., 2018), including direct reactivators of mutant p53 (e.g. PRIMA-1MET/APR-246) and drugs designed to return functionality to wild-type p53 by inhibiting its upstream regulators (e.g. MDM2/X inhibitors) (Sanz et al., 2019). Interestingly, despite the impact on transcription of genes associated with DNA repair, CENP-A overexpression did not affect the rate of DNA repair (Jeffery et al., 2021), suggesting that sensitization or resistance observed is not related to repair efficiency.

Whether CENP-A can serve as a biomarker to improve stratification of cancer patients is also a crucial question. CENP-A overexpression has already been used as a general biomarker of poor patient prognosis and as a predictive biomarker for chemotherapy (Ma et al., 2003; Sun et al., 2016; Zhang et al., 2016). It has been proposed as a biomarker for tumor aggressiveness in ovarian (Qiu et al., 2013), osteosarcoma (Gu et al., 2014), lung (Wu et al., 2012; Liu et al., 2018), and breast estrogen receptor positive (McGovern et al., 2012; Montes de Oca et al., 2015) cancers. Interestingly, in breast cancer, identifying high levels of the CENP-A chaperone, HJURP, has been proposed as a prognostic marker of poor patient outcome, distinguishing aggressive tumors within the luminal A subtype (Montes de Oca et al., 2015). In addition to the use of CENP-A level, measured as a total amount in a bulk population to serve as a biomarker, given the discrete pattern observed, its nuclear distribution should also be considered. Indeed, CENP-A nuclear localization pattern in patient samples allows to directly interrogate the chromatin architecture in the nucleus by following centromeres and in breast could reveal changes between healthy, non-neoplastic and neoplastic lesions (Verrelle et al., 2021). CENP-A subnuclear pattern could also reveal clear alterations in chromatin architecture in the nucleus associated with resistance to treatments. The application of this strategy in head and neck squamous cell carcinoma (HNSCC) enabled to reveal a nuclear CENP-A localization pattern assessed by immunohistochemistry, as a predictive marker of local disease control at 2 years by concurrent chemoradiation therapy (CCRT) with 96% accuracy (Verrelle et al., 2021). This distinct CENP-A pattern, termed "Pattern-C" provided a strong prognostic marker of overall survival advantage, outperforming all other tumor characteristics usually examined including proliferation, HPV status and tumor stage. Given the general nature of CENP-A subnuclear patterns across tissues, extending the use of this simple staining method to predict sensitivity to concurrent chemoradiation may prove of interest for other cancers treated with genotoxic agents.

CONCLUDING REMARKS

CENP-A is key for centromere function, a chromosome region with a fundamental role in cell division. However, recent work has demonstrated that beyond its centromeric role in mitosis, CENP-A may be related to tumor status through an impact on chromatin organization in interphase. We have presented recent studies concerning the regulation of CENP-A, and how aberrant expression affects mammalian cells in the context of cancer. The role of CENP-A in cancer progression is multifaceted, affecting both genome integrity and transcriptional reprogramming. These changes facilitate cancer progression and the acquisition of properties promoting metastasis. Furthermore, CENP-A levels could contribute to guiding therapy choice, notably when taking p53 status into account. Interestingly, in addition, CENP-A subnuclear pattern visualized on tissue sections represents a biomarker of potential prognostic value. Future work with new technological advances enabling to follow at a single cell level an integrated analysis of proteins, transcripts and spatial distribution in a tissue should help to further characterize the molecular mechanisms underlying the connections between CENP-A and cancer.

AUTHOR CONTRIBUTIONS

GA defined the scope of the review in interactions with CR-P, J-PQ, and ML. CR-P wrote the draft of the manuscript and prepared figures with inputs from GA and J-PQ. J-PQ and ML wrote subsections of the manuscript. J-PQ and GA reviewed and edited the manuscript and figures. All authors contributed to manuscript revision, read, and approved the submitted version.

FUNDING

Our work is supported by the fundings from la Ligue Nationale contre le Cancer (labellisation), Labex DEEP-PSL (ANR-11-LABX-0044_DEEP, ANR-10-IDEX-0001-02), ERC-2015-ADG-694694 ChromADICT. CR-P PhD is funded by SU. ML has been funded on the ERC and the ARC.

ACKNOWLEDGMENTS

We thank Shauna Katz for critical reading as well as the Chromatin Dynamics team for their advice.

REFERENCES

Aitken, S. J., Ibarra-Soria, X., Kentepozidou, E., Flicek, P., Feig, C., Marioni, J. C., et al. (2018). CTCF Maintains Regulatory Homeostasis of Cancer Pathways | Genome Biology. Available at: https://genomebiology.biomedcentral.com/articles/10.1186/s13059-018-1484-3 (Accessed January 19, 2022).

Alcobia, I., Dilão, R., and Parreira, L. (2000). Spatial Associations of Centromeres in the Nuclei of Hematopoietic Cells: Evidence for Cell-type-specific Organizational Patterns. *Blood* 95, 1608–1615. doi:10.1182/blood.v95.5.1608.005k32_1608_1615

Ali-Ahmad, A., Bilokapić, S., Schäfer, I. B., Halić, M., and Sekulić, N. (2019). CENP-C Unwraps the Human CENP-A Nucleosome through the H2A C-Terminal Tail. *EMBO Rep.* 20, e48913. doi:10.15252/embr.201948913

Allu, P. K., Dawicki-McKenna, J. M., Van Eeuwen, T., Slavin, M., Braitbard, M., Xu, C., et al. (2019). Structure of the Human Core Centromeric Nucleosome Complex. *Curr. Biol.* 29, 2625–2639. e5. doi:10.1016/j.cub.2019.06.062

Amato, A., Schillaci, T., Lentini, L., and Di Leonardo, A. (2009). CENPA Overexpression Promotes Genome Instability in pRb-Depleted Human Cells. *Mol. Cancer* 8, 119. doi:10.1186/1476-4598-8-119

Amor, D. J., Bentley, K., Ryan, J., Perry, J., Wong, L., Slater, H., et al. (2004). Human Centromere Repositioning "in Progress". *Proc. Natl. Acad. Sci. U.S.A.* 101, 6542–6547. doi:10.1073/pnas.0308637101

Arimura, Y., Tachiwana, H., Takagi, H., Hori, T., Kimura, H., Fukagawa, T., et al. (2019). The CENP-A Centromere Targeting Domain Facilitates H4K20 Monomethylation in the Nucleosome by Structural Polymorphism. *Nat. Commun.* 10, 576. doi:10.1038/s41467-019-08314-x

Ariyoshi, M., Makino, F., Watanabe, R., Nakagawa, R., Kato, T., Namba, K., et al. (2021). Cryo-EM Structure of the CENP-A Nucleosome in Complex with Phosphorylated CENP-C. *EMBO J.* 40, e105671. doi:10.15252/embj.2020105671

Athwal, R. K., Walkiewicz, M. P., Baek, S., Fu, S., Bui, M., Camps, J., et al. (2015). CENP-A Nucleosomes Localize to Transcription Factor Hotspots and Subtelomeric Sites in Human Cancer Cells. *Epigenetics Chromatin* 8. doi:10.1186/1756-8935-8-2

Barnhart, M. C., Kuich, P. H. J. L., Stellfox, M. E., Ward, J. A., Bassett, E. A., Black, B. E., et al. (2011). HJURP Is a CENP-A Chromatin Assembly Factor Sufficient to Form a Functional De Novo Kinetochore. *J. Cell Biol.* 194, 229–243. doi:10.1083/jcb.201012017

Bassett, E. A., DeNizio, J., Barnhart-Dailey, M. C., Panchenko, T., Sekulic, N., Rogers, D. J., et al. (2012). HJURP Uses Distinct CENP-A Surfaces to Recognize and to Stabilize CENP-A/histone H4 for Centromere Assembly. *Dev. Cell* 22, 749–762. doi:10.1016/j.devcel.2012.02.001

Blandino, G., and Di Agostino, S. (2018). New Therapeutic Strategies to Treat Human Cancers Expressing Mutant P53 Proteins. *J. Exp. Clin. Cancer Res.* 37, 30. doi:10.1186/s13046-018-0705-7

Bonev, B., and Cavalli, G. (2016). Organization and Function of the 3D Genome. *Nat. Rev. Genet.* 17, 661–678. doi:10.1038/nrg.2016.112

Bykov, V. J. N., Eriksson, S. E., Bianchi, J., and Wiman, K. G. (2018). Targeting Mutant P53 for Efficient Cancer Therapy. *Nat. Rev. Cancer* 18, 89–102. doi:10.1038/nrc.2017.109

Carty, B. L., and Dunleavy, E. (2021). *Truly Epigenetic: A Centromere Finds a "Neo" Home | Journal of Cell Biology*. Rockefeller University Press. Available at: https://rupress.org/jcb/article/220/3/e202101027/211780/Truly-epigenetic-A-centromere-finds-a-neo (Accessed January, 19, 2022).

Cerami, E., Gao, J., Dogrusoz, U., Gross, B. E., Sumer, S. O., Aksoy, B. A., et al. (2012). The cBio Cancer Genomics Portal: An Open Platform for Exploring Multidimensional Cancer Genomics Data: Figure 1. *Cancer Discov.* 2, 401–404. doi:10.1158/2159-8290.CD-12-0095

Chardon, F., Japaridze, A., Witt, H., Velikovsky, L., Chakraborty, C., Wilhelm, T., et al. (2022). CENP-B-mediated DNA Loops Regulate Activity and Stability of Human Centromeres. *Mol. Cell* 82, 1751–1767. doi:10.1016/j.molcel.2022.02.032

Chen, X., Müller, G. A., Quaas, M., Fischer, M., Han, N., Stutchbury, B., et al. (2013). The Forkhead Transcription Factor FOXM1 Controls Cell Cycle-dependent Gene Expression through an Atypical Chromatin Binding Mechanism. *Mol. Cell. Biol.* 33, 227–236. doi:10.1128/MCB.00881-12

Dambacher, S., Deng, W., Hahn, M., Sadic, D., Fröhlich, J., Nuber, A., et al. (2012). CENP-C Facilitates the Recruitment of M18BP1 to Centromeric Chromatin. *Nucleus* 3, 101–110. doi:10.4161/nucl.18955

Dunleavy, E. M., Almouzni, G., and Karpen, G. H. (2011). H3.3 Is Deposited at Centromeres in S Phase as a Placeholder for Newly Assembled CENP-A in G1phase. *Nucleus* 2, 146–157. doi:10.4161/nucl.2.2.15211

Dunleavy, E. M., Roche, D., Tagami, H., Lacoste, N., Ray-Gallet, D., Nakamura, Y., et al. (2009). HJURP Is a Cell-Cycle-dependent Maintenance and Deposition Factor of CENP-A at Centromeres. *Cell* 137, 485–497. doi:10.1016/j.cell.2009.02.040

Earnshaw, W. C., and Rothfield, N. (1985). Identification of a Family of Human Centromere Proteins Using Autoimmune Sera from Patients with Scleroderma. *Chromosoma* 91, 313–321. doi:10.1007/BF00328227

Engeland, K. (2018). Cell Cycle Arrest through Indirect Transcriptional Repression by P53: I Have a DREAM. *Cell Death Differ.* 25, 114–132. doi:10.1038/cdd.2017.172

Fachinetti, D., Diego Folco, H., Nechemia-Arbely, Y., Valente, L. P., Nguyen, K., Wong, A. J., et al. (2013). A Two-step Mechanism for Epigenetic Specification of Centromere Identity and Function. *Nat. Cell Biol.* 15, 1056–1066. doi:10.1038/ncb2805

Feodorova, Y., Falk, M., Mirny, L. A., and Solovei, I. (2020). Viewing Nuclear Architecture through the Eyes of Nocturnal Mammals. *Trends Cell Biol.* 30, 276–289. doi:10.1016/j.tcb.2019.12.008

Filipescu, D., Naughtin, M., Podsypanina, K., Lejour, V., Wilson, L., Gurard-Levin, Z. A., et al. (2017). Essential Role for Centromeric Factors Following P53 Loss and Oncogenic Transformation. *Genes Dev.* 31, 463–480. doi:10.1101/gad.290924.116

Finn, E. H., and Misteli, T. (2019). Molecular Basis and Biological Function of Variability in Spatial Genome Organization. *Science* 365, eaaw9498. doi:10.1126/science.aaw9498

Fischer, M., Grossmann, P., Padi, M., and DeCaprio, J. A. (2016). Integration of TP53, DREAM, MMB-FOXM1 and RB-E2f Target Gene Analyses Identifies Cell Cycle Gene Regulatory Networks. *Nucleic Acids Res.* 44, 6070–6086. doi:10.1093/nar/gkw523

Foltz, D. R., Jansen, L. E. T., Bailey, A. O., Yates, J. R., Bassett, E. A., Wood, S., et al. (2009). Centromere-Specific Assembly of CENP-A Nucleosomes Is Mediated by HJURP. *Cell* 137, 472–484. doi:10.1016/j.cell.2009.02.039

Fritz, A. J., Sehgal, N., Pliss, A., Xu, J., and Berezney, R. (2019). Chromosome Territories and the Global Regulation of the Genome. *Genes. Chromosom. Cancer* 58, 407–426. doi:10.1002/gcc.22732

Gao, J., Aksoy, B. A., Dogrusoz, U., Dresdner, G., Gross, B., Sumer, S. O., et al. (2013). Integrative Analysis of Complex Cancer Genomics and Clinical Profiles Using the cBioPortal. *Sci. Signal.* 6. doi:10.1126/scisignal.2004088

Gascoigne, K. E., Takeuchi, K., Suzuki, A., Hori, T., Fukagawa, T., and Cheeseman, I. M. (2011). Induced Ectopic Kinetochore Assembly Bypasses the Requirement for CENP-A Nucleosomes. *Cell* 145, 410–422. doi:10.1016/j.cell.2011.03.031

Goldberg, A. D., Banaszynski, L. A., Noh, K.-M., Lewis, P. W., Elsaesser, S. J., Stadler, S., et al. (2010). Distinct Factors Control Histone Variant H3.3 Localization at Specific Genomic Regions. *Cell* 140, 678–691. doi:10.1016/j.cell.2010.01.003

Gu, X.-M., Fu, J., Feng, X.-J., Huang, X., Wang, S.-M., Chen, X.-F., et al. (2014). Expression and Prognostic Relevance of Centromere Protein A in Primary Osteosarcoma. *Pathology - Res. Pract.* 210, 228–233. doi:10.1016/j.prp.2013.12.007

Hasson, D., Panchenko, T., Salimian, K. J., Salman, M. U., Sekulic, N., Alonso, A., et al. (2013). The Octamer Is the Major Form of CENP-A Nucleosomes at Human Centromeres. *Nat. Struct. Mol. Biol.* 20, 687–695. doi:10.1038/nsmb.2562

Hickman, E., Moroni, M. C., and Helin, K. (2002). The Role of P53 and pRB in Apoptosis and Cancer. *Curr. Opin. Genet. Dev.* 12, 60–66. doi:10.1016/S0959-437X(01)00265-9

Hori, T., Amano, M., Suzuki, A., Backer, C. B., Welburn, J. P., Dong, Y., et al. (2008). CCAN Makes Multiple Contacts with Centromeric DNA to Provide Distinct Pathways to the Outer Kinetochore. *Cell* 135, 1039–1052. doi:10.1016/j.cell.2008.10.019

Jansen, L. E. T., Black, B. E., Foltz, D. R., and Cleveland, D. W. (2007). Propagation of Centromeric Chromatin Requires Exit from Mitosis. *J. Cell Biol.* 176, 795–805. doi:10.1083/jcb.200701066

Jansz, N., and Torres-Padilla, M.-E. (2019). Genome Activation and Architecture in the Early Mammalian Embryo. *Curr. Opin. Genet. Dev.* 55, 52–58. doi:10.1016/j.gde.2019.04.011

Jeffery, D., Gatto, A., Podsypanina, K., Renaud-Pageot, C., Ponce Landete, R., Bonneville, L., et al. (2021). CENP-A Overexpression Promotes Distinct Fates in Human Cells, Depending on P53 Status. *Commun. Biol.* 4, 1–18. doi:10.1038/s42003-021-01941-5

Katainen, R., Dave, K., Pitkänen, E., Palin, K., Kivioja, T., Välimäki, N., et al. (2015). CTCF/cohesin-binding Sites Are Frequently Mutated in Cancer. *Nat. Genet.* 47, 818–821. doi:10.1038/ng.3335

Kemp, C. J., Moore, J. M., Moser, R., Bernard, B., Teater, M., Smith, L. E., et al. (2014). CTCF Haploinsufficiency Destabilizes DNA Methylation and Predisposes to Cancer. *Cell Rep.* 7, 1020–1029. doi:10.1016/j.celrep.2014.04.004

Krijger, P. H., and de Laat, W. (2013). Identical Cells with Different 3D Genomes; Cause and Consequences? *Curr. Opin. Genet. Dev.* 23, 191–196. doi:10.1016/j.gde.2012.12.010

Lacoste, N., Woolfe, A., Tachiwana, H., Garea, A. V., Barth, T., Cantaloube, S., et al. (2014). Mislocalization of the Centromeric Histone Variant CenH3/CENP-A in Human Cells Depends on the Chaperone DAXX. *Mol. Cell* 53, 631–644. doi:10.1016/j.molcel.2014.01.018

Lagana, A., Dorn, J. F., De Rop, V., Ladouceur, A.-M., Maddox, A. S., and Maddox, P. S. (2010). A Small GTPase Molecular Switch Regulates Epigenetic Centromere Maintenance by Stabilizing Newly Incorporated CENP-A. *Nat. Cell Biol.* 12, 1186–1193. doi:10.1038/ncb2129

Lever, E., and Sheer, D. (2010). The Role of Nuclear Organization in Cancer. *J. Pathol.* 220, 114–125. doi:10.1002/path.2651

Li, Y., Zhu, Z., Zhang, S., Yu, D., Yu, H., Liu, L., et al. (2011). ShRNA-Targeted Centromere Protein A Inhibits Hepatocellular Carcinoma Growth. *PLOS ONE* 6, e17794. doi:10.1371/journal.pone.0017794

Liu, G., Stevens, J., Horne, S., Abdallah, B., Ye, K., Bremer, S., et al. (2014). Genome Chaos: Survival Strategy during Crisis. *Cell Cycle* 13, 528–537. doi:10.4161/cc.27378

Liu, S.-T., Rattner, J. B., Jablonski, S. A., and Yen, T. J. (2006). Mapping the Assembly Pathways that Specify Formation of the Trilaminar Kinetochore Plates in Human Cells. *J. Cell Biol.* 175, 41–53. doi:10.1083/jcb.200606020

Liu, W.-T., Wang, Y., Zhang, J., Ye, F., Huang, X.-H., Li, B., et al. (2018). A Novel Strategy of Integrated Microarray Analysis Identifies CENPA, CDK1 and CDC20 as a Cluster of Diagnostic Biomarkers in Lung Adenocarcinoma. *Cancer Lett.* 425, 43–53. doi:10.1016/j.canlet.2018.03.043

Ma, X.-J., Salunga, R., Tuggle, J. T., Gaudet, J., Enright, E., McQuary, P., et al. (2003). Gene Expression Profiles of Human Breast Cancer Progression. *Proc. Natl. Acad. Sci. U.S.A.* 100, 5974–5979. doi:10.1073/pnas.0931261100

Maehara, K., Takahashi, K., and Saitoh, S. (2010). CENP-A Reduction Induces a P53-dependent Cellular Senescence Response to Protect Cells from Executing Defective Mitoses. *Mol. Cell. Biol.* 30, 2090–2104. doi:10.1128/MCB.01318-09

Mahlke, M. A., and Nechemia-Arbely, Y. (2020). Guarding the Genome: CENP-A-Chromatin in Health and Cancer. *Genes* 11, 810. doi:10.3390/genes11070810

Mai, S. (2019). The Three-Dimensional Cancer Nucleus. *Genes. Chromosom. Cancer* 58, 462–473. doi:10.1002/gcc.22720

Maison, C., Quivy, J. P., Probst, A. V., and Almouzni, G. (2010). Heterochromatin at Mouse Pericentromeres: a Model for De Novo Heterochromatin Formation and Duplication during Replication. *Cold Spring Harb. Symposia Quantitative Biol.* 75, 155–165. doi:10.1101/sqb.2010.75.013

Malvezzi, F., Litos, G., Schleiffer, A., Heuck, A., Mechtler, K., Clausen, T., et al. (2013). A Structural Basis for Kinetochore Recruitment of the Ndc80 Complex via Two Distinct Centromere Receptors. *EMBO J.* 32, 409–423. doi:10.1038/emboj.2012.356

Marshall, A. D., Bailey, C. G., Champ, K., Vellozzi, M., O'Young, P., Metierre, C., et al. (2017). CTCF Genetic Alterations in Endometrial Carcinoma Are Pro-tumorigenic. *Oncogene* 36, 4100–4110. doi:10.1038/onc.2017.25

Marshall, O. J., Chueh, A. C., Wong, L. H., and Choo, K. H. A. (2008). Neocentromeres: New Insights into Centromere Structure, Disease Development, and Karyotype Evolution. *Am. J. Hum. Genet.* 82, 261–282. doi:10.1016/j.ajhg.2007.11.009

McGovern, S. L., Qi, Y., Pusztai, L., Symmans, W. F., and Buchholz, T. A. (2012). Centromere Protein-A, an Essential Centromere Protein, Is a Prognostic Marker for Relapse in Estrogen Receptor-Positive Breast Cancer. *Breast Cancer Res.* 14, R72. doi:10.1186/bcr3181

McKinley, K. L., and Cheeseman, I. M. (2014). Polo-like Kinase 1 Licenses CENP-A Deposition at Centromeres. *Cell* 158, 397–411. doi:10.1016/j.cell.2014.06.016

Mendiratta, S., Gatto, A., and Almouzni, G. (2019). Histone Supply: Multitiered Regulation Ensures Chromatin Dynamics Throughout the Cell Cycle. *J. Cell Biol.* 218, 39–54. doi:10.1083/jcb.201807179

Montes de Oca, R., Gurard-Levin, Z. A., Berger, F., Rehman, H., Martel, E., Corpet, A., et al. (2015). The Histone Chaperone HJURP Is a New Independent Prognostic Marker for Luminal A Breast Carcinoma. *Mol. Oncol.* 9, 657–674. doi:10.1016/j.molonc.2014.11.002

Moree, B., Meyer, C. B., Fuller, C. J., and Straight, A. F. (2011). CENP-C Recruits M18BP1 to Centromeres to Promote CENP-A Chromatin Assembly. *J. Cell Biol.* 194, 855–871. doi:10.1083/jcb.201106079

Moroi, Y., Peebles, C., Fritzler, M. J., Steigerwald, J., and Tan, E. M. (1980). Autoantibody to Centromere (Kinetochore) in Scleroderma Sera. *Proc. Natl. Acad. Sci. U.S.A.* 77, 1627–1631. doi:10.1073/pnas.77.3.1627

Muller, H., Gil, J., and Drinnenberg, I. A. (2019). The Impact of Centromeres on Spatial Genome Architecture. *Trends Genet.* 35, 565–578. doi:10.1016/j.tig.2019.05.003

Murillo-Pineda, M., Valente, L. P., Dumont, M., Mata, J. F., Fachinetti, D., and Jansen, L. E. T. (2021). Induction of Spontaneous Human Neocentromere Formation and Long-Term Maturation. *J. Cell Biol.* 220, e202007210. doi:10.1083/jcb.202007210

Nardi, I. K., Zasadzińska, E., Stellfox, M. E., Knippler, C. M., and Foltz, D. R. (2016). Licensing of Centromeric Chromatin Assembly through the Mis18α-Mis18β Heterotetramer. *Mol. Cell* 61, 774–787. doi:10.1016/j.molcel.2016.02.014

Nechemia-Arbely, Y., Miga, K. H., Shoshani, O., Aslanian, A., McMahon, M. A., Lee, A. Y., et al. (2019). DNA Replication Acts as an Error Correction Mechanism to Maintain Centromere Identity by Restricting CENP-A to Centromeres. *Nat. Cell Biol.* 21, 743–754. doi:10.1038/s41556-019-0331-4

Nye, J., Sturgill, D., Athwal, R., and Dalal, Y. (2018). HJURP Antagonizes CENP-A Mislocalization Driven by the H3.3 Chaperones HIRA and DAXX. *PLoS ONE* 13, e0205948. doi:10.1371/journal.pone.0205948

Palmer, D. K., O'Day, K., Trong, H. L., Charbonneau, H., and Margolis, R. L. (1991). Purification of the Centromere-specific Protein CENP-A and Demonstration that it Is a Distinctive Histone. *Proc. Natl. Acad. Sci. U.S.A.* 88, 3734–3738. doi:10.1073/pnas.88.9.3734

Palmer, D., O'Day, K., Wener, M., Andrews, B., and Margolis, R. (1987). A 17-kD Centromere Protein (CENP-A) Copurifies with Nucleosome Core Particles and with Histones. *J. Cell Biol.* 104, 805–815. doi:10.1083/jcb.104.4.805

Pan, D., Klare, K., Petrovic, A., Take, A., Walstein, K., Singh, P., et al. (2017). CDK-regulated Dimerization of M18BP1 on a Mis18 Hexamer Is Necessary for CENP-A Loading. *eLife* 6, e23352. doi:10.7554/eLife.23352

Pan, D., Walstein, K., Take, A., Bier, D., Kaiser, N., and Musacchio, A. (2019). Mechanism of Centromere Recruitment of the CENP-A Chaperone HJURP and its Implications for Centromere Licensing. *Nat. Commun.* 10, 4046. doi:10.1038/s41467-019-12019-6

Panchenko, T., Sorensen, T. C., Woodcock, C. L., Kan, Z.-y., Wood, S., Resch, M. G., et al. (2011). Replacement of Histone H3 with CENP-A Directs Global Nucleosome Array Condensation and Loosening of Nucleosome Superhelical Termini. *Proc. Natl. Acad. Sci. U.S.A.* 108, 16588–16593. doi:10.1073/pnas.1113621108

Perpelescu, M., Nozaki, N., Obuse, C., Yang, H., and Yoda, K. (2009). Active Establishment of Centromeric CENP-A Chromatin by RSF Complex. *J. Cell Biol.* 185, 397–407. doi:10.1083/jcb.200903088

Przewloka, M. R., Venkei, Z., Bolanos-Garcia, V. M., Debski, J., Dadlez, M., and Glover, D. M. (2011). CENP-C Is a Structural Platform for Kinetochore Assembly. *Curr. Biol.* 21, 399–405. doi:10.1016/j.cub.2011.02.005

Qiu, J.-J., Guo, J.-J., Lv, T.-J., Jin, H.-Y., Ding, J.-X., Feng, W.-W., et al. (2013). Prognostic Value of Centromere Protein-A Expression in Patients with Epithelial Ovarian Cancer. *Tumor Biol.* 34, 2971–2975. doi:10.1007/s13277-013-0860-6

Ray-Gallet, D., and Almouzni, G. (2021). "The Histone H3 Family and its Deposition Pathways," in Histone Mutations and Cancer *Advances in Experimental Medicine and Biology*. Editors D. Fang and J. Han (Singapore: Springer), 17–42. doi:10.1007/978-981-15-8104-5_2

Saha, A. K., Contreras-Galindo, R., Niknafs, Y. S., Iyer, M., Qin, T., Padmanabhan, K., et al. (2020). The Role of the Histone H3 Variant CENPA in Prostate Cancer. *J. Biol. Chem.* 295, 8537–8549. doi:10.1074/jbc.RA119.010080

Sanz, G., Singh, M., Peuget, S., and Selivanova, G. (2019). Inhibition of P53 Inhibitors: Progress, Challenges and Perspectives. *J. Mol. Cell Biol.* 11, 586–599. doi:10.1093/jmcb/mjz075

Schlesinger, S., and Meshorer, E. (2019). Open Chromatin, Epigenetic Plasticity, and Nuclear Organization in Pluripotency. *Dev. Cell* 48, 135–150. doi:10.1016/j.devcel.2019.01.003

Screpanti, E., De Antoni, A., Alushin, G. M., Petrovic, A., Melis, T., Nogales, E., et al. (2011). Direct Binding of Cenp-C to the Mis12 Complex Joins the Inner and Outer Kinetochore. *Curr. Biol.* 21, 391–398. doi:10.1016/j.cub.2010.12.039

Sekulic, N., Bassett, E. A., Rogers, D. J., and Black, B. E. (2010). The Structure of (CENP-A-H4)2 Reveals Physical Features that Mark Centromeres. *Nature* 467, 347–351. doi:10.1038/nature09323

Shang, W.-H., Hori, T., Martins, N. M. C., Toyoda, A., Misu, S., Monma, N., et al. (2013). Chromosome Engineering Allows the Efficient Isolation of Vertebrate Neocentromeres. *Dev. Cell* 24, 635–648. doi:10.1016/j.devcel.2013.02.009

Shelby, R. D., Vafa, O., and Sullivan, K. F. (1997). Assembly of CENP-A into Centromeric Chromatin Requires a Cooperative Array of Nucleosomal DNA Contact Sites. *J. Cell Biol.* 136, 501–513. doi:10.1083/jcb.136.3.501

Shrestha, R. L., Ahn, G. S., Staples, M. I., Sathyan, K. M., Karpova, T. S., Foltz, D. R., et al. (2017). Mislocalization of Centromeric Histone H3 Variant CENP-A Contributes to Chromosomal Instability (CIN) in Human Cells. *Oncotarget* 8, 46781–46800. doi:10.18632/oncotarget.18108

Shrestha, R. L., Rossi, A., Wangsa, D., Hogan, A. K., Zaldana, K. S., Suva, E., et al. (2021). CENP-A Overexpression Promotes Aneuploidy with Karyotypic Heterogeneity. *J. Cell Biol.* 220, e202007195. doi:10.1083/jcb.202007195

Shuaib, M., Ouararhni, K., Dimitrov, S., and Hamiche, A. (2010). HJURP Binds CENP-A via a Highly Conserved N-Terminal Domain and Mediates its Deposition at Centromeres. *Proc. Natl. Acad. Sci. U.S.A.* 107, 1349–1354. doi:10.1073/pnas.0913709107

Silva, M. C. C., Bodor, D. L., Stellfox, M. E., Martins, N. M. C., Hochegger, H., Foltz, D. R., et al. (2012). Cdk Activity Couples Epigenetic Centromere Inheritance to Cell Cycle Progression. *Dev. Cell* 22, 52–63. doi:10.1016/j.devcel.2011.10.014

Skalníková, M., Kozubek, S., Lukásová, E., Bártová, E., Jirsová, P., Cafourková, A., et al. (2000). Spatial Arrangement of Genes, Centromeres and Chromosomes in Human Blood Cell Nuclei and its Changes during the Cell Cycle, Differentiation and after Irradiation. *Chromosome Res. Int. J. Mol. Supramol. Evol. Asp. Chromosome Biol.* 8, 487–499. doi:10.1023/a:1009267605580

Smoak, E. M., Stein, P., Schultz, R. M., Lampson, M. A., and Black, B. E. (2016). Long-term Retention of CENP-A Nucleosomes in Mammalian Oocytes Underpins Transgenerational Inheritance of Centromere Identity. *Curr. Biol.* 26, 1110–1116. doi:10.1016/j.cub.2016.02.061

Spiller, F., Medina-Pritchard, B., Abad, M. A., Wear, M. A., Molina, O., Earnshaw, W. C., et al. (2017). Molecular Basis for Cdk1-Regulated Timing of Mis18 Complex Assembly and CENP-A Deposition. *EMBO Rep.* 18, 894–905. doi:10.15252/embr.201643564

Stankovic, A., Guo, L. Y., Mata, J. F., Bodor, D. L., Cao, X.-J., Bailey, A. O., et al. (2017). A Dual Inhibitory Mechanism Sufficient to Maintain Cell-Cycle-Restricted CENP-A Assembly. *Mol. Cell* 65, 231–246. doi:10.1016/j.molcel.2016.11.021

Sullivan, K. F., Hechenberger, M., and Masri, K. (1994). Human CENP-A Contains a Histone H3 Related Histone Fold Domain that Is Required for Targeting to the Centromere. *J. Cell Biol.* 127, 581–592. doi:10.1083/jcb.127.3.581

Sun, X., Clermont, P.-L., Jiao, W., Helgason, C. D., Gout, P. W., Wang, Y., et al. (2016). Elevated Expression of the Centromere protein-A(CENP-A)-encoding Gene as a Prognostic and Predictive Biomarker in Human Cancers. *Int. J. Cancer* 139, 899–907. doi:10.1002/ijc.30133

Szenker, E., Lacoste, N., and Almouzni, G. (2012). A Developmental Requirement for HIRA-dependent H3.3 Deposition Revealed at Gastrulation in Xenopus. *Cell Rep.* 1, 730–740. doi:10.1016/j.celrep.2012.05.006

Tachiwana, H., Kagawa, W., and Kurumizaka, H. (2012). Comparison between the CENP-A and Histone H3 Structures in Nucleosomes. *Nucleus* 3, 6–11. doi:10.4161/nucl.18372

Tachiwana, H., Kagawa, W., Shiga, T., Osakabe, A., Miya, Y., Saito, K., et al. (2011). Crystal Structure of the Human Centromeric Nucleosome Containing CENP-A. *Nature* 476, 232–235. doi:10.1038/nature10258

Thiru, P., Kern, D. M., McKinley, K. L., Monda, J. K., Rago, F., Su, K.-C., et al. (2014). Kinetochore Genes Are Coordinately Up-Regulated in Human Tumors as Part of a FoxM1-Related Cell Division Program. *MBoC* 25, 1983–1994. doi:10.1091/mbc.E14-03-0837

Tomonaga, T., Matsushita, K., Yamaguchi, S., Oohashi, T., Shimada, H., Ochiai, T., et al. (2003). Overexpression and Mistargeting of Centromere Protein-A in Human Primary Colorectal Cancer. *Cancer Res.* 63, 3511–3516.

Tromer, E. C., van Hooff, J. J. E., Kops, G. J. P. L., and Snel, B. (2019). Mosaic Origin of the Eukaryotic Kinetochore. *Proc. Natl. Acad. Sci. U.S.A.* 116, 12873–12882. doi:10.1073/pnas.1821945116

Tyler-Smith, C., Gimelli, G., Giglio, S., Floridia, G., Pandya, A., Terzoli, G., et al. (1999). Transmission of a Fully Functional Human Neocentromere through Three Generations. *Am. J. Hum. Genet.* 64, 1440–1444. doi:10.1086/302380

Uhlén, M., Fagerberg, L., Hallström, B. M., Lindskog, C., Oksvold, P., Mardinoglu, A., et al. (2015). Tissue-based Map of the Human Proteome. *Science*. 347(6220) doi:10.1126/science.1260419

Van Hooser, A. A., Ouspenski, I. I., Gregson, H. C., Starr, D. A., Yen, T. J., Goldberg, M. L., et al. (2001). Specification of Kinetochore-Forming Chromatin by the Histone H3 Variant CENP-A. *J. Cell Sci.* 114, 3529–3542. doi:10.1242/jcs.114.19.3529

Verrelle, P., Meseure, D., Berger, F., Forest, A., Leclère, R., Nicolas, A., et al. (2021). CENP-A Subnuclear Localization Pattern as Marker Predicting Curability by Chemoradiation Therapy for Locally Advanced Head and Neck Cancer Patients. *Cancers* 13, 3928. doi:10.3390/cancers13163928

Wang, I.-C., Chen, Y.-J., Hughes, D., Petrovic, V., Major, M. L., Park, H. J., et al. (2005). Forkhead Box M1 Regulates the Transcriptional Network of Genes Essential for Mitotic Progression and Genes Encoding the SCF (Skp2-Cks1) Ubiquitin Ligase. *Mol. Cell. Biol.* 25, 10875–10894. doi:10.1128/MCB.25.24.10875-10894.2005

Wang, J., Liu, X., Dou, Z., Chen, L., Jiang, H., Fu, C., et al. (2014). Mitotic Regulator Mis18β Interacts with and Specifies the Centromeric Assembly of Molecular Chaperone Holliday Junction Recognition Protein (HJURP). *J. Biol. Chem.* 289, 8326–8336. doi:10.1074/jbc.M113.529958

Wang, Q., Xu, J., Xiong, Z., Xu, T., Liu, J., Liu, Y., et al. (2021). CENPA Promotes Clear Cell Renal Cell Carcinoma Progression and Metastasis via Wnt/β-Catenin Signaling Pathway. *J. Transl. Med.* 19, 417. doi:10.1186/s12967-021-03087-8

Watanabe, R., Hara, M., Okumura, E.-i., Hervé, S., Fachinetti, D., Ariyoshi, M., et al. (2019). CDK1-mediated CENP-C Phosphorylation Modulates CENP-A Binding and Mitotic Kinetochore Localization. *J. Cell Biol.* 218, 4042–4062. doi:10.1083/jcb.201907006

Weierich, C., Brero, A., Stein, S., von Hase, J., Cremer, C., Cremer, T., et al. (2003). Three-dimensional Arrangements of Centromeres and Telomeres in Nuclei of Human and Murine Lymphocytes. *Chromosome Res. Int. J. Mol. Supramol. Evol. Asp. Chromosome Biol.* 11, 485–502. doi:10.1023/a:1025016828544

Weimer, R., Haaf, T., Krüger, J., Poot, M., and Schmid, M. (1992). Characterization of Centromere Arrangements and Test for Random Distribution in G0, G1, S, G2, G1, and Early S′ Phase in Human Lymphocytes. *Hum. Genet.* 88, 673–682. doi:10.1007/BF02265296

Wu, Q., Chen, Y.-F., Fu, J., You, Q.-H., Wang, S.-M., Huang, X., et al. (2014). Short Hairpin RNA-Mediated Down-Regulation of CENP-A Attenuates the Aggressive Phenotype of Lung Adenocarcinoma Cells. *Cell Oncol.* 37, 399–407. doi:10.1007/s13402-014-0199-z

Wu, Q., Qian, Y.-M., Zhao, X.-L., Wang, S.-M., Feng, X.-J., Chen, X.-F., et al. (2012). Expression and Prognostic Significance of Centromere Protein A in Human Lung Adenocarcinoma. *Lung Cancer* 77, 407–414. doi:10.1016/j.lungcan.2012.04.007

Xu, Y., Liang, C., Cai, X., Zhang, M., Yu, W., and Shao, Q. (2020). High Centromere Protein-A (CENP-A) Expression Correlates with Progression and Prognosis in Gastric Cancer. *Ott* 13, 13237–13246. doi:10.2147/OTT.S263512

Yang, J., Antin, P., Berx, G., Blanpain, C., Brabletz, T., Bronner, M., et al. (2020). Guidelines and Definitions for Research on Epithelial-Mesenchymal Transition. *Nat. Rev. Mol. Cell Biol.* 21, 341–352. doi:10.1038/s41580-020-0237-9

Ye, X., Brabletz, T., Kang, Y., Longmore, G. D., Nieto, M. A., Stanger, B. Z., et al. (2017). Upholding a Role for EMT in Breast Cancer Metastasis. *Nature* 547, E1–E3. doi:10.1038/nature22816

Zaidi, S. K., Fritz, A. J., Tracy, K. M., Gordon, J. A., Tye, C. E., Boyd, J., et al. (2018). Nuclear Organization Mediates Cancer-Compromised Genetic and Epigenetic Control. *Adv. Biol. Regul.* 69, 1–10. doi:10.1016/j.jbior.2018.05.001

Zasadzińska, E., Barnhart-Dailey, M. C., Kuich, P. H. J. L., and Foltz, D. R. (2013). Dimerization of the CENP-A Assembly Factor HJURP Is Required for Centromeric Nucleosome Deposition. *EMBO J.* 32, 2113–2124. doi:10.1038/emboj.2013.142

Zasadzińska, E., Huang, J., Bailey, A. O., Guo, L. Y., Lee, N. S., Srivastava, S., et al. (2018). Inheritance of CENP-A Nucleosomes during DNA Replication Requires HJURP. *Dev. Cell* 47, 348–362. e7. doi:10.1016/j.devcel.2018.09.003

Zhang, W., Mao, J.-H., Zhu, W., Jain, A. K., Liu, K., Brown, J. B., et al. (2016). Centromere and Kinetochore Gene Misexpression Predicts Cancer Patient Survival and Response to Radiotherapy and Chemotherapy. *Nat. Commun.* 7, 12619. doi:10.1038/ncomms12619

Zhao, H., Winogradoff, D., Bui, M., Dalal, Y., and Papoian, G. A. (2016). Promiscuous Histone Mis-Assembly Is Actively Prevented by Chaperones. *J. Am. Chem. Soc.* 138, 13207–13218. doi:10.1021/jacs.6b05355

Conflict of Interest: The authors declare that the research was conducted in the absence of any commercial or financial relationships that could be construed as a potential conflict of interest.

Publisher's Note: All claims expressed in this article are solely those of the authors and do not necessarily represent those of their affiliated organizations, or those of the publisher, the editors and the reviewers. Any product that may be evaluated in this article, or claim that may be made by its manufacturer, is not guaranteed or endorsed by the publisher.

Copyright © 2022 Renaud-Pageot, Quivy, Lochhead and Almouzni. This is an open-access article distributed under the terms of the Creative Commons Attribution License (CC BY). The use, distribution or reproduction in other forums is permitted, provided the original author(s) and the copyright owner(s) are credited and that the original publication in this journal is cited, in accordance with accepted academic practice. No use, distribution or reproduction is permitted which does not comply with these terms.

News & Views

OPEN ACCESS CHECK FOR UPDATES

THE EMBO JOURNAL

Tipping the balance in histone supply puts genome stability at stake

Charlène Renaud-Pageot & Geneviève Almouzni ✉

Specific localization of the histone H3 variant CENP-A at centromeres is key for faithful chromosome segregation during cell division, with CENP-A mislocalization being associated with chromosomal instability and cancer. New work in *The EMBO Journal* identifies the H3-H4 chaperone DNAJC9 as a factor restricting CENP-A localization, underscoring the importance of balancing H3 and CENP-A histone levels for ensuring proper CENP-A localization and maintaining genome stability.

See also: V Balachandra et al (April 2024)

Histones exist as distinct variants marking chromatin with unique properties. Dedicated histone chaperones regulate the distribution of each variant within the genome. As a prime example of this regulation, the presence at centromeres of a specific variant of histone H3, termed CENP-A (Centromere Protein A) in mammals, is central to direct kinetochore assembly during cell division. The specific deposition of CENP-A into centromeric chromatin involves a dedicated histone chaperone called HJURP (Dunleavy et al, 2009; Foltz et al, 2009). However, ectopic incorporation of CENP-A at non-centromeric regions occurs upon an imbalance in the proportions of histone H3 variants available, as shown in human cells overexpressing CENP-A (Lacoste et al, 2014; Athwal et al, 2015; Nye et al, 2018). Overexpression of CENP-A also leads to mitotic defects and chromosomal instability (CIN), possibly due to the trapping of kinetochore components away from the native centromeres by ectopic CENP-A nucleosomes (Shrestha et al, 2017). CENP-A overexpression and CIN are common characteristics of aggressive cancers that can impact tumor evolution and response to therapy (Renaud-Pageot et al, 2022). A critical question was whether factors that can perturb the specific localization of CENP-A without acting on CENP-A levels could also lead to a similar outcome, an important aspect to consider more broadly in cancer.

Previous studies found that when CENP-A was overexpressed, its mislocalization depended on DAXX (Lacoste et al, 2014) or HIRA (Nye et al, 2018), histone chaperones that are normally involved in the deposition of the H3.3 histone variant. Consistent with the view that overexpressed CENP-A may have saturated its chaperone HJURP, re-establishing the balance between levels of CENP-A and HJURP was able to abrogate ectopic incorporation of CENP-A (Nye et al, 2018). Thus, the dosage of CENP-A relative to its dedicated chaperone proved important to restrict its localization at the centromere. CENP-A mislocalization also occurred in human cells upon depletion of CHAF1B (p60), a subunit of the CAF-1 complex involved in the deposition of the histone variants H3.1 and H3.2. Here, the global defect in H3.1/H3.2 deposition upon CHAF1B depletion may have allowed the mislocalization of CENP-A, again through the H3.3 chaperone DAXX (Shrestha et al, 2023).

Two major questions ensue: first, can a reduction of the proportions of non-centromeric H3 variants cause CENP-A mislocalization, and second, what factors are involved in such deregulation? In a recent *EMBO Journal* article, Balachandra et al (2024) investigated these questions, and identified key factors that either promote or prevent CENP-A mislocalization in human cells. They performed a genome-wide RNAi screen, using image-based detection of CENP-A enrichment in chromatin as readout for mislocalized CENP-A. Amongst their top candidates, they found factors regulating deposition of other H3 variants, in line with an important role of H3-H4 homeostasis in preventing CENP-A mislocalization. The authors identified CHAF1A/B as one of the top candidates, consistent with previous findings (Shrestha et al, 2023). Most importantly, their screening revealed a new potential regulator, DNAJC9 (member of the J-domain containing heat shock protein HSP40 family), a co-chaperone that assists proper folding of non-centromeric histone H3 variants (Hammond et al, 2021). Balachandra and colleagues confirmed DNAJC9's importance by depleting it, or by mutating its catalytic J-domain required for proper H3-H4 folding. Indeed, DNAJC9 depletion or loss-of-function both led to stable incorporation of CENP-A particles at non-centromeric chromatin in HeLa as well as RPE-1 cell lines. Notably, the authors did not observe higher CENP-A mRNA levels, indicating that CENP-A deregulation does not occur at the transcriptional level. Furthermore, CENP-A mislocalization phenotypes were comparable in cells depleted for DNAJC9 or overexpressing CENP-A: both displayed weakened kinetochores at native centromeres and increased chromosomal instability with higher incidence of micronuclei and defective chromosome segregation.

Finally, Balachandra et al (2024) also explored the interactome of CENP-A in DNAJC9-depleted cells. They found increased CENP-A association with MCM2, a DNA replication-associated H3 chaperone. MCM2 likely contributes to CENP-A mislocalization since co-depletion of both MCM2 and DNAJC9 abrogated CENP-A mislocalization. Since MCM2 has been implicated in the recycling of all H3 (Groth et al, 2007), it would be interesting

Institut Curie, CNRS, PSL Research University, Sorbonne University, Nuclear Dynamics Unit, Équipe Labellisée Ligue contre le Cancer, Paris, France.
✉E-mail: genevieve.almouzni@curie.fr
https://doi.org/10.1038/s44318-024-00112-6 | Published online: 2 May 2024

© The Author(s)

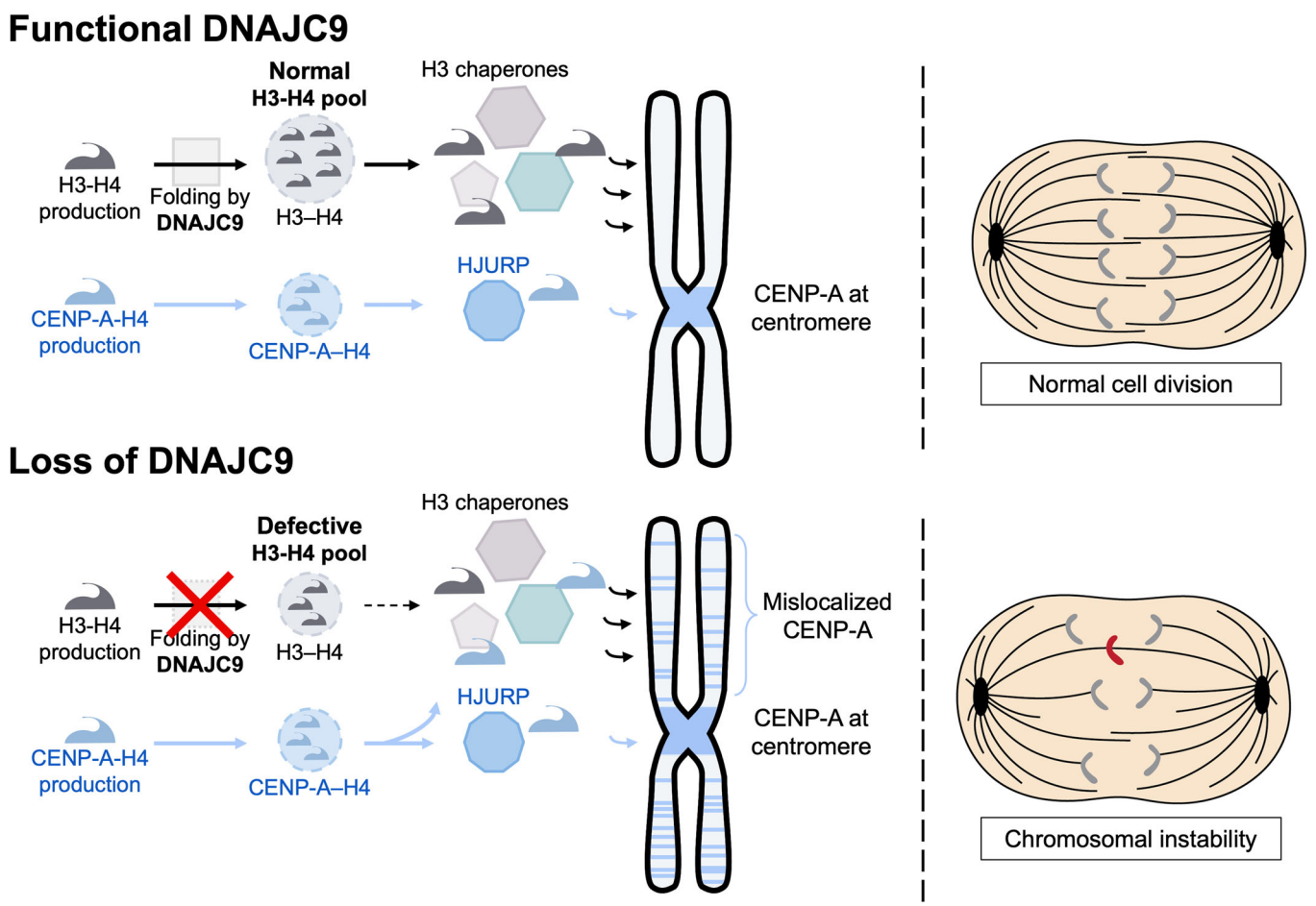


Figure 1. Model for DNAJC9 importance in H3-H4 supply with impact on CENP-A localization and chromosome segregation.

In the presence of functional DNAJC9, a proper balance of folded H3-H4 and CENP-A-H4 pools allows CENP-A to localize at centromere, ensuring proper centromere function and chromosome segregation (top panel). Loss of DNAJC9 reduces folded H3-H4 dimers, tipping the balance in histone supply towards aberrant deposition of CENP-A, and chromosomal instability (bottom panel).

to determine if its effect on CENP-A misincorporation also involves recycling or new deposition of ectopic CENP-A.

Collectively, the study by Balachandra et al (2024) demonstrates that disrupting the function of DNAJC9, which normally supplies folded H3.1-H4, H3.2-H4, and H3.3-H4 dimers, can cause CENP-A mislocalization. A general model for DNAJC9's importance in H3-H4 supply with impact on CENP-A localization and chromosome segregation is depicted in Fig. 1. Upon reduction of the pool of folded H3-H4 dimers, there would be a higher probability of inappropriate interactions between H3-H4 chaperones and CENP-A. In turn, the chaperones would deposit CENP-A at ectopic chromosomal sites. This model is further supported by the fact that partial reduction of H3.3 levels in HeLa cells also led to CENP-A mislocalization. Balachandra et al thus unveil not only the importance of a novel factor, DNAJC9, for restricting CENP-A at centromeres, but also open new avenues for how to consider the network of chaperones and H3 variants in cancer. Indeed, CENP-A mislocalization may be a broader issue, if it depends on imbalance in the proportions of soluble variants. This imbalance can have multiple origins comprising not only overexpression of CENP-A, but also interference in the H3-H4 histone supply chain. Forthcoming research considering the histone chaperone/variant balance in patient tumors may provide avenues to better identify vulnerabilities with a therapeutic potential.

References

Athwal RK, Walkiewicz MP, Baek S, Fu S, Bui M, Camps J, Ried T, Sung MH, Dalal Y (2015) CENP-A nucleosomes localize to transcription factor hotspots and subtelomeric sites in human cancer cells. Epigenetics Chromatin 8:2. https://doi.org/10.1186/1756-8935-8-2

Balachandra V, Shrestha RL, Hammond CM, Lin S, Hendriks IA, Sethi SC, Chen L, Sevilla S, Caplen NJ, Chari R et al (2024) DNAJC9 prevents CENP-A mislocalization and chromosomal instability by maintaining the fidelity of histone supply chains. EMBO J 43. https://doi.org/10.1038/s44318-024-00093-6

Dunleavy EM, Roche D, Tagami H, Lacoste N, Ray-Gallet D, Nakamura Y, Daigo Y, Nakatani Y, Almouzni-Pettinotti G (2009) HJURP is a cell-cycle-dependent maintenance and deposition factor of CENP-A at centromeres. Cell 137:485–497. https://doi.org/10.1016/j.cell.2009.02.040

Foltz DR, Jansen LE, Bailey AO, Yates 3rd JR, Bassett EA, Wood S, Black BE, Cleveland DW (2009) Centromere-specific assembly of CENP-a nucleosomes is mediated by HJURP. Cell

 © The Author(s)

137:472–484. https://doi.org/10.1016/j.cell.2009.02.039

Groth A, Corpet A, Cook AJ, Roche D, Bartek J, Lukas J, Almouzni G (2007) Regulation of replication fork progression through histone supply and demand. Science 318:1928–1931. https://doi.org/10.1126/science.1148992

Hammond CM, Bao H, Hendriks IA, Carraro M, García-Nieto A, Liu Y, Reverón-Gómez N, Spanos C, Chen L, Rappsilber J et al (2021) DNAJC9 integrates heat shock molecular chaperones into the histone chaperone network. Mol Cell 81:2533–2548.e9. https://doi.org/10.1016/j.molcel.2021.03.041

Lacoste N, Woolfe A, Tachiwana H, Garea AV, Barth T, Cantaloube S, Kurumizaka H, Imhof A, Almouzni G (2014) Mislocalization of the centromeric histone variant CenH3/CENP-A in human cells depends on the chaperone DAXX. Mol Cell 53:631–644. https://doi.org/10.1016/j.molcel.2014.01.018

Nye J, Sturgill D, Athwal R, Dalal Y (2018) HJURP antagonizes CENP-A mislocalization driven by the H3.3 chaperones HIRA and DAXX. PLoS ONE 13:e0205948. https://doi.org/10.1371/journal.pone.0205948

Renaud-Pageot C, Quivy JP, Lochhead M, Almouzni G (2022) CENP-A regulation and cancer. Front Cell Dev Biol 10:907120. https://doi.org/10.3389/fcell.2022.907120

Shrestha RL, Ahn GS, Staples MI, Sathyan KM, Karpova TS, Foltz DR, Basrai MA (2017) Mislocalization of centromeric histone H3 variant CENP-A contributes to chromosomal instability (CIN) in human cells. Oncotarget 8:46781–46800. https://doi.org/10.18632/oncotarget.18108

Shrestha RL, Balachandra V, Kim JH, Rossi A, Vadlamani P, Sethi SC, Ozbun L, Lin S, Cheng KC, Chari R et al (2023) The histone H3/H4 chaperone CHAF1B prevents the mislocalization of CENP-A for chromosomal stability. J Cell Sci 136:jcs260944. https://doi.org/10.1242/jcs.260944

Acknowledgements

Our work is supported by the ERC-2015-ADG 694694 "ChromADICT," the Ligue Nationale contre le Cancer (Équipe labellisée Ligue), the ANR-11-LABX-0044 DEEP, and the ANR-10-IDEX-0001-02 PSL. C.R.-P. PhD is funded by Sorbonne University and the FRM (Fondation pour la Recherche Médicale).

Disclosure and competing interests statement

The authors declare no competing interests.

Open Access This article is licensed under a Creative Commons Attribution 4.0 International License, which permits use, sharing, adaptation, distribution and reproduction in any medium or format, as long as you give appropriate credit to the original author(s) and the source, provide a link to the Creative Commons licence, and indicate if changes were made. The images or other third party material in this article are included in the article's Creative Commons licence, unless indicated otherwise in a credit line to the material. If material is not included in the article's Creative Commons licence and your intended use is not permitted by statutory regulation or exceeds the permitted use, you will need to obtain permission directly from the copyright holder. To view a copy of this licence, visit http://creativecommons.org/licenses/by/4.0/. Creative Commons Public Domain Dedication waiver http://creativecommons.org/publicdomain/zero/1.0/ applies to the data associated with this article, unless otherwise stated in a credit line to the data, but does not extend to the graphical or creative elements of illustrations, charts, or figures. This waiver removes legal barriers to the re-use and mining of research data. According to standard scholarly practice, it is recommended to provide appropriate citation and attribution whenever technically possible.

© The Author(s) 2024